Sea-Floor Observations and Subbottom Seismic Characteristics of OAK and KOA Craters, Enewetak Atoll, Marshall Islands

U.S. GEOLOGICAL SURVEY BULLETIN 1678

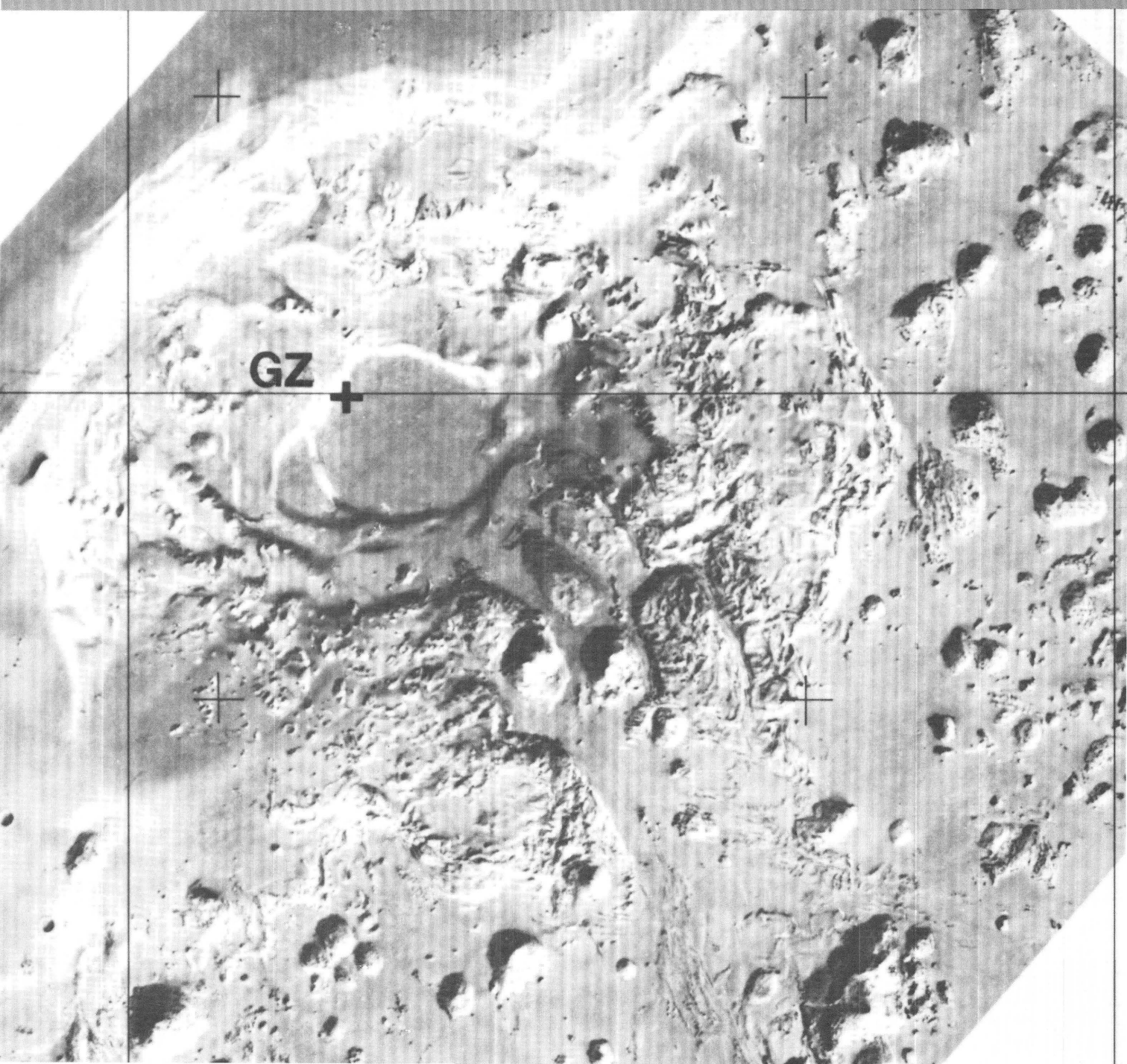

COVER:

Airbrush-enhanced image of OAK crater based on sidescan-sonar, bathymetry, and sea-floor observations. GZ=ground zero.

Sea-Floor Observations and Subbottom Seismic Characteristics of OAK and KOA Craters, Enewetak Atoll, Marshall Islands

Edited by D. W. FOLGER

A study conducted by the U.S. Geological Survey for the Defense Nuclear Agency

This volume is published as chapters A through H. These chapters are not available separately.

U.S. GEOLOGICAL SURVEY BULLETIN 1678

DEPARTMENT OF THE INTERIOR
DONALD PAUL HODEL, Secretary

U.S. GEOLOGICAL SURVEY
Dallas L. Peck, Director

UNITED STATES GOVERNMENT PRINTING OFFICE: 1986

For sale by the Book and Open-File Reports Section, U.S. Geological Survey,
Federal Center, Box 25425, Denver, CO 80225

Library of Congress Cataloging-in-Publication Data

Sea-floor observations and subbottom seismic characteristics of OAK and KOA craters, Enewetak Atoll, Marshall Islands.
"A Study conducted by the U.S. Geological Survey for the Defense Nuclear Agency."
Bibliography : p. 7, A26, B18, C51, D46, E18, F17, G11, H39
Supt. of Docs. no.: I 19.3:1678
1. Nuclear weapons—Testing. 2. Ocean Bottom—Marshall Islands—Enewetak Atoll. 3. Seismic reflection method. I. Folger, David W. II. Geological Survey (U.S.) III. United States. Defense Nuclear Agency.
U264.S417 1986 623.4'5119'0287 86-600112

CONTENTS

[Letters designate chapters]

GLOSSARY

[Most definitions were taken from: Bates, R. L., and Jackson, J. A., Editors, 1980, Glossary of geology, 2d edition: American Geological Institute, Falls Church, Va. 749 p.]

A-Frame. The "A"-shaped steel frame mounted on the stern of a vessel from which oceanographic instruments are towed.

Acoustics. The study of sound and characteristics of its transmission through various media.

Airgun. A sound source for seismic reflection and refraction profiling powered by compressed air.

Anemone. A marine organism, often attached to the bottom, related to corals, jellyfish, and plant-like colonies of hydroids.

Apparent crater. The locus of the zero-difference contour surrounding a crater; that is, the locus of points along which the effects of an explosion can no longer be detected when the preevent contours are compared with the postevent contours.

Apparent velocity. In refraction seismic surveys, the velocity obtained with one unreversed profile.

Arrival. Refers to the appearance of energy on a seismic record.

Backreef. In this study, the side of the reef away from the sea and toward the lagoon.

Bathymetry. In this volume, depth of the sea floor beneath the sea surface.

Beachrock. A friable to well-cemented sedimentary rock, formed in the intertidal zone in a tropical or subtropical region, consisting of calcareous debris (from corals and coralline algae) cemented with calcium carbonate; often a thin, clearly stratified, seaward-dipping calcareous sandstone found on sandy coral beaches.

Bench. A long, narrow, relatively level or gently inclined strip or platform of land, earth, or rock, bounded by steeper slopes above and below.

Check shots. In this volume, air-gun shots fired in the water above a hole drilled in the crater or lagoon bottom while a hydrophone was lowered down the borehole with the objective of obtaining the sound velocity of the drilled strata.

Chronostratigraphy. The branch of stratigraphy (the study of sedimentary rock layers) that interprets the geologic record by determining the age and time sequence of the rock strata.

Cobble. A rock fragment larger than a pebble and smaller than a boulder, having a diameter in the range of 64 to 256 mm (2.5–10 in.).

Common depth point (CDP) shooting. A type of seismic profiling designed for multiple subsurface coverage to establish common depth points to key mappable horizons (reflectors) using several hydrophones in a long, linear array. The data acquired using this technique require computer processing and give better results in most cases than less sophisticated techniques.

Coral knoll. In this volume, small patch reefs.

Cuesta. A hill or ridge with a gentle slope on one side and steep slope on the other, created by the outcrop of a dipping sedimentary layer.

Debris. Used in this volume for sedimentary material that has been moved from its original position and deposited elsewhere by a nuclear explosion.

Decibel (dB). A unit of sound intensity equal to 20 times the common logarithm of the ratio of the pressure produced by the sound wave to a reference pressure.

Deconvolution. A data-processing technique applied to seismic-reflection for the purpose of improving the visibility and resolution of reflections.

Diffraction. A record of seismic data produced by diffracted energy. Such records commonly result from a termination of reflectors and are characterized on seismic records and sections by a distinctive curved alignment pattern of reflections.

Disconformity. An unconformity in which the bedding planes above and below the break are essentially parallel, indicating a significant interruption in the orderly deposition of sedimentary rocks, generally by a considerable interval of erosion or nondeposition, and usually marked by a visible and irregular erosion surface of low relief.

Distal. Sedimentary deposits formed farthest from the source area; in this volume debris derived from the explosion that is farther away from ground zero than the remainder of the debris. (*See* proximal.)

Ejecta. Airborne debris from an explosion.

Eocene. An epoch in the lower Tertiary Period, after the Paleocene and before the Oligocene, about 38 to 55 m.y. before the present.

Event. A nuclear explosion.

Fault. A fracture along which there has been displacement of the sides relative to one another parallel to the fracture.

Fish. In this context an instrument containing electronic equipment, such as a sidescan sonar, usually towed in the water behind the ship.

Fluted. Scalloped

Fold. A bend in strata or any planar structure.

Forereef. The seaward side of a reef.

Frequency spectrum. A description of the distribution of energy within a frequency range; used to characterize acoustic or seismic devices.

Galvo-camera. A device that records seismic signals; commonly used for evaluating performance during operations.

Geometric center. In this volume, the point that is equidistant from points of equal elevation that lie on opposite sides of the crater.

Geomorphology. The study of the shape of the sea floor or land forms.

Grainstone. A mud-free (less than 1 percent of material with diameters less than 20 micrometers), grain-supported, carbonate sedimentary rock.

Granule. A rock fragment larger than a very coarse sand grain and smaller than a pebble, having a diameter in the range of 2 to 4 mm.

Grooves. *See* spur and groove structure.

Ground zero. The point directly under an explosion.

Gully. A small ravine.

Hogback. A ridge produced by highly tilted strata.

Holmes and Narver datum. Equivalent to mean low water spring minus 0.18 m, or 0.6 ft. *See* mean lower low water.

Holocene. One of two epochs in the Quaternary Period of geologic time that dates from final retreat of the ice sheet, about 8,000 years ago, to the present.

Horizon. An interface indicative of a particular position in a stratigraphic sequence, commonly a distinctive very thin bed.

Hydrophone. A pressure-sensitive acoustic detector designed for use in liquid elastic wave-propagating media such as water. An underwater microphone.

IVY grid. A geographic-rectangular coordinate system, devised in 1951, named after Project IVY of the nuclear test program and used for subsequent testing and surveys of the atoll. Coral head OSCAR, about 4 miles west of Runit Island in the Enewetak lagoon, was selected as the source of the IVY grid and was given a value of 100,000 N. and 100,000 E., in international feet.

Isobath. A line on the bottom of equal depth below the sea surface.

Julian Day. The day of the year in sequence to 365, or 366 in leap year.

Laser theodolite. A surveying instrument that measures distances to a high level of precision.

Line-of-sight tube. In this volume, a helium-filled tube used for photographing nuclear explosions from several kilometers away.

Lithostratigraphy. Sequence of sedimentary rock layers that are defined by physical or mineralogic characteristics.

Mean lower low water (MLLW). A reference level to which soundings are corrected. In this volume, MLLW is equivalent to mean low water spring minus 0.6 feet, which is the Holmes and Narver datum for Enewetak.

Micrometer (μm, or micron). One millionth of a meter.

Millisecond (ms). One thousandth of a second.

Miocene. An epoch of the upper Tertiary Period, following the Oligocene and before the Pliocene; 5 to 22.5 m.y. ago.

Morphology. The physical form of the sea floor or exposed lands.

Multichannel seismic system. A seismic system that records returned seismic energy on several hydrophones spaced along a linear array. In this study, 12-channel and 24-channel systems were used.

Multiple reflection. A seismic wave that has been reflected more than once, commonly used for the trace of a seismic echo that has reflected from the water surface and back from the sea bottom.

Norwegian floats. In this study buoys to which the hydrophones were attached during the refraction seismic study.

Nose. The projecting end of a hill. Usually, in this volume, a projection on the wall of a crater.

Nuclear device. Any device capable of producing a nuclear explosion.

Operation Crossroads. An extensive study of the physical characteristics of Bikini and Enewetak Atolls intiated in 1946 prior to testing of nuclear devices.

OSCAR. A patch reef in the Enewetak lagoon assigned as the origin of the IVY grid used during operations and later mapping to locate most structures, vessels, and so on.

Overburden. Loosely consolidated upper part of a sedimentary deposit.

Overwash deposit. Sediment deposited by water landward of a berm crest that does not flow directly back into the sea.

Packstone. A sedimentary carbonate rock whose granular material is arranged in a self-supporting framework but that also contains some matrix of calcareous mud.

Patch reef. Small, thick, generally unbedded lenses of limestone and dolomite that rise from the lagoon floor up to several tens of meters and occasionally reach the sea surface.

Pebble. A rock fragment larger than a granule and smaller than a cobble, having a diameter in the range of 4 to 64 mm.

Physiography. The study of the genesis and evolution of land forms.

Pleistocene. One of two epochs in the Quaternary Period of geologic time that dates from approximately 8,000 to 1.8 m.y. before the present.

Profile. A cross-sectional representation. A subbottom profile, or seismic-reflection profile, is a cross-sectional image of subsurface sediments created by a series of acoustic echoes. The reflections of a sound pulse at the sea surface, or within the water column, are recorded and displayed next to each other. The sea bottom and reflecting surfaces within the bottom sediments are depicted as dark lines or areas that indicate subbottom stratigraphy and structure. Acoustic-, or seismic-reflection profiles are usually somewhat distorted because the vertical scale is a measure of reflection time rather than vertical distance and the speed of sound is variable in different media, varying with density and with porosity of sediments, for example.

Promontory. In this volume, a bluff or prominent hill of sediment projecting from the crater wall.

Proximal. Closer; in this context, debris from the explosion that is closer to ground zero than the remainder of the debris. (*See* distal.)

Ray. Lineament of debris usually extending radially from the center of a crater.

Raypath. The imaginary line along which wave energy travels—always perpendicular to the wave front in an isotropic medium.

Reef flat. A stony platform of dead reef-rock, commonly strewn with coral fragments and coral sand, generally dry at low tide and formed as the summit of the reef above low tide.

Reef plate. Rock formed of cemented reef rubble that occurs in a band several hundred meters wide lagoonward of the living reef.

Reef rock. A resistant massive unstratified rock consisting of the calcareous remains of reef-buiding organisms, often intermingled with with carbonate sand and shingle, the whole deposit cemented by calcium carbonate.

Reentrants. Any indentation in a landform whether above or below the water surface.

Reflector. A velocity discontinuity that reflects seismic energy.

Riprap. A layer of large, durable fragments of broken rock specially selected and graded, thrown together irregularly or fitted together to prevent erosion by waves or currents.

Scarp. An escarpment, cliff, or steep slope of some extent along the margin of plateau, terrace, or bench.

Secondary crater. Small crater formed by falling ejecta from an explosion.

Seismic. Commonly used as an adjective to describe sound in frequency ranges of about 20 Hertz to 500 Hertz.

Seismic refraction shooting. A type of seismic survey based on the measurement of the travel times of seismic waves that have moved nearly parallel to the bedding in high-velocity rock layers, to obtain the depth to the layer and velocity of sound in the layer.

Seismic streamer. A linear array of hydrophones towed behind a ship to receive the energy from a sound source that has been reflected from rock layers below the bottom. The geometry of the array suppresses noise relative to seismic signals.

Seismogram. The record made by a seismograph whether recording natural earthquake waves or sound waves generated by an explosion or other sound source.

Seismology. The study of the structure of the Earth by both natural and artificially generated seismic waves.
Side echoes. Sound echoes from a reflector off to the side rather than directly below a hydrophone. Side echoes are usually unwanted and confusing signals.
Sidescan sonar. An acoustic device that sends signals out to each side and receives echoes from the sea floor that are then mapped. The oceanographic equivalent of airborne side-looking radar.
Sideswipe. Spurious data occurring in seismic refraction shooting when sound energy that travels along a transmission path beside the source-receiver set-up arrives before signals that traveled directly beneath it.
Single-channel seismic system. Usually a high-resolution seismic system that records only on one channel.
Solution unconformity. A break in the sedimentary record produced by dissolution of carbonate strata during subaerial erosion.
Sonobuoy. A buoy, usually free-floating, that contains a hydrophone and a radio transmitter that broadcasts acoustic signals received by the hydrophone. Used in seismic refraction surveying.
Source signature. The wave form of the outgoing pulse from an acoustic source such as an air or water gun.
Spur and groove structure. A comb-tooth structure common to many reef fronts, best developed on the windward side, and consisting of elongate channels or grooves a few meters wide and deep, separated by seaward-extending ridges or spurs.
Stacking velocity. In seismic reflection surveys, the constant velocity for an overlying medium that would most nearly give the observed normal moveout for a horizontal reflector. It is determined from normal moveout values in velocity analysis. *Also called* normal moveout velocity.
Strike. The direction or bearing of a horizontal line in the plane of an inclined stratum, joint, fault, or other structural plane.
Structure-contour map. A map that portrays subsurface configuration by means of structure-contour lines (lines of equal depth).
Subcrop. The areal extent of a truncated subsurface rock unit that succeeds an unconformity.
Swale. A slight depression in a generally level surface.
Syncline. Generally concave-upward fold of which the core contains stratigraphically younger rocks.
Talus slope. A steep slope formed by accumulation of loose rock fragments; especially such a slope at the base of a cliff, formed by the coalescence of several rockfalls or alluvial cones.
Terrace. Relatively flat, horizontal or gently inclined surface, sometimes long and narrow, bounded by a steeper ascending slope on one side and by a steeper descending slope on the other.
Thalweg. A line joining the deepest points of a channel.
Track lines. The representation on a map of the path of the survey vessel.
Transient crater. That part of the crater removed during the first few milliseconds of an explosion.
Transparent. Used to describe rocks that contain insufficient velocity discontinuities to cause seismic energy to be reflected.
Transponder. A device which can transmit and receive signals.
Unconformity. A break or gap in the sedimentary record where a rock unit is overlain by another that is not next in stratigraphic succession, that is, some strata are missing either due to nondeposition or erosion.
Wackestone. A mud-supported carbonate sedimentary rock containing more than 10 percent grains (particles with diameters greater than 62 micrometers).
Watergun. A source of acoustic energy for marine seismic surveying that creates a signal by rapidly forcing water under high pressure into the ocean.

Selected Abbreviations Used in this Report

cm, centimeter
cm/s, centimeters per second
dB, decibel
ft, feet
gal/min, gallons per minute
G.m.t., Greenwich mean time
Hz, hertz
in., inch
kg, kilogram
kHz, kilohertz
kJ, kilojoule
km, kilometers
kn, knots
kW, kilowatt
lb, pound
L/min, liters per minute
m, meters
MLLW, mean lower low water
mm, millimeter
ms, millisecond
m/s, meters per second
nmi, nautical miles
psi, pounds per square inch
s, second
V.E., vertical exaggeration
μm, micrometer
UTM, Universal Transverse Mercator

Introduction to the Volume

By D. W. FOLGER

U.S. GEOLOGICAL SURVEY BULLETIN 1678

SEA-FLOOR OBSERVATIONS AND SUBBOTTOM SEISMIC CHARACTERISTICS OF OAK AND KOA CRATERS, ENEWETAK ATOLL, MARSHALL ISLANDS

CONTENTS

FIGURES

TABLES

Introduction to the Volume

By D. W. Folger

Abstract

From June 17 to September 20, 1984, the physiographic and subsurface effects of thermonuclear explosions were studied in two submarine craters created during nuclear testing in 1958 at Enewetak Atoll, Marshall Islands. The first of a three-phase field program included echo-sounding, sidescan-sonar, and single-channel seismic-reflection profiles; the second included sea-floor observations and bottom sampling by scuba and research submersible; and the third included multichannel seismic-reflection profiles, seismic-refraction profiles, and additional sea-floor observations and sampling. In this report are the results of the 1984 field work supplemented with some preliminary data acquired during an extensive follow-up drilling program conducted during 1985.

OAK Crater

OAK crater is a large circular depression that has a maximum radius to the 5-m (16 ft) isobath of about 600 m (1,970 ft) and a maximum depth of 60 m (197 ft). The geometric center of the crater lies about 100 m (328 ft) southeast (lagoonward) of ground zero where the 8.9-megaton device was exploded on a barge located at the lagoonward edge of the reef in 4 m (13 ft) of water. Both bathymetric and sidescan imagery show that a flat, circular crater floor is surrounded by a complex of hummocks and terraces probably formed by slumps and mass movement that took place after the initial crater was formed. Along the reef, the crater is bordered by a series of scarps several meters high. Around much of the lagoonward side, a blanket of debris extends about 850 m (2,789 ft) from ground zero. An estimate of crater volume based on preblast and postblast bathymetry is 23.6×10^6 m^3 (833×10^6 ft^3). High-resolution single-channel seismic-reflection profiles reveal the detailed geometry of two strongly reflecting layers that are shallower than about 60 m (197 ft) below sea level and less than 20 m (66 ft) subbottom in the area around the crater. The upper of these reflectors in most areas cannot be traced closer to ground zero than 600 m (1,970 ft) except to the south where an inward-dipping flap extends as close as 400 m (1,310 ft). The lower reflector commonly can be traced about 550 m (1,804 ft) from ground zero but may extend as close as 440 m (1,444 ft). With multichannel seismic-reflection data a small segment of the lower reflector can be traced within 250 m (820 ft) of ground zero.

The multichannel profiles define the distribution and deformation of deeper reflectors. These profiles show that an acoustically transparent pond of sediments, apparently chaotically mixed debris and postevent deposits, in the crater center extends to a depth of 110 m (361 ft) below sea level or 50 m (164 ft) below bottom. In most of the crater the transparent sediments extend 400 to 500 m (1,312–1,640 ft) from ground zero and are inferred to outline the transient crater. A zone of intense fracturing extends 70 m (230 ft) below the base of the transparent sediments to 180 m (591 ft) below sea level. A strong acoustic reflector that lies about 95 m (312 ft) below sea level outside the crater is downwarped to 115 m (377 ft) about 300 m (984 ft) from ground zero, where it becomes too fractured to map. Downwarping of deeper reflectors decreases to about 10 m (33 ft) at a depth of 280 m (919 ft) below sea level. Seismic refraction data suggest that fracturing may extend as deep as 425 m (1,394 ft).

Extensive diving by submersible and scuba revealed a transition from fine sediments in the center of the crater to boulder-sized detritus in talus slopes on the reefward side of the crater. In the hummocky area between the crater floor and rim are small hills consisting of coarse, dark-brown detritus which is similar to sediment cored about 230 m (755 ft) below the crater floor. This material may have been transported upward through fractures during dewatering due to the compressional effects of the blast and postevent subsidence. Evaluation of analytical methods for correlating debris samples with cored samples suggests that the original depths of the debris samples may be estimated to within 6 m (20 ft) using strontium isotopes.

Scuba observations in waters less than 30 m deep (98 ft) show that the reefward margin of the crater subsided as much as 21 m (69 ft). Rock strata along the reefward rim of the crater most commonly dip toward ground zero. In one area west of ground zero they dip away from the crater and may be part of an upturned flap. This dip implies that the transient crater margin in that area may be as large as 550 m (1,804 ft).

KOA Crater

The crater was excavated entirely from reef rock, reef plate, and beachrock by a 1.4-megaton device mounted in a water tank on Teteiripucchi Island. Five other nuclear tests were conducted nearby including the largest (10.4 megatons) exploded in the atoll. The radius of KOA crater from ground zero to the 5-m (16 ft) isobath averages about 500 m (1,640 ft), and its maximum depth is 33 m (108 ft). Bathymetric maps and sidescan-sonar imagery show that the crater floor is elliptical with the long axis oriented northeast. Between the crater floor and rim, the bottom is hummocky and comprises numerous slump masses. Some manmade objects that were emplaced as part of the original testing program are clearly visible in sidescan-sonar imagery on the southeastern side of the crater.

Multichannel seismic-reflection profiles show that a transparent pond of sediments in the center of the crater extends to a depth of about 80 m (262 ft) below sea level or 47 m (154 ft) below bottom. As at OAK, these sediments are interpreted to be chaotically mixed debris and postevent deposits that filled the transient crater. The profiles do not define the perimeter of these deposits. A zone of intense fracturing

appears to extend to a depth of 140 m (459 ft) below sea level and laterally 300 to 500 m (984–1,640 ft) from ground zero. A reflector at 75 m (246 ft) below sea level warps downward at about 500 m (1,640 ft) from ground zero to a depth of 100 m (328 ft) at about 200 m (656 ft) from ground zero; beyond 200 m from ground zero the reflector is obscured by intense fracturing. Deeper-lying reflectors that correlate across the crater suggest that acoustically detectable fractures and downwarp are not present below 230 m (755 ft); cores indicate that fractures may persist as deep as 297 m (974 ft).

Submersible and scuba observations revealed only a few scarps around the margin of KOA. The crater floor is covered with coarser sediment than at OAK because of the continuing influx of abundant detritus from the adjacent reef to windward. The dives also documented the locations of manmade objects on the southeastern side of the crater, including a concrete test platform, a line-of-sight tube support, vertically emplaced railroad rails that had been used to support causeways and a collimator station, and other debris such as cables and riprap. Two sets of rails, one found in water as deep as 18 m (59 ft), and another in about 6 m (20 ft) of water, apparently were originally continuous but were separated by postevent slumping. By moving the deep set eastward and joining it to the shallow set, the effects of the postevent slump can be eliminated. This places riprap west of the last rail about 430 m (1,411 ft) from ground zero, which probably is a good estimate for the maximum transient crater radius in the southeast quadrant of the crater.

PURPOSE

The thermonuclear explosions, detonated in the Marshall Islands from 1952 to 1958, were the only events conducted at or near sea level before the nuclear test-ban treaty required that all further testing be conducted underground. Thus, these are the only sites available to assess the effects of such large explosions on surface and subsurface geology.

This study was initiated at the request of the Defense Nuclear Agency (DNA) to acquire detailed information on the size, morphology, and deformation depth of two submarine nuclear craters, OAK and KOA, located on the north side of Enewetak Atoll (fig. 1). The report represents the first part of a two-part study that responded to the DNA request. It comprises a geological and geophysical assessment of the surface and subsurface geology based on data collected at Enewetak from June 17 to September 20, 1984. The second part comprises mainly a drilling and coring program carried out from January to August 1985. Only preliminary results from the second part are included in this report.

DATA ACQUISITION

Sea-floor and subbottom characteristics discussed include: (1) bathymetry (depth below the sea surface), physiography, and the distribution and character of materials on the bottom or to a depth of about 10 m (33 ft) below bottom, and (2) the depth, distribution, extent, continuity, and seismic velocity of acoustic reflectors below the bottom. We acquired bathymetric data, sidescan-sonar imagery, and single-channel seismic profiles on the first leg (June 17 to July 4, 1984); sea-floor descriptions, bottom samples, and cores on the second leg (July 14 to August 12, 1984); and multichannel and refraction seismic profiles and additional sea-floor descriptions and bottom samples on the third leg (August 21 to September 20, 1984).

Vessels used to support the program included *Egabrag II, Delta, Halimeda,* the "Mike" boat, and various whalers (fig. 2).

Preliminary data from the second part of the study concerning the character and age of subsurface samples are integrated mainly into chapters C, D, E, and G.

SETTING

Part of the Marshall Islands group, Enewetak Atoll lies approximately 4,600 km (2,500 nmi) southwest of Honolulu; it is elliptical in shape with its long (40 km, or 22 nmi) axis oriented northwest and the short (28 km, or 15 nmi) axis northeast. Most islands in the atoll are located along the northeast side, which faces the prevailing trade winds (fig. 1). More detailed discussions of settings that pertain specifically to acquisition of different data sets are included in each chapter.

During this study, positions on Enewetak Atoll were determined using the IVY grid as well as geographic coordinates of latitude and longitude. The IVY grid is a planar coordinate system established during the postwar nuclear testing program, which has been used subsequently to locate structures and test sites. It is an orthogonal grid, measured in feet, based on site OSCAR, a coral head in Enewetak lagoon (fig. 1), which was assigned the position of 100,000 ft N. and 100,000 ft E.

As the result of satellite observations used to locate five transponder stations, we relocated the geodetic position of site OSCAR. (See table 1.) This position will be further refined by the Defense Mapping Agency (DMA) through analyses of the corrected satellite orbits. The former position of OSCAR is 11°32′20.254″ N., and 162°17′10.944″ E. The new position of OSCAR is 11°32′07.432″ N., and 162°16′49.408″ E. or, in space, 762.21 m (2,500.7 ft) southwest of the old position. The latitude and longitude of the atoll and craters on our maps have been changed accordingly and do not agree with positions shown on older charts.

We have used the names of islands after Tobin (1973) in Freisen (1982). (See table 1.) Of the 43 nuclear tests conducted on Enewetak Atoll, we include in table 2 a list of the 8 craters studied or referred to in this volume.

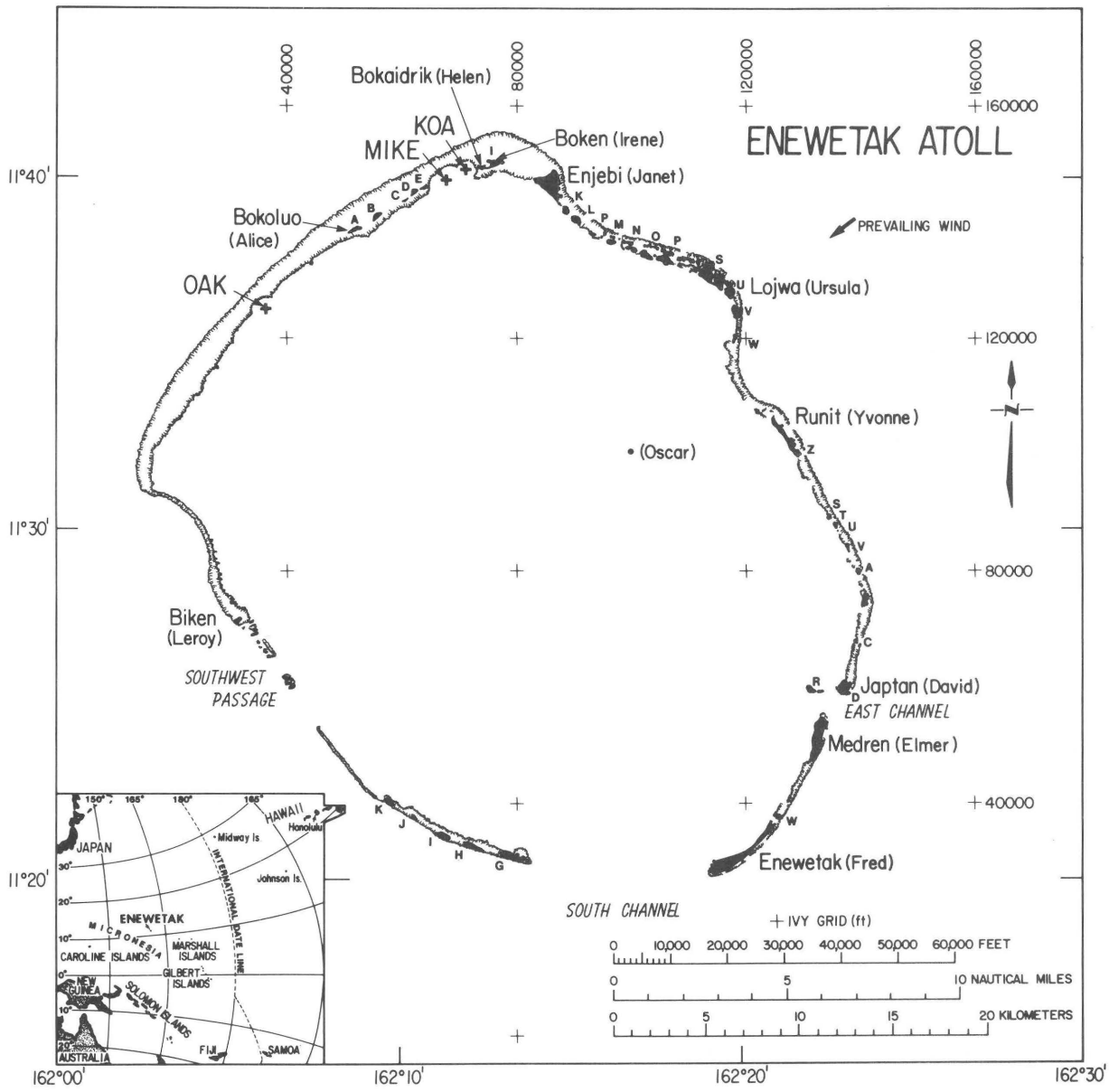

Figure 1. Map showing the location of Enewetak Atoll, the locations of craters (shown by crosses), and of islands (in black) on submerged reef. Names in parentheses are site names, which are listed in table 1. Letters, such as A, B, and C, are the first initials of each site name.

PREVIOUS WORK

Operation Crossroads, initiated in 1946 prior to testing of nuclear devices on Bikini and Enewetak Atolls, included extensive geologic, geophysical, oceanographic, and biologic studies of the area. The principal products of these investigations were many papers assembled as U.S. Geological Survey Professional Paper 260. The first of these appeared in 1954 (Emery and others, 1954); others were published over the next 15 years. This enormous volume of papers and the references cited include most of the scientific work concerned with the area prior to 1970. Subsequently, in addition to many studies concerning radiation effects on biota (see Friesen, 1982, and references cited), geologic and geophysical surveys of the craters and crater areas were conducted during a series of projects designed to understand the mechanisms of cratering (Circeo and Nordyke, 1964; Henny and others, 1974; Couch and others, 1975; Ristvet and others, 1978; Tremba and others, 1982). Their work documented many characteristics of the craters vital to understanding cratering mechanisms, but it also left many questions unresolved concerning the geometry of craters. This study was designed and carried out to provide answers to these unresolved questions.

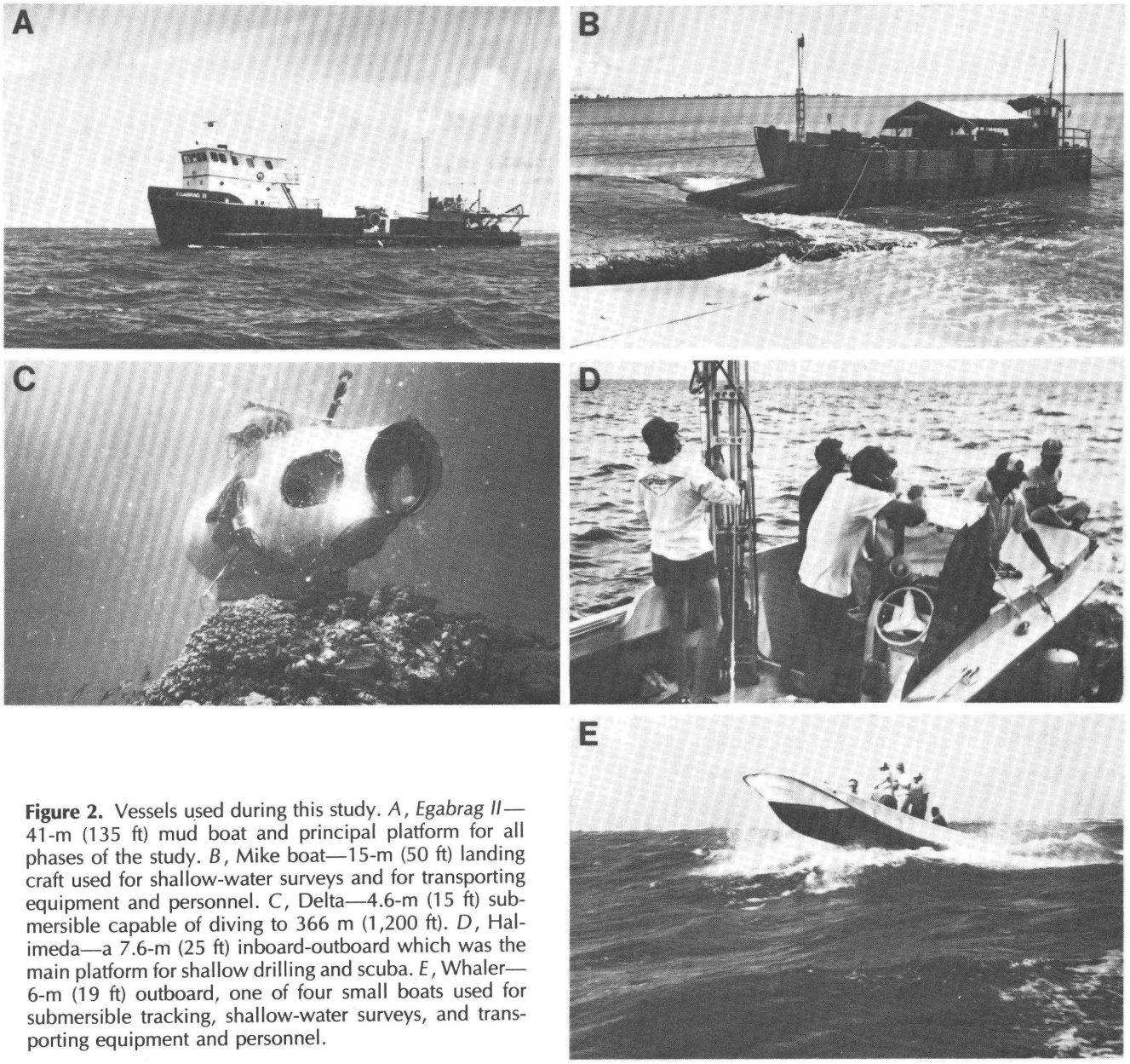

Figure 2. Vessels used during this study. *A*, *Egabrag II*—41-m (135 ft) mud boat and principal platform for all phases of the study. *B*, Mike boat—15-m (50 ft) landing craft used for shallow-water surveys and for transporting equipment and personnel. *C*, Delta—4.6-m (15 ft) submersible capable of diving to 366 m (1,200 ft). *D*, Halimeda—a 7.6-m (25 ft) inboard-outboard which was the main platform for shallow drilling and scuba. *E*, Whaler—6-m (19 ft) outboard, one of four small boats used for submersible tracking, shallow-water surveys, and transporting equipment and personnel.

PARTICIPANTS

On the first leg of the cruise, U.S. Geological Survey (USGS) personnel included D. W. Folger and J. M. Robb, cochief scientists, and G. K. Miller, K. F. Parolski, and D. S. Blackwood. Navigators from Meridian Ocean Systems, Inc. (MOS), included R. C. Hollar, party chief, and A. Pearce, S. L. Thoresen, and M. Milburn. E. L. Tremba and B. L. Ristvet were observers for DNA. H. V. Woodworth of the Defense Mapping Agency, with the assistance of E. L. Tremba, helped to calibrate the navigation system transponders, and he also relocated several critical positions on Enewetak and Lojwa Islands within the IVY grid at the outset of the first leg. On the second leg, U.S. Geological Survey personnel included E. A. Shinn, chief scientist, and R. B. Halley, J. H. Hudson, J. L. Kindinger, M. W. Hempenius, D. W. Folger, and D. J. Roddy. Operators of the submersible included R. A. Slater of GEOCUBIC, Inc., and D. N. Privitt of MARFAB. Because of his experience in submarine carbonate terrains, Slater also served as a principal scientist. The Defense Nuclear Agency observer was B. L. Ristvet. Navigators from MOS included R. C. Hollar, R. F. Johnson, and S. L. Thoresen. Many observers from the Defense community made orientation dives on the submersible during this leg (see appendix, chap. F). Between legs 2 and 3, at DNA's request, additional sidescan and bathymetric surveys were conducted in nearshore areas with the Mid-Pacific Laboratory's Mike boat (landing craft). D. W. Folger and K. F. Parolski of USGS and S. L.

Table 1. Comparison of names of islands and coral heads (site names) assigned before and during nuclear tests with those used by the natives

[Table is taken from Freisen (1982). Names used before nuclear testing are from Bryan (1971). The native names from Tobin (1973) are used in this report]

Site	Native Names From U.S. Hydrographic Office 1946	1968	From Bryan 1971	From Tobin, 1973 Native names [a]
ALICE	Bogallua	Bogallua	Peony	BOKOLUO
BELLE	Bogombogo	Bogombogo	Petunia	BOKOMBAKO
CLARA	Ruchi	Eybbiyae	Poinsettia	KIRUNU
DAISY	b	Lidilbut	Primrose	LOUJ
EDNA*	b	b	Rambler	BOCINWOTME[c]
EDNA'S DAUGHTER	b	b	b	b
FLORA*	Elugelab	b	Sagebrush	b
GENE*	Teiteiripucchi	b	Sunflower	b
HELEN*	Bogairikk	Bogeirik	Violet	BOKAIDRIK
IRENE	Bogon	Bogon	Zinnia	BOKEN
JANET	Engebi	Engebi	Fragile	ENJEBI
KATE	Muzinbaarikku	Mujinkarikku	Arbutus	MIJIKADREK
LUCY	Kirinian	Billee	Aster Blossom	KIDRINEN
PERCY	b	b	b	TAIWEL
MARY	Bokonaarappu	Bokonarppu	Bitterroot	BOKENELAB
MARY'S DAUGHTER	b	b	Bluebonnet	b
NANCY	Yeiri	Yeiri	Buttercup	ELLE
OLIVE	Aitsu	Aitsu	Camellia	AEJ
PEARL	Rujoru	Rujiyoru	Canna	LUJOR
PEARL'S DAUGHTER	b	b	Carnation	b
RUBY*	Eberiru	Eberiru	Columbine	ELELERON
SALLY	Aomon	Aomon	Clover	AOMON
SALLY'S CHILD	b	b	Dandelion	b
TILDA	Biijiri	Biijire	Daisy	BIJILE[c]
URSULA	Rojoa	Rojoa	Delphinium	LOJWA
VERA	Aaraanbiru	Arambiru	Gardenia	ALEMBEL
WILMA	Piiraai	Piirai	Goldenrod	BILLAE
YVONNE	Runit	Runit	Hawthorn	RUNIT
SAM	b	b	b	BOKO
TOM	b	b	b	MUNJOR
URIAH	b	b	b	INEDRAL
VAN	b	b	b	b
ALVIN	Chinieero	b	b	JINEDROL
BRUCE	Aniyaanii	Japtan	Jasmine	ANANIJ
CLYDE	Chinimi	Chinimi	Lavender	JINIMI
DAVID	Japtan	Muti	Ladyslipper	JAPTAN
REX	Jieroru	Bogen	Lilac	JEDROL
ELMER	Parry	Parry	Heartstrings	MEDREN
WALT	b	b	b	BOKANDRETOK
FRED	Eniwetok	Eniwetok	Privilege	ENEWETAK
GLENN	Igurin	Igurin	Lantana	IKUREN
HENRY	Mui	Buganegan	Mimosa	MUT
IRWIN	Pokon	Bogan	Mistletoe	BOKEN
JAMES	Ribaion	Libiron	Oleander	RIBEWON
KEITH	Giriinien	Grinem	Oca	KIDRENEN
LEROY	Rigili	Rigile	Posy	BIKEN
OSCAR (coral head)	b	b	b	DREKATIMON
MACK (coral head)	b	b	b	UNIBOR

[a] As confirmed by the Enewetak people during the Ujelang field trip of July 1973.

[b] No name reported.

[c] BOKINWOTME and BIJIRE are preferred according to current literature and are so spelled in this report.

*Original island destroyed by nuclear tests except for small portions of EDNA, HELEN, and RUBY.

Table 2. List of nuclear test events cited in this volume

[Characteristics after Freisen, 1982; B. L. Ristvet and K. L. Mills III, written commun., July 1985; E. L. Tremba, oral commun., July 1985. ---, no information available]

Event	Date	Location	Height of burst	Yield (kilotons)	Average apparent radius	IVY grid co-ordinates
MIKE	Oct. 31, 1952	Surface, Flora	3.1 m (10 ft)	10,400	887 m (2,910 ft)	147,754 N. 67,789 E.
NECTAR	May 13, 1954	Barge, Mike crater	---	1,700	---	147,750 N. 67,790 E.
LACROSSE	May 4, 1956	Surface, Yvonne	2.4 m (8.0 ft)	40	61 m (200 ft)	106,885 N. 124,515 E.
SEMINOLE	June 6, 1956	Surface, Irene	2.1 m (7.0 ft)	13.7	99 m (324 ft)	149,897 N. 75,237 E.
APACHE	July 8, 1956	Barge, Mike crater	---	---	---	148,063 N. 69,227 E.
HURON	July 21, 1956	Barge, Mike crater	---	---	---	148,304 N. 70,015 E.
KOA	May 12, 1958	Surface, Gene	0.8 m (2.67 ft)	1,400	658 m (2,160 ft)	149,360 N. 71,120 E.
OAK	June 28, 1958	Barge, lagoon	1.75 m (5.75 ft)	8,900	875 m (2,870 ft)	124,981 N. 36,108 E.

Thoresen of MOS carried out the work. On the third leg, USGS personnel included J. A. Grow, chief scientist, J. J. Miller, T. F. O'Brien, D. R. Nichols, and D. H. Mason and, from Seismic Data Systems, Inc., T. Owens. During the latter part of the leg, Shinn, Halley, Hudson, and Kindinger returned to complete the scuba observations. In addition, a bottom sampling program was carried out from a 6.4-m (21 ft) whaler by USGS personnel T. W. Henry and B. R. Wardlaw. MOS navigators included R. F. Johnson and S. L. Thoresen. DNA observers included E. L. Tremba and R. F. Couch. Captain R. L. Wilson was master of the *Egabrag II* during the entire field program.

Shore personnel who played large roles in the processing, analysis, and synthesis of data included H. D. Ackermann, J. C. Hampson, L. A. Tavares, D. S. Foster, R. A. Woellner, V. F. Paskevich, E. L. Wright, J. E. Dodd, B. H. Lidz, M. W. Lee, W. F. Agena, J. M. Williams, P. A. Davis, P. M. Bridges, R. P. Major, K. R. Ludwig, and Z. L. Peterman of USGS and R. A. Goldsmith, S. B. Volkmann, and J. R. McCullough of the Woods Hole Oceanographic Institution, and R. K. Matthews of Brown University.

ACKNOWLEDGMENTS

We are particularly indebted to W. J. Stanley, Director, Pacific Area Support Office (PASO), Department of Energy, in Honolulu, and to his staff, including especially H. U. Brown, PASO Deputy for this project. P. R. Haggerty of Holmes and Narver, Inc., and his staff at Honolulu, particularly J. H. Matthewman, were of invaluable assistance in arranging contracts and transportation. S. S. Miyasato and his staff at Enewetak offered every assistance to solve the many on-site technical and logistical problems during the project. E. L. Tremba, B. L. Ristvet, and A. S. Melzer provided us with much information that was useful in the planning and execution of the work. C. E. Otterman, owner of *Egabrag II*, also provided us with valuable suggestions. H. V. Woodworth of DMA has supplied us with much important information concerning the precise locations of our transponder stations and of submerged objects that we located with the submersible and scuba. V. E. Zadnik of USGS helped to write many contracts for equipment and services and shepherded them through the system. P. L. Forrestel, J. A. Zwinakis, and D. S. Blackwood drafted and photographed most of the illustrations. P. A. Davis prepared the three-dimensional computer images for both craters. M. W. Hempenius typed the entire manuscript and appendices. P. B. Worl typed drafts of chapters D and E. D. M. Morton, R. F. Couch, E. L. Tremba, B. L. Ristvet and B. R. Wardlaw kindly reviewed the manuscript.

REFERENCES

Bryan, E. H., Jr., 1971, Guide to place names in the Trust Territory of the Pacific Islands: Pacific Scientific Information Center, Bishop Museum, Honolulu, Hawaii, not paginated.

Circeo, L. J., and Nordyke, M. D., 1964, Nuclear cratering experience at the Pacific proving grounds: Livermore, University of California, Lawrence Radiation Laboratory, TID–4500, UC–35, (UCRL)–12172, 88 p.

Couch, R. F., Jr., Fetzer, J. A., Goter, E. R., Ristvet, B. L., Tremba, E. L., Walter, D.R., and Wendland, V. P., 1975, Drilling operations on Eniwetok Atoll during Project EXPOE: Air Force Weapons Laboratory Technical Report TR–75–216, Kirtland Air Force Base, New Mexico, 87117, 270 p.

Emery, K. O., Tracey, J. I., Jr., and Ladd, H. S., 1954, Geology of Bikini and nearby atolls: U.S. Geological Survey Professional Paper 260–A, 259 p.

Freisen, Bert, ed., 1982, Enewetak Radiological Support Project, final report: U.S. Department of Energy, Nevada Operations Office, Las Vegas, Nevada, NVO 213, 349 p.

Henny, R. W., Mercer, J. W., Zbur, R. T., 1974, Near-surface geologic investigations at Eniwetok Atoll: Air Force Weapons Laboratory Technical Report TR–74–257, Kirtland Air Force Base, New Mexico 87117, 36 p.

Ristvet, B. L., Tremba, E. L., Couch, R. F., Jr., Fetzer, J. A., Goter, E. R., Walter, D. R., and Wendland, V. P., 1978, Geologic and geophysical investigations of the Eniwetok nuclear craters: Air Force Weapons Laboratory Technical Report TR–77–242, Kirtland Air Force Base, New Mexico 87117.

Tobin, J. A., 1973, The Enewetak Atoll people: A special report for the radiological survey of 1972–73: Atomic Energy Commission, Washington, D.C., not paginated.

Tremba, E. L., Couch, R. F., Ristvet, B. L., 1982, Enewetak Atoll Seismic Investigation (EASI): Phases I and II (final report): Air Force Weapons Laboratory Technical Report TR–82–20, Kirtland Air Force Base, New Mexico 87117.

Chapter A

Bathymetry of OAK and KOA Craters

By D. W. FOLGER, J. C. HAMPSON, J. M. ROBB
R. A. WOELLNER, D. S. FOSTER, and L. A. TAVARES

U.S. GEOLOGICAL SURVEY BULLETIN 1678

SEA-FLOOR OBSERVATIONS AND SUBBOTTOM SEISMIC CHARACTERISTICS OF OAK AND KOA CRATERS, ENEWETAK ATOLL, MARSHALL ISLANDS

CONTENTS

FIGURES

Chapter A
Bathymetry of OAK and KOA Craters

By D. W. Folger, J. C. Hampson, J. M. Robb, R. A. Woellner, D. S. Foster, *and* L. A. Tavares[1]

INTRODUCTION

Purpose

Bathymetric data, collected as part of Project EASI (Enewetak Atoll Seismic Investigation) by Tremba and others (1982), provided definition of most geomorphological features in OAK and KOA craters. However, a bathymetric survey was requested with much closer line spacing so that greater data density could be exploited by sophisticated image-processing techniques developed at the U.S. Geological Survey's (USGS) Branch of Astrogeological Studies in Flagstaff, Ariz. These techniques have the potential to provide much more resolution to assess the extent, distribution, and thickness of debris, and to define the characteristics of the crater rims, walls, and floors in greater detail. Therefore, we acquired bathymetric data on 25-m-spaced (82-ft-spaced) lines, which was the closest spacing practicable in view of the echo-sounder beam width, navigation errors, and ship maneuverability. Our purpose was to integrate bathymetry with sidescan-sonar data, so that more detailed information on the morphology of these submarine craters could be provided. The bathymetric data were used as guides for the acquisition of all other geophysical data, submersible and scuba observations, and siting of sample stations and drill sites.

Setting

The 48 small islands and coral heads that rise above the reef make up an area of only 7 km^2 (2 nmi^2), contrasting markedly with the area of the lagoon which totals about 1,000 km^2 (292 nmi^2) (fig. 1). The bottom of the lagoon, sounded in 1944 by the U.S. Navy (Emery and others, 1954), comprises three physiographic provinces: (1) a terrace, as wide as 4.8 km (2.6 nmi); (2) an almost perfectly elliptical, flat-floored basin that has a maximum depth of 62 m (210 ft) in its northwestern half, and (3) several thousand patch reefs or coral knolls. Some of these knolls come within a few meters of the lagoon's surface; most, however, lie below about 36 m (120 ft) of water (Emery and others, 1954) (fig. 1).

Both OAK and KOA craters lie on the north side of the atoll. The 8.9-megaton OAK device formed the westernmost of the craters; it was detonated over the terrace close to the reef, on a barge that was anchored in water approximately 4 m (13 ft) deep. Present depth of ground zero is close to 60 m (197 ft). OAK was created in an area which has been little disturbed by other blasts. The nearest other crater, MIKE, which was not studied in detail, lies about 12 km (6.5 nmi) to the northeast. The much smaller (1.4-megaton) KOA device was fired on Teiteiripucchi (Gene) Island close to the sites where five other tests had taken place—of which MIKE was the largest (10.4 megatons) fired in the atoll. KOA obliterated the island, and ground zero now lies under slightly more than 33 m (108 ft) of water.

Previous work

The extent of echo sounding by the Germans, or subsequently by the Japanese when they were in possession of the atoll, is unknown. In 1944, the U.S.S. *Bowditch* conducted an extensive survey of the entire atoll, and more than 180,000 sounding depths were plotted (Emery and others, 1954) (fig. 1). Some additional data were added during Operation Crossroads in 1946. Lead line and echo-sounding surveys were conducted in the area of OAK crater prior to and after the test in 1958. This survey apparently consisted of at least 23 lines run normal to the reef at about 90-m-spacing (300-ft-spacing) that were rerun subsequent to the detonation. At KOA, three lines were run through ground zero before and after the detonation, but apparently there was some problem with navigation as the before-and-after lines were not in the same locations (B. L. Ristvet, oral commun., October 1984). The most extensive and most recent survey conducted prior to this study took place during Project EASI, which started in 1979. Approximately 260 km (140 nmi) of data in a grid with line spacing ranging from 100 to 140 m (328–450 ft) were collected in the OAK and KOA crater areas and near Enjebi (Janet) Island (Tremba and others, 1982).

[1]All authors are with the U.S. Geological Survey, Branch of Atlantic Marine Geology, Woods Hole, Mass. 02543.

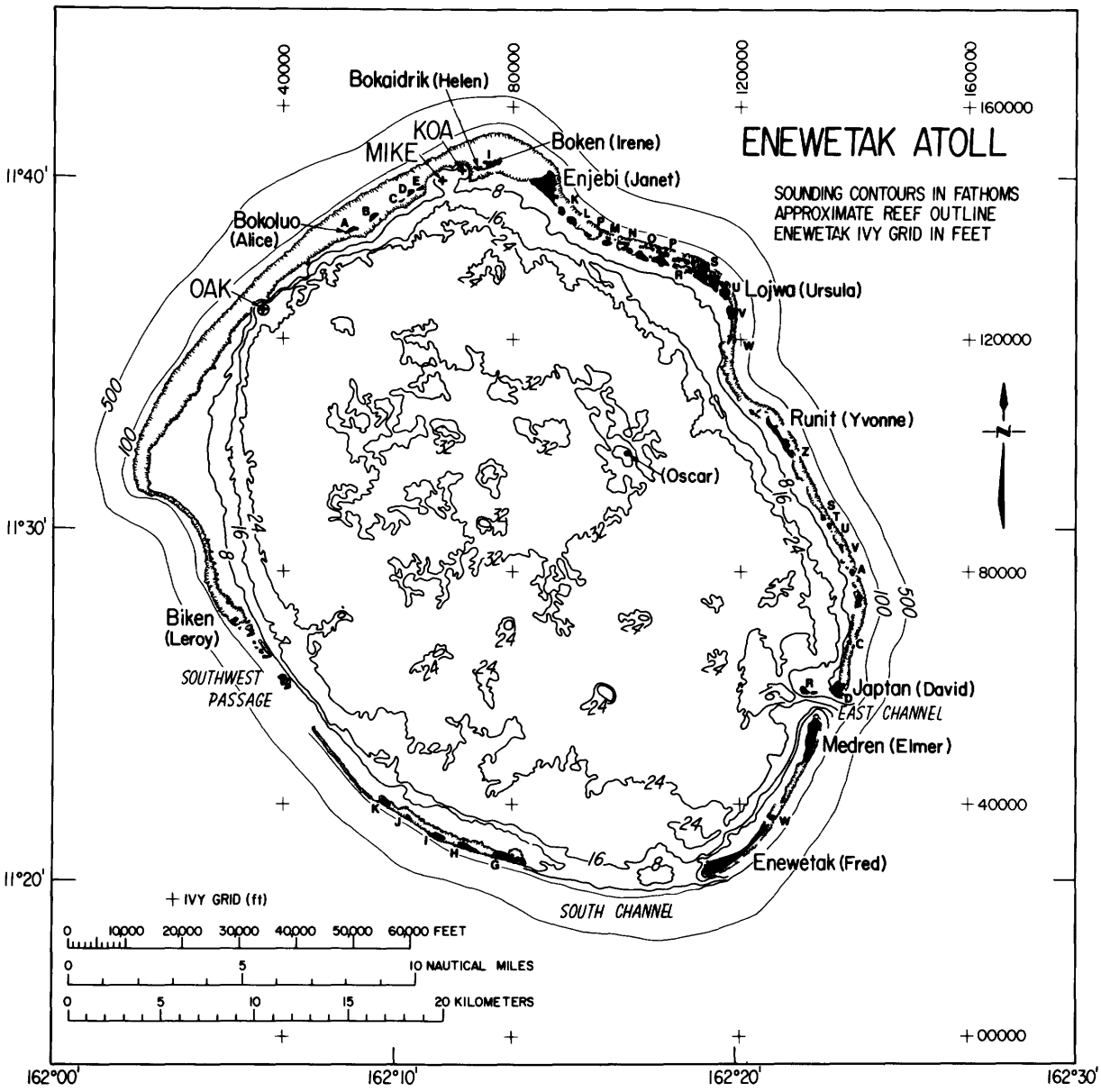

Figure 1. Map showing bathymetry of Enewetak Atoll. Letters (A, B, and C) next to islands represent the first letters of site names. (See table 1, Introduction to the volume.) The map has been generalized and simplified after Emery and others (1954) on the basis of soundings collected by U.S.S. *Bowditch*. Contours in OAK, MIKE, and KOA are based on soundings collected in this study.

METHODS

Echo-sounding data (figs. 2, 3) were acquired in both craters from three different vessels: MS *Egabrag II*, Mike boat (landing craft), and a 6.4-m (21 ft) whaler (fig. 2, Introduction to the volume). Most data were collected from *Egabrag II* along 25-m-spaced (82-ft-spaced) lines during the first leg of the cruise. Data collected during the multichannel leg augmented the data base. Smaller vessels were used mainly nearshore in shallow water. Each vessel was positioned with a Motorola FALCON-IV Miniranger System (accuracy ±3 m, or 10 ft) which was set up and operated by Meridian Ocean Systems of Ventura, Calif. The navigation net was controlled by five transponders located atop towers on Biken (Leroy), Bokoluo (Alice), Enjebi (Janet), Lojwa (Ursula), and Enewetak (Fred) Islands (fig. 1). The transponder towers were tied into the IVY grid net by H. V. Woodworth of the Defense Mapping Agency using a laser theodolite and were found to be consistently within 4.5 m (15 ft) of the positions previously established by Meridian personnel using Motorola Satellite Navigation Systems.

We mounted an Atmospheric Instrumentation Research (Model AIR–DB–1A) digital barometer aboard *Egabrag II* to record variations in atmospheric pressure. To

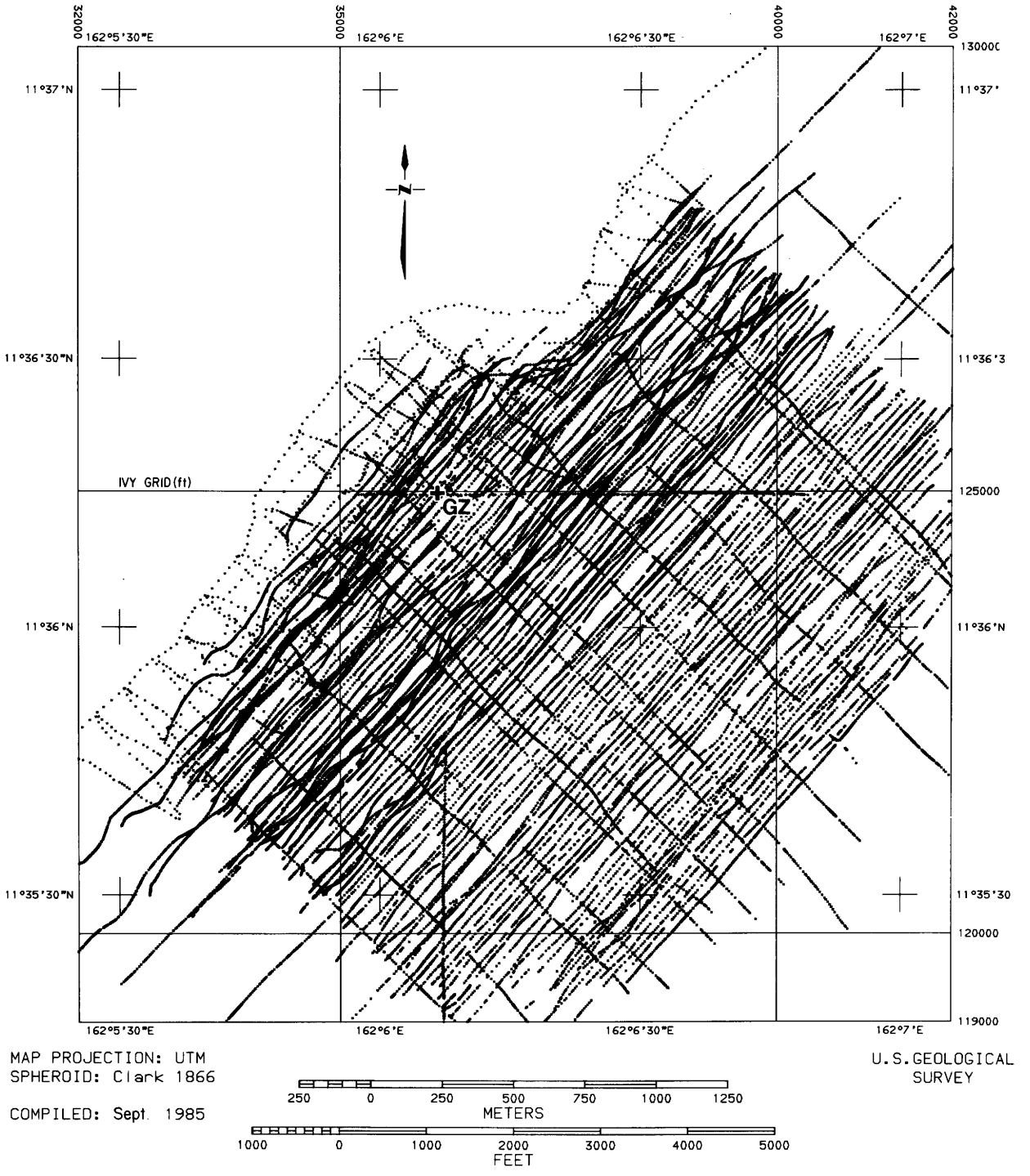

Figure 2. Point plots of echo soundings along tracks of all vessels used to acquire bathymetric data in OAK crater. Closer points in spacing most often reflect areas of more variable bathymetry. GZ=ground zero.

monitor the 1.5-m (5 ft) tidal fluctuations, we deployed two Sea Data tide gauges, one in OAK crater and one in KOA crater. No atmospheric pressure correction was necessary because variations were too small to affect the level of the water in the lagoon significantly or to require a correction to the pressure-depth acquired with the tide gauges. We also found that measured values differed by as much as 0.6 m (2 ft) from NOAA (National Oceanographic and Atmospheric Administration) tide table predictions for the Enewetak lagoon.

To acquire bathymetric data, we used a Raytheon 719B depth-recording system (200 kHz, 534 pulses/minute, accuracy of ±2.5 cm, with a beam width of 18° at −10dB). Echo-sounding data were processed in the USGS laboratory

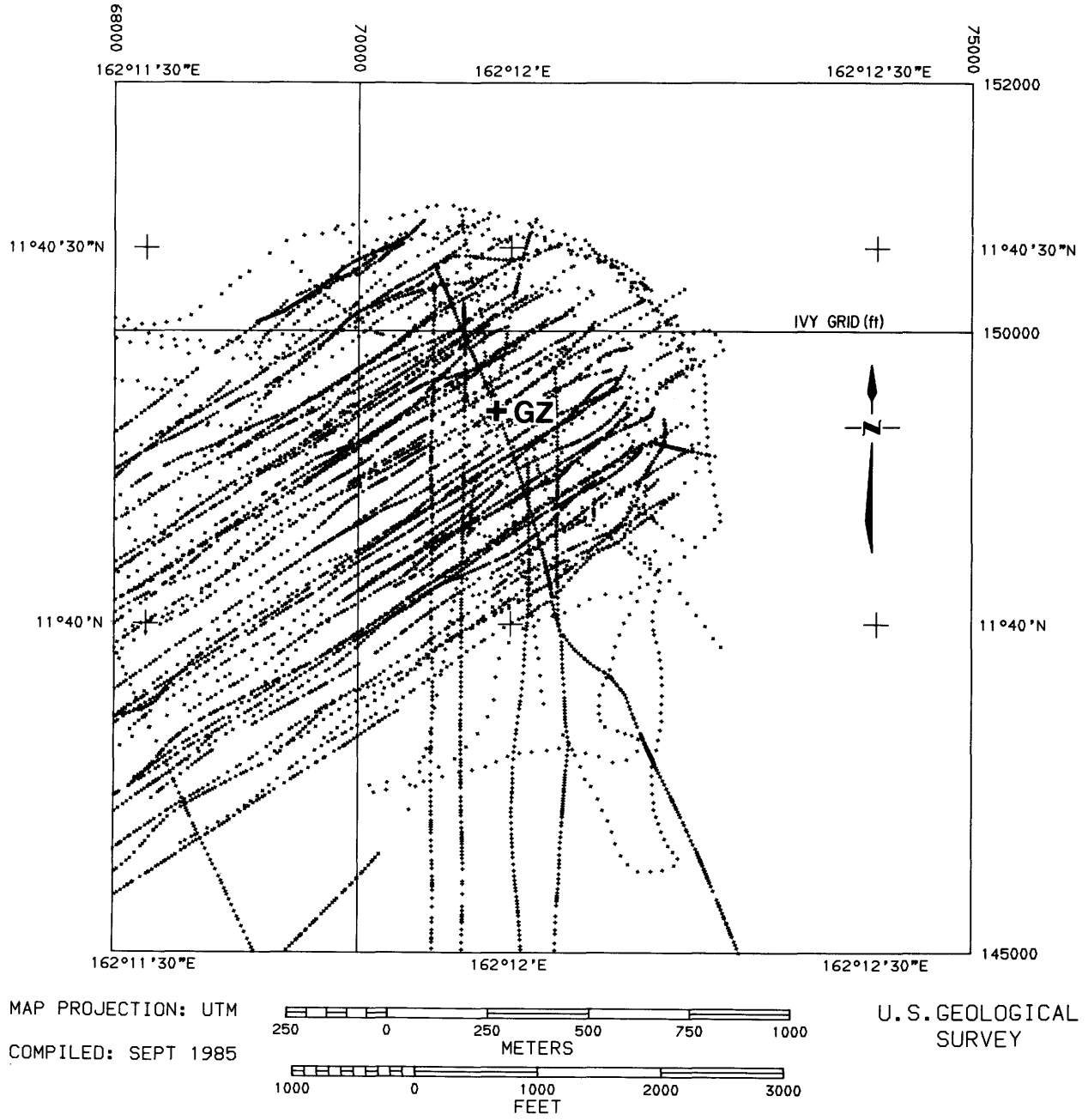

Figure 3. Point plots of echo soundings along tracks of all vessels used to acquire bathymetric data in KOA crater. Closer point spacing most often reflects areas of more variable bathymetry. GZ=ground zero.

at Woods Hole, Mass., to create a digital data base and detailed bathymetric maps. The procedure, as shown in figure 4, begins with three data sets: (1) a computer data base of time (G.m.t.) and depth pairs from the echo-sounding records (bathymetric data); (2) tide-gauge data (also in time and depth); and (3) navigation data (time and position). The separate data sets merge when the tide data are used to standardize the depths to mean lower low water (MLLW) (mean low water spring minus 0.18 m, or 0.6 ft) and when the navigation data are used to interpolate a position for each tide-corrected, time-depth pair. The resulting position-depth pairs were further edited on the basis of map-crossings and computer contouring. Figure 4 shows a loop for this stage that can be repeated until all data have been processed and errors minimized. In the last phase, we used the corrected position-depth data to create a final contour map and a digital data base on magnetic tape for further processing. Appendix 1 describes the programs used in processing.

The echo-sounding data were digitized on a magnetic graphics tablet linked to a Hewlett-Packard HP–1000 computer and were processed using an in-house package of seismic data analysis programs. The echo-sounding profiles collected in the field are printed in feet, based on a built-in

conversion using 4,800 ft/s (1,463 m/s) as the speed of sound in water. The conversion to meters was applied by recalculating travel time and then converting to meters on the basis of a sound velocity of 1,542 m/s (5,060 ft/s). This velocity was derived from tables published by Chen and Millero (1977) and from water temperature (isothermal at 28.5 °C) measured aboard the submersible.

The tidal variations in KOA and OAK craters, shown in figure 5, are within a few centimeters of each other. Most of the bathymetric data were collected within the time period

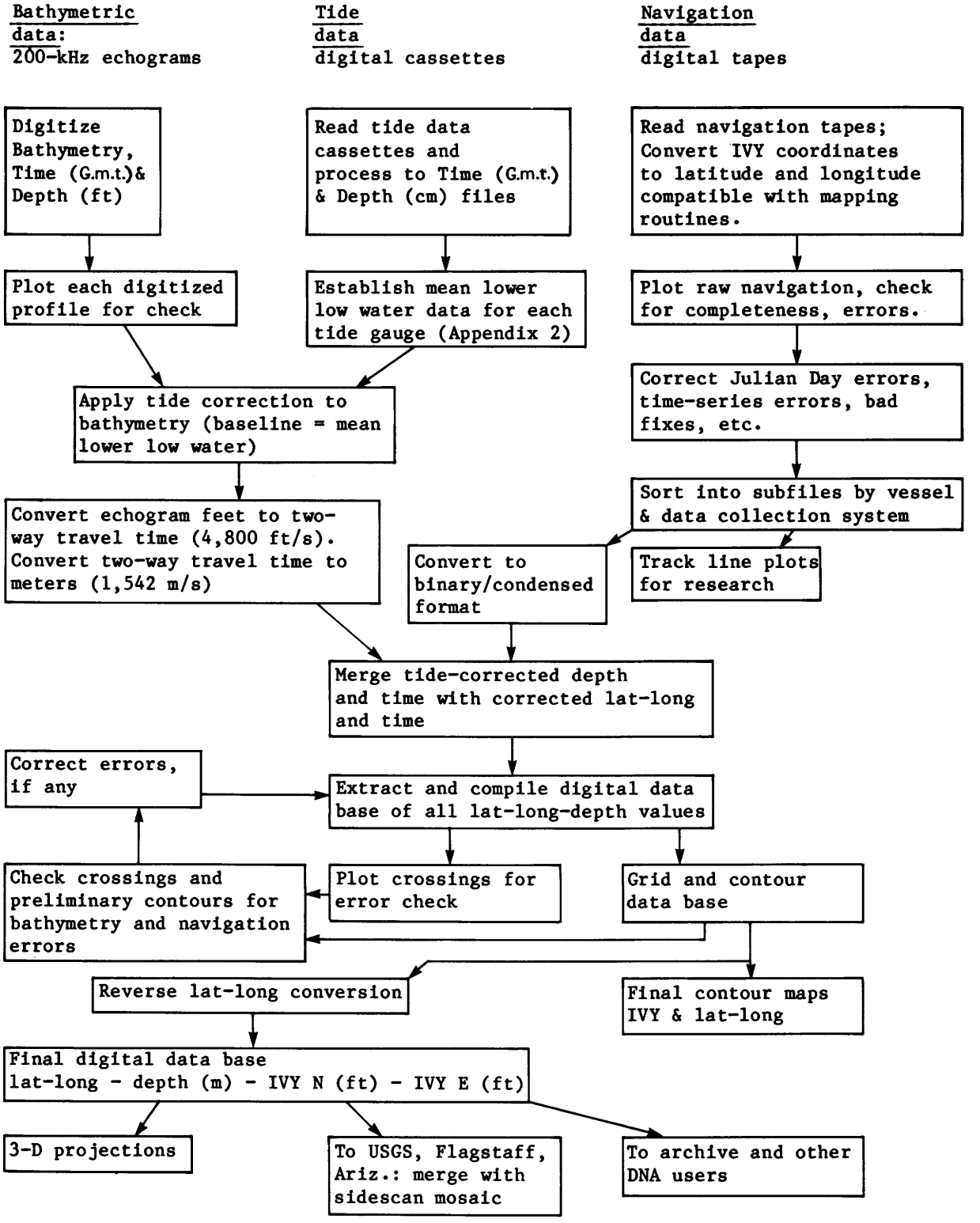

Figure 4. Procedure used to process bathymetric data.

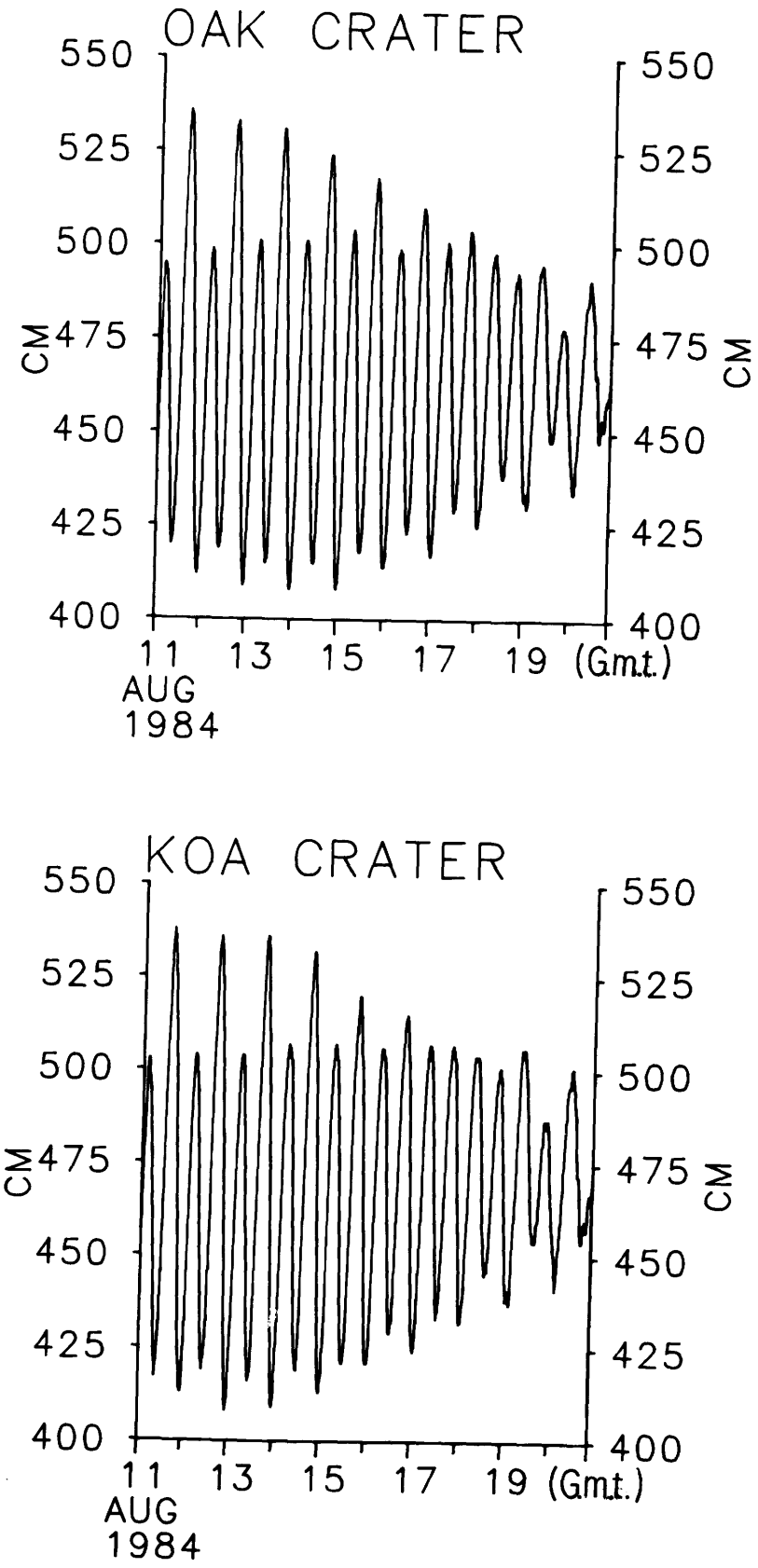

Figure 5. Tide-gauge data acquired in OAK and KOA craters. Note the similarity of the two profiles. G.m.t.=Greenwich mean time.

of the tide record shown in figure 6. The maximum tide range is about 1.3 m (4.25 ft). The tide-gauge data were linked to MLLW by tide tables for Enewetak supplied by D. Simpson (written commun., October 1984) of NOAA (appendix 2). This is within 0.03 m (0.1 ft) of the Holmes and Narver datum. In figure 6, MLLW falls at 720 cm, yielding a tide correction from −0.25 m (−0.82 ft) to −1.55 m (−5.08 ft).

The navigation data were converted from IVY grid coordinates to latitude and longitude to be compatible with the USGS processing and mapping programs. The results were identical to latitude and longitude conversions provided by the navigation contractor, Meridian Ocean Systems. The conversion was reversed in the final phase, and IVY coordinates were added to the position-depth pairs in the digital data base.

A few maps in subsequent chapters contain generalized versions of 5-m (16 ft) bathymetry for orientation only. These may differ in some areas by as much as 50 cm (1.5 ft) from the versions that appear throughout this chapter, which should be used as the reference for any questions regarding water depth.

In OAK crater we collected 400 km (216 nmi) of bathymetric profiles, and in KOA we collected 150 km (82 nmi). Additional lines not in the crater areas both inside and outside the atoll totalled 717 km (388 nmi).

RESULTS

OAK Crater

OAK crater is a large circular depression (fig. 7) with an average apparent diameter of 1,750 m (5,740 ft) and a

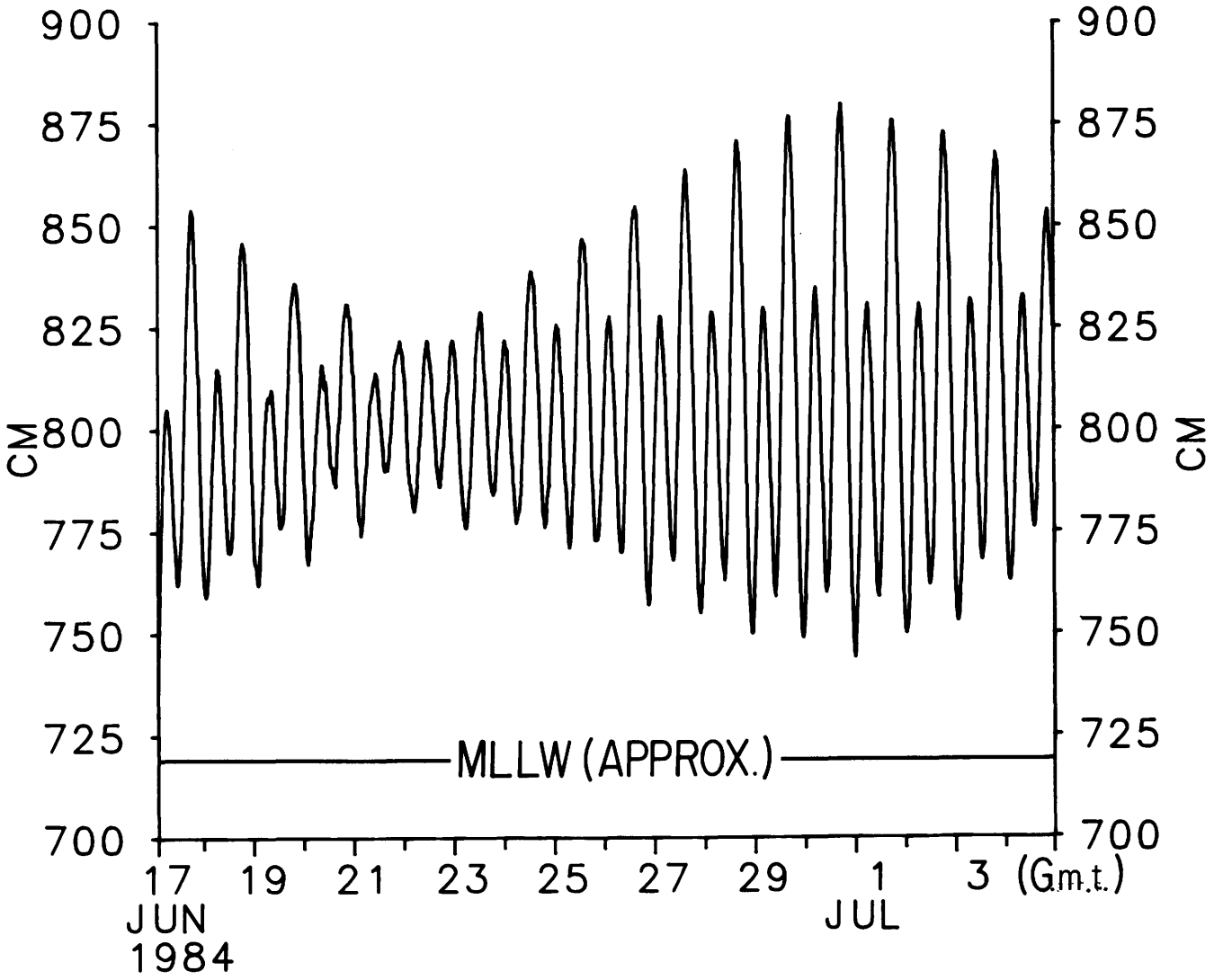

Figure 6. Tide-gauge data from KOA crater used to correct all of the echo-sounding records collected during the first leg of the survey to approximate mean lower low water (MLLW), which is equivalent to mean low water spring minus 0.18 m (0.6 ft). G.m.t.=Greenwich mean time.

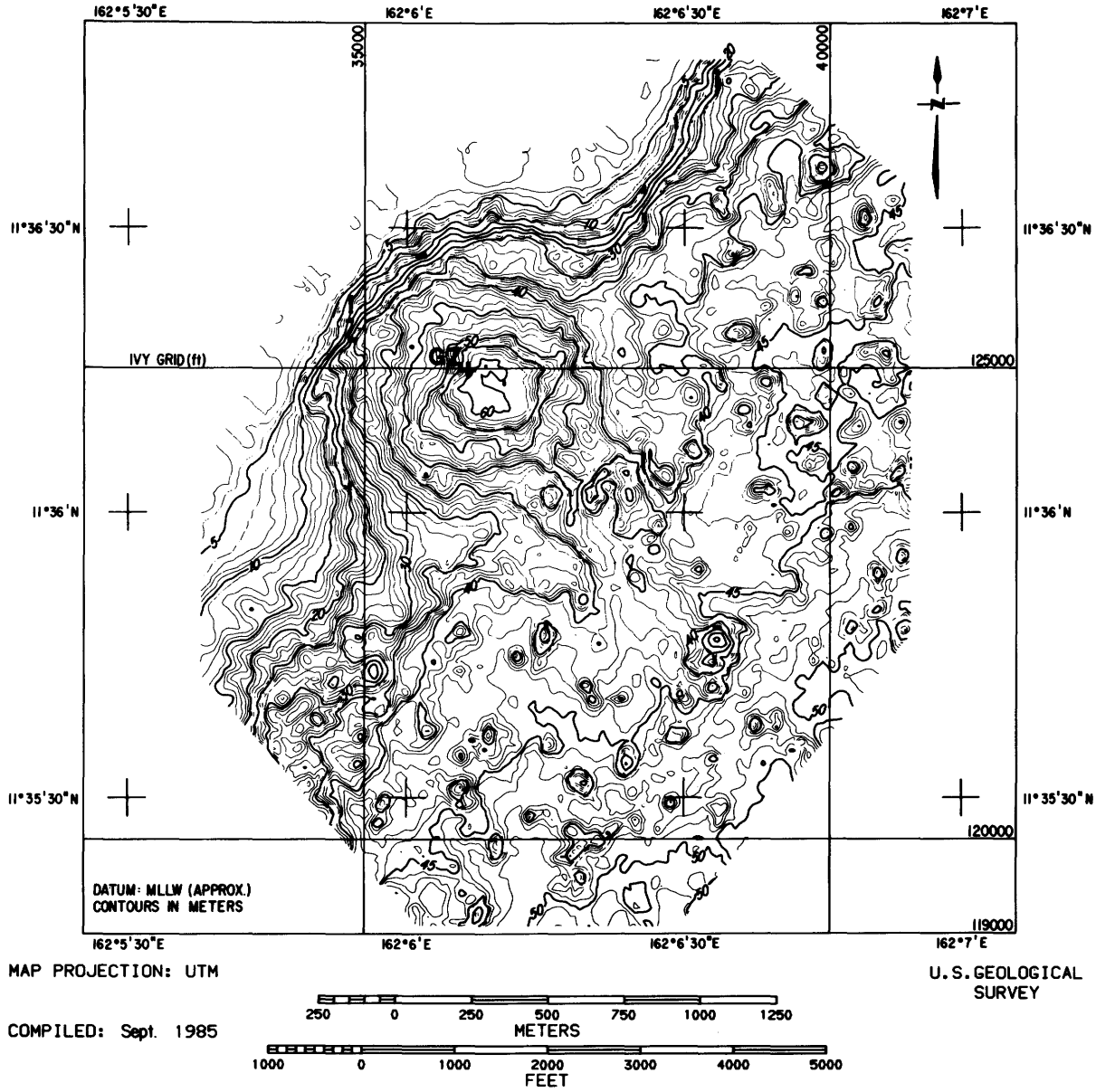

Figure 7. Map showing the bathymetry of OAK crater. Contour interval is 1 m. GZ=ground zero.

maximum depth of 60 m (197 ft) (B. L. Ristvet and K. L. Mills, III, written commun., July 1985). The 8.9-megaton device that formed the crater was fired on a barge moored in 4 m (13 ft) of water (Circeo and Nordyke, 1964). The reported location of ground zero is at IVY grid coordinates 124981.4 N. (11°36′14.9″ N.) and 36108.02 E. (162°06′6.6″ E.). However, the geometric center of the crater for all isobaths as shallow as 40 m (130 ft) lies about 100 m (330 ft) southeast of ground zero as noted previously by Tremba and others (1982). Examples of similar offsets between ground zero and the geometric center for high-explosive craters generated on slopes have been observed (R. F. Couch and B. L. Ristvet, oral commun., June 1985).

Preevent Bathymetry

Preevent and postevent bathymetric maps for the OAK area, constructed by Holmes and Narver, were based on lead-line and echo-sounding data apparently acquired along 90-m-spaced (300-ft-spaced) lines laid out at right angles to the reef. The preevent bathymetric map (fig. 8), digitized from a copy of the Holmes and Narver map provided by B. L. Ristvet, covers an area of 3.24 km^2 (0.94 nmi^2), and includes all of the crater but little of the surrounding area.

The northwest half (reef side) of the preevent map comprises reef plate with superimposed sand bars. At the breaker line was a 0.5-m (1.6 ft), almost linear scarp which

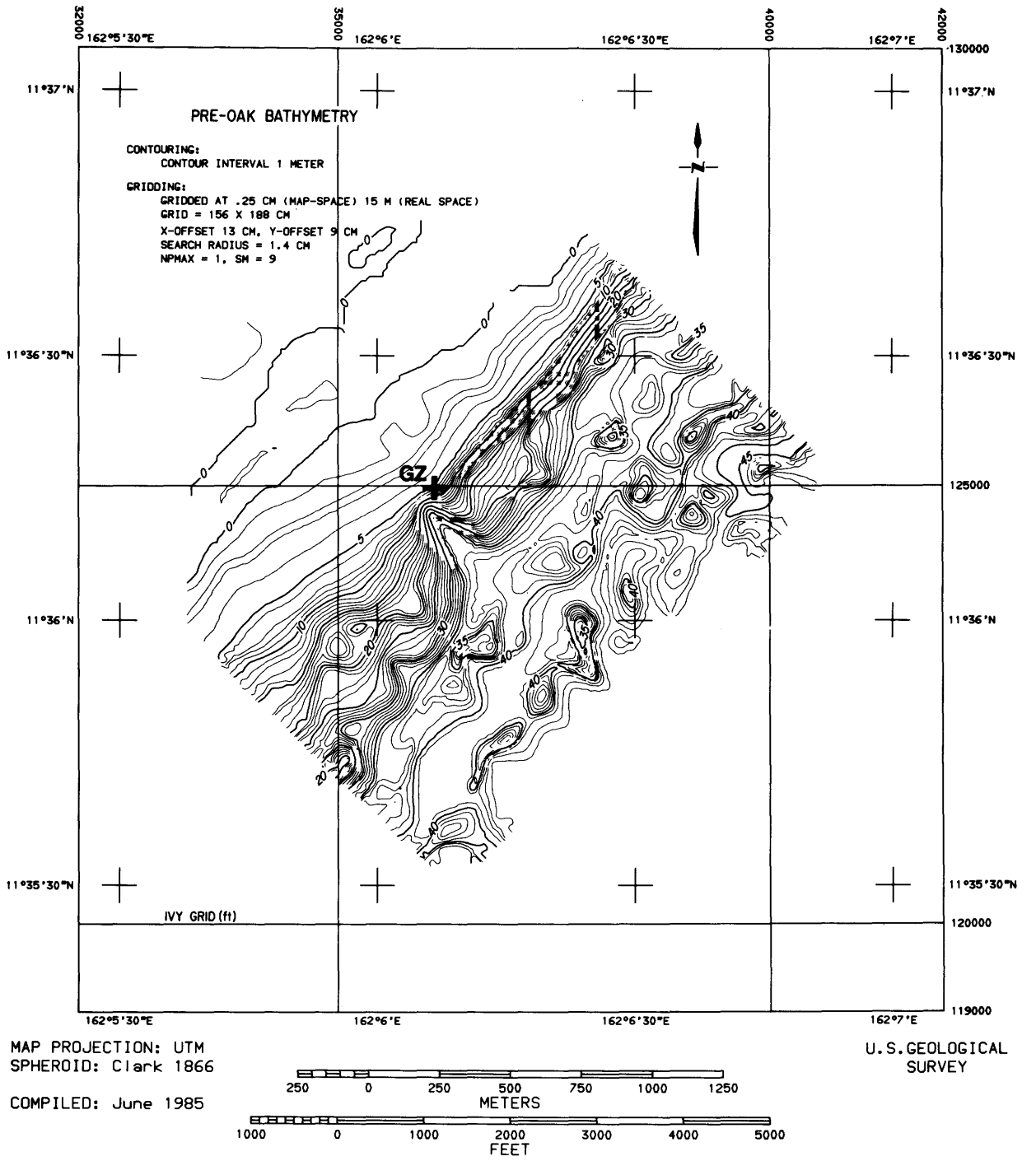

Figure 8. Map showing the preblast bathymetry in the area of the OAK site (taken from Holmes and Narver, Topography and Hydrology, Site 25, Alice Reef, July 31, 1956). Gridding parameters are described in appendix 1 of this chapter. GZ=ground zero.

was indented by a small embayment (fig. 8) beside a promontory of similar size. From the 1.5-m to 6-m (5–20 ft) isobaths, a narrow, gently sloping (1.6°) shelf ranged in width from 107 m (350 ft) to 290 m (950 ft).

The southeast half of the map comprises the reef slope, lagoon floor, and numerous mounds, which were probably mostly patch reefs. The slope was steepest (15°) in the northeast part of the map area and more gentle (4°) to the southwest where it descended to the lagoon floor as a series of terraces. According to the Holmes and Narver map (fig. 8), it was incised by a 15-m-deep (50-ft-deep) gully with a steep (23°) headwall; the gully flattened out over a

distance of about 305 m (1,000 ft) to lose its identity in 38 m (125 ft) of water. At the foot of the slope, the bottom slopes gently (0.8°) toward the center of the lagoon where it is interrupted by 19 mounds, or patch reefs, that rise as high as 12 m (40 ft) above the bottom and range in diameter from about 60 m (200 ft) to 300 m (1,000 ft). These appear to vary in shape from elliptical to triangular, a result which is doubtless in part due to the sampling density.

Present Bathymetry

We have contoured the crater on 1-m (3 ft) spacing, but we have thinned out some isobaths in the steeply dipping areas so that the reader can see details that otherwise would have been masked by the concentration of lines (fig. 7). However, on the annotated versions (figs. 9, 10), we have included all the contours to accentuate the variations in slope. Note that ground zero lies on the extreme northwest-

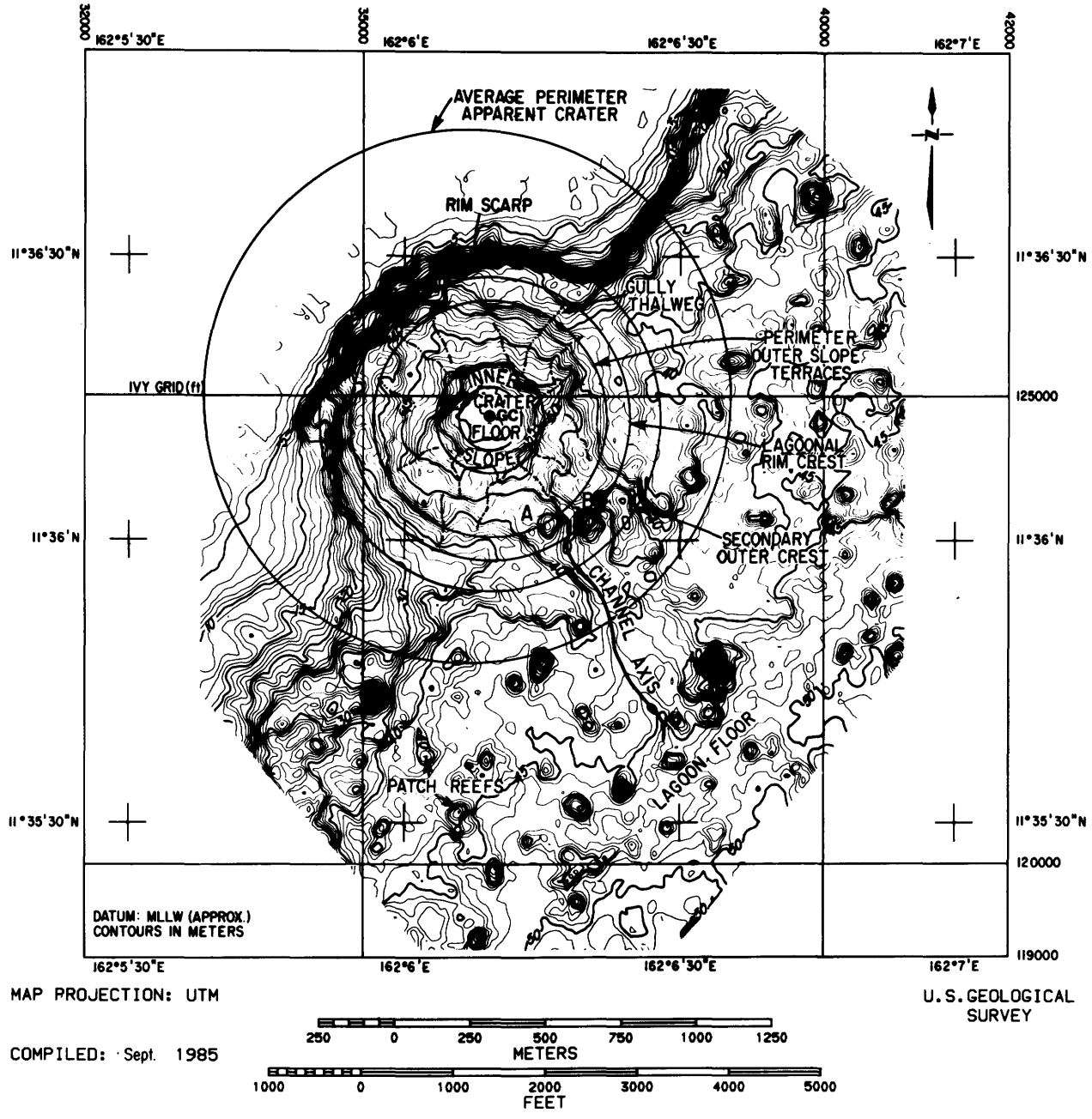

Figure 9. Map showing the bathymetry of OAK crater, the locus of some isobaths used to locate the geometric center (GC) of the crater, and other important physiographic features. Average perimeter of apparent crater is after B. L. Ristvet and K. L. Mills, written commun., July 1985. Letters A and B are localities referred to in the text.

ern edge of the crater floor. The crater is almost equally divided through its geometric center with half extending into the reef and half extending into the lagoon. This symmetry about the geometric center of the crater is worth highlighting and is illustrated in figure 9.

The crater floor is almost perfectly circumscribed by the 59-m (194 ft) isobath which has a radius of 100 m (330 ft) from the geometric center. Similarly, northwest and southeast of the geometric center, much of the 50-m (164 ft) isobath, which outlines the top of a slope (inner slope, fig. 10) surrounding the crater floor, lies along a circle with a radius of 183 m (600 ft). The distance of the 50-m (164 ft) isobath from the geometric center increases equally in both southwest and northeast directions (symmetrically) to 250 m (820 ft) due to the presence of two broad terraces.

Farther up the crater side, the approximate top of the outer slope (fig. 10) lies in waters 35 to 40 m (115–131 ft) deep and varies little from a circle with a radius of 390 m (1,280 ft) from the geometric center. Another circle with a radius of 463 m (1,520 ft) lies close to the bottom of the main scarp that surrounds the reefward edge of the crater and also follows closely the crest of the lagoonal crater rim; and another with a radius of 573 m (1,880 ft) lies close to the top of the same scarp and follows a lower secondary

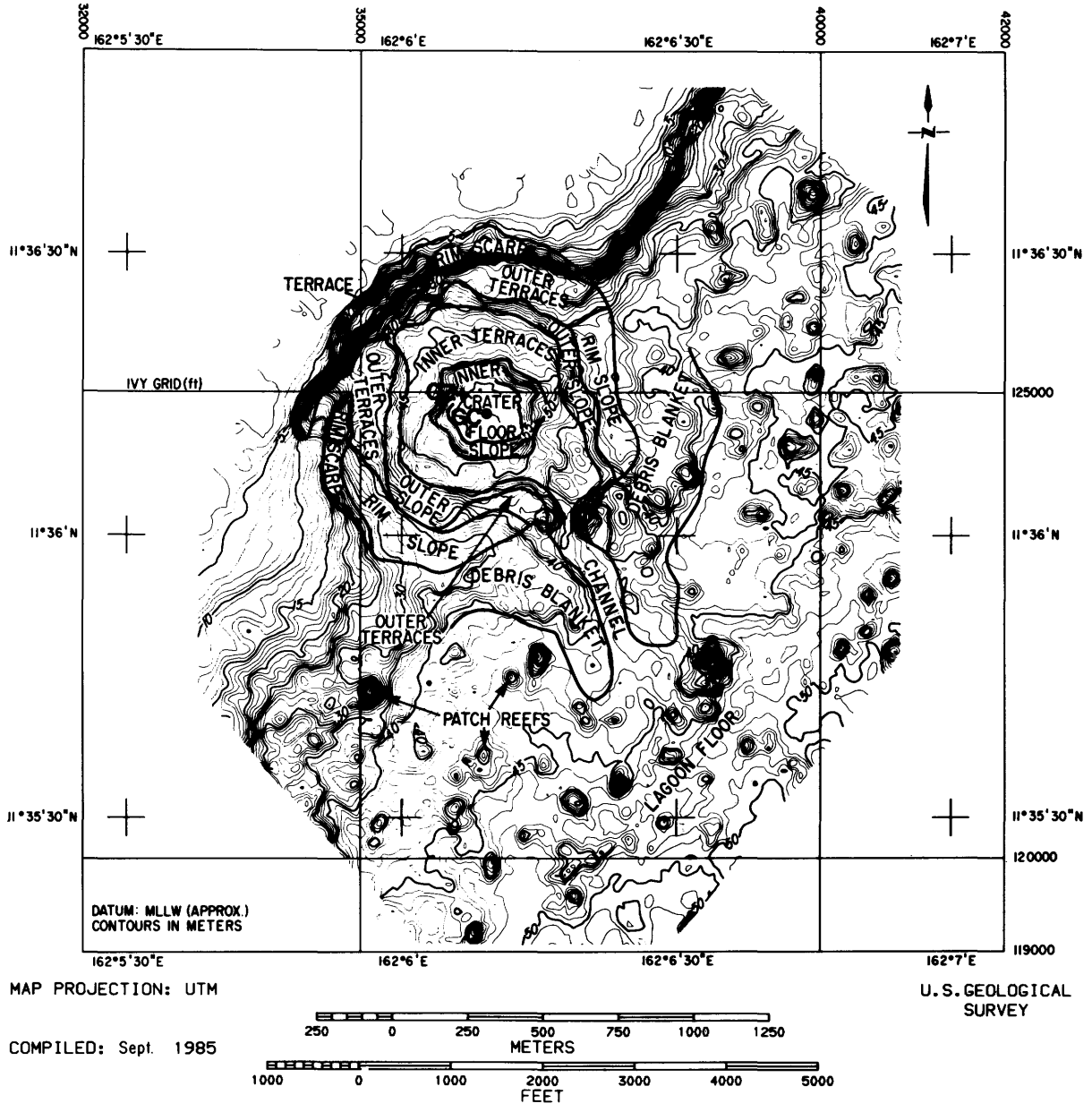

Figure 10. Map showing bathymetry of OAK crater with physiographic provinces outlined. GZ=ground zero. GC=geometric center.

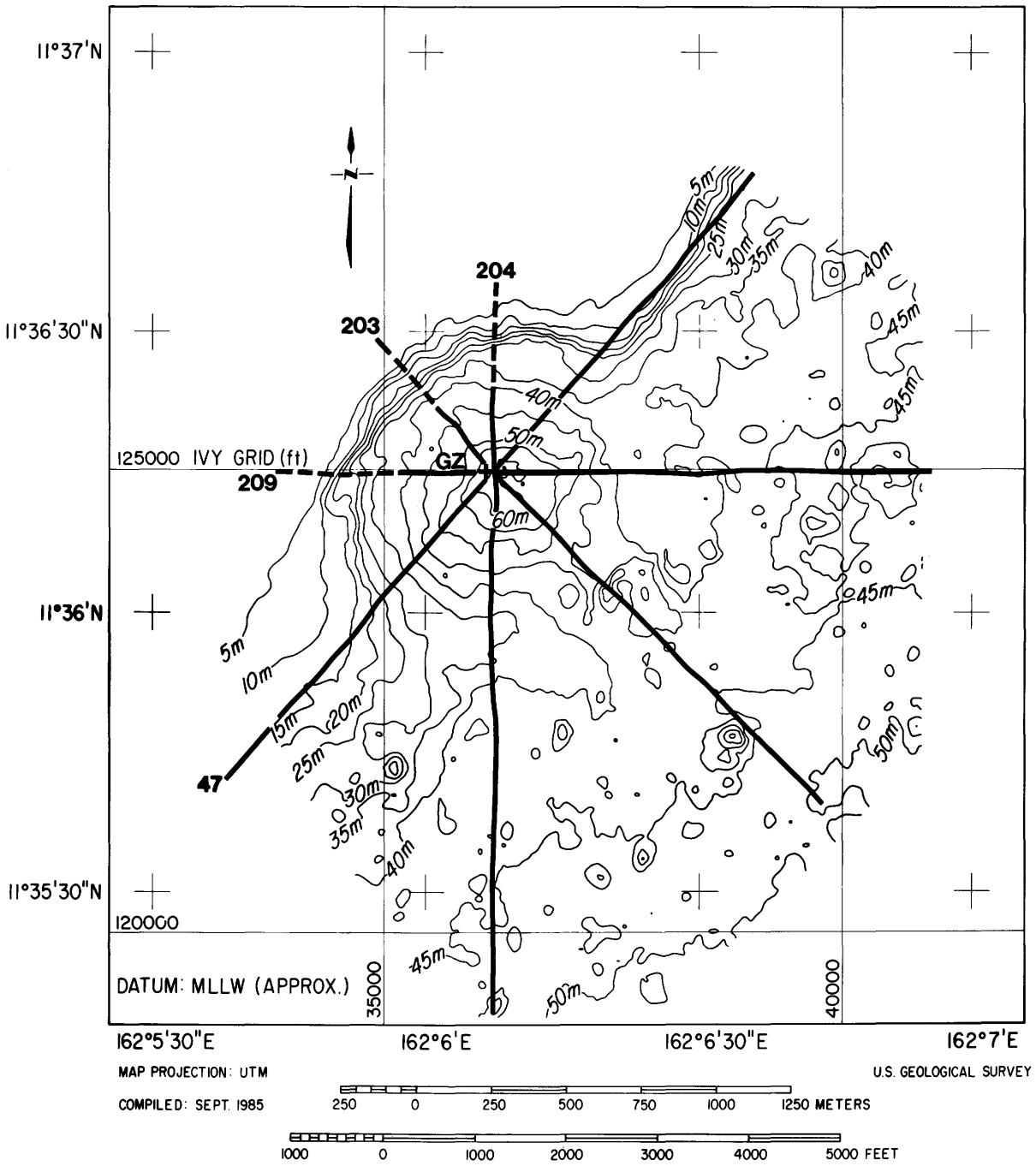

Figure 11*A*. Map showing bathymetric profiles that pass through or close to ground zero (GZ) in OAK crater. Dashed where inferred from bathymetric map.

ridge lagoonward of the rim crest. These circles all illustrate that many of the physiographic characteristics of the crater are symmetrical about the geometric center.

We also have shown on figure 9 the average perimeter of the apparent crater, with a radius of 875 m (2,870 ft), from ground zero as defined by B. L. Ristvet and K. L. Mills, III (written commun., July 1985).

On the basis mainly of slope changes, we have divided the crater area into eight major physiographic provinces (fig. 10) and will discuss each in sequence from the crater center outward.

Crater Floor

The flat to gently undulating floor of the crater has a diameter of 200 m (650 ft) and reaches a maximum depth of 60 m (197 ft) below MLLW, which is the Holmes and Narver datum (figs. 10; 11, lines 203, 204; 12, line 75). The crater is circumscribed by the nearly circular 59-m (194 ft)

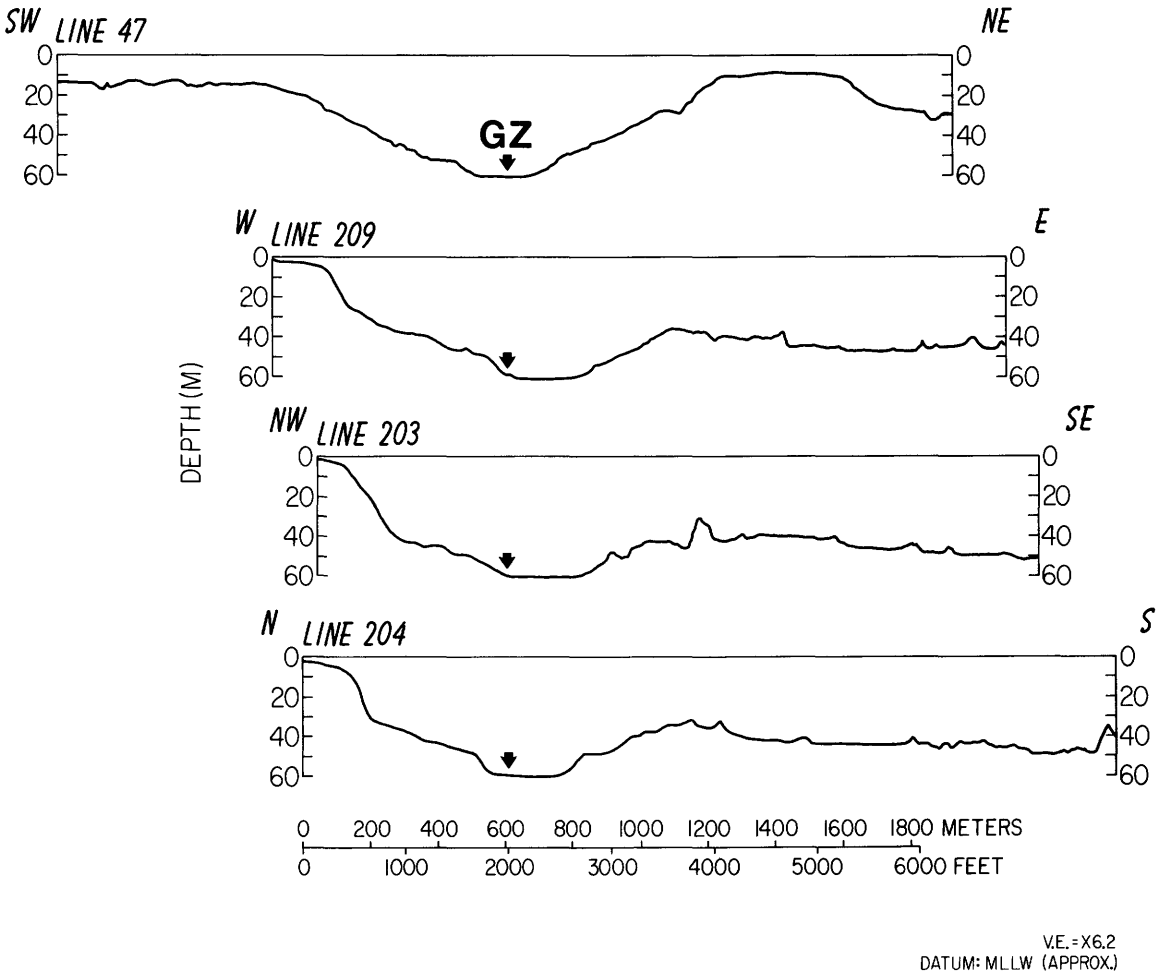

Figure 11*B*. Ground zero location projected orthogonally into lines. Contour interval is 5 m.

isobath (figs. 9, 10). As noted above, ground zero lies on the northwest edge of the crater floor, and the geometric center lies almost precisely at its center. A low ridge extends across the crater floor close to the geometric center (see figs. 7; 12, line 75) possibly representing a central crater uplift.

Inner Slope

Surrounding the crater floor is a slope that rises as steeply as 17° to a depth of 50 m (164 ft) along much of the crater's northwest and southeast sides (figs. 7; 10; 11, line 204; 12, line 75). The steepness of this slope is only exceeded by the steepness of the scarps that lie along the reefward margin of the crater edge in much shallower water (5–30 m, or 16–98 ft) and of a scarp on the craterward side of a debris mound that lies about 425 m (1,394 ft) southeast of the geometric center. The area ranges in width from 37 to 95 m (120–310 ft) and is well defined on both its lower and upper boundaries. At the upper boundary, the steep slope flattens out abruptly into the area of inner terraces where slopes are as low as 1°.

Inner Terraces

This area ranges in depth from about 40 to 50 m (130–164 ft), and the distance from lower to upper boundary, or width of the province, ranges from 61 to 220 m (200–720 ft). The long axis of the upper boundary is oriented northwest-southeast and lies about 427 m (1,400 ft) symmetrically on either side of the geometric center; the short, equally symmetrical axis lies about 340 m (1,115 ft) on either side of the geometric center.

The area is characterized by variable bathymetry that ranges from flat to reversed slopes, that is, slopes that dip away from the geometric center, to a few areas where slopes are as great as 10° into the crater (figs. 7; 10; 11, lines 203, 204, 209; 12, lines 75, 77). The noses and reentrants all suggest that the area comprises overlapping slumped bodies of sediment. The finer details of the bathymetry observed from the submersible, and their significance to cratering mechanics, are discussed in chapter F of this volume.

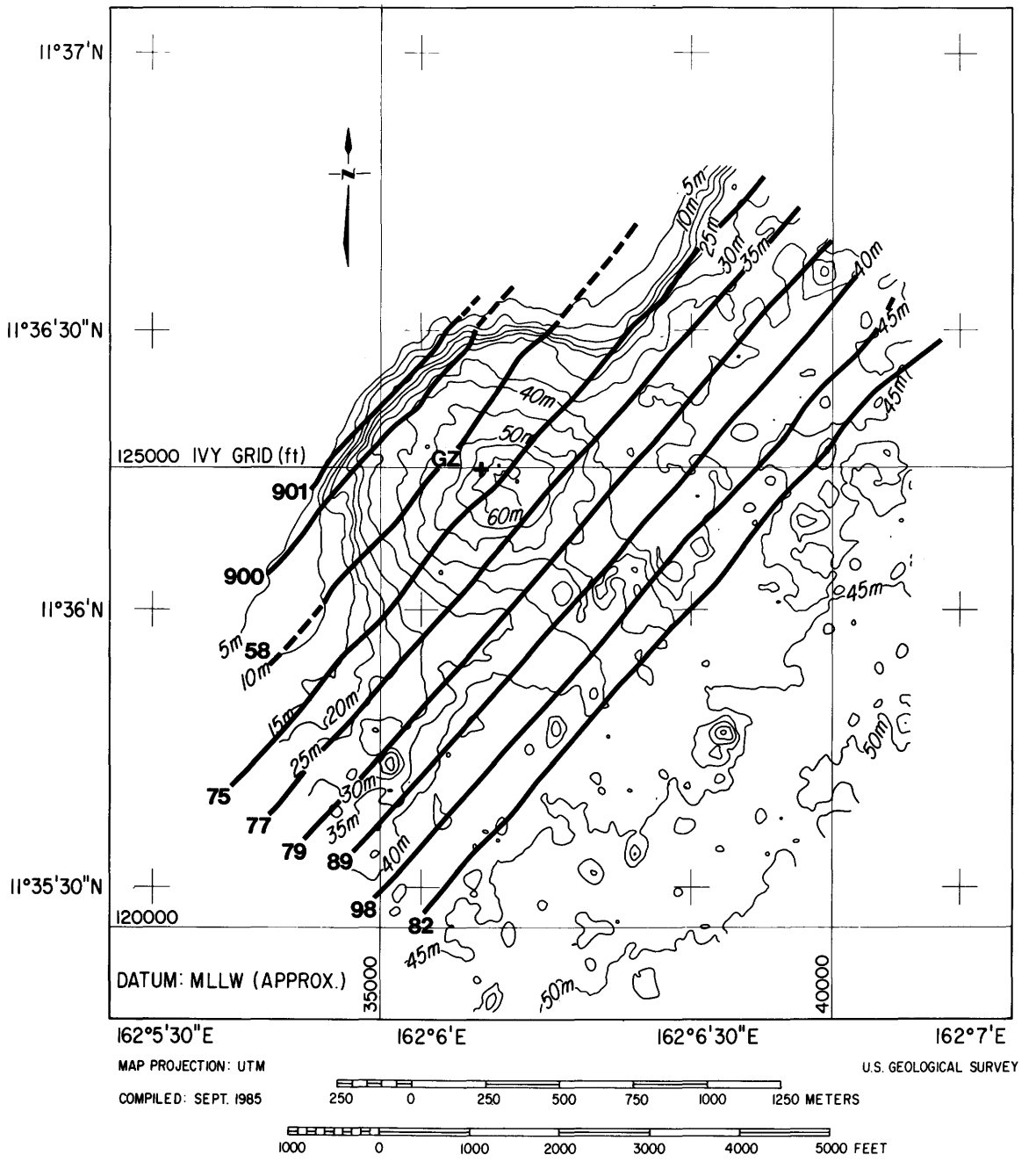

Figure 12*A*. Map of OAK crater showing location of bathymetric profiles in and around the crater that are oriented parallel to the reef. GZ=ground zero. Contour interval is 5 m.

Outer Slope

This is a narrow area 10 to 128 m (33–420 ft) wide in which average slopes are steeper (approx 5°) than in adjacent areas. It does not represent a major discontinuity in the physiography of the crater, but it clearly separates the hummocky terraced areas on either side of it (figs. 10; 11, line 204). It may represent a poorly developed or partially buried slump scarp. On the reefward side of ground zero, it appears to be truncated by the bottom of the rim scarp. The steepest slopes (28°) lie on the southeast side of the crater where a large debris mound (fig. 9, site B) rises abruptly from the terraced area. Adjacent to it, a flat-floored channel about 30 m (100 ft) wide cuts through the outer slope and extends from the crater more than 500 m (1,640 ft) into the lagoon (figs. 9, 10).

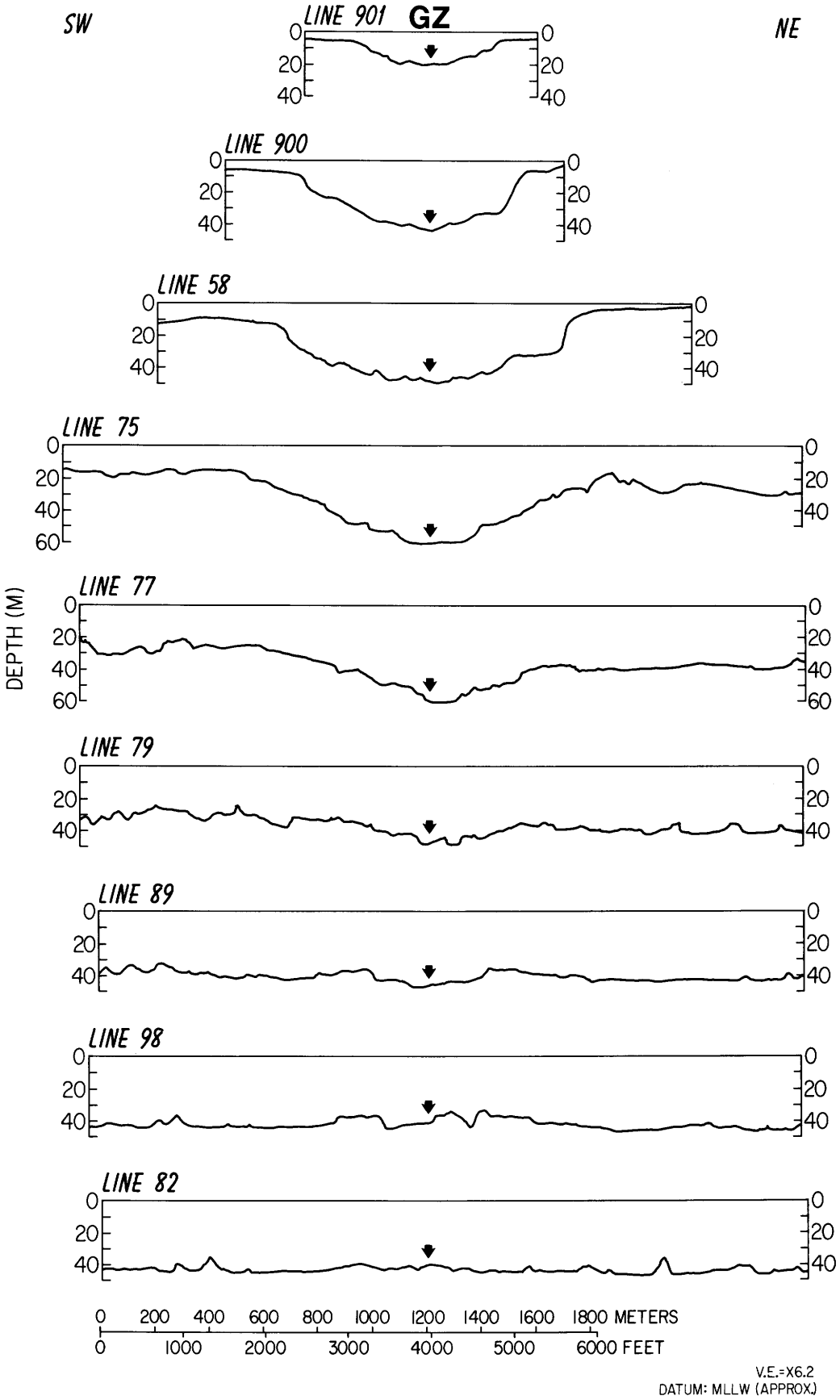

Figure 12*B*. Ground Zero (GZ) location projected orthogonally into lines.

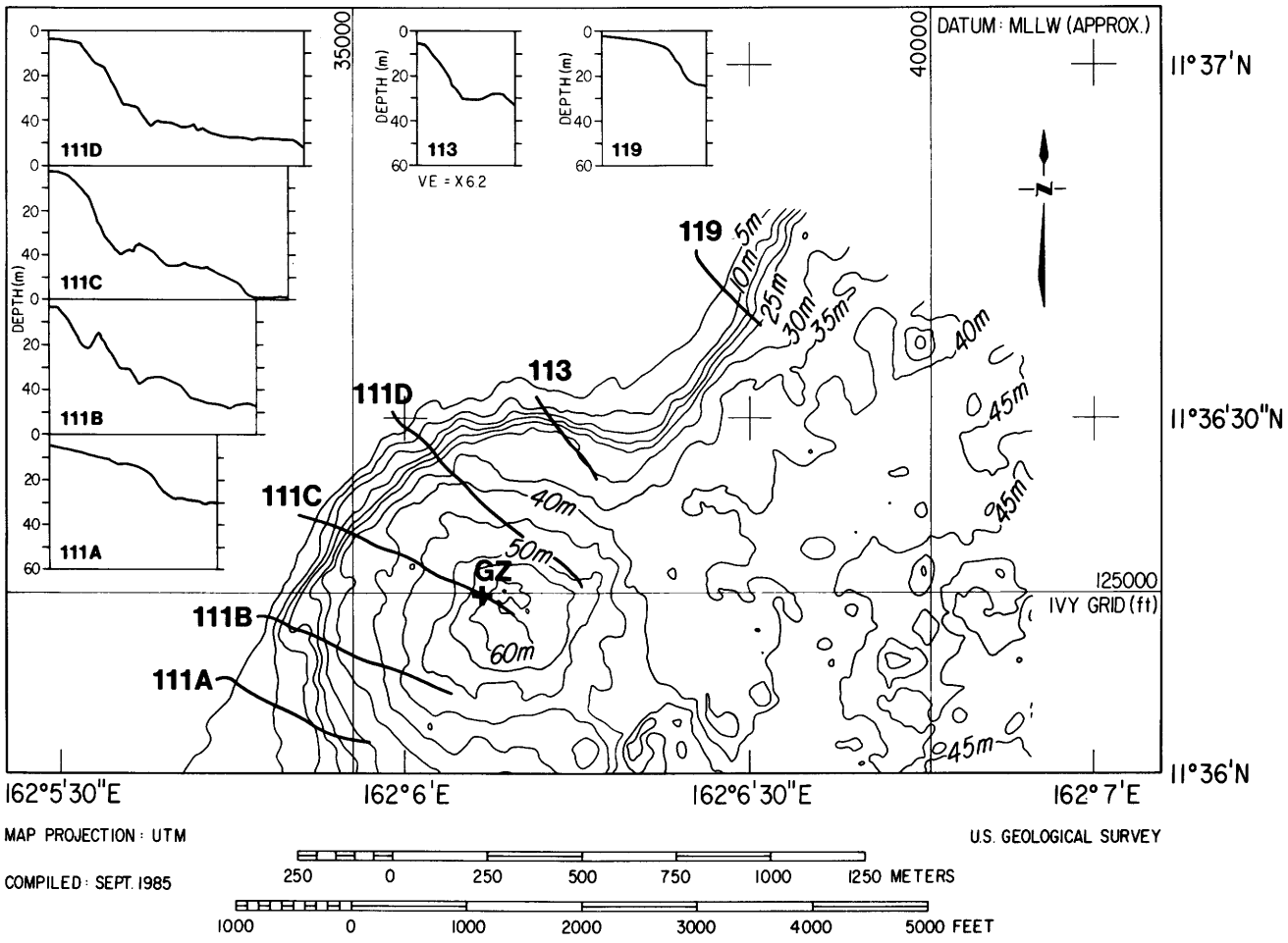

Figure 13. Bathymetric profiles collected nearshore around the reef margin of OAK crater. GZ=ground zero. Contour interval is 5 m. Vertical exaggeration for all profiles is ×6.2.

Outer Terraces

Much of this area is similar in bathymetric expression to the inner terraces. It lies at the foot of the steepest scarp in the crater and probably also represents a melánge of slumped material. It comprises three areas that are as wide as 150 m (500 ft) in which slopes range from flat, to a few degrees away from the geometric center, to as much as 9° toward the geometric center (figs. 10; 11, line 204). The upper boundary of this area is the most abrupt in the crater where it abuts the steep rim scarp. However, the boundary between it and the adjacent rim slope on the lagoonward side of the crater is more arbitrary, and we have drawn it on the basis of both slope change and isobath orientation.

About 12 poorly developed gullies incise the sides of the crater from the outer terraces to the crater floor (fig. 9). Most extend into waters that are no shallower than 40 m (130 ft). Their positions may be structurally controlled. (See chap. C, this volume.)

Rim Scarp

The steepest slopes in the crater, up to 30°, lie along its reefward side (figs. 9; 10; 11, lines 203, 204; 12, lines 900, 58; 13, lines 111B–D, 113). In some areas, submersible and scuba observations revealed that the

slope comprises vertical to overhanging ledges and talus slopes. (See chap. F and H, this volume.)

The inner margin of the scarp ranges from 400 to 520 m (1,300–1,700 ft) from the geometric center, and the outer margin ranges from 590 to 640 m (1,930–2,100 ft). However, the width is misleading because the scarp is separated on the western side of the crater by a terrace that is about 60 m (200 ft) wide. The large, southwestern segment of the crater rim appears to have moved toward the geometric center, presumably in at least two parts. A similar terrace broadens the rim scarp on the northwestern side of the crater (fig. 10).

Rim Slope

These two areas are bounded on the upper or outward sides by a line connecting the highest points along the crater's lagoonward rim, except along the base of the rim scarp on its western side (fig. 10; 11, line 209). Its outer margin lies about 400 to 500 m (1,300–1,640 ft) from the geometric center, which is close to the distance (550 m, or 1,800 ft) that Tremba and others (1982) found it from ground zero. On the east side of the crater, the highest point on the rim is at or slightly shallower than 35 m (115 ft); on the southeast side, the top of a large debris mound lies at 32 m (105 ft), and on the south-southwest side the crest lies at the same depth.

The two arcs thus form the lagoonward crater rim and doubtless consist of abundant debris from the crater possibly uplifted in part by thrusting. (See chap. C and D, this volume.)

Debris Blanket

This large area of irregular bathymetry or rough bottom is physiographically little different from the rim slope; thus, both areas are probably underlain by abundant debris from the crater (figs. 10; 11, lines 203, 204, 209; 12, lines 79, 89). The outer perimeter of much of this material lies on a circle about 750 m (2,460 ft) from the geometric center and 850 m (2,800 ft) from ground zero. On the southeastern side, two lobes that border the 90-m-wide (300-ft-wide) channel (figs. 9, 10) extend to the southeast about 1,000 m (3,300 ft) from the geometric center.

The physiography of the debris blanket suggests that much debris was blown out into the lagoon directly opposite from the reef. This is not surprising, considering the relative elevation and resistivity of the two sides. Delineating the debris on the basis of bathymetry alone in the lagoon is difficult because of the 80-or-so patch reefs that are present in the area (figs. 7, 9); however, the physiographic analyses are supported by the subbottom data. (See chap. C, this volume.)

The circular to elliptically shaped patch reefs range in maximum diameter from 46 m to 243 m (150–800 ft) and range in height from a few meters to 19 m (62 ft) above the lagoon floor. The patch reef or debris mound (fig. 9, site A) nearest the crater center lies about 390 m (1,280 ft) from it and rises about 9 m (30 ft) above the adjacent channel floor. It may be capped by debris. East of it, on the other side of the channel, lies a larger complex of debris (fig. 9, site B) and patch reefs.

Comparison of Preevent and Postevent Bathymetry

Features in the preevent Holmes and Narver bathymetric map correlate well with those on our map outside the crater area. For example, the contours on the slope northeast and southwest of the crater are in close alignment on both maps, and eight of the patch reefs are close to the same location and height, although their shapes differ significantly (fig. 8). The character of the crater area shows many differences.

The blast removed most of the slope area, including the deep gully shown on the preevent map near ground zero. Almost 600 m (1,970 ft) of reef or reef plate northwest of the crater center were disrupted, blown away or downfaulted. The only manifestation of the gully in the present bathymetry may be at the southwest corner of the box-shaped valley on the southeast side of the crater where the flat-floored channel cuts through the crater rim. Although that channel may show some structural control (see chap. C, this volume), it probably developed because two large patch reefs (305 m (1,000 ft) long, 10–12 m (35–40 ft) high) (fig. 8) funnelled some of the blast between them. The westernmost of the two patch reefs appears to have been mostly destroyed or buried, whereas part of the eastern one appears to be intact. The large (150 m long by 90 m wide, or 490 ft by 300 ft) mound of material noted above (see fig. 9, site B), now lies adjacent to it on its craterward side and rises 9 m (30 ft) above the preblast surface. Neither this additional material nor the mound (debris or patch reef) at site A, figure 9, appear on the preevent map.

The preevent map does not extend far enough to the southeast to evaluate the two long ridges (rays?) that appear to terminate about 1,200 m (3,937 ft) from the crater center. On the opposite side of the crater (reef side), the box-shaped valley at 40 m (131 ft) coincides almost precisely with the peculiar reentrant on the preblast reef. Why, or if, this occurrence influenced the crater geometry is not clear.

We have constructed an isopach map (fig. 14) that shows the difference in terrain between the Holmes and Narver digitized preevent bathymetric map (fig. 8) and our bathymetric map (fig. 7). In the unstippled area, our depths are greater than the values shown by Holmes and Narver; material has been removed and(or) the bottom depressed. In the stippled area, depths are less than those shown by Holmes and Narver; material has been added and(or) the bottom has been uplifted or bowed up outside the crater area. Our computer-calculated value of 23.6×10^6 m^3 for the total volume of the crater is close to the crater volume estimated by Mills and Ristvet (in Ristvet and others, 1978).

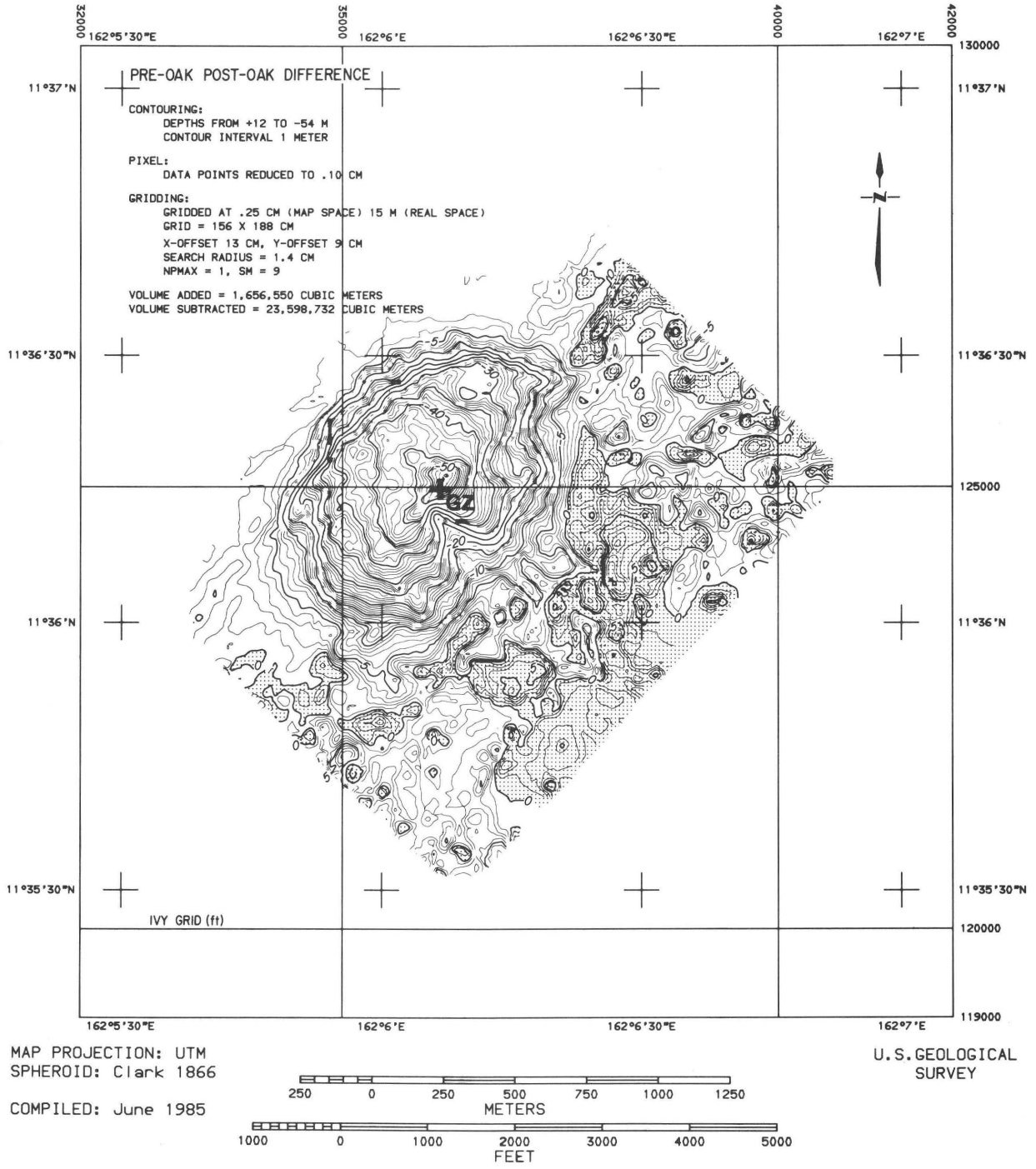

Figure 14. An isopach map showing the difference in terrain between the Holmes and Narver preshot bathymetry (fig. 8) and the postshot bathymetry (fig. 7) acquired during this study. In the area not stippled, our values are deeper than those of Holmes and Narver, whereas in the area stippled, our values are shallower than those of Holmes and Narver. Gridding parameters are described in appendix 1 of this chapter. GZ=ground zero.

Three-Dimensional Computer Images of OAK Crater

Perspective views of OAK crater are shown in figure 15. To accentuate the relief of the saucer-shaped crater, we have used a vertical exaggeration (5×).

The views from the southwest and northeast clearly show the large volume of material removed from the reef. They also show the difference in the reef slope on either side of the crater—steep to the northeast, more gradual to the southwest, which, based on the Holmes and Narver map (fig. 8), is close to the precrater physiography of the slope.

Views from the southwest, and particularly from the southeast (fig. 15*B*), highlight the terrace, which has the

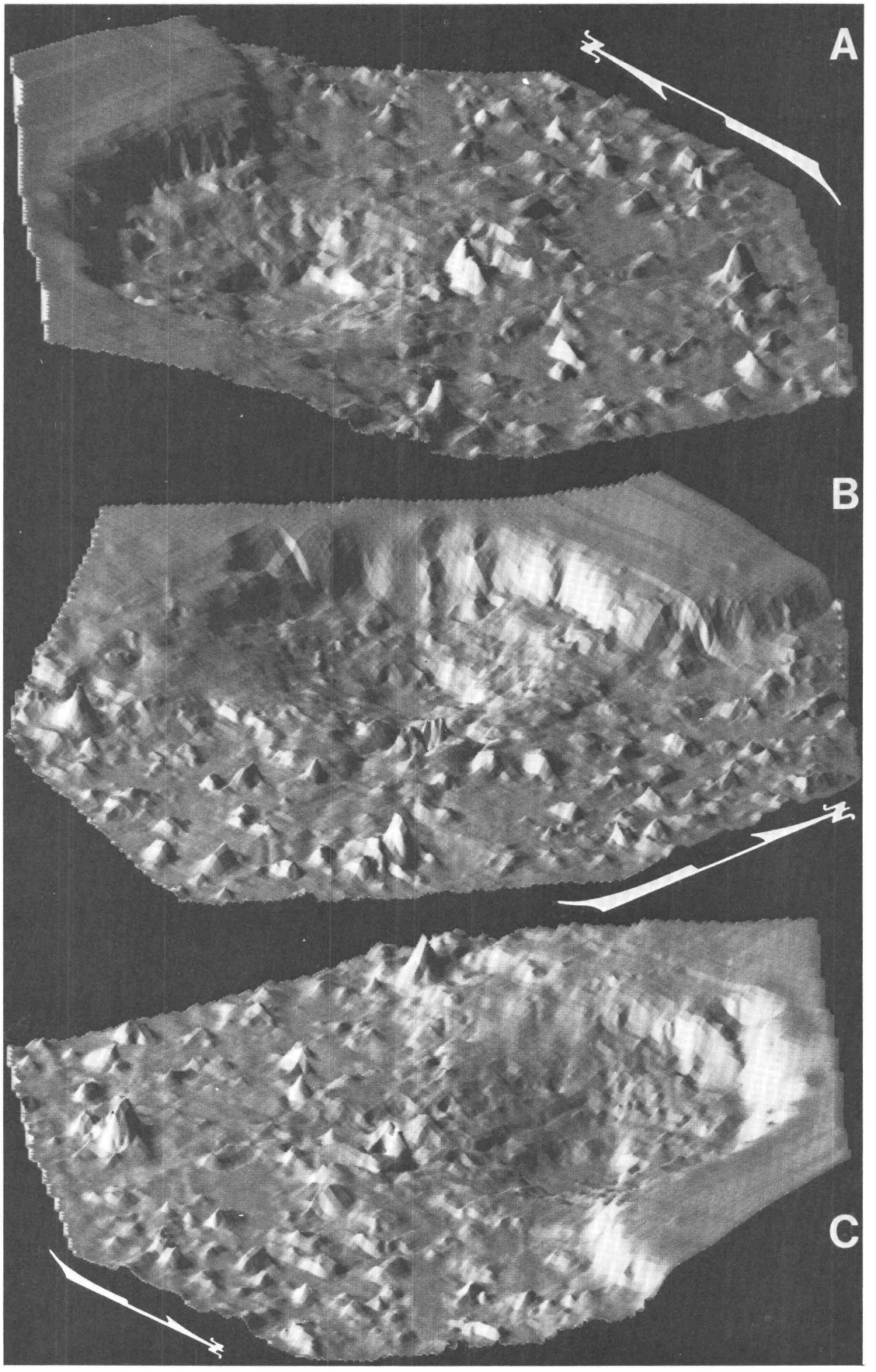

Figure 15. Three-dimensional images of OAK crater: *A*, from the southwest, *B*, from the southeast, and *C*, from the northeast. Vertical exaggeration is ×5.

appearance of slumped material on the reefward side of the crater.

All four views show the thickest part of the debris blanket around the lagoonward side of the crater and the physiography of the apparent inner and outer rim crests (fig. 9). The extent of thinner debris accumulation may coincide with the 40- to 45-m (131–148 ft) depth range outside the thick debris at the crater edge. The channel through the crater rim opposite the reef that crosses this area also is well depicted on all four images. The integrated sidescan-sonar-bathymetry data in chapter B (this volume) clearly show greater detail and texture of the crater, debris, and patch reefs.

KOA Crater

This nearly circular crater was formed in 1958 by a 1.4-megaton device detonated in a water tank on Teiteiripucchi (Gene) Island. The crater, now covered by a maximum of 33 m (108 ft) of water, was excavated entirely in the lagoon terrace and has an average apparent radius of 658 m (2,160 ft) (B. L. Ristvet and K. L. Mills, III, written commun., July 1985) (fig. 17). The adjacent MIKE crater, southwest of KOA, was formed by a 10.4-megaton device 6 years previously. Three smaller devices, NECTAR in 1954 and APACHE and HURON in 1956, were detonated subsequently in or at the edge of MIKE crater (fig. 17). SEMINOLE, also detonated in 1956, lies just east of the map area (fig. 17).

KOA ground zero is located at IVY grid coordinates N. 149360; E. 71120 (11°40′17″ N.; 162°11′59″ W.). The bathymetry of the crater is less complex than that at OAK crater because the blast excavated the KOA crater entirely from reef rock instead of from reef and lagoon sediments. Much of the debris blanket fell on the reef and nearby islands. Some of it, especially on the shallowly submerged southeast margin, probably was swept back into the crater immediately after the blast by rushing water and subsequently by waves associated with storms. Little information can be drawn from the debris blocks because their source in the area could have been from any of five events.

The radius from ground zero to the 5-m (16 ft) isobath along the northeast crater rim averages about 500 m (1,640 ft). The crater is fairly symmetrical about ground zero, but isobaths deeper than 25 m (82 ft) are elliptical with the long axis oriented parallel to the reef trend (northeast). The 30-m (98 ft) isobath, for example, is about 210 m (690 ft) from ground zero in the northeast and southwest directions but only about 110 m (360 ft) from ground zero in the southeast and northwest directions, whereas the 15-m (50 ft) isobath is almost circular about ground zero. Bathymetry is complex at the southwest margin of the crater where it abuts MIKE crater (figs. 16, 17).

We have divided the crater into four major physiographic provinces, from the crater center outward. These include: (1) the crater floor; (2) the inner slope; (3) terraces; and (4) rim scarp. In addition, other scarps, debris mounds, and an intercrater channel have been outlined (fig. 18).

Crater Floor

We have included the gently sloping area below the 30-m (100 ft) isobath as the crater floor. The flattest part of the floor lies mostly southwest of ground zero. To the northeast, it rises to the 30-m (100 ft) isobath in a 0.9° slope from ground zero over a distance of about 200 m (656 ft). The crater floor is elliptical in shape and symmetrical about ground zero, with the long axis extending about 200 m (656 ft) to the northeast and southwest and the short axis extending about 100 m (328 ft) to the northwest and southeast (figs. 16; 18; 19*A*,*B*).

Inner Slope

The transition from the crater floor to the inner slope is easy to define. Slopes increase to as much as 9° southeast of ground zero and about 4–5° elsewhere (figs. 18; 19*A*,*B*: lines 116, 304). The slope change that characterizes the outer boundary of this area is well defined except northeast of ground zero where our choice of its position is somewhat arbitrary because it changes little from crater floor to rim scarp (figs. 19*A*,*B*: line 507). The outer boundary is asymmetric about ground zero—335 m (1,100 ft) to the northeast and only about 235 m (770 ft) to the southwest. The width of the area varies from about 120 m (400 ft) northeast of ground zero to zero southeast of ground zero where the toe of a probable slump impinges on the crater floor (fig. 18).

Terraces

Most of the crater bottom lies within the area designated as terraces. It is complex physiographically, having slopes as steep as 6° ranging to slopes in the more common terraces and low mounds where the bottom is flat and sometimes even slopes away from ground zero (figs. 18; 19*A*,*B*: lines 116, 304; 20*A*,*B*: lines 541, 539, 538, 507). These terraces are similar to those in OAK crater and, as there, appear to make up a complex of slumped material.

Most of the flatter areas lie northwest and southeast of ground zero. These broaden the crater in this direction so that much of the upper boundary is almost equidistant from ground zero. The area thus is as narrow as 20 m (66 ft) to the southwest and as wide as 300 m (985 ft) to the northwest (fig. 18). The outer perimeter of the northwest, northeast, and southeast quadrants lies between 400 and 475 m (1,300–1,550 ft) from ground zero. However, it is interrupted by small scarps and offset by the position of the broken rim scarp above it. About 10 poorly developed gullies incise the area more or less evenly around the crater (fig. 17).

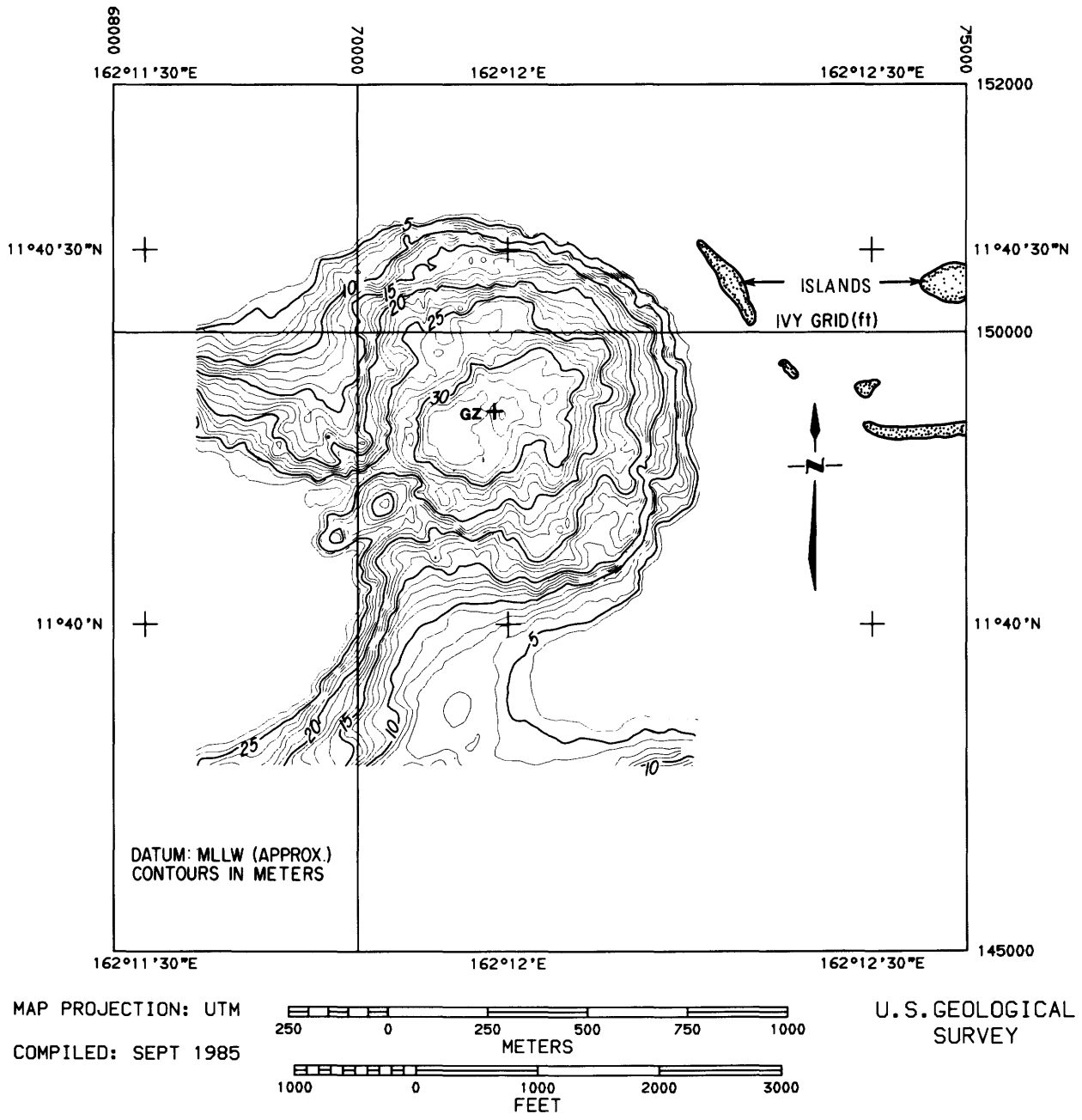

Figure 16. Map showing the bathymetry of KOA crater. GZ=ground zero. Contour interval is 1 m.

Rim Scarp

The change in slope between the terraces and the rim scarp is the most abrupt in the crater, ranging up to a maximum of 18° and commonly about 12° (figs. 16; 18; 19*A*,*B*: lines 115, 116, 120). The area is mostly between 30 and 60 m (100–200 ft) wide, although broader areas are present along the transition into MIKE crater. The scarp is continuous around the northern margin of the crater where its outer perimeter lies consistently close to 500 m (1,640 ft) from ground zero. It appears to have deepened about 15 m (50 ft) on the western side of the crater. On the southeast and south sides of the crater, the scarp is broken and offset into the crater to within about 365 m (1,200 ft) of ground zero; due south of ground zero, it is apparently buried or undeveloped.

The terrace between the broken part of the scarp is about 75 m (246 ft) wide, which is close to the distance (60 m, or 197 ft) that the rim scarp is offset on the west side of OAK crater. Presumably, it was continuous in both craters and has been separated by faulting. Of particular relevance to this interpretation is the separation of railroad

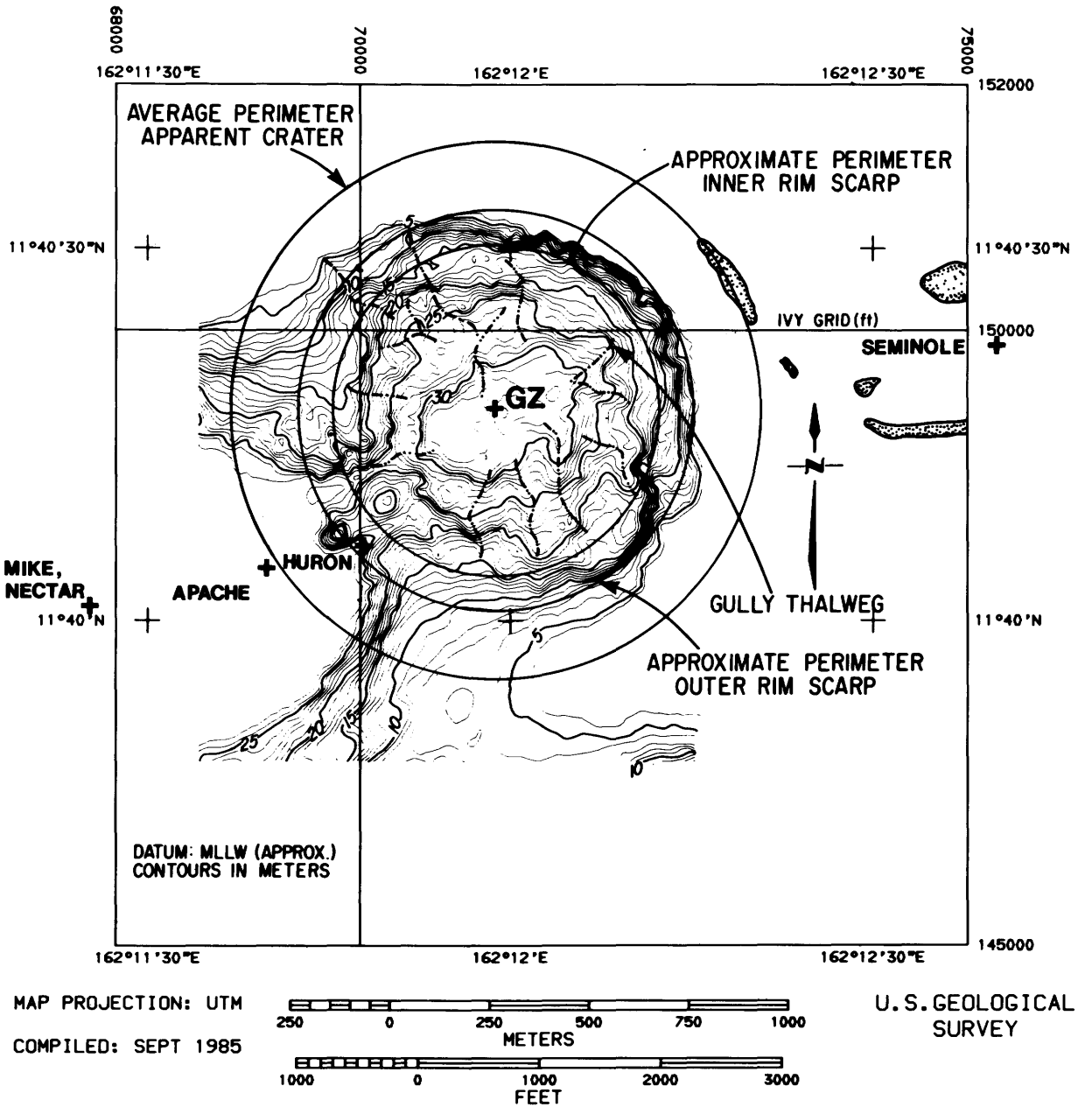

Figure 17. Map showing the bathymetry of KOA crater, the circularity of some isobaths, and some important physiographic features. Crosses show ground zero (GZ) locations of KOA and other events. The average perimeter of the apparent crater is after B. L. Ristvet and K. L. Mills, III, written commun., July 1985. Contour interval is 1 m.

rails discovered and mapped on the bottom of KOA crater by the submersible and by scuba divers. (See chap. H, this volume.) These rails appear to have been in a continuous line when they were set prior to the blast. They now are separated by a distance of about 50 m (164 ft) on the bottom of the crater in the same sense and in the same area that the rim scarp apparently is offset.

Two smaller scarps, one outlined in the northern part and one outlined in the southwestern part of the terraces area (fig. 18), may have been part of the rim scarp complex.

Debris Mounds

Two large debris mounds project into the southwest side of the area of terraces (fig. 18). They both rise to about 15 m (50 ft) above the floor of KOA and 8 m (26 ft) above the floor of MIKE. Within the 25-m (82 ft) isobath, the two mounds are about 300 m (985 ft) wide in the northeast direction and about 130 m (425 ft) wide in the southwest direction (fig. 18). The site of the test known as HURON (fig. 17; see also table 2 of the Introduction to the volume)

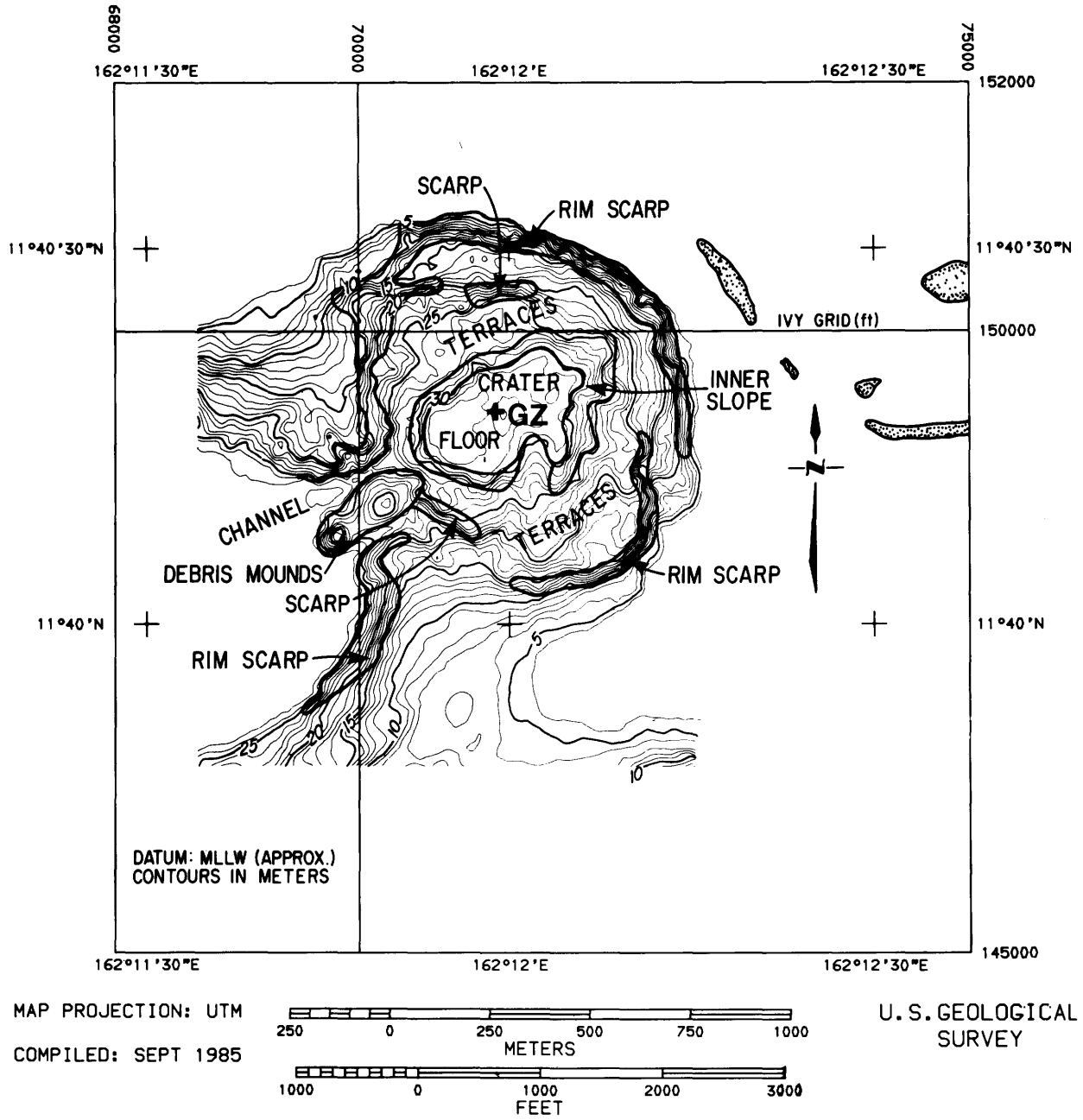

Figure 18. Map showing bathymetry of KOA crater with physiographic provinces outlined. GZ=ground zero. Contour interval is 1 m.

which was fired in 1956, 2 years prior to the KOA event, lies only 60 m (200 ft) southeast of the smaller of the two debris mounds. If a crater was formed, it apparently has been obliterated by KOA's blast and debris. The top of this mound lies 500 m (1,640 ft) from KOA's ground zero, the same distance as does most of the outer edge of the rim scarp (figs. 17, 18). Southeast of the mounds, the bottom rises at about 2–3° in the broad expanse of reef plate that forms the southern margin of the crater. One part of it that rises more steeply (8–9°) may be part of the rim scarp between KOA and MIKE (fig. 18).

Inter-Crater Channel

This narrow (21 m, or 70 ft) channel rises 6 m (20 ft) above KOA's crater floor to a depth of between 25 and 26 m (82–85 ft) which is only a meter or two above the flat floor of MIKE crater (figs. 16; 18; 20*A*,*B*: line 507) to the southwest. Why it has not filled with sediment is not clear; perhaps it is kept open by tidal currents. To the northwest, the steep (9–10°) slope appears to be part of the deepened rim scarp, above which the bottom flattens out in the gradual (2°) ascent to the exposed reef and islands.

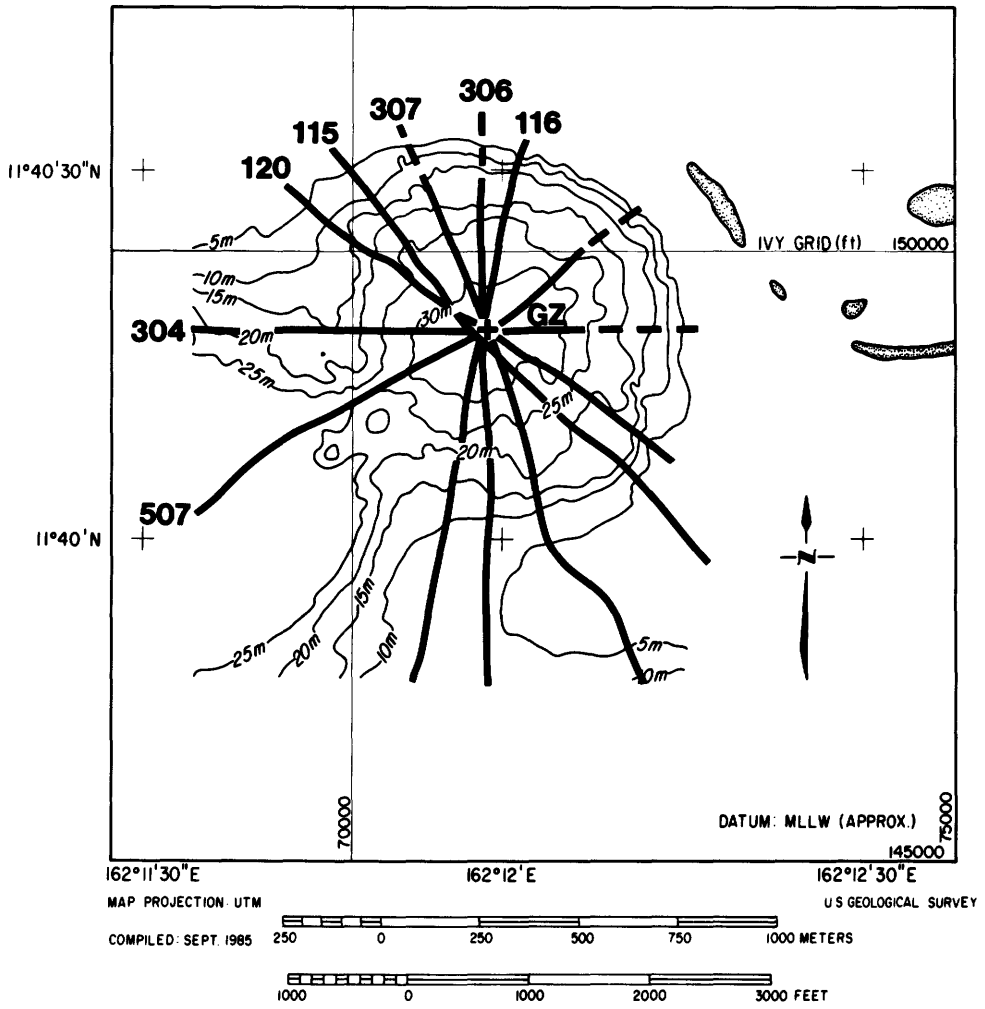

Figure 19*A*. Map showing locations of bathymetric profiles passing through or close to ground zero (GZ) in KOA crater. Profiles are dashed where inferred from bathymetric map based on other data. Contour interval is 5 m.

Three-Dimensional Computer Images of KOA Crater

Perspective images of KOA are shown in figures 21*A*–*C*. A 5× vertical exaggeration was used to accentuate the details of the physiography.

The view from the southwest (fig. 21*A*) depicts the relation of MIKE to KOA and shows more features on the crater walls than the others. The terraces are perhaps the most striking features. The impression that the terraces are related to slumps, particularly those on the northeast and southwest sides of the crater, is clearer in the perspective images.

SUMMARY

The radii of the two craters from their ground zero (KOA) or geometric center (OAK) to the 5-m (16 ft) isobath differ by about 90 m (295 ft); OAK's radius is 590 m (1,935 ft), and KOA's 500 m (1,640 ft). OAK is almost twice as deep (60 m, or 197 ft) as KOA (33 m, or 108 ft). Mainly because of the depth difference, the average slope from the floor of OAK to the 5-m (16 ft) isobath is 5.2°, whereas in KOA it is only 3°. However, on the southeast side of OAK, where water was 40 m (131 ft) deep before the blast, the average slope is only about 4°. Both crater walls are steepest around the outer parts, but in OAK, the slope is steeper and extends deeper around the reefward side.

Much of OAK is symmetrical about a point that is 100 m (330 ft) southeast of ground zero. KOA's ground zero is the symmetrical center of the crater, but below 15 m (49 ft) of depth, isobaths are elliptical with the long axis oriented northeast-southwest. The scarps and terraces on the walls of KOA and OAK suggest that faulting and slumping are common and have affected the shape and size of both craters.

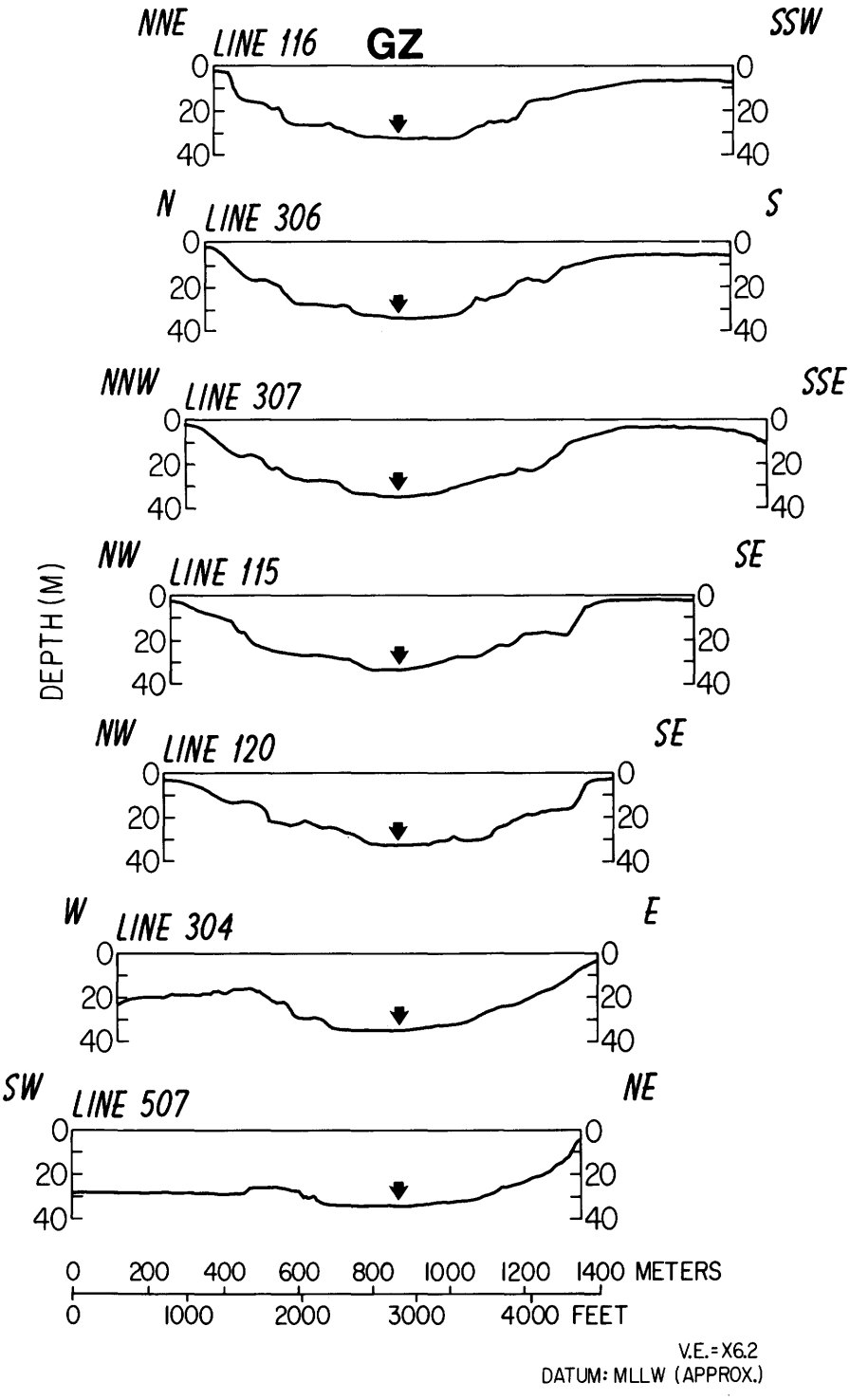

Figure 19*B*. Ground zero location projected orthogonally into lines. Vertical exaggeration is ×6.2

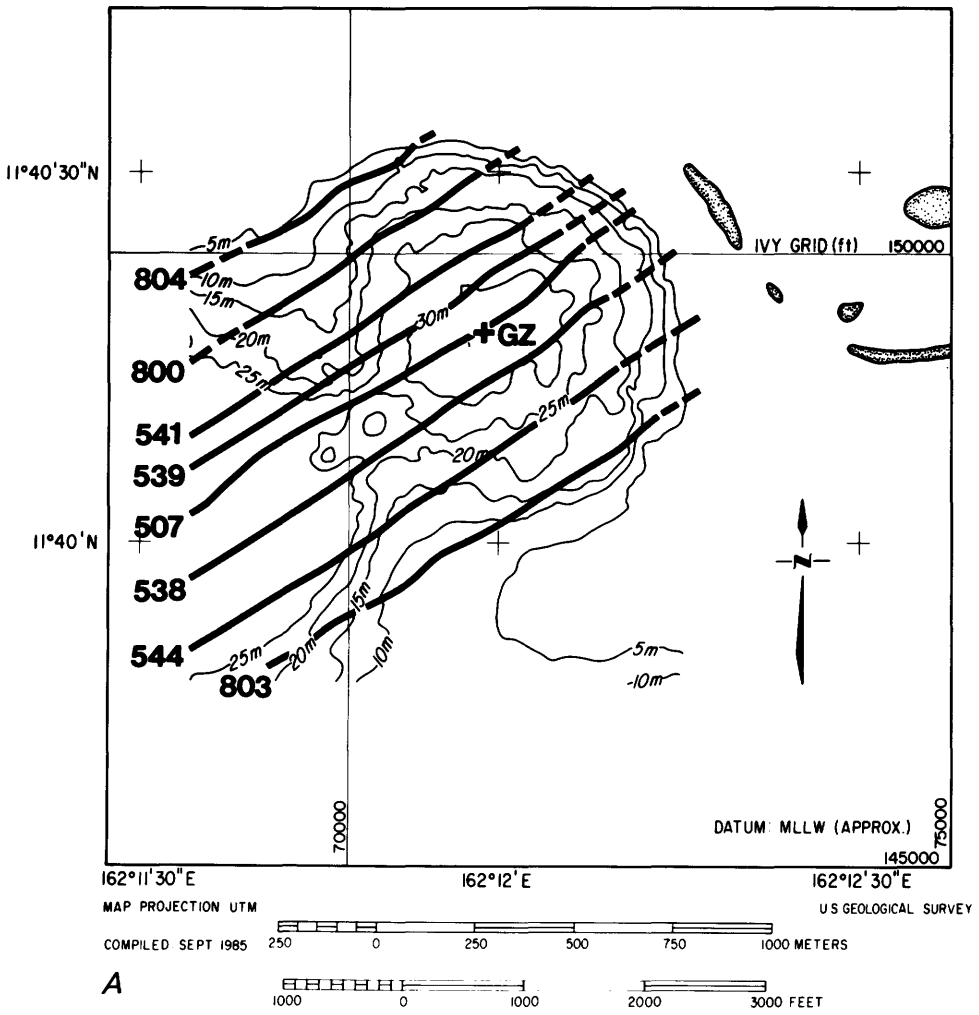

Figure 20. *A* (above), Map showing locations of bathymetric profiles of KOA crater that are oriented parallel to the trend of the reef. Profiles are dashed where inferred from bathymetric map based on other data. Contour interval is 5 m. *B* (right), Ground zero (GZ) location projected orthogonally into lines.

REFERENCES

Chen, C.-T., and Millero, F. J., 1977, Speed of sound in sea water at high pressures: Journal of the Acoustic Society of America, v. 62, no. 6, p. 1129–1135.

Circeo, L. J., Jr., and Nordyke, M. D., 1964, Nuclear cratering experience at the Pacific proving ground Livermore, University of California, Lawrence Radiation Laboratory, TID–4500, UC–35, (UCRL)–12172, 88 p.

Emery, K. O., Tracey, J. I., Jr., and Ladd, H. S., 1954, Geology of Bikini and nearby atolls: U.S. Geological Survey Professional Paper 260–A, 259 p.

Freisen, Bert, ed., 1982, Enewetak Radiological Support Project, final report: U.S. Department of Energy, Nevada Operations Office, Las Vegas, Nevada, NVO 213, 349 p.

Ristvet, B. L., Tremba, E. L., Couch, R. F., Jr., Fetzer, J. A., Goter, E. R., Walter, D.. R., and Wendland, V. P., 1978, Geologic and geophysical investigations of the Eniwetok nuclear craters: Air Force Weapons Laboratory Technical Report TR–77–242, Kirtland Air Force Base, New Mexico 87117, 298 p.

Tremba, E. L., Couch, R. F., and Ristvet, B. L., 1982, Enewetak Atoll Seismic Investigation (EASI): Phases I and II (final report): Air Force Weapons Laboratory Technical Report TR–82–20, Kirtland Air Force Base, New Mexico 87117, 124 p.

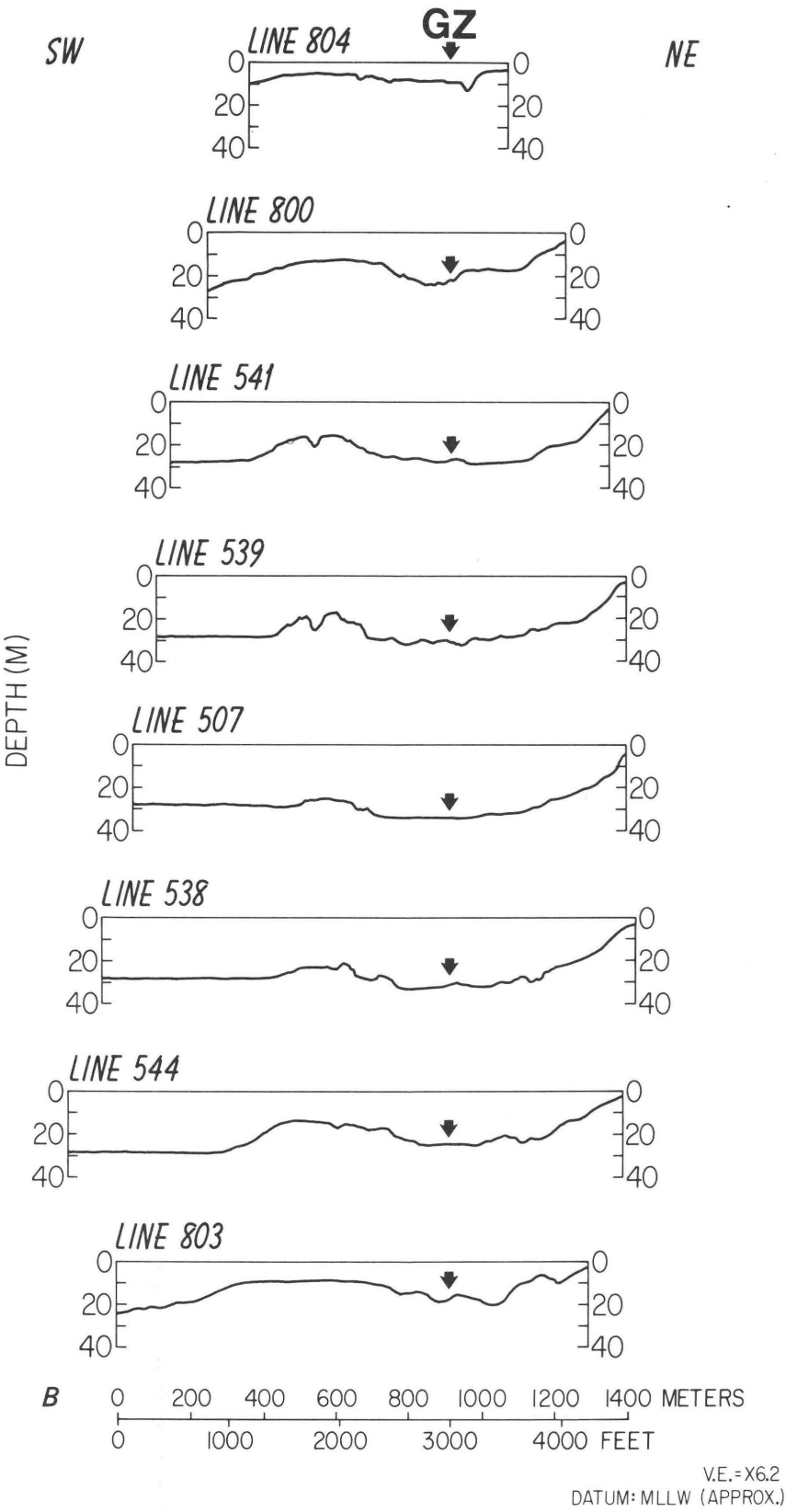
SW
GZ
NE
LINE 804
LINE 800
LINE 541
LINE 539
LINE 507
LINE 538
LINE 544
LINE 803
DEPTH (M)
0
20
40
B
0 200 400 600 800 1000 1200 1400 METERS
0 1000 2000 3000 4000 FEET
V.E.=X6.2
DATUM: MLLW (APPROX.)

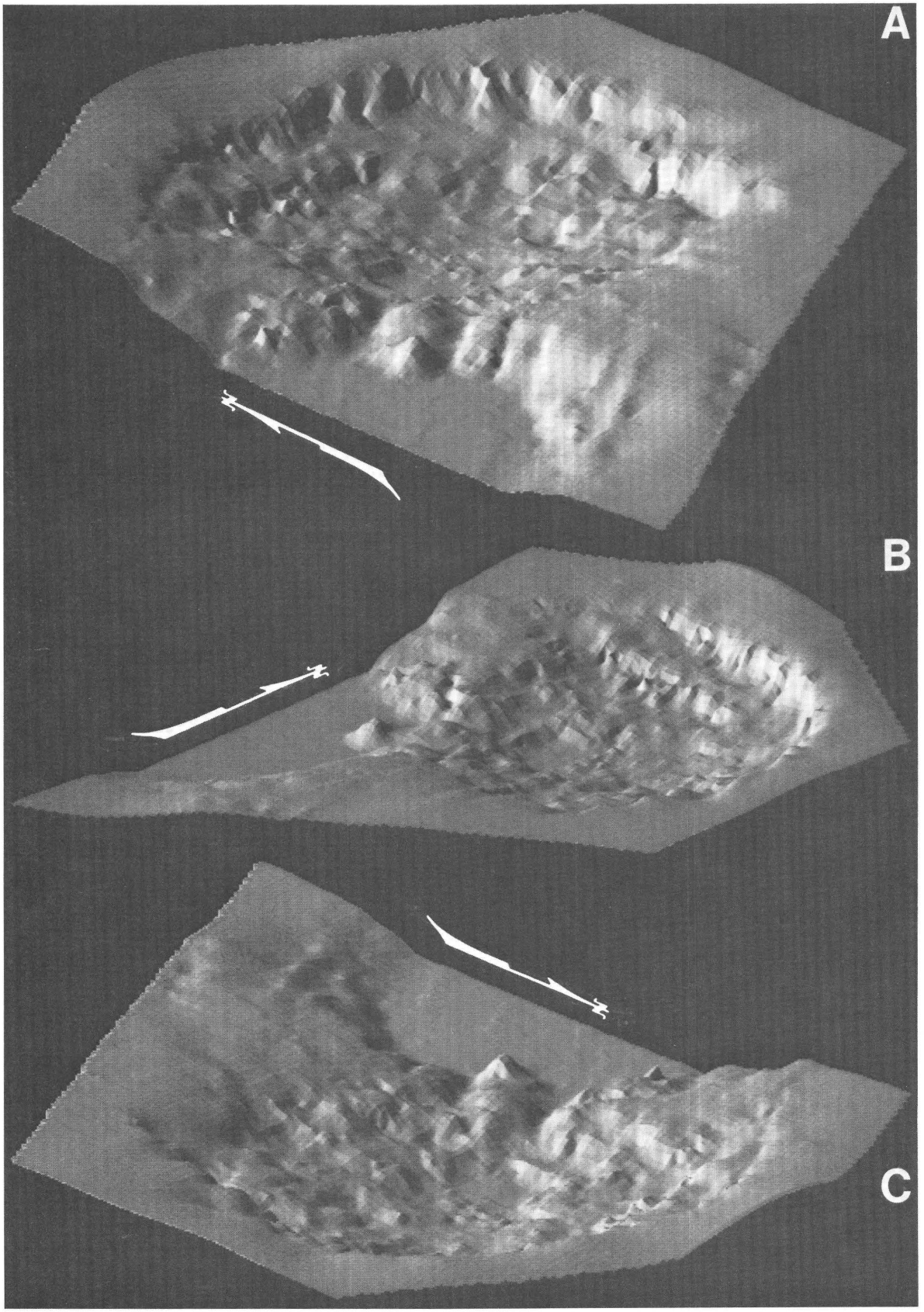

Figure 21. Three-dimensional images of KOA crater: *A*, from the southwest, *B*, from the southeast, and *C*, from the northeast. Vertical exaggeration is ×5.

APPENDICES

Appendix 1. Annotated flow chart showing procedure used to process bathymetric data and description of depth-data contouring

Appendix 2. NOAA tide tables for Enewetak

APPENDIX 1: Annotated Flow Chart

Key: upper case annotations = programs on USGS, Woods Hole HP-1000 computers
lower case annotations = programs on USGS, Woods Hole Pacifics computers
comments in parentheses

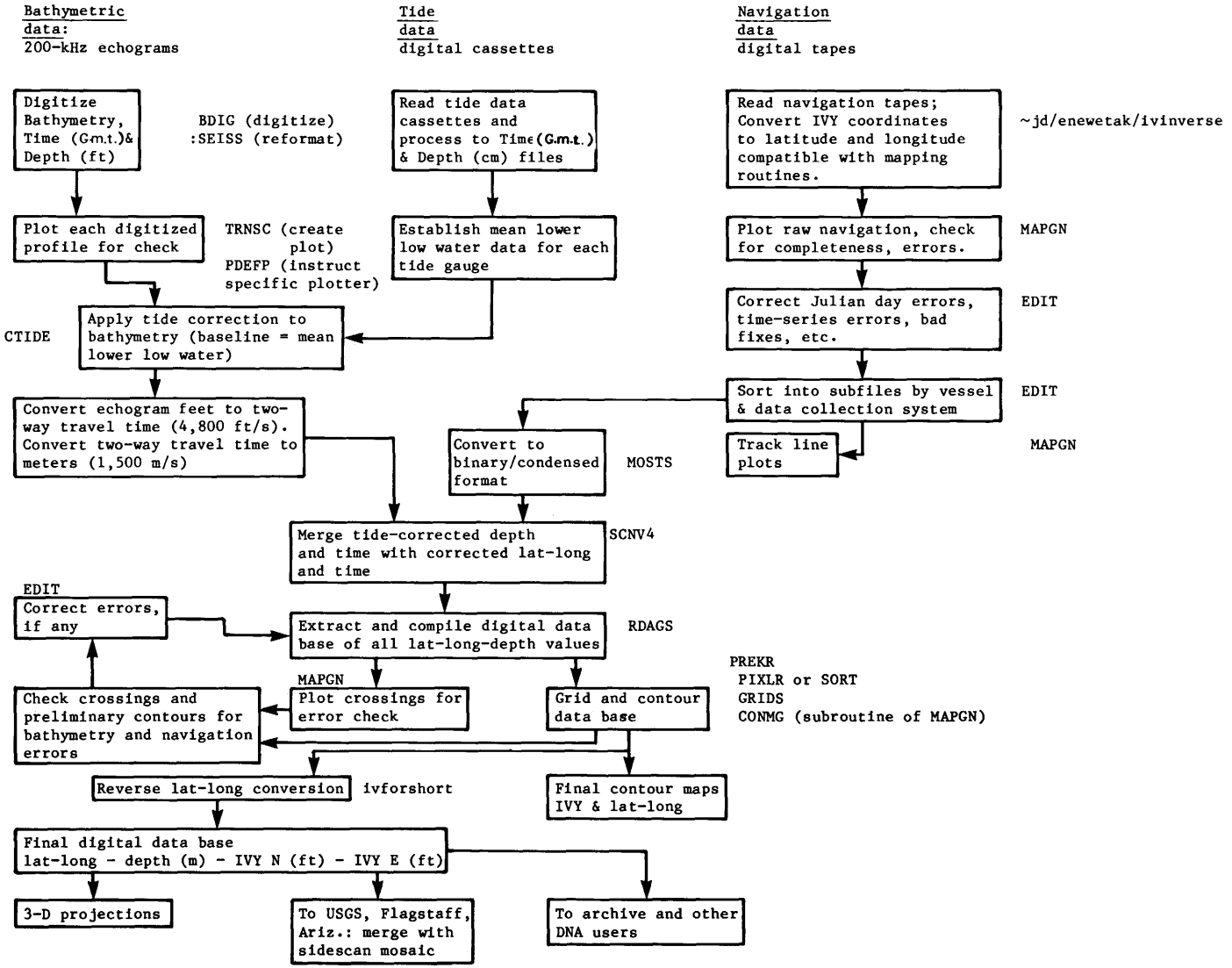

APPENDIX 1: DEPTH-DATA CONTOURING

Computer gridding and contouring have been the primary techniques used in creating maps of depth data; this includes bathymetry, structure contours and unit thickness. Gridding encompasses a body of statistical techniques used for interpolating depths between track lines in order to create a "grid" of evenly spaced values. Contouring is the mathematical technique for examining groups of values in the "grid" and "fitting" a surface, represented by contours, to those values. Note that even a single contour represents a surface, because it has an upslope and a downslope side.

GRIDS, a program written at the U.S. Geological Survey, Woods Hole, Mass., is used for gridding depth data. The user must first select and create a specific map base (that is, one with scale, projection, boundaries, and margin widths). The map base is created by the mapping program, MAPGN. The depth data are then projected onto the map base using the program PREKR. In addition, the user must decide on grid parameters including (1) the size of grid matrix squares in centimeters (appropriate for the map scale being used), (2) the overall size of the grid, as number of squares in the X and Y directions, and (3) the positioning of the grid on the map base, as an offset in centimeters from the bottom (Y-offset) and from the left side (X-offset) of the map (including margin widths).

GRIDS must handle large arrays of depths in order to interpolate values for any given square in the grid. Because of limitations in the HP–1000 computer's working memory, the data is sorted in the Y direction and read in strips, moving up the Y scale by adding a row at the top of the strip and dropping a row from the bottom. The HP–1000 memory capacity determines how many rows may be searched at once, on the basis of data density within each row. In cases where some sections of the data are very dense, the number of rows that can be searched may be of insufficient width to achieve smooth interpolation. This situation is improved using the program PIXLR which averages redundant or duplicate points, thinning out the densest portions of the data, and sorting.

GRIDS permits varying the interpolation parameters. These are: (1) RMAX, (2) IOCT, (3) NPMAX, (4) SM. (1) RMAX is the maximum radius to search for points to interpolate a depth. RMAX also defines half the number of rows to be loaded into computer memory, and hence it is limited by the memory capacity. RMAX was always at least 6 times the size of the grid squares. (2) IOCT is a 0/1 off/on switch that determines whether GRIDS searches in a simple circle (=0) or searches each octant (eighth circle) individually (=1). We always use a 1. (3) NPMAX, with IOCT=1, represents the maximum number of points to find from each octant for the interpolation. (4) SM is the smoothing factor, indicating how to weight points according to distance from center of the search radius. "0" is no weighting for distance; that is, simply an average of all the points gathered based on RMAX and NPMAX. This translates into maximum smoothing, averaging out small details of terrain. "10" is a steep weighting for distance, where points found within approximately 0.1 RMAX completely outweigh distal values, and smoothing is minimized. We used SM=8 for bathymetry, which translates to: any soundings found within a grid square override soundings from outside that grid square.

With the grid parameters and interpolation control values set, GRIDS proceeds to create what is in essence a piece of graph paper with numbers (depths) in all squares located within RMAX of a sounding. These maps of depth data created by GRIDS can be contoured or compared with other grids. Specifically, two grids created with the same grid parameters can be subtracted, square for square (using the program SUBGD::3302). This technique was applied to arrive at a map showing the difference between preblast and postblast bathymetry and the maps of unit thickness above reflectors 10 and 20.

CONMG, a subroutine of the mapping program MAPGN, creates the contour maps. CONMG reads the output of GRIDS or SUBGD and creates a MAPGN file of contours. CONMG permits selection of the contour interval, the contour labeling interval, the label size and format, and the angularity of contours connecting points. In addition, contouring can be restricted to selected portions of the grid or selected depth ranges. With the exception of the contour angularity control, called DEL, the variables are straightforward. DEL varies the curvature put on a contour connecting three or more points that are not in a straight line. Setting DEL equal to 2 yielded smooth curves without causing interference between adjacent contours.

Based on the above information, the precision of computer contours on a map is seen to depend on the size of the grid squares that were contoured and on the distribution of the data used to interpolate values for these squares. This information is derived from the gridding parameters and by examination of the point plot (that is, data distribution) for the specific region and data set in question.

APPENDIX 2: NOAA Tide Tables for Enewetak

ENEWETAK (MARSHALL ISLANDS) T.M. 180 E. DATUM = MLLW
TIDE PREDICTIONS (HIGH AND LOW WATERS) JUNE, 1984
REFERENCE STATION IS: KWAJALEIN ATOLL, MARSHALL IS. T.M. 180 E.
HWTIME = -7 HWHT = .00 HWR = +.77
LWTIME = -3 LWHT = .00 LWR = +.77
CONS = .30
NOAA, NATIONAL OCEAN SERVICE

STANDARD TIME

DAY	TIME	HT.	TIME	HT.	TIME	HT.	TIME	HT.
1 F	451 H	4.9	1123 L	.8	1713 H	3.9	2304 L	1.0
2 SA	528 H	4.9	1204 L	.9	1753 H	3.7	2341 L	1.2
3 SU	606 H	4.7	1247 L	1.1	1836 H	3.5		
4 M	24 L	1.4	651 H	4.5	1338 L	1.3	1931 H	3.3
5 TU	111 L	1.6	744 H	4.2	1438 L	1.5	2037 H	3.2
6 W	217 L	1.9	851 H	4.0	1553 L	1.6	2207 H	3.2
7 TH	353 L	2.1	1015 H	3.7	1713 L	1.6	2338 H	3.4
8 F	534 L	2.0	1143 H	3.7	1819 L	1.5		
9 SA	44 H	3.7	656 L	1.7	1253 H	3.7	1915 L	1.3
10 SU	137 H	4.1	757 L	1.4	1353 H	3.8	2000 L	1.2
11 M	222 H	4.4	848 L	1.2	1441 H	3.9	2042 L	1.1
12 TU	303 H	4.7	933 L	1.0	1523 H	3.9	2119 L	1.0
13 W	342 H	4.9	1012 L	.9	1603 H	3.9	2156 L	1.0
14 TH	417 H	4.9	1051 L	.9	1640 H	3.8	2232 L	1.0
15 F	454 H	4.9	1128 L	.9	1715 H	3.7	2305 L	1.1
16 SA	529 H	4.8	1208 L	1.1	1753 H	3.6	2339 L	1.3
17 SU	604 H	4.6	1242 L	1.2	1830 H	3.4		
18 M	16 L	1.5	641 H	4.3	1322 L	1.4	1910 H	3.3
19 TU	55 L	1.7	718 H	4.0	1404 L	1.6	1958 H	3.2
20 W	138 L	1.9	803 H	3.8	1455 L	1.7	2058 H	3.1
21 TH	239 L	2.1	900 H	3.5	1555 L	1.8	2217 H	3.1
22 F	403 L	2.3	1012 H	3.3	1703 L	1.9	2336 H	3.2
23 SA	540 L	2.2	1133 H	3.3	1806 L	1.8		
24 SU	39 H	3.5	656 L	2.0	1244 H	3.3	1859 L	1.7
25 M	129 H	3.7	752 L	1.8	1340 H	3.4	1944 L	1.5
26 TU	209 H	4.1	837 L	1.5	1428 H	3.5	2026 L	1.4
27 W	249 H	4.3	919 L	1.2	1510 H	3.7	2103 L	1.2
28 TH	326 H	4.6	959 L	1.0	1550 H	3.8	2143 L	1.1
29 F	403 H	4.8	1039 L	.8	1631 H	3.8	2221 L	1.0
30 SA	443 H	4.9	1120 L	.8	1711 H	3.8	2302 L	1.0

ENEWETAK (MARSHALL ISLANDS) T.M. 180 E. DATUM = MLLW
TIDE PREDICTIONS (HIGH AND LOW WATERS) JULY, 1984
REFERENCE STATION IS: KWAJALEIN ATOLL, MARSHALL IS. T.M. 180 E.
HWTIME = -7 HWHT = .00 HWR = +.77
LWTIME = -3 LWHT = .00 LWR = +.77
CONS = .30
NOAA, NATIONAL OCEAN SERVICE

STANDARD TIME

DAY	TIME	HT.	TIME	HT.	TIME	HT.	TIME	HT.
1 SU	523 H	5.0	1200 L	.8	1753 H	3.8	2344 L	1.0
2 M	604 H	4.9	1242 L	.8	1836 H	3.7		
3 TU	26 L	1.2	649 H	4.7	1327 L	1.0	1925 H	3.7
4 W	116 L	1.4	734 H	4.4	1415 L	1.2	2019 H	3.6
5 TH	212 L	1.6	829 H	4.1	1510 L	1.4	2122 H	3.5
6 F	324 L	1.8	933 H	3.7	1614 L	1.5	2239 H	3.5
7 SA	452 L	1.9	1054 H	3.4	1724 L	1.6	2359 H	3.7
8 SU	627 L	1.9	1218 H	3.3	1830 L	1.6		
9 M	108 H	3.9	744 L	1.7	1329 H	3.3	1931 L	1.5
10 TU	204 H	4.2	842 L	1.4	1430 H	3.4	2021 L	1.4
11 W	249 H	4.4	928 L	1.2	1515 H	3.5	2106 L	1.3
12 TH	331 H	4.6	1010 L	1.1	1558 H	3.6	2146 L	1.2
13 F	408 H	4.7	1045 L	1.0	1632 H	3.7	2222 L	1.1
14 SA	445 H	4.8	1120 L	.9	1708 H	3.7	2258 L	1.1
15 SU	518 H	4.7	1153 L	1.0	1741 H	3.7	2333 L	1.1
16 M	552 H	4.6	1224 L	1.0	1814 H	3.7		
17 TU	7 L	1.2	625 H	4.5	1255 L	1.1	1848 H	3.7
18 W	41 L	1.4	656 H	4.2	1325 L	1.3	1923 H	3.6
19 TH	117 L	1.6	728 H	4.0	1359 L	1.5	2002 H	3.5
20 F	159 L	1.8	806 H	3.7	1436 L	1.6	2047 H	3.4
21 SA	247 L	2.0	851 H	3.4	1524 L	1.8	2151 H	3.3
22 SU	405 L	2.2	957 H	3.2	1628 L	1.9	2315 H	3.3
23 M	548 L	2.2	1134 H	3.0	1751 L	1.9		
24 TU	39 H	3.5	723 L	2.0	1308 H	3.1	1904 L	1.8
25 W	140 H	3.9	824 L	1.7	1414 H	3.3	2005 L	1.6
26 TH	230 H	4.2	911 L	1.3	1502 H	3.5	2051 L	1.3
27 F	315 H	4.6	952 L	1.0	1545 H	3.7	2135 L	1.1
28 SA	356 H	4.9	1031 L	.7	1625 H	3.9	2218 L	.9
29 SU	437 H	5.0	1110 L	.6	1703 H	4.1	2257 L	.8
30 M	515 H	5.1	1147 L	.5	1742 H	4.2	2339 L	.8
31 TU	555 H	5.0	1224 L	.6	1822 H	4.2		

ENEWETAK (MARSHALL ISLANDS) T.M. 180 E. DATUM = MLLW
TIDE PREDICTIONS (HIGH AND LOW WATERS) AUGUST, 1984
REFERENCE STATION IS: KWAJALEIN ATOLL, MARSHALL IS. T.M. 180 E.
HWTIME = -7 HWHT = .00 HWR = +.77
LWTIME = -3 LWHT = .00 LWR = +.77
CONS = .30
NOAA, NATIONAL OCEAN SERVICE

STANDARD TIME

DAY		TIME		HT.	TIME		HT.	TIME		HT.	TIME		HT.
1	W	21	L	.9	633	H	4.8	1301	L	.7	1902	H	4.1
2	TH	103	L	1.1	715	H	4.5	1340	L	1.0	1947	H	4.0
3	F	151	L	1.4	758	H	4.0	1423	L	1.3	2037	H	3.8
4	SA	249	L	1.7	848	H	3.6	1510	L	1.6	2141	H	3.6
5	SU	409	L	2.0	959	H	3.2	1618	L	1.9	2309	H	3.6
6	M	606	L	2.1	1148	H	2.9	1750	L	2.0			
7	TU	47	H	3.7	747	L	1.9	1335	H	3.0	1918	L	1.9
8	W	156	H	3.9	850	L	1.6	1438	H	3.2	2018	L	1.7
9	TH	247	H	4.2	930	L	1.3	1521	H	3.4	2104	L	1.5
10	F	326	H	4.5	1002	L	1.1	1553	H	3.6	2143	L	1.2
11	SA	401	H	4.6	1033	L	1.0	1625	H	3.8	2216	L	1.1
12	SU	432	H	4.7	1059	L	.9	1653	H	4.0	2248	L	1.0
13	M	502	H	4.8	1127	L	.8	1722	H	4.1	2320	L	.9
14	TU	530	H	4.7	1152	L	.8	1747	H	4.1	2348	L	1.0
15	W	558	H	4.6	1218	L	.9	1816	H	4.1			
16	TH	18	L	1.1	625	H	4.4	1245	L	1.1	1843	H	4.0
17	F	47	L	1.3	651	H	4.1	1309	L	1.3	1913	H	3.9
18	SA	119	L	1.5	721	H	3.8	1338	L	1.5	1947	H	3.7
19	SU	159	L	1.8	750	H	3.5	1410	L	1.7	2032	H	3.5
20	M	252	L	2.1	835	H	3.1	1455	L	2.0	2144	H	3.4
21	TU	439	L	2.3	1018	H	2.8	1627	L	2.2	2350	H	3.4
22	W	712	L	2.1	1300	H	2.9	1841	L	2.1			
23	TH	124	H	3.7	818	L	1.7	1414	H	3.2	1957	L	1.8
24	F	222	H	4.2	903	L	1.3	1459	H	3.6	2045	L	1.4
25	SA	305	H	4.6	938	L	.9	1534	H	3.9	2128	L	1.0
26	SU	344	H	4.9	1015	L	.6	1611	H	4.2	2210	L	.7
27	M	422	H	5.1	1049	L	.4	1647	H	4.5	2248	L	.5
28	TU	500	H	5.2	1122	L	.3	1721	H	4.6	2326	L	.5
29	W	535	H	5.1	1155	L	.4	1758	H	4.6			
30	TH	5	L	.6	612	H	4.8	1229	L	.6	1833	H	4.5
31	F	44	L	.9	649	H	4.4	1301	L	.9	1910	H	4.3

ENEWETAK (MARSHALL ISLANDS) T.M. 180 E. DATUM = MLLW
TIDE PREDICTIONS (HIGH AND LOW WATERS) SEPTEMBER, 1984
REFERENCE STATION IS: KWAJALEIN ATOLL, MARSHALL IS. T.M. 180 E.
HWTIME = -7 HWHT = .00 HWR = +.77
LWTIME = -3 LWHT = .00 LWR = +.77
CONS = .30
NOAA, NATIONAL OCEAN SERVICE

STANDARD TIME

DAY	TIME	HT.	TIME	HT.	TIME	HT.	TIME	HT.
1 SA	125 L	1.2	725 H	3.9	1335 L	1.3	1950 H	4.0
2 SU	215 L	1.7	803 H	3.4	1410 L	1.7	2045 H	3.7
3 M	326 L	2.1	901 H	2.9	1500 L	2.1	2217 H	3.4
4 TU	611 L	2.2	1159 H	2.6	1715 L	2.3		
5 W	39 H	3.5	808 L	1.9	1404 H	2.9	1933 L	2.2
6 TH	156 H	3.8	853 L	1.6	1446 H	3.2	2024 L	1.8
7 F	241 H	4.1	919 L	1.3	1515 H	3.5	2103 L	1.5
8 SA	315 H	4.4	946 L	1.1	1541 H	3.8	2134 L	1.2
9 SU	344 H	4.6	1008 L	.9	1603 H	4.1	2204 L	1.0
10 M	411 H	4.7	1032 L	.8	1628 H	4.3	2231 L	.8
11 TU	437 H	4.7	1055 L	.7	1653 H	4.4	2258 L	.8
12 W	504 H	4.7	1117 L	.7	1718 H	4.5	2325 L	.8
13 TH	527 H	4.6	1141 L	.8	1743 H	4.5	2352 L	.9
14 F	553 H	4.4	1202 L	1.0	1806 H	4.4		
15 SA	18 L	1.1	617 H	4.1	1224 L	1.1	1833 H	4.2
16 SU	47 L	1.3	643 H	3.8	1247 L	1.4	1902 H	4.0
17 M	122 L	1.6	710 H	3.5	1314 L	1.7	1939 H	3.8
18 TU	210 L	2.0	750 H	3.1	1346 L	2.0	2043 H	3.5
19 W	358 L	2.3	928 H	2.7	1513 L	2.3	2309 H	3.4
20 TH	704 L	2.1	1308 H	2.8	1830 L	2.3		
21 F	108 H	3.7	803 L	1.6	1407 H	3.3	1947 L	1.8
22 SA	205 H	4.2	842 L	1.2	1444 H	3.8	2034 L	1.3
23 SU	246 H	4.6	917 L	.8	1518 H	4.2	2117 L	.9
24 M	326 H	4.9	948 L	.5	1550 H	4.6	2154 L	.6
25 TU	403 H	5.1	1021 L	.3	1624 H	4.9	2232 L	.4
26 W	438 H	5.1	1053 L	.3	1657 H	5.0	2309 L	.3
27 TH	513 H	4.9	1123 L	.4	1729 H	5.0	2346 L	.5
28 F	548 H	4.6	1155 L	.6	1804 H	4.8		
29 SA	24 L	.8	620 H	4.2	1223 L	1.0	1838 H	4.6
30 SU	103 L	1.2	654 H	3.7	1250 L	1.4	1915 H	4.2

Chapter B

Sidescan-Sonar Survey of OAK and KOA Craters

By D. W. FOLGER, J. M. ROBB, J. C. HAMPSON, P. A. DAVIS, P. M. BRIDGES, and D. J. RODDY

U.S. GEOLOGICAL SURVEY BULLETIN 1678

SEA-FLOOR OBSERVATIONS AND SUBBOTTOM SEISMIC CHARACTERISTICS OF OAK AND KOA CRATERS, ENEWETAK ATOLL, MARSHALL ISLANDS

CONTENTS

FIGURES

Chapter B
Sidescan-Sonar Survey of OAK and KOA Craters

By D. W. Folger[1], J. M. Robb[1], J. C. Hampson[1], P. A. Davis[2], P. M. Bridges[2], *and* D. J. Roddy[2]

INTRODUCTION

Purpose

The sidescan-sonar survey provided critical information on the distribution, trends, and texture of scarps, fractures, slumps, and bottom sediments associated with the craters and the debris accumulation around OAK crater. The sidescan-sonar survey also provided an on-site map-quality image (a field-prepared mosaic) to guide submersible and scuba surveys.

Echo soundings provide quantitative measurements of the surface of a submarine crater, but such data are limited to points directly beneath the tracks of a ship. Information needed to fill in details between ship tracks requires another technique. Side-looking radar or even oblique aerial photographs are appropriate for subaerial craters. Radar cannot be used for submarine features, however, and sophisticated submarine optical systems such as Angus (Ballard and others, 1984) could not be used in this study due to poor visibility (as reported by Tremba and others, 1982). Therefore, we used a sidescan-sonar system, the acoustic equivalent of side-looking radar.

Previous Work

The sidescan-sonar survey that was undertaken as part of the EASI (Enewetak Atoll Seismic Investigation) project provided no useful data. To our knowledge, no other sidescan-sonar observations in the craters have been made.

Field Methods

Most of the sidescan-sonar data were collected aboard *Egabrag II* on tracks spaced 75 m (246 ft) apart. We acquired data along a total distance of 75 km (40 nmi) in OAK and 19.6 km (10 nmi) in KOA (figs. 1, 2). Additional tie lines were run in the lagoon between the craters, and short extensions of lines were run into shallow water by the landing craft (Mike boat) in both craters. Most data were acquired with a Klein Model 422S-101 AF transducer unit mounted in a 545-kg (1,200 lb) fish. Data from the landing craft were acquired with similar transducers, but they were mounted on a smaller fish. The port and starboard transducers have a horizontal beam width of 1°, a vertical beam width of 40°, an output frequency of 100 kHz, a 0.1-ms pulse length, and a resolution of 0.15 m. The stability of the large transducer vehicle in the water was a major contributor to the excellent record quality that allowed us to construct usable mosaics in the field. We used 100 m (330 ft) of range on either side of the fish, giving us about 30 percent overlap in each direction from line to line. Data were displayed on a Klein 531T three-channel wet-paper recorder. Analog signals were recorded on magnetic tape using a Honeywell 14-track recorder and 1-inch (2.54 cm) magnetic tape.

Although the best detail is generally obtained by towing the transducer fish close to the bottom at 10 percent of the instrument's range, we were forced to run it at shallower than optimal depths in the confined space of KOA and among the many patch reefs surrounding OAK. During cloudy weather, coral heads were difficult to see, maneuvering room for *Egabrag II* was constrained, and we had to terminate lines short of some critical nearshore areas in both craters. To overcome this problem, we subsequently mounted the sidescan-sonar system on the Mike boat (fig. 2, Introduction to the volume), and used a smaller, less stable fish that could be controlled quickly by hand. However, rapid changes in depth produced noisier records in some areas, especially within KOA.

Following the *Egabrag* phase of the sidescan-sonar survey, the analog paper records were photographed at the Mid-Pacific Laboratory on Enewetak by D. S. Blackwood, and photographs were assembled into mosaics. These were then rephotographed and printed at Enewetak at scales appropriate for immediate field use aboard *Egabrag, Delta,* and *Halimeda.*

Image Processing

Subsequent to field operations, to enhance the sidescan-sonar images and to create map-quality mosaics using processed navigation and bathymetric data, the analog recordings of sidescan-sonar data on magnetic tape were digitized using a MASSCOMP MC-500 computer. A 30-kHz digitizing rate was used over 180 ms of the 200-ms scan interval, with every third point recorded, giving about 1,800 points per scan, for an average lateral pixel dimension of about 7.5 cm (3 in.). At the usual ship speed of 4 kn (about

[1]U.S. Geological Survey, Branch of Atlantic Marine Geology, Woods Hole, Mass. 02543

[2]U.S. Geological Survey, Branch of Astrogeological Studies, Flagstaff, Ariz. 86001

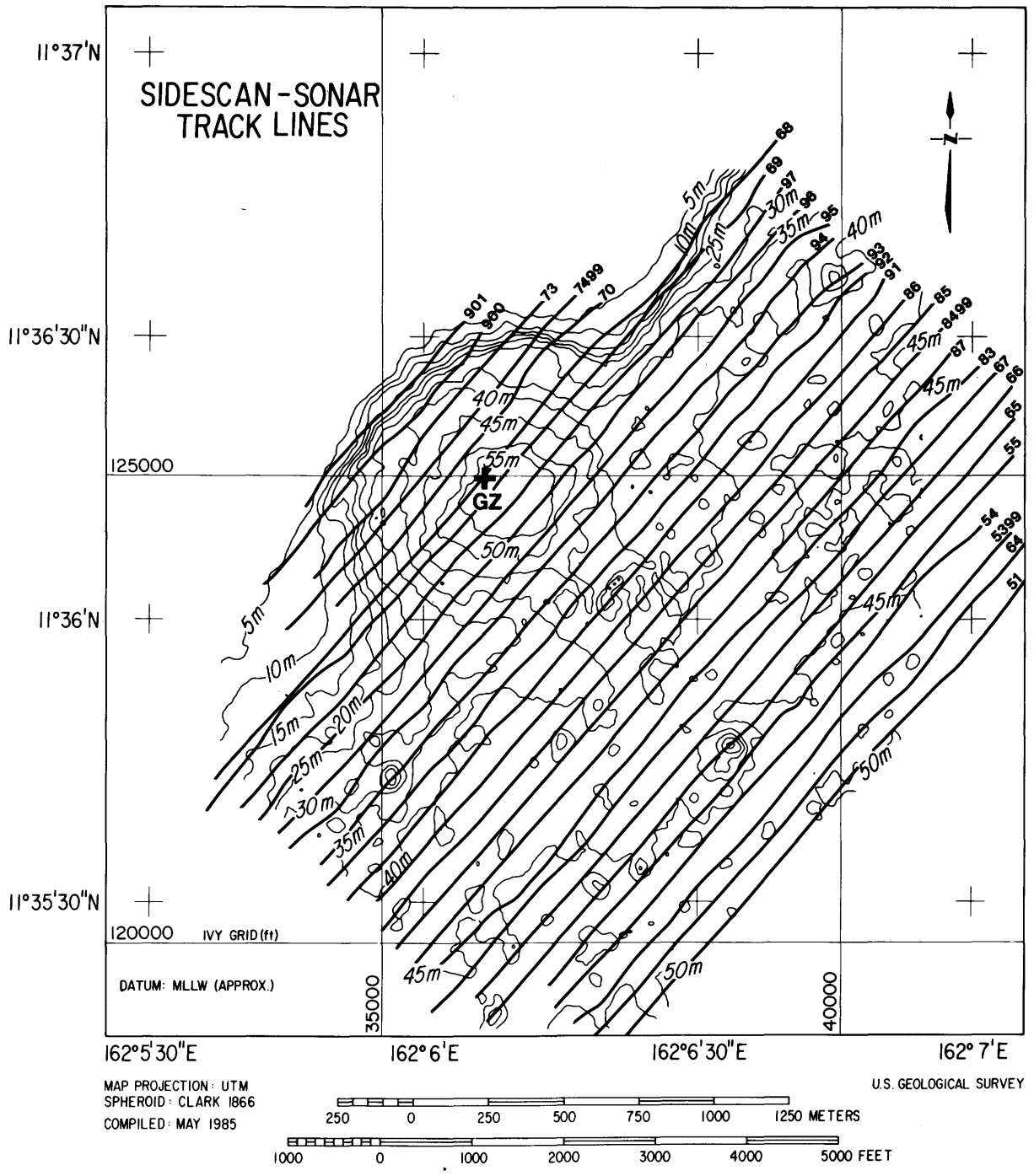

Figure 1. Tracks of vessels along which sidescan-sonar data were acquired in OAK crater. GZ=ground zero. Contour interval is 5 m.

2 m per second), the vertical, or along-track, pixel dimension was about 40 cm (16 in.).

The digital sidescan-sonar data were processed at the U.S. Geological Survey's (USGS) laboratories in Flagstaff, Ariz., using a VAX-11/750-based computer system and a Ramtek interactive display unit. The computer programs used have been developed primarily within the USGS.

Processing steps included noise removal, slant-range correction, aspect-ratio correction, and application of a constant contrast stretch so the data could be assembled in a mosaic. Film transparencies of each sonar track were prepared at scales appropriate for airbrushing.

The noise removed took the form of (1) random electronic noise introduced by various hardware systems, and (2) speckle noise that is inherent in all sonar and radar data. Most of the random noise was visible as solid white or black horizontal lines and, with the Mike-boat data, some vertical lines. The position of either line or sample noise was deter-

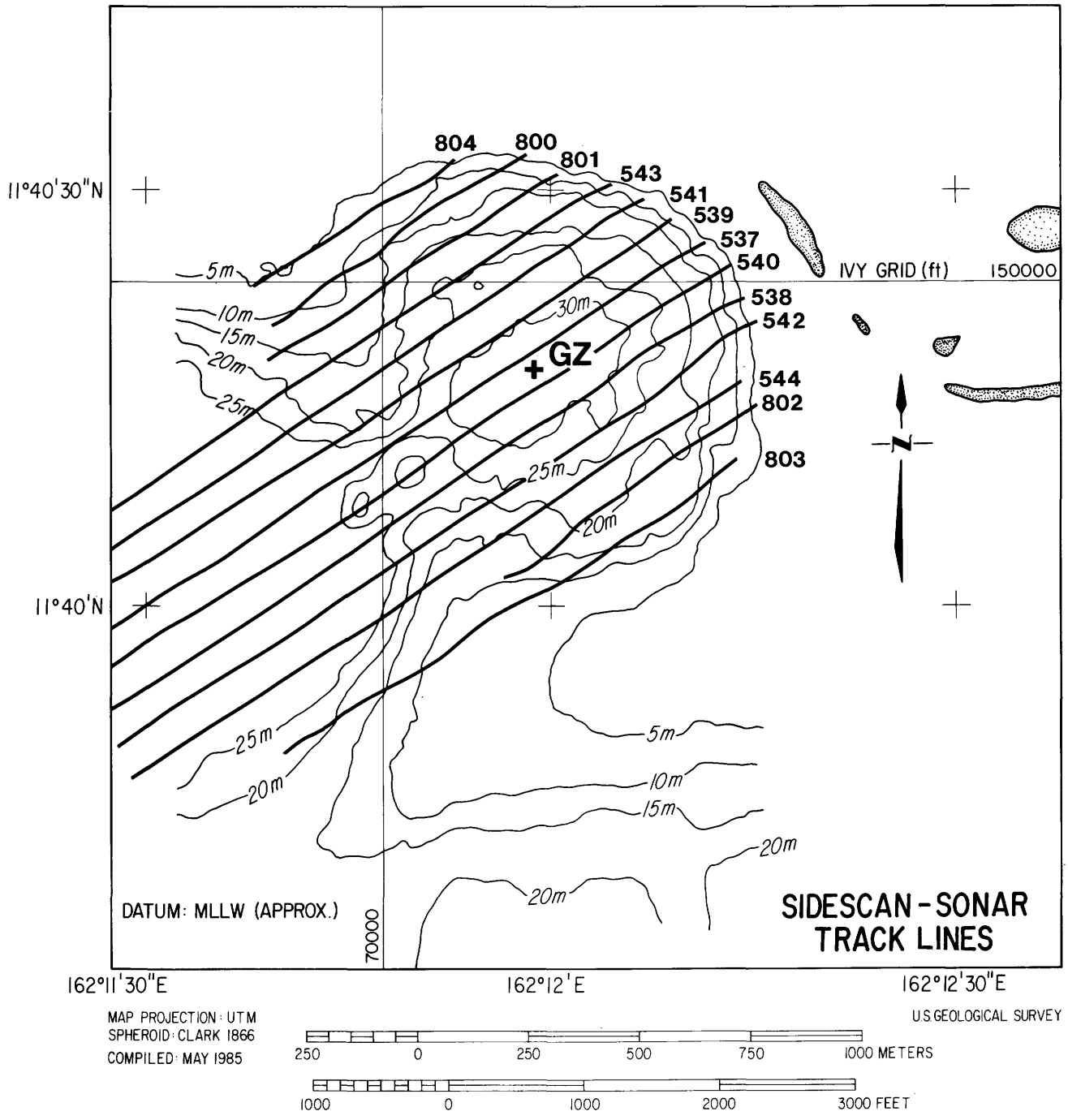

Figure 2. Tracks of vessels along which sidescan-sonar data were acquired in KOA crater. GZ=ground zero. Contour interval is 5 m.

mined and recorded by examination using an interactive display screen coupled to the computer. The line noise was removed from the digital data by duplication of adjacent lines (either vertical or horizontal). The duplication is unnoticeable in the image because of the high resolution of the data, but the duplication must be done prior to the slant-range correction because the latter would distort the noise and make its later removal extremely difficult.

The speckle noise was removed by applying a median digital filter to the data. Preliminary tests showed that the minimum-sized boxcar filter (2-by-2) was sufficient to remove this noise. A 2-by-2 boxcar refers to the imaginary box configuration of the filter that runs laterally along each line of image data from the top to the bottom of the image. During this moving filter process, the value of each pixel (known as the digital number, or DN) in the four-pixel box

is taken from the original image data base and accumulated in computer memory, and a median DN is selected. The resultant median value represents the new DN value for the upper left corner value of the box. This value is then placed in a blank image database at the original image position of the upper left pixel of the box. The advantage of the median filter over other digital filters is that it eliminates DN spikes, either as anomalously high or low values in the original data, but maintains as much of the information content of the original data as possible.

The next step was slant-range correction, which requires knowledge of the height of the sidescan fish over bottom. Because the height over bottom varied and the built-in altimeter unit in the sidescan-sonar fish had failed near the start of the operation, we recovered these values by digitizing the first arrival of the sonar image. This procedure produced a file of across-track pixel positions for each line of image data, which was then used in the slant-range calculation to determine where pixels within a particular line of original image data should be located in an undistorted image. These positions were then used to extract pixels along a particular line of original image data and to place them at their true relative positions in a blank image file. The across-track resolution of the resultant image data was degraded to about 30 cm (12 in.) from the original 7.5 cm (3 in.).

RESULTS

The sidescan data from OAK were of significantly better quality than those from KOA crater. This result probably was due to several factors that included: (1) restricted area in KOA for maneuvering the ship; (2) more reverberation noise in KOA data due to the crater's smaller size and enclosed geometry; and (3) more use in KOA of the smaller fish which had to be raised and lowered rapidly and was consequently more noisy. To illustrate the quality of the field sidescan-sonar data, we have included the mosaics of the two craters that were constructed at Enewetak from the analog records (figs. 3, 4). The mosaics include 5-m bathymetric overlays for orientation. The field mosaics show many characteristics that make interpretation of sidescan data difficult, such as the boundaries between strips of imagery recorded along each track, variations in directions of shadows depending on fish location, and complex patterns of noise. Digitizing and processing has minimized these characteristics and enhanced the definition of targets, especially in such areas as the inner crater. The processed, digitized sidescan data provided the principal input to the airbrush-enhanced sea-floor images of the two craters (figs. 5*A–C*; 6*A–C*).

OAK Crater

For the field mosaic, photographs of sidescan-sonar images were glued up with the look direction toward the reef. Accordingly, more details are visible on the northwest side of the crater than on the southeast side (fig. 3*A*). Most major features are present on this mosaic, but many smaller features are not. The steep slopes on the reefward side of the crater show as the most intense reflections in the area. Few details of the numerous scarps that make up the slope are resolved. The debris blanket surrounding the lagoonward side of the crater is defined by a texture that is unique and appears nowhere else in the image. The flat-floored valley that cuts through the crater wall and broadens as it crosses the debris blanket is clearly apparent southeast of ground zero. Outside the debris blanket the ubiquitous patch reefs appear as conical mounds. In contrast to these features, the crater floor and crater walls out to a distance of about 260 m (850 ft) from the geometric center of the crater show few targets or reflectors.

The airbrush-enhanced version of the sidescan-sonar data (fig. 5*A*) was also set up with lighting from the southeast. Light areas thus represent, for the most part, surfaces that slope toward the viewer, and dark areas represent surfaces that slope away from the viewer. Intermediate between the two are areas with relatively flat, smooth bottom.

The third step was the correction for aspect ratio. Because the speed of the ship varies, the along-track spatial resolution of pixels in the original data set also varies and does not match the across-track resolution. This discrepancy gives the effect of different vertical and horizontal scales, and the slant-range correction alone will not produce an undistorted image. The aspect-ratio correction was calculated using the navigation data associated with each scan line to compress or expand the along-track data, setting the output-image data to an aspect ratio of 1.0, so that along-track and across-track scales were equal.

After noise, slant-range, and aspect-ratio corrections, the resultant data were interactively examined to determine the digital stretches necessary to make images of overlapping strips appear to be taken under the same electronic "lighting" conditions. These stretch values were then employed by the electronic photowrite device to make film transparencies of each sonar strip at the appropriate scale for preparation of airbrush maps.

Airbrush maps of the digitally processed data were constructed at Flagstaff, Ariz. The maps were created by overlaying the film transparencies of the digitally processed data and the navigation track lines and the 1-m contour bathymetric map, and reproducing the locations and shadings of features shown on the digitally processed data strips as a single mosaic having a constant lighting direction. To construct the airbrush maps, the relief shading of the grander features of the areas, the craters and the reef or reef plate, was derived from the bathymetric contours as well as from the sidescan-sonar images. The true position of individual features, such as the patch reefs around OAK crater, were taken from the bathymetric maps because the position of echo-soundings below the transducer mounted in the ship's

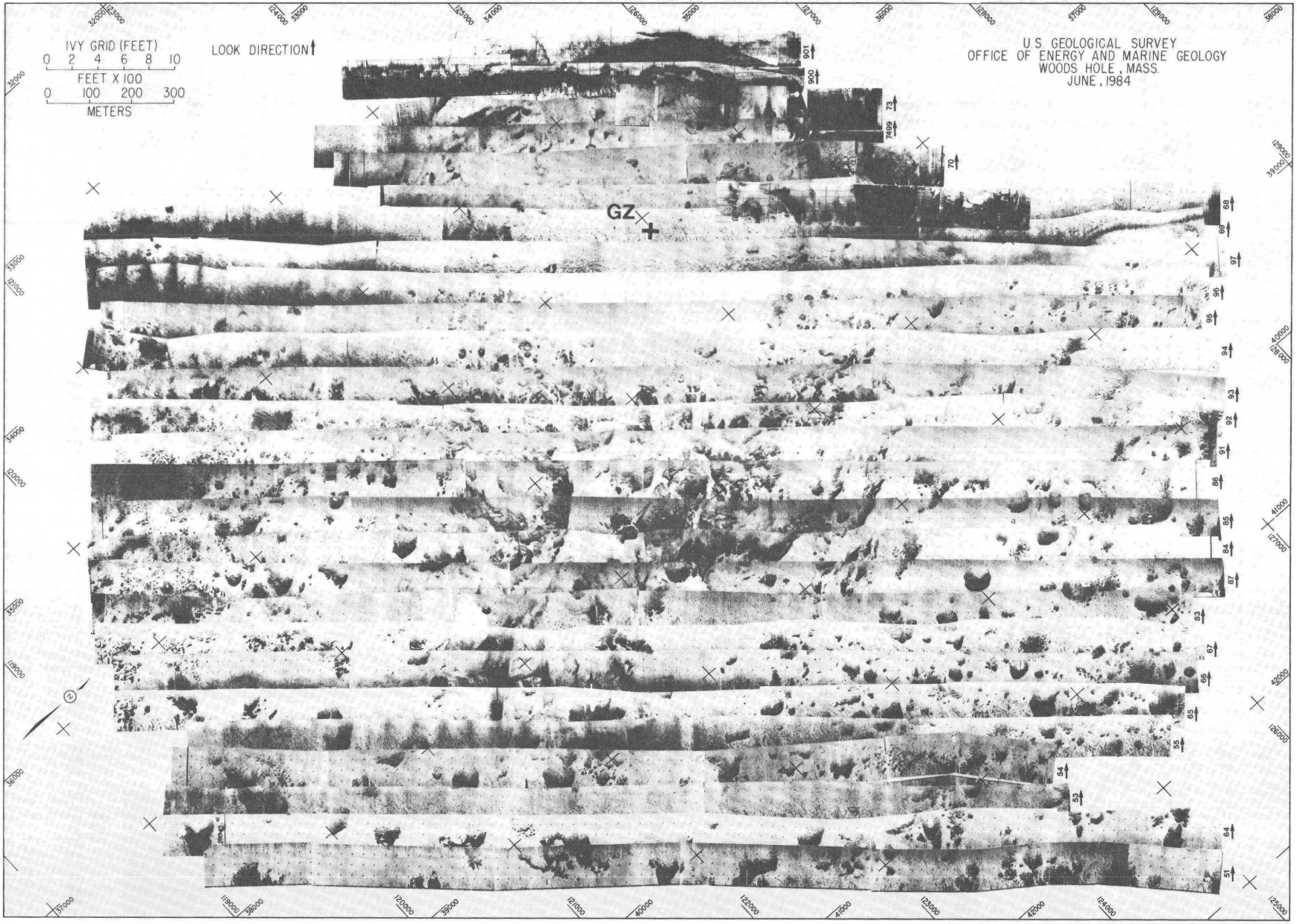

Figure 3*A*. Sidescan-sonar mosaic of OAK crater prepared from analog field records. GZ=ground zero.

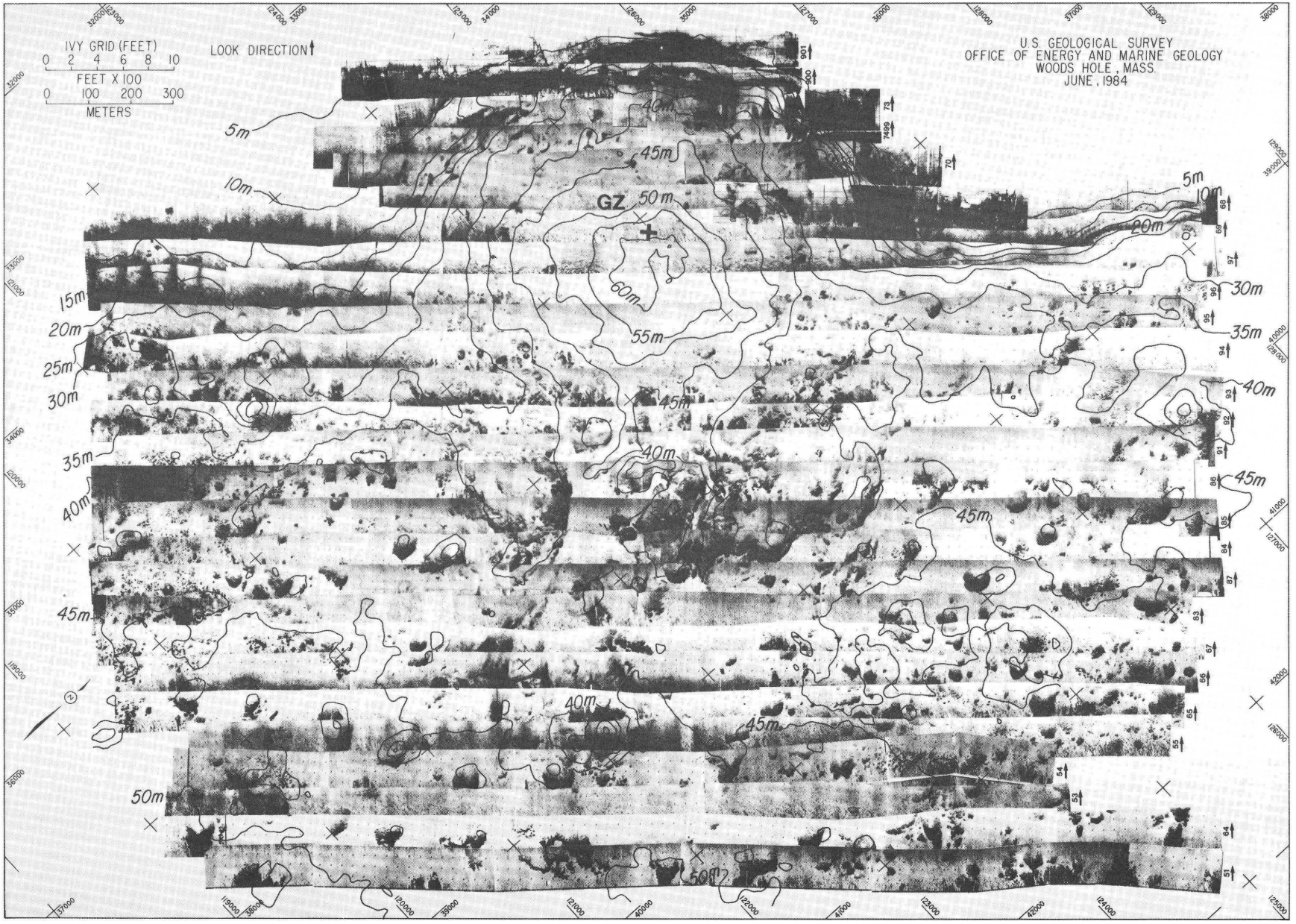

Figure 3*B*. Sidescan-sonar mosaic of OAK crater prepared with 5-m bathymetric overlay. GZ=ground zero.

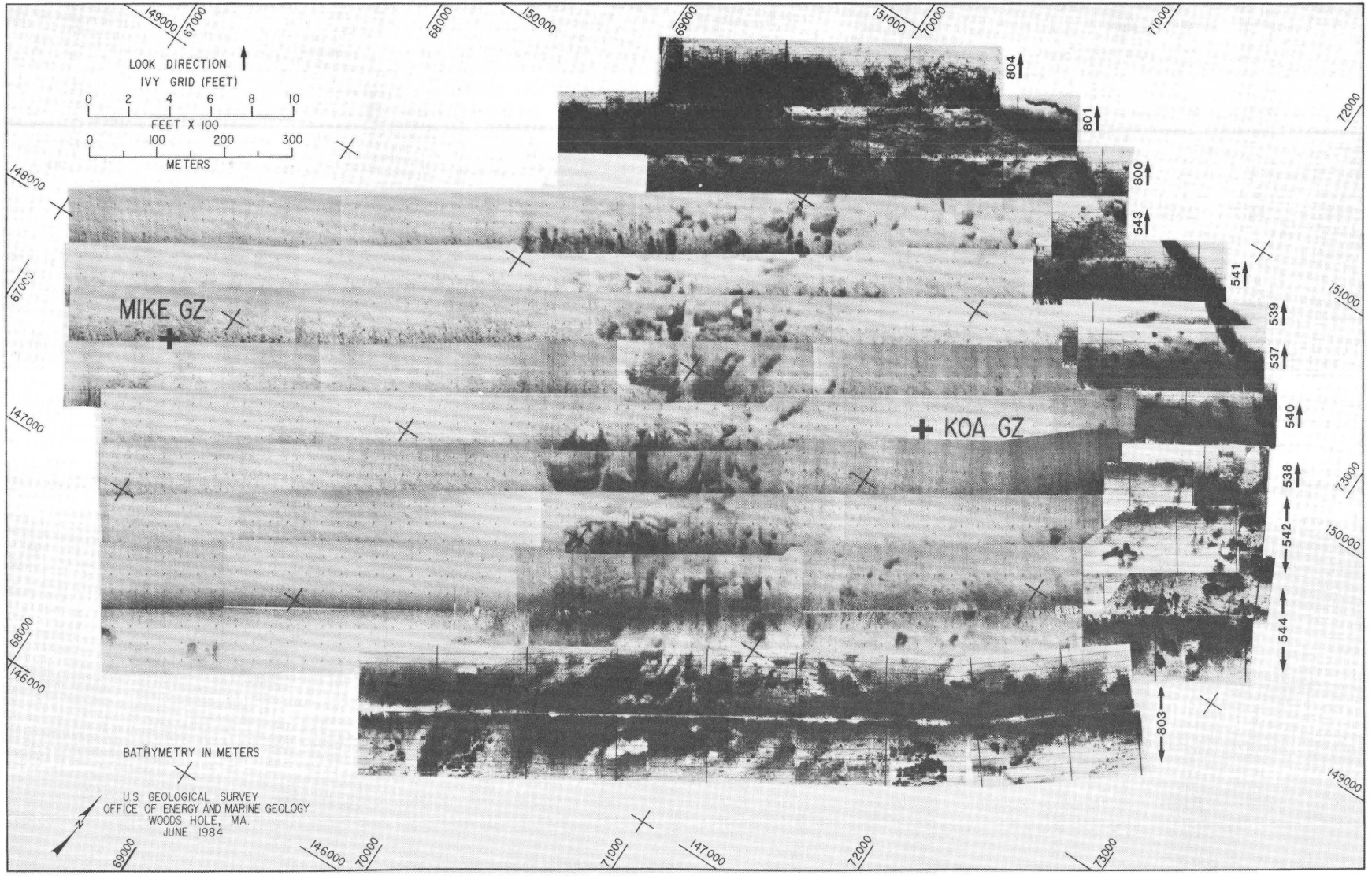

Figure 4*A*. Sidescan-sonar mosaics of KOA crater prepared from analog field records. GZ=ground zero.

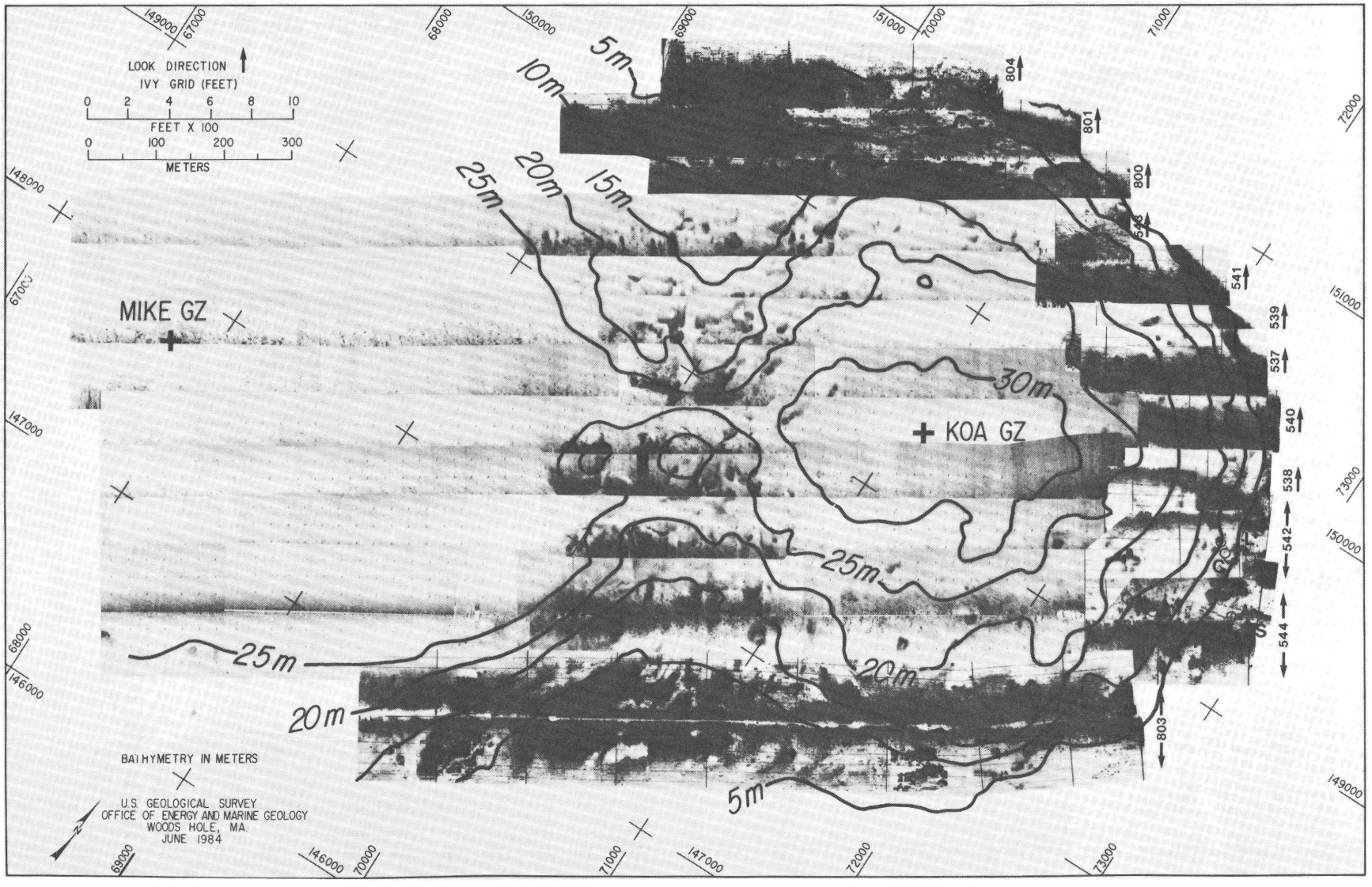

Figure 4*B*. Sidescan-sonar mosaic of KOA crater prepared with 5-m bathymetric overlay. GZ=ground zero.

hull was more closely controlled than were the sidescan-sonar data, which were taken from a submerged fish at the end of a variable-length cable. The locations of features on the airbrush maps are probably within about twice the specified navigational error, or within about 10 m (33 ft) of their true positions. The images were reviewed and modified for compatibility with sea-floor observations made from the submersible and by scuba divers. Thus the airbrush-enhanced images represent the most comprehensive integration of data in the report.

The excellent quality of these products will greatly enhance the interpretation of the other data sets. They come too late to modify figures in other chapters prepared for this report, but they should provide valuable input to future analyses of these and other craters.

We shall discuss the details of the airbrush-enhanced sidescan-sonar map of OAK in sequence from the crater floor outward, on the basis of the physiographic provinces defined by the bathymetry in chapter A of this volume. Those provinces include the crater floor, inner slope, inner terraces, outer slope, outer terraces, rim slope, rim scarp, debris blanket, and lagoon floor (fig. 5*C*). For purposes of this discussion, we have not altered the boundaries determined from the bathymetric map to fit the features depicted on the airbrush map except for the outer boundary of the debris blanket. Five-meter (16 ft) bathymetric contours have been overlain on the airbrush map for orientation (fig. 5*B*).

Crater Floor

Inside the boundary of the crater floor, the bottom appears to be flat and featureless (fig. 5*C*). The small rise near its center, shown by the bathymetry, apparently is of insufficient relief to be detected by the sidescan-sonar. The perimeter of the crater, drawn on the basis of the bathymetric change in slope, lies slightly inside the steepest slopes interpreted from the sidescan data.

Inner Slope

The steep sides of this province are clearly defined on the airbrush map, particularly near its inside perimeter, where they have greater sonar expression than near its outer perimeter (fig. 5*C*). Valleys incise the slope, particularly on the southern and eastern sides. About half of the valleys revealed here are coincident with valley thalwegs shown in figure 9 of chapter A (this volume). The eastern side of the crater's inner slope appears to be breached, as if debris had flowed in that direction, whereas the western side is complicated by what appear to be downdropped areas. These areas probably reflect variations in the style of mass-wasting from the lagoon side to the reef side of the crater.

Inner Terraces

This broad area is characterized mostly by smooth bottom in the northeast, northwest, and southwest quadrants of the crater (fig. 5*C*). In the southeast quadrant the bottom texture more closely resembles that of the debris blanket farther from ground zero. The airbrush map shows three channels that cut through the eastern side of this area. The westernmost channel is obvious on the bathymetry, but the other two are not as clearly defined. All three join into the main channel that cuts through many of the major provinces on the southeastern side of the crater. A large mass 310 m (1,017 ft) long and 150 m (490 ft) wide of what probably is mostly debris separates the main channel from its neighbor to the north. In the other three quadrants of the area, probable debris mounds are mostly no larger than 120 m (394 ft) long and 60 m (197 ft) wide.

Outer Slope

The outer slope has a distinctive texture on the sidescan data (fig. 5*C*) that is surprising, considering the subtle change in slope that defines it on the bathymetry. Only in a small part of the area east of ground zero is the bottom smooth. Elsewhere, radially subparallel linear to arcuate features crenulate most of the bottom. These are commonly 30 to 60 m (100–197 ft) long and are found around the southwest side of the outer slope. Similar but fewer features are present on the northeast and southeast sides. These features are probably the promontories discussed by Halley and others in chapter F (this volume) that give the slope a fluted appearance from the submersible. On the north side of the crater is an area about 140 m (450 ft) wide that appears to be incised by small, subradial ravines or gullies.

Outer Terraces

The outer terraces of the northern and western areas are characterized by a smooth bottom, like the inner terraces in those quadrants (fig. 5*C*). South of ground zero, however, the area is about 50 percent rougher, more like a debris surface, and contains several small, arcuate scarps up to 130 m (426 ft) long. In the northwest quadrant of the crater, the natural reef slope projects into the area of inner terraces about 375 m (1,230 ft) from ground zero, and no outer terraces region is present. The western area appears to be complex, having reverse slopes and narrow scarps. The boundary between the outer terraces and the rim slope is marked by a change from smooth to rough relief and is clear on the northeast flank of the crater but less clear on the southwest flank.

Rim Slope

The two areas of the rim slope east and west of ground zero are similar in texture, each showing about 50 to 70 percent smooth bottom. Both have scattered debris mounds, which are mostly less than 18 m (60 ft) in diameter (fig. 3*C*). However, in the southern part of the eastern area, a large debris or patch-reef complex about 100 m (330 ft) in diameter occupies most of the rim slope. A secondary crater

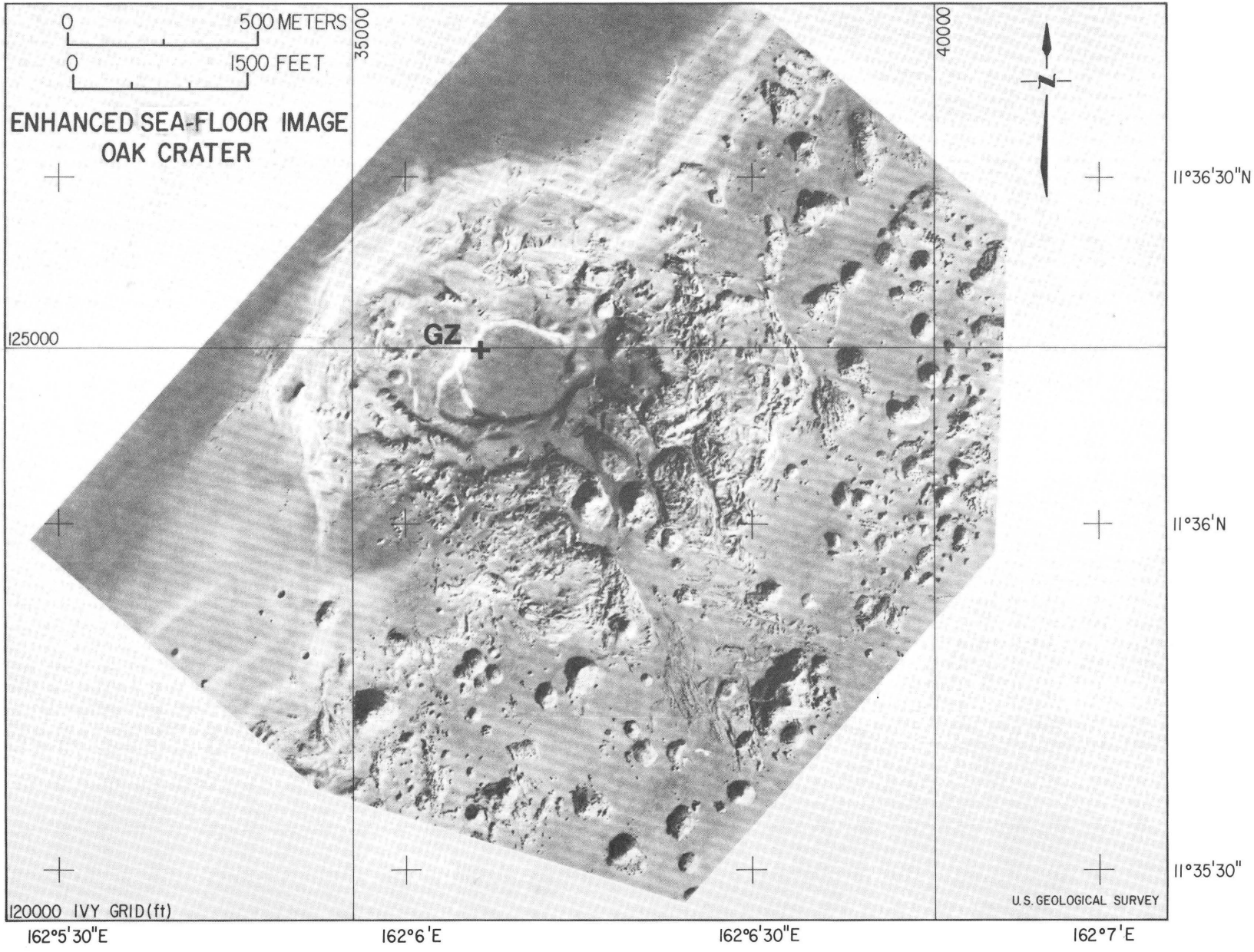

Figure 5A. Airbrush-enhanced image of OAK crater based on sidescan-sonar, bathymetry, and sea-floor observations. GZ=ground zero.

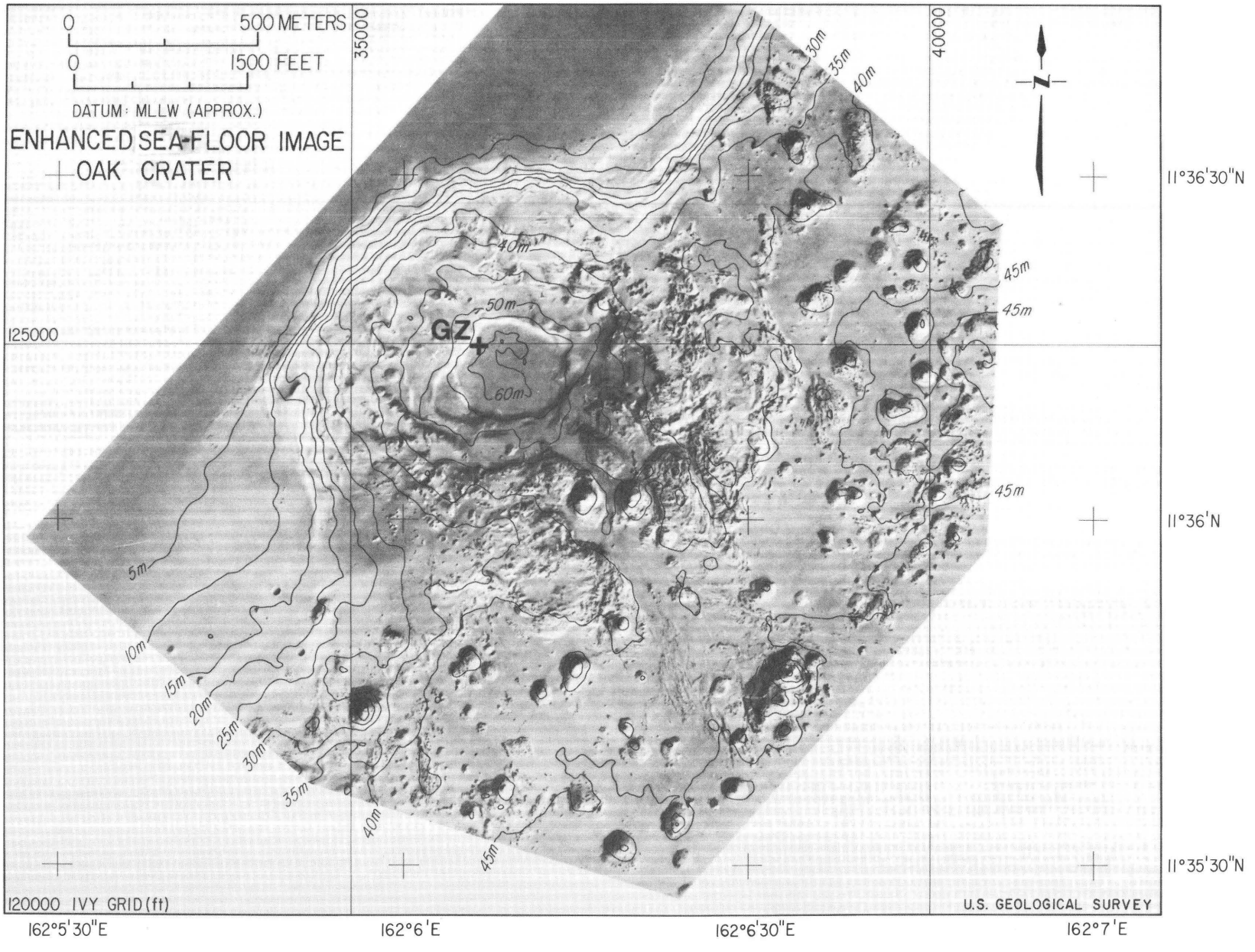

Figure 5*B*. Airbrush-enhanced image of OAK crater prepared with a 5-m bathymetric overlay. GZ=ground zero.

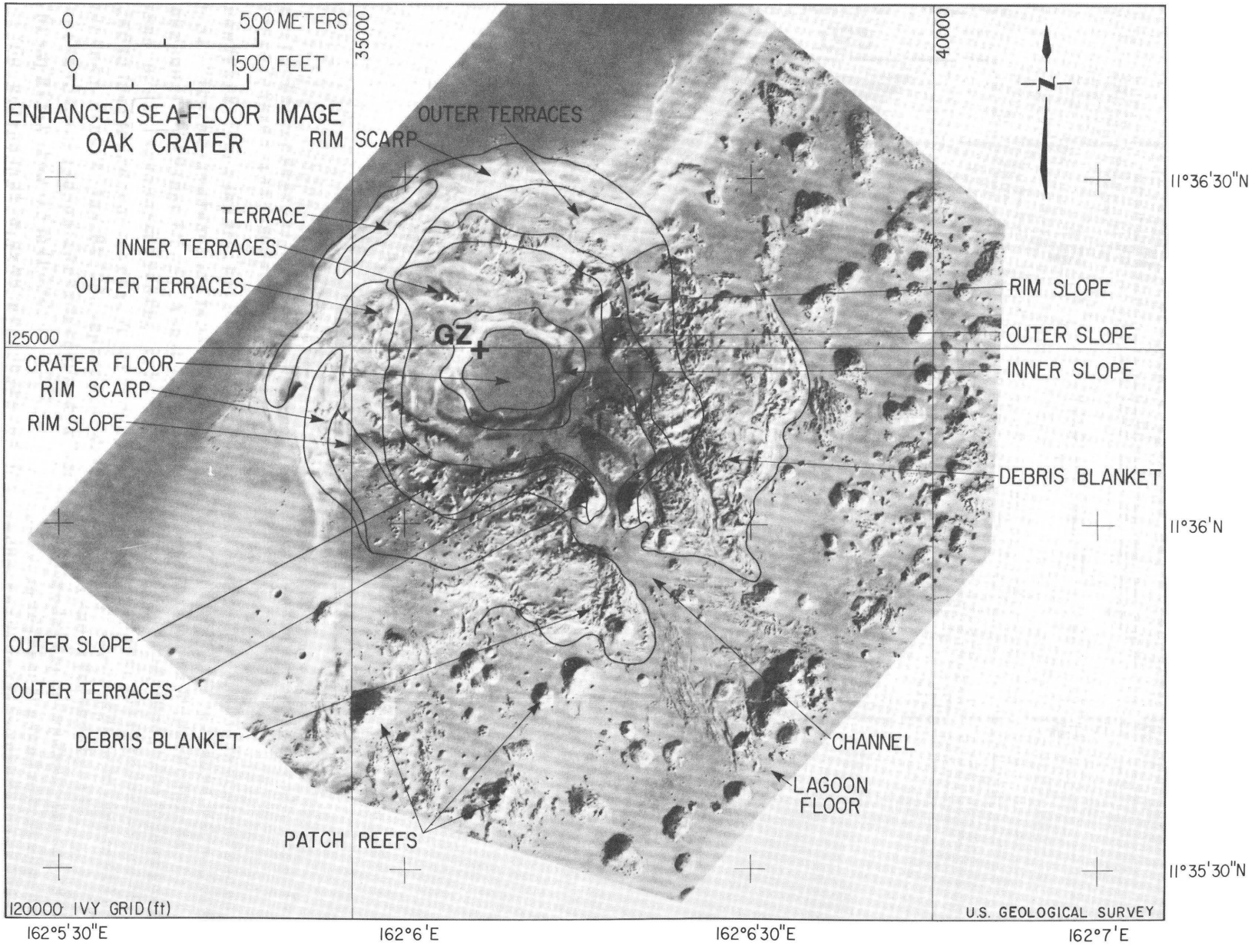

Figure 5C. Airbrush-enhanced image of OAK crater including a province map overlay derived mostly from bathymetric data. GZ=ground zero.

about 20 m (65 ft) in diameter lies almost due south of ground zero.

Rim Scarp

The high reflectivity of the rim scarp clearly depicts the area of steepest slopes in the crater (fig. 5*C*). Alternating light and dark bands, commonly only 6 to 8 m (20–25 ft) wide, mark the scarps and terraces observed by submersible and by scuba divers. These smaller scarps and terraces contrast with the areas where major terraces, as large as 60 m (200 ft) by 375 m (1,230 ft), break the scarp into steps west and northwest of ground zero.

The uppermost scarp west of ground zero shows about 40 small reflectors, less than 3 m (10 ft) in diameter, which may be pieces of reef plate that have slumped into the crater.

Debris Blanket

The debris blanket is made up mainly of two arcuate ridges rimming the lagoonward side of the crater. These compose a broad debris complex that is more extensive to the northeast than to the southwest and is divided by the broad, flat-floored channel southeast of ground zero (fig. 5*C*).

The boundaries of the debris blanket visible on the airbrush map coincide well with those we could define using the bathymetric map, except at the blanket's southern extremity. There, according to the interpretation of the sidescan data, the rough bottom typical of most of the debris blanket terminates as much as 250 m (820 ft) closer to ground zero than we drew it on the basis of bathymetry. Figure 5*C* shows the boundary that conforms with the airbrush-map interpretation.

Farther to the southeast, about 1,150 m (3,770 ft) from ground zero, sea bottom having a similar texture to the debris blanket covers an isolated area 325 m (1,070 ft) long and 250 m (820 ft) wide. This area may be a mass of debris that swept through the main channel to be slowed down or stopped by several patch reefs, which it now mantles or abuts.

Lagoon Floor

The predominantly smooth lagoon floor within the study area is dotted by about 75 patch reefs (fig. 5*C*). The diameter of the reefs varies greatly from 10 to 20 m (33–65 ft) to greater than 100 m (330 ft). The fine-textured bottom of the lagoon floor also comprises some complexes of mounds similar to those in the debris blanket that may consist of debris from the crater.

Farther than about 800 m (2,600 ft) southeast of ground zero, the channel separates into two legs that extend to either side of the large mass of debris noted above. There, the channel floor is lineated with what appear to be erosional furrows and grooves. Because the subbottom profiles show the lagoon floor there to be underlain by chaotic reflectors, those features do not appear to represent truncations of horizontal bedding.

Two circular depressions, which appear to be secondary craters about 25 m (83 ft) in diameter, lie about 900 m (3,000 ft) southwest of ground zero, on probable reef plate.

KOA Crater

Because KOA crater was blown out of an island, land or reef plate makes up much of its perimeter. Debris accumulations, similar to those at OAK, lie in shallow water or on land where they cannot be seen; therefore the sidescan-sonar mosaic only portrays the central part of the crater complex.

The same kind of strong echoes associated with the scarps that are present along the reef side of OAK extend around the north, east, and south sides of KOA (fig. 4). On its southwest side KOA crater adjoins MIKE in an area of complex topography where a third test, HURON, was conducted in 1956 (Circeo and Nordyke, 1964; chap. A, fig. 17, this volume).

In KOA only a few, small (less than 40 m, or 131 ft, in diameter) targets were recorded on the analog records deeper than the 25-m (82 ft) isobath (fig. 4). This is probably due in part to sediment infilling of the crater center but also in part to the height off-bottom of the *Egabrag*-towed transponder. Targets are more common on the analog records especially to the southwest in the hummocky area between MIKE and KOA. There, however, even the two large conical mounds, which are so apparent on the bathymetric map, are not well defined.

Targets are abundant in water shallower than 20 m (66 ft). The increased frequency of targets is, in part, a result of having the transponder towed closer to the bottom from the MIKE boat, but it is also due to the presence of small scarps and debris from the main scarp that surrounds much of the crater between the 5- and 20-m (16- and 66-ft) isobaths.

In the northeast quadrant, the upper edge of the main scarp is well defined near the 5-m (16 ft) isobath. In the southeast quadrant, however, targets are complex and, except for a few segments, show little coherence. The airbrush-enhanced image was modified little with input from submersible and scuba observations in the deep areas of the crater because underwater visibility there was so limited. However, around the margins of the crater, seafloor observations were useful in identifying and defining some targets in detail, particularly the manmade structures. As for OAK, the airbrush-enhanced image for KOA (fig. 6*A*) was set up with lighting from the southeast.

We shall discuss the features portrayed on the airbrush map in sequence from the crater floor outward, on the basis of physiographic provinces defined by the bathymetry in chapter A, figure 18, of this volume. These provinces include the crater floor, inner slope, terraces, rim scarp, debris mounds, and channel. None of the province

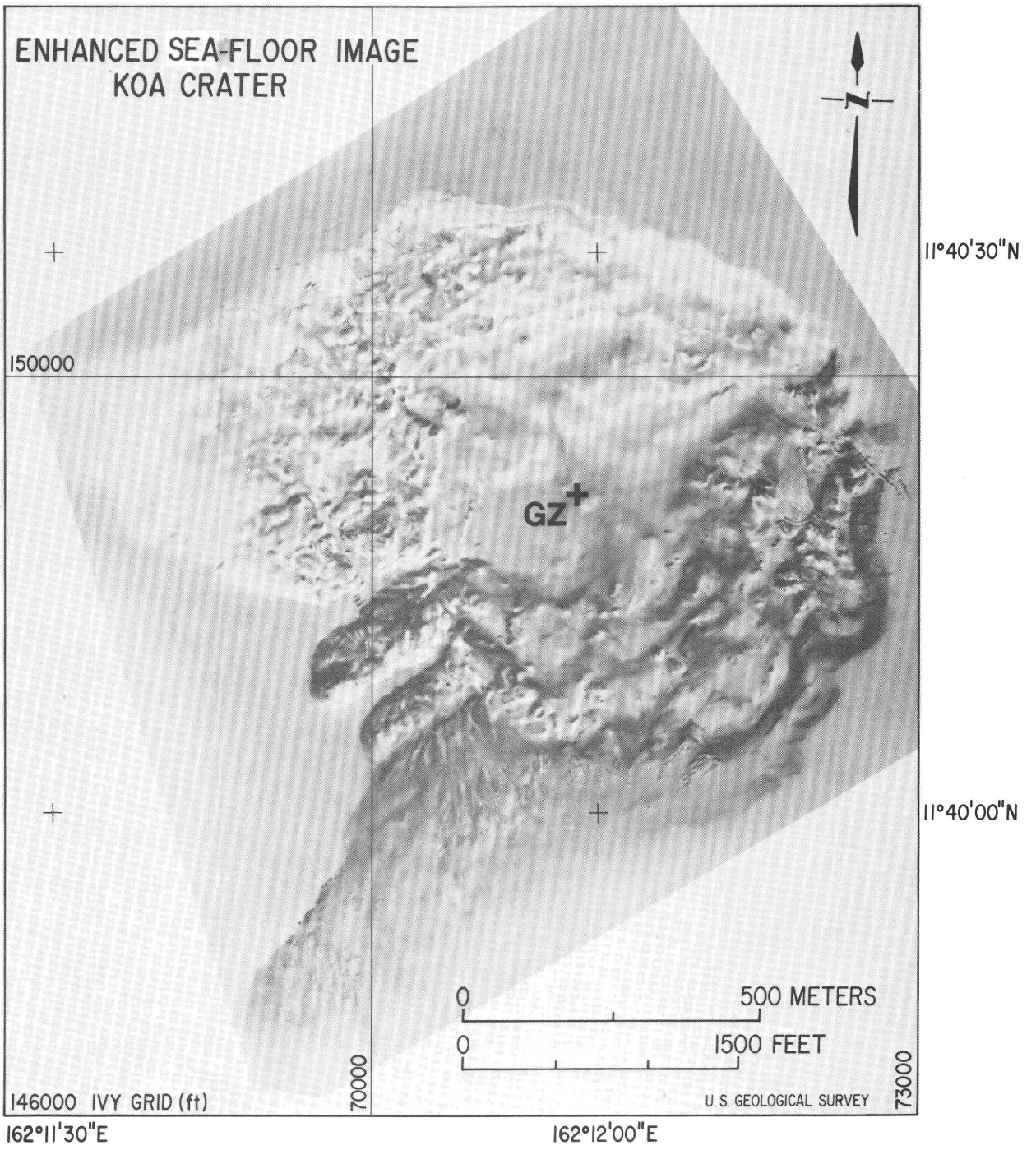

Figure 6A. Airbrush-enhanced image of KOA crater based on sidescan-sonar, bathymetry, and sea-floor observations. GZ=ground zero.

boundaries in KOA crater have been altered for this discussion of the sidescan data, but the boundaries of the rim scarp and of the debris mounds have been modified slightly on the eastern margin of MIKE crater (fig. 6*C*). We show the airbrush map with a 5-m bathymetric-contour overlay for orientation and have labeled some of the target-echoes from manmade structures on the eastern margin of the crater (fig. 6*B*).

Crater Floor

The crater floor is smooth and subdued, doubtless owing in part to the influx of material continually being swept from the reef by the trade winds. The smoothest, most featureless area appears to be southwest of ground zero, suggesting that some material may be flowing from the

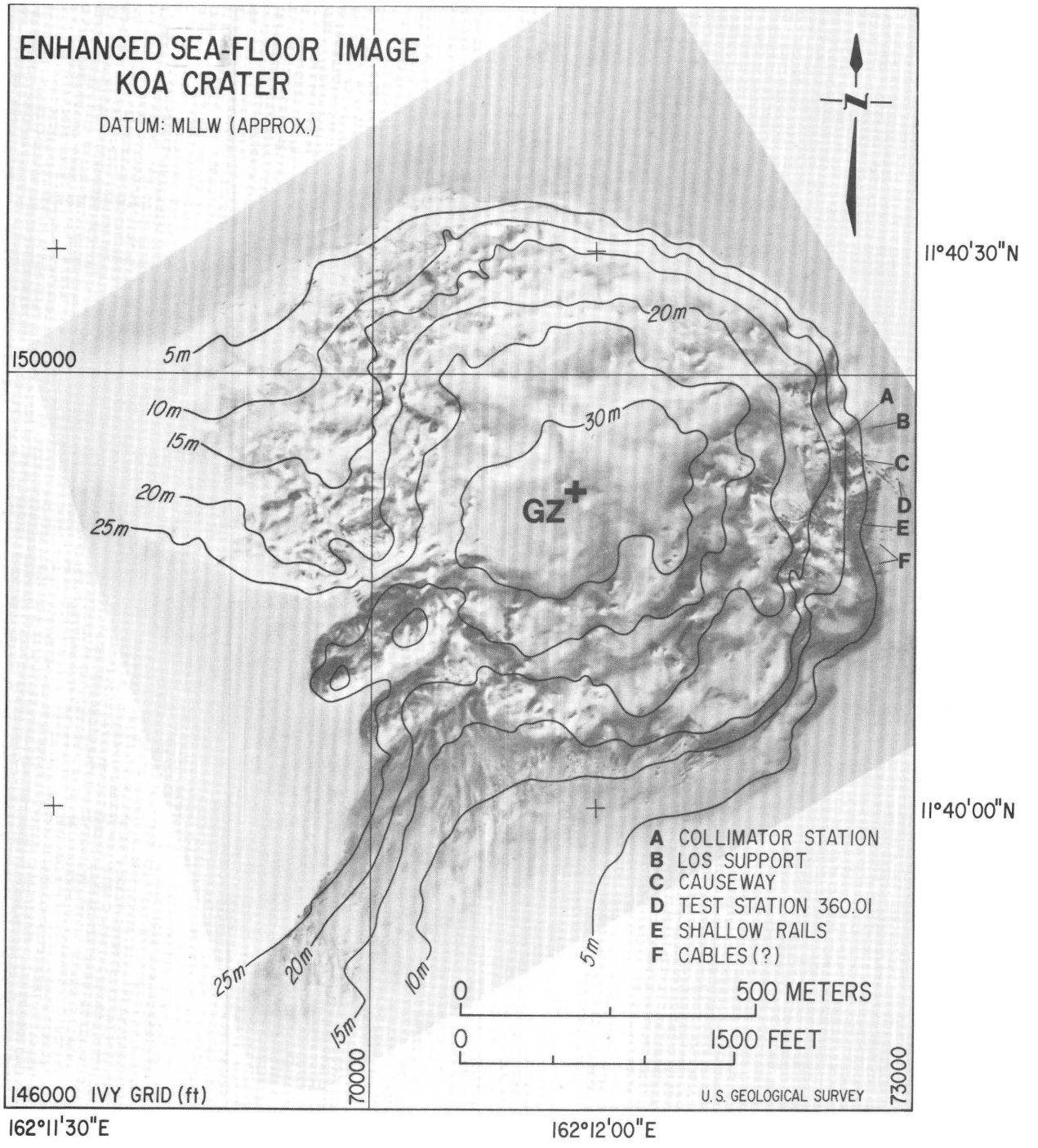

Figure 6*B*. Airbrush-enhanced image of KOA crater prepared with a 5-m bathymetric overlay and showing manmade structures. GZ=ground zero. LOS=line of sight.

shallower floor of MIKE crater into KOA through the narrow channel that connects them (fig. 6*C*).

Southeast and northwest of ground zero, the bottom relief is more variable. To the southeast this variability is apparently due to the toe of a slump which can be traced up the crater side to the south-southeast across the inner slope and terraces. Three possible blocks of debris about 10 m (30 ft) in diameter that may have been derived from the slump protrude above the crater floor in this area. To the northeast a small channel, which may be another conduit for the influx of detritus, debouches onto the crater floor. Relief is more subdued to the northeast than near ground zero and appears to be part of a sediment cone or slump associated with a scarp that cuts across the inner slope and terraces and

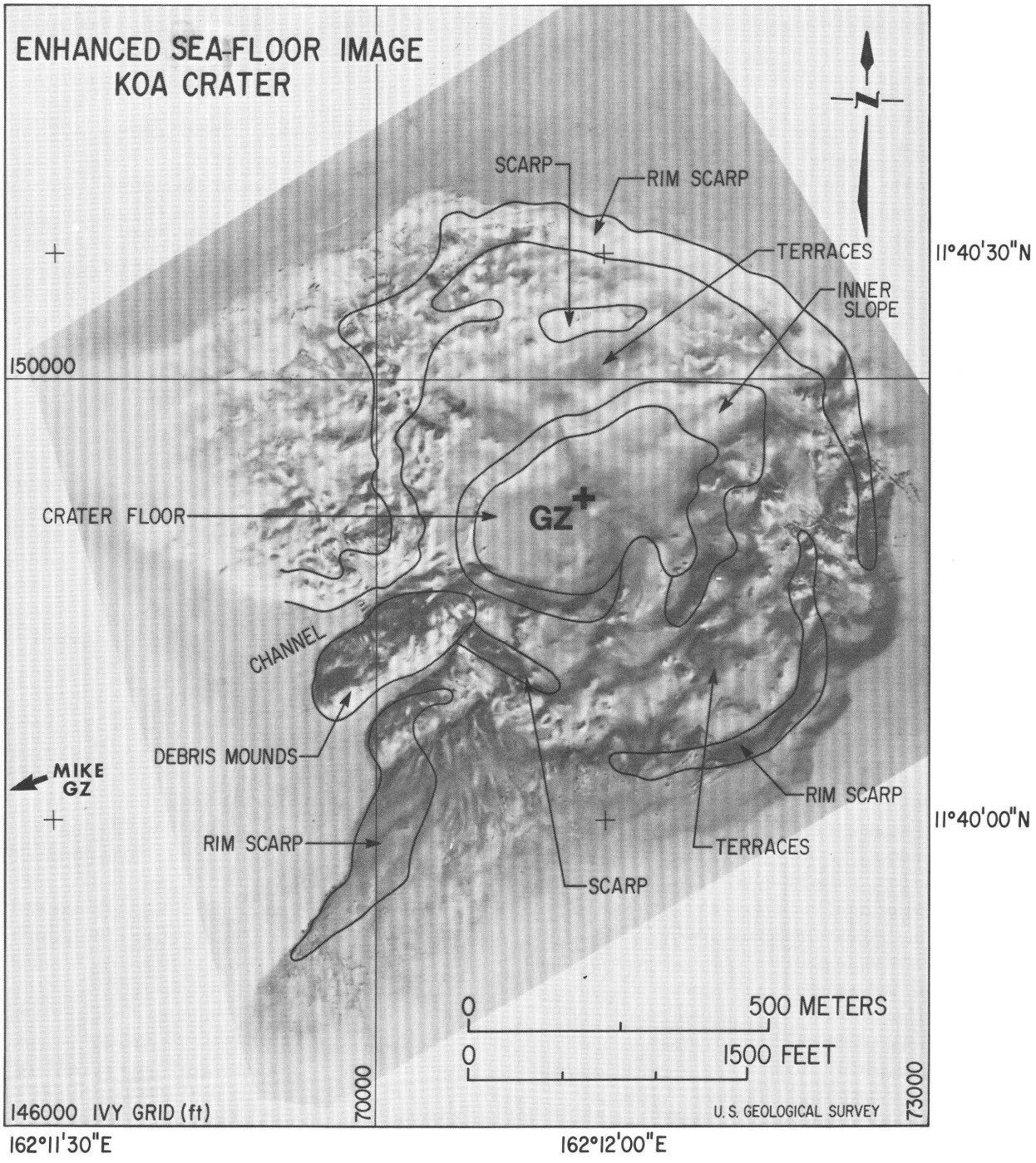

Figure 6*C*. Airbrush-enhanced image of KOA crater including a province map overlay derived mostly from bathymetric data. GZ=ground zero.

joins with the scarp that forms the northwest inner slope. We might have drawn the perimeter of the crater floor farther to the northeast, along the base of that scarp, if it had shown better bathymetric expression.

Inner Slope

The province is clearly distinguishable on the sidescan images, and its boundaries correlate closely with those of the area as bathymetrically defined (fig. 6*C*). Only along the northwest side does the airbrush map show a steeper slope extending closer to ground zero. As noted above, the sidescan data suggest that the lower boundary could have been extended farther to the northeast than it was, on the basis of bathymetry. Northwest of ground zero, the inner slope shows low relief except for a small channel. East of ground zero, bathymetry is more complicated where slumping apparently has taken place. Southeast of ground zero,

the province is apparently broken by a slide that impinges on the crater floor and obscures the slope. To the southwest, the province could be broken again by the narrow channel that connects the floor of KOA and MIKE, but the character of that channel, both on sidescan and bathymetry, is not distinctive close to the crater floor.

Terraces

The hummocky, complex nature of this large area is clearly apparent on the airbrush sidescan image (fig. 6*C*). West and northwest of ground zero, the inner half of the province is relatively smooth, having only a few, low-relief channels and mounds. The outer half is much rougher with numerous scarps and hills. These two areas of contrasting texture could be separated perhaps into inner and outer terraces by an outer slope as is the case in OAK. The large scarp which has been outlined due north of ground zero could be included within an outer slope province, but the continuity of such a province is not as clear as it is for OAK. East of that large scarp the relief smoothes out somewhat where the area of the terraces is narrower and marked only by sinuous features 30 to 60 m (100–200 ft) long. To the northeast are indications of possible grooves and furrows that trend northwest. East of ground zero, where the rim scarp is broken or separated, are two hummocky ridges oriented northwest, separated by a 10-m-wide (30-ft-wide) channel. The physiography of this area is apparently complicated by mass movement of sediment. Southeast of ground zero are broad terraces about 60 m (200 ft) wide. Superimposed on them are widely scattered mounds most often less than 15 m (50 ft) in diameter.

The shallow boundary of the province southwest of ground zero is not clear probably because the rim scarp either didn't develop or because it has been obscured by sediment. A significant scarp projects in a southeast direction from the mounds into the terraces; it may be part of the rim scarp.

Rim Scarp

West and northwest of ground zero, the bathymetry of the rim scarp is complex and comprises many hills and mounds that range from 3 to 40 m (10–130 ft) in diameter. To the north are three narrow (10 m, or 30 ft) scarps that make up the main scarp; east of them, details are lost in an area of high reflectivity. East of ground zero, the rim scarp appears to be offset by faulting or slumping. The sidescan data reveal that hummocky masses extend for almost 150 m (500 ft) south of the offset area. This hummocky area is probably made up of slump blocks that moved toward ground zero into deeper water. Whether or not it should be included as the rim scarp is open to question. The dark shadow of a scarp lies along the crater margin in a fishhook shape, but the slope there is much less than within adjoining segments which have been included within the rim scarp province (fig. 6*C*). Southwest of the offset, the southern section of the scarp is coherent for about 330 m (1,000 ft). Then it breaks up into about three noses and reentrants and loses its identity south of ground zero. The rim scarp based on bathymetry was continued around the southeastern margin of MIKE, but that picture doesn't fit the airbrush interpretation well (fig. 6*C*). To the east of MIKE, the adjacent flank of the large submarine ridge, which separates the craters from the lagoon, is characterized by northwest-trending furrows and ridges having a wavelength of about 15 m (50 ft).

Debris Mounds

The airbrush image of the debris mounds between KOA and MIKE craters does not portray the mounds as clearly as they are defined by the bathymetric contours (fig. 6*C*; see also chap. A, fig. 18, this volume). The southwestern hill, which projects into MIKE crater, is better defined than the northeastern hill, which appears to be made up of a complex of smaller mounds. The mounds are flanked on the northwest and southeast sides by two channels. The southwestern hill terminates against a scarp on the southwest side of KOA crater, whereas the one on the northwest side connects the crater floors of KOA and MIKE.

Channel

The flat floor of the channel northwest of the mounds is well depicted on the airbrush image, narrowing from about 50 m (165 ft) wide in MIKE to only about 10 m (30 ft) wide where it enters KOA (fig. 6*C*). A smaller tributary channel joins the larger channel at a right angle from the northwest and cuts through complex hummocky terrain that probably consists mostly of debris.

Manmade Structures

The digitally processed sidescan data clearly show echoes from several of the structures that were discovered by the submersible and the scuba divers along the eastern margin of KOA. These are identified in figure 6*B*. The clearest targets are the vertically emplaced railroad rails that retained the causeway leading to the collimator station. (See chap. H, figs. 33–36, this volume.) Though the rails on the northeastern side of the causeway were best documented by the scuba divers, enough material apparently was left on the southwestern side to produce sonar echoes. Thus the sidescan-sonar imagery appears to portray much of the causeway. Similarly, parts of the concrete base of the collimator station itself seem to be outlined (fig. 6*B*; see also chap. H, figs. 33, 36, this volume). A line-of-sight tube support is visible in shallow water (fig. 6*B*; see also chap. H, fig. 33, this volume) as are various parts of the concrete test station 360.01 (fig. 6*B*; see also chap. H, figs. 29–33, this volume). To the south, the railroad rails in about 6 m (20 ft) of water are well depicted (shallow rails in

figs. 6*B*; see also chap. H, fig. 33, this volume), but the rails in deeper water apparently are at least partly obscured by other echoes (chap. H, figs. 33, 38, this volume), some of which may be due to the abundant coral thickets surrounding them. In the same area two linear features trend roughly toward ground zero (fig. 6*B*); these features may be cables that were observed by the scuba divers but were not surveyed precisely. Several echoes similar to those derived from the rails appear in other areas on the airbrush image. Additional scuba observations must be carried out to identify them.

CONCLUSIONS

The airbrush-enhanced images based on sidescan-sonar surveys, bathymetry, and sea-floor observations have provided a comprehensive view of the physiography of the two submarine craters that could not have been obtained by any other combination of techniques.

In OAK crater, for instance, bottom texture, visible on the sidescan imagery, clearly depicts the spatial distribution of the debris blanket. Similarly, the detailed characteristics of the main channel southeast of ground zero that cuts through the crater side provides important evidence that the significant amount of material was transported from the excavation to the adjacent lagoon floor. The clear portrayal of the distribution of scarps, not only where they are most common on the reefward side of the crater but within the inner and outer terraces, will provide good evidence for the mechanisms responsible for late-stage deformation of the crater.

In KOA, the airbrush-enhanced image presents a good picture of the distribution of slumped debris especially in the southeast quadrant. It also suggests that the offset of the rim scarp east of ground zero may be a complex of slump blocks rather than a more simple offset as interpreted from the bathymetry alone. Finally, the image provides a comprehensive view of some of the important manmade structures that were surveyed by submersible and by scuba divers and indicates the locations of other objects, not identified, that might be equally useful in determining the absolute sense and magnitude of ground displacement during and following the KOA event.

REFERENCES

Ballard, R. D., Hekinian, Roger, Francheteau, Jean, 1984, Geological setting of hydrothermal activity at 12 degrees 50′ North on the East Pacific Rise: a submersible study: Earth and Planetary Science Letters, v. 69, p. 176–186.

Circeo, L. J., and Nordyke, M. D., 1964, Nuclear cratering experience at the Pacific proving grounds: Livermore, University of California, Lawrence Radiation Laboratory, TID–4500, UC–35, (UCRL)-12172, 88 p.

Tremba, E. L. Couch, R. F., and Ristvet, B. L., 1982, Enewetak Atoll Seismic Investigation (EASI): Phases I and II (final report): Air Force Weapons Laboratory Technical Report TR–82–20, Kirtland Air Force Base, New Mexico 87117, 124 p.

Chapter C

Single-Channel Seismic Survey of OAK and KOA Craters

By J. M. ROBB, D. S. FOSTER, D. W. FOLGER,
J. C. HAMPSON, and R. A. WOELLNER

U.S. GEOLOGICAL SURVEY BULLETIN 1678

SEA-FLOOR OBSERVATIONS AND SUBBOTTOM SEISMIC CHARACTERISTICS OF OAK AND KOA CRATERS, ENEWETAK ATOLL, MARSHALL ISLANDS

CONTENTS

FIGURES

Chapter C
Single-Channel Seismic Survey of OAK and KOA Craters

By J. M. Robb, D. S. Foster, D. W. Folger, J. C. Hampson, *and* R. A. Woellner[1]

INTRODUCTION

Purpose

In and around the craters, the upper 30 m (100 ft) of sediment includes a complex of debris distorted by folds, faults, and slumps. Distinguishing the debris from naturally deposited sediment and delineating the stratigraphy and geometry of both components is essential to understanding the cratering mechanics of the Enewetak nuclear events. For this purpose, we used a Huntec Hydrosonde Deep-Towed Seismic System.

Previous Work

Previous attempts to acquire useful shallow subbottom seismic profiles of OAK and KOA craters apparently were not successful. A 3.5-kHz high-resolution single-channel seismic system was used during Project EXPOE (Exploratory Program on Enewetak), but Ristvet and others (1978) included no profiles in their report. Subsequently, a 3.5-kHz EDO-Western Model-315 subbottom profiler with 8 kW of power output was used during Project EASI (Enewetak Atoll Seismic Investigations). No profiles of these data were presented by Tremba and others (1982), although some illustrations of the profiles were included in a classified report (E. Tremba, oral commun., July 1985).

METHODS

The Huntec Hydrosonde DTS (Deep-Towed-Seismic) profiling system (fig. 1) produces a 500-Hz to 6-kHz wide-band acoustic signal by using an air-backed, depth-corrected, impulse-driven piston as a sound source. A 10-element hydrophone having a 3-m (10 ft) aperture is towed about 2 m (6.5 ft) behind the sound source; both are towed at depth on a 545-kg (1,200 lb) fish. The signal insonifies an area of the bottom within about a 60° cone below the fish. Towing both the source and receiver close to the bottom achieves a better signal-to-noise ratio and horizontal resolution than conventional surface-towed profiling systems. The transducers for the Klein 100-kHz sidescan-sonar system are mounted on the same fish. The two systems can operate simultaneously, although we operated them independently for the most part to eliminate crosstalk and because the optimum tow depths in the crater areas for the two systems were not the same.

During operations, the Huntec fish was lowered over the stern A-frame of *Egabrag II* (fig. 1). Its depth was continuously monitored from a digital readout of a pressure sensor on the fish and from the incoming paper record and was controlled by the winch operator to avoid coral heads and patch reefs.

The high-resolution seismic survey was carried out on the first leg of *Egabrag II* operations during June and July in 1984. Rain and clouds often reduced the visibility of underwater hazards, resulting in the shortening or elimination of some desirable nearshore profiles. Low visibility was less of a problem during subsequent legs when weather was better and the crew more familiar with the area. However, most of the time the wind was light and seas low, providing ideal conditions for towing the fish at slow speeds (150–200 cm/s, or 3–4 kn).

The Huntec boomer was fired at half-second intervals, corresponding to about 1 m (3 ft) of advance at the usual 200-cm/s (4 kn) speed. Data were electronically corrected for fish depth and for heave, filtered between 1,000 and 2,500 Hz, and recorded on an EPC 3200 recorder at a 0.125-s sweep and on 1/2-inch analog magnetic tape.

Interpretation Procedure

The towed submarine source-receiver configuration of the Huntec system, while effective in acquiring shallow subbottom data, produced a complex pattern of water-surface and water-bottom multiples (figs. 2, 3). The sequence of signals includes a direct echo from the water surface, a direct echo from the bottom surface, subbottom reflections, then a second bottom and subbottom sequence from the sound wave that had first echoed from the water surface. These signals were followed by the more usually encountered water-surface and bottom-surface multiples. In most places, the second arrival (the pulse that had first reflected from the water surface) obscured deeper subbottom data.

Subbottom profiles were interpreted by tracing reflectors on overlays that had been prepared using bathymetry from the echo-sounding data. The bottom profile was matched on the two data sets. This procedure corrected the single-channel data to the navigational reference point under

[1]All authors are with the U.S. Geological Survey, Branch of Atlantic Marine Geology, Woods Hole, Mass. 02543.

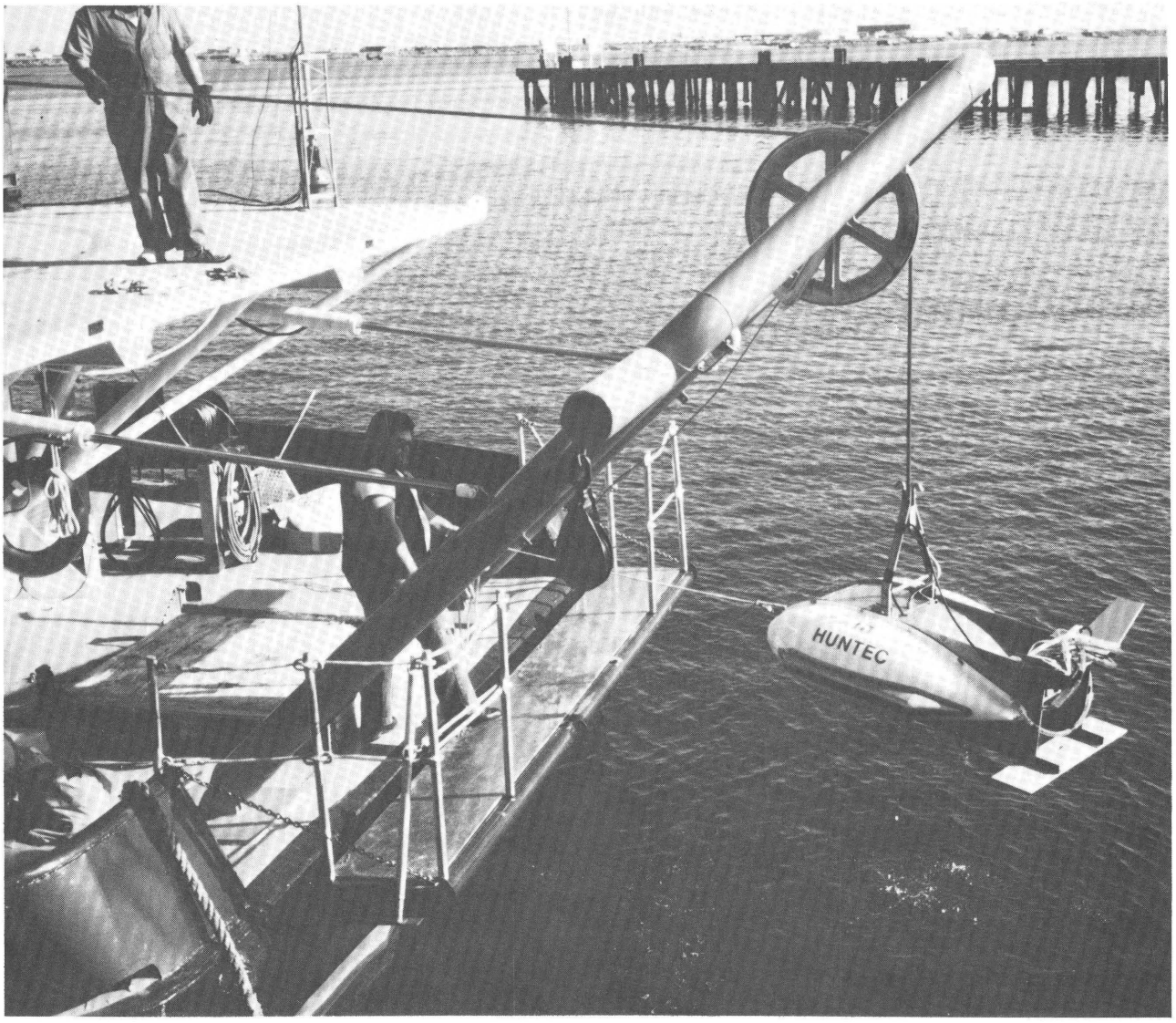

Figure 1. Huntec towfish suspended from stern A-frame aboard MS *Egabrag II*. San Diego harbor is in background.

the echo-sounder and eliminated any water-depth discrepancies between the two systems due to minor differences in datum or artifacts of the electronic adjustments that were made to compensate for changes in Huntec fish depth. Multiples were identified first and marked on the overlays to avoid confusion with subbottom reflections.

We correlated reflectors from line to line by direct comparison of depths and sediment thicknesses at line crossings, and we closed correlation traverses to ensure consistent interpretations. We digitized reflectors for machine plotting using an automated digitizing table. For plots of depths and sediment thicknesses, sound velocity was taken as 1,542 m/s (5,060 ft/s) in seawater and as 1,650 m/s (5,413 ft/s) in the shallow subbottom sediments.

RESULTS AND DISCUSSION

Grids of single-channel profiles were acquired in both craters and on long tie lines between OAK and KOA crater areas and Enjebi (Janet) island (fig. 4).

At KOA crater, because of the enclosing reef and limited maneuvering room, data were only acquired along eight lines, 75 m (250 ft) apart, parallel to the axis between KOA and MIKE craters, and along two radial lines through KOA ground zero on other azimuths (fig. 5). Copies of the data are illustrated in figures 6*A*–*F*.

At OAK crater, we acquired data along 25 lines parallel to the reef (strike lines), spaced 75 m (250 ft) apart; along 7 lines perpendicular to the reef (dip lines), spaced 305 to

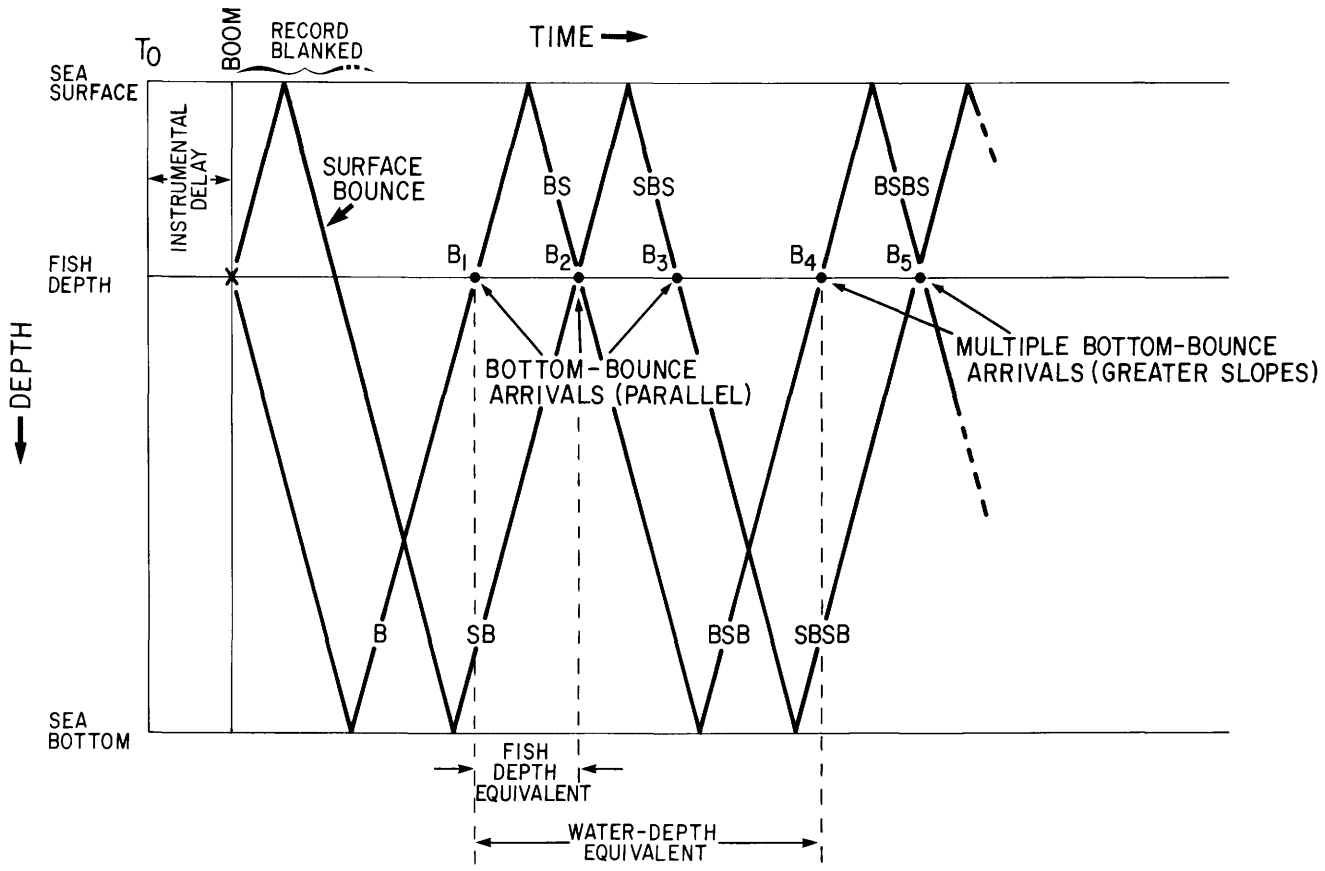

Figure 2. Huntec mid-water boomer: ray path with time. Diagram explains the sequence of reflections that are received from the sea floor and water surface by using a midwater-towed sound source and hydrophone. The profiles have three parallel traces (B1, B2, B3) and subsequent multiples (B4, B5, and so on) that result from the illustrated ray paths. B2, which arrives simultaneously from two paths, commonly appears strongest and obscures subbottom reflectors of the B1 path. B3 is usually weak. B4 and B5 are conventional multiples and show greater slopes than the first arrivals. B=bottom reflecton; S=surface reflection.

366 m (1,000–1,200 ft) apart; and on two lines through ground zero that lie at about 45° to the other two sets (fig. 7). These profiles are shown in figures 8*A*–*HH*, in sequence from reef to lagoon so that structure from line to line can be compared. Each profile is shown as recorded at sea, displayed by time along the ship's track; hence some are reversed in geographical orientation compared to others. Line drawings of digitized interpreted profiles, corrected to constant scale, are included with the photographs of the raw data from OAK crater area.

The lagoon profiles, whose tracks are shown in figure 4, are illustrated in figures 9*A*–*I*.

KOA Crater

The event that created KOA crater was fired on a small island that was obliterated by the explosion. Because five other devices were fired in the area (MIKE, NECTAR, APACHE, HURON, and SEMINOLE—see chap. A, fig. 17, this volume), any debris that is mappable cannot be attributed uniquely to the KOA event.

The profiles of KOA crater revealed only scattered subbottom reflections; none could be mapped as a surface. According to E. Tremba (oral commun., July 1985), data acquired during the EASI project show mappable reflectors below the shallow water outside KOA crater to the south, in an area where we did not acquire any subbottom profiles. Figure 10 shows the location of the fragmental reflections detected during this study and the depth below bottom of those reflections. Figure 11 shows line 701, which contains the only strong subbottom reflector. This reflector lies between 8 and 12 ms (about 6–9 m, or 20–30 ft) below the crater floor and apparently represents a change in the character of the postshot deposits, possibly from debris to natural sediments. The location of dipping acoustic patterns whose source is not clear are also plotted on figure 10.

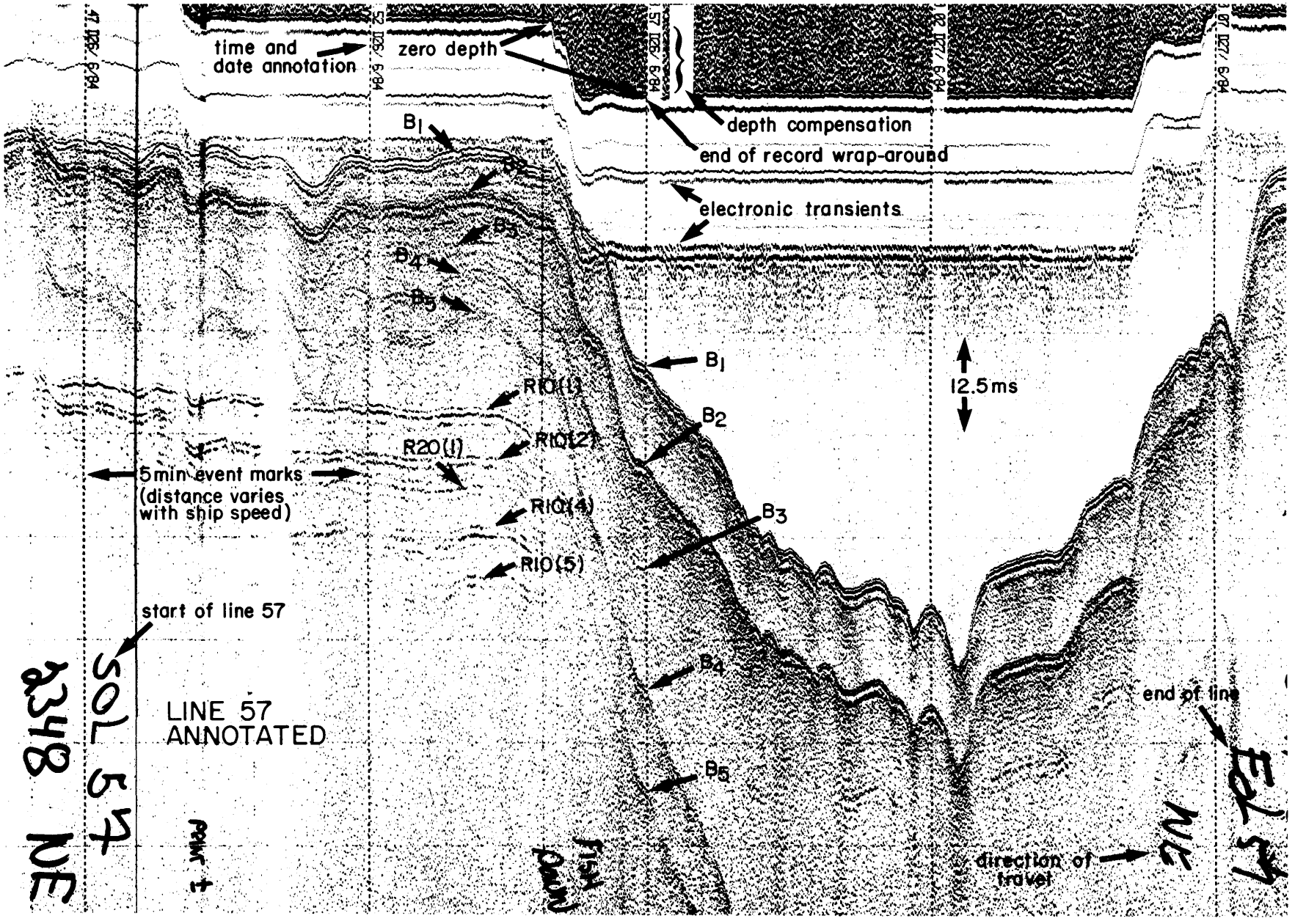

Figure 3. An example profile across OAK crater (line 57). Labels point out features of the record, including reflections, multiples, field annotation conventions, time of day, and horizontal and vertical scales. This illustration shows the changes in the spacing of the multiples resulting from changes in the tow-depth of the fish. Note that changes in fish depth caused aberrant appearance of records during times that the fish was descending or ascending because the automatic adjustment mechanism took a few moments to reestablish equilibrium. B=reflection from sea floor; R10(1–5)=reflections and multiple reflections from reflector R10. R20(1)=reflection from subsurface reflector R20.

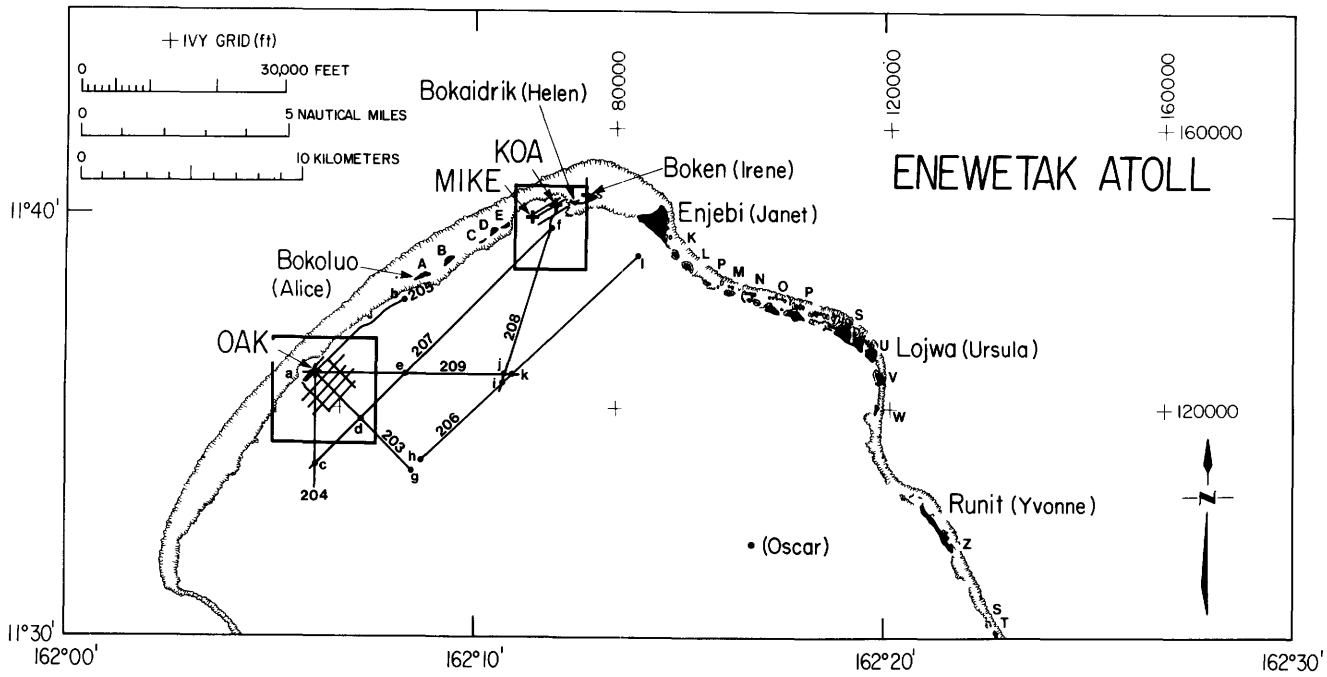

Figure 4. Location map of single-channel subbottom survey aboard MS *Egabrag II*, northern part of Enewetak Atoll, June and July 1984. For track lines within KOA and OAK crater areas, see figures 5 and 7. Subbottom profiles acquired within those areas are shown in figures 6 and 8. Subbottom profiles along tie lines in the atoll are shown in figure 9. Points a-l locate points marked on subbottom profiles illustrated in figure 9. Uppercase letters are first letters of site names (table 1 of the Introduction of the volume).

OAK Crater

Reflecting Surfaces

We mapped two reflectors that underlie the back reef and lagoon area surrounding the crater. They have been disrupted or blown away near ground zero. The two reflectors, termed R10 and R20, probably represent extensive, buried solution unconformities. R10, the shallower of the two surfaces, is a strong reflector and can be picked with confidence. It is clearly traceable below sediments of the lagoon floor to distances greater than 4.5 km (15,000 ft) from the crater and even below many large patch reefs. R10 correlates with the Holocene-Pleistocene boundary (disconformity "1" between sediment packages 1 and 2; B. R. Wardlaw, written commun., July 15, 1985).

Figure 12 shows point locations, and figure 13 shows structure contours (elevation below sea level) on R10. Figure 14 shows thickness of overburden above R10.

The R10 surface ranges in depth from 3 m to 25 m (10–82 ft) below bottom; most commonly, it lies about 4 to 5 m (13–16 ft) below bottom. It has subdued relief (see dip profiles, figures 8*Z–HH*) and slopes from the reef into the lagoon. It overlies a sequence of sediments marked by weak and discontinuous reflectors and locally incised by small channels. The thickness of sediment between R10 and R20 ranges from 3 to 14 m (10–46 ft) (fig. 15).

The deeper surface, R20, is a weak reflector, obscured in many places by multiples. It is best identified where it truncates lagoonward-dipping sedimentary units and is marked by apparent cuestas or hogbacks and depressions of 1 to 4 m (3–13 ft), which appear to be parallel to the reef. (See dip profiles, figs. 8*Z–HH*, especially line 201, fig. 8*AA*). Figure 16 is a point plot showing the locations of digitized picks. Figure 17 shows structure contours drawn on the top of the R20 reflector. R20 lies within upper Pleistocene sediments (disconformity "2" within the uppermost part of sediment package 2; B. R. Wardlaw, written commun., July 15, 1985).

Deformation of R10 and R20 Surfaces

Figure 18 is a summary interpretive map showing the craterward extent of R10 and R20 and some structural characteristics of R10. It can be compared with the structure-contour maps (figs. 13, 17).

R10 and R20 are folded near the crater. In most places, they dip toward the crater, and terminate below the accumulation of surface debris that surrounds the crater on its lagoonward side; we also identified small upturned areas of R10 (for example, line 203, about 0046, fig. 8*CC*; line 210, about 2307, fig. 8*DD*; also shown by symbols on fig. 18).

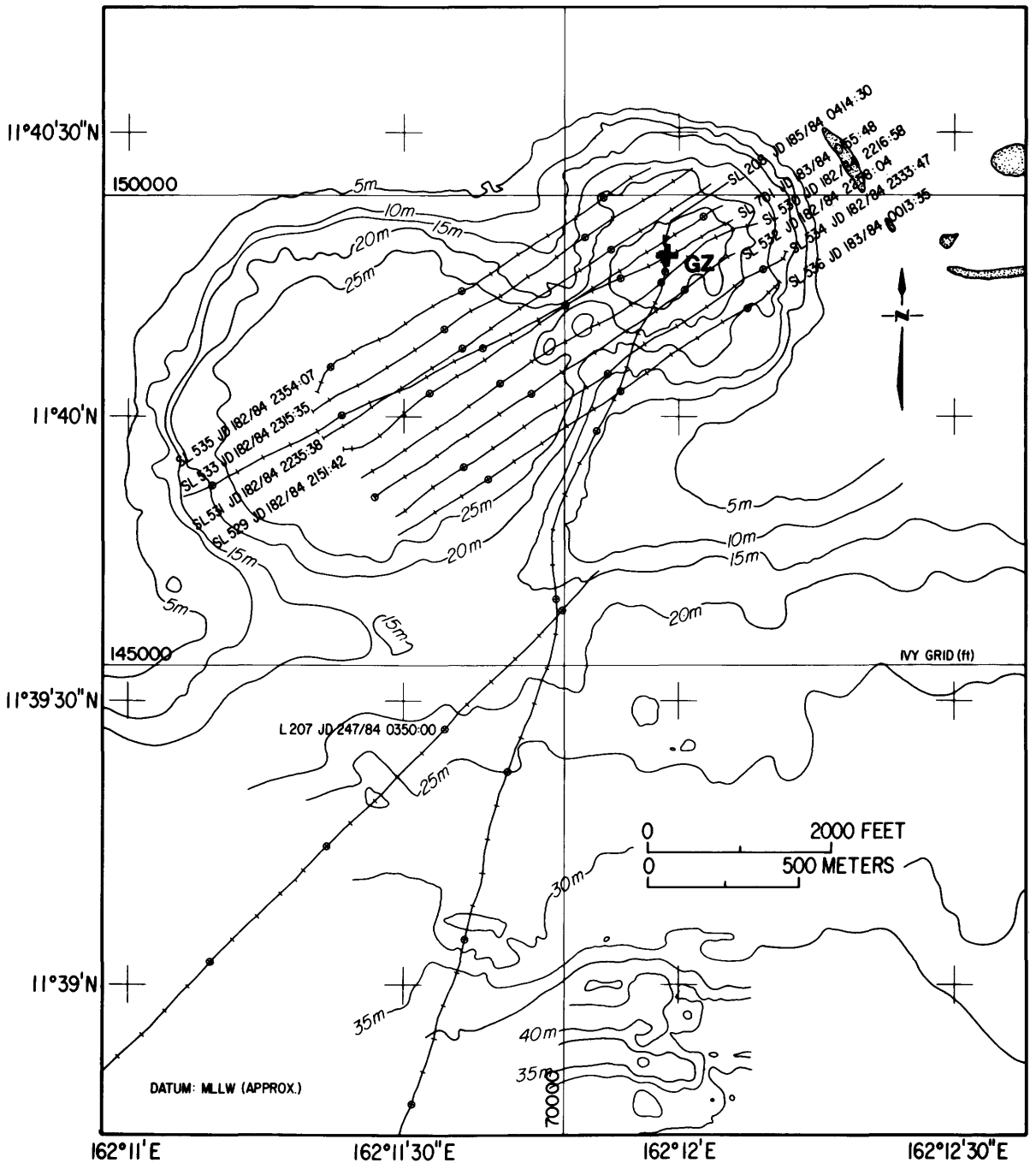

Figure 5. Track lines, single-channel subbottom profiles, KOA crater area. Tics indicate 1-minute intervals; circled tics indicate 5-minute intervals. Labels include: SL (start of line), line no., JD (Julian day/year); numerals (for example, 0350:00) are time of day. Some of the bathymetric contours of the area outside the crater are adapted from Tremba and others, 1982. GZ=ground zero. Contour interval is 5 m.

The R10 surface can be classified by seismic character as continuous (for example, line 89 from 0354–0359, fig. 8*K*), disturbed (for example, line 77, 0410–0414, fig. 8*G*), and fragmented (for example, line 79, 0578–0520, fig. 8*I*). We can identify some sites of probable fractures (for example, line 89, 0359–0400, fig. 8*K*; see also symbols on fig. 18). In most places, the R20 reflector is not recorded clearly enough to evaluate its deformation.

Shallow water prevented us from profiling the reef and near-reef parts of the northwest quadrant of the crater, but we were able to define the shallow structure of the southwest, southeast, and northeast quadrants (fig. 18). The

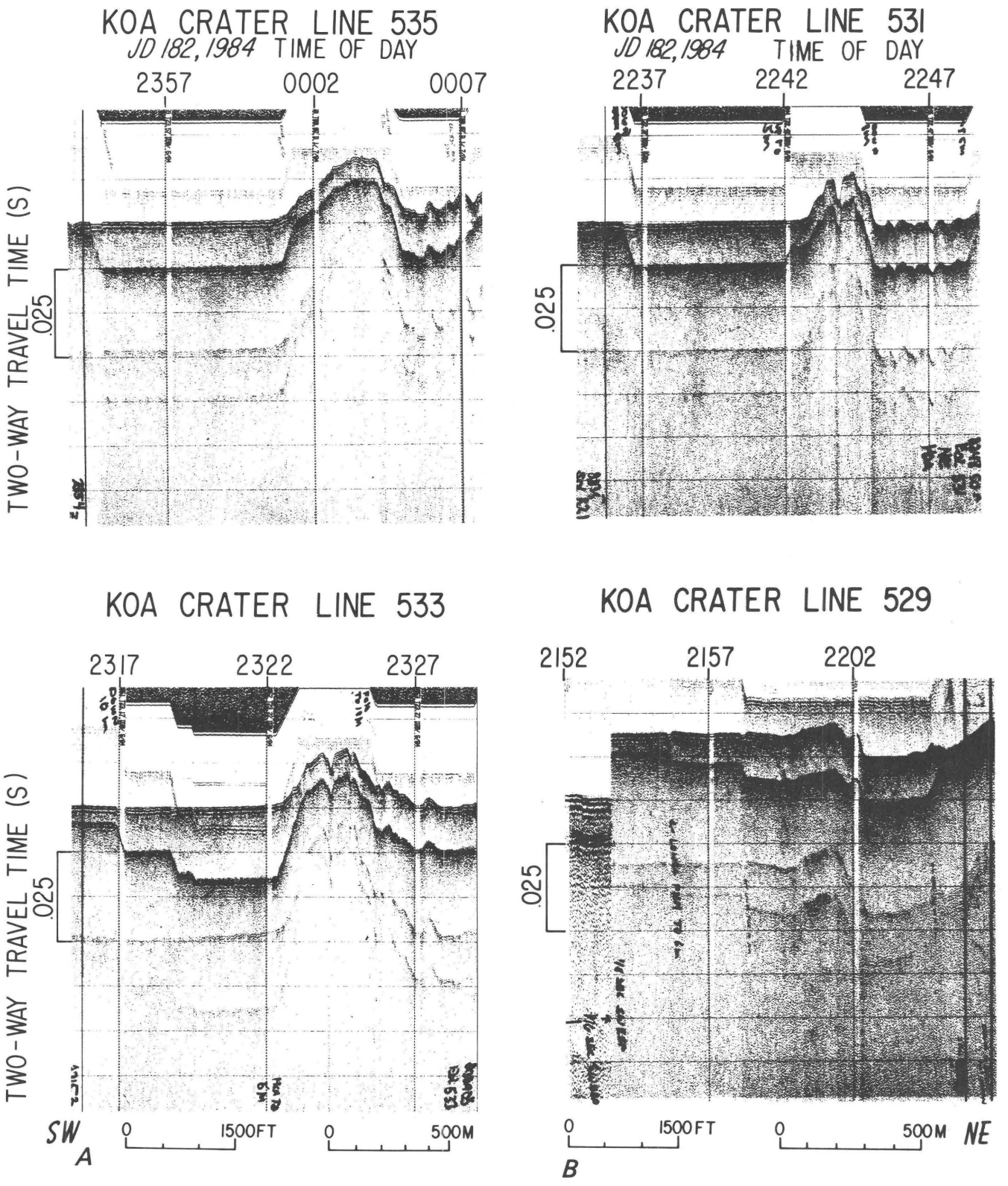

Figure 6. *A–F*. Subbottom profiles from KOA crater. Horizontal scale is time along track. Vertical scale is 12.5 ms between scale lines. Note that absolute depth can have slight errors in correction for fish depth, and that for precise depths the reader should refer to chapter A of this volume. Subbottom thickness measurements are correct in time units. *A*, lines 535, 533; *B*, lines 531, 529; *C*, lines 530, 532; *D*, lines 534, 536; *E*, line 701; *F*, line 208. Date given is Julian day (JD) and year.

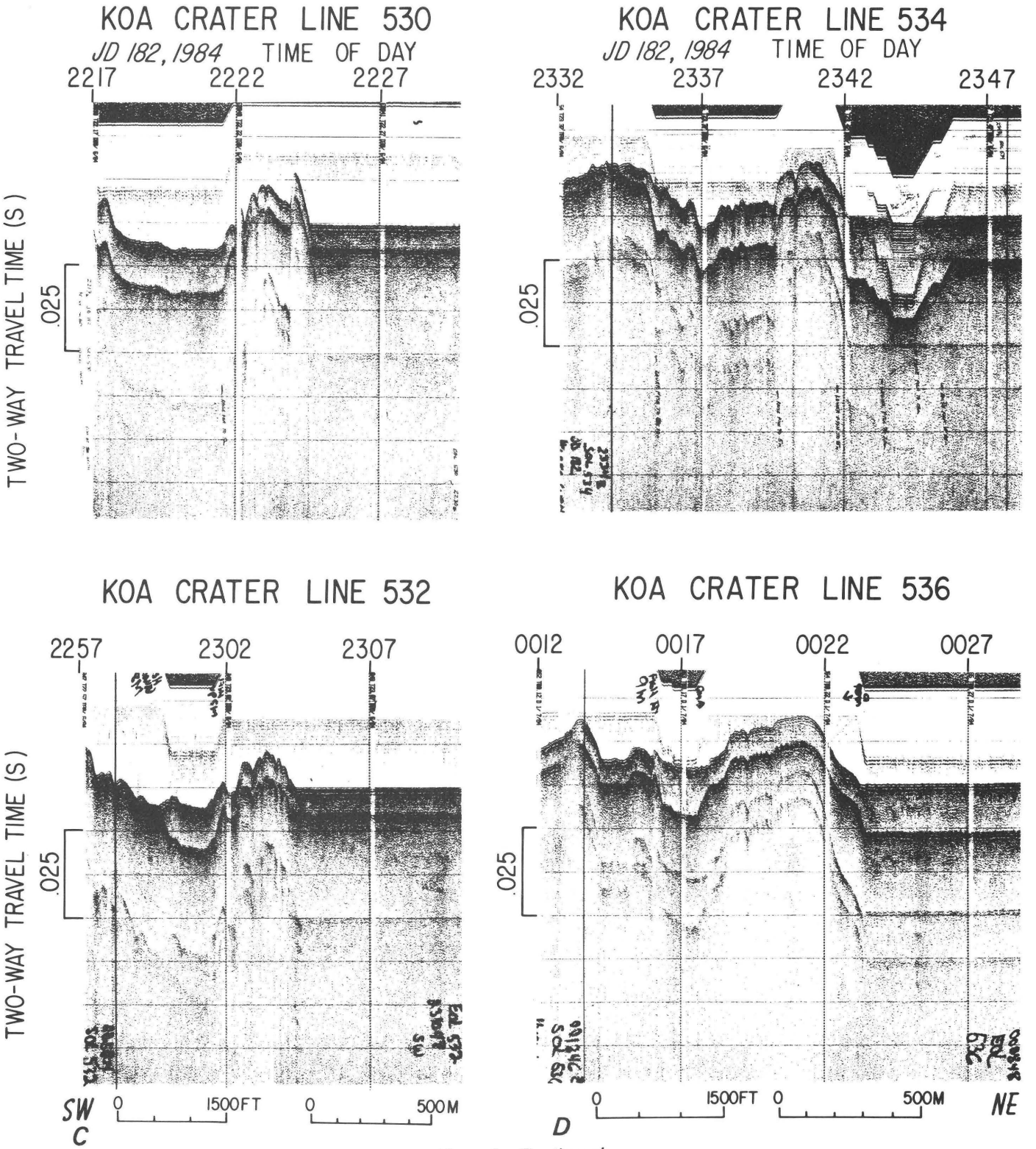

Figure 6—*Continued*

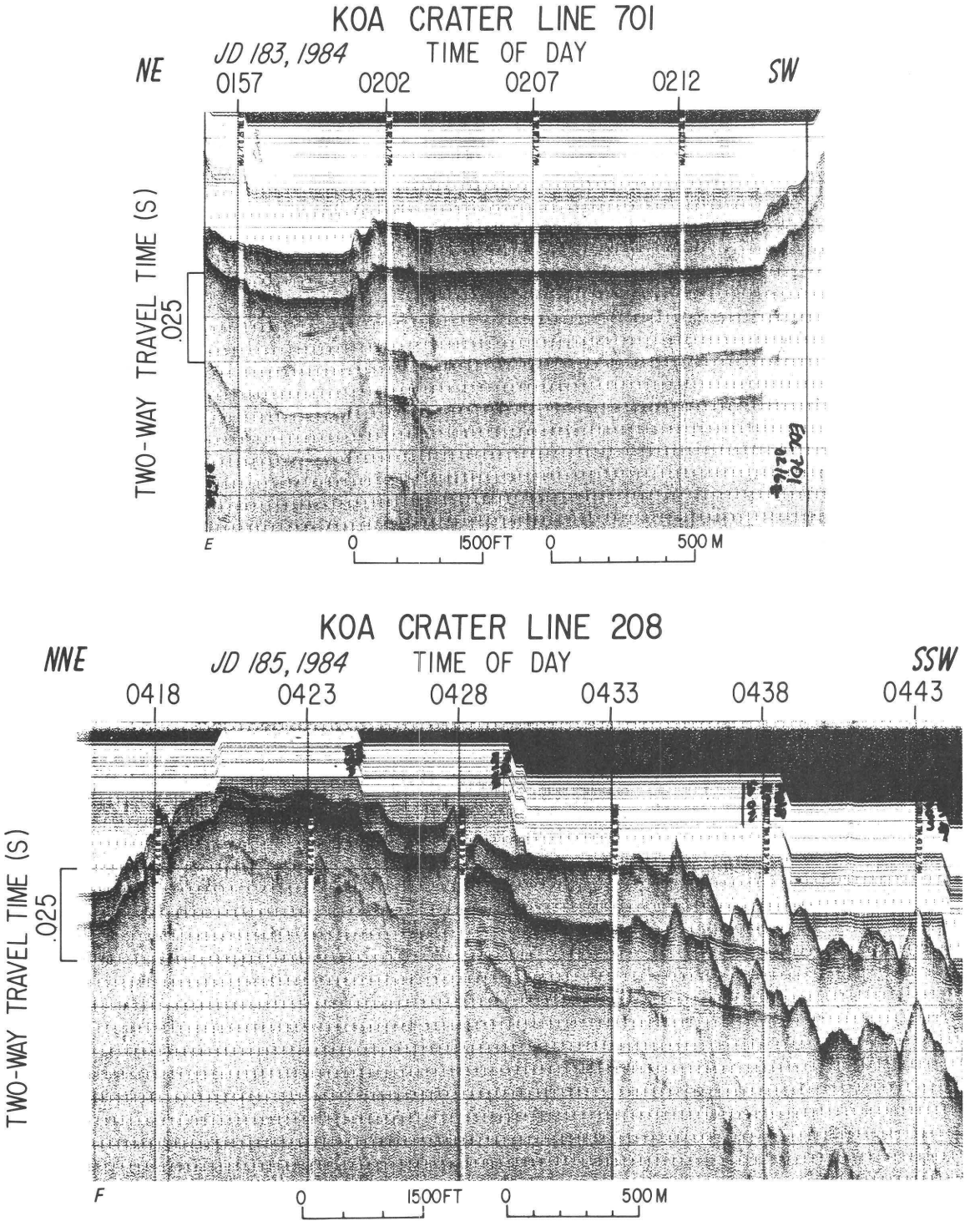

Figure 6—*Continued*

southwest quadrant is marked by extensive downturning of R10 into the crater. The outermost point of initial inflection ranges from 720 m (2,400 ft) from ground zero near the reef on lines 5899 and 57 to about 870 m (2,850 ft) from ground zero along line 77 (fig. 18). The R10 reflector dips craterward, measured radially toward ground zero, for distances between 60 and 425 m (200–1,400 ft) from the initial zone of inflection, before it terminates. Termination points in the southwest quadrant lie between 790 m (2,590 ft) from ground zero on line 56 and 390 m (1,280 ft) from ground zero on line 79. Near terminations, disturbed or fragmented reflectors are common. The large downturned area along

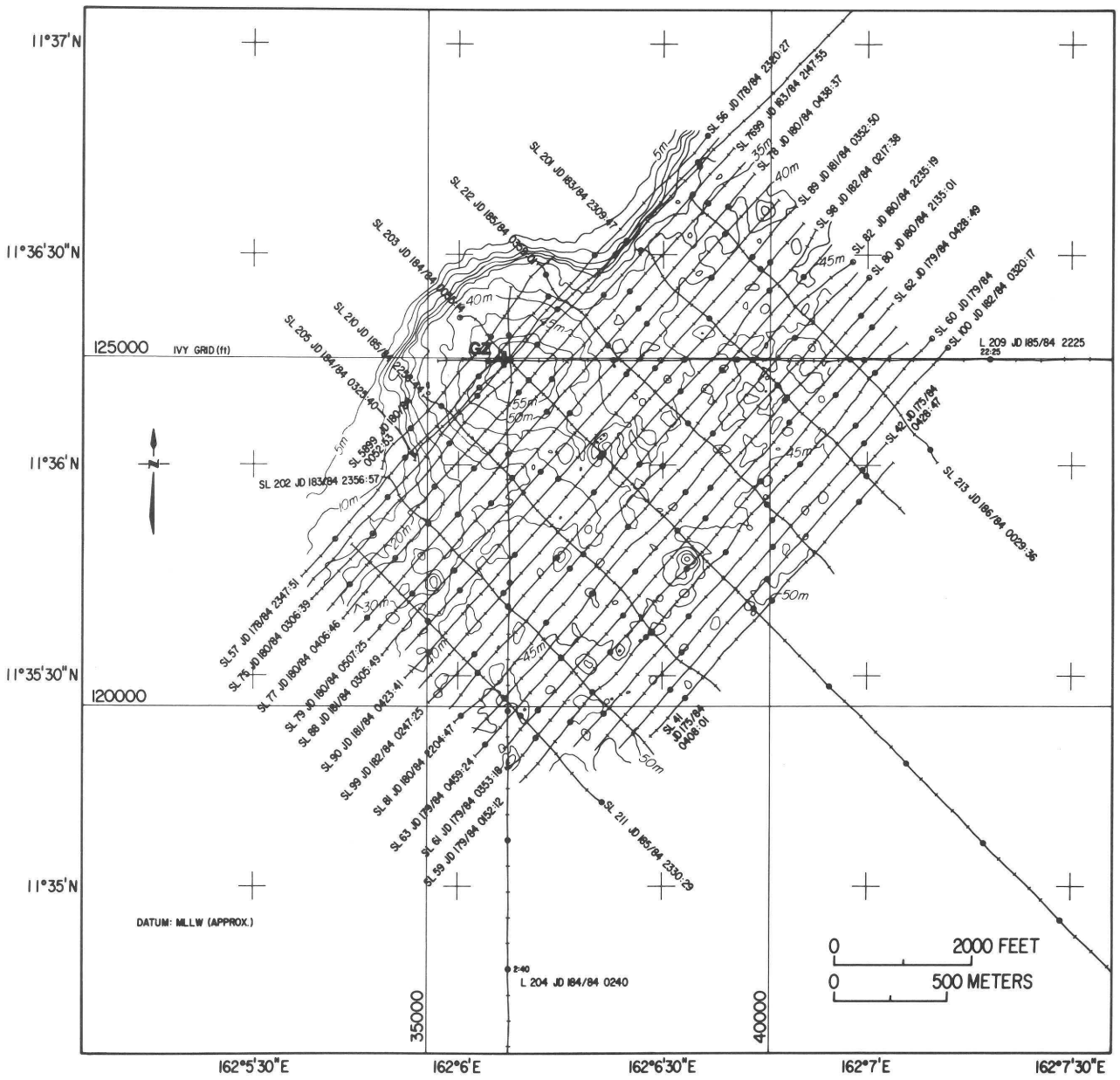

Figure 7. Track lines, single-channel subbottom profiles, OAK crater area. Tics indicate 1-minute intervals; circled tics indicate 5-minute intervals. Labels include: SL (start of line), **line no.**, JD (Julian day/year); and numerals (for example, 0350:00) are time of day. GZ=ground zero. Contour interval is 5 m.

Figure 8. *A–HH*. Profiles and interpretations of Huntec subbottom profiles for OAK crater. Note that the correction for depth of the fish can have slight errors and that echo-sounding data were used for water-depth measurements. Vertical-scale lines on the profiles are 12.5 ms apart. Time markers (vertical dashed lines) are at 5-minute intervals. Date given as Julian day (JD) and year. R10, R20 refer to subbottom reflectors.

A, line 5899
B, line 57
C, line 56
D, line 205
E, line 75
F, line 7699
G, line 77
H, line 78
I, line 79
J, line 88
K, line 89
L, line 90
M, line 98
N, line 99
O, line 82
P, line 81
Q, line 80
R, line 63
S, line 62
T, line 61
U, line 59
V, line 60
W, line 100
X, line 42
Y, line 41
Z, line 213
AA, line 201
BB, line 212
CC, line 203
DD, line 210
EE, line 202
FF, line 211
GG, line 209
HH, line 204

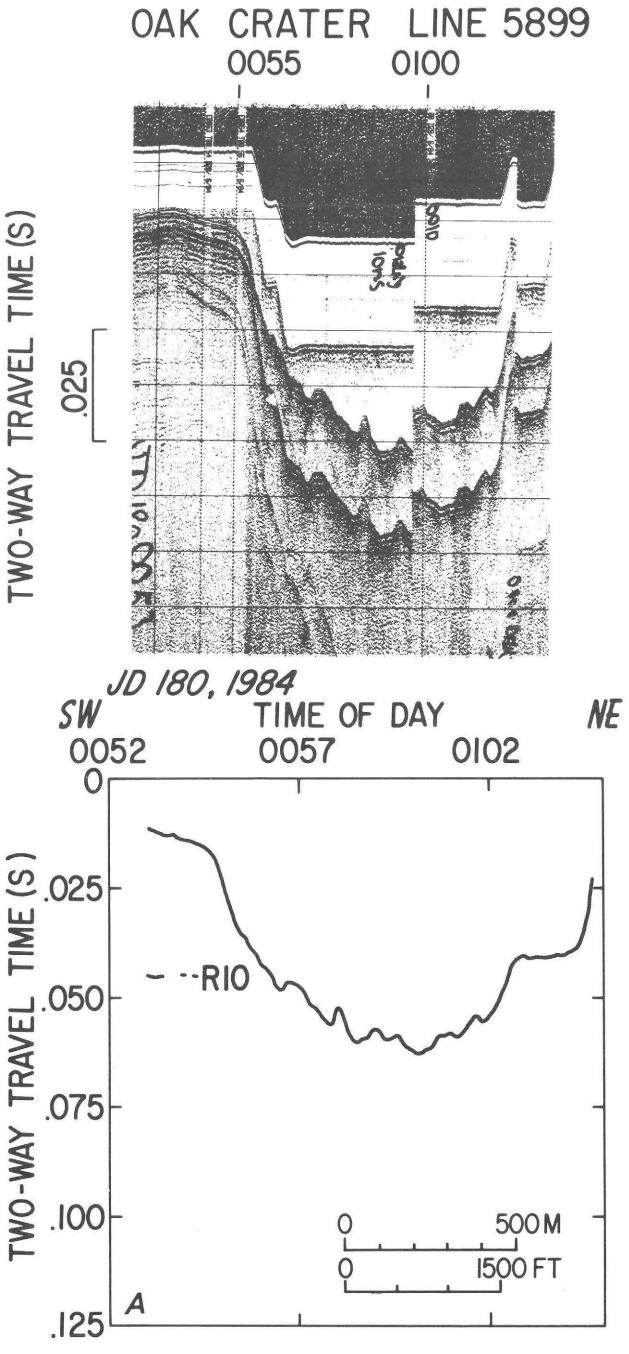
OAK CRATER LINE 5899
0055
0100
TWO-WAY TRAVEL TIME (S)
.025
JD 180, 1984
SW
TIME OF DAY
NE
0052
0057
0102
0
.025
.050
.075
.100
.125
R10
0
500M
0
1500 FT
A

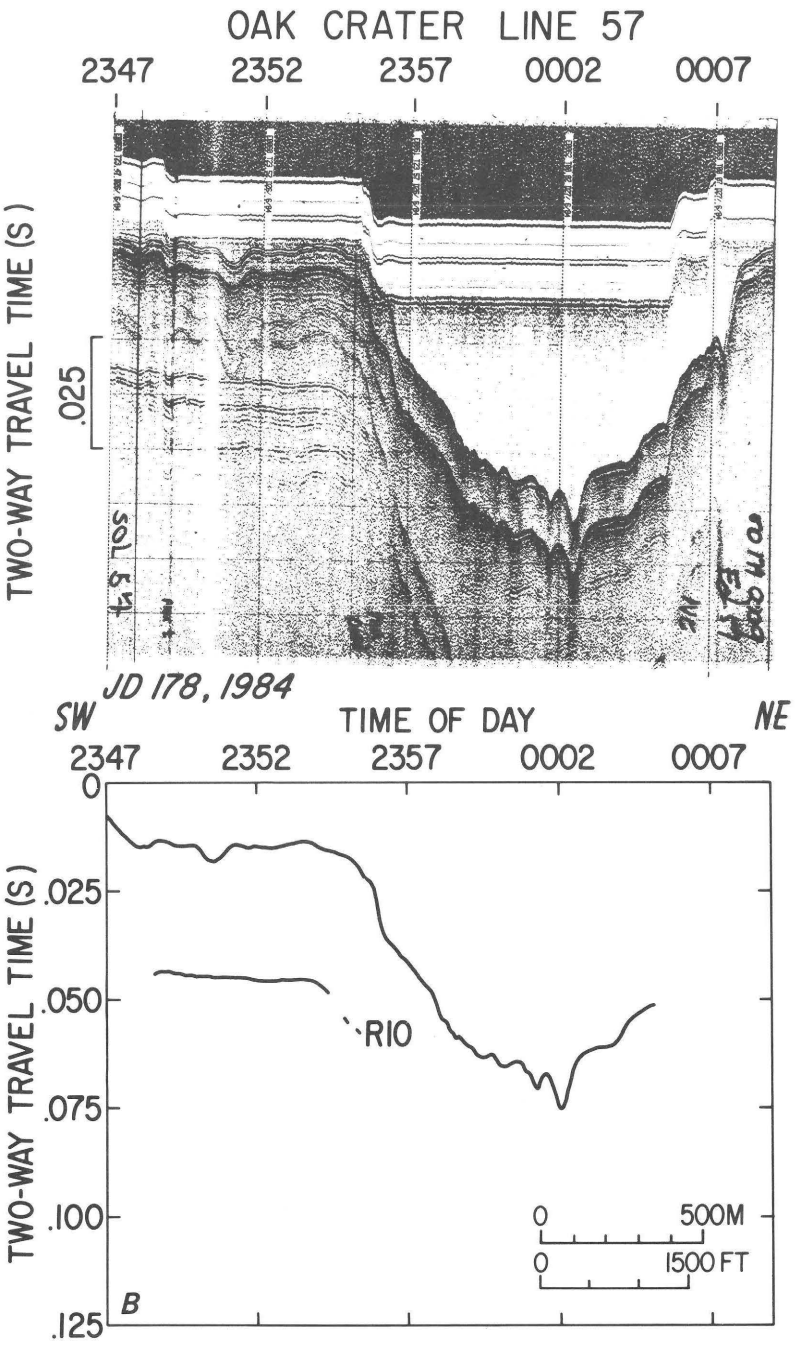
OAK CRATER LINE 57
2347
2352
2357
0002
0007
TWO-WAY TRAVEL TIME (S)
.025
JD 178, 1984
SW
TIME OF DAY
NE
2347
2352
2357
0002
0007
0
.025
.050
.075
.100
.125
R10
0
500M
0
1500 FT
B

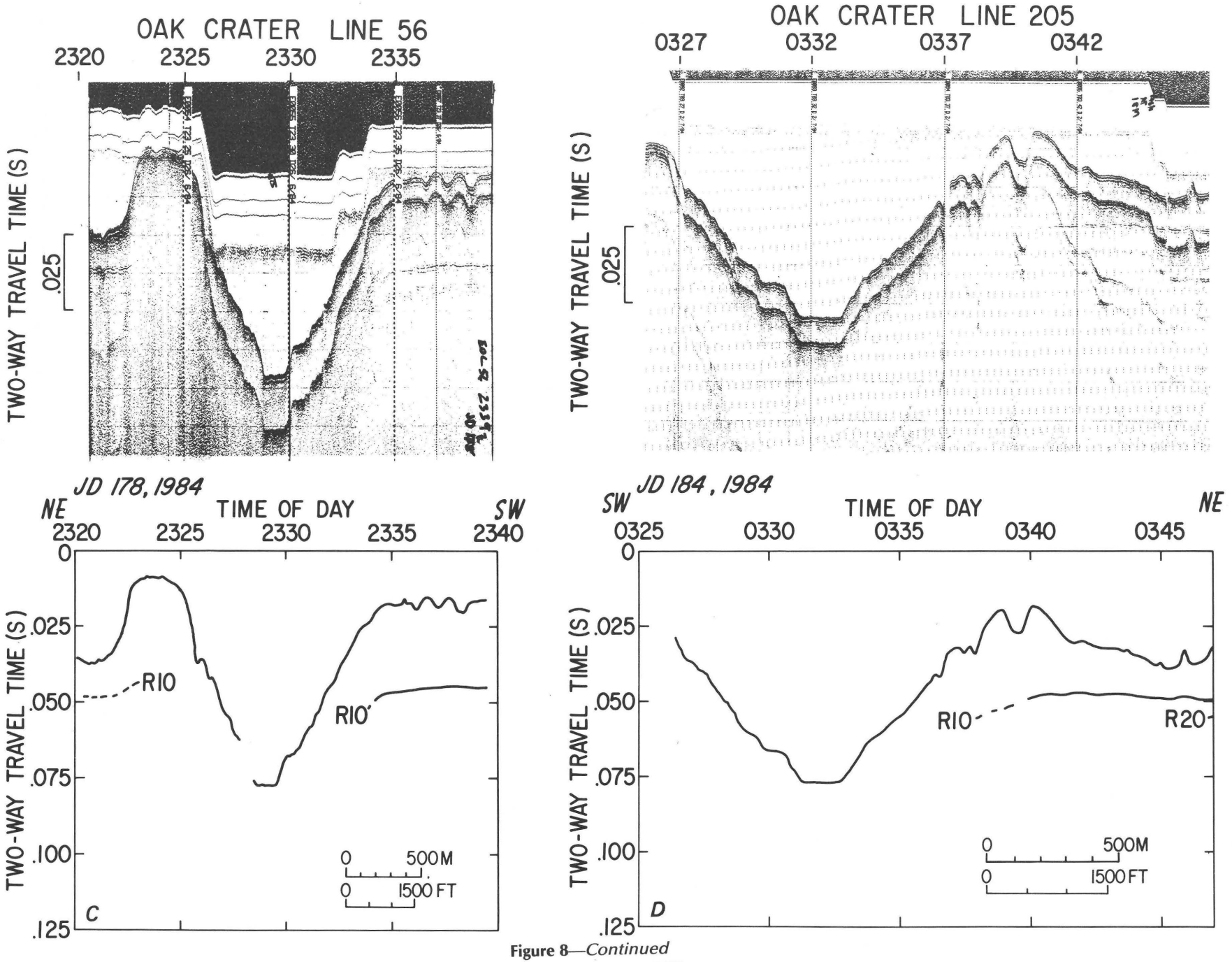

Figure 8—*Continued*

Figure 8—*Continued*

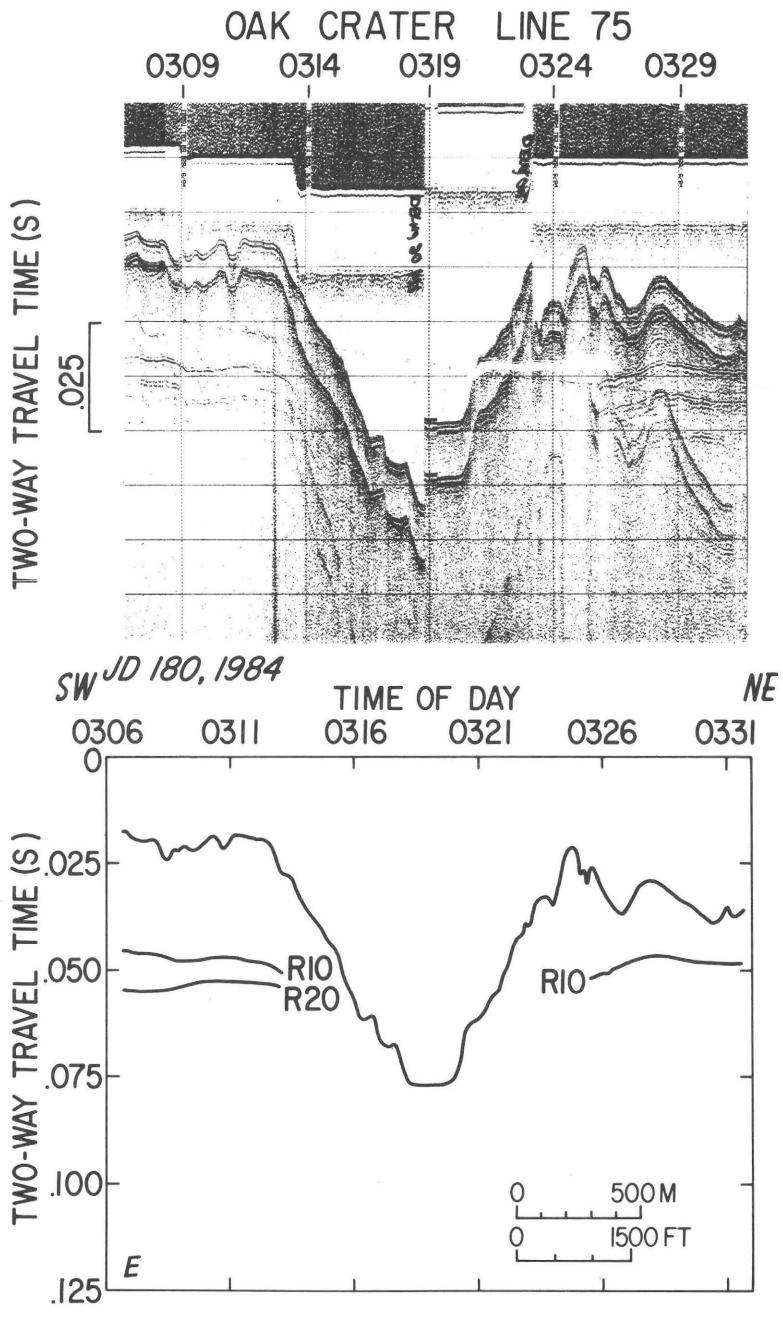

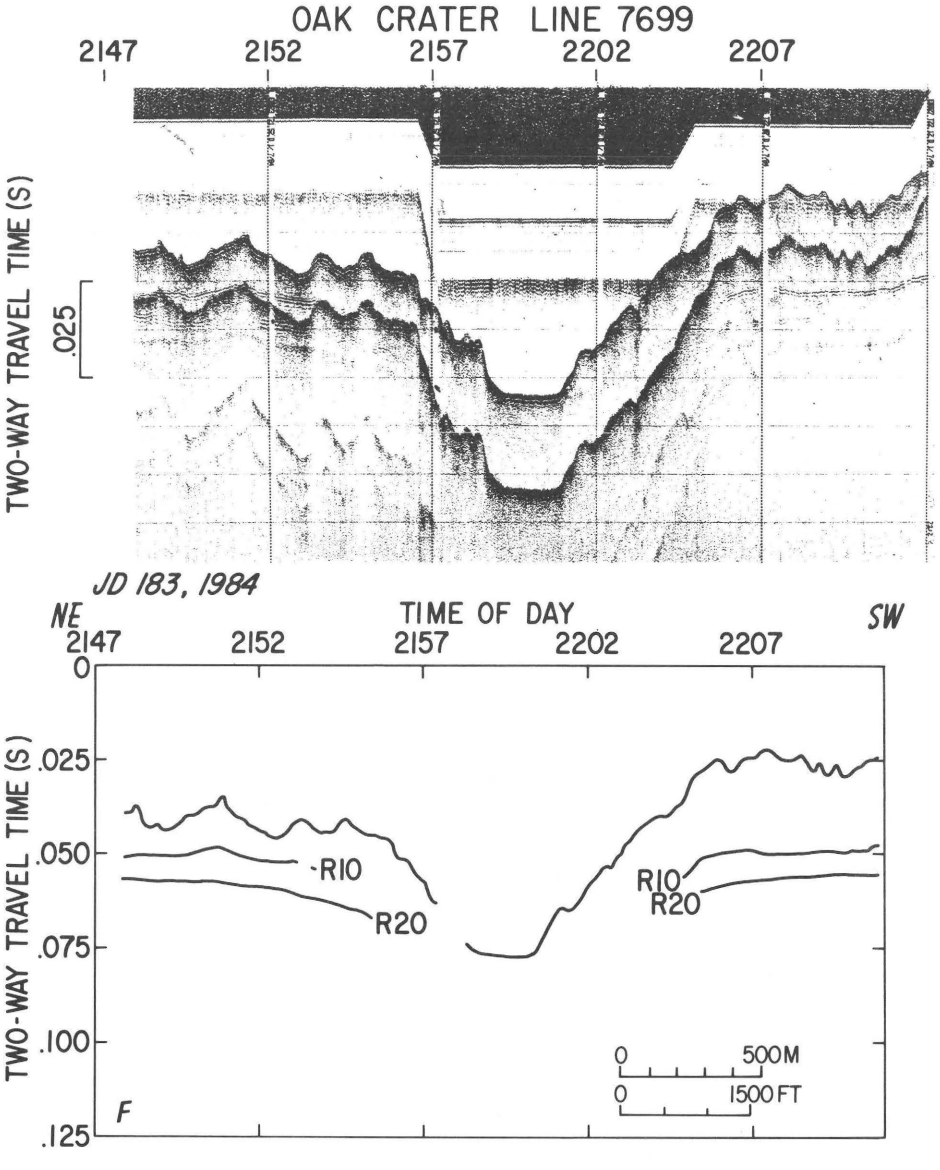

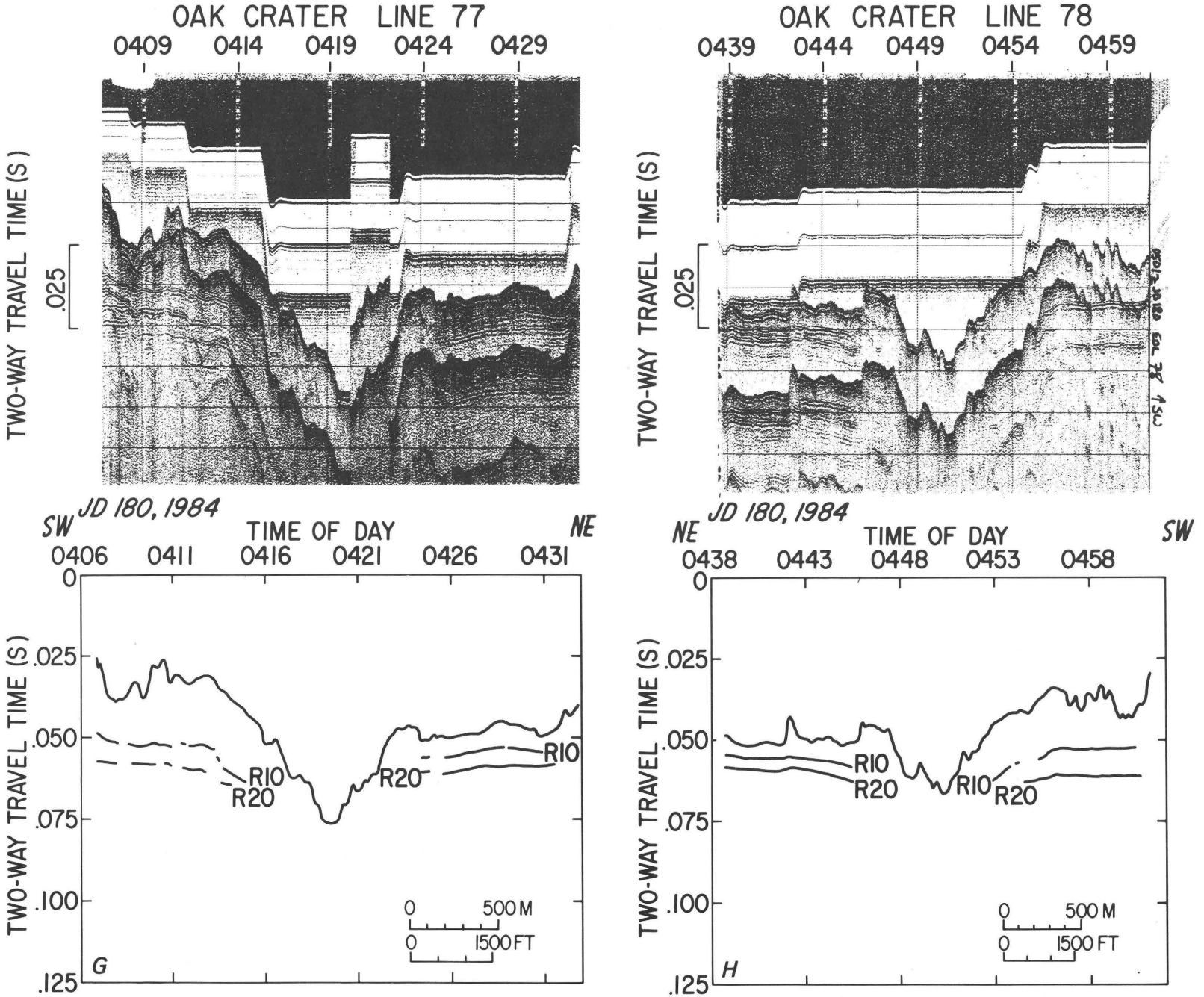
OAK CRATER LINE 77
0409
0414
0419
0424
0429
TWO-WAY TRAVEL TIME (S)
.025
SW
JD 180, 1984
NE
TIME OF DAY
0406
0411
0416
0421
0426
0431
0
.025
.050
.075
.100
.125
R10
R20
R10
R20
0
500 M
0
1500 FT
G
OAK CRATER LINE 78
0439
0444
0449
0454
0459
TWO-WAY TRAVEL TIME (S)
.025
NE
JD 180, 1984
SW
TIME OF DAY
0438
0443
0448
0453
0458
0
.025
.050
.075
.100
.125
R10
R20
R10
R20
0
500 M
0
1500 FT
H

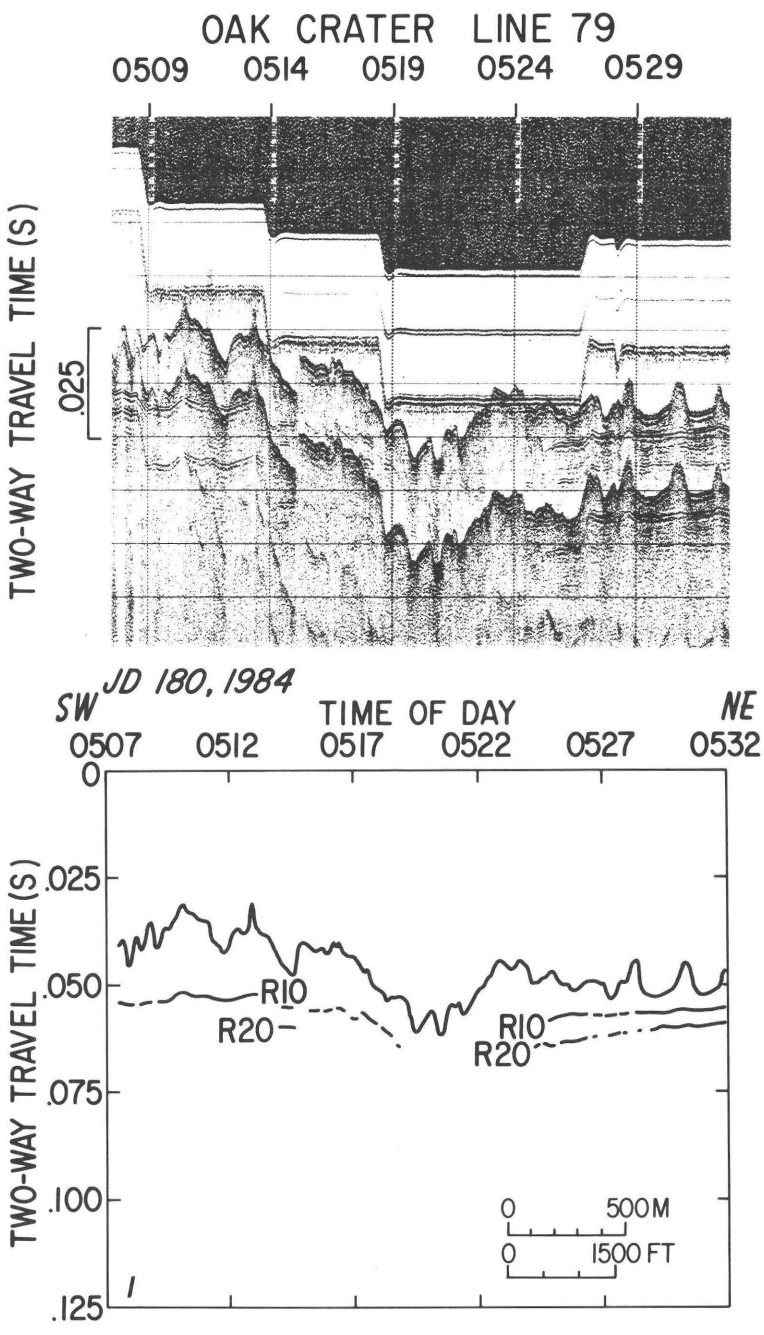

Figure 8—*Continued*

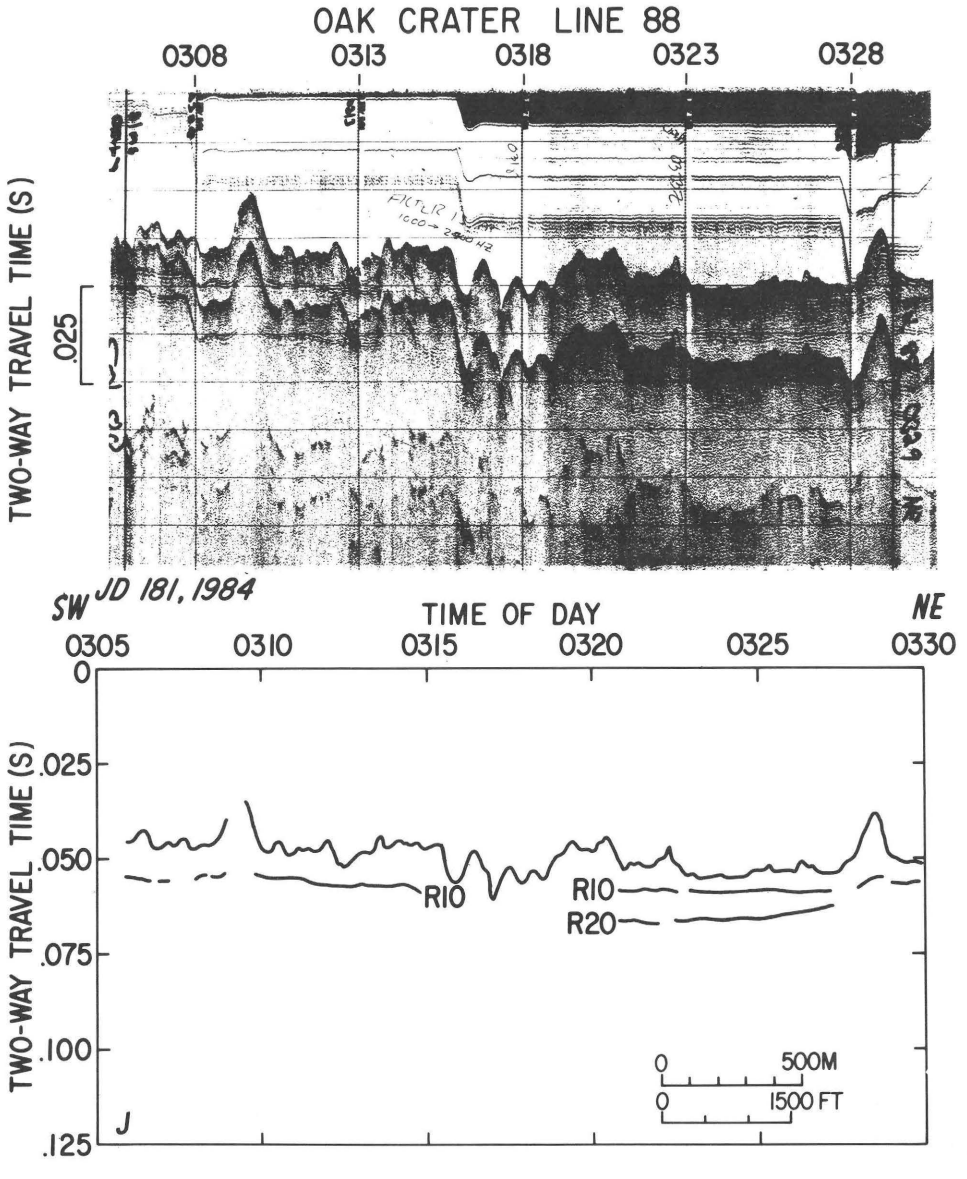

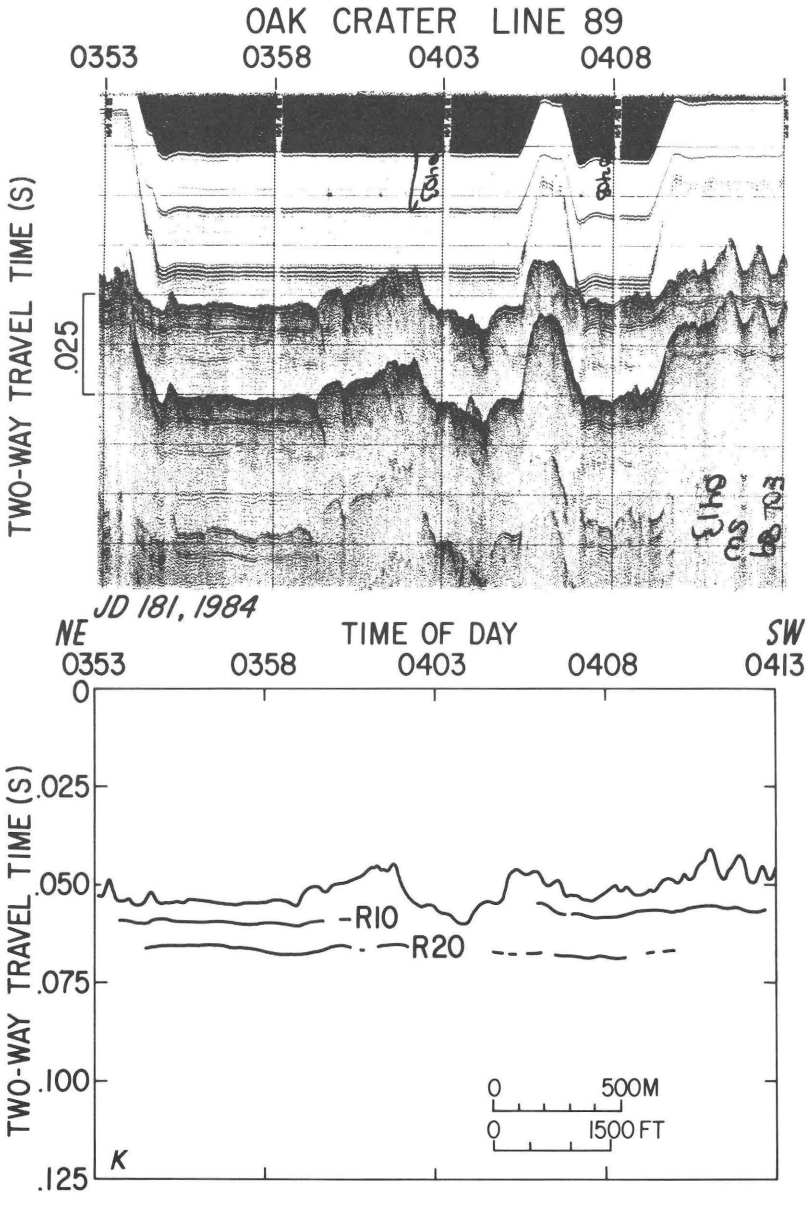
OAK CRATER LINE 89
0353
0358
0403
0408
TWO-WAY TRAVEL TIME (S)
.025
JD 181, 1984
NE
SW
TIME OF DAY
0353
0358
0403
0408
0413
0
.025
.050
.075
.100
.125
R10
R20
0 500M
0 1500 FT
K

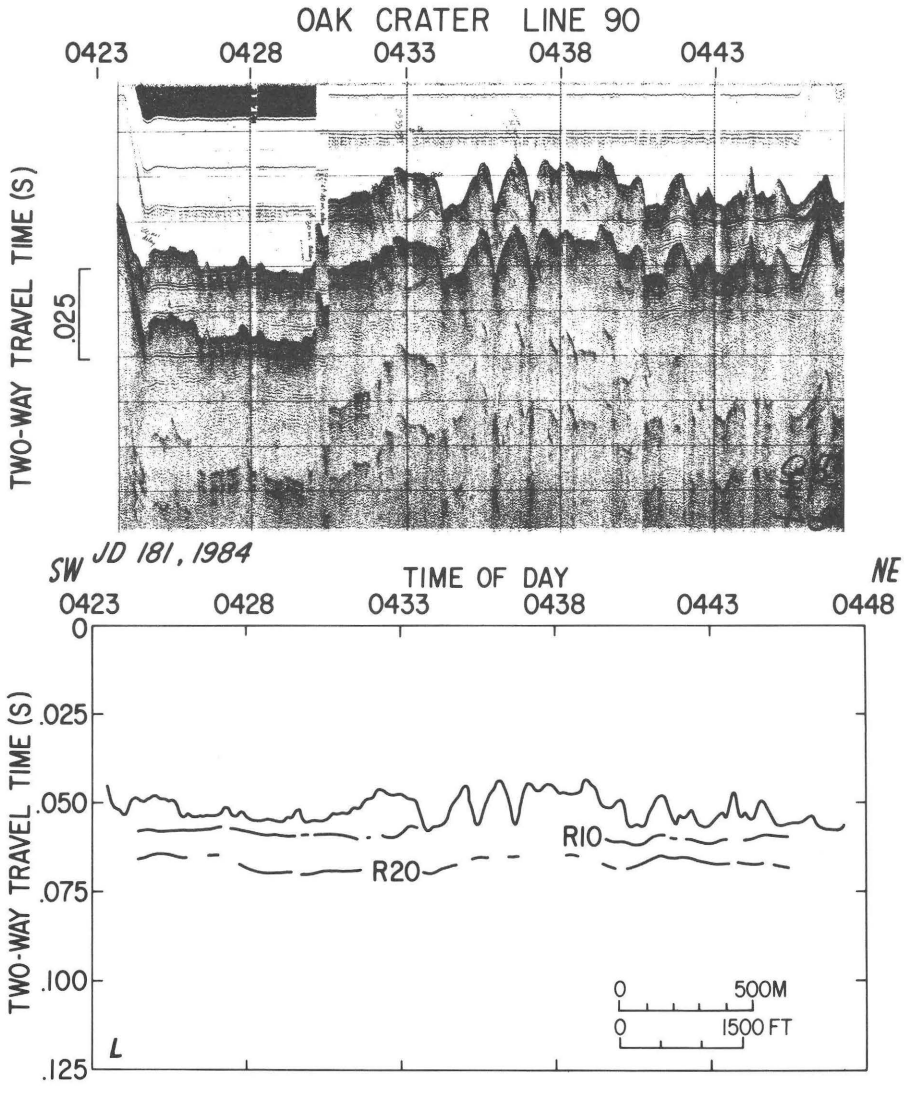
OAK CRATER LINE 90
0423
0428
0433
0438
0443
TWO-WAY TRAVEL TIME (S)
.025
SW
JD 181, 1984
NE
TIME OF DAY
0423
0428
0433
0438
0443
0448
0
.025
.050
.075
.100
.125
R10
R20
0 500M
0 1500 FT
L

Figure 8—*Continued*

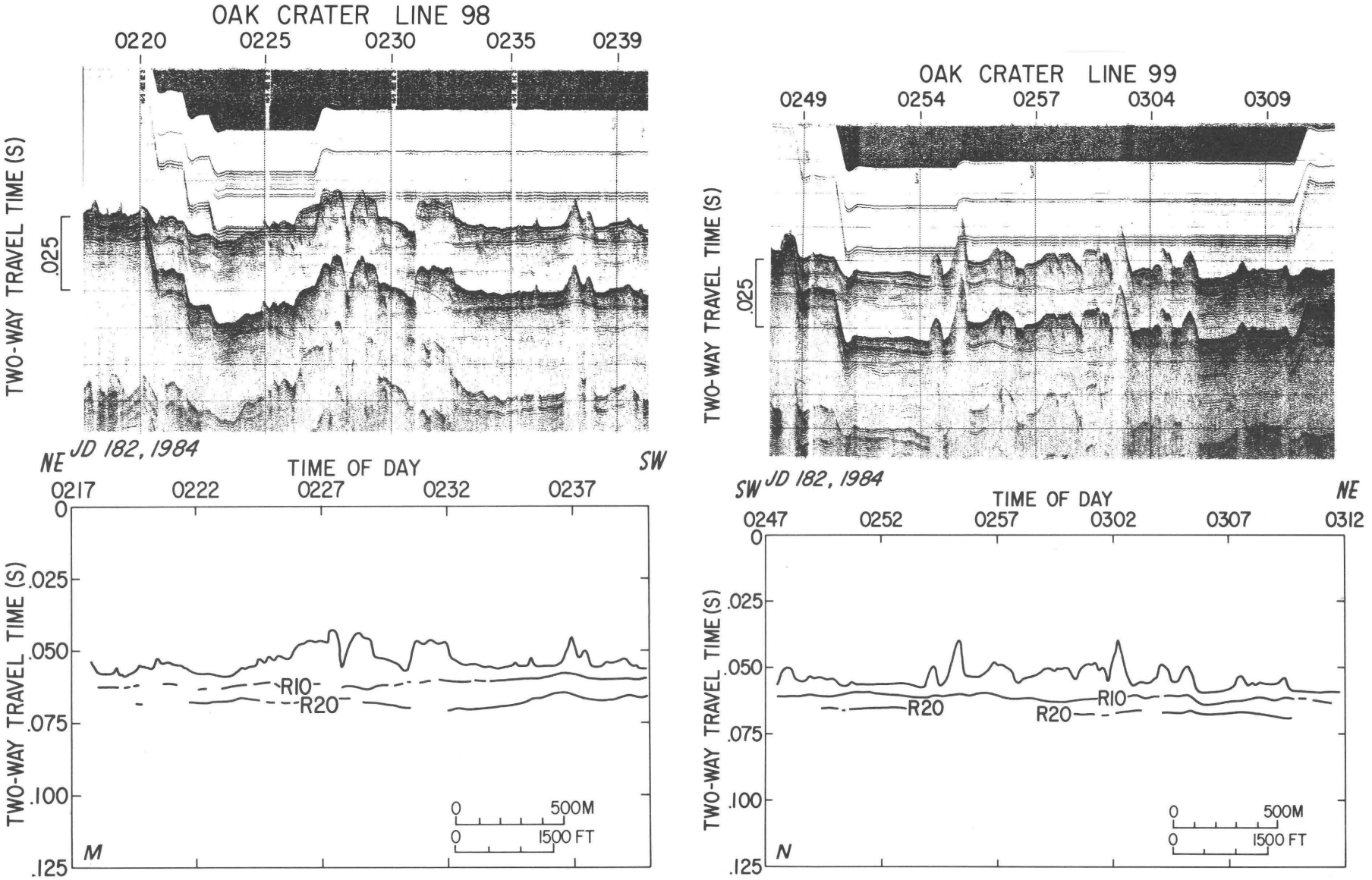

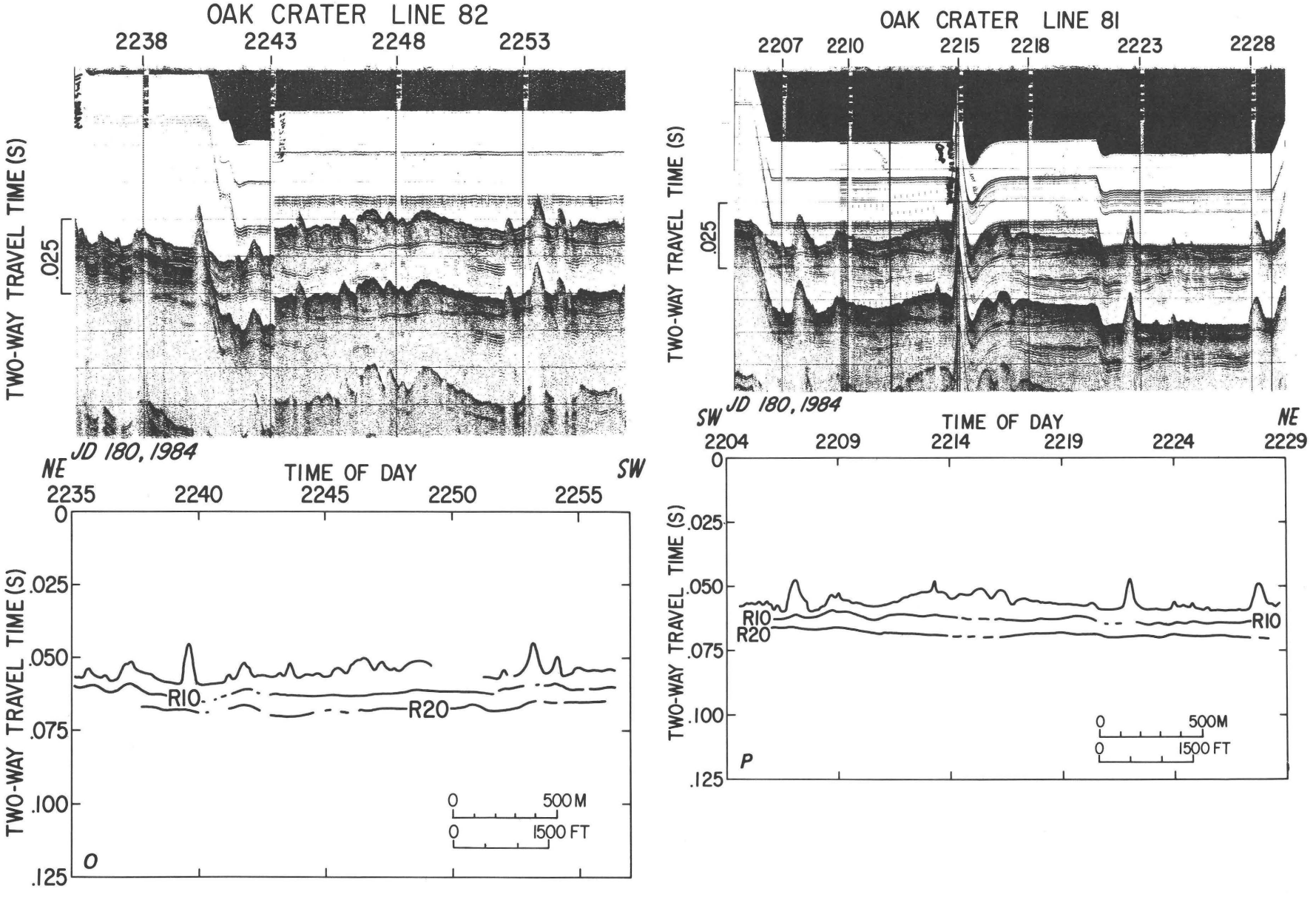

Figure 8—*Continued*

Figure 8—*Continued*

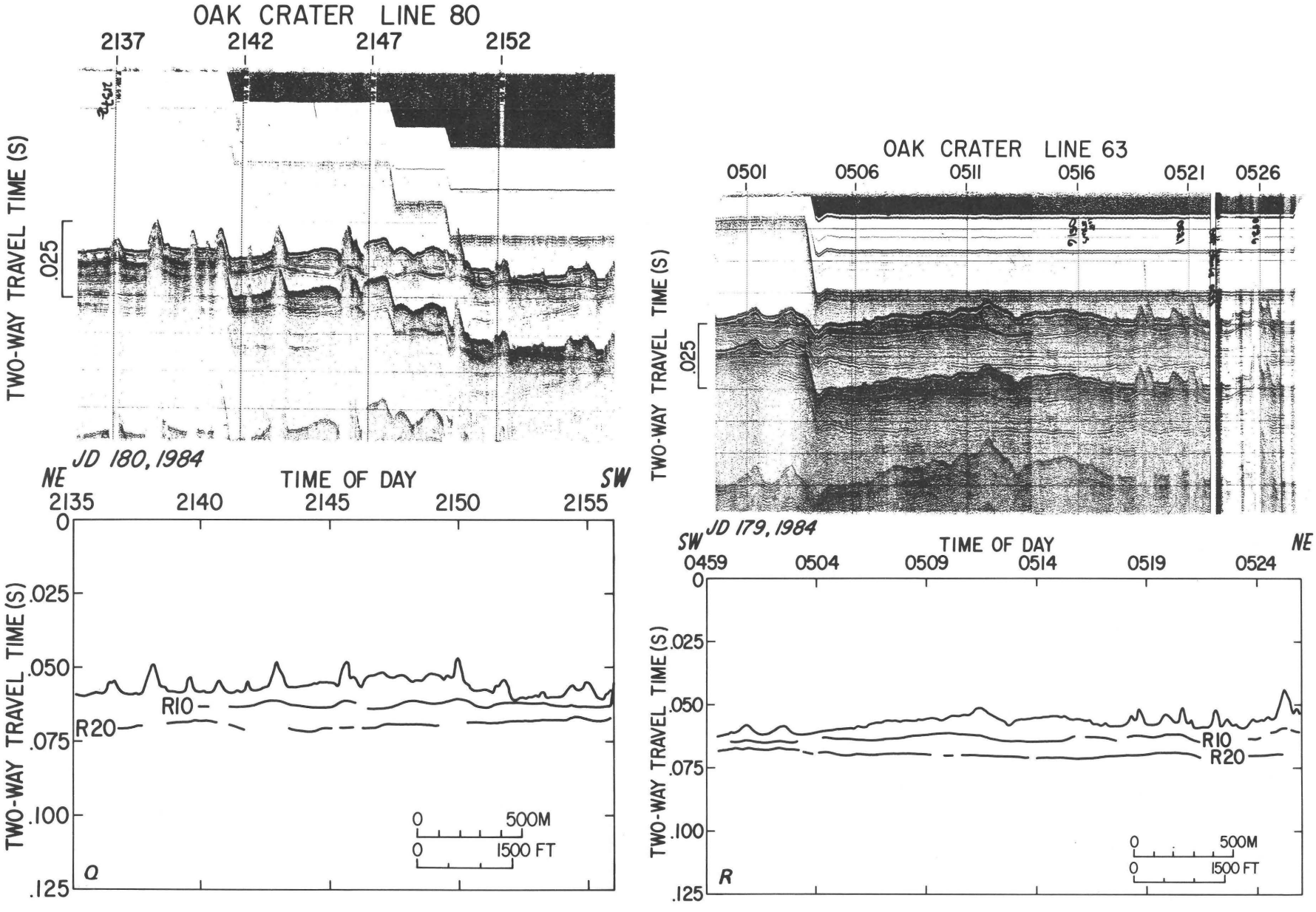

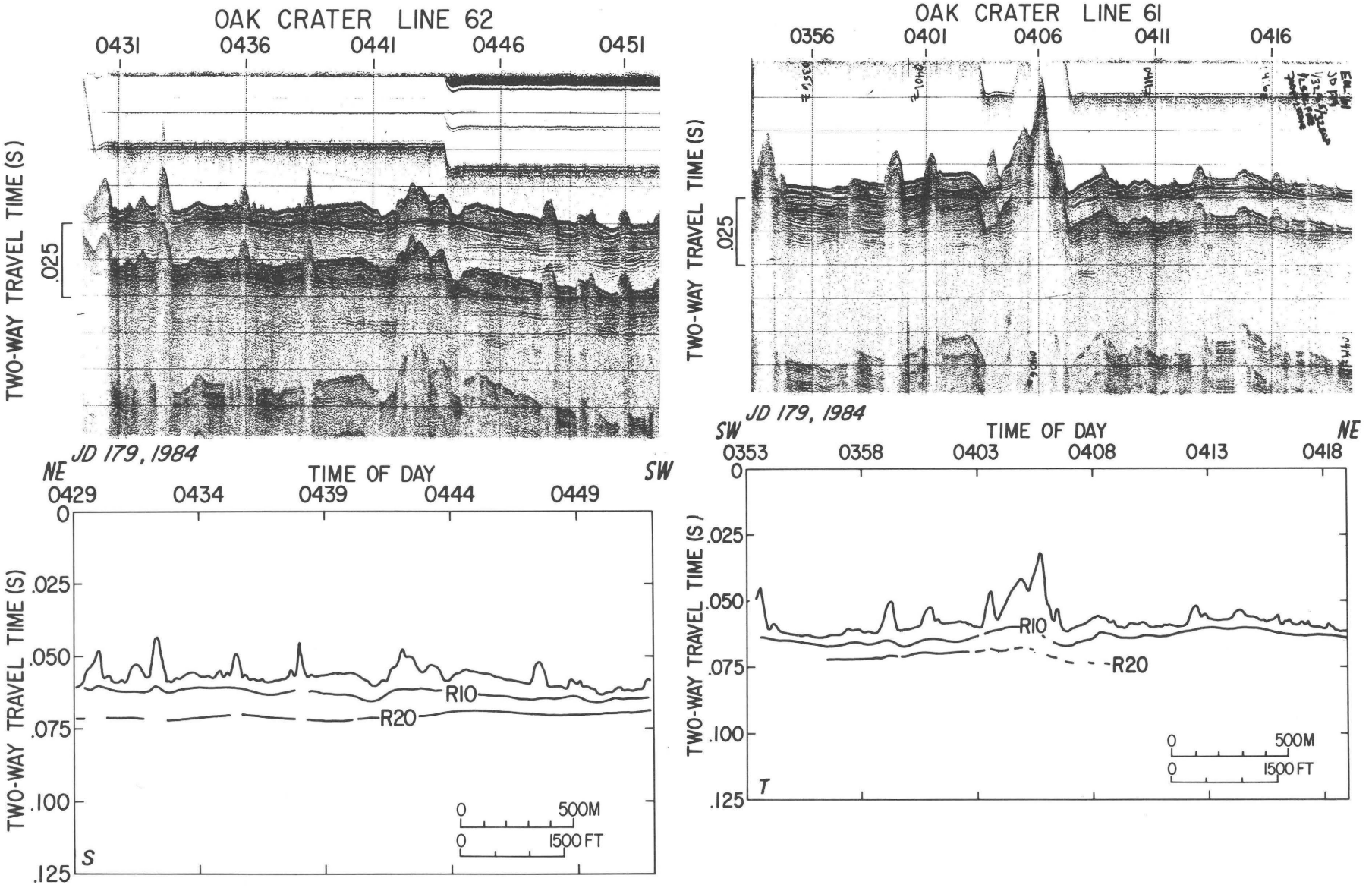

Figure 8—*Continued*

Figure 8—*Continued*

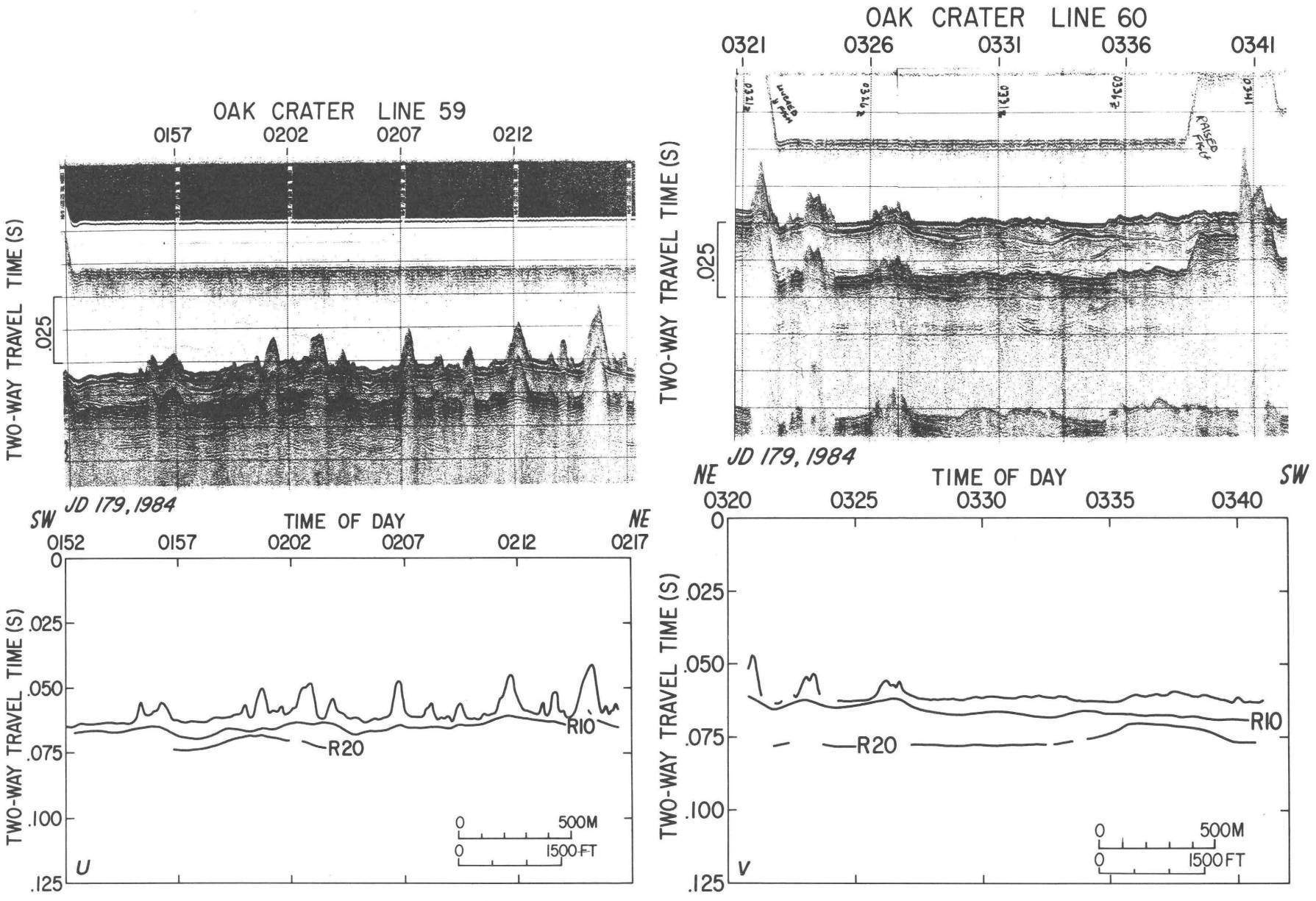

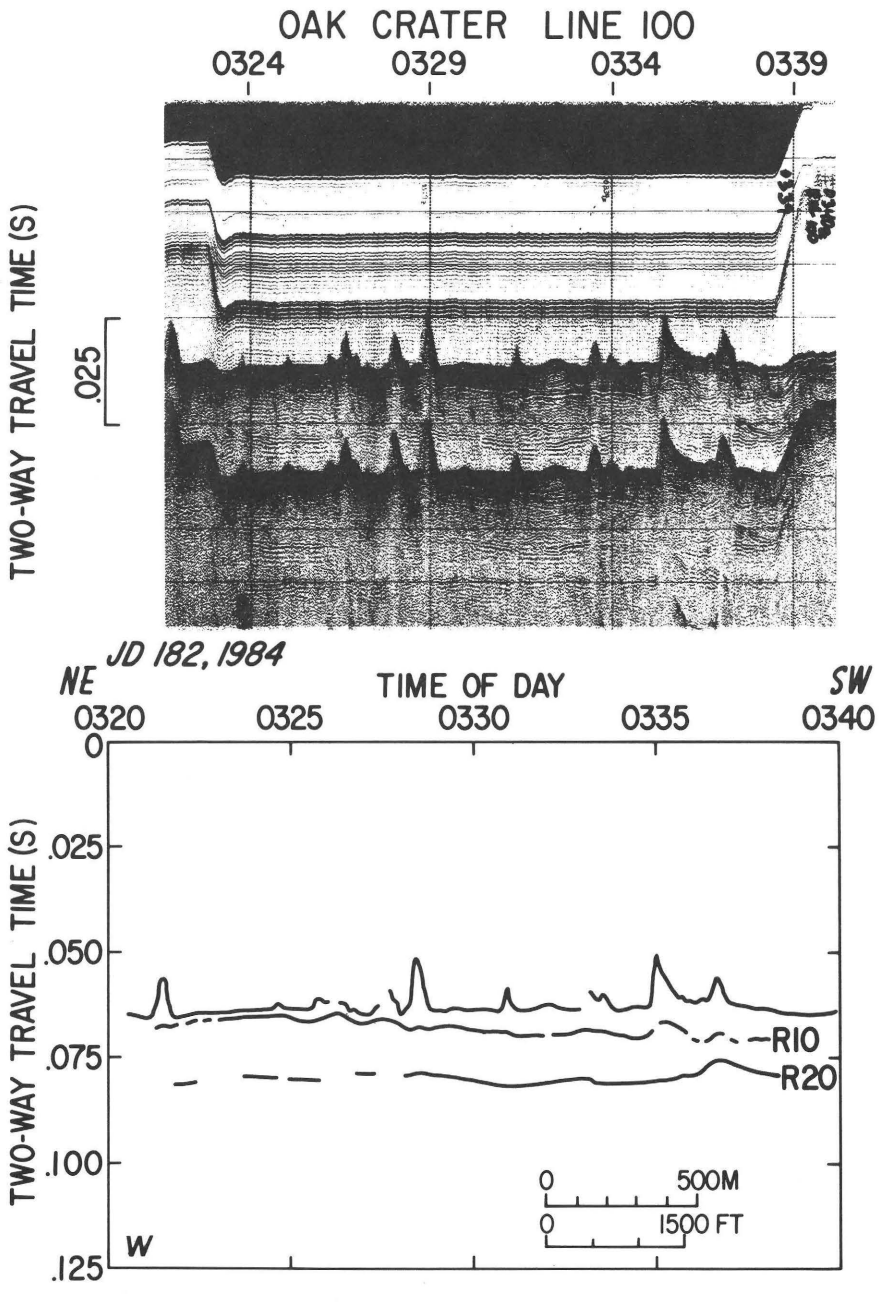

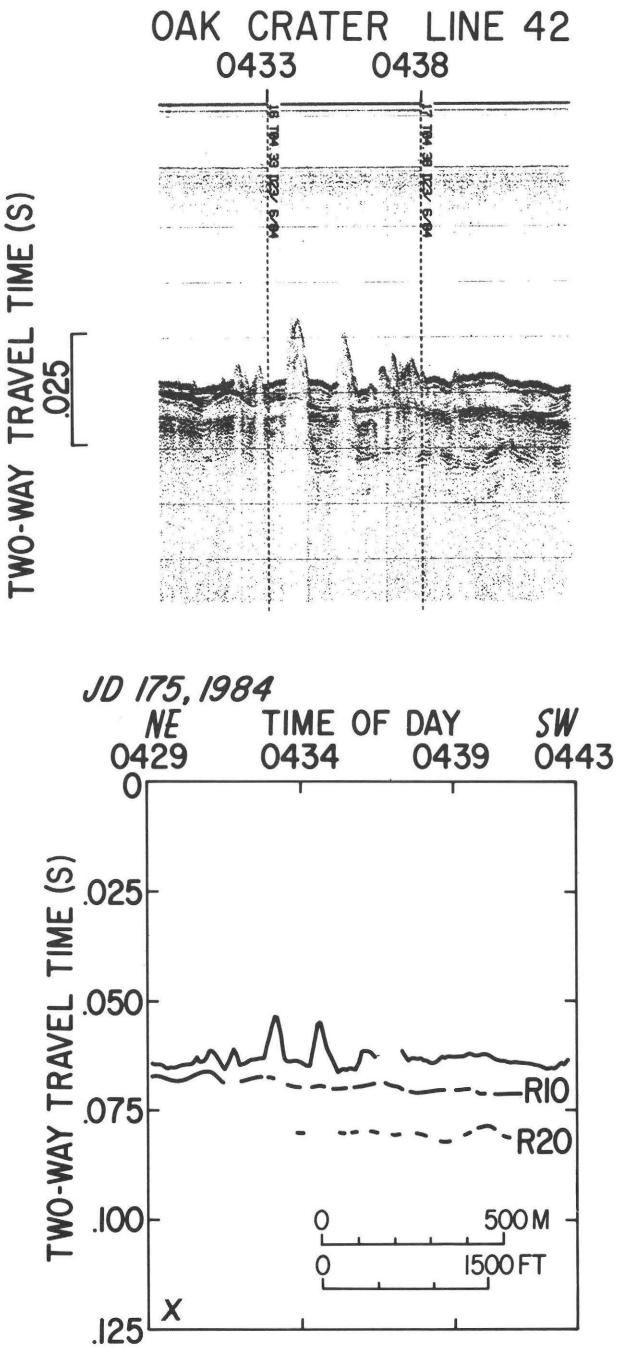

Figure 8—*Continued*

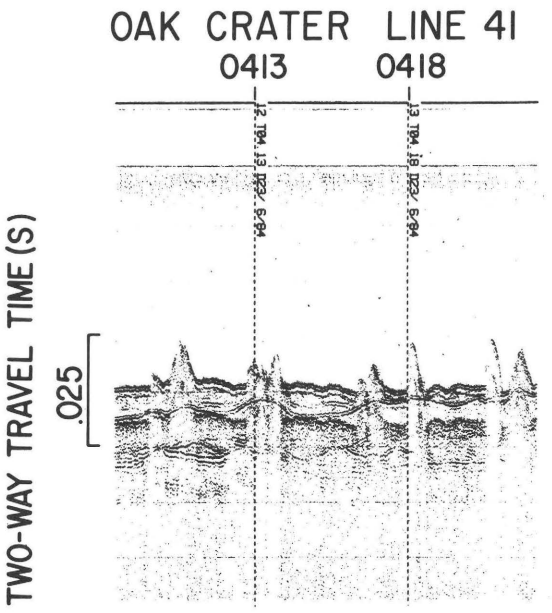
OAK CRATER LINE 41
0413
0418
TWO-WAY TRAVEL TIME (S)
.025

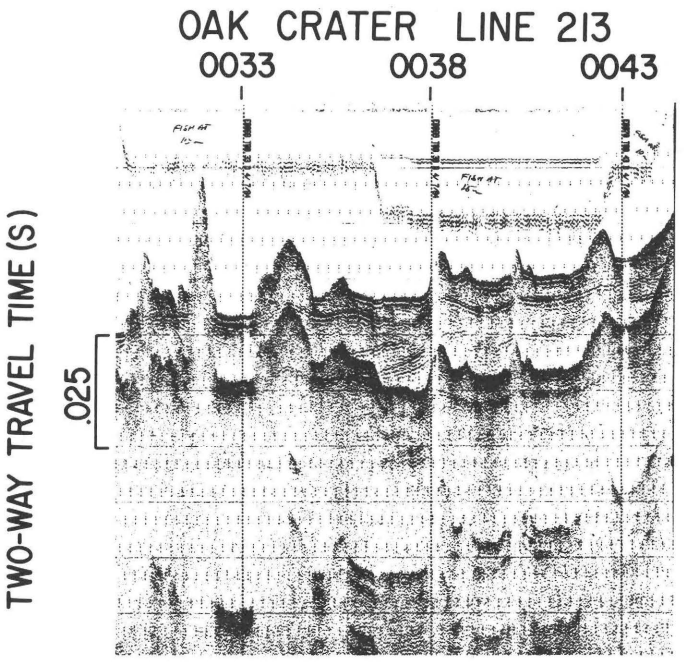
OAK CRATER LINE 213
0033
0038
0043
TWO-WAY TRAVEL TIME (S)
.025

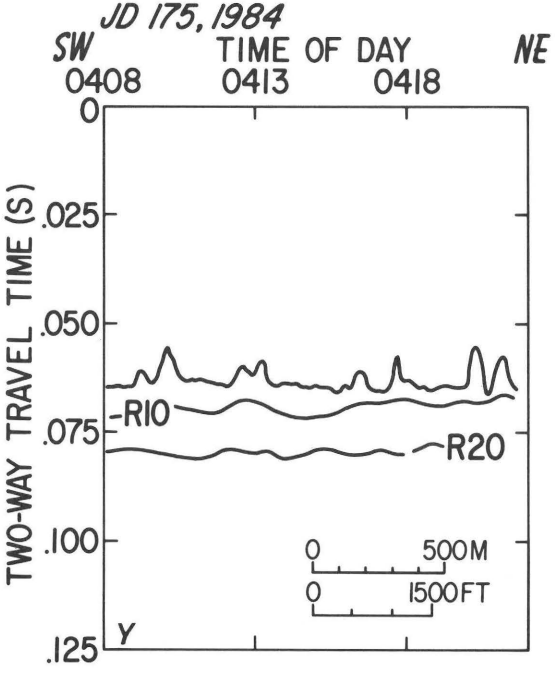
JD 175, 1984
SW
TIME OF DAY
NE
0408
0413
0418
TWO-WAY TRAVEL TIME (S)
0
.025
.050
.075
.100
.125
R10
R20
0
500M
0
1500FT
Y

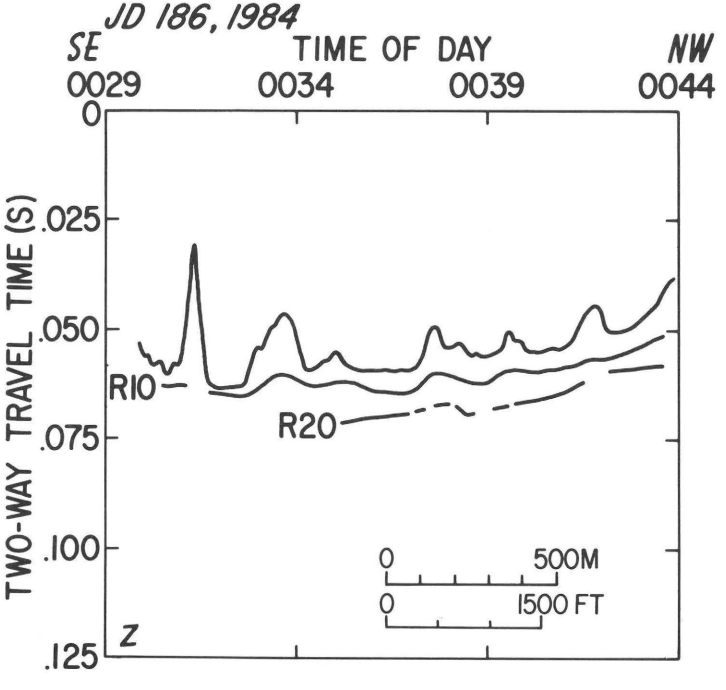
JD 186, 1984
SE
TIME OF DAY
NW
0029
0034
0039
0044
TWO-WAY TRAVEL TIME (S)
0
.025
.050
.075
.100
.125
R10
R20
0
500M
0
1500 FT
Z

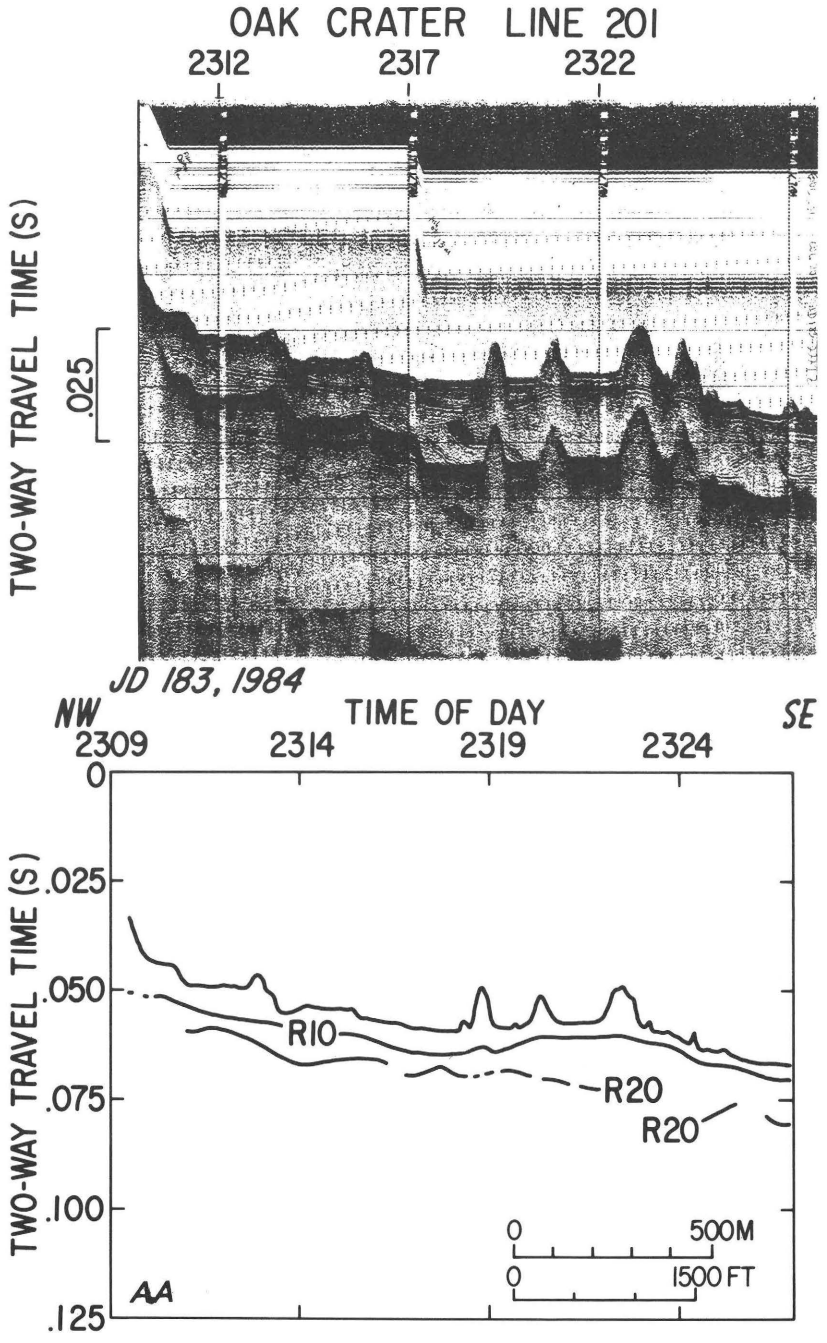
OAK CRATER LINE 201
2312
2317
2322
TWO-WAY TRAVEL TIME (S)
.025
JD 183, 1984
NW
TIME OF DAY
SE
2309
2314
2319
2324
0
.025
.050
.075
.100
.125
R10
R20
R20
0
500M
0
1500 FT
AA

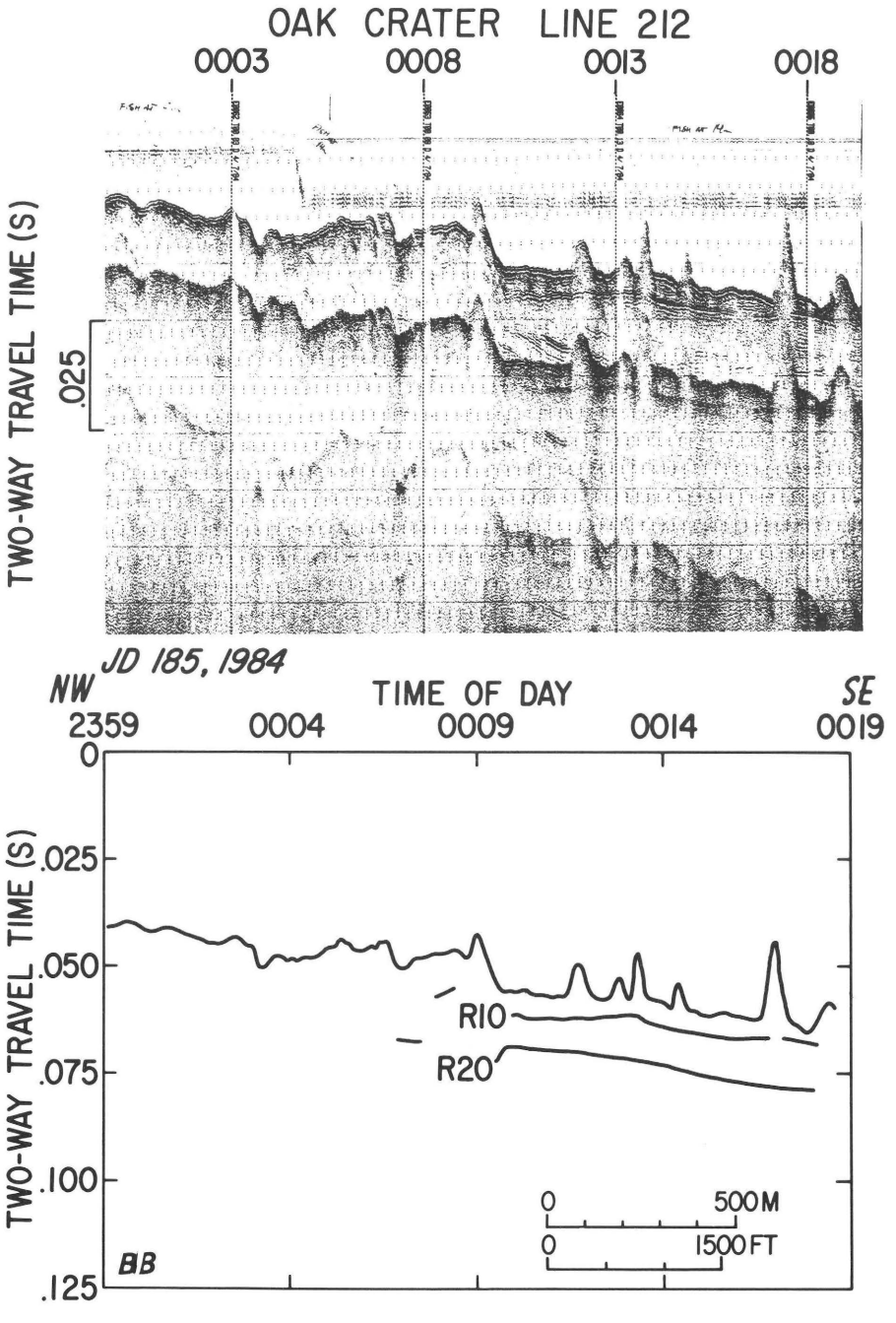
OAK CRATER LINE 212
0003
0008
0013
0018
TWO-WAY TRAVEL TIME (S)
.025
JD 185, 1984
NW
TIME OF DAY
SE
2359
0004
0009
0014
0019
0
.025
.050
.075
.100
.125
R10
R20
0
500M
0
1500 FT
BB

Figure 8—*Continued*

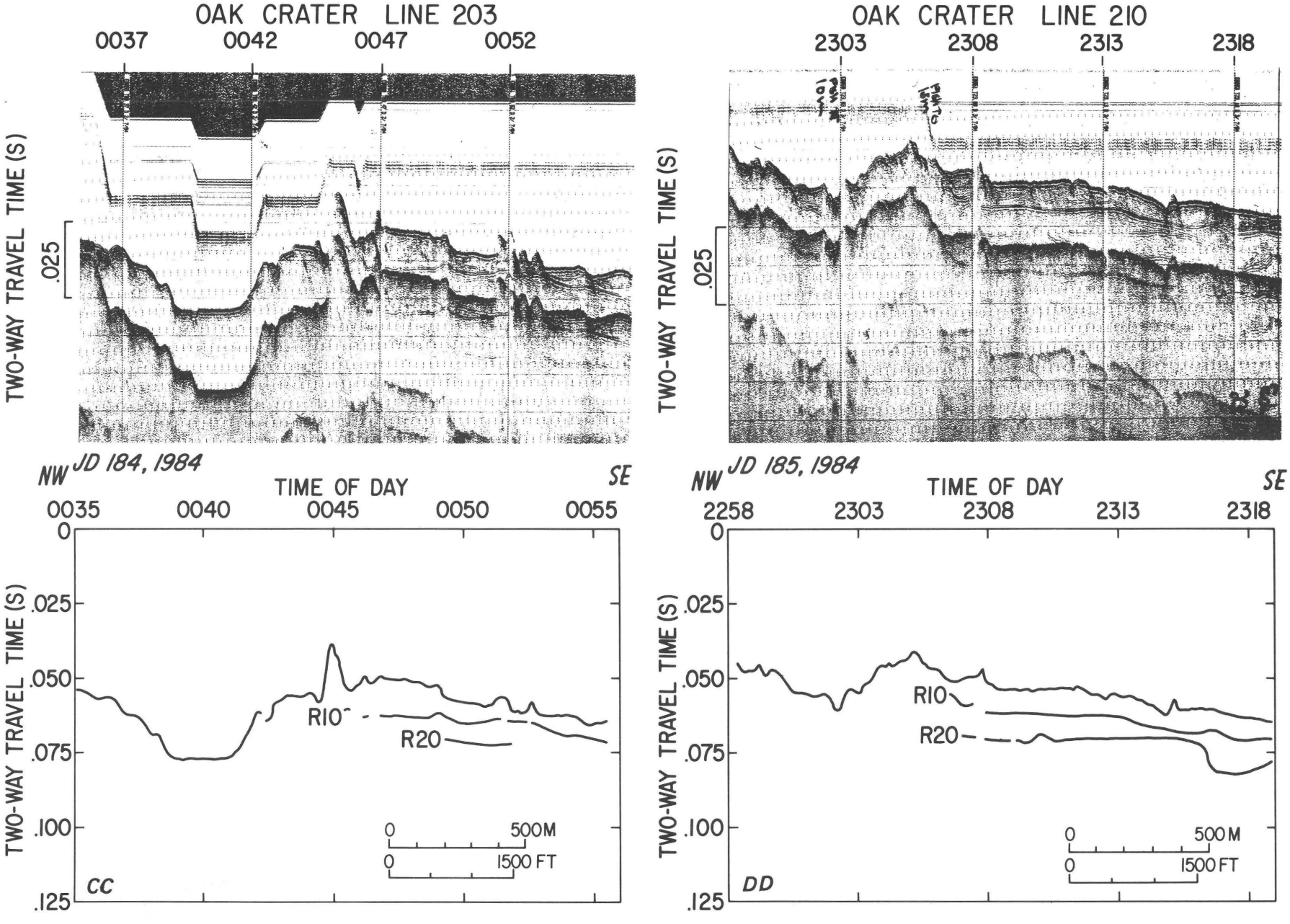

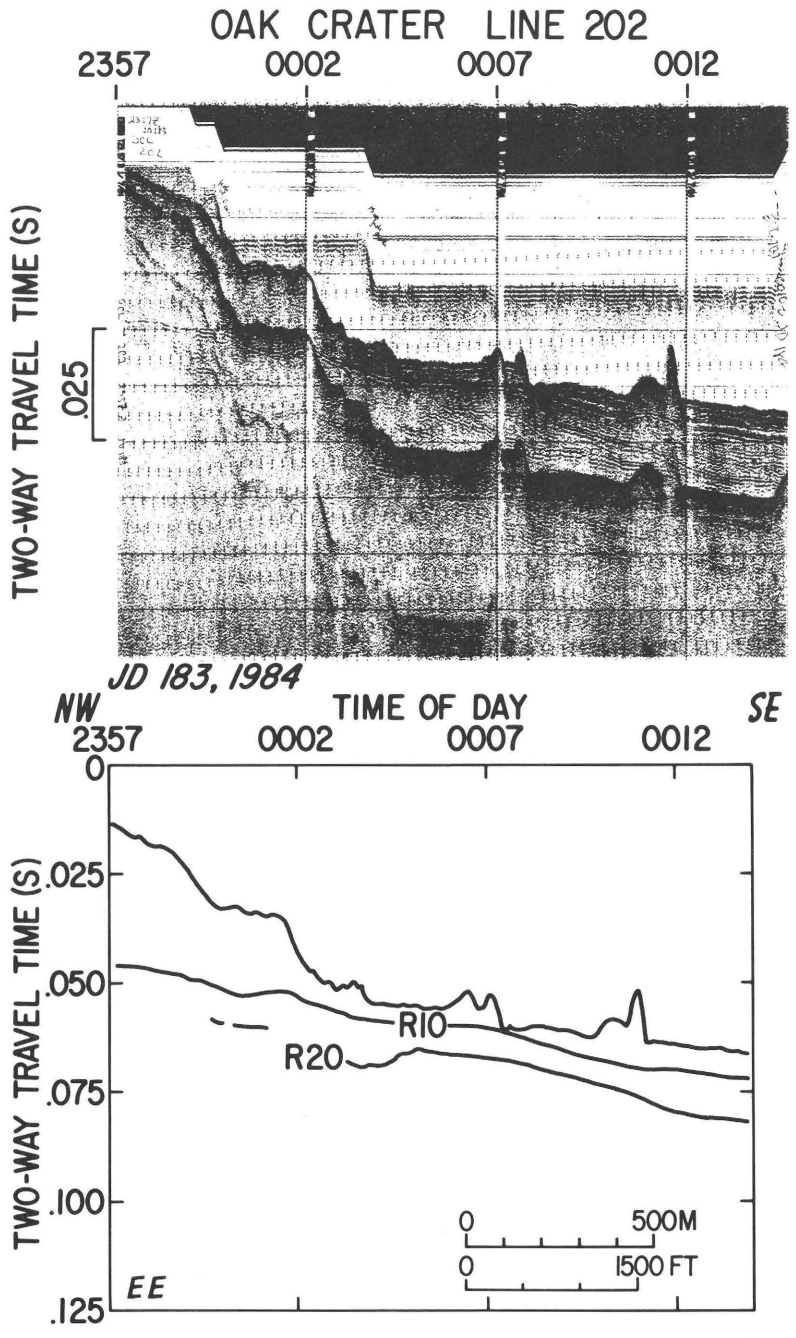
OAK CRATER LINE 202
2357
0002
0007
0012
TWO-WAY TRAVEL TIME (S)
.025
JD 183, 1984
NW
TIME OF DAY
SE
2357
0002
0007
0012
0
.025
.050
.075
.100
.125
R10
R20
0
500M
0
1500 FT
EE

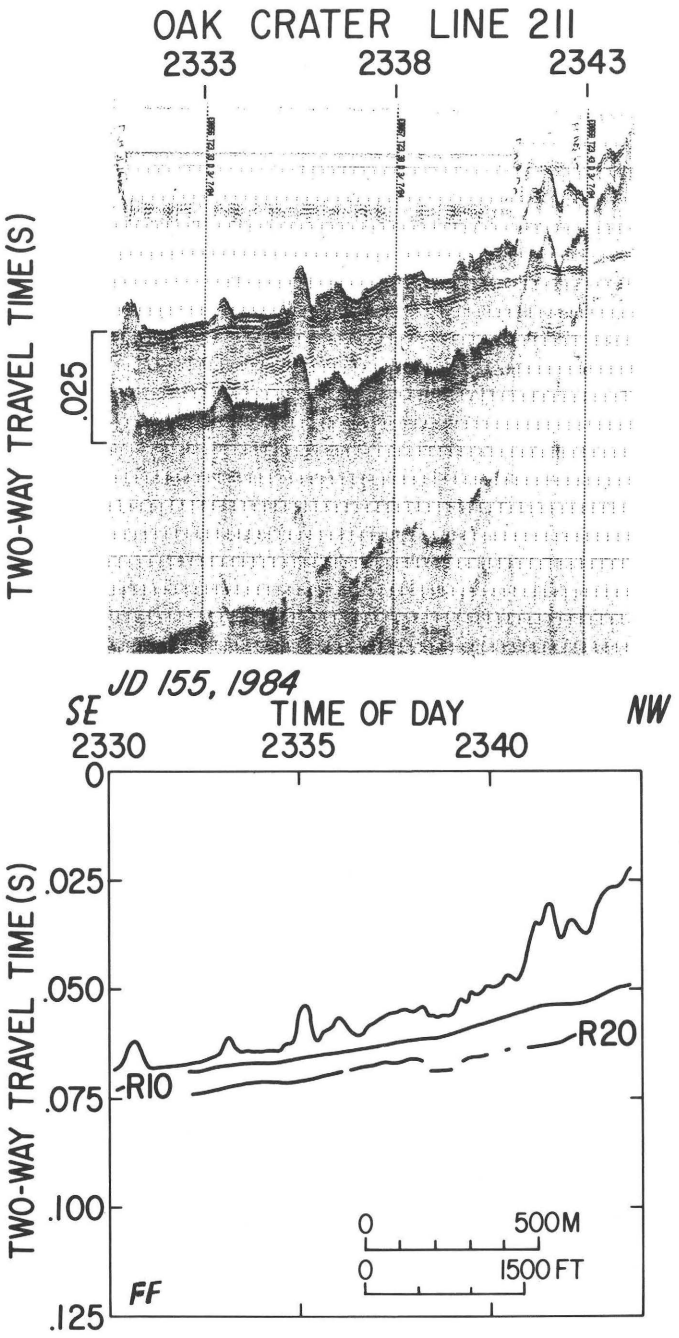
OAK CRATER LINE 211
2333
2338
2343
TWO-WAY TRAVEL TIME (S)
.025
JD 155, 1984
SE
TIME OF DAY
NW
2330
2335
2340
0
.025
.050
.075
.100
.125
R10
R20
0
500M
0
1500 FT
FF

Figure 8—*Continued*

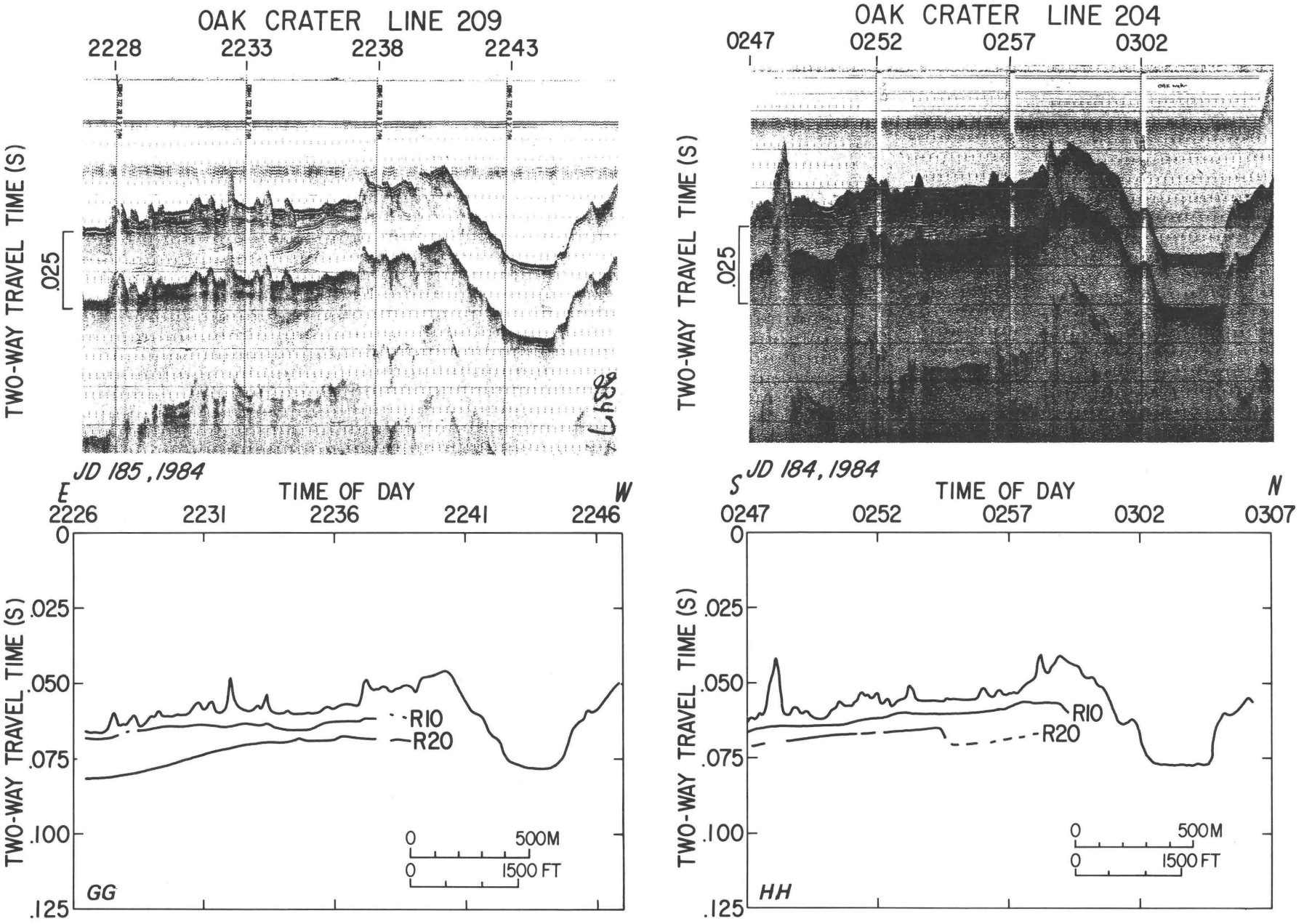

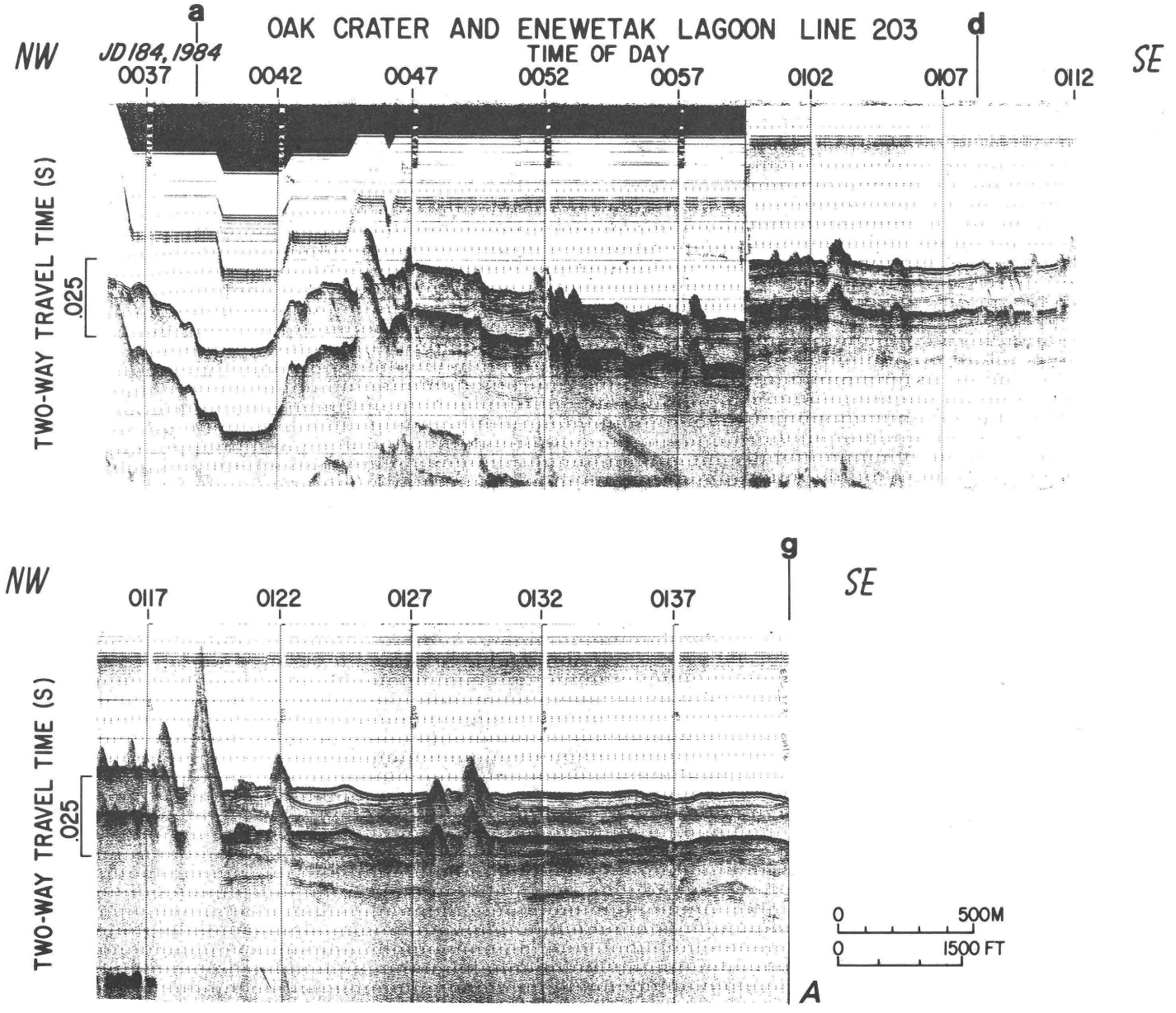

Figure 9. *A–I*, Subbottom profiles of lagoon areas. Tracks and locations a–*I* are shown on figure 4. *A*, line 203; *B*, line 204; *C*, line 205; *D*, line 209; *E* and *F*, line 206; *G* and *H*, line 207; *I*, line 208. Date given in Julian day (JD) and year.

Figure 9—*Continued*

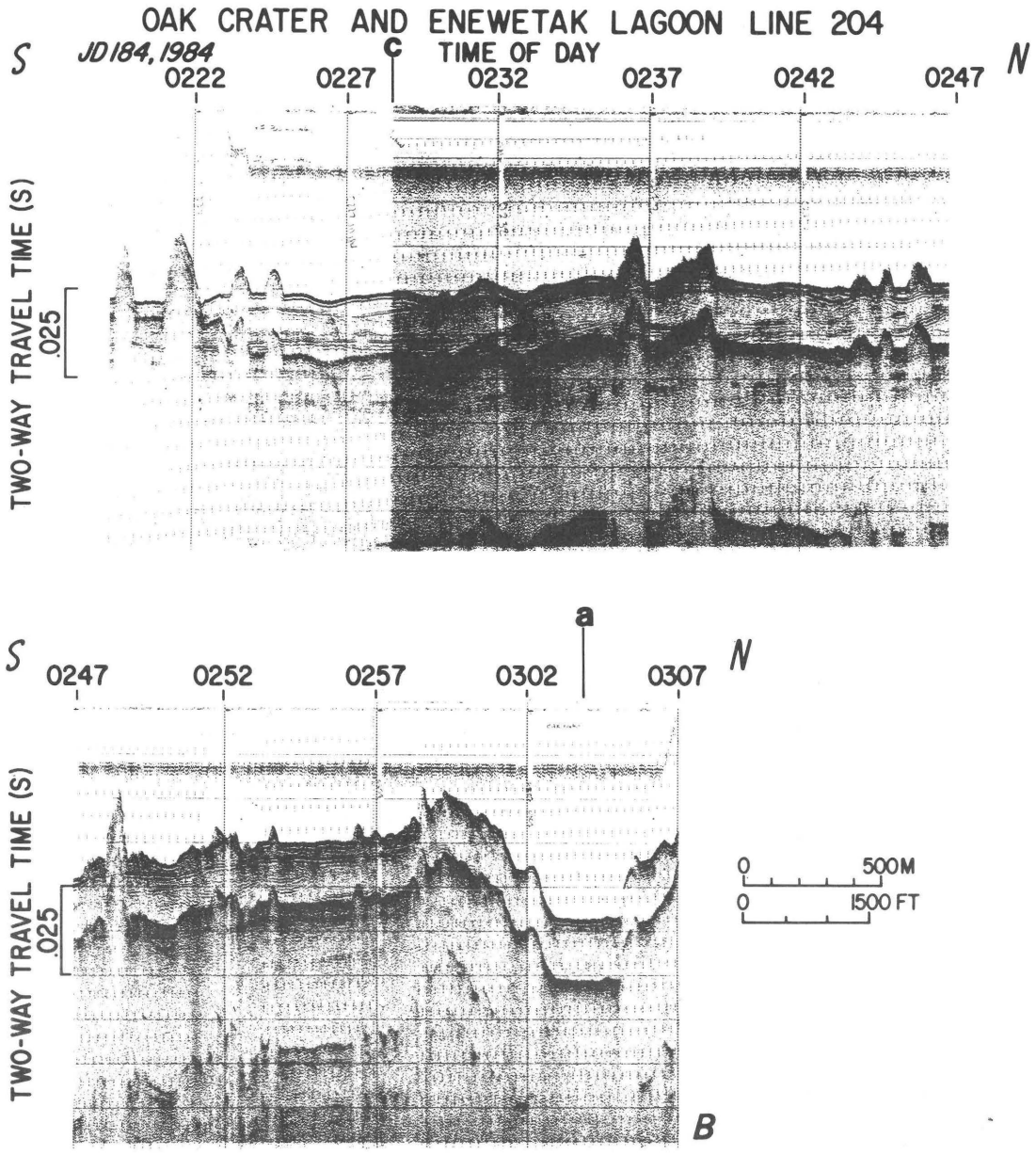

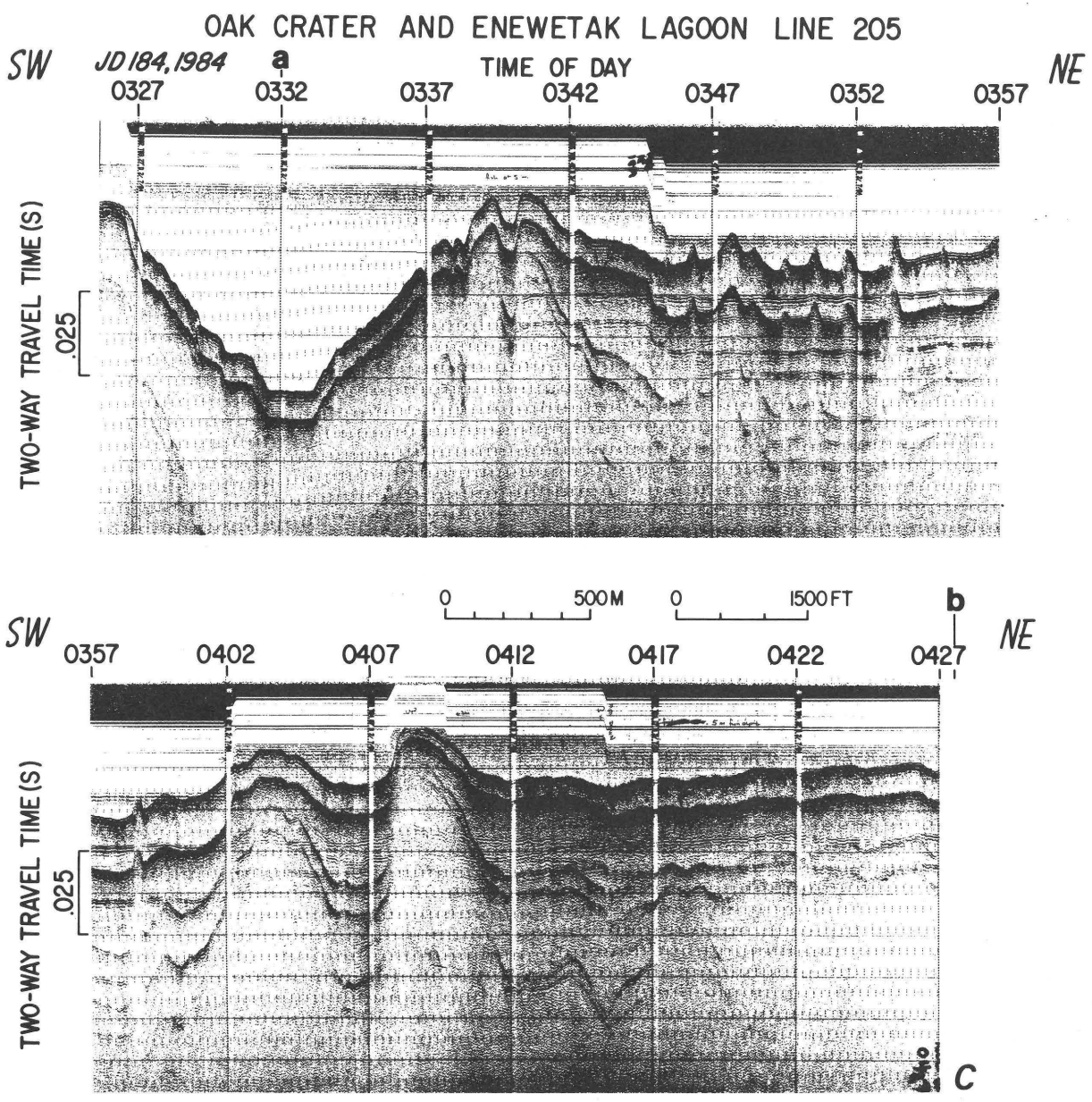

Figure 9—*Continued*

Figure 9—*Continued*

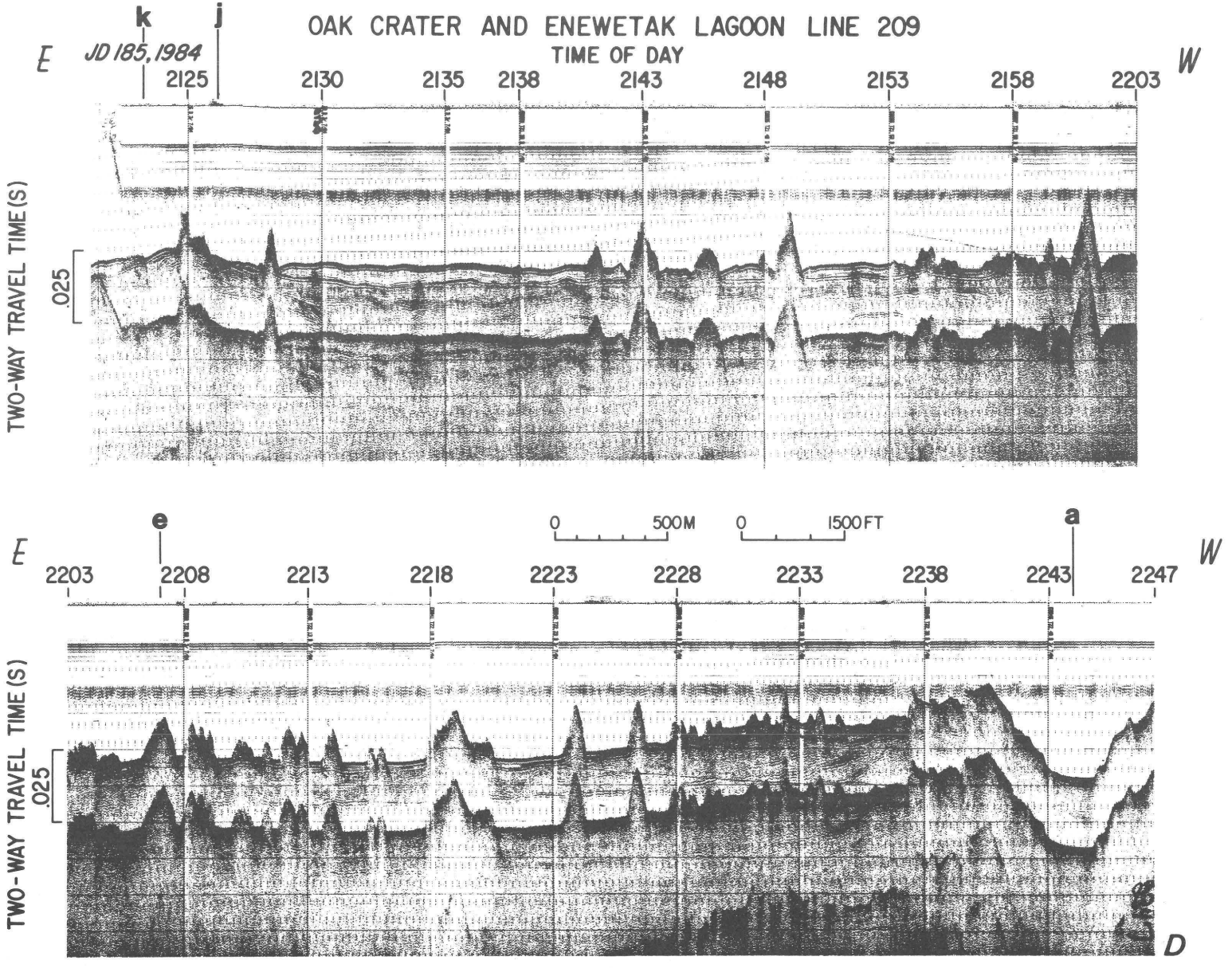

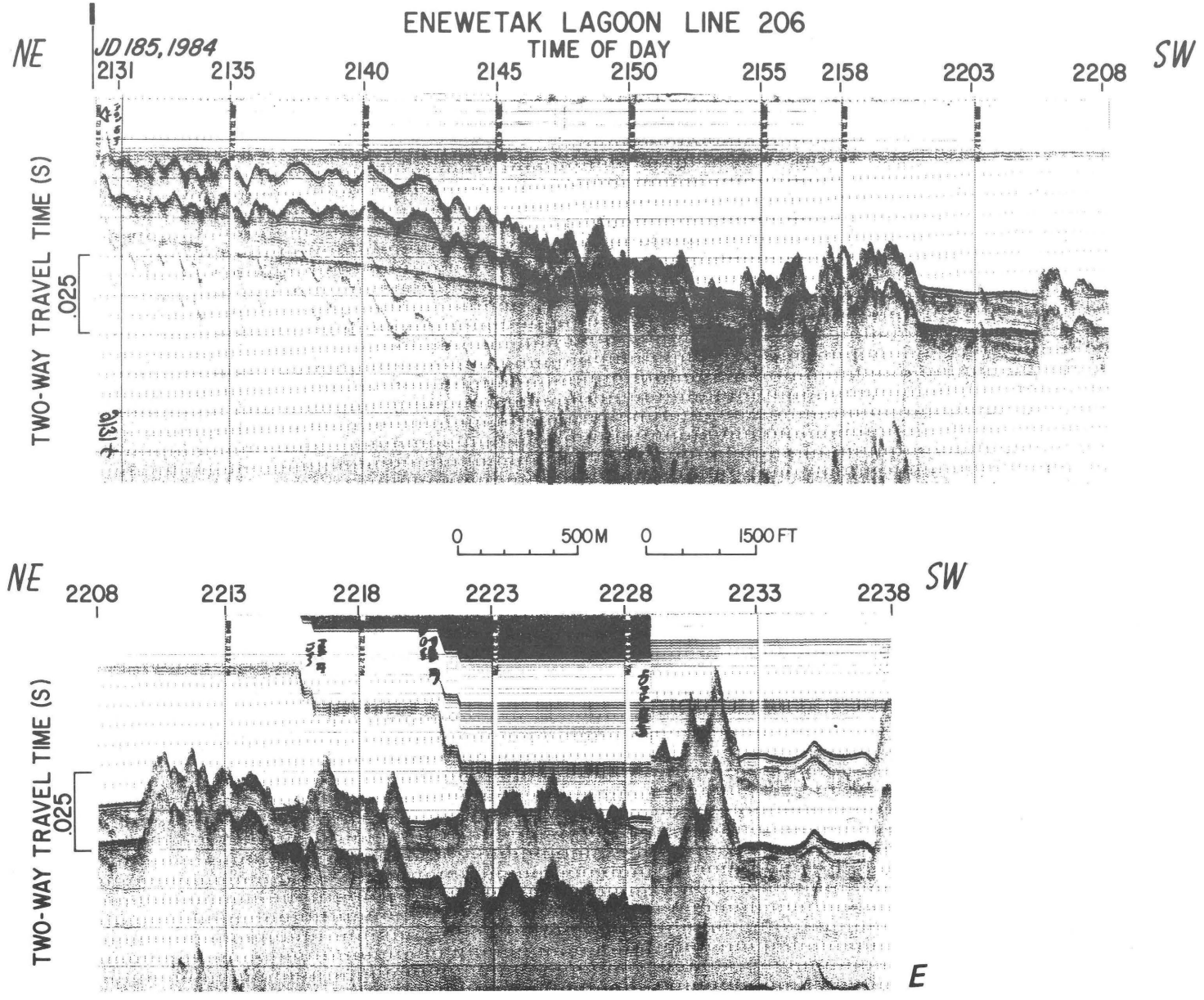

Figure 9—*Continued*

Figure 9—*Continued*

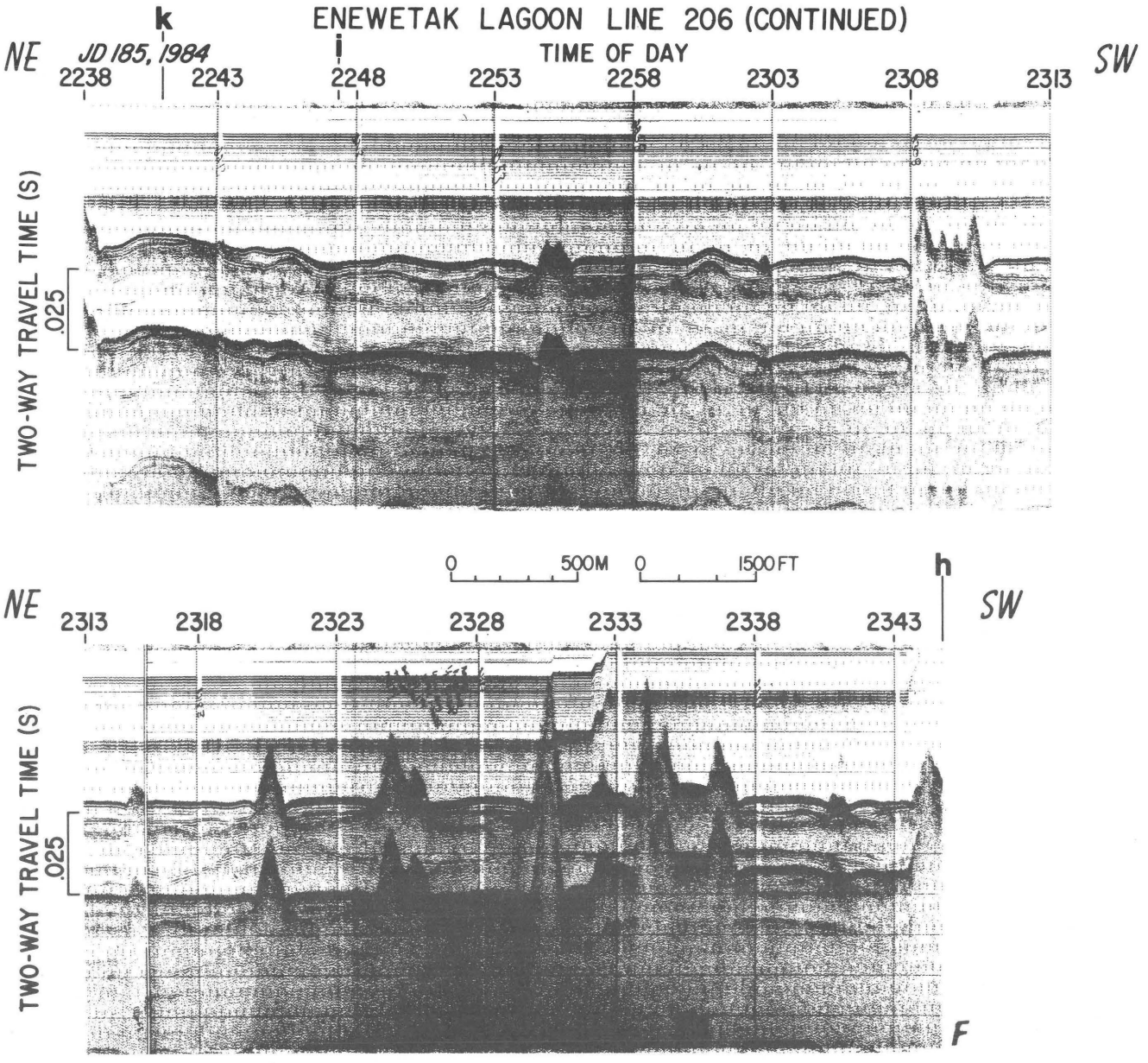

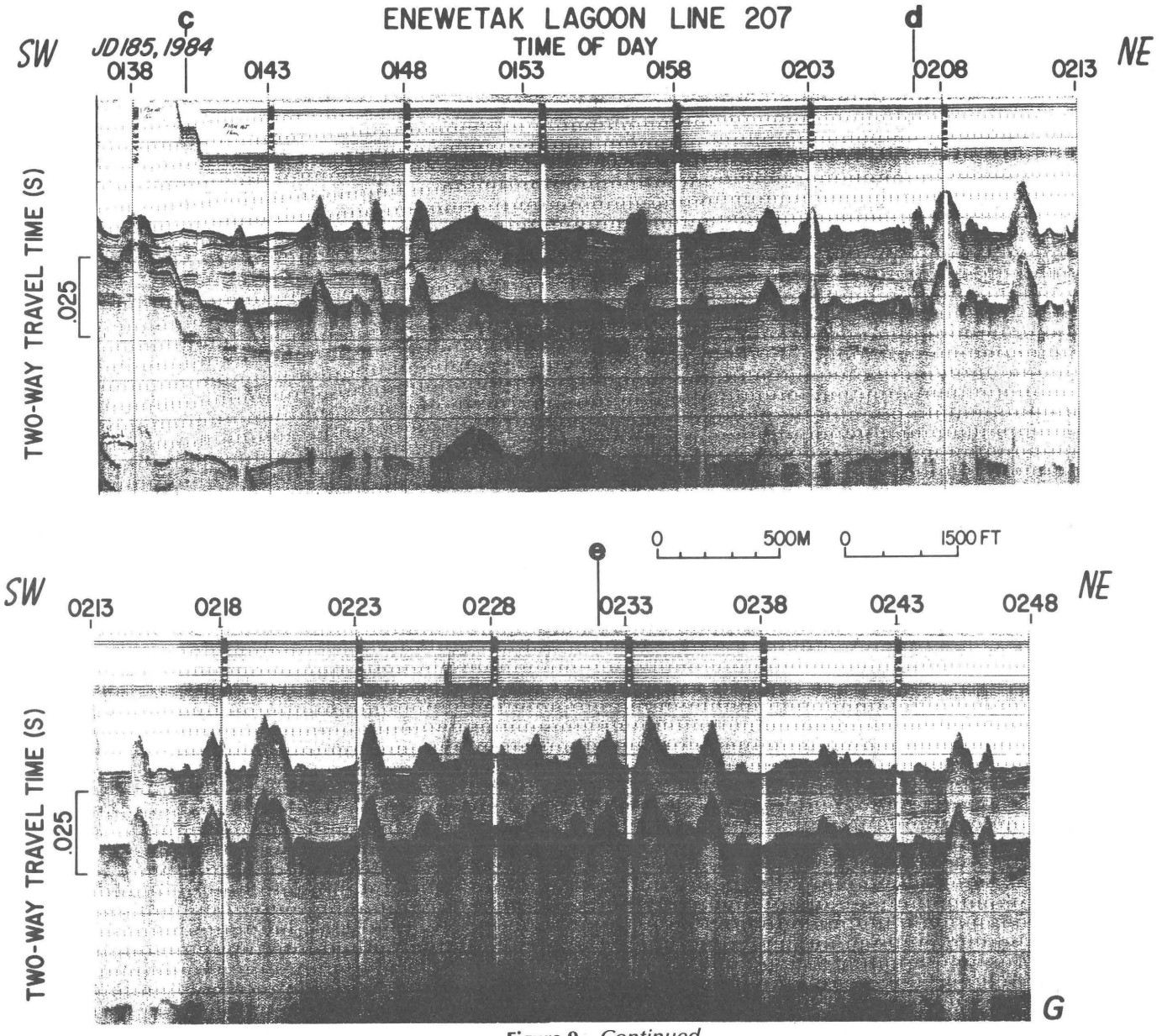

Figure 9—*Continued*

Figure 9—*Continued*

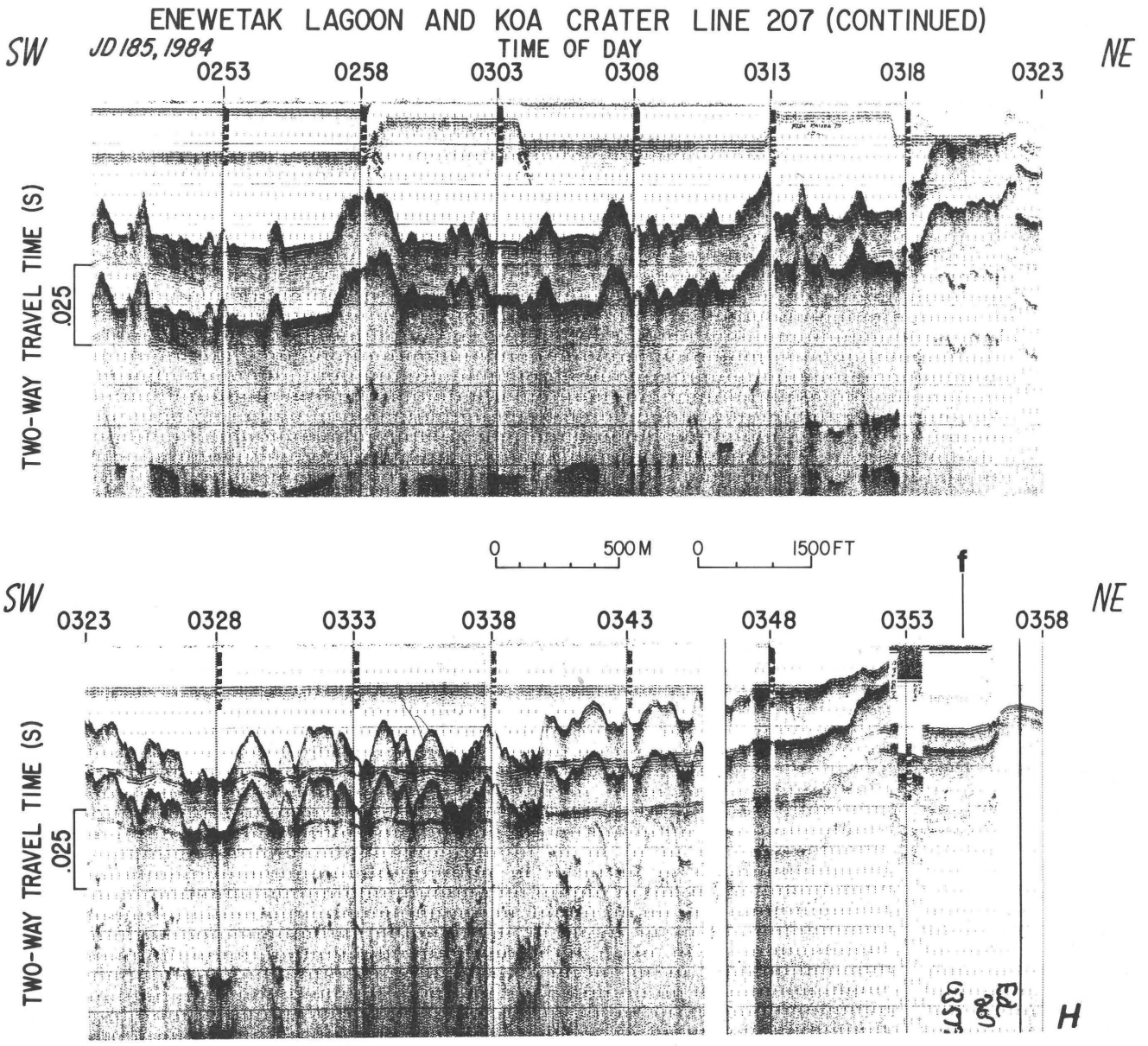

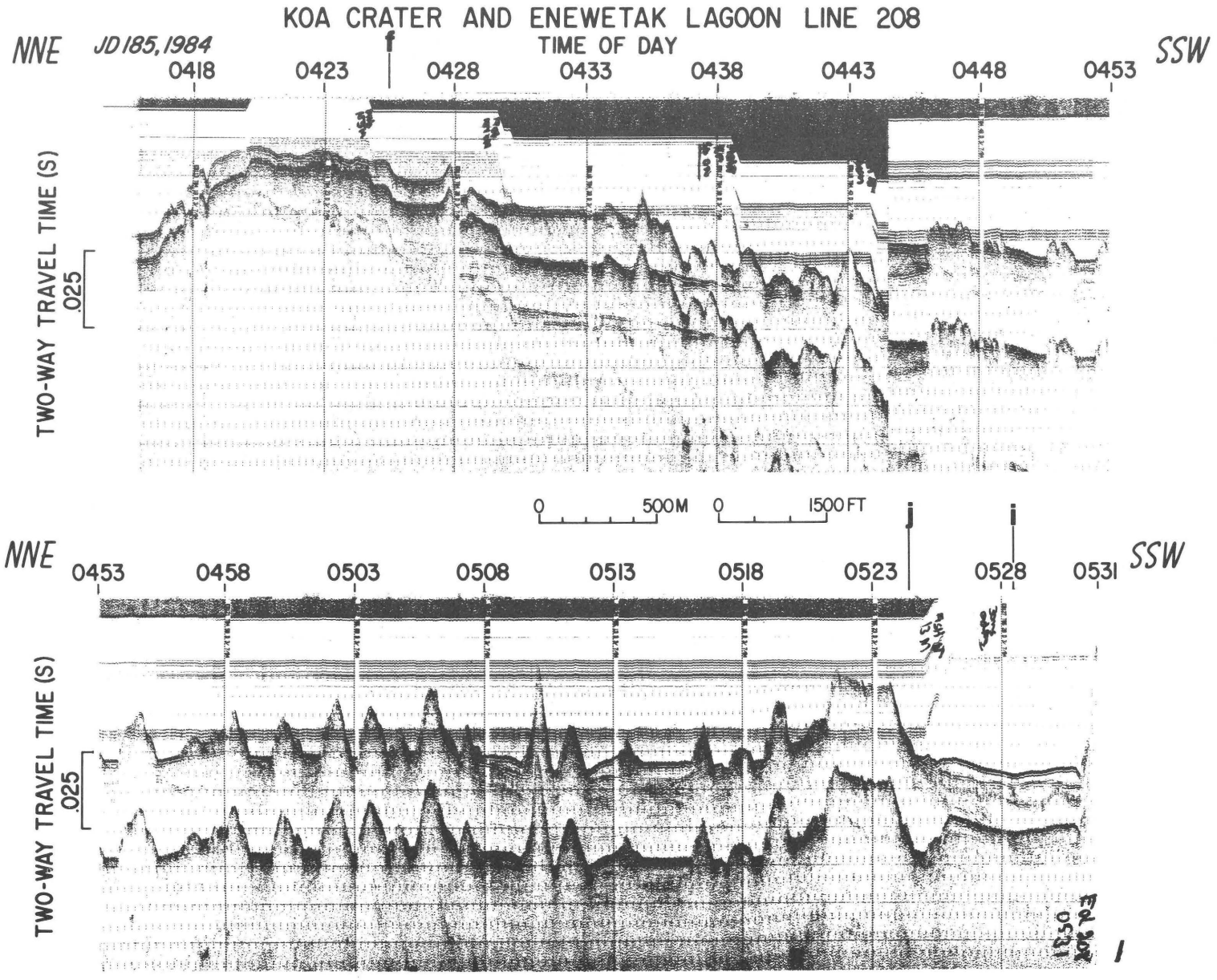

Figure 9—*Continued*

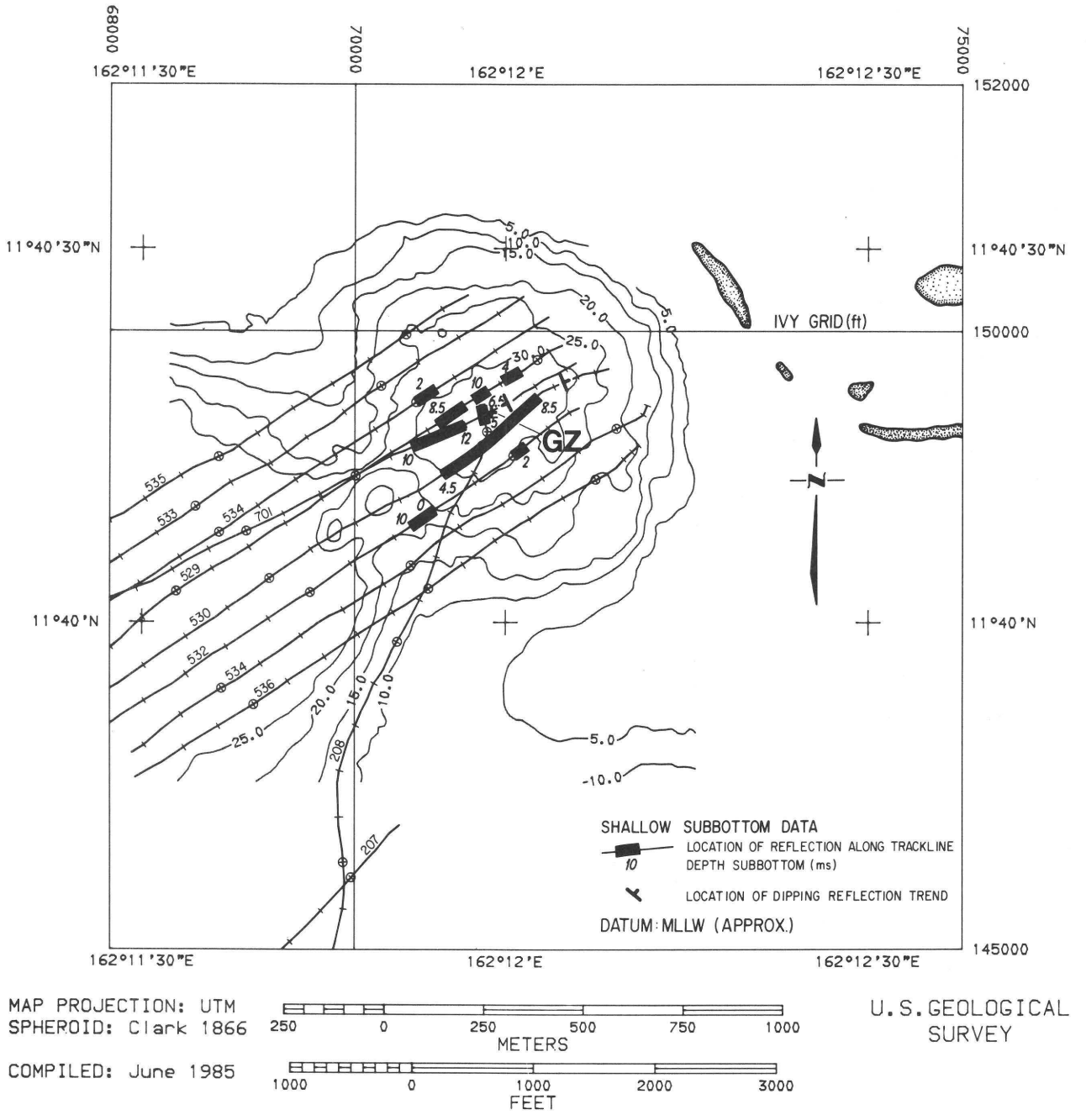

Figure 10. Locations and spot depths of subbottom reflectors shown by Huntec profiles in KOA crater. GZ=ground zero. Contour interval is 5 m. Datum is mean lower low water (approx).

lines 77, 78, and 79 appears highly fragmented to discontinuous in its inner part (figs. 8*G–I*) and is absent from the middle of line 89, although a weak trace of R20 is present (line 89, figs. 8*K*, 18). A small segment of R10 may have overridden itself a few meters in small thrusts or reverse faults that dip toward ground zero. (See line 79, fig. 8*I* at 0517; and line 88, fig. 8*J* at 0313.)

In the southeast quadrant, R10 is less downturned than in the southwest quadrant, but it is disturbed at 870 m (2,850 ft) from ground zero along line 82 (fig. 8*O*, 2242–2245; fig. 18). Clear deformation and fractures of the R10 surface are found 640 m (2,100 ft) from ground zero on line 203 (fig. 8*CC*, 0047–0048). Probable fragments of R10 lie only 580 m (1,900 ft) from ground zero (fig. 18, and line 90, fig. 8*L*, 0434–0438). However, R10 appears to be absent within 730 m (2,400 ft) of ground zero in a salient to the east-southeast. Apparently, fragments of R20 are present in this quadrant at distances as close as 490 m (1,600 ft) from ground zero (line 89, fig. 8*K*). The geometry cannot be described in detail because the profiles are

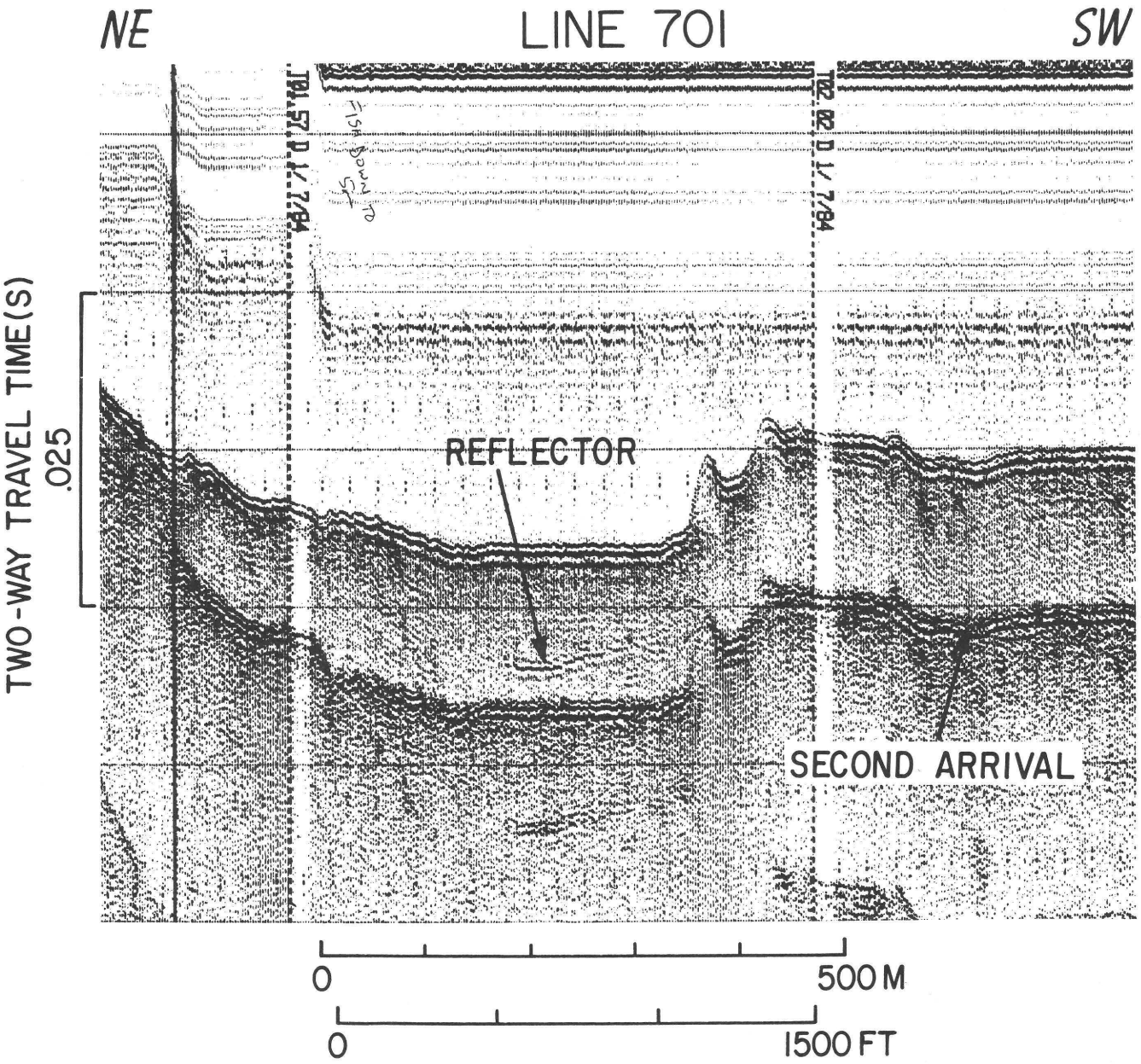

Figure 11. Reflector below southwest wall and floor (line 701), KOA crater. Vertical scale markers are 12.5 m apart. Dashed event marks are 5 minutes apart. Compare figures 6*E* and 10.

primarily strike lines in this area; line 203 is the only crossing line. There are crenulations and breaks in R10 in the central part of line 89 (figs. 8*K*, 19). A small graben in the bottom of the southeastward-trending valley 760 m (2,500 ft) from ground zero (see chap. A, fig. 9, this volume) shown in line 99 (figs. 8*N*, 20), appears to be about 60 m (200 ft) across, to displace the sea bottom by about 1 m (3 ft) and R10 by about 0.5 m (1.5 ft).

The northeast quadrant shows abrupt termination of R10 accompanied by little downturning (fig. 18). Fractured segments 60 to 150 m (200–500 ft) in extent are found along lines 205, 77, and 90 (figs. 8*D*,*G*,*L*) before terminating in the crater. An outer limit of deformation (folding) can be picked at 1,040 m (3,410 ft) from ground zero on lines 7699 and 77 (figs. 8*F*–*G*) or at about 800 m (2,620 ft) from ground zero on lines 89 and 90 (figs. 8*K*–*L*). Termination points of R10 lie at 550 m (1,800 ft) from ground zero on line 77 to 580 m (1,900 ft) on lines 79 and 89. Separated fragments, perhaps of R20, lie as close as 410 m (1,350 ft) to ground zero in this area (fig. 18).

Especially in the southeast quadrant, R10 and R20 can be traced closer to ground zero on some multichannel profiles than on the single-channel profiles. This is probably due to the greater power and depth of penetration of the multichannel system as well as to acquisition and processing techniques which enhance horizontal reflectors. (See chap. D, this volume.)

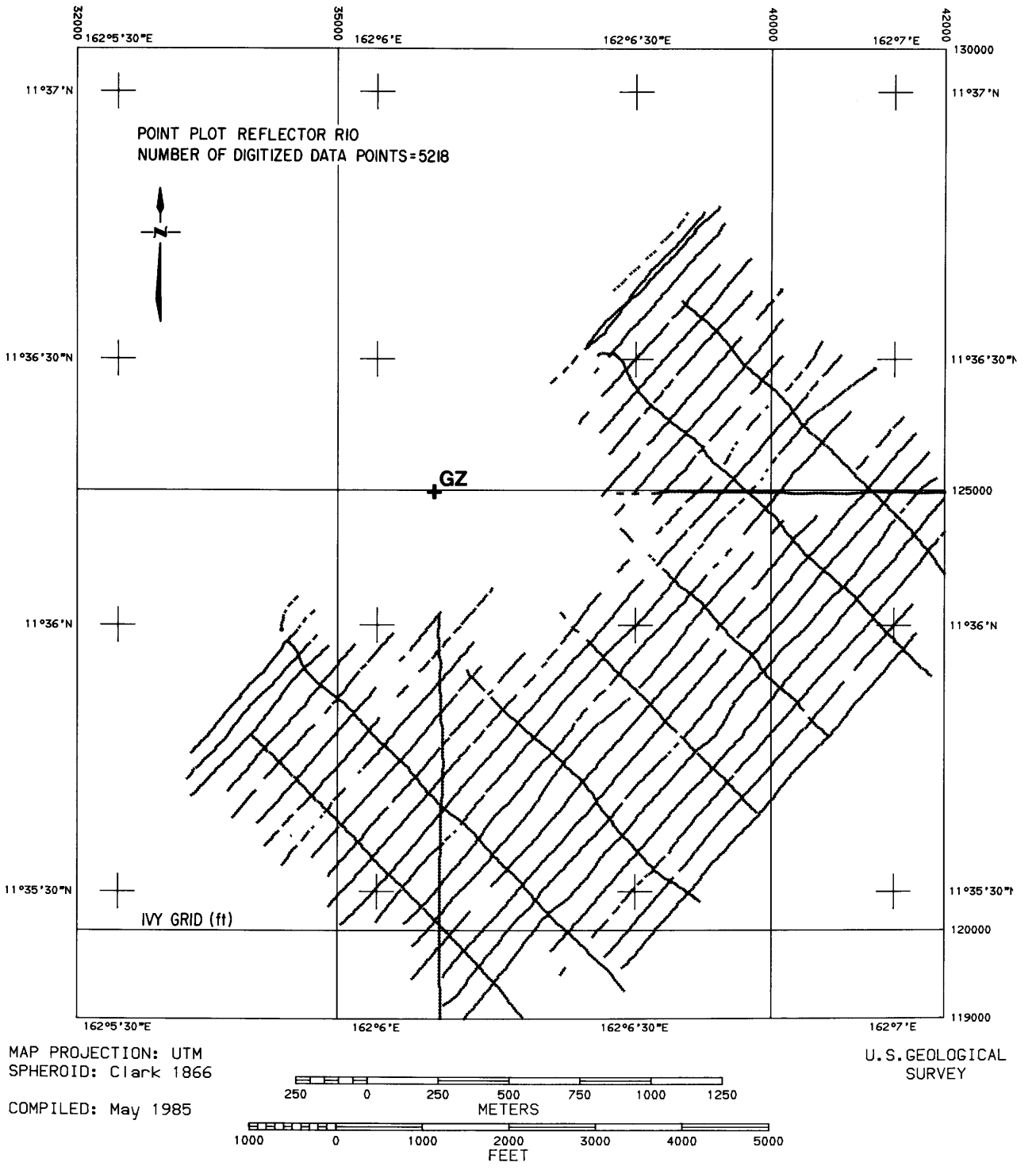

Figure 12. Locations of digitized points on reflector R10 surface, OAK crater, used to prepare structure maps and thickness contours. GZ=ground zero.

Shallow Subsurface Character of the Central Part of OAK Crater

The crater is crossed by nine lines parallel to the reef, one line orthogonal to the reef, and two diagonal lines. Within the bowl of the crater, the Huntec profiles show only weak reflectors. Some dim subbottom laminations that may represent postevent deposits (figs. 21, 22) extend to at least 13 ms (10.5 m, or 35 ft) subbottom under the crater floor, or to about 8 ms (6.4 m, or 21 ft) in places on the crater slopes.

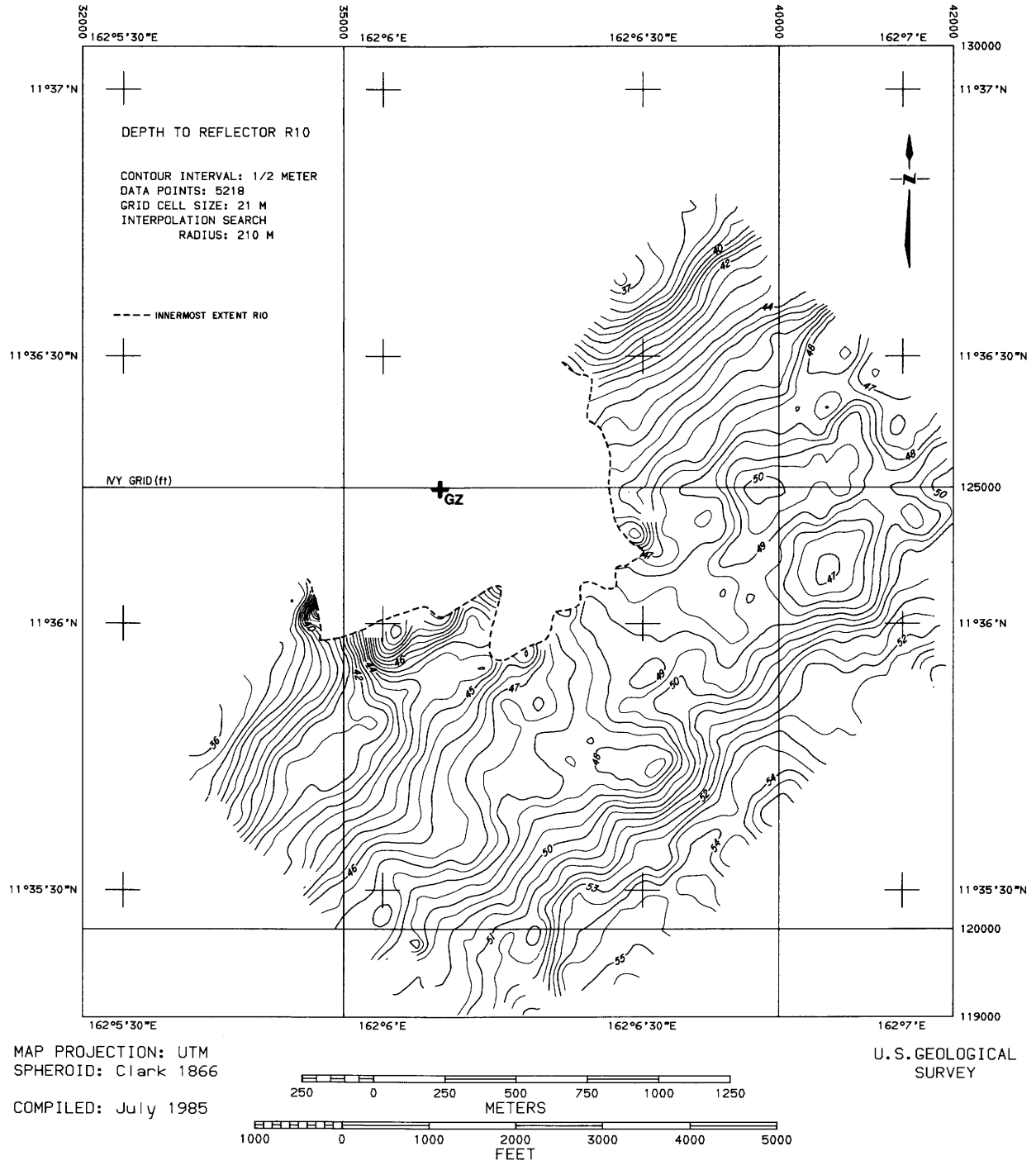

Figure 13. Structure contours (depth below sea level) for OAK crater, reflector R10 surface, constructed assuming velocities of 1,542 m/s in seawater and 1,650 m/s subbottom.

Our mapping of arcuate faults or slide blocks and terraces within the crater is based on interpretations of the subbottom profiles integrated with bathymetric data. (See fig. 18.) Because of the orientation of the profiles, such features are delineated better on the northeast and southwest slopes than on the southeastern slope. One example of displacement of subsurface reflectors is illustrated on line 75 (figs. 8*E*, 22) and on line 205, where a terrace-like surface was formed by a downslid block on the southwest slope (fig. 8*D*, about 0331).

Surficial Debris

We classified surficial deposits around OAK crater into proximal and distal debris on the basis of morphology and seismic signature (fig. 23).

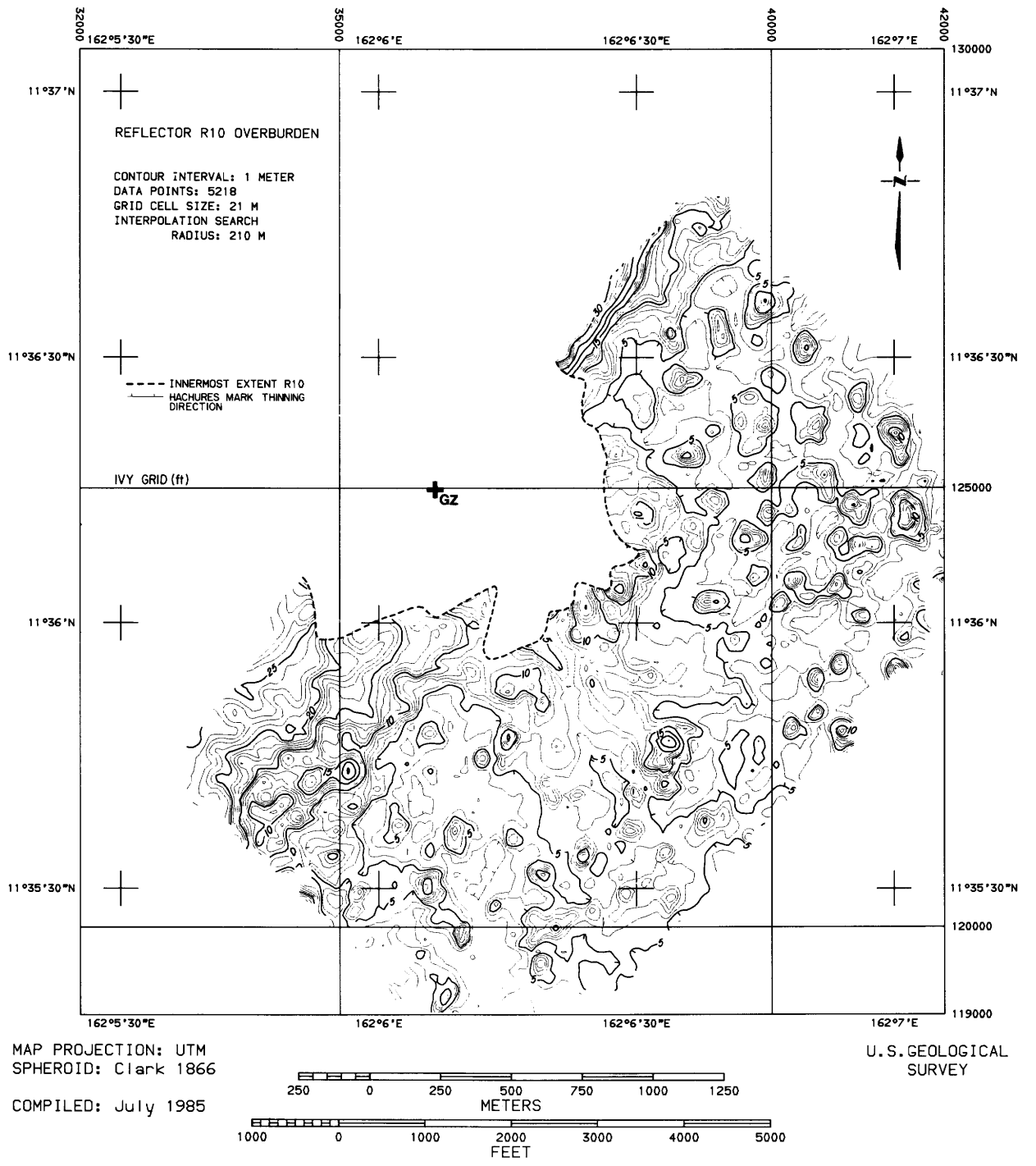

Figure 14. Thickness of overburden (isopach) over reflector R10, OAK crater, constructed assuming 1,650 m/s sound velocity. GZ=ground zero.

The proximal accumulations of debris form mounds locally around the crater; R10 is deeply buried (for example, line 98, fig. 8*M*, southwest of crater). Debris mounds have a rough surface compared to surrounding areas. Patch reefs are absent or covered. Acoustically, the material is commonly amorphous or chaotic. The boundaries of the deposits that we identify as proximal debris coincide closely with areas of net accumulation determined from comparison of preshot and postshot bathymetry (chap. A, fig. 14, this volume).

Deposits of distal debris, in contrast to the proximal debris, are thinner; R10 is less deeply buried, and the bottom is rough (for example, line 63, fig. 8*R*, 0507–0512). In the subsurface, distal debris deposits are acoustically chaotic. They overlie a poorly definable surface and lap onto patch reefs.

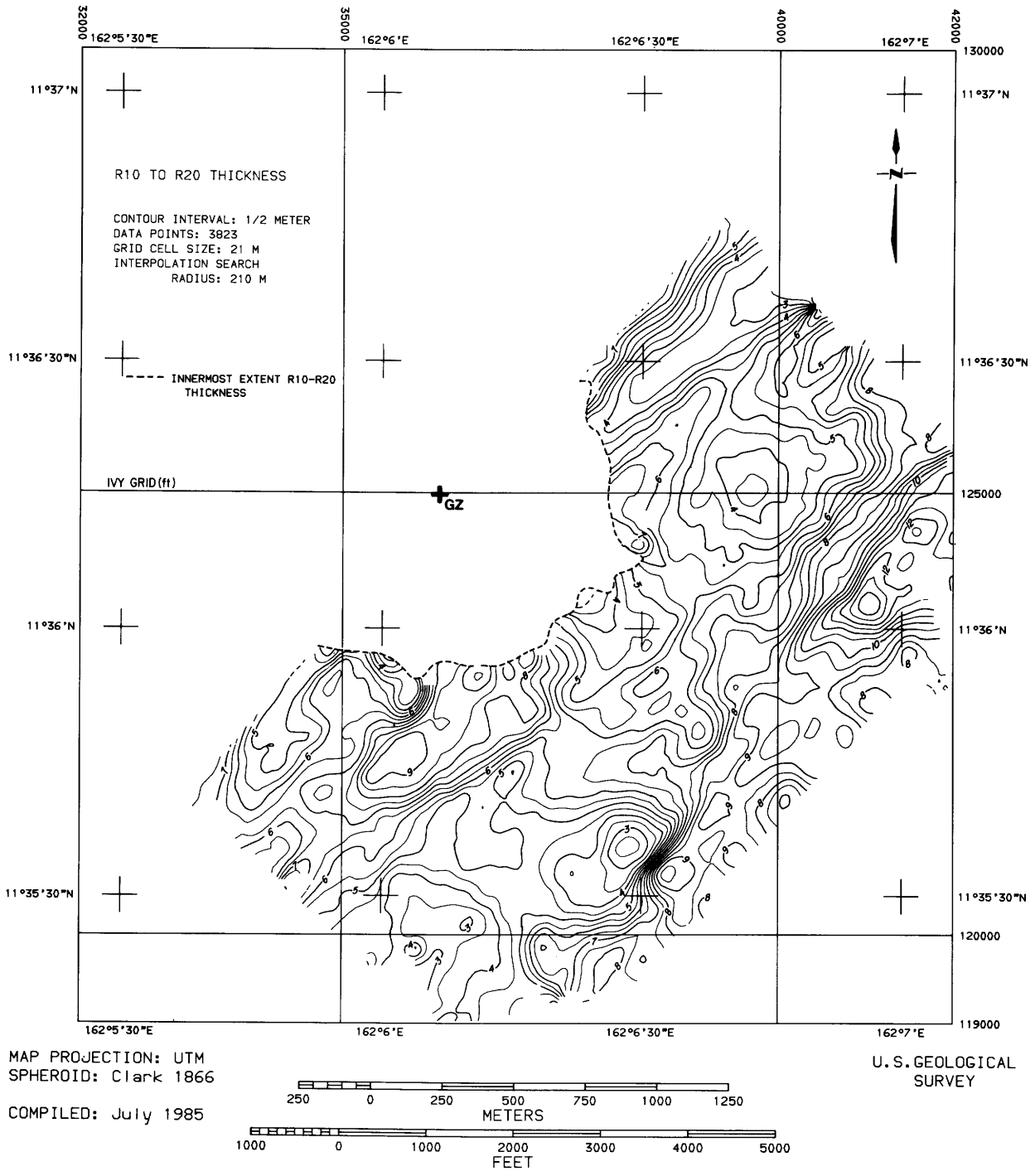

Figure 15. Thickness (isopach) of sediment between reflectors R10 and R20, OAK crater, constructed assuming 1,650 m/s sound velocity. GZ=ground zero.

Surficial deposits outside the main area of debris accumulation, as shown by profiles in the lagoon, are commonly characterized by a smooth surface and even bedding (for example, line 209, fig. 9*D*). Some are ponded sediments and local overwash deposits. Because they are thin, R10 is close to the sea floor.

A relatively strong and consistent reflecting horizon was recorded within several mounds of otherwise amorphous or chaotic proximal debris that encircles the southeastern part of the crater (fig. 23). It crops out on both the inner and outer slopes of those mounds. (See lines 88, 89, 90, 98, 99, and 203, figs. 8*J–N,CC*; especially line 98 in fig. 8*M* between 0226–0232 and line 203 in fig. 8*CC* from 0047–0049). It is not detected near the reef in the northeast or southwest quadrants. The location of this intradebris reflector corresponds to areas of thick net accumulation

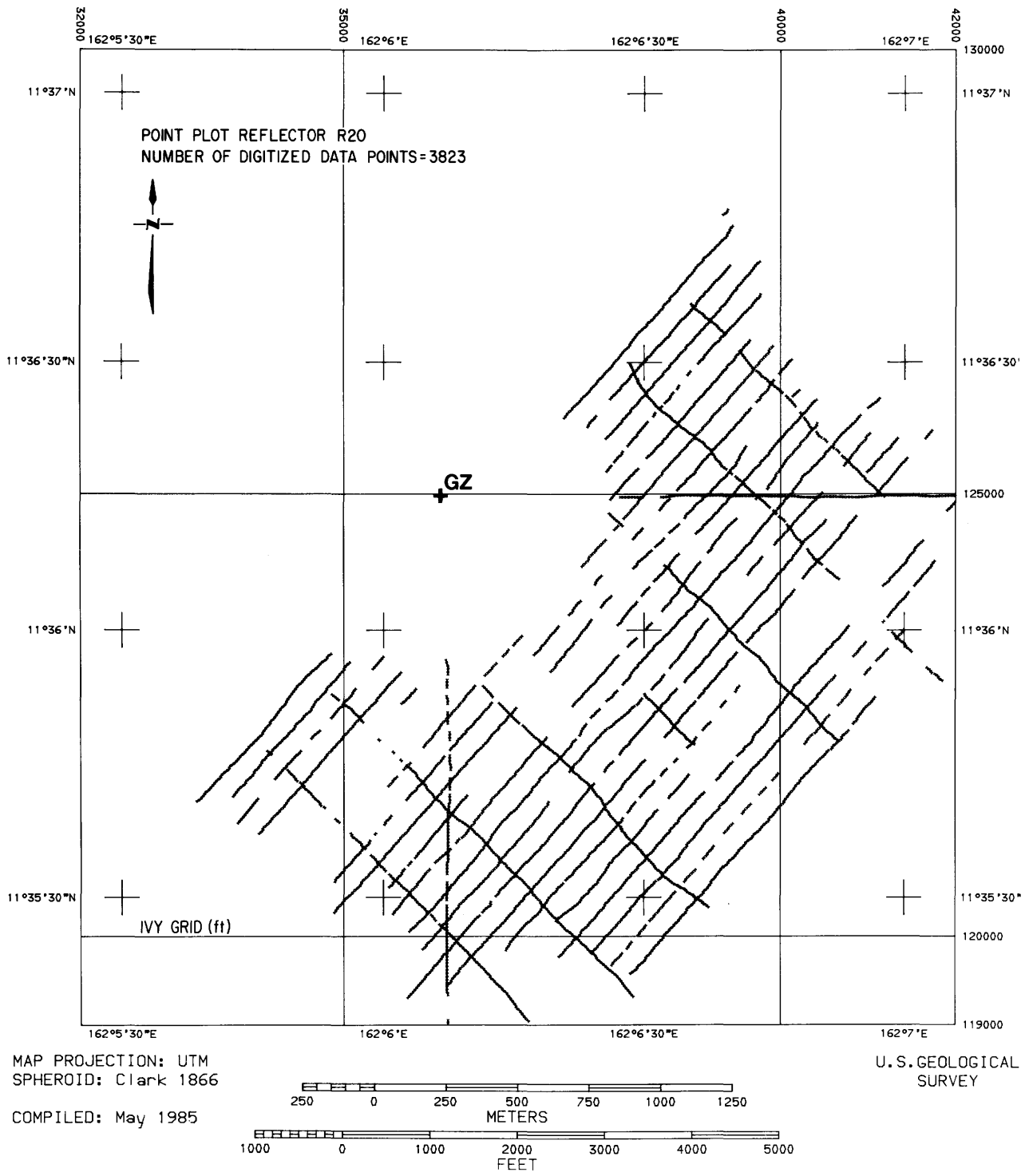

Figure 16. Locations of digitized points on reflector R20 surface, OAK crater, used to prepare structure maps and thickness contours. GZ=ground zero.

derived from the comparison of preshot and postshot bathymetry. (See chap. A, fig. 14, this volume.)

We suggest that this reflector may result from overthrust debris, or from an overturned flap (note especially line 203, 0047–0049, fig. 8*CC*). Further analysis of borehole samples may positively identify this important intradebris horizon.

Patch Reefs

Patch reefs are common features on the lagoon bottom. Our subbottom profiles show that most are young and have developed since the R10 surface was formed. Some appear to penetrate the R10 and R20 surfaces and hence are older. Shinn and others (chap. H, this volume) found that

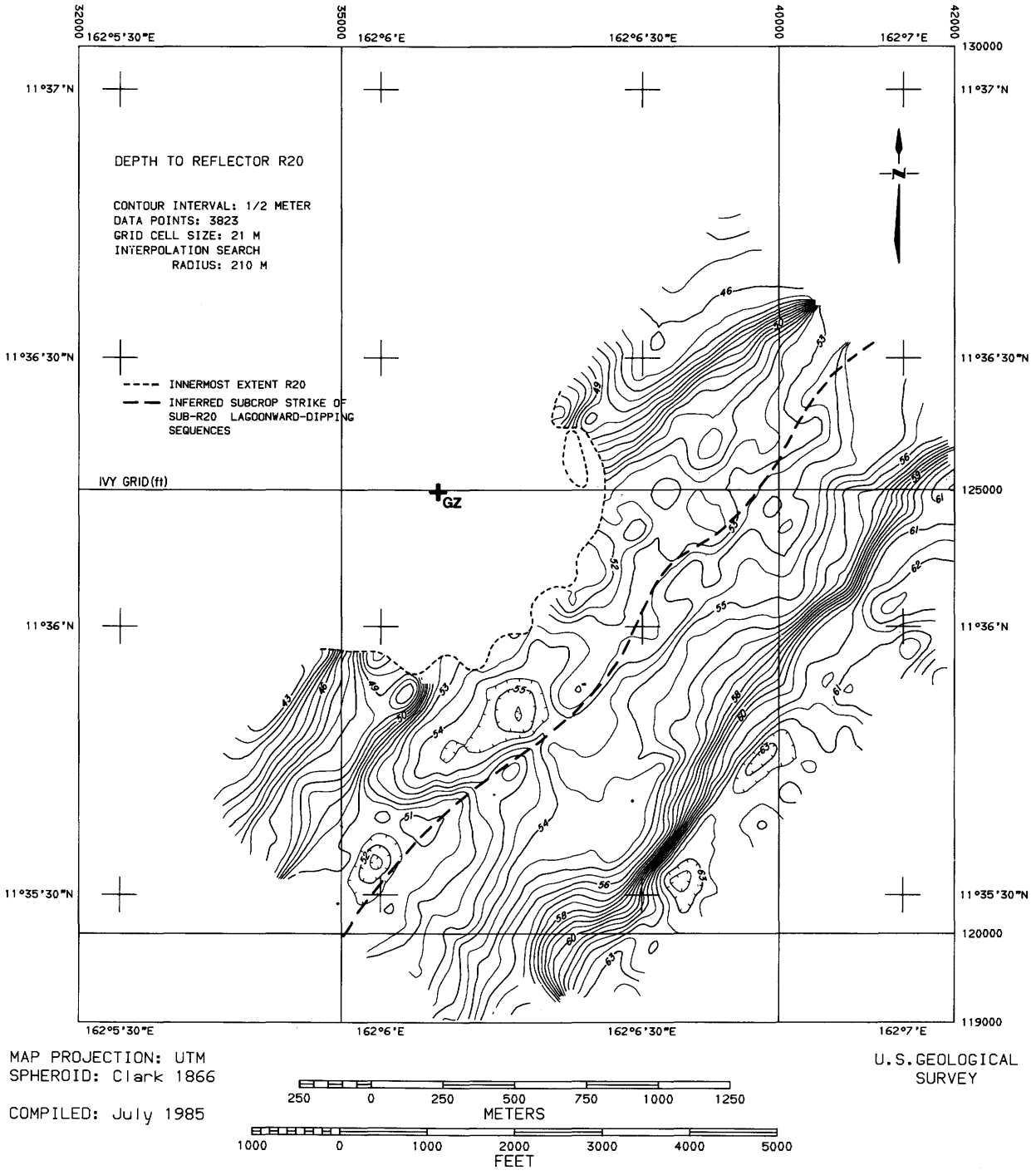

Figure 17. Structure contours for reflector R20 surface, OAK crater, constructed assuming velocities of 1,542 m/s in seawater and 1,650 m/s subbottom. Dashed line shows inferred strike of lagoonward-dipping sub-R20 sequences. GZ=ground zero.

one patch reef 2 km (1.1 nmi) southwest of ground zero is capped with a thick section of Holocene deposits. The patch reefs presumably are all preevent features.

Debris accumulations lap onto or bury patch reefs around the crater, whereas in the lagoon farther from the crater, some are surrounded by moats. Patch reefs at the outer parts of the crater area in the southeast quadrant may have served as buttresses that, in part, controlled the movement of debris.

Physiography of R20 Surface and Geologic Characteristics of the Pre-R20 Deposits

Lagoonward-dipping sequences below R20, which form its topography along the back reef, are best seen on the

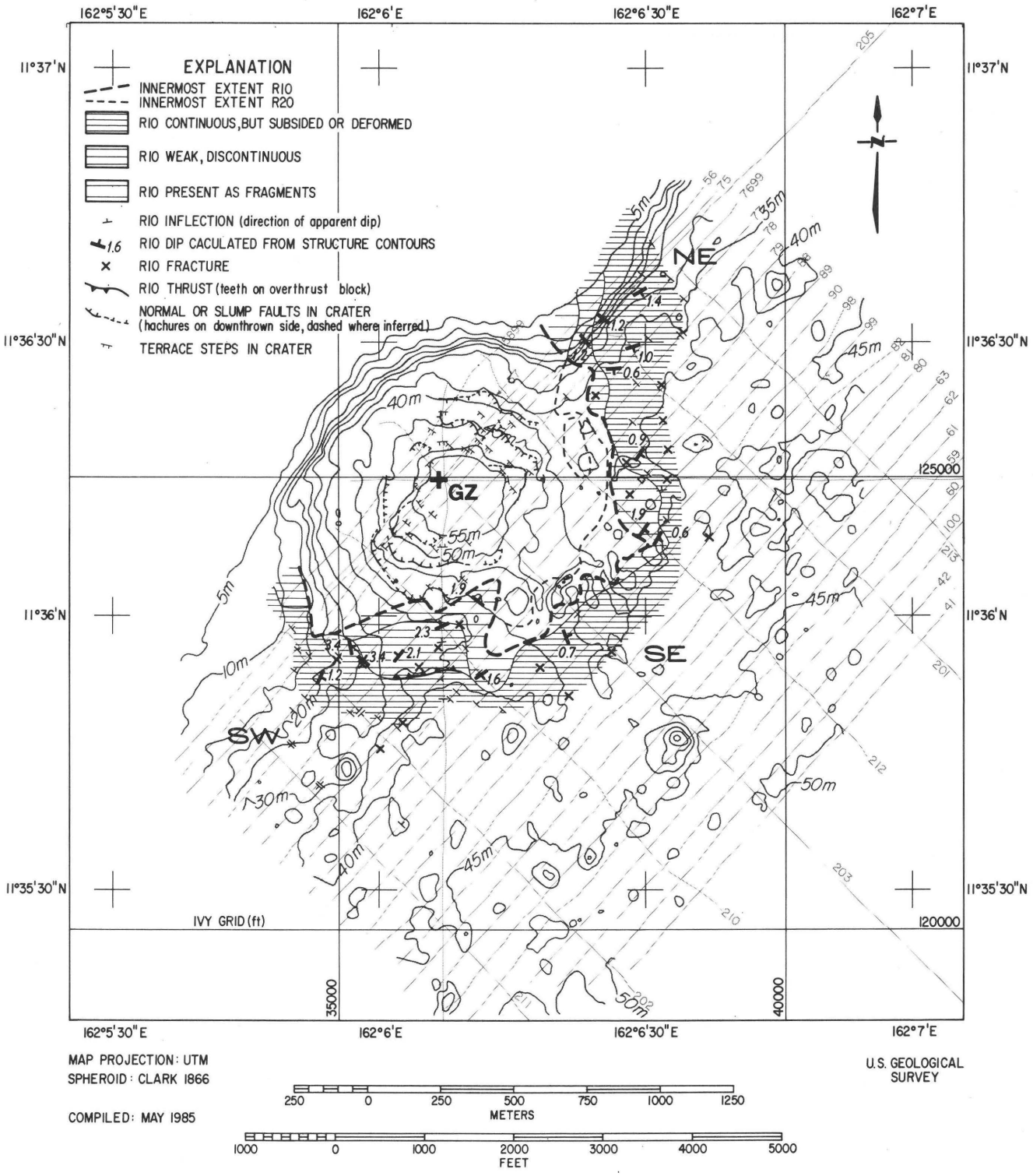

Figure 18. In-crater faulting and structural features of reflector R10 surface, OAK crater, GZ=ground zero. Track lines are screened. Bathymetry contour interval is 5 m.

seven profiles perpendicular to the reef. The R20 reflector appears to be an erosional surface that truncates two or three or more separate sequences that dip lagoonward along the trend of the back reef (for example, line 201, fig. 8*AA*). The resistant members of these sequences are expressed as cuestas and hogbacks, which are associated with depressions or swales and probably a wave-cut terrace in the lagoonward part of the area. The trends of these features are reflected by

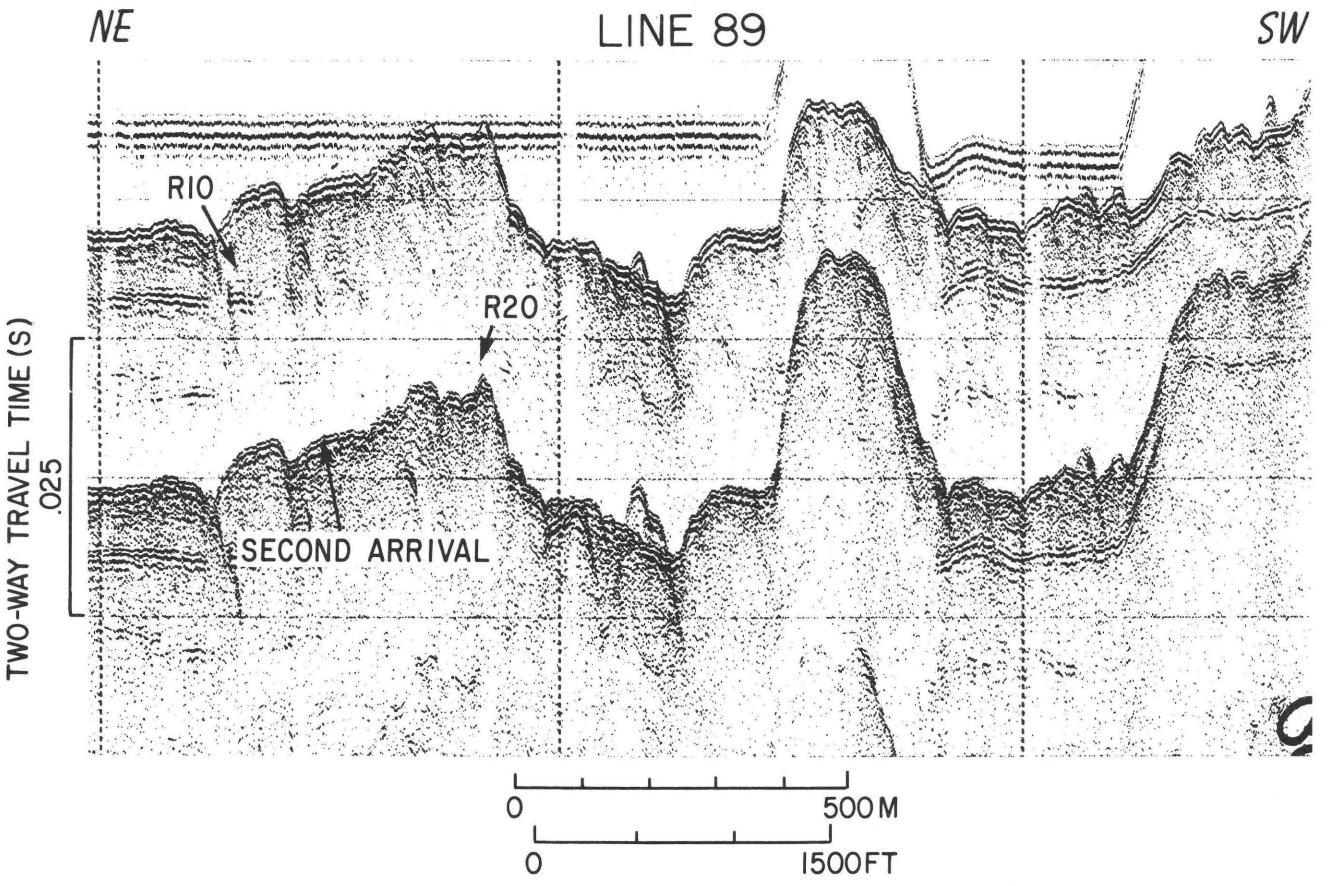

Figure 19. Weak trace of reflector R20 along line 89, southwest quadrant.

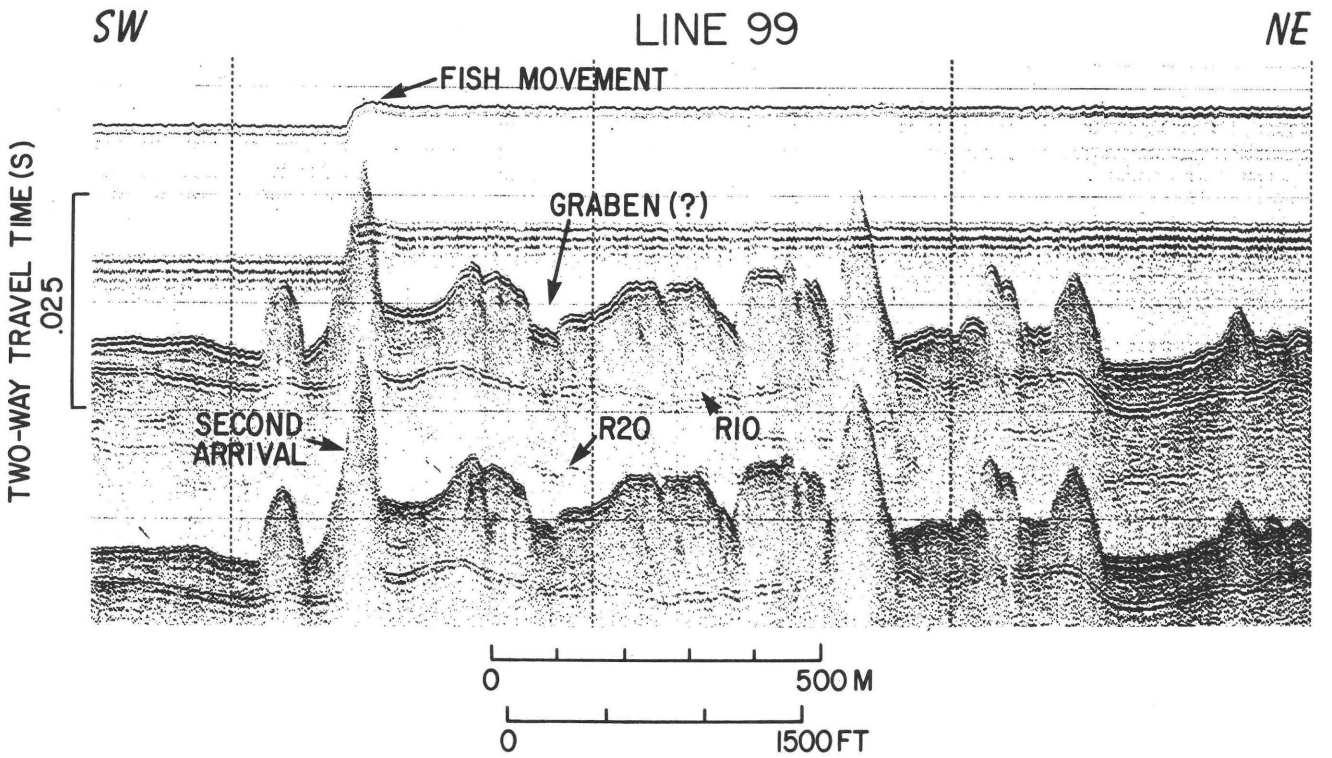

Figure 20. Graben(?) forming valley floor on line 99, southwest quadrant. R10 and R20 surfaces are also shown.

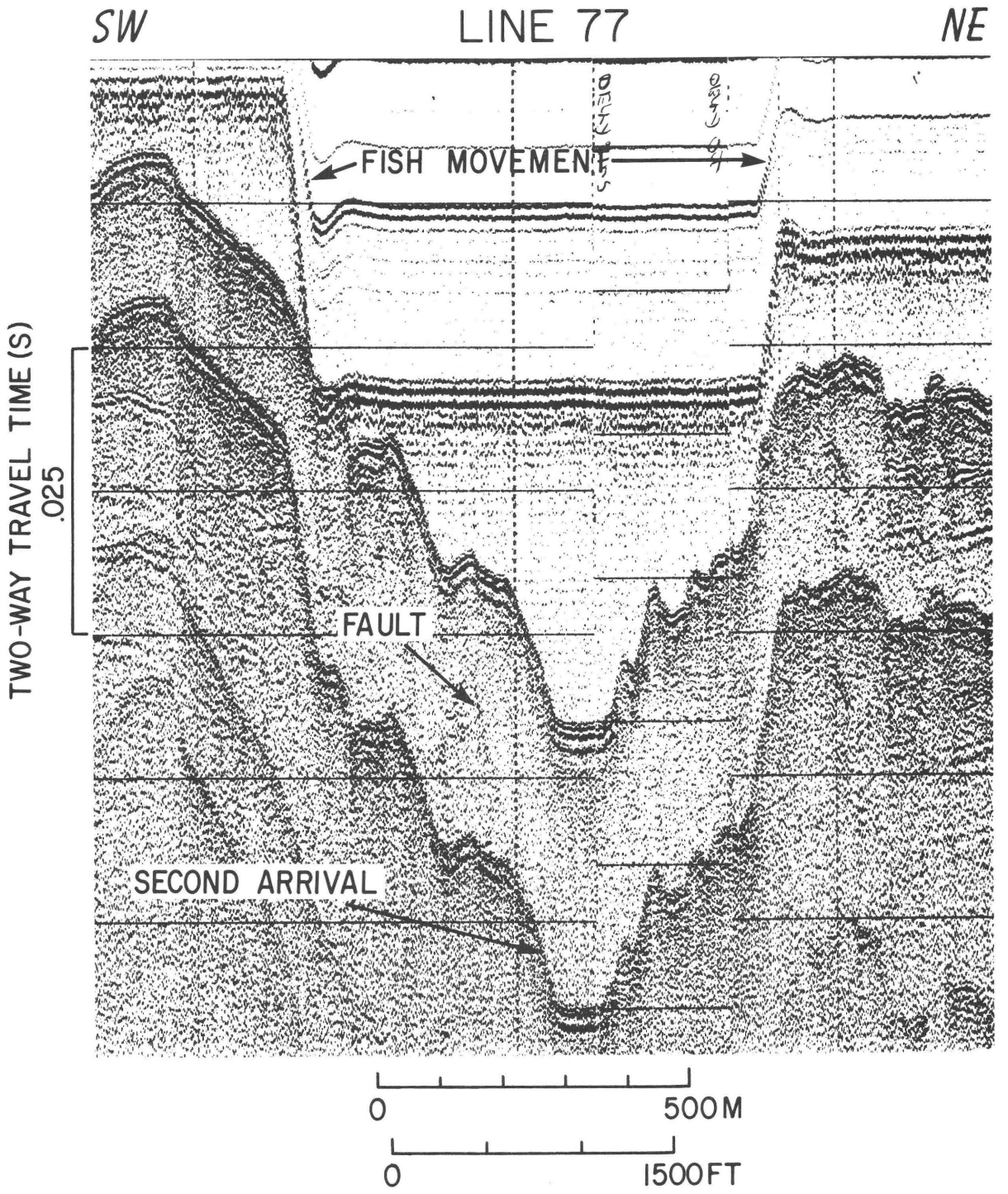

Figure 21. Postevent fill and fault in the central part of OAK crater (line 77). See also line 75, figure 22.

the structure contours of figure 17. Also shown is the inferred subcrop strike of the lagoonward-dipping sequences. The pre-R20 sequences probably include beachrock, which is more indurated than surrounding sediments. These sequences are discontinuous, similar to present-day deposits of beachrock on the lagoonward beaches of the islands of the atoll (fig. 24).

Geologic Control of Patch-Reef Locations

Some of the patch reefs appear to have grown upon topographic highs on strata resistant to erosion, such as the cuestas and hogbacks of the pre-R20 sequences. Consequently, beach ridges inundated by rising sea level may serve as bases for patch-reef growth, explaining why some

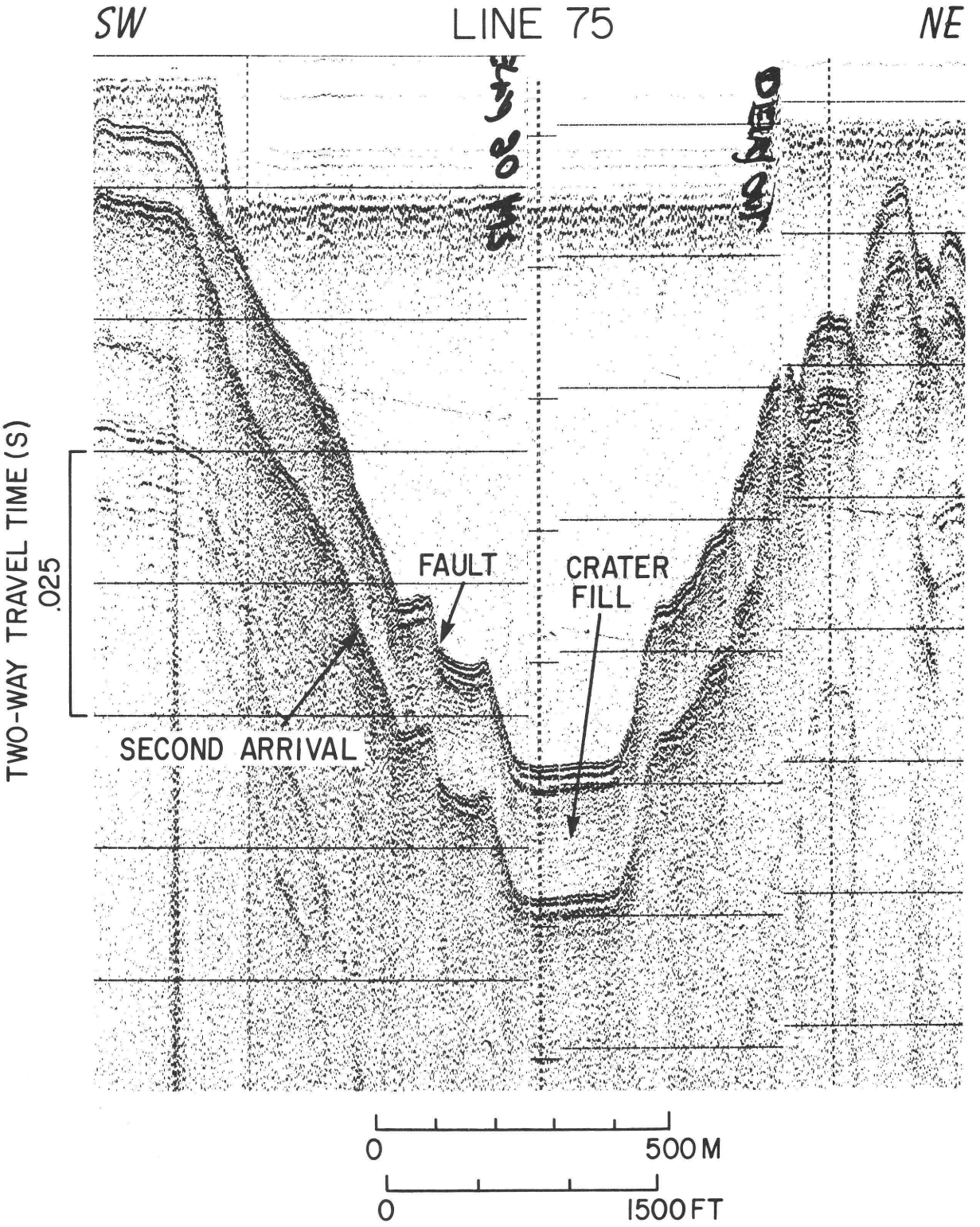

Figure 22. Fault in central part of OAK crater; note displacement of subsurface reflectors and terrace at surface (line 75). Faint reflectors from crater fill may represent postevent deposits.

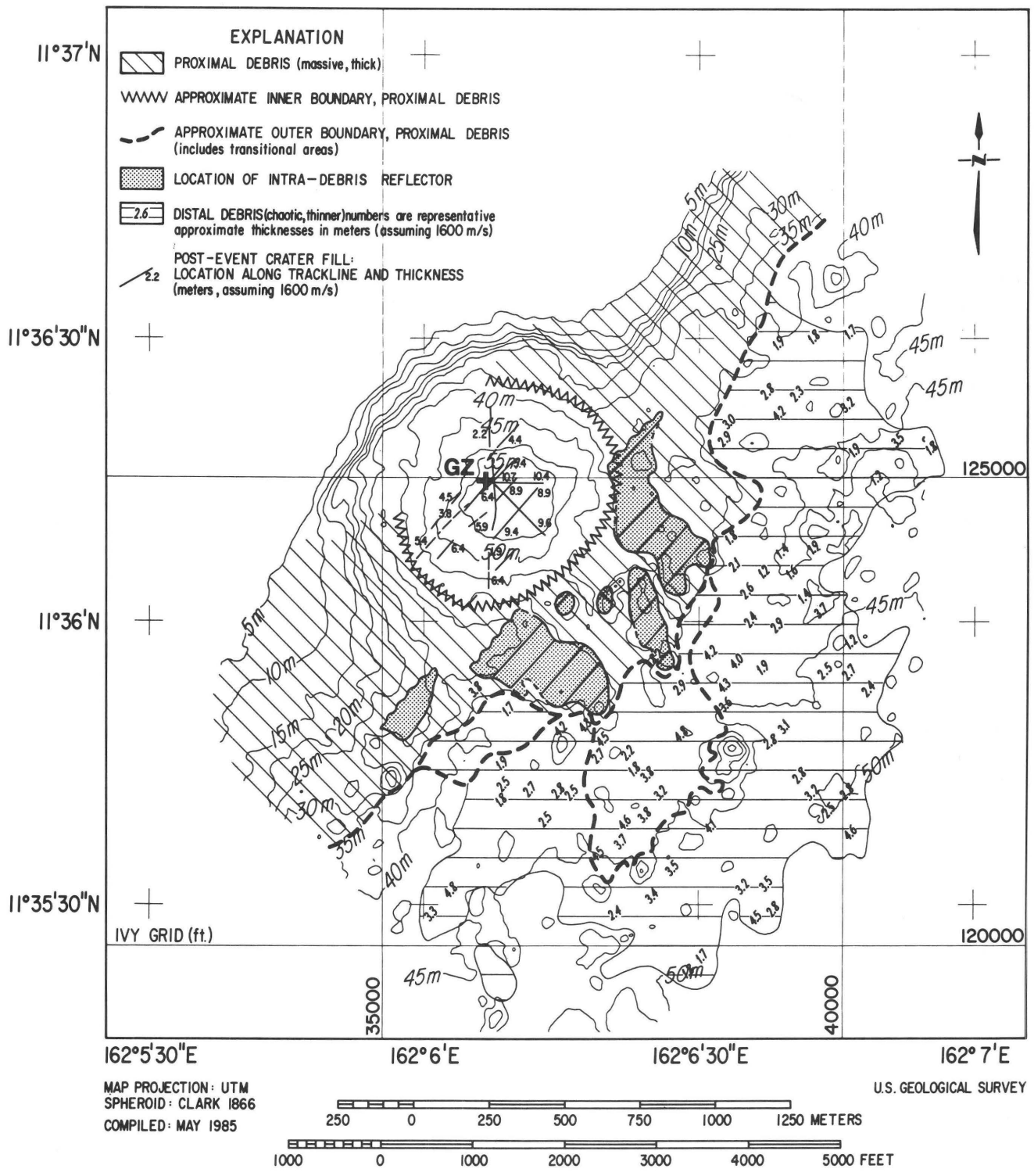

Figure 23. Surface sediments of OAK crater area showing distribution and thickness of debris and postevent fill in crater. Intradebris reflector may be inverted surface of R10 in an overturned flap, or it may be R10 thrust over the southeastern edge of the crater. GZ=ground zero. Bathymetry contour interval is 5 m.

Figure 24. Beachrock on lagoon side of Bokoluo (Alice) Island.

patch reefs appear to be in lines subparallel to the reef. (See chap. A, fig. 7, this volume.)

SUMMARY

In summary, two seismically reflecting layers, R10 and R20, which predate the OAK nuclear event, were mapped in the subsurface around the crater. These are shallower than about 60 m (200 ft) below sea level and are less than 20 m (65 ft) subbottom. The R10 reflector is absent within about 600 m (1,970 ft) of ground zero in most areas, but one inward-dipping segment extends as close as 400 m (1,310 ft) southwest of ground zero. The termination of the deeper lying R20 reflector is commonly about 550 m (1,800 ft) from ground zero, but ranges between 440 and 700 m (1,500–2,300 ft) from it.

The debris deposits surrounding the crater have characteristics that can be distinguished seismically from the surrounding naturally deposited sediments. The debris deposits are amorphous, chaotic, or not clearly structured and have a rough surface at the sea bottom. Deposits proximal to the present crater are about 10 m (33 ft) thick, but their base cannot be clearly distinguished seismically. They extend as far as 1,400 m (4,593 ft) from ground zero along the reef and about 800 m (2,625 ft) into the lagoon. Distal deposits make up a thinner outer apron, 1.5 to 5 m (5–16 ft) thick, that can be recognized as far as 1,700 m (5,577 ft) from ground zero.

REFERENCES

Ristvet, B. L., Tremba, E, L., Couch, R. F., Fetzer, J. A., Goter, E. R., Walter, D. R., and Wendland, V. P., 1978, Geological and geophysical investigations of the Eniwetok nuclear craters: Air Force Weapons Laboratory Technical Report TR–77–242, Kirtland Air Force Base, New Mexico 87117, 263 p.

Tremba, E. L., Couch, R. F., and Ristvet, B. L., 1982, Enewetak Atoll Seismic Investigation (EASI): Phases I and II (final report): Air Force Weapons Laboratory Technical Report TR–82–20, Kirtland Air Force Base, New Mexico 87117, 124 p.

Chapter D

Multichannel Seismic-Reflection Survey of KOA and OAK Craters

By J. A. GROW, M. W. LEE, J. J. MILLER, W. F. AGENA, J. C. HAMPSON, D. S. FOSTER, and R. A. WOELLNER

U.S. GEOLOGICAL SURVEY BULLETIN 1678

SEA-FLOOR OBSERVATIONS AND SUBBOTTOM SEISMIC CHARACTERISTICS OF OAK AND KOA CRATERS, ENEWETAK ATOLL, MARSHALL ISLANDS

CONTENTS

FIGURES

Chapter D
Multichannel Seismic-Reflection Survey of KOA and OAK Craters

By J. A. Grow[1], M. W. Lee[1], J. J. Miller[1], W. F. Agena[1], J. C. Hampson[2], D. S. Foster[2], *and* R. A. Woellner[2]

INTRODUCTION

Purpose

Because postevent processes obscure depth, diameter, and ejecta debris of submarine nuclear craters, high-resolution multichannel seismic reflection data are essential to define their subsurface geometry. To optimize the field data, we mobilized a Phoenix Seismic Processing Computer System for on-site processing. The primary goal of the multichannel seismic survey was to acquire data on the distribution, continuity, and structure of subsurface reflectors to a depth of at least 500 m (1,640 ft) below bottom. A secondary goal was to provide data for the selection of drilling sites.

Shallow (0–30 m, or 0–100 ft) subsurface reflectors were mapped with the single-channel seismic system (chap. C, this volume), and deeper reflectors were mapped with the multichannel seismic system.

Setting

During the period of the survey (August 21-September 20, 1984), the lagoon provided us with light winds and low seas, an ideal meteorologic and oceanographic setting for a multichannel survey. However, the physiographic and geologic settings were far from ideal. Handling a long seismic streamer in shallow water close to the reef at OAK crater was difficult to impossible in some areas. KOA was even more confining because of the shoal on the lagoonward side of the crater (chap. A, fig. 16, this volume). The number of lines that could be run was limited by the *Egabrag*'s size and by the length of the seismic streamer needed to acquire the desired penetration and resolution.

Previous Work

Reflection seismic profiling in the lagoon has apparently been limited to studies associated with the craters. The first subbottom reflection profiling was part of project EXPOE (Exploratory Program on Enewetak) (Ristvet and others, 1978). Twelve reflection profiles (two-way travel time) collected in OAK, MIKE, and KOA craters with an 8-kJ sparker system and 20-element single-channel analog streamer array (length not reported) revealed reflectors depressed toward the crater center; these reflectors become discontinuous and lose their identity at a distance of 0.5 to 0.75 apparent crater radii (chap. A, figs. 9, 17, this volume; table 2, Introduction to the volume). One successful profile was run off Medren (Elmer) Island. However, the authors expressed reservations about the usefulness of the data due to limitations in the accuracy of navigation, high noise levels aboard ship, and abundant multiples in the data. To resolve these problems, an extensive multichannel seismic-reflection program using an 8-kJ sparker source and a 12-channel, 75-m streamer was carried out by Fairfield Industries in late 1979 during Project EASI (Enewetak Atoll Seismic Investigation) (Tremba and others, 1982).

Approximately 260 km (140 nmi) of seismic lines were shot during Project EASI in three grids controlled by a Motorola Miniranger navigation system. The grid in OAK and the grid in MIKE and KOA had line spacings of about 140 m (450 ft) near ground zero, whereas the grid in the control area off Enjebi (Janet) Island had line spacings of about 600 m (970 ft). The data acquired in the EASI survey show strong reflectors at about 0.3 s (two-way travel time) in many areas, but the 8-kJ sparker had a very complex source signature, and the 75-m streamer did not have enough offset to resolve the velocity structure accurately. However, EASI multichannel seismic data were useful for developing the design of the USGS multichannel program.

GEOPHYSICAL METHODS

Acquisition

We experimented with four different streamer configurations and acoustic sources to determine what system

[1]U.S. Geological Survey, Branch of Oil and Gas Resources, Denver, Colo. 80225.

[2]U.S. Geological Survey, Branch of Atlantic Marine Geology, Woods Hole, Mass. 02543.

would give optimum penetration and resolution of the complex atoll strata. These included: (1) a 75-m (246 ft) streamer cable with 12 channels in 6.25-m (21 ft) groups; (2) a 150-m (492 ft) cable with 24 channels in 6.25-m (21 ft) groups; (3) a 300-m (984 ft) cable with 24 channels in 12.5-m (41 ft) groups; and (4) a 300-m (984 ft) cable with 12 channels in 25-m (82 ft) groups. The acoustic sources included 15- and 80-in^3 waterguns, and 1-, 20-, 40-, and 540-in^3 airguns. The digital recording system had the option of recording either 12 channels at a 0.5-ms sampling rate or 24 channels at a 1.0-ms sampling rate. The data were recorded aboard ship using a Texas Instruments DFS–V seismic-data-acquisition system and ANSI (American National Standards Institute) standard nine-track magnetic tape at 1,600 BPI (bits per inch).

Based on 4 days of testing and processing, one combination of sound-source and receiving systems gave best results in the craters, and another combination gave best results for regional work. Best for the detailed crater work was a 15-in^3 watergun and a 150-m (492 ft) streamer cable with 24 channels in 6.25-m (21 ft) groups at a sampling rate of 1.0 ms and a recording time of 1.0 s. Best for regional lines across and outside the atoll was an 80-in^3 watergun and a 300-m (984 ft) cable with 24 channels in 12.5-m (41 ft) groups at a sampling rate of 1 ms and a recording time of 2.0 s. Shot-spacing for the 15-in^3 watergun was 3.1 m (10.2 ft) for 24-fold common-depth-point (CDP) coverage, while the shot-spacing for the 80-in^3 watergun was 12.5 m (41 ft) for 12-fold CDP coverage.

We collected 53 km (29 nmi) of data adjacent to the lagoonward side of KOA and southwest of Enjebi Island (200-series lines, fig. 1), 34 km (18 nmi) in KOA crater (300-series lines, fig. 2), and 69 km (37 nmi) of data in OAK crater (100-series lines, fig. 3). Tie lines between OAK and KOA craters (lines 401–404, fig. 1) totaled 45 km (24 nmi). Regional lines across and outside the reef (lines 405–415, fig. 1) totaled 181 km (98 nmi). The combined total of all multichannel seismic lines was 382 km (206 nmi).

As many as five passes were made along parts of some lines. The profiles are designated, for example, OAK line 405V2, for the second pass on line 405.

Multichannel Processing Techniques

Field tapes from Enewetak were processed on a VAX 11/780 computer in Denver, Colo., using Digicon DISCO software. While the 15- and 80-in^3 waterguns were considerably cleaner sound sources than the 8-kJ minisparker used in the EASI multichannel seismic survey, source-signature deconvolution before stack was desirable to remove a low-frequency precursor and small oscillations following the main pulse. USGS software, developed in-house for the signature deconvolution, was successful in collapsing the watergun signature into a clean spike. Watergun signature deconvolution was implemented by applying Gray's (1979) variable-norm deconvolution technique to the original seismic data. A single-source signature for each seismic line was extracted from a CDP gather. On the basis of the extracted wavelet, a deconvolution operator was derived and applied to the corresponding seismic line. When this source signature deconvolution was applied within the craters, a seismically transparent sedimentary unit could be clearly identified. Drilling confirmed that the base of this transparent layer marked the probable base of the transient crater (B. Wardlaw, written commun., July 15, 1985).

Seismic Velocities and Check-Shot Surveys

Multichannel velocities (interval velocities derived from the stacking velocity) were erratic until a careful analysis of water-bottom reflections and multiple times indicated that 6 ms needed to be subtracted from the raw data to correct for cumulative phase shifts within the acquisition and processing systems. Subsequent velocity analyses showed much-improved precision, and two sediment layers were resolved. Sediments between the sea floor and 100 m (330 ft) had an average interval velocity of 1,752 m/s (5,748 ft/s) in KOA and 1,687 m/s (5,535 ft/s) in OAK. Sediments between 100 and 300 m (328–984 ft) had an average interval velocity of 2,095 m/s (6,873 ft/s) at KOA and 1,995 m/s (6,545 ft/s) at OAK. Scatter within the data suggested that the accuracy was within ±5 percent. No consistent velocity anomaly was detected within either crater. Check shots from subsequent drilling within and outside KOA crater did show a 7-percent velocity decrease between 100- and 220-m (328–722 ft) depth, but the average velocities were within the range predicted by the multichannel analyses. Check shots from subsequent drilling at OAK showed good agreement with the multichannel velocities outside the crater. A large velocity decrease was observed in the check shots between 100- and 300-m (328–984 ft) depth within the crater not detected by the multichannel velocities. A complete analysis of this discrepancy is beyond the scope of this report, but the diffraction effects of fractured discontinuous reflectors and side echoes from the slopes around the crater are probably major factors.

After the source-signature deconvolution and 6-ms time-shift corrections were applied, a conventional processing sequence was effective. Water-bottom multiples were not severe, but a poststack predictive deconvolution was applied and improved the data in many cases. All OAK and KOA lines were migrated and converted to depth using check-shot velocities.

Depths refer to sea level at the time profiles were run. Resolution of the data is not sufficient to warrant correcting depths to the Holmes and Narver datum (mean low water spring minus 0.18 m (0.6 ft)).

Both EASI and USGS reflection profiles over OAK crater recorded a band of discontinuous strong reflectors at

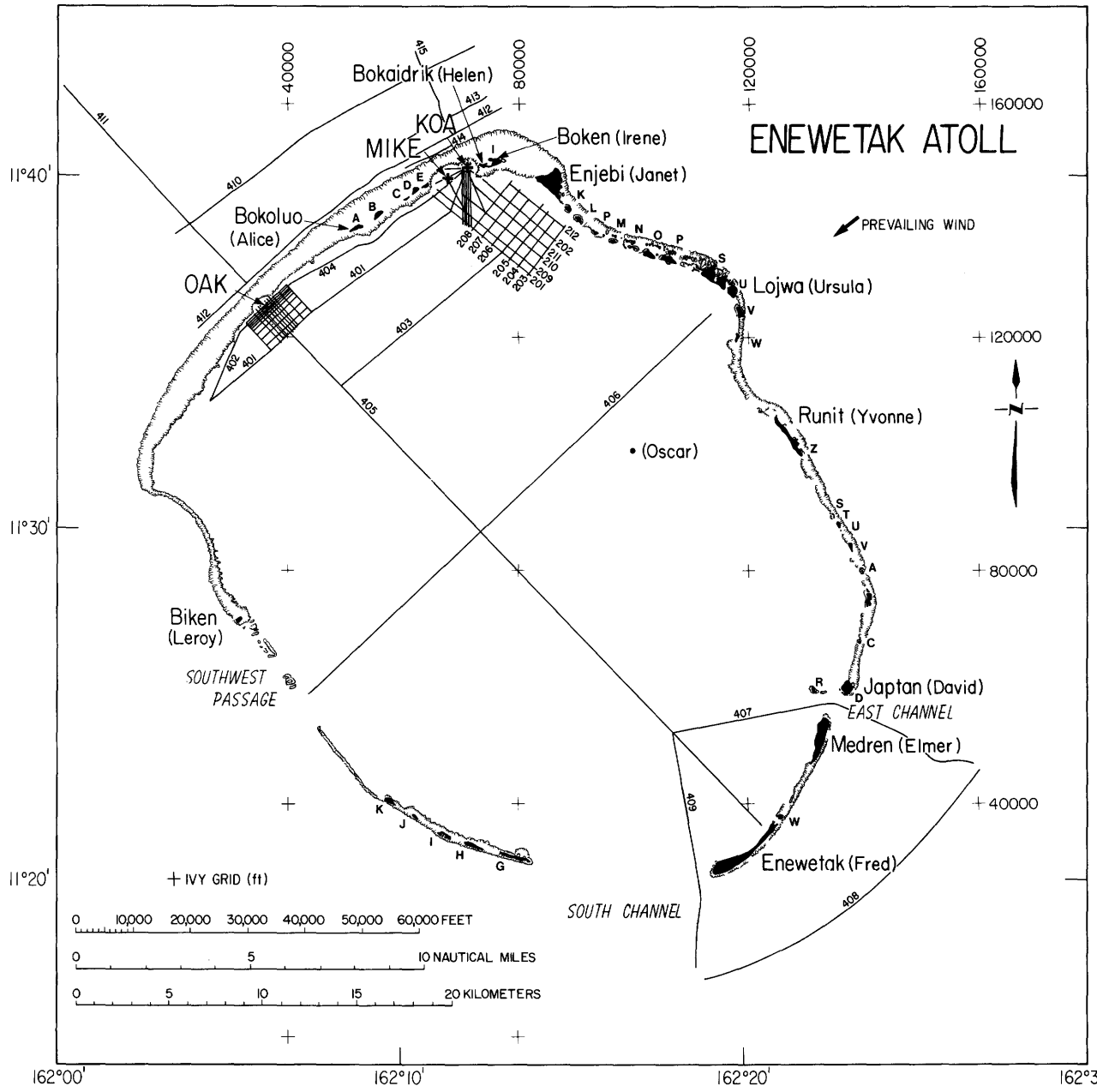

Figure 1. Sites of USGS refraction profiles and multichannel seismic-reflection profiles in Enewetak Atoll, 1984. Uppercase letters are first letters of site names. (See table 1 of the Introduction to the volume.)

approximately a 300-ms depth outside the crater; these reflectors are delayed by up to 50 ms beneath ground zero. The 75-m (246 ft) streamer used by Fairfield Industries was too short to obtain reliable velocities even outside the craters. We anticipated that the 150- and 300-m (492- and 984-ft) streamers used during this survey might provide velocities that would yield depths accurate to approximately 5 percent. This approach would allow us to determine what part of the time delay beneath OAK crater was due to velocity decreases (or increases?) beneath ground zero and what part was due to actual depression of the rocks. Calibration of the seismic velocities by check-shot surveys were run in the drill holes at ground zero and reference holes for both KOA and OAK craters (figs. 4, 5). In addition to allowing a more accurate time-to-depth conversion of the reflection profiles, the interval velocities derived from the check shots provide a direct measure of the depth of detonation effects on rock properties.

A plot of one-way seismic travel time versus seismometer depth in the KOA drill holes shows a delay below ground zero of up to 8 ms in one-way travel-time at approximately a 220-m (721 ft) depth (fig. 4). Between the sea floor and approximately a 130-m (426 ft) depth, the observed values of both reference and crater holes appear to be similar within the scatter of the data. Between 130 and 220 m of depth (426–721 ft), the ground zero hole (KBZ–4)

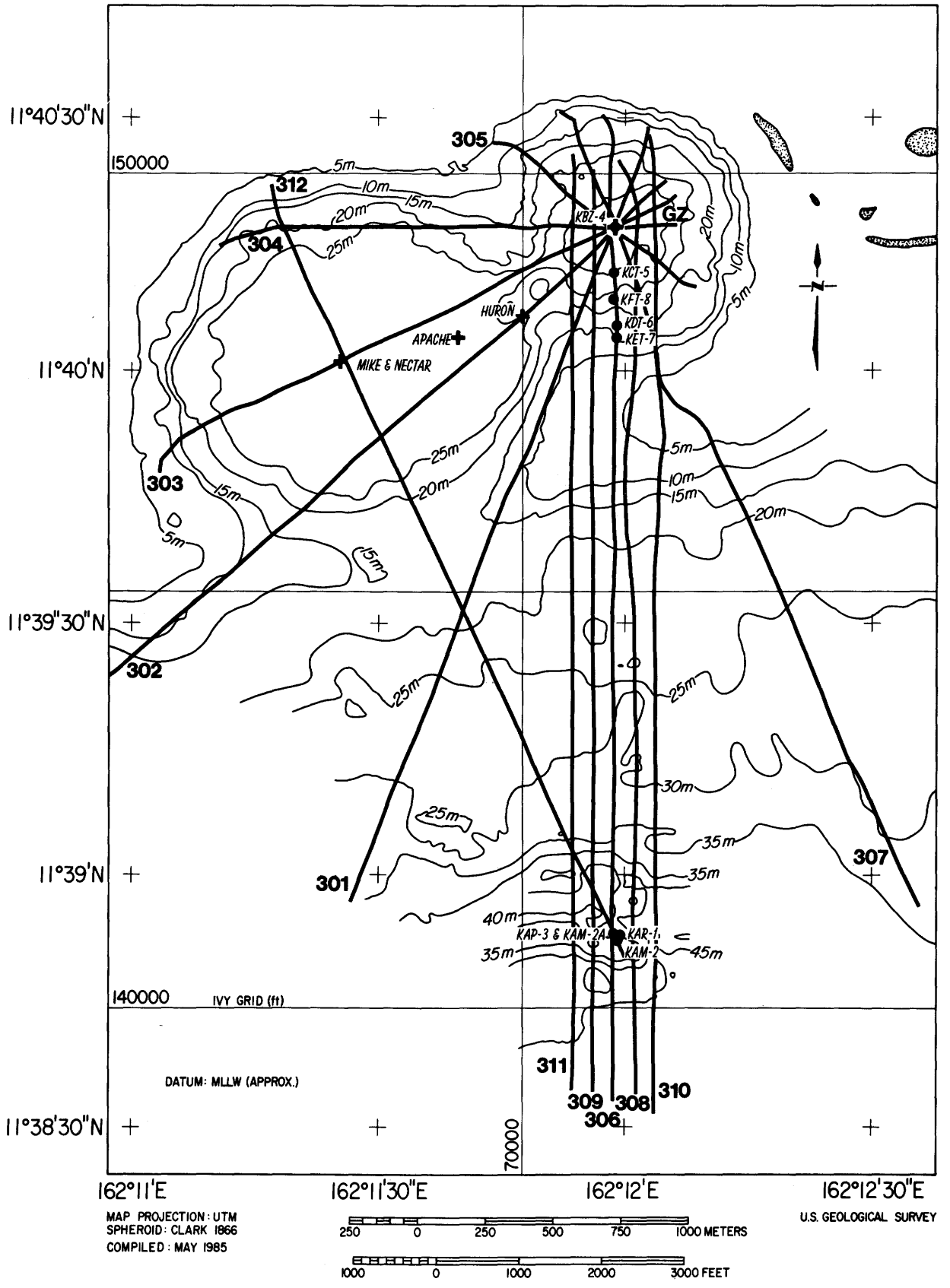

Figure 2. Multichannel seismic-reflection track lines and drill sites, KOA crater. GZ=ground zero. Contour interval is 5 m.

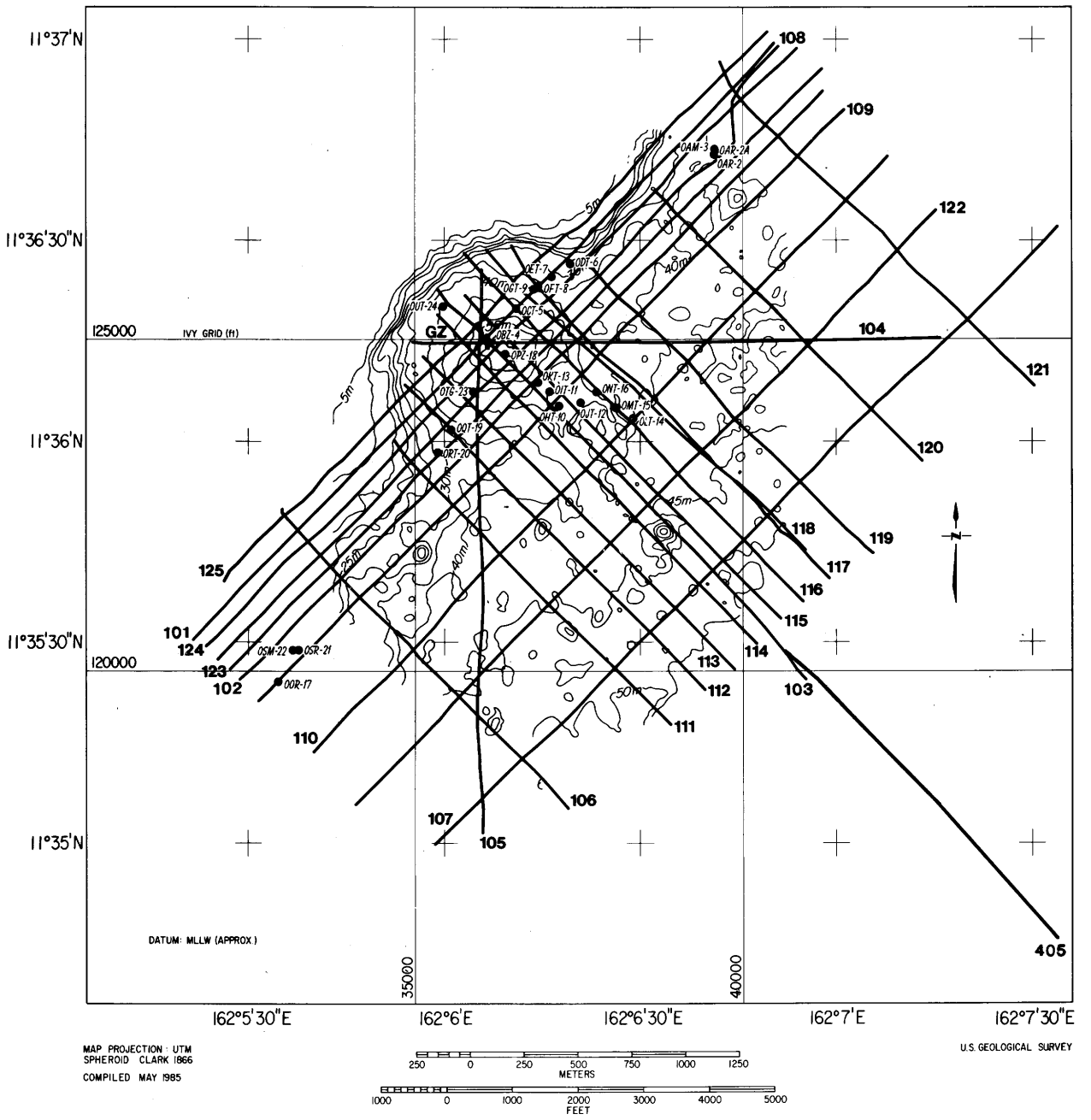

Figure 3. Multichannel seismic-reflection track lines and drill sites, OAK crater. GZ=ground zero. Contour interval is 5 m.

value is progressively delayed with respect to the reference hole (KAR–1) value. Between 220 and 350 m (721–1,148 ft) of depth, the delay decreases to about 2 ms. With possible errors of ±1 m (3.3 ft) in depth and ±1 ms of time, interval velocities from individual pairs of readings at 10-m (33 ft) intervals were noisy. Therefore, interpreted curves were averaged over 50-m (164 ft) intervals.

Plots of interval velocity versus depth averaged over 50-m (164 ft) depth intervals for KOA show large velocity decreases between 100 and 200 m (328–656 ft) beneath KOA crater (fig. 6). Between a depth of 200 and 250 m (650–820 ft), the KOA interval velocities are similar. Both KOA sites show small velocity inversions between 250 and 300 m (820-984 ft) in a zone reported in preliminary drilling reports to be organic-rich. Between a depth of 300 and 350 m (984–1,138 ft), the KOA ground zero velocities are approximately 400 m/s (1,312 ft/s) faster than those of the reference hole. This effect is probably due to a natural facies transition from unconsolidated sediments in the lagoon at KAR–1 to more massive consolidated reef facies at KBZ–4 (ground zero at KOA). The lack of any measureable time delays or velocity anomalies in the upper 130 m (427 ft) at

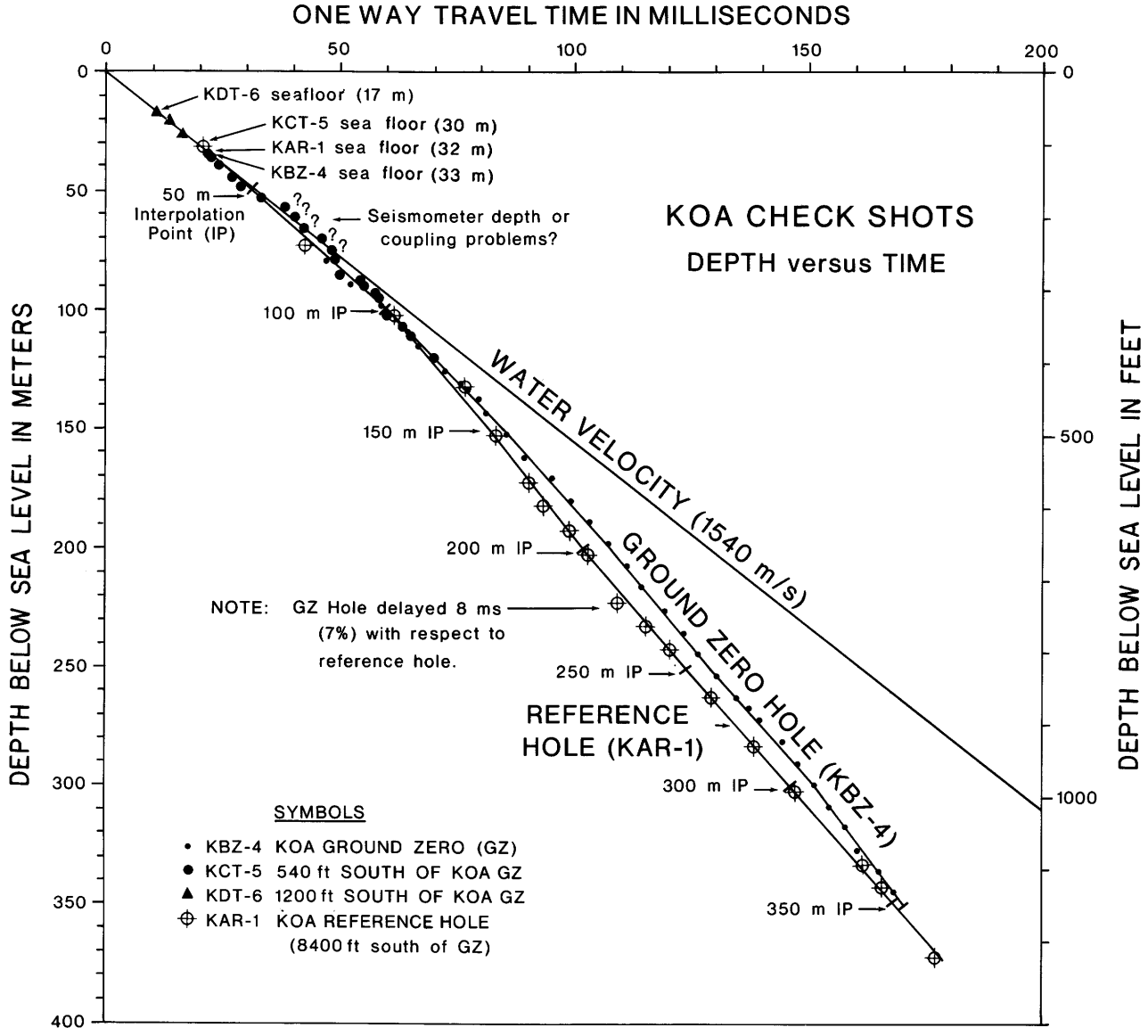

Figure 4. Seismic velocity check shots, KOA crater.

KOA ground zero is probably due to the absence of lithification at KAR–1. The significant velocity decrease between 100 and 200 m (328–658 ft) deep beneath KOA ground zero is not easily explained by natural geologic facies changes and is probably due to fracture effects of the KOA detonation.

A plot of one-way seismic time versus depth for OAK shows an increasing delay between 100 and 300 m (328–984 ft) of depth where a remarkable 20-ms delay was observed (fig. 5). Interval velocities averaged over 50-m bands for OAK are also shown in figure 6 for comparison with KOA. Check shots for the OAK reference holes (OAM–1, OAR–2) only reached 295 m (968 ft), while the ground zero hole (OBZ–4) reached a depth of 540 m (1,772 ft). As in KOA, no significant delays or velocity anomalies were observed in the upper 100 m (328 ft) of OAK crater. Both the OAK reference and ground zero holes have approximately the same position with respect to the reef, and the large velocity decreases at OAK ground zero between 100 and 300 m (328–984 ft) of depth are probably due mostly to detonation effects, although some geologic facies changes are probably present. A sharp increase in velocity at OBZ–4 (ground zero, KOA) between 300 and 350 m (984–1,148 ft) suggests that the detonation effects below 300 m (984 ft) are probably less significant.

For the purpose of time-to-depth conversion of the multichannel seismic-reflection profiles, reflection time versus interval-velocity tables for KOA and OAK were derived from the time-versus-depth plots (figs. 4, 5). Examination of downwarping reflectors around the craters suggests that the lateral effect around KOA extends out to a 457-m (1,500 ft) radius, while around OAK it extends out

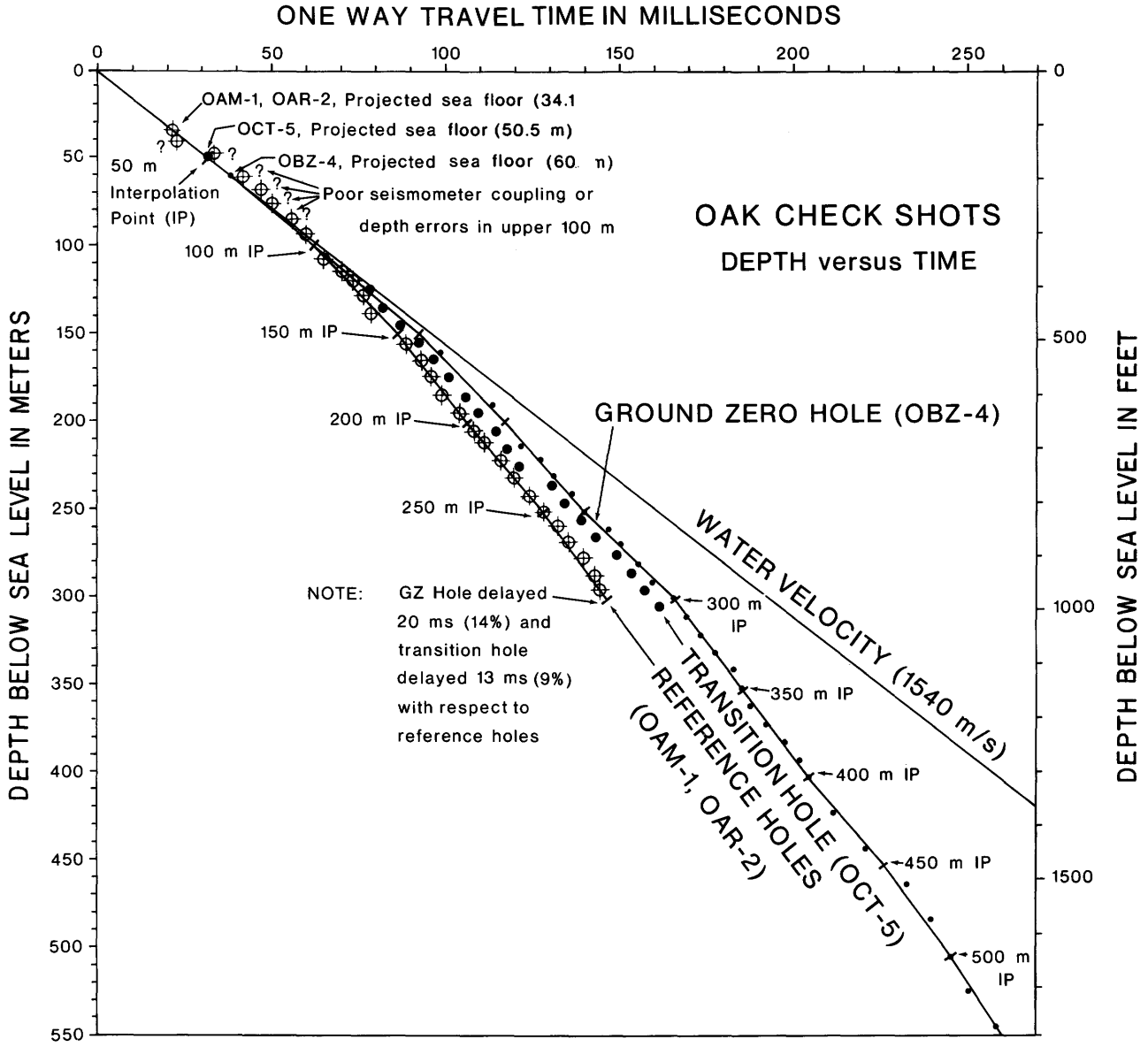

Figure 5. Seismic velocity check shots, OAK crater. GZ=ground zero.

to 610 m (2,000 ft). Therefore, the appropriate reference-hole velocities were applied outside 457 m and 610 m (1,500 and 2,000 ft) at KOA and OAK, respectively, and linear transition to ground zero was assumed. Line 109 in OAK crater (fig. 3) was run parallel to the reef and approximately 427 m (1,400 ft) southeast of ground zero, and it showed no beds deeper than 50 m (subbottom) disrupted or significantly delayed by velocity decreases near the crater. Therefore, during the depth conversion of the OAK seismic profiles, OAK reference velocities were assumed to apply all along line 109. This assumption required that the transition from OAK ground zero to OAK reference velocities take place over 427 m (1,400 ft) on the southeast side of OAK, while the transition was assumed to take place over 610 m (2,000 ft) on the southwest, northwest, and northeast sides of OAK. For OAK lines southeast of line 109 (fig. 3), interval velocities were gradually reduced to take into account the increasing water depth, assuming that the underlying velocity layers dipped to the southeast, parallel to the sea floor.

Preliminary results from check shots at the OOR–17 reference drill site on the southwest end of line 109 (fig. 3) show the same trend as OAR–2 and confirm the assumption of OAR–2 velocities for line 109.

Concern over the accuracy of the OOR–17 check shots was expressed on the basis of shipboard analysis, and an 8-ms error was suspected because the check shots at the sea floor appeared too slow. No analog or digital magnetic tapes were recorded by the contractor, and the paper galvo-camera records from the field do not have the resolution

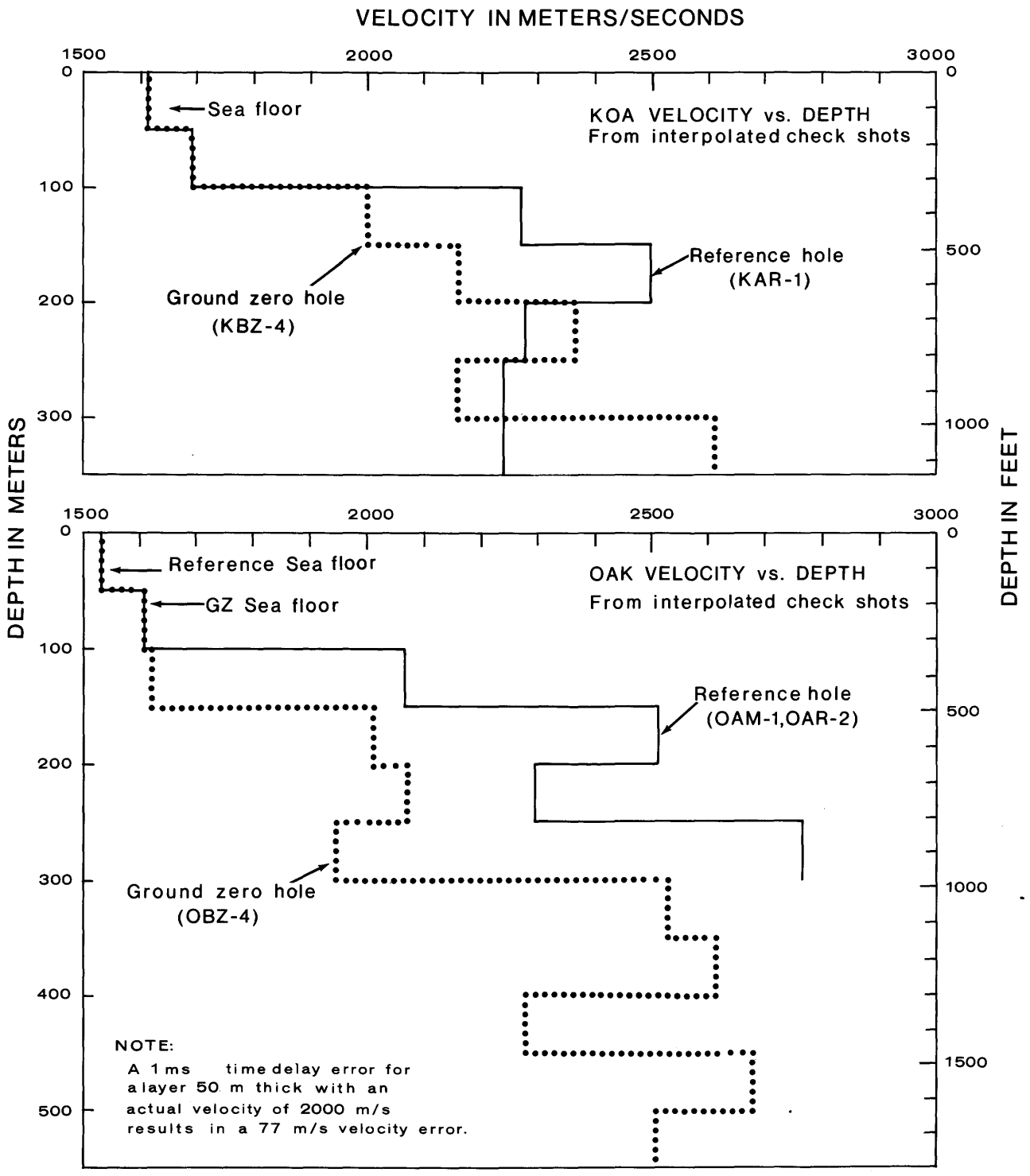

Figure 6. Interval velocities, KOA and OAK craters.

necessary to resolve this issue. However, a visual examination of the galvo-camera records from KAR–1, OCT–5, and OOR–17 does *not* confirm any obvious 8-ms error and implies that no relative change occurred between the first and last check-shot surveys. A systematic error might still occur if electrical crosstalk between the airgun firing wire and the shot-detector hydrophone wire took place. Alternatively, if the shot-detector hydrophone was too sensitive, it might pick up the airgun solenoid or shuttle motion in advance of the main pressure pulse from the airgun. However, because we lack magnetic tapes for a more detailed analysis, the galvo-camera records must be accepted as the best available

data source, and in the absence of more conclusive evidence, the contractor's check shots have been applied without a systematic 8-ms correction.

Side-Echo Problems

Conventional multichannel seismic-reflection-profiling techniques are based on an assumption of two-dimensional topography and structure; reflections of topography or buried structures from outside the plane of the profile result in side echoes that cannot be easily corrected with presently available acquisition and processing techniques.

In Enewetak, side echoes off the main reef, crater rims, and random pinnacle reefs presented difficult interference problems, especially on profiles parallel to the main reef or those grazing the crater rims. While the reflection profiles cannot be corrected for these effects, computer models using simplified topography illustrate these problems. For instance, a circular model of OAK crater with an inner crater and an intermediate terrace (fig. 7) illustrates the side-echo and diffraction effects that complicate the interpretation of the multichannel seismic data from Enewetak.

The first layer of the model simulates the sea floor of the apparent OAK crater. The second layer models a shallow-subsurface reflector which is truncated beneath the inner crater. The third layer simulates a deep reflector which is down-dropped beneath the inner crater. The impulse-like strong seismic response under the center of the crater (fig. 7*B*) results from the focused diffractions from the edges of the discontinuous subsurface layer. Numerous diffraction tails, some originating from the topographic relief of the apparent crater and others from the truncational edge of the second layer, can be clearly observed under the crater. This diffraction effect is a major side-echo problem in interpreting seismic data.

Figure 7*C* shows the seismic response when the seismic line is offset 35 m (115 ft) from the center of the crater. Notice the synclinal appearance of the diffraction tails under the crater. When the line-offset distance is 75 m (246 ft) (fig. 7*D*), the truncated second layer appears as a continuous reflector, and the water-bottom reflection reveals a very complicated interference pattern. The seismic responses of the deep crater have a synclinal appearance. Similar side-echo problems due to the three-dimensional topographic and subsurface effects mentioned above can be observed in multichannel seismic data from Enewetak.

Because of the side-echo problems, caution is required in making overly detailed interpretations of the records. The least contaminated lines are those directly through the topographic center of the crater, while lines even 35 m (115 ft) away from the crater center are partially contaminated.

SEISMIC CHARACTER OF CRATERS AND ADJACENT LAGOON

Profiles using the 80-in^3 watergun and the 24-channel 300-m (984 ft) streamer were recorded to 2 s on a north-south profile through KOA ground zero, approximately perpendicular to the reef, and both parallel and perpendicular to the reef at OAK. Strong reflectors were observed to approximately a 1.0-s depth in both areas, the deepest of which are inferred to correspond with the volcanic rock drilled at 1,405 m (4,610 ft) on Elugelab (Flora) Island prior to the MIKE detonation (fig. 8). Profile 306V1, the north-south line through KOA ground zero, has been converted to depth using the check-shot velocities in the upper 350 m (1,148 ft) and assuming that the reflector at approximately 1.0 s is the volcanic horizon. This approach assumes an average interval velocity of 3,200 m/s (10,490 ft/s) between 0.350 and 1.000 s. The unmigrated data for line 306V2 had better signal-to-noise ratio than the migrated data for depth conversion, and several strong reflecting zones can be seen between the volcanic basement at 1,400- to 1,500-m (4,593–4,921 ft) depth and the present sea floor (fig. 8).

A band of shallow reflectors between 60 and 120 m (197–394 ft) deep can be seen across the entire profile except where the reflectors are downwarped or terminated near KOA ground zero. The most obvious pattern observed within the sedimentary section on profile 306V2 is a series of highly reflective zones at approximately 300-m (984 ft), 600-m (1,968 ft), and 800-m (2,624 ft) depths, which appear to migrate from south to north (fig. 8). The band of reflectors between approximately 280- and 400-m (919-1,312 ft) depth has much stronger amplitude in the north near KOA crater than in the south. The shingled pattern of the deeper reflecting zones between 600 and 1,000 m (1,968–3,280 ft) also shows large horizontal variations of reflectivity. The shallowing of these high-amplitude reflectors from south to north is interpreted to be evidence of a prograding reef system where the strong reflectors are probably well-cemented reef plate or back-reef facies and their weaker reflecting equivalents to the south are a deeper water lagoon facies. The absence of obvious forereef reflectors on the north side may be due to the steepness of the forereef or to masking by the strong reflectors shallower in the section.

Profiles perpendicular and parallel to the reef at OAK ground zero are shown in profiles 405V2 and 101V5, respectively (figs. 3, 9, 10). Line 405V2 shows a similar pattern of shingled reflectors prograding away from the lagoon as depths become shallower. Line 101V5 is parallel to the reef and displays much better lateral continuity of reflectors than the lines perpendicular to the reef. Note that the resolution on line 101V5 is not as good as on line 405V2. This "wormy" low-resolution pattern is common to most of the profiles run parallel and close to the reef. While the continuity of reflectors is good, probably because of similar lithologic facies, the resolution appears to be degraded by

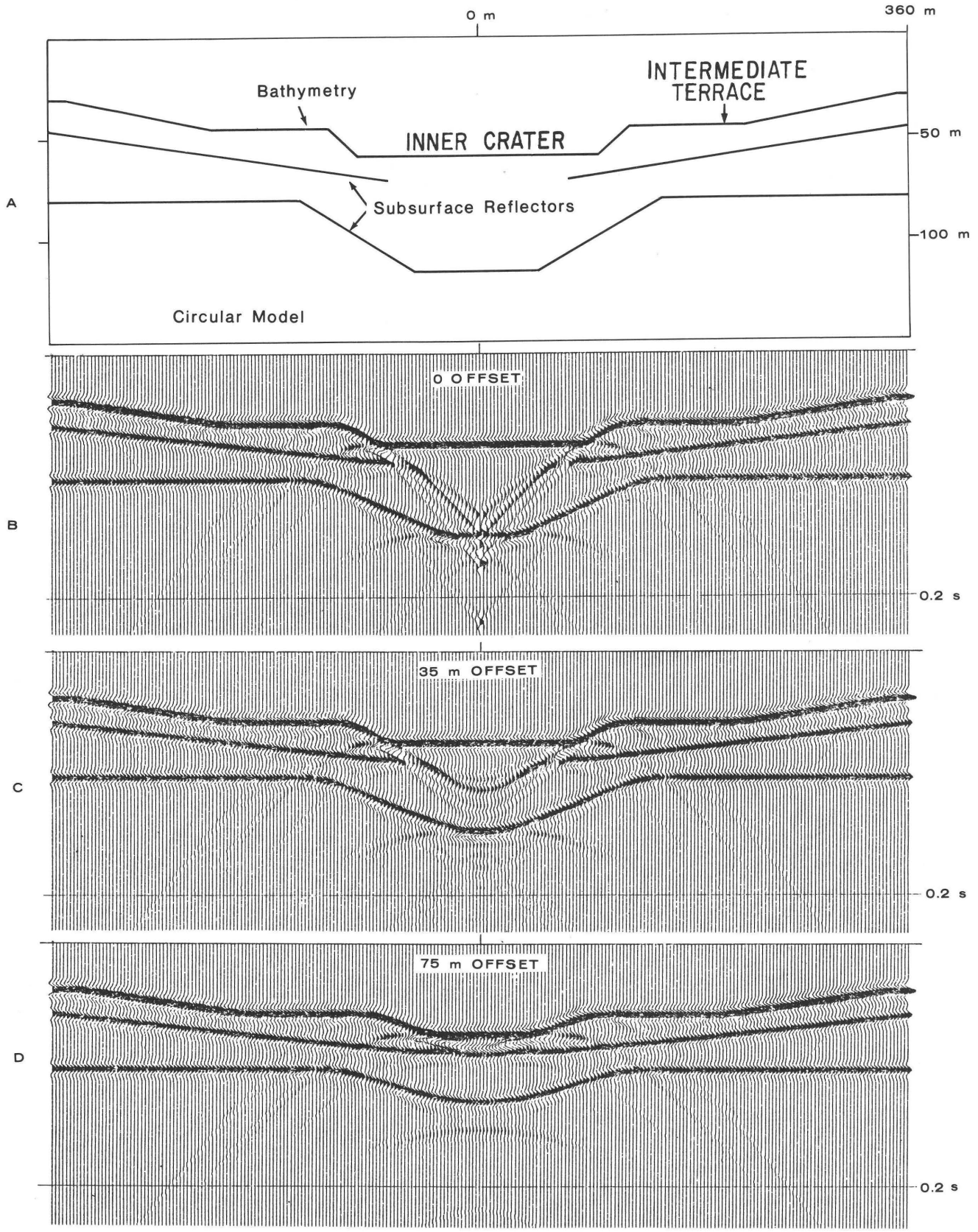

Figure 7. Three-dimensional circular model of OAK crater. *A*, Cross-section of model. *B*, Modeled reflectors at 0 offset. *C*, Modeled reflectors at 35-m (115 ft) offset. *D*, Modeled reflectors at 75-m (246 ft) offset. Horizontal distance scale in meters. Depth in *A* is in meters; in *B*, *C*, and *D*, is in seconds.

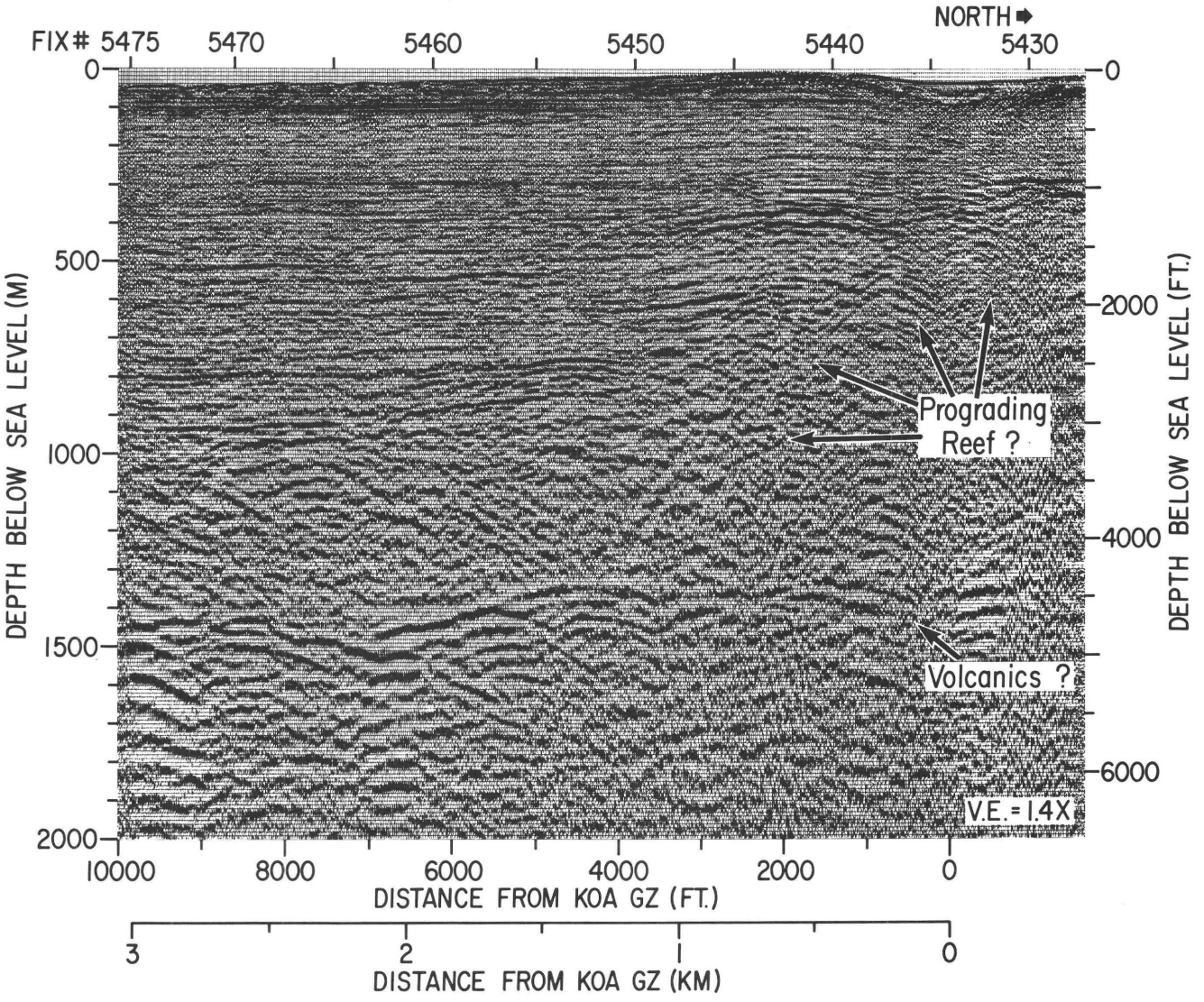

Figure 8. Deep-penetration seismic profile of KOA crater (line 306V2). V2 designates the second pass along line 306 with an 80-in^3 watergun and 300-m streamer. GZ=ground zero.

side echoes off the reef topography and subsurface structures on the reef side of the profile.

While strong reflection bands are observed down to basement, the lateral continuity of individual seismic wavelets is relatively poor, even on lines perpendicular to the reef. The lack of contrasting lithologies within the homogeneous carbonate reef environment results in generally poorer impedance contrasts and reflection quality than in typical continental margin sediments. Because of the poor lateral continuity of individual seismic wavelets, relatively few horizons can be mapped around and into the craters with a high degree of confidence.

In summary, KOA and OAK craters are located within a reef-lagoon system where seismic amplitudes change rapidly perpendicular to the reef and very slightly parallel to the reef. High-amplitude reflecting areas only 0.5 to 1 km (0.3–0.5 nmi) wide can be seen prograding from the lagoon toward the ocean. In spite of the poor continuity of individual seismic wavelets and side-echo problems, a few groups of reflectors within the sedimentary section allow the general character of deformation within and adjacent to the craters to be mapped with reasonable confidence.

RESULTS: KOA CRATER

Depth of Penetration of Multichannel Seismic Profiles at KOA

Because of reefs and shoals in the north, east, and southeast side of KOA crater (figs. 1, 11), and a badly

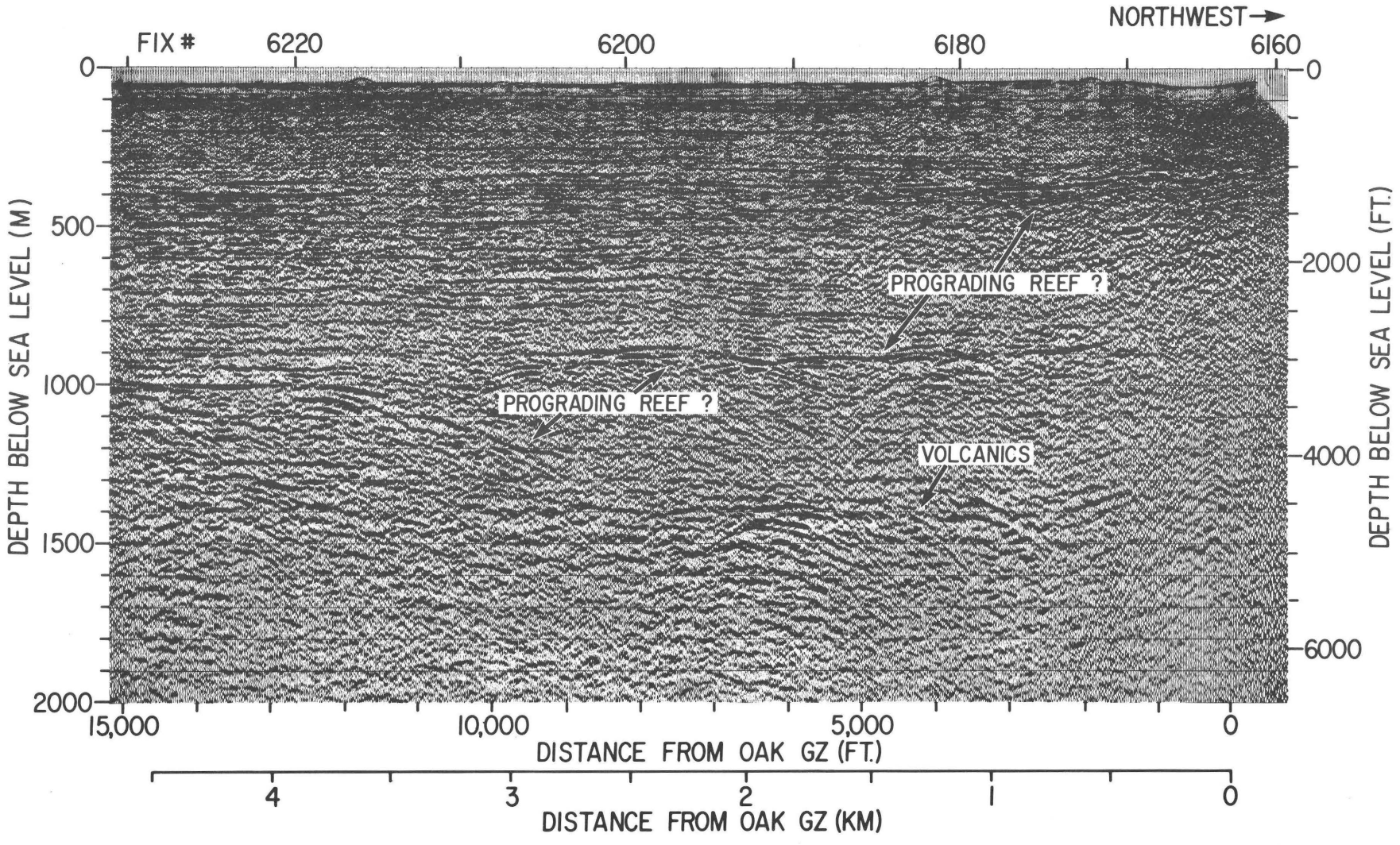

Figure 9. Seismic-reflection profile 405V2 across OAK crater acquired with an 80-in^3 watergun and 300-m streamer. GZ=ground zero. Vertical exaggeration is ×1.3

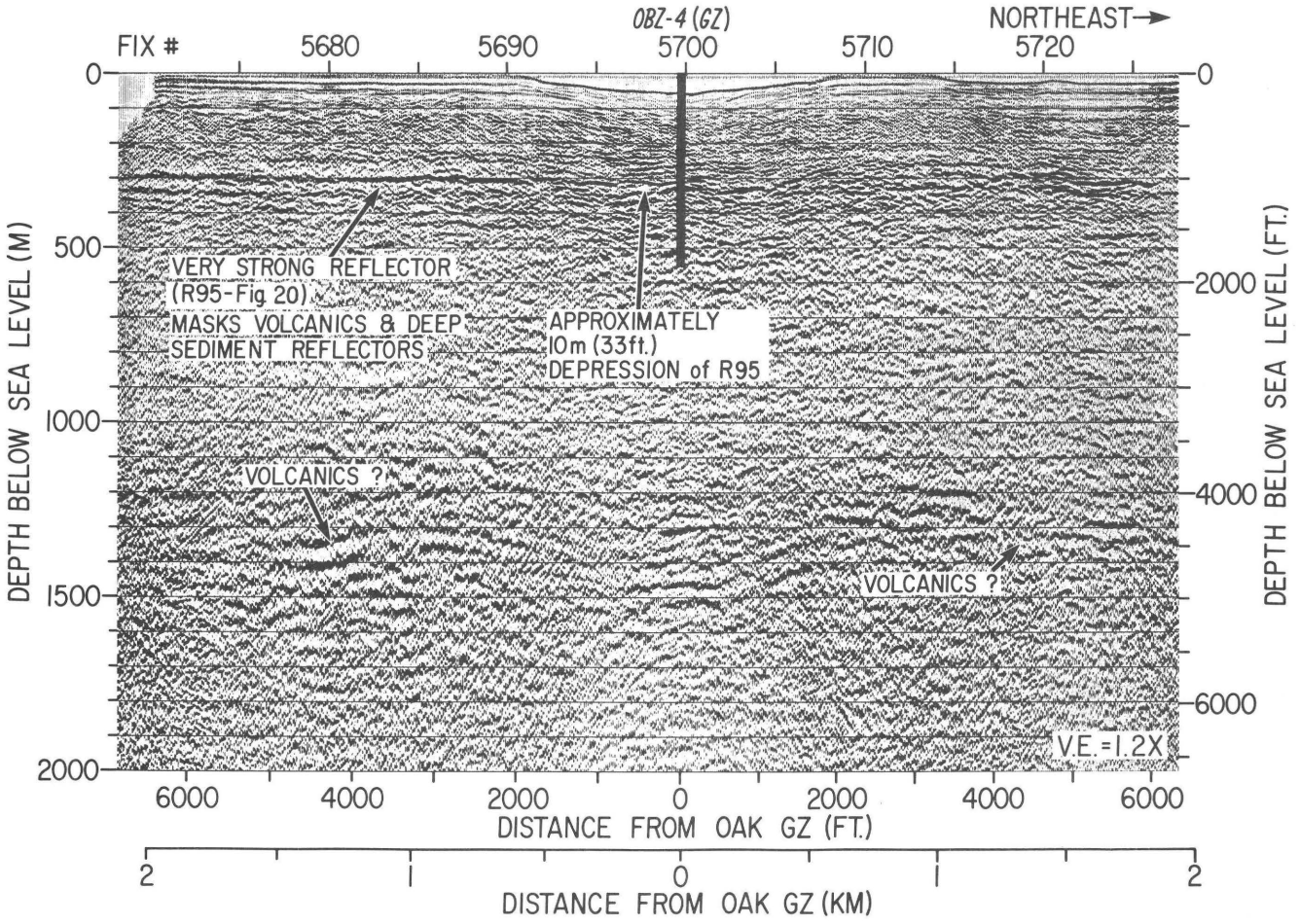

Figure 10. Seismic-reflection profile 101V5 across OAK crater acquired with an 80-in^3 watergun and 300-m streamer. GZ=ground zero.

disturbed zone in MIKE crater to the west and southwest side of KOA, most of the 1984 multichannel seismic lines were run near a north-south heading. The production lines were acquired using the 15-in^3 watergun source and 24-channel, 150-m (492 ft) streamer. Shots were fired at 2-s intervals and the ship speed was held as close as possible to 3.0 kn (5,556 m/hr) so that shot distances averaged 3.09 m (10.1 ft), a close approximation to the 3.125 m (10.25 ft) needed for 24-fold CDP coverage. Digital recordings at 1-ms sampling rate were recorded to 1.0 s. Good reflections were observed all the way to 1.0 s.

A sharp, single pulse from the crater floor near KOA ground zero demonstrates the highly successful signature deconvolution that was possible with the 1984 data. The seismically transparent sediments between the crater floor (34 m, or 111 ft) and 80 m (262 ft) probably represent transient crater fill beneath the inner bathymetric crater (fig. 11). The overall depth of penetration and the resolution within the crater itself gives confidence that the discontinuous reflectors and lateral amplitude transitions are evident in the seismic lines in spite of the expected side-echo and facies-change difficulties.

Correlation of Seismic Profiles to KOA Drill Holes

Six drill holes at KOA were sited along north-south profile 306V1 through KOA ground zero (figs. 2, 11–13). Reference hole KAR–1 was located 2,594 m (8,509 ft) south of KOA ground zero in an area assumed to be undisturbed by KOA or any of the other nuclear weapons tests in Enewetak (fig. 12). The five other drill sites were located at KOA ground zero (KBZ–4) and between KOA ground zero and 404 m (1,326 ft) south of ground zero (sites KCT–5, KDT–6, KET–7, and KFT–8). Portions of seismic line 306V1 at KAR–1 and the five drill sites near KOA ground zero are displayed in figures 12 and 13, respectively. Eleven reflectors with considerable lateral continuity have been annotated with labels R10, R20, and so forth, down through

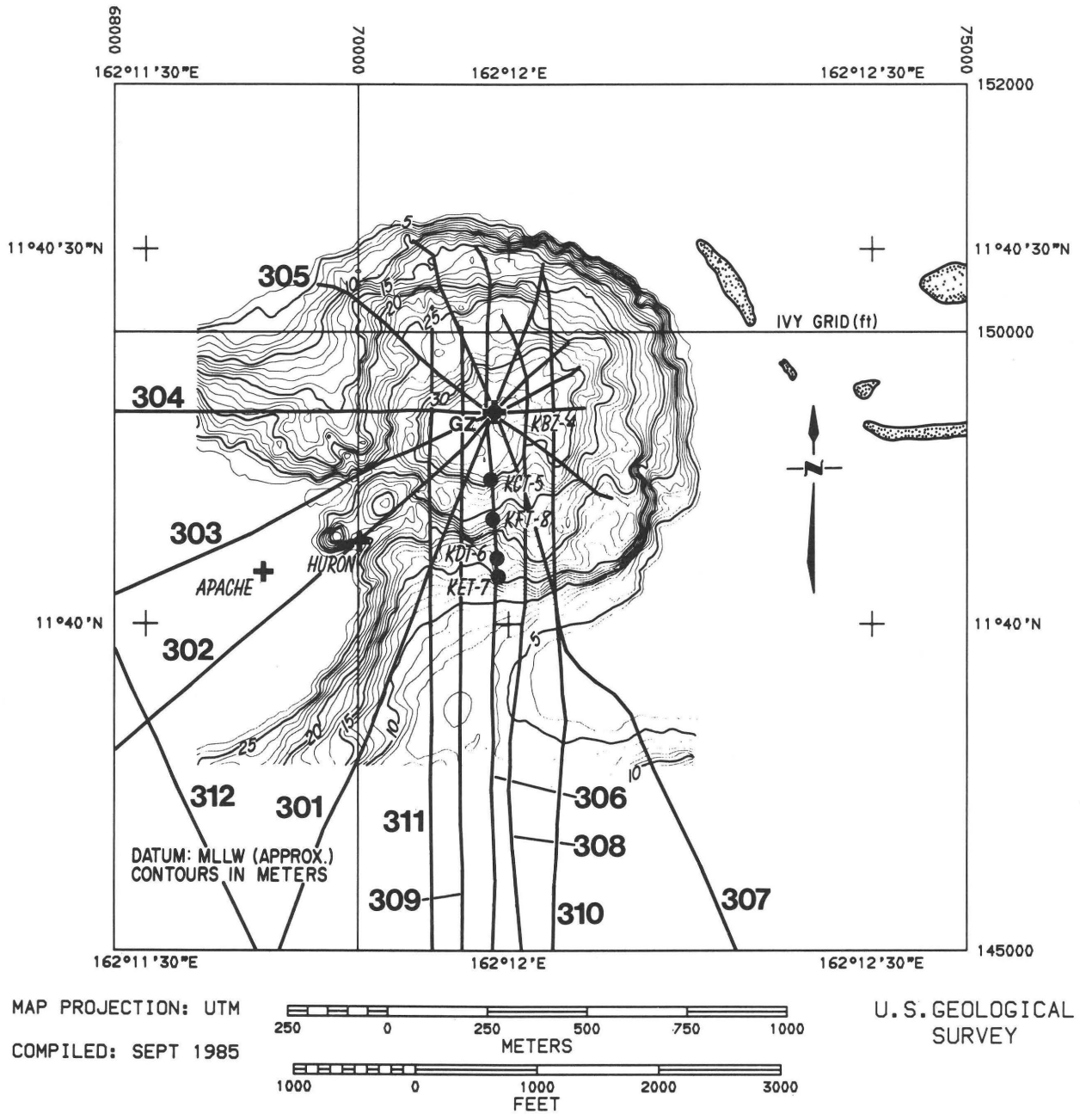

Figure 11. Bathymetry and track lines, KOA crater, with drill sites. Contours are in meters. GZ=ground zero.

R110 (fig. 12*B*). Some of these reflectors correlate with disconformities and sediment package boundaries identified in the preliminary drilling results (B. Wardlaw, written commun., July 15, 1985). Intermediate reflectors (R45, R75, and R95) are discussed later.

At the KAR–1 drill site (figs. 2, 12), R10 occurs at a depth of 47 m (154 ft) below sea level and correlates with the boundary between Holocene and Pleistocene sediments (disconformity "1," separating sediment packages 1 and 2; B. Wardlaw, written commun., July 15, 1985). R20 occurs at 55 m (180 ft) and correlates with Wardlaw's disconformity "2" within the Pleistocene (sediment package 2). R30 is a weak reflector at 80 m (262 ft) near KAR–1 and correlates with Wardlaw's disconformity "5" within the Pleistocene. R30 becomes a much stronger reflector near KOA ground zero. R40 occurs at 98 m (321 ft) and correlates well with Wardlaw's disconformity "8" within the Pleistocene. R50 occurs at 115 m (377 ft) and falls between Wardlaw's disconformities "11" and "12". R60 occurs at 124 m (407 ft) near Wardlaw's disconformity "12" which separates Pleistocene and Pliocene sediments (sediment packages 2 and 3,

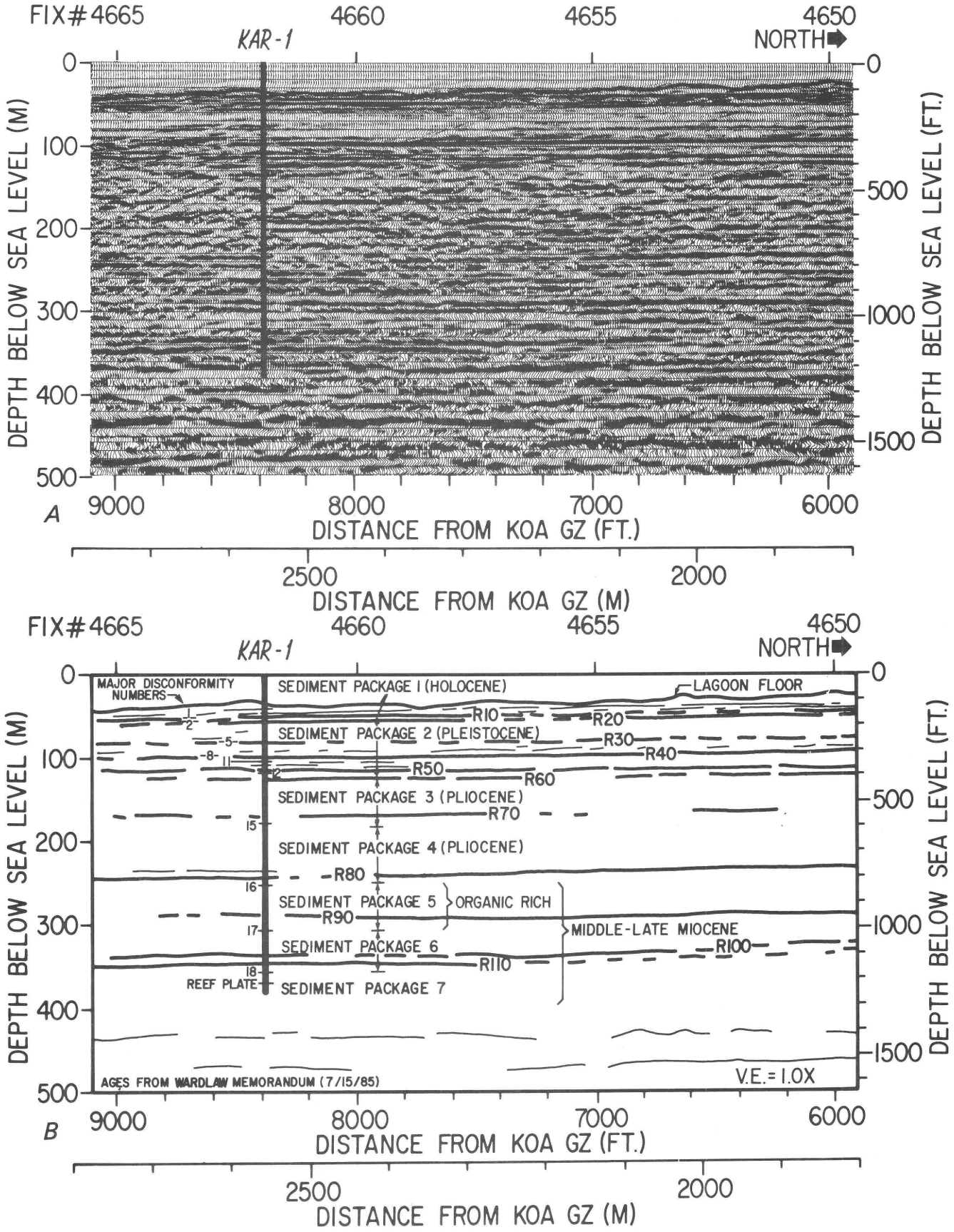

Figure 12. North-south profile 306V1 at drill site KAR–1, KOA crater. *A*, Migrated depth section; *B*, Interpretation. GZ=ground zero.

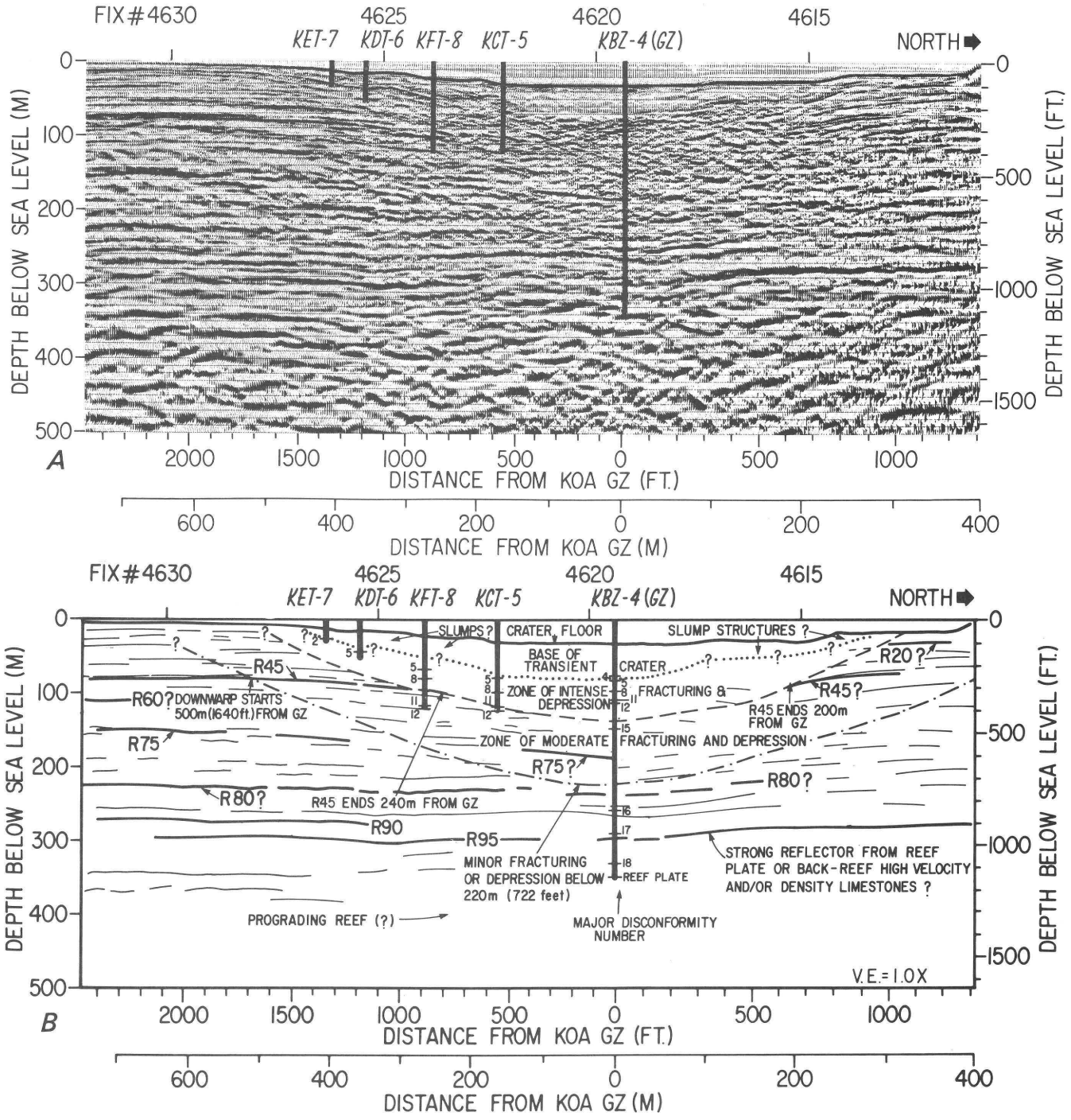

Figure 13. North-south profile 306V1 through KOA ground zero (GZ). *A*, Seismic display. *B*, Interpretation. Major disconformity numbers from B. Wardlaw, written commun., July 15, 1985.

respectively). R70 occurs at 168 m (551 ft), 11 m (36 ft) above disconformity "15" which separates sediment packages 3 and 4, both Pliocene. R80 occurs at 245 m (804 ft), 9 m (29 ft) above disconformity "16," which separates sediment package 4 from the underlying organic-rich sediment package 5. R90 occurs at 280 m (919 ft), within sediment package 5. R100 occurs at 334 m (1,096 ft), within the lower part of sediment package 6. R110 occurs at 343 m (1,125 ft), 13 m (43 ft) above disconformity "18" which separates sediment packages 6 and 7 (middle-to-late Miocene). R90, R100, and R110 are part of a band of strong, discontinuous reflectors between 280 and 350 m (918–1,148 ft) which increase in reflectivity near the reef, suggesting paleo-reef and back-reef facies.

While some reflectors correspond to disconformities drilled at KAR–1, there are no strong reflectors that can be

correlated easily between the six drill holes. The relatively homogeneous carbonate composition of the Enewetak sediments appears to result in small velocity and density contrasts related to subtle depositional and diagenetic effects which appear to have limited lateral continuity.

Projection of the reflectors from KAR–1 (fig. 12) into KOA crater (fig. 13) was hampered also by reverberation beneath the shoal south of the crater, and only reflectors R60, R80, and R90 tie to Wardlaw's disconformities in the crater holes within ±10 m. While most of the reflectors were obviously weak and discontinuous, R30 appeared to be a good reflector beneath the shoal. However, R30 projected into the KDT–6 well approximately 35 m (115 ft) deeper than disconformity "5" with which it should have tied. The cause of the mis-tie is uncertain, but it might be due to the seismic reflector following a diagenetic boundary rather than a primary depositional boundary. Alternatively, thrusting and uplift of disconformity "5" may have occurred during the cratering process. Since the drilling results have not supported any evidence of thrusting or uplift of disconformity "5," a mis-tie must be assumed, and the reflector under KOA crater has been relabeled from R30 to R45. R45 is a relatively good reflector beneath KOA and appears to downwarp into the crater on many of the seismic profiles.

Reflectors R10, R20, R50, R70, R100, and R110 from KAR–1 could not be reliably tied into KBZ–4, and intermediate reflectors R75 and R95, which are mappable within KOA, have been identified. Structure-contour maps were prepared for R45, R75, R80, and R95. However, before discussion of the maps, the deformation effects seen on seismic lines 306, 304, 305, and 302 (fig. 11) will be interpreted in detail.

While the absolute ties between KAR–1 and KBZ–4 for the reflectors have been difficult, the relative downwarping, fracturing, and truncation of R45, R75, and other intermediate reflectors are still valid indications of deformational effects within KOA crater.

Deformational Effects: North-South Profile 306V1 through KOA Ground Zero

Within the center of KOA crater, transparent sediments are seen between the crater floor (34 m, or 111 ft, below sea level) and 80 m (262 ft) (fig. 13*A*,*B*). The bottom of this transparent zone is interpreted as the base of the transient crater, and the preliminary drilling reports indicate that drilling lithologies and age units are unstratified and mixed above this level (B. Wardlaw, written commun., July 15, 1985). Below this level, a stratified mixed rubble was encountered.

R10 and R20, approximately 47 and 55 m (154 and 180 ft) deep at KAR–1 (fig. 12*A*,*B*), could not be traced with any confidence within 600 m (1,968 ft) south of KOA ground zero, but a few shallow reflectors (which may be R10 or R20) are present between 300 and 400 m (984 and 1,312 ft) to the north of KOA ground zero. These shallow reflectors are difficult to discriminate from water-bottom multiples. Scattered reflecting points occur at 10- to 30-m (33–98 ft) depth beneath the terraces beginning 100 m (328 ft) north and 200 m (656 ft) south of ground zero. These may be chaotic slump masses or coherent down-dropped fault blocks.

R45 forms the most mappable shallow reflector around KOA crater (fig. 13*A*,*B*). As discussed in the previous section, R45 within KOA crater and R30 at KAR–1 appeared to be the same reflector, but this possibility did not agree with the stratigraphic drilling results. In spite of the correlation problem to KAR–1, R45 is a good mappable surface within KOA crater and can show relative deformational effects. Beginning about 500 m (1,640 ft) south of KOA ground zero, R45 drops from 77 m (253 ft) to a depth of 92 m (302 ft) at a distance of 240 m (787 ft) from KOA ground zero, where it is too broken to be closely followed. On the north side of KOA ground zero, a shallow reflector, perhaps R45, slopes from 65 m (213 ft) at the north end of the profile, 400 m (1,312 ft) from ground zero to a depth of 89 m (292 ft) at a point 200 m (668 ft) from ground zero. The effects of the KOA detonation on R45 are slightly asymmetric with intense fracturing and downward depression extending approximately 40 m (131 ft) further from ground zero on the south side (240 m, or 787 ft) than on the north side (200 m, or 656 ft) (fig. 13*B*).

R75 forms an intermittent horizon toward KOA crater (fig. 13*A*,*B*). South of ground zero, it occurs at a depth of approximately 145 m (476 ft) at a point 700 m (2,296 ft) south of ground zero and drops to 162 m (531 ft) at a distance of 380 m (1,246 ft). A strong reflector at 180-m (590 ft) depth, directly below KOA ground zero and out to 100 m (328 ft) south of it, may correlate with R75. The apparent deformation on R75 is deeper than reported in the preliminary drilling reports (B. Wardlaw, written commun., July 15, 1985). The interpreted 180-m (590 ft) reflector may be a side echo. However, a similar strong event occurs on several KOA profiles. Possibly the drilling disconformities "12" and "15" (fig. 13*B*), which appear uplifted near KOA ground zero, are underlain by more depressed strata. This would require rebound at a shallow level, but complexities of this sort may be possible in craters. For the present analysis, our preferred interpretation is that the downwarped R75 is a valid seismic reflector.

Below a depth of approximately 220 m (722 ft), R80, R90, and R95 appear to pass beneath KOA ground zero with little disruption (figs. 13*A*,*B*). While the preliminary drilling report (B. Wardlaw, written commun., July 15, 1985) indicates that some fracturing extended to 297 m (975 ft) below KOA ground zero, the travel-time and velocity anomalies beneath KOA ground zero in the check shots (figs. 4, 6) only extended down to approximately 220 m (722 ft). Before discussing a more general interpretation of crater deformation at KOA, presentation of profiles 304V1, 305V1, and 302V1 is appropriate.

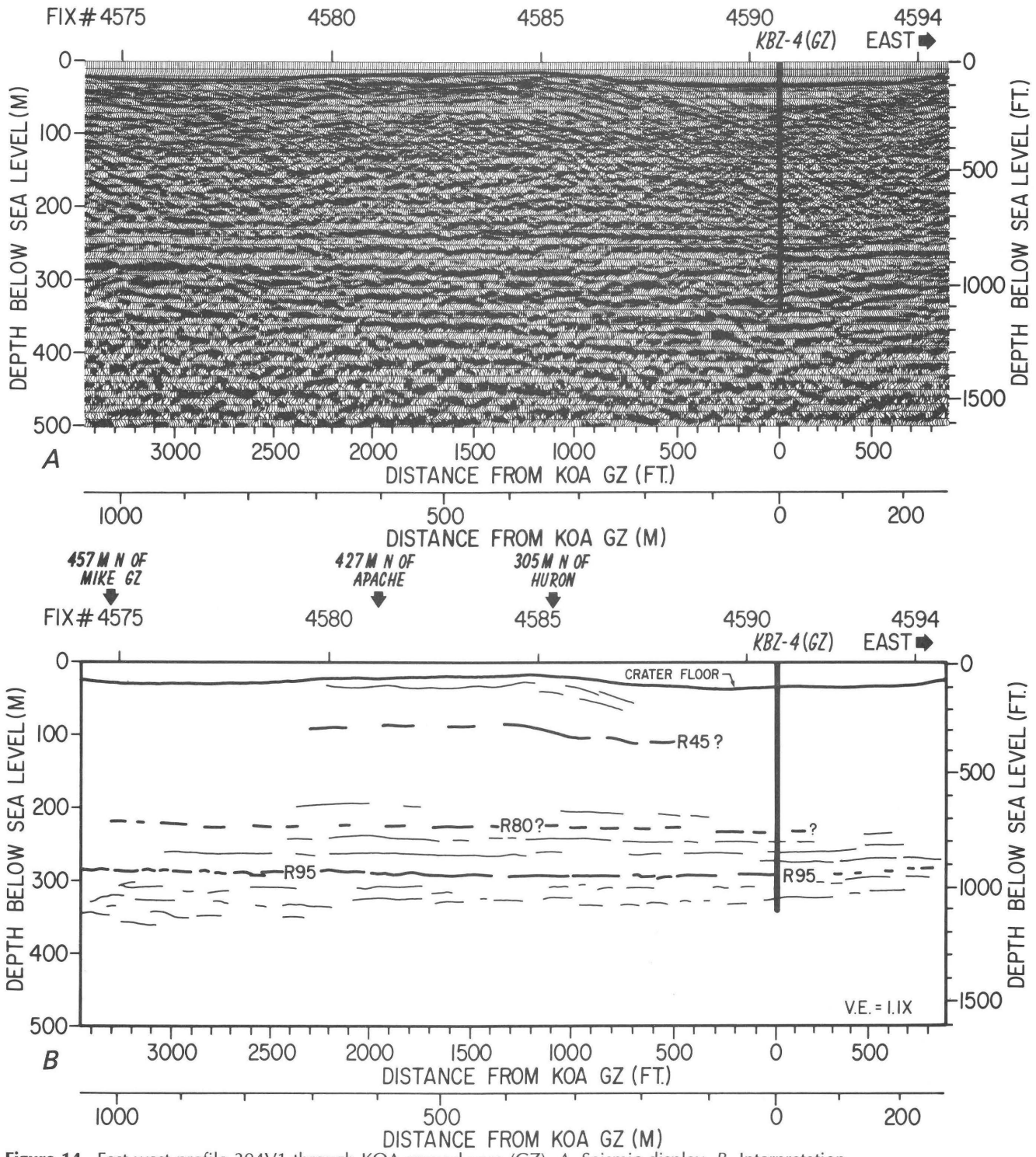

Figure 14. East-west profile 304V1 through KOA ground zero (GZ). *A*, Seismic display. *B*, Interpretation.

Deformational Effects: East-West Profile 304V1 through KOA Ground Zero

A portion of line 304V1, beginning approximately 1,000 m (3,280 ft) west of KOA ground zero and extending approximately 200 m (656 ft) east of ground zero, is shown in figures 14*A*,*B*. The shallow reflectors west of KOA ground zero are difficult to interpret and have probably been disturbed by MIKE, APACHE, and HURON in addition to KOA. A reflector possibly equivalent to R45 may be present, but it is too weak to interpret confidently. R75 is not obvious as a mappable horizon on line 304V1.

R80 and R95 are mappable beneath KOA ground zero on line 304V1 at depths of 230 m (754 ft) and 285 m (935 ft), respectively. They are relatively flat, having little or no downward depression or major fracturing.

In summary, line 304V1 shows that R80 and R95 at depths greater than 230 m (754 ft) below KOA ground zero are relatively undisturbed and agrees with the observations at that depth derived from the north-south line 306V1 (figs. 13*A*,*B*).

Deformational Effects: Northwest-Southeast Profile 305V1 through KOA Ground Zero

Line 305V1 begins approximately 600 m (1,968 ft) northwest of KOA ground zero and extends 300 m (984 ft) southeast of ground zero. R45 appears as a weak reflector on both ends of the profile (figs. 15*A*,*B*). Beginning about 450 m (1,476 ft) northwest of KOA ground zero, R45 begins to drop from 80 m (262 ft) to a depth of 98 m (321 ft) 200 m (656 ft) from ground zero, where it is too broken to be followed more closely to ground zero. On the southeast side of KOA ground zero, another reflector, apparently R45, can be identified approximately 200 m (656 ft) from ground zero. The interpreted R45 on line 305V1 terminates approximately 200 m (656 ft) from KOA ground zero as did R45 on the north end of line 306V1 (figs. 13*A*,*B*).

A weak northwest-dipping reflector between depths of 150 and 180 m (492–590 ft) southeast of ground zero on line 305V1 may be R75. R80 and R95 appear at 230- and 290-m (754 and 951 ft) depth below KOA ground zero on line 305V1 (fig. 15*B*) and are relatively undisturbed except for a gentle apparent southeast dip.

When compared to line 306V1 (fig. 13), line 305V1 (fig. 15) shows the best seismic resolution of R45 and confirms that R45 begins to bend down about 450 m (1,476 ft) northeast of KOA ground zero and is intensely fractured within 200 m (656 ft) of ground zero. Over this 250-m (820 ft) interval, R45 is downwarped from 80 m (267 ft) to 95 m (312 ft). Within 200 m (656 ft) of ground zero, R45 is apparently too severely fractured to provide a mappable seismic reflector.

Deformational Effects: Northeast-Southwest Line 302V1 through KOA Ground Zero

The portion of line 302V1 shown in figures 16*A* and *B* starts 800 m (2,024 ft) southwest of KOA ground zero and extends 300 m (984 ft) northeast of ground zero. On the southwest end, line 302V1 passes south of MIKE ground zero and APACHE ground zero and over HURON ground zero (fig. 2). Shallow reflectors on this line are too broken to provide a mappable horizon. Deep reflectors, R80 and R95, again are relatively flat and undisturbed below KOA ground zero.

The most interesting feature on line 302V1 is a reflector, apparently R75, on the southwest side of ground zero. It is flat at about 145 m (476 ft) in the southwest but begins to downwarp 300 m (984 ft) southwest of ground zero and drops to 180 m (590 ft) at ground zero. Although this downwarp of R75 is most clearly seen on line 302V1, it also downwarps on the southwest side of KOA ground zero on lines 301V1, 303V1, 306V1, and 309V1 (not shown).

The downwarp of R75 to 180 m (590 ft) beneath ground zero is in conflict with the preliminary drilling data from KOA ground zero hole KBZ–4, where the deepest horizon with apparent downwarp is disconformity "12" at 112 m (369 ft) (B. Wardlaw, written commun., July 15, 1985). Although it is possible that the apparent downwarp of R75 on line 302V1 is a side echo or other interference effect, a reexamination of the drill log between 112 and 180 m (369–591 ft) at KOA ground zero is recommended. Although data conflict on this issue, the R75 downwarp appears to be real. Within KOA crater, at drill site KBZ–4 (ground zero), disconformity "12" appears to be uplifted 8 m (26 ft) above its depth at sites KFT–8 and KCT–5 (fig. 13*B*) (B. Wardlaw, written commun., July 15, 1985). Even if disconformities "12" and "15" are level or slightly uplifted near KOA ground zero (fig. 13*B*), this uplifting could be a rebound phenomenon leaving deeper horizons, such as R75, still depressed. No disconformities were reported between 147 and 258 m (481–847 ft) at KBZ–4, and rebound within this zone may be possible.

Structure-Contour Maps

Using migrated depth sections of KOA lines 301V1, 303V1, 308V1, 309V1, 310V1, 311V1, and 312V1 in addition to the four lines discussed above, structure-contour maps of R45, R75, R80, and R95 have been prepared that depict the three-dimensional warping or termination of these four reflectors (figs. 17–20).

The R45 map (fig. 17) shows a relatively flat surface 75 m (246 ft) deep at distances more than 500 m (1,640 ft) south of KOA ground zero. The surface downwarps to more than 110 m (361 ft) 240 m (787 ft) south of ground zero where R45 becomes too fractured to map. Southwest of KOA ground zero and south of MIKE ground zero and APACHE ground zero, R45 appears to downwarp to approximately 120 m (394 ft). North of KOA ground zero, R45 (or a slightly shallower reflector on line 306V1, fig. 13) downwarps to a depth of 90 to 100 m (295–328 ft) at a distance approximately 200 m (656 ft) from ground zero. Within 200 m (656 ft) of ground zero, R45 is too fractured to map.

The R75 map (fig. 18) shows mappable events primarily in the area south-southwest of KOA ground zero. R75 lies between 140 and 150 m (459–492 ft) at distances more than 300 m (984 ft) from ground zero and then drops to 180 m (590 ft) directly below ground zero.

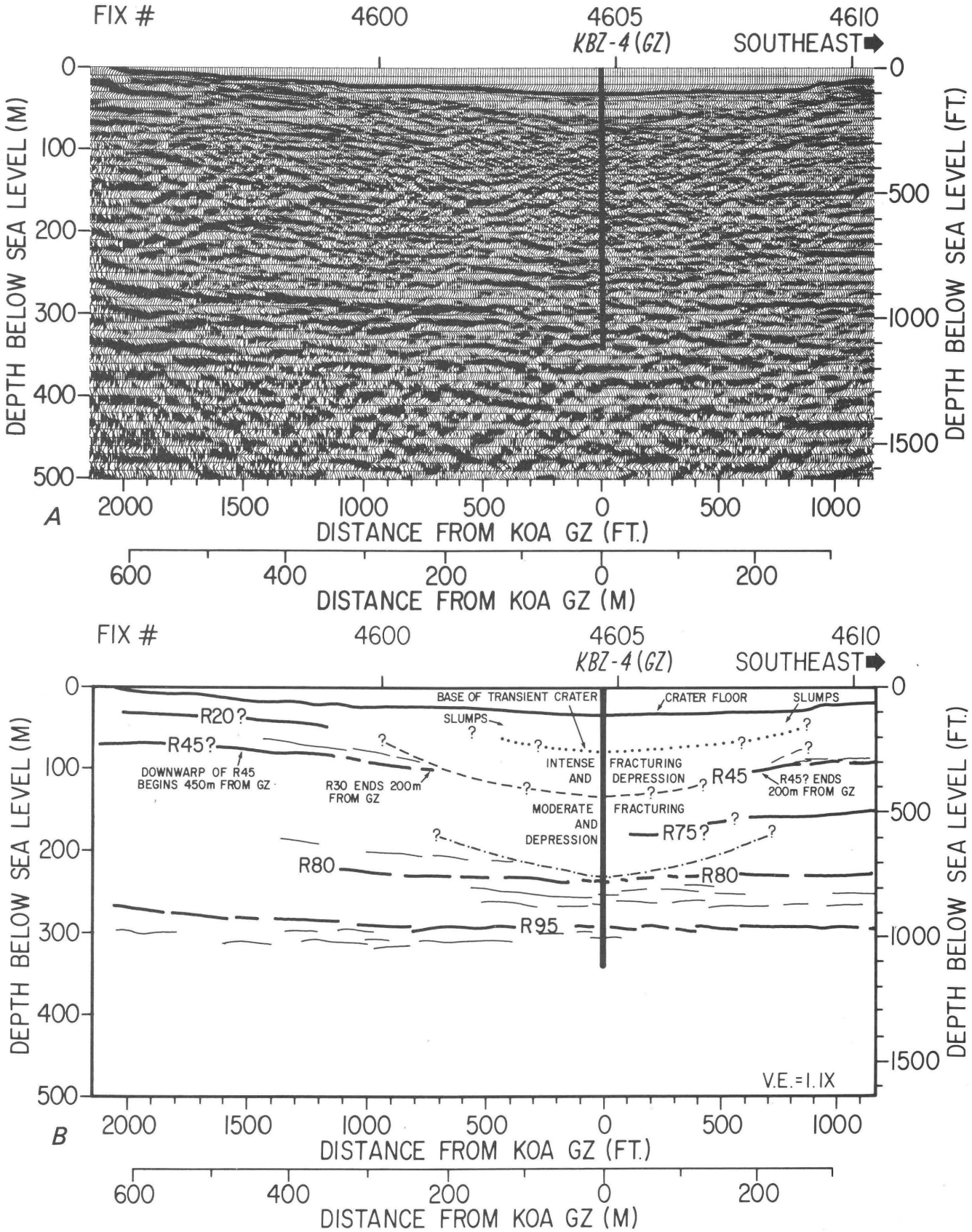

Figure 15. Northwest-southeast profile 305V1 through KOA ground zero (GZ). *A*, Seismic display. *B*, Interpretation.

Figure 16 (right). Northeast-southwest profile 302V1 through KOA ground zero (GZ). *A*, Seismic display. *B*, Interpretation.

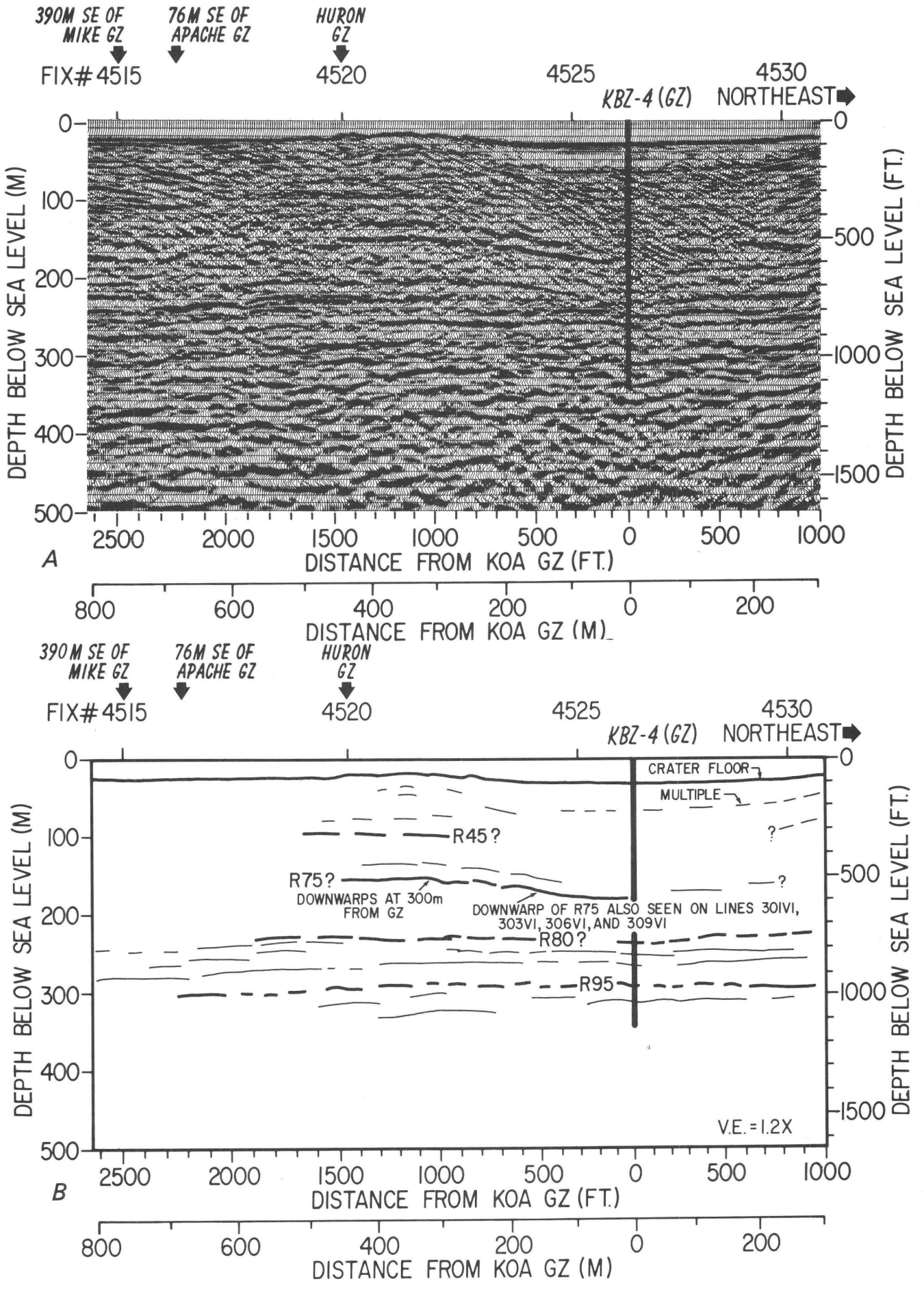
390M SE OF MIKE GZ
76M SE OF APACHE GZ
HURON GZ
FIX# 4515
4520
4525
4530
KBZ-4 (GZ)
NORTHEAST
DEPTH BELOW SEA LEVEL (M)
DEPTH BELOW SEA LEVEL (FT.)
0
100
200
300
400
500
500
1000
1500
2500
2000
1500
1000
500
0
500
1000
A
DISTANCE FROM KOA GZ (FT.)
800
600
400
200
0
200
DISTANCE FROM KOA GZ (M)
390M SE OF MIKE GZ
76M SE OF APACHE GZ
HURON GZ
FIX# 4515
4520
4525
4530
KBZ-4 (GZ)
NORTHEAST
CRATER FLOOR
MULTIPLE
R45?
R75?
DOWNWARPS AT 300m FROM GZ
DOWNWARP OF R75 ALSO SEEN ON LINES 301VI, 303VI, 306VI, AND 309VI
R80?
R95
V.E. = 1.2X
DEPTH BELOW SEA LEVEL (M)
DEPTH BELOW SEA LEVEL (FT.)
B
DISTANCE FROM KOA GZ (FT.)
DISTANCE FROM KOA GZ (M)

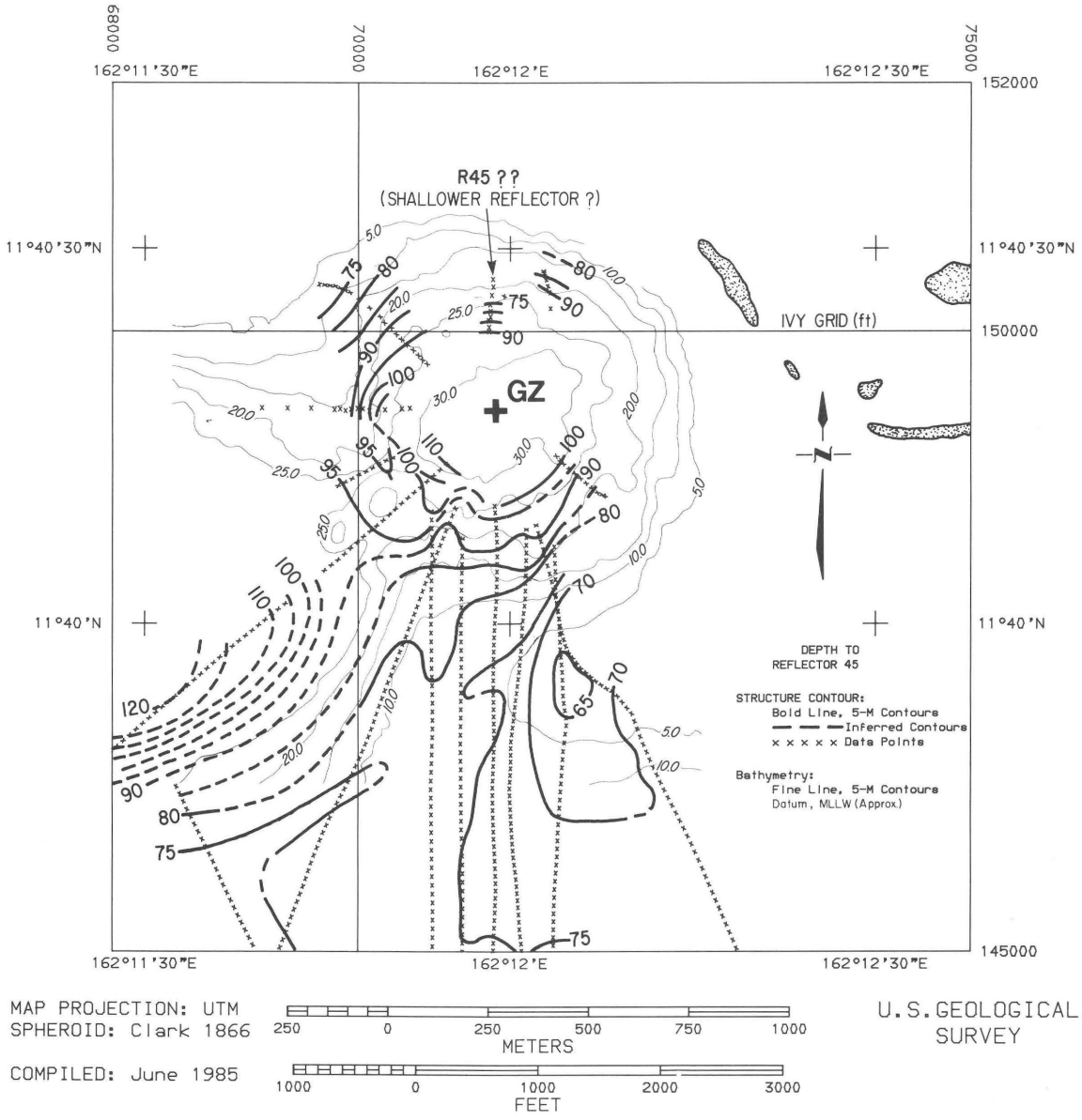

Figure 17. Structure-contour map, reflector R45, KOA crater. GZ=ground zero.

The structure-contour map of R80 (fig. 19) shows variations between 215 and 245 m (705–804 ft) of depth with less than a 10-m (33 ft) downwarp beneath KOA ground zero and no simple trend outside KOA crater.

The structure-contour map of R95 (fig. 20) shows variations from 280 to 335 m (918–1,099 ft) with no obvious downwarp at KOA ground zero and a generally southward dip in the southern half of the map area.

Structural Summary of KOA Crater Based on Multichannel Seismic Data

Seven multichannel seismic radial lines over KOA ground zero show a transparent pond of sediments in the center of the crater which extends down to an average depth of approximately 80 m (262 ft). In a water depth of about 34 m (111 ft) (33 m, or 108 ft, corrected to Holmes and Narver datum), this 46-m-thick (151-ft-thick) transparent sediment layer is interpreted as chaotically mixed debris and postevent sediment fill. Results from drilling this transparent sediment at KBZ–4 were in good agreement with the seismic data. Mapping of the lateral extent of this debris has been hampered by the numerous side echoes off the crater rim and may have been further complicated by low-angle sediment slumps (fig. 13*B*). Unfortunately, the Huntec near-bottom sonar (single-channel) system was also unsuccessful in KOA and, therefore, neither seismic system has produced a clear picture in the upper 50 m (164 ft) of the lateral extent of the transient crater.

A zone of intense fracturing can be inferred on reflector R45 within 200 m (656 ft) of KOA ground zero. R45 is last seen at a depth of approximately 100 m (328 ft), but on

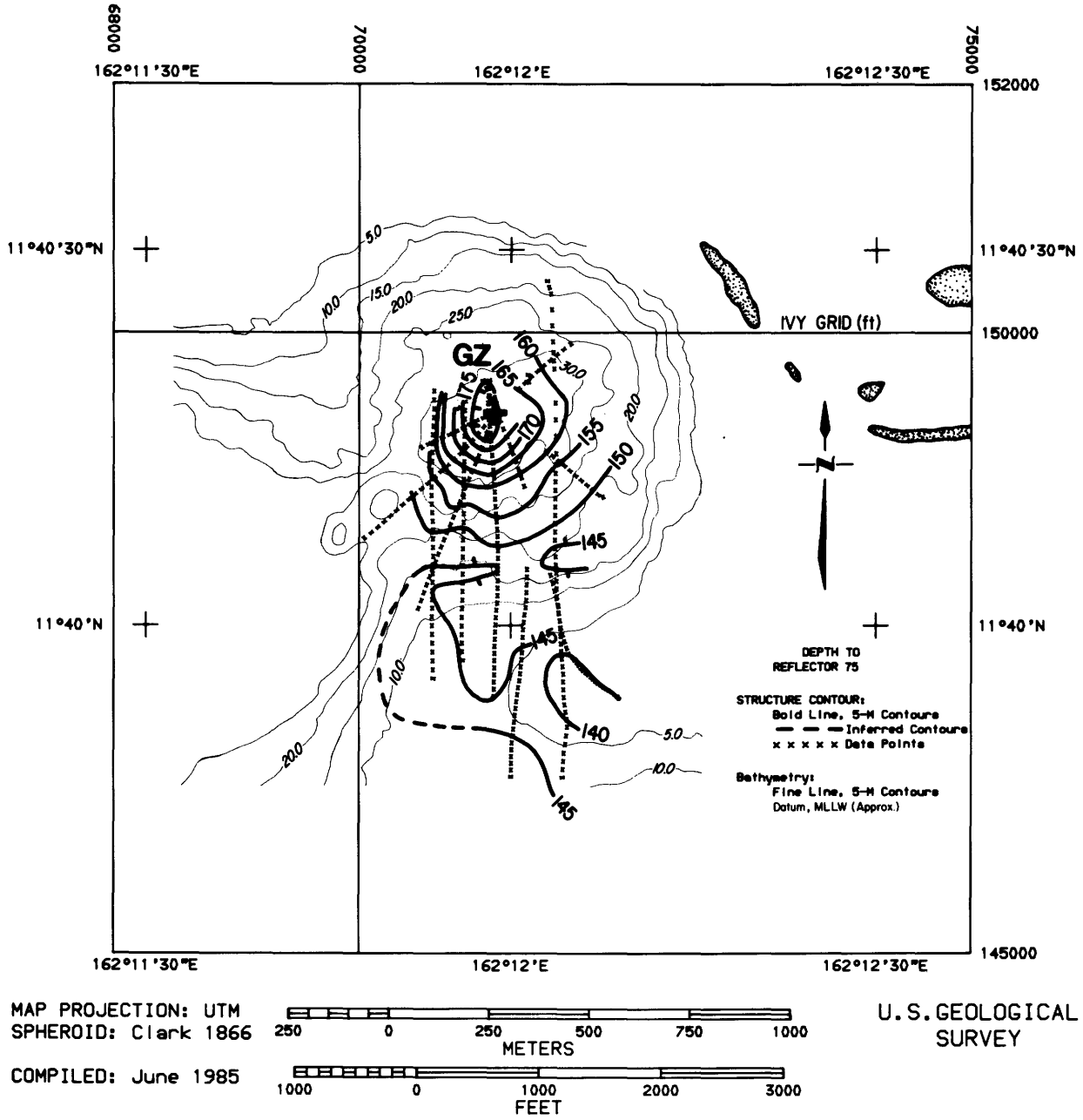

Figure 18. Structure-contour map, reflector R75, KOA crater.

the basis of the general absence of reflectors on line 306V1 near KOA ground zero (fig. 13*B*), the intensely fractured zone may project to a depth of 140 m (459 ft) directly beneath ground zero. Because good marker reflectors shallower than R45 are lacking, the lateral extent of the intensely fractured zone above R45 beyond 200 m (656 ft) from ground zero is speculative and is based only on the multichannel seismic data. On line 306V1 (fig. 13*B*), intense fracturing extends laterally out to a distance of about 500 m (1,640 ft) on the south side and at least 300 m (984 ft) on the north side of KOA ground zero.

The downwarping of the R45 and R75 reflectors indicates an outer zone of deformation where coherent reflectors are depressed downward and fracturing effects are only moderate. For R45, this downwarp begins at approximately 500 m (1,640 ft) from ground zero, and it drops from 75 to 100 m (246–328 ft) before intense fracturing occurs within 200 m (656 ft) of ground zero. For R75, the apparent downwarp begins 300 m (984 ft) from ground zero, and it drops from 150 to 180 m (492–590 ft) (fig. 18). The relatively undisturbed reflectors R80 and R95 suggest that moderate fracturing and downwarp do not occur below 230 m (754 ft).

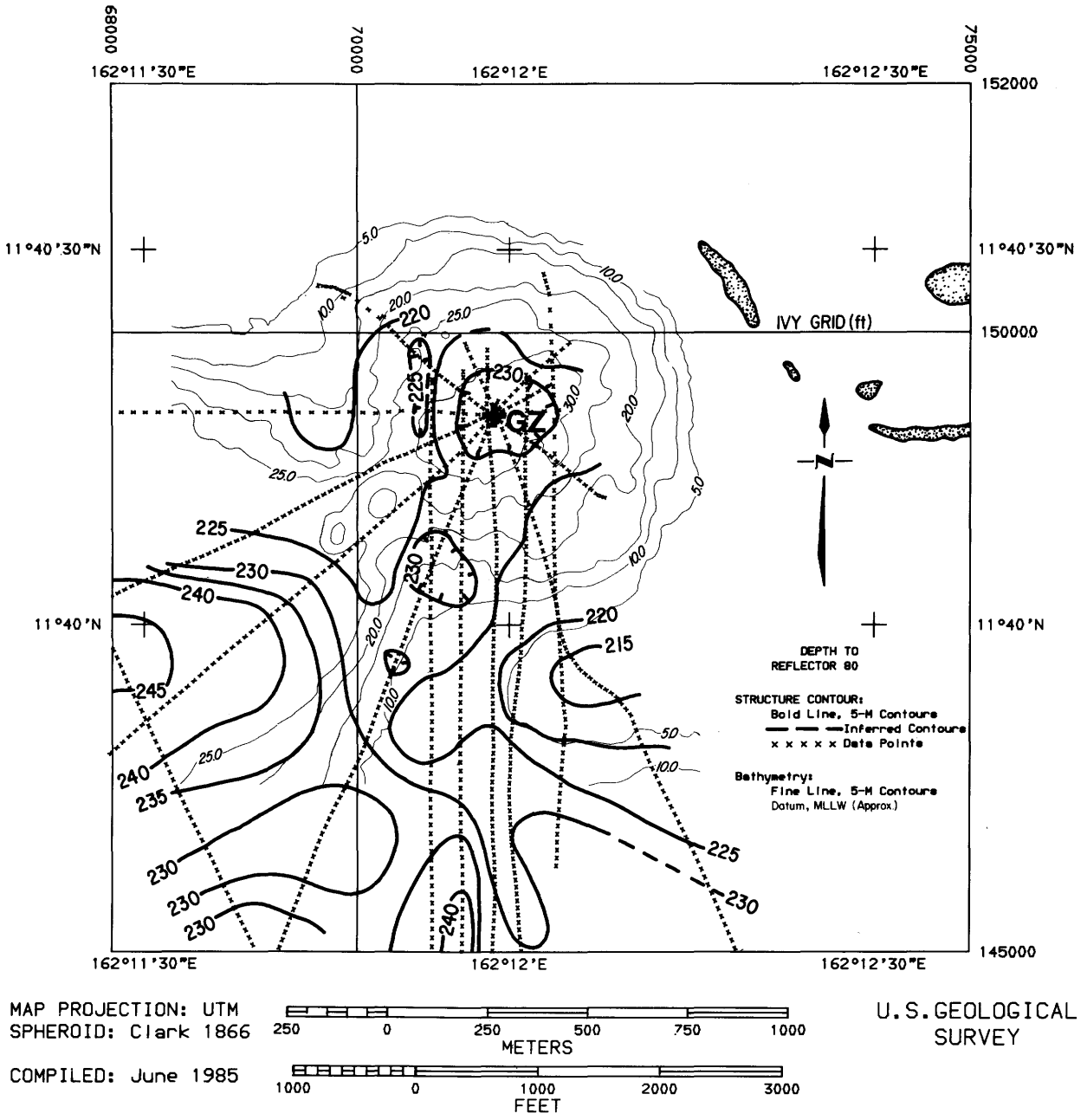

Figure 19. Structure-contour map, reflector R80, KOA crater.

The check-shot surveys from the KOA drill holes indicated an increasing travel-time delay down to a depth of 220 m (722 ft) below KOA ground zero (fig. 4). The interval velocities, which were averaged over depth intervals of 50 m (164 ft), show a major velocity anomaly down to at least 200 m (625 ft) (fig. 6). The preliminary drilling reports (B. Wardlaw, written commun., July 15, 1985) indicate some fracturing down to 297 m (975 ft) beneath KOA ground zero. The interpretation of line 306V1 over KOA ground zero (fig. 13*B*) assumes that the base of the moderately fractured and depressed zone corresponds with the maximum time delay in the check shots, that is, 220 m (722 ft). While some fracturing may occur to a depth of 297 m (975 ft) in the core samples, the effects appear minor in the check-shot and multichannel seismic data below 220 m (722 ft).

In spite of limited success in tying the individual seismic reflectors to the disconformities in the KAR–1, KBZ–4, and other KOA drill sites, the relative warping, fracturing, truncation of reflectors, and the transparent

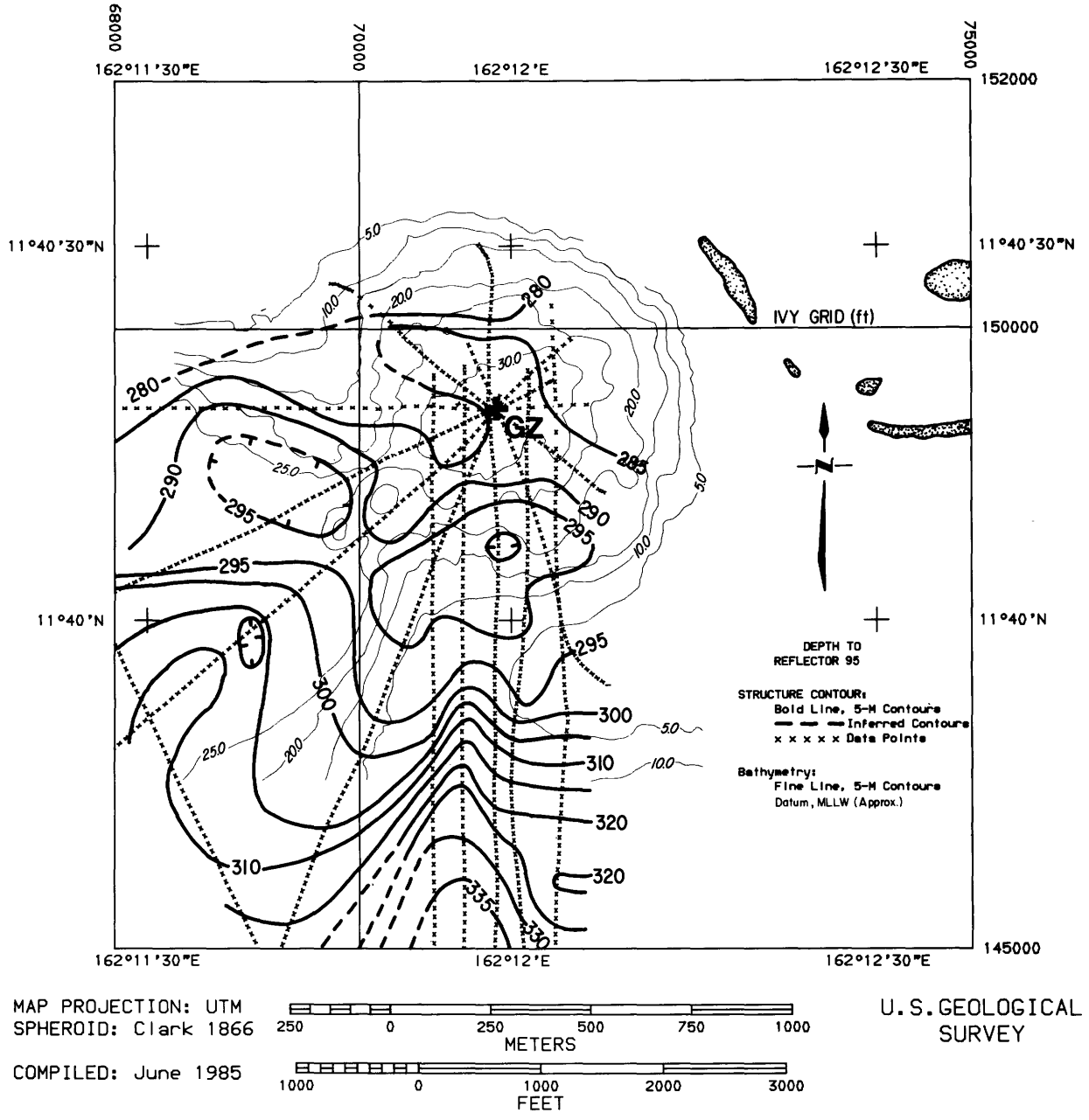

Figure 20. Structure-contour map, reflector R95, KOA crater.

crater fill within KOA crater observed in the multichannel seismic reflection data are valid evidence for the deformation effects within the crater.

In terms of first-order deformational effects at KOA, both the multichannel seismic reflection and drill-hole results indicate a transient crater depth of 75 to 80 m (246–262 ft). Moderate fracturing effects can be identified to a depth of 220 m (722 ft) in the reflection and check-shot data, while fracturing was observed to 297 m (974 ft) in the drilling results. Downwarp of horizons directly beneath ground zero varies between 112 m (369 ft) for the drilling results and 180 m (590 ft) for the seismic profiles; internal rebound effects may be responsible for this apparent discrepancy. The lateral effects of the KOA event can be seen in downwarp of the R45 reflector out to distances of 500 m (1,640 ft) from ground zero, and the drilling results indicate fracturing down to a depth of 27 m (88 ft) at the southernmost drilling site (KET–7, fig. 13), which is 404 m (1,326 ft) south of KOA ground zero.

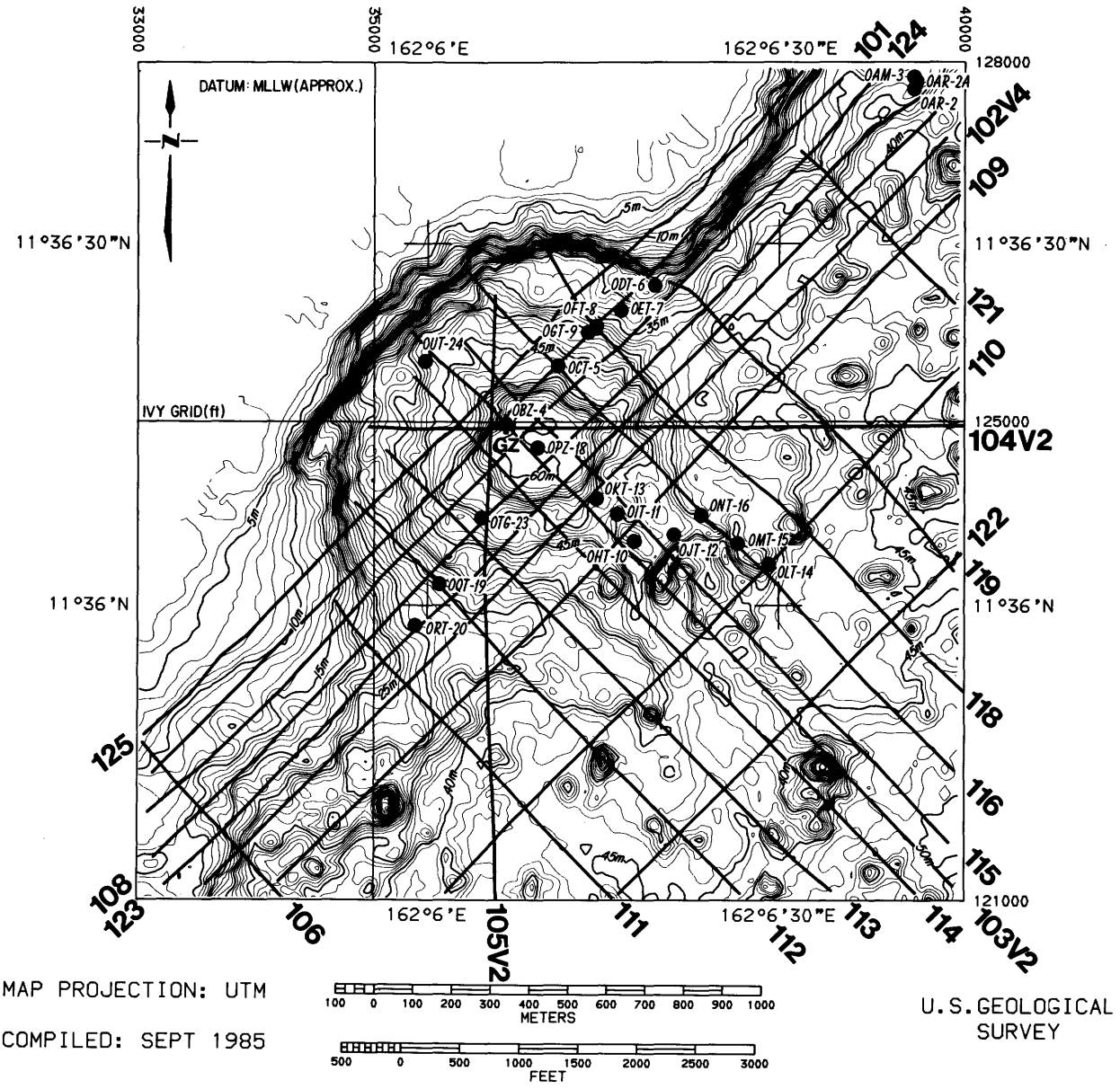

Figure 21. Bathymetry with multichannel seismic-reflection track lines and drill sites, OAK crater. GZ=ground zero. Bathymetric contour interval is 1 m.

RESULTS: OAK CRATER

Because one side of OAK crater lies mostly in deep water open to the lagoon, *Egabrag II* was able to maneuver successfully with the long streamer. A grid of 25 profiles was acquired with the 15-in^3 watergun and 24-channel, 150-m streamer (figs. 3, 21). Good-quality reflections were generally observed to the base of the recording window at 1.0 s. The primary lines perpendicular and parallel to the reef through OAK ground zero are lines 103V2 and 101V4, respectively (figs. 22, 23). Because the geometric center of OAK crater lies 100 m (330 ft) southeast of ground zero, line 101V4 grazes the northwest flanks of the crater and has more severe side echoes than line 124V1, which also lies parallel to the reef but passes closer to the geometric center. Therefore, lines 103V2 and 124V1 are the reef-perpendicular and reef-parallel lines which pass closest to the geometric and physiographic center of OAK crater. Clean pulses off the crater floor at approximately 60 m (197 ft) are observed on both lines 103V2 and 124V1, and a transparent zone can be observed down to approximately 110 m (361 ft). We interpret this zone as the base of the transient crater (figs. 22*B*, 24*B*). In OAK, as in KOA, we observed good reflections down to 1.0 km (3,280 ft), but the lateral continuity of individual reflectors was usually limited.

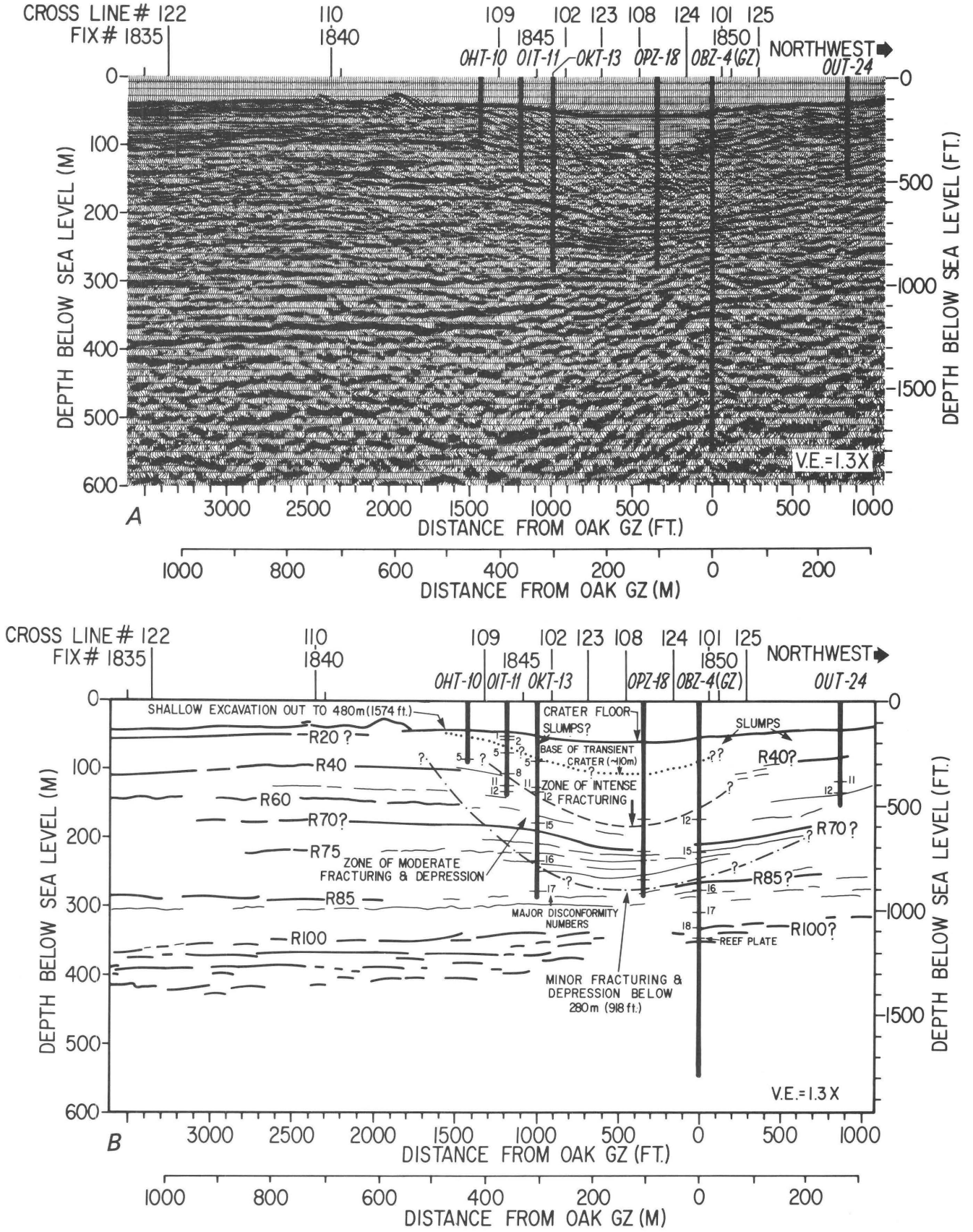

Figure 22. Northwest-southeast profile 103V2 through OAK ground zero (GZ). *A*, Seismic display. *B*, Interpretation. Major disconformity numbers after B. Wardlaw, written commun., July 15, 1985.

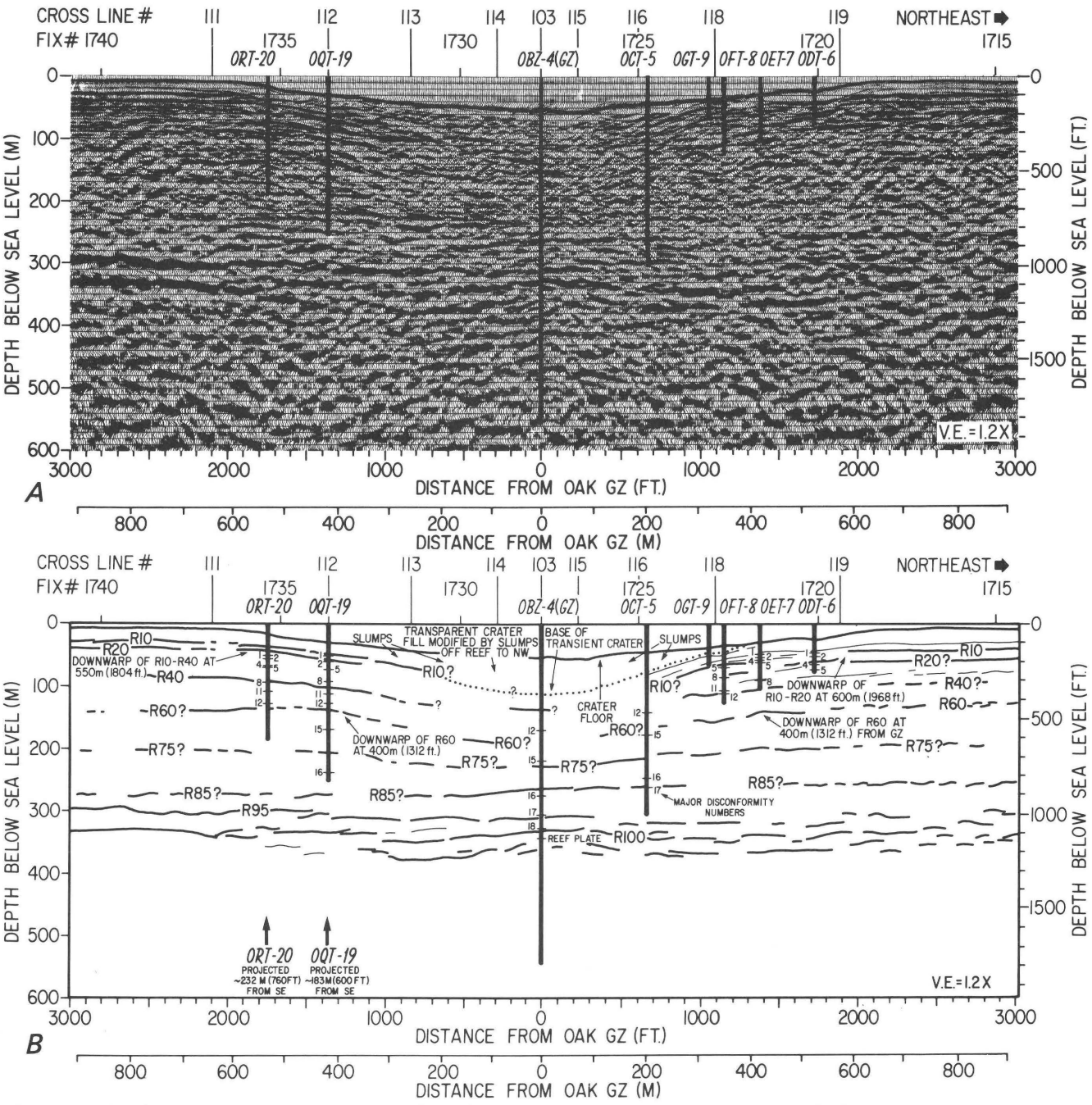

Figure 23. Southwest-northeast profile 101V4 through OAK ground zero (GZ). *A*, Seismic display. *B*, Interpretation. Major disconformity numbers after B. Wardlaw, written commun., July 15, 1985.

Key Seismic Horizons at OAK: Reference Drill Sites OAR–2 and OOR–17

Reference drill sites were located near the reef, both northeast and southwest of OAK crater, at sites OAR–2 and OOR–17, respectively (fig. 3). OAR–2 was located near the northeast end of seismic line 108V1 (fig. 25) and OOR–17 on the southwest end of line 109V1 (fig. 26). The most continuous reflectors observed outside OAK crater are shown on the northeast end of line 109V1, which is parallel to the reef and 412 m (1,350 ft) southeast of ground zero (fig. 27). Reflectors R10 and R20 correlate with shallow horizons mapped by the Huntec sonar (chap. C, this volume), and preliminary drilling results indicate that R10 is the Holocene-Pleistocene boundary. Reflectors R40, R60, R75, R80, and R100 are interpreted as the most correlatable seismic horizons. Line 121V1 illustrates the character of a profile perpendicular to the reef well northeast of OAK ground zero and OAR–2 (fig. 28).

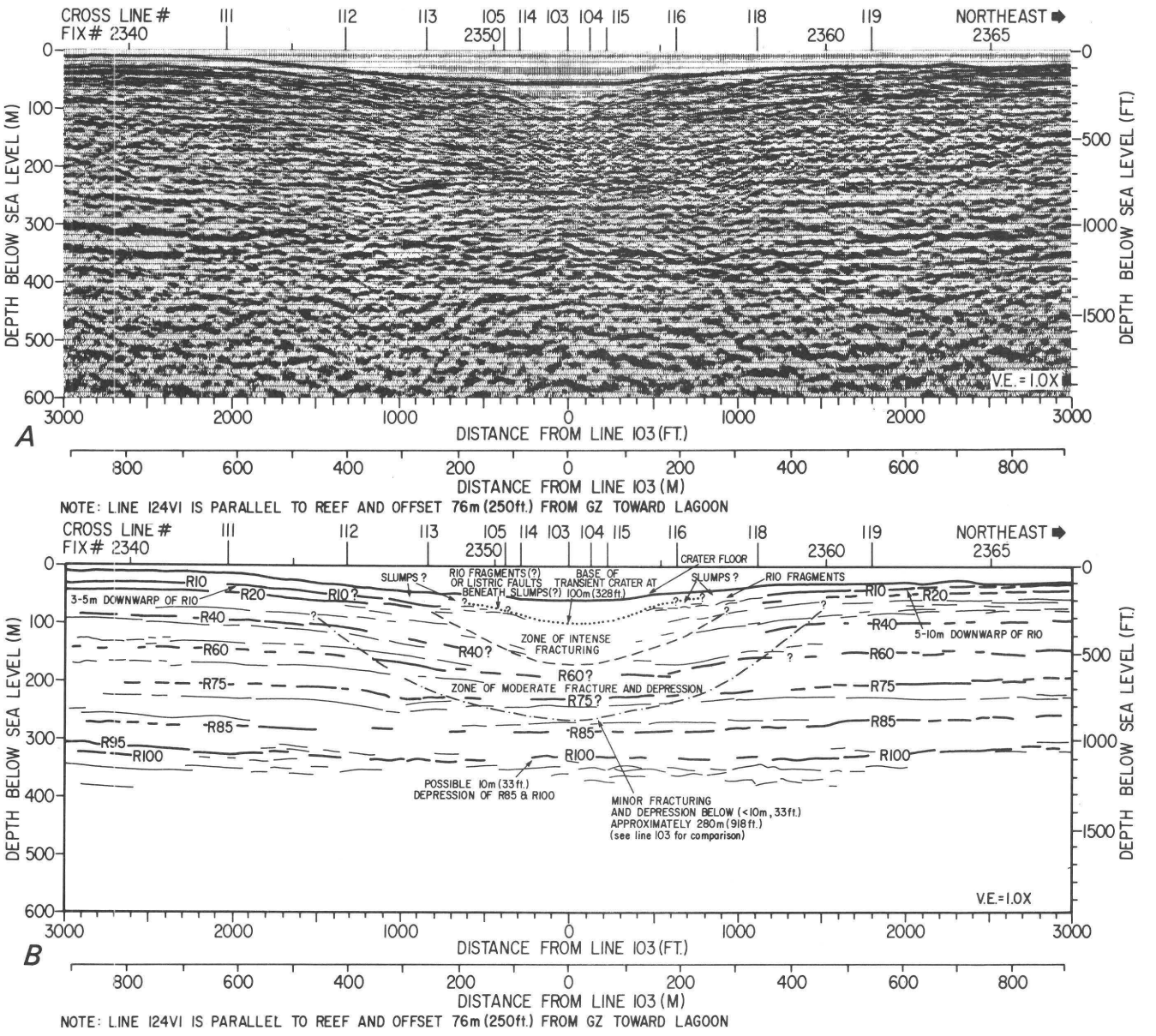

Figure 24. Southwest-northeast profile 124V1 offset 76 m (250 ft) southeast of OAK ground zero (GZ). *A*, Seismic display. *B*, Interpretation. Line 124 is parallel to the reef and offset 76 m (250 ft) from ground zero toward the lagoon.

The major disconformities identified in the preliminary drilling reports at sites OAR–2 and OOR–17 (B. Wardlaw, written commun., July 15, 1985) are shown in figures 25, 26, and 28. While there are some mappable reflection horizons, their lateral continuity is only fair, at best. This appears to be an inherent characteristic of the relatively homogeneous carbonates throughout the lagoon at Enewetak. Mapping the reflectors into OAK crater is difficult but not impossible. While any single reflector may die out laterally, others above or below it can be followed which allows the general deformational character within the crater to be mapped with a reasonable degree of assurance.

Deformational Effects: Northwest-Southeast Profile 103V2 through OAK Ground Zero

The most revealing single profile over OAK crater is the northwest-southeast line perpendicular to the reef through ground zero (line 103V2, fig. 22). The key reflectors, as well as numerous intervening beds, are well represented. The greatest downwarp of subsurface reflectors lies about 120 m (394 ft) southeast of ground zero, close to the geometric center of the crater based on bathymetry. The transient crater extends to a depth of 110 m (361 ft) beneath the geometric center and appears to extend laterally for a

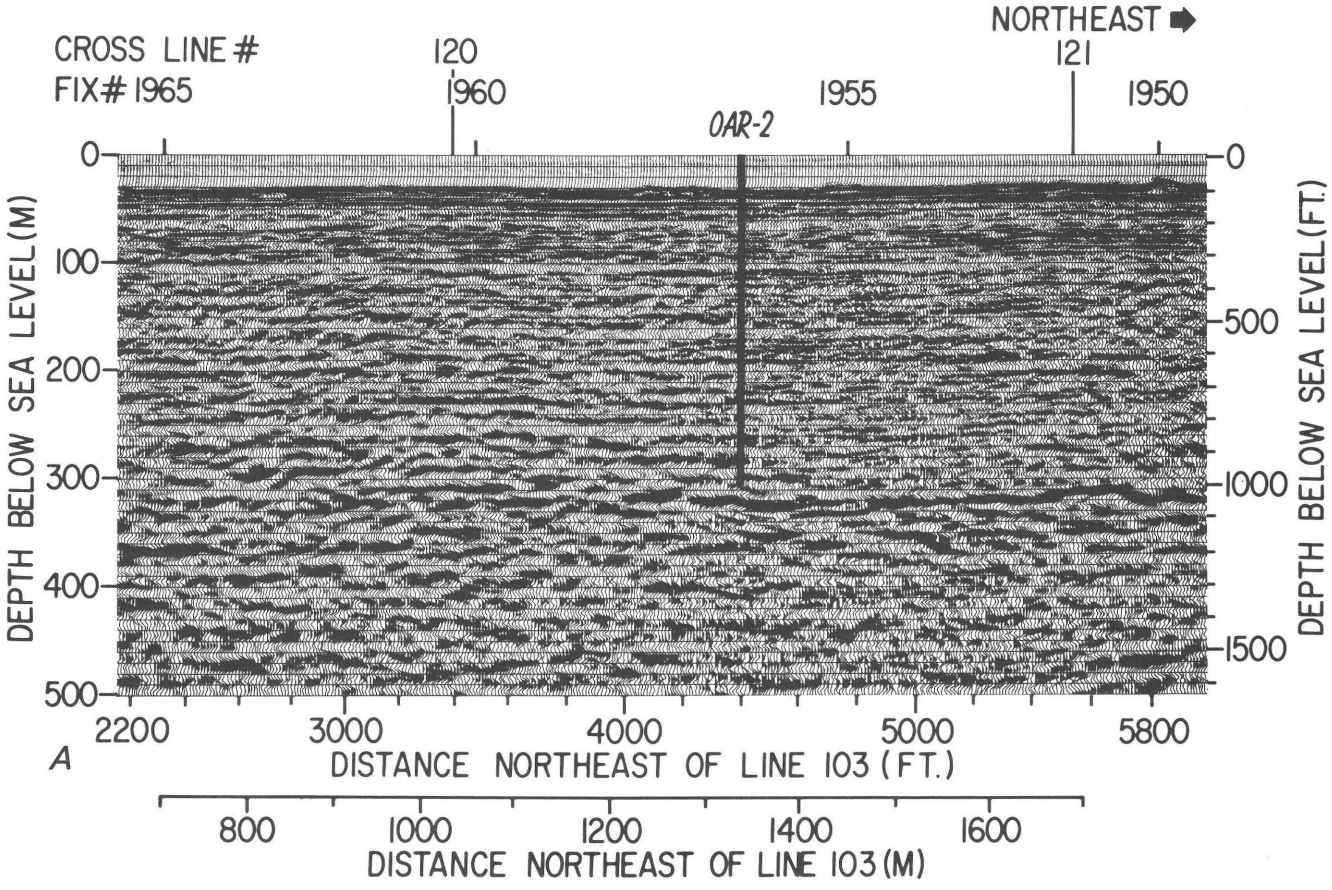

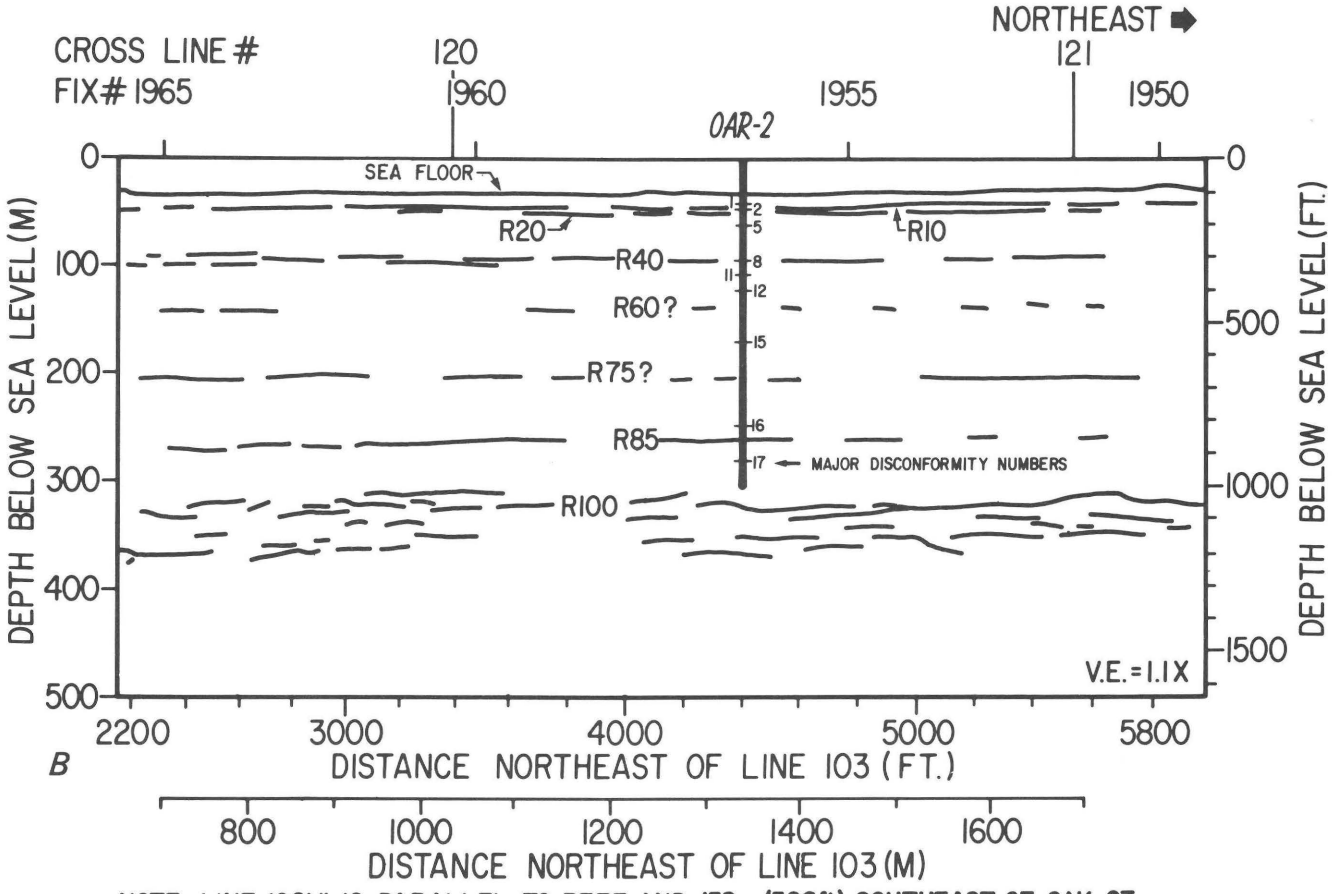

NOTE: LINE 108VI IS PARALLEL TO REEF AND 152 m (500ft) SOUTHEAST OF OAK GZ

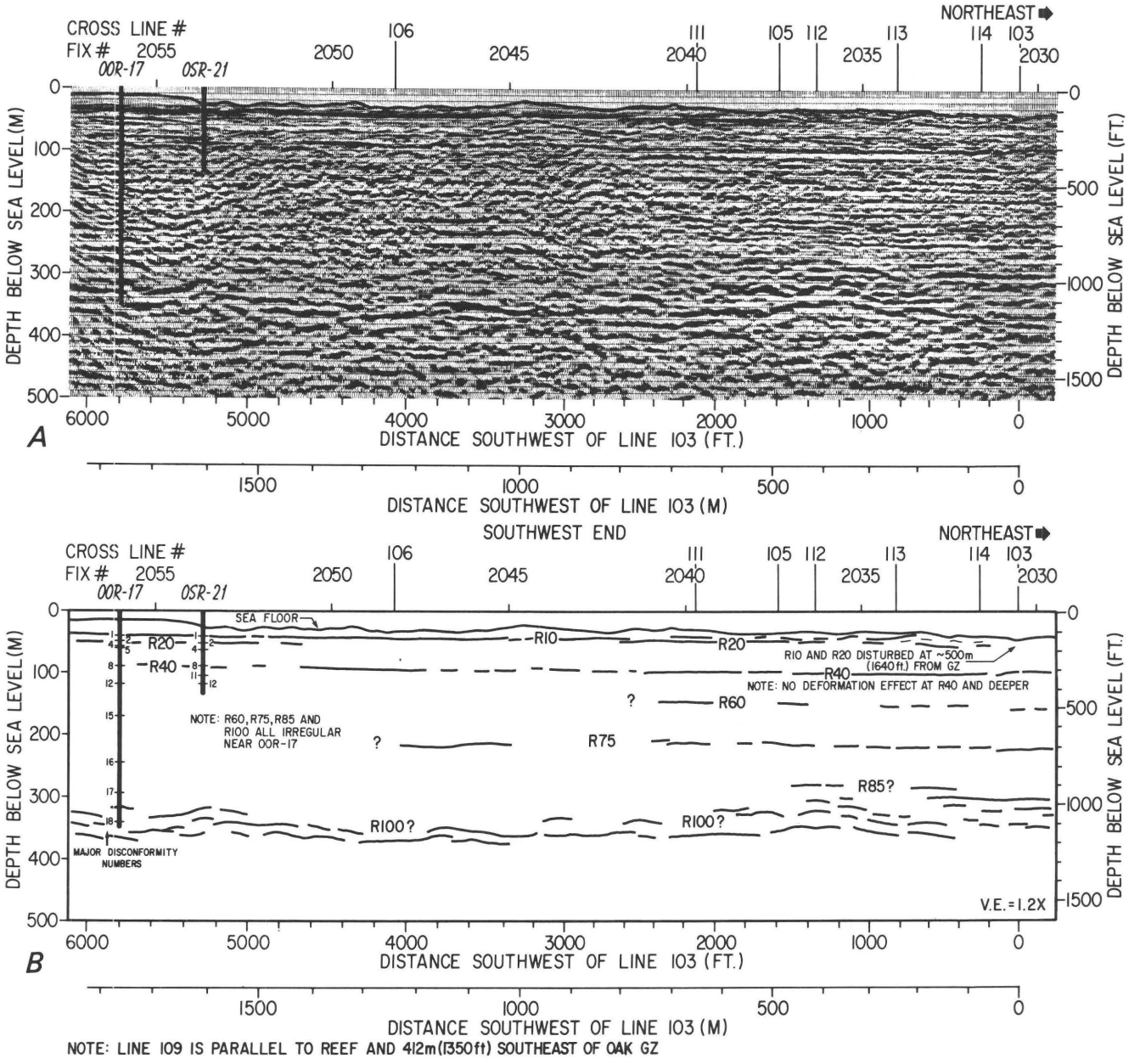

Figure 26. Southwest-northeast profile 109V1 at OOR–17, OAK crater. *A*, Seismic display. *B*, Interpretation. Line 109 is parallel to the reef and 412 m (1,350 ft) southeast of OAK ground zero (GZ). Major disconformity numbers after B. Wardlaw, written commun., July 15, 1985.

distance of 480 m (1,575 ft) southeast of ground zero. The profile extends only 300 m (984 ft) northwest of ground zero toward the reef where possible shallow slumping makes interpretation and correlation more uncertain.

From the lagoon (southeast) side of OAK crater, the R40 horizon begins to downwarp at a distance of 500 m (1,640 ft) and then appears to become severely fractured at 360 m (1,181 ft) from ground zero. On the reef (northwest) side of the crater, R40 may come to within 120 m (394 ft) of ground zero before becoming severely fractured. Beneath the geometric center of the crater, the absence of coherent reflectors between approximately 110 and 180 m (361-590

Figure 25 (left). Southwest-northeast profile 108V1 at drill site OAR–2, OAK crater. *A*, Seismic display. *B*, Interpretation. Line 108 is parallel to the reef and 152 m (500 ft) southeast of OAK ground zero (GZ). Major disconformity numbers after B. Wardlaw, written commun., July 15, 1985.

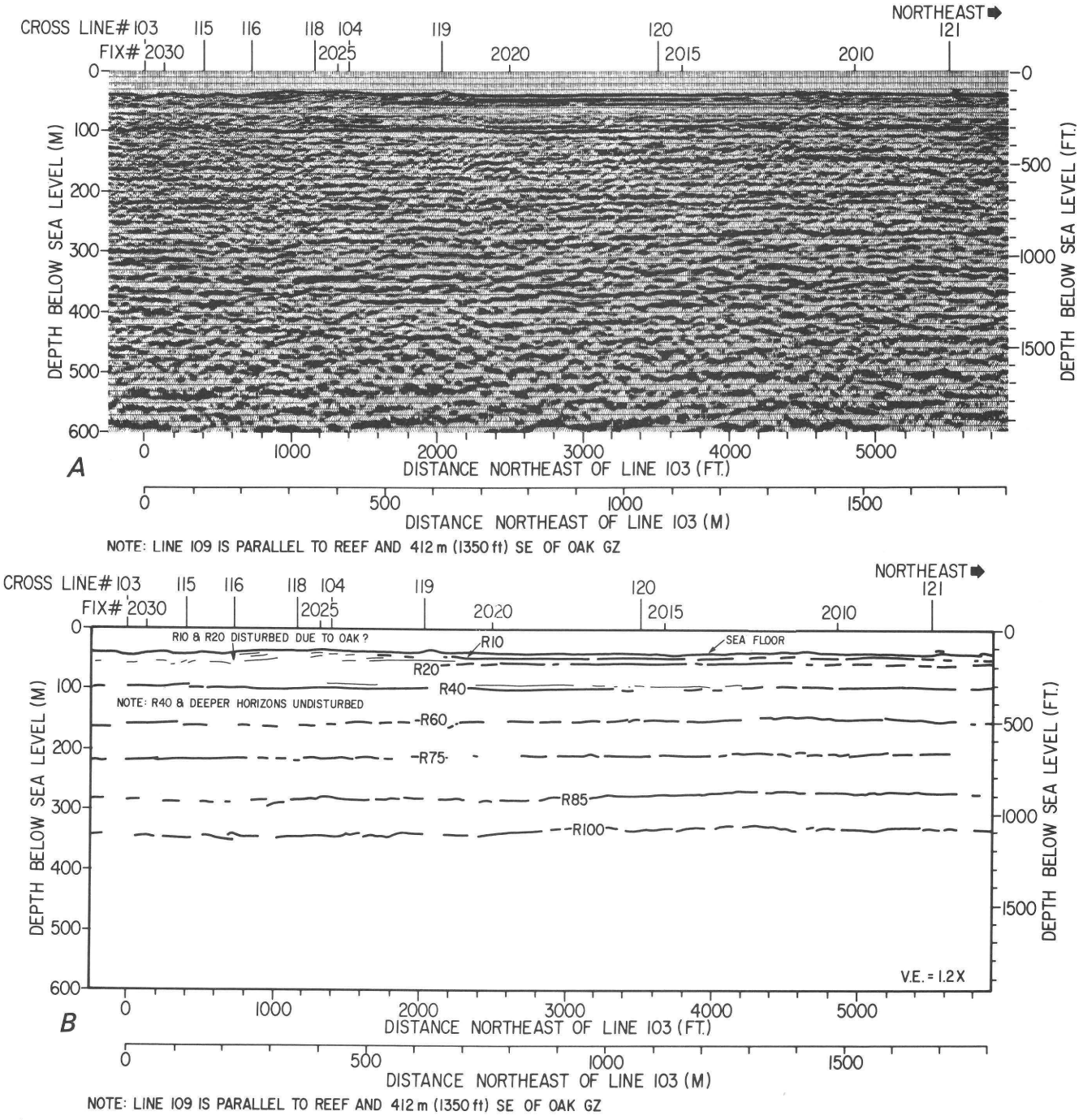

Figure 27. Southwest-northeast profile 109V1 (northeast end), OAK crater. *A*, Seismic display. *B*, Interpretation. Line 109 is parallel to the reef and 412 m (1,350 ft) southeast of OAK ground zero (GZ). Major disconformity numbers after B. Wardlaw, written commun., July 15, 1985.

ft) suggests that rocks are intensely fractured as deep as 180 m (590 ft). Horizons R60, R70, and underlying reflectors have been downwarped by 10 to 40 m (33–131 ft), down to a depth of approximately 280 m (918 ft). Because reflectors R85 and R100 dip slightly toward the lagoon even outside the crater area (see profile 121V1, fig. 28), downwarps of 10 m (33 ft) or less are difficult to resolve. However, the deep penetration seismic line parallel to the reef

Figure 28 (right). Southeast-northwest profile 121V1, OAK crater. *A*, Seismic display. *B*, Interpretation. Line 121 is perpendicular to the reef and 1,615 m (5,300 ft) northeast of OAK ground zero (GZ). Major disconformity numbers after B. Wardlaw, written commun., July 15, 1985.

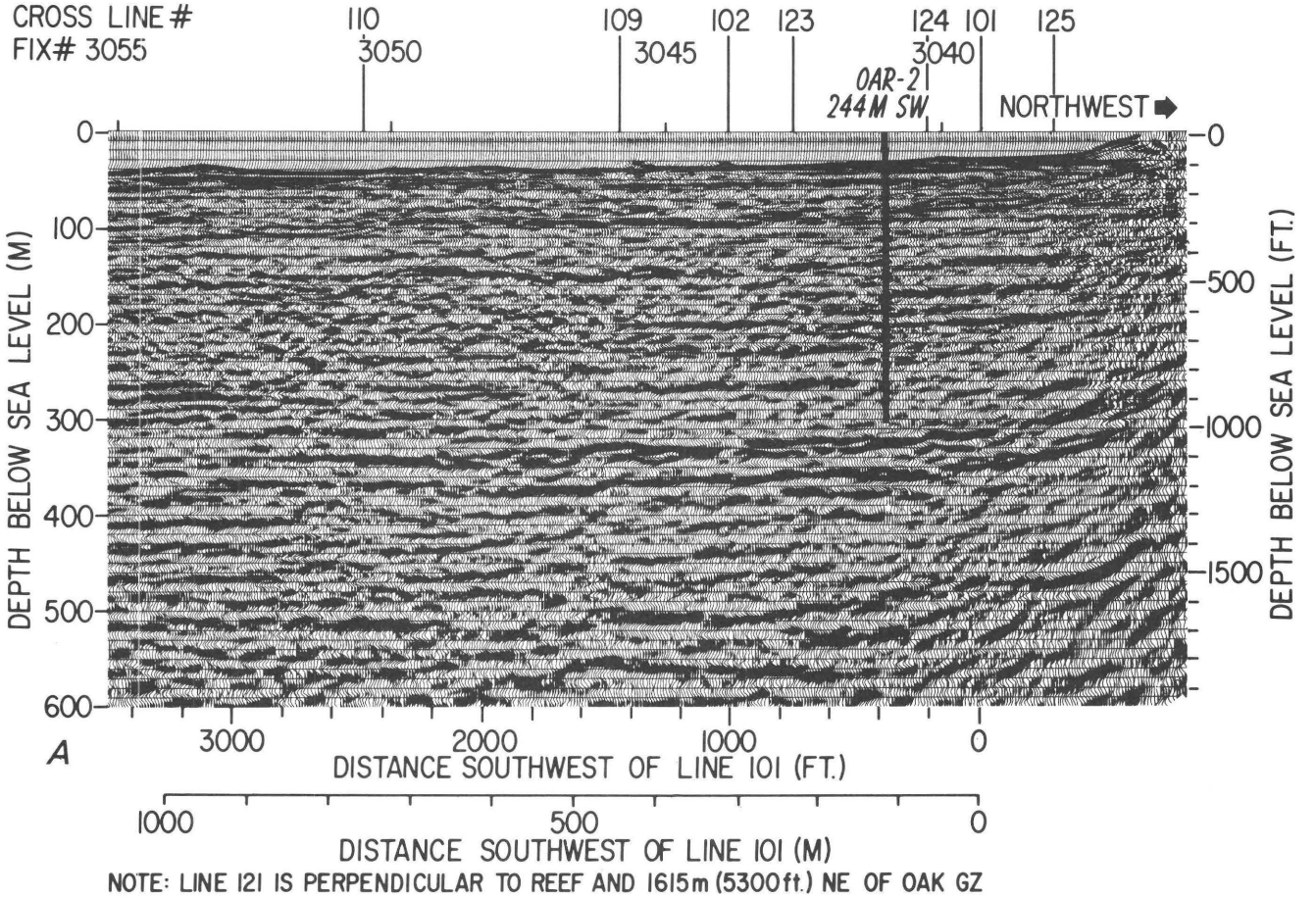

NOTE: LINE 121 IS PERPENDICULAR TO REEF AND 1615m (5300ft.) NE OF OAK GZ

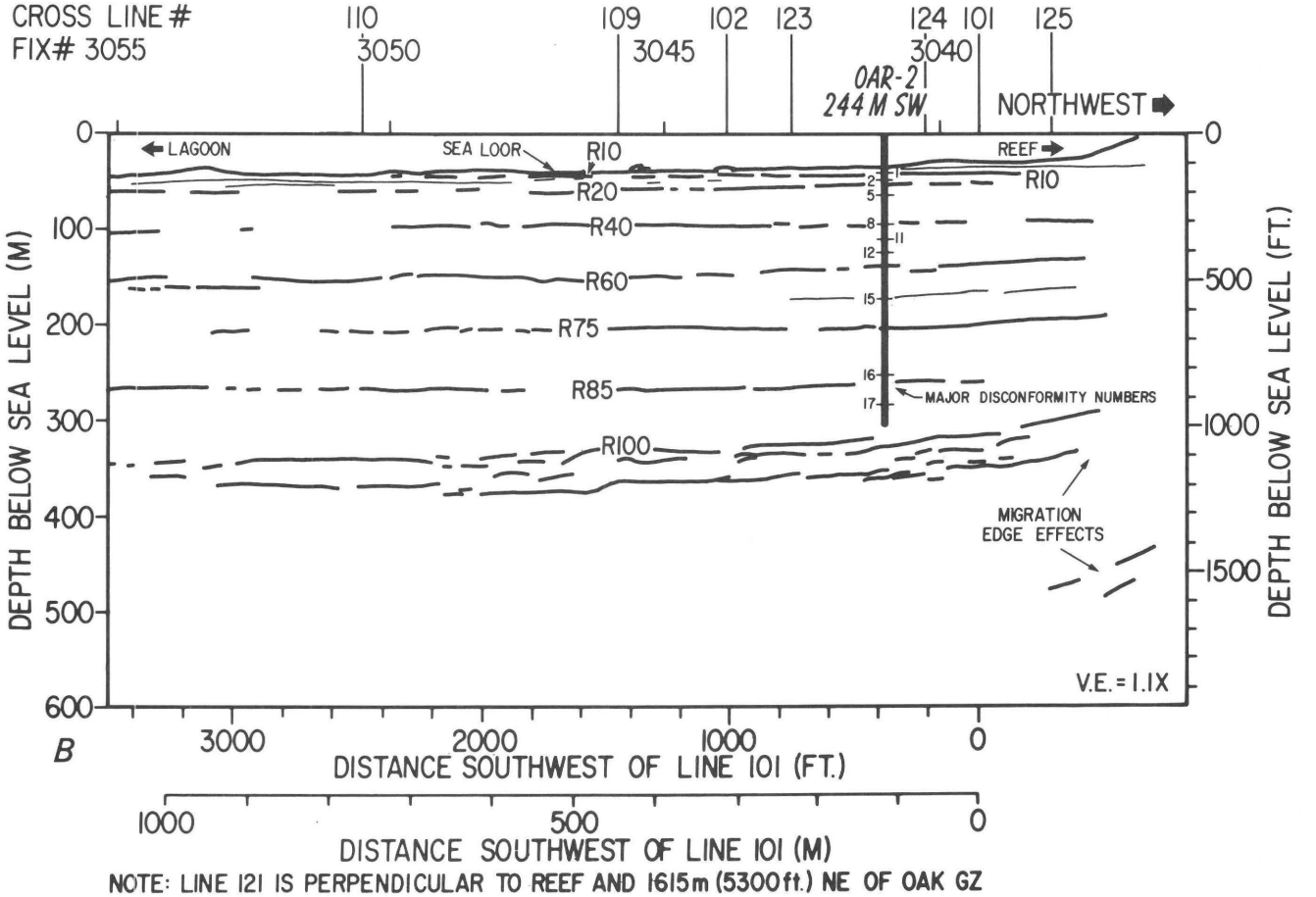

NOTE: LINE 121 IS PERPENDICULAR TO REEF AND 1615m (5300ft.) NE OF OAK GZ

(line 101V5, fig. 10) suggests that reflectors 300 m (984 ft) deep are downwarped about 10 m (33 ft) beneath OAK ground zero. Note also that the check-shot velocities between 250 and 300 m (820–984 ft) at OAK ground zero are approximately 30 percent slower than at reference site OAR–2 (fig. 6). Since the OAK reference hole only went to 305 m (1,000 ft) below sea level, reduced velocities at ground zero may extend deeper. Therefore, while the seismic reflection data (line 103V2, fig. 22) suggests minor fracturing or depression effects below 280 m (918 ft), it should be noted that the check-shot velocities suggest that reduced velocities, presumably due to significant fracturing, may extend to depths of 300 m (984 ft) or greater. Finally, the refraction data (chap. E, fig. 19, this volume) suggest that the velocities beneath OAK may be lowered at depths of more than 400 m (1,312 ft).

Deformational Effects: Southwest-Northeast Profile 101V4 through OAK Ground Zero

Line 101V4 is parallel to the reef and passes almost directly over OAK ground zero (fig. 23). Because of the offset of the geometric center of the crater to the southeast of ground zero, side echoes off the reef and crater rim create more severe noise problems on this profile than the side echoes present on line 103V2 (fig. 22), which is perpendicular to the trend of the reef. Line 101V4 grazes the crater slope on the northwest (reef) side of the crater (fig. 21), where slumps appear to have transported debris into the crater. (See chap. A, fig. 15*B*, this volume.) Therefore, the acoustically transparent sediment pond seen on line 103V2, which marks the base of the transient crater, is not obvious on line 101V4.

The shallow R10 and R20 reflectors are clearly apparent on this line and begin to downwarp at distances of 550 to 600 m (1,804–1,968 ft) from ground zero. R10 appears to drop from 40 m (131 ft) down to approximately 80 m (262 ft) at distances of 220 m (722 ft) from ground zero, where the reflectors appear to be truncated by the excavation. The R40, R60, and R75 reflectors are not as clear on line 101V4 as on the perpendicular line, but R40 appears to begin downwarping 400 m (1,312 ft) from ground zero. Reflectors R85, R95, and R100 lie between 260 and 340 m (853–1,115 ft) deep. Although all reflectors show considerable depositional variability along the line, R100 appears to be downwarped approximately 10 to 20 m (33–66 ft) beneath ground zero due to the OAK detonation.

Deformational Effects: Southwest-Northeast Profile 124V1, Offset 76 m (250 ft) from OAK Ground Zero

Line 124V1 is parallel to the reef and passes nearly through the geometric center of the crater (fig. 24) approximately 76 m (250 ft) southeast of OAK ground zero. As on line 103V2 perpendicular to the reef, the transparent crater fill can be observed down to 100 m (328 ft). Reflectors R10 and R20 are relatively clear on the line and appear to have some downwarp (3–10 m, or 10–33 ft) at distances beyond 600 m (1,968 ft) from ground zero. They are downwarped as much as 70 m (230 ft) at a distance of 300 m (984 ft) from ground zero, and possibly fragments of R10 and R20 can be traced down to depths of 90 m (236 ft) at a distance of 100 m (328 ft) from ground zero.

Downwarps of reflectors R40, R60, and R75 begin between 400 and 500 m (1,312–1,640 ft) from ground zero with 20 to 40 m (66–131 ft) downward displacement suggested beneath ground zero. Reflectors R85 and R100 appear to have downwarps of less than 10 m (33 ft) beneath ground zero.

Deformational Effects: North-South Line 105V2 through OAK Ground Zero

Line 105V2 illustrates complexities within the excavated zone and shallow reflectors not observed on the previously discussed lines (fig. 29). While the base of the transient crater appears to be at 110 m (361 ft) just south of ground zero, line 105V2 reveals a buried block that rises to a depth of 85 m (279 ft) directly beneath OAK ground zero. The R20 reflector on the south side of ground zero also has remarkable coherence and can be traced to within 300 m (984 ft) of ground zero. R10 and R20 appear to begin their downwarp about 600 m (1,968 ft) south of ground zero. R40 begins to downwarp approximately 500 m (1,640 ft) south of ground zero. The downwarps on reflectors R60 and R75 are not as clear as on line 103V2 but appear to be on the order of 20 m (66 ft) beneath ground zero. Reflectors R85 and R100 are again a discontinuous band of reflectivity which appears to have been downwarped 10 m (33 ft) or less.

Line 105V2 displays the same dramatic offset of deepest deformation to the southeast of ground zero, as is observed on line 103V2.

Deformational Effects: East-West Line 104V2 through OAK Ground Zero

Line 104V2 recorded a broad transparent zone down to a depth of 110 m (361 ft) which marks the base of the transient crater and extends to over 400 m (1,312 ft) east of ground zero (fig. 30). Reflectors R40 and R60 are also relatively undisturbed at a distance of 400 m (1,312 ft) or more from ground zero. Downwarps of R60 and R75 are difficult to measure accurately, but they appear to be in the range of 10 to 40 m (33–131 ft) beneath ground zero. R85 and R100 are relatively flat, and they lie at depths of 280 m (918 ft) and deeper. The line confirms the offset of deepest deformation southeast of ground zero, seen on line 103V2 (fig. 22) and line 105V2 (fig. 29).

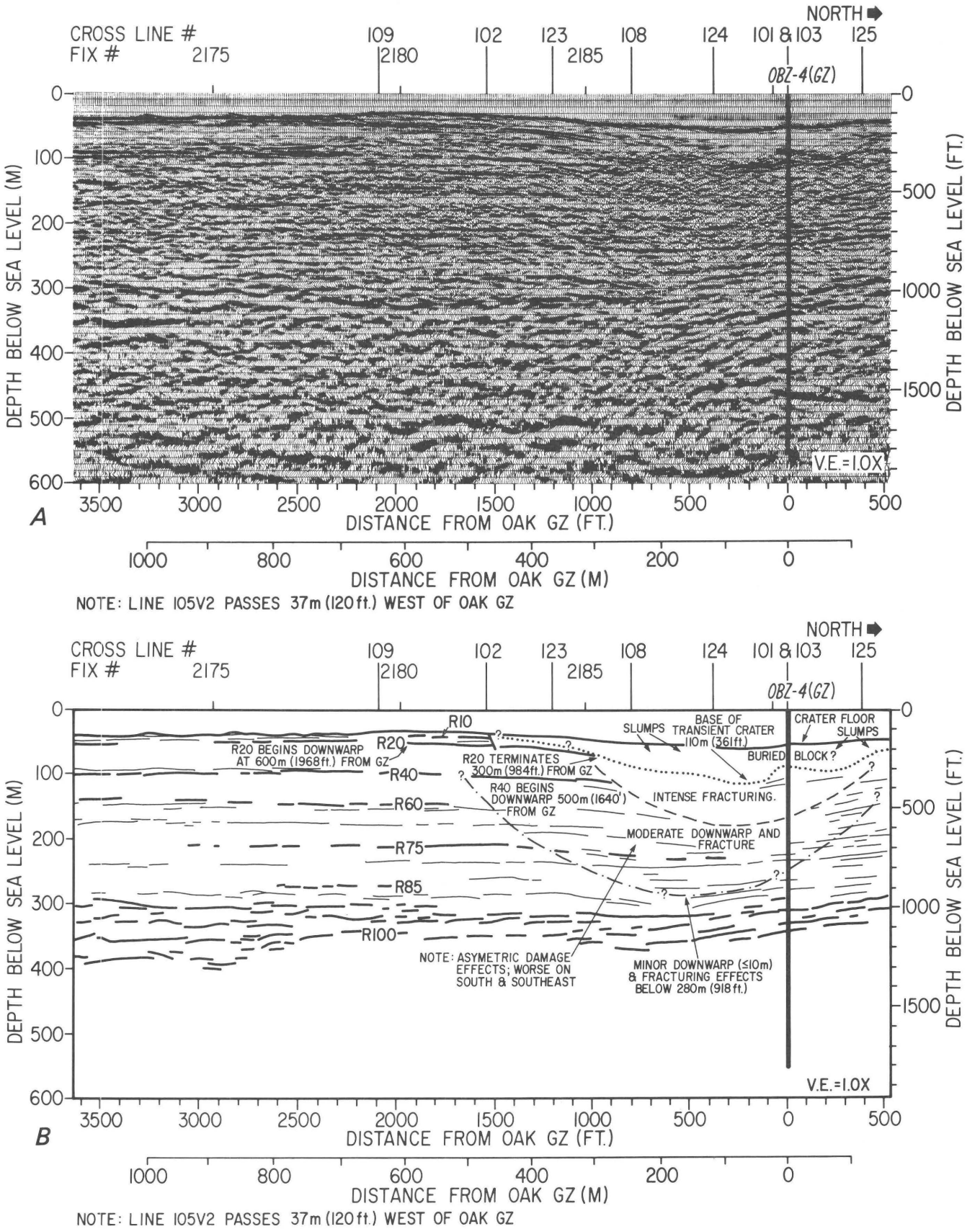

Figure 29. North-south profile 105V2 through OAK ground zero (GZ). *A*, Seismic display. *B*, Interpretation. Line 105V2 passes 37 m (120 ft) west of OAK ground zero.

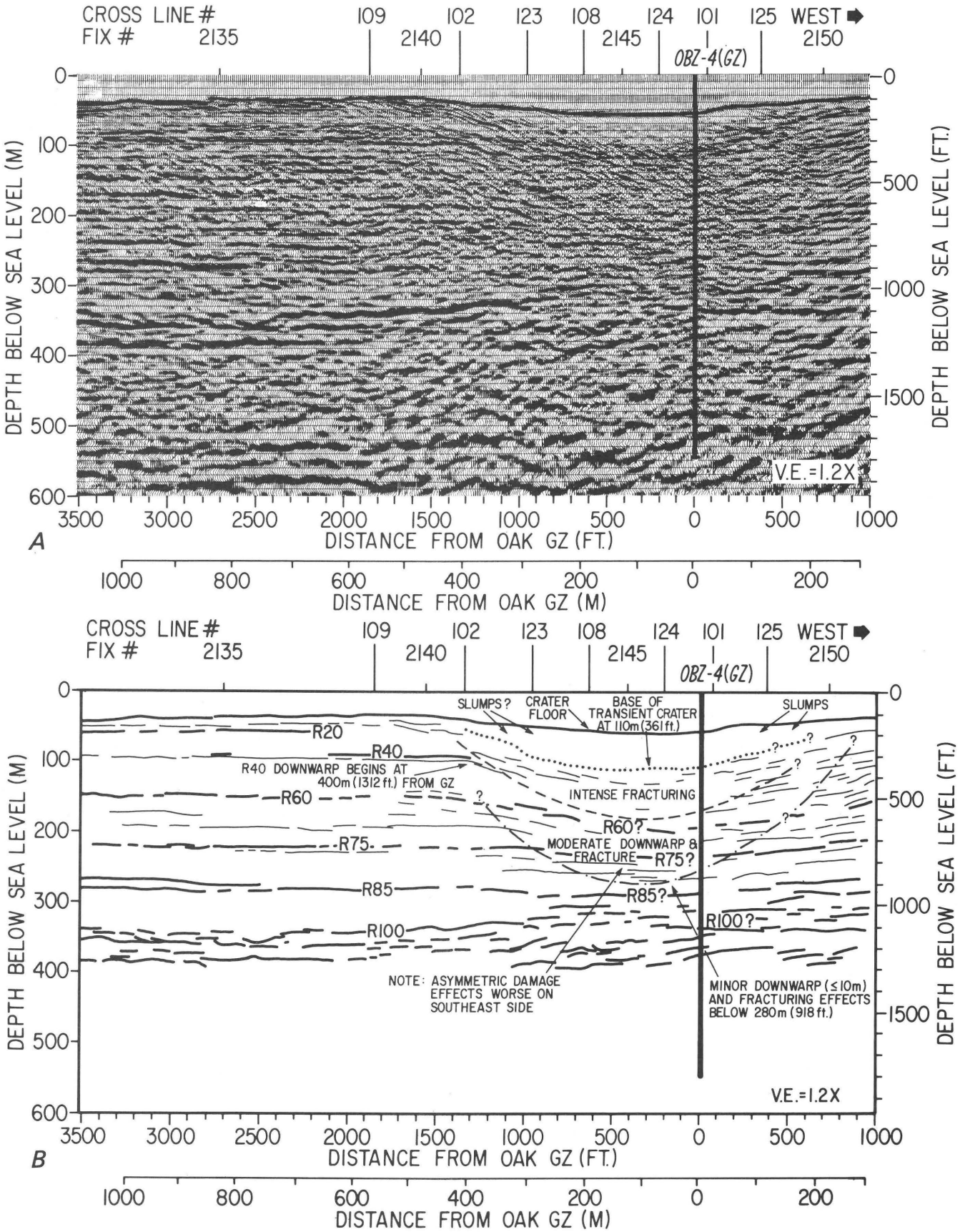

Figure 30. East-west profile 104V2 through OAK ground zero (GZ). *A*, Seismic display. *B*, Interpretation.

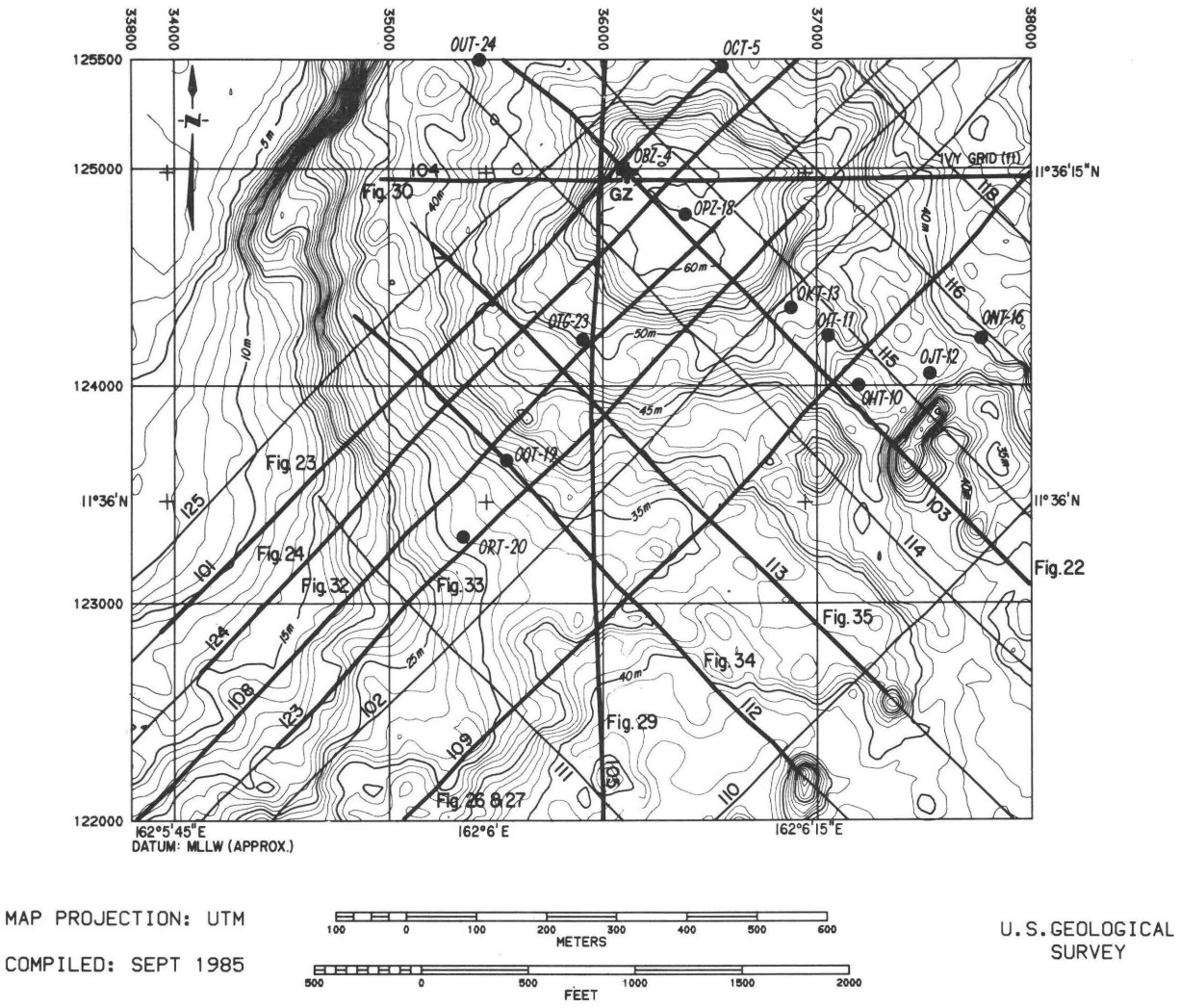

Figure 31. Map of OAK showing location of multichannel seismic-reflection profiles, drill sites, figure numbers for profiles, and 1-m bathymetry.

Structure-Contour Maps

Reflectors R20, R40, R75, and R100 were coherent enough to map. The single-channel data were used to prepare structure-contour maps for both R10 and R20 (chap. C, figs. 13, 17, this volume). Both single-channel and multichannel data were generally in close agreement for these two reflectors, except for the area south of ground zero where they could be carried much closer toward ground zero on the multichannel data. Prior to discussing the R20 structure contour map, we will interpret four more key profiles south of ground zero (fig. 31).

The area southwest of OAK ground zero had extremely coherent and continuous R10 and R20 reflectors. Line 108V1 (fig. 32), which is parallel to the reef and offset 152 m (500 ft) toward the lagoon from line 101V4 (fig. 23), shows very clear R10 and R20 reflectors at about 38 and 45 m (125 and 148 ft), respectively, at the southwest end of the line. Beginning at about 750 m (2,460 ft) southwest of ground zero, R10 and R20 start downwarping toward ground zero to depths of 55 and 62 m (180 and 203 ft), respectively, near the OQT–19 drill site at approximately 400 m (1,328 ft) southwest of ground zero. Fragments of R10 and R20 continue at a depth of approximately 80 m (262 ft) at a distance of 250 m (820 ft) south of ground zero. Very similar R10 and R20 reflectors can be observed on the next line toward the lagoon, line 123V1 (fig. 33). R10 and R20 correlate with disconformities "1" and "2" at the ORT–20 and OQT–19 wells. Lines 112V1 and 113V1 are perpendicular to the reef, crossing the previously discussed line 108V1 and 123V1. Line 112 is 415 m (1,360 ft) southwest of ground zero and shows that R10 and R20 dip toward the

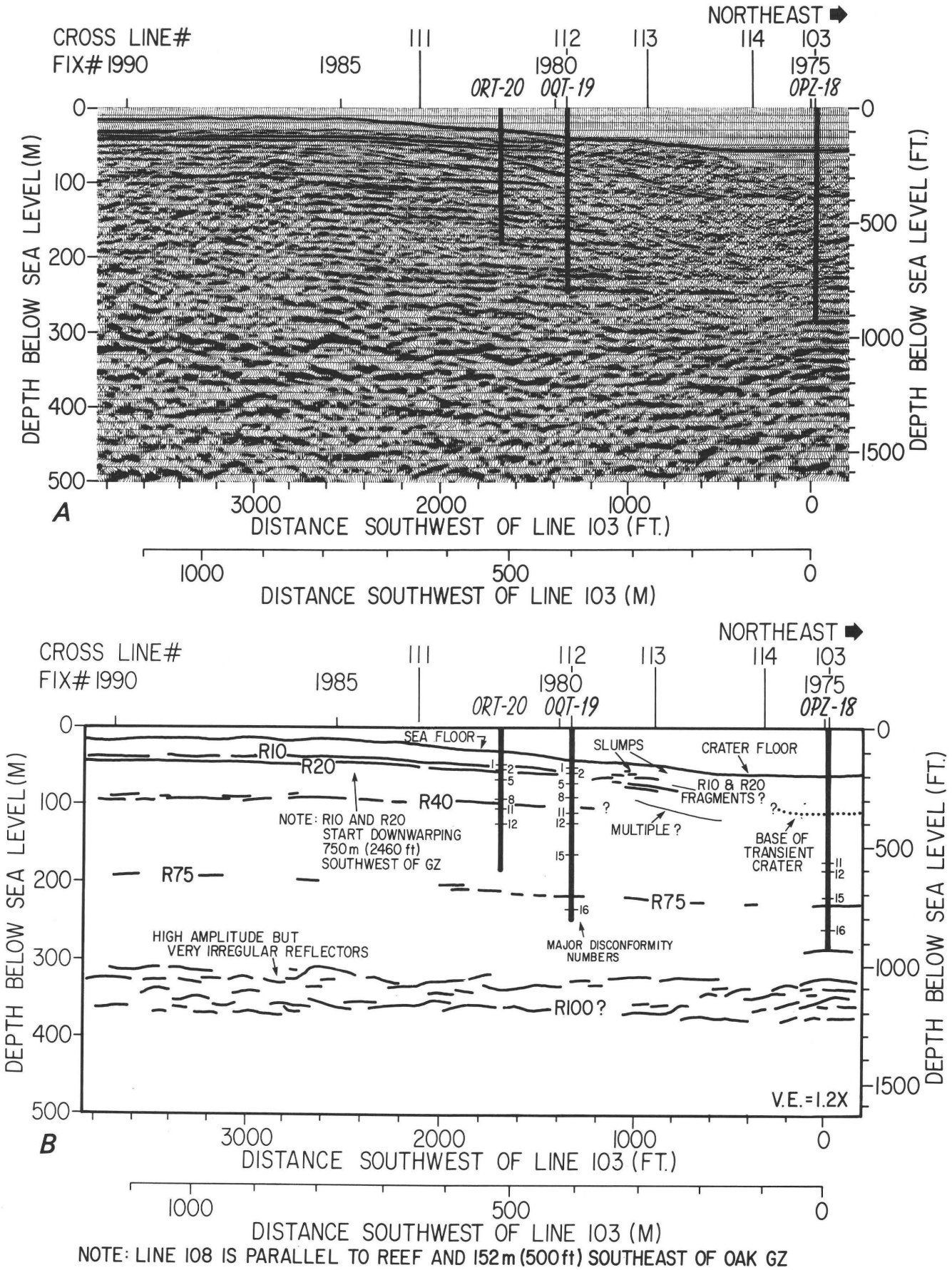

Figure 32. Southwest-northeast profile 108V1 at drill site OQT–19, OAK crater. *A*, Seismic display. *B*, Interpretation. Line 108 is parallel to the reef and 152 m (500 ft) southeast of OAK ground zero (GZ). Major disconformity numbers after B. Wardlaw, written commun., July 15, 1985.

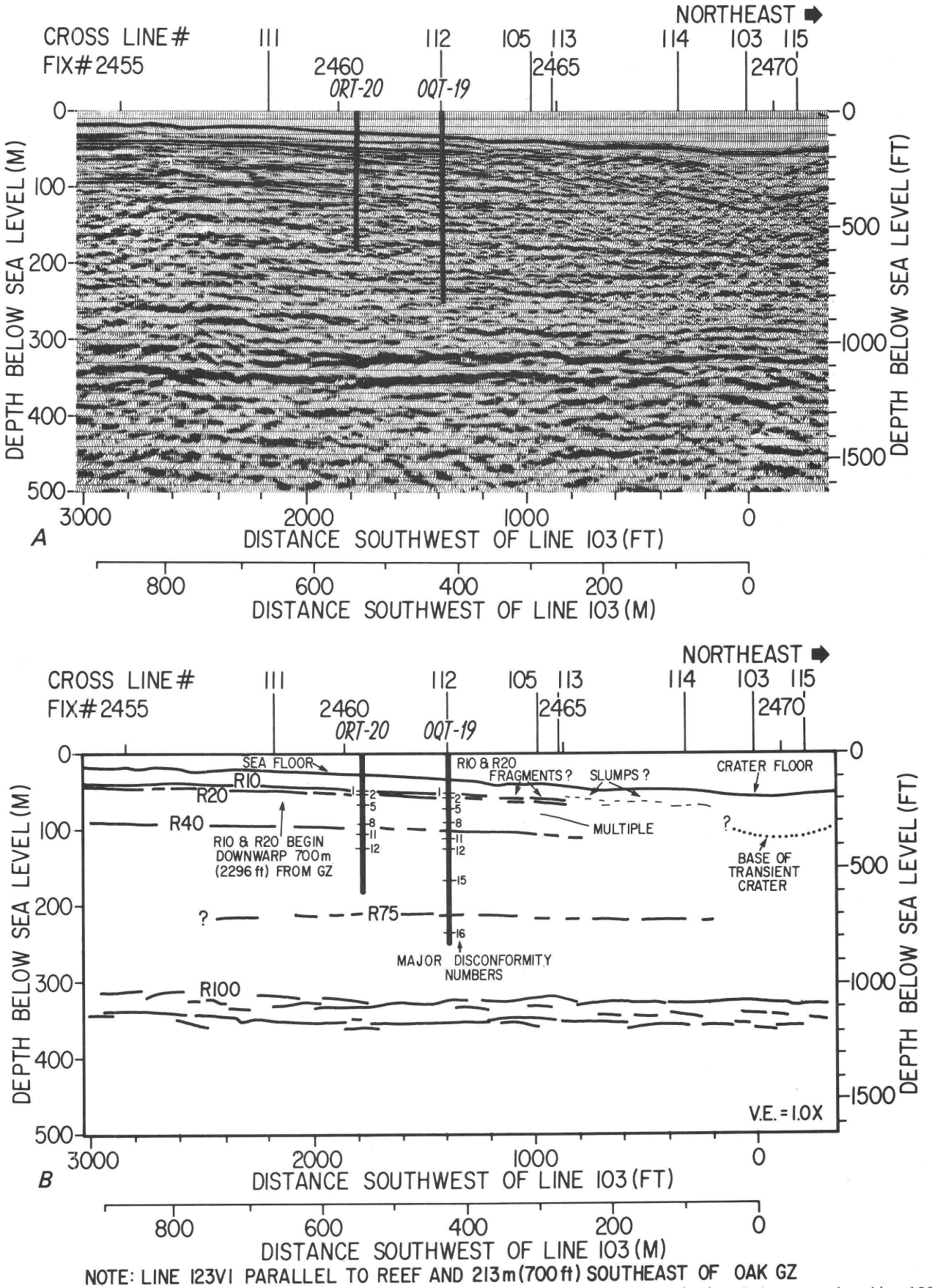

Figure 33. Southwest-northeast profile 123V1 at drill site ORT–20, OAK crater. *A*, Seismic display. *B*, Interpretation. Line 123 is parallel to the reef and 213 m (700 ft) southeast of OAK ground zero (GZ). Major disconformity numbers after B. Wardlaw, written commun., July 15, 1985.

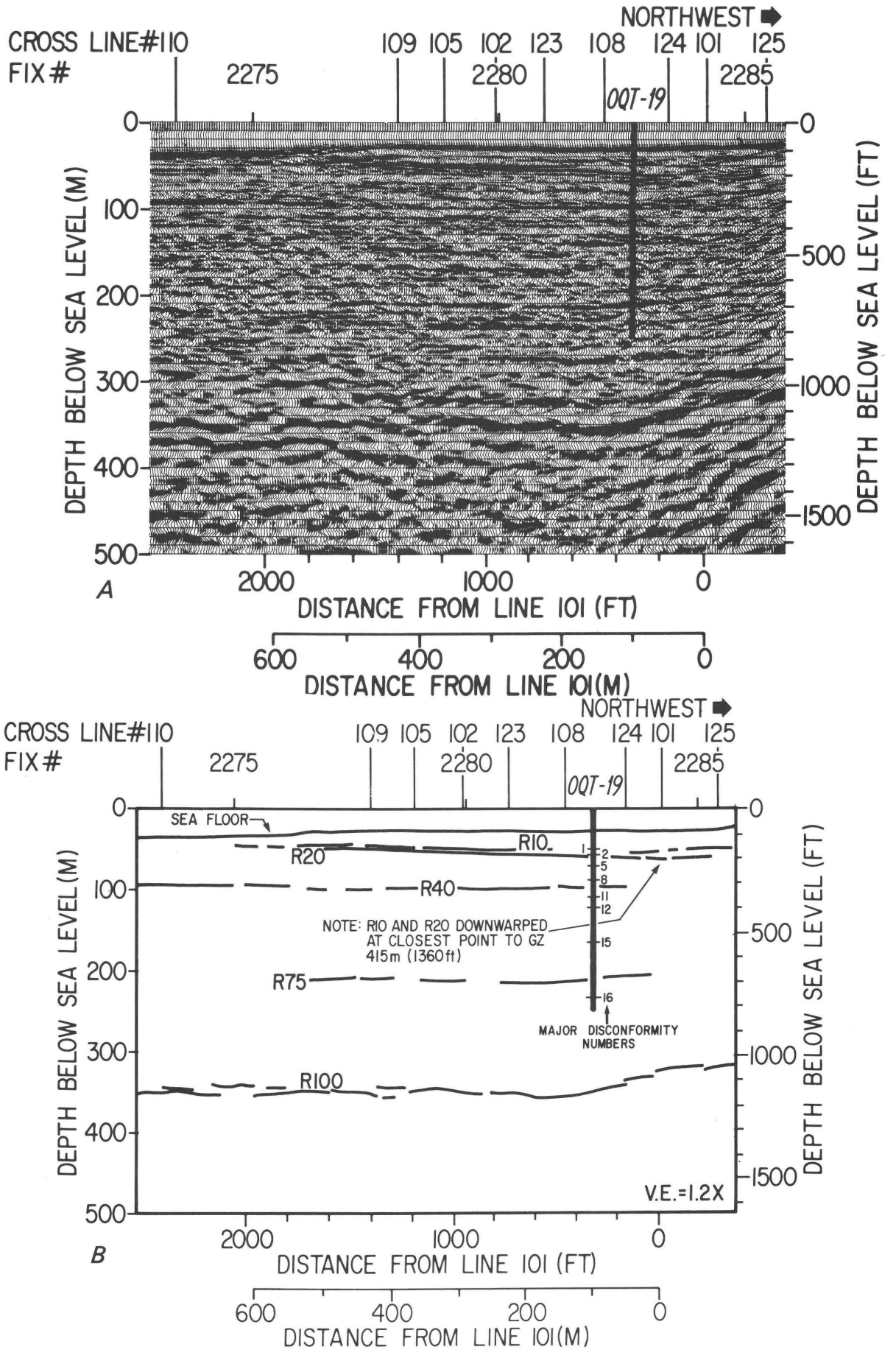
NORTHWEST
CROSS LINE#110
FIX#
109 105 102 123 108 124 101 125
2275
2280
2285
OQT-19
DEPTH BELOW SEA LEVEL (M)
DEPTH BELOW SEA LEVEL (FT)
0
100
200
300
400
500
1000
1500
A
2000
1000
0
DISTANCE FROM LINE 101 (FT)
600
400
200
0
DISTANCE FROM LINE 101(M)
NORTHWEST
CROSS LINE#110
FIX#
109 105 102 123 108 124 101 125
2275
2280
2285
OQT-19
SEA FLOOR
R10
R20
R40
R75
R100
NOTE: R10 AND R20 DOWNWARPED AT CLOSEST POINT TO GZ 415m (1360ft)
1
2
5
8
11
12
15
16
MAJOR DISCONFORMITY NUMBERS
V.E.=1.2X
DEPTH BELOW SEA LEVEL (M)
DEPTH BELOW SEA LEVEL (FT)
B
2000
1000
0
DISTANCE FROM LINE 101 (FT)
600
400
200
0
DISTANCE FROM LINE 101(M)

reef and reach their greatest depths, 53 and 60 m (174 and 197 ft), respectively, near the crossing of lines 101V4 and 112 (fig. 34). Line 113V1 is 262 m (860 ft) southwest of ground zero and also shows R10 and R20 dipping toward the reef (fig. 35). On line 113V1, two small normal faults can be resolved that downfault both R10 and R20 to the northwest to a depth of 78 m (256 ft) before the reflectors terminate in an intensely fractured zone near ground zero. Lines 108V1, 123V1, 112V1, and 113V1 (figs. 31–35) show that R10 and R20 on the southwest side of OAK ground zero begin to downwarp at a distance of at least 700 m (2,296 ft) from ground zero; this observation is in excellent agreement with the single-channel map of R20 (chap. C, fig. 17, this volume). While the single-channel data can follow R10 and R20 to within 400 m (1,328 ft) of ground zero, the multichannel data follow downwarped fragments of R10 and R20 to within 250 m (820 ft) of ground zero. Closer to ground zero, R10 and R20 are intensely fractured and probably were partly excavated during the formation of the transient crater. A structure-contour map of R20 on the southwest side of ground zero summarizes the downwarping and truncation of R20 (fig. 36).

Reflector R40 correlates with disconformity "8" at a depth of approximately 92 m (302 ft) in the OAR–2 and OOR–17 OAK reference sites. Mapping of R40 into OAK crater was successful to within 300 to 400 m (984–1,328 ft) of ground zero (fig. 37) where it drops down to a depth of approximately 110 m (361 ft) before becoming too fractured to follow. While the correlation of R40 with disconformity "8" was good at OIT–11 (southeast of ground zero on line 103V2, fig. 22) and at ORT–20 and OQT–19 (southwest of ground zero on line 108V1, fig. 32), R40 is 10 to 25 m (33–82 ft) too deep on the northeast side of the crater near drill sites OFT–8 and OET–7 (line 101V4, fig. 23). Although the discrepancy may be due to the weak, discontinuous character of R40 along the northeast end of line 101V4 (fig. 23), it also may be due to thrusting. The structure-contour map for R40 notes other possible areas where thrusting may have occurred. Subsequent analysis of the drill-hole samples and logs can probably clarify this discrepancy. However, for this report, we have noted only where the seismic data do or do not agree with the drilling data.

In summary, R40 comes in to about 300 m (984 ft) before becoming too fractured to map. Surprisingly, the overlying R10 and R20 group was mapped into 250 m (820 ft) before breaking up. The difference is probably due to R10 and R20 being extremely strong formations relative to R40 and other reflectors around OAK. The outer limit of downwarp for R40 is not as clear as for R20 but varies from 400 m (1,312 ft) on line 104V2 (fig. 30) to 500 m (1,640 ft) on line 103V2 (fig. 22) to as much as 550 m (1,804 ft) on the southwest end of line 101V4 (fig. 23). The net vertical downwarp for R40 is only from 90 m (295 ft) down to a maximum of 115 m (377 ft) within distances of 600 and 300 m from ground zero (1,968 and 984 ft). Drilling results from sites OBZ–4, OPZ–18, OKT–13, and OCT–5 (figs. 22, 23) have not reported disconformity "8," but have reported "mixed rubble" down to 127 m (415 ft) and "stratified, unmixed rubble" down to 229 m (752 ft). The shallowest disconformity reported at OBZ–4 is "12" at 166 m (546 ft), within the "stratified, unmixed rubble." Disconformity "8" was 29 m (95 ft) shallower than disconformity "12" in OAR–2, so disconformity "8" and R40 might be expected at 136 m (446 ft) at OBZ–4, that is, within the "stratified, unmixed rubble." The failure to identify disconformity "8" at OBZ–4 may be due to the intense fracturing within the "stratified, unmixed rubble."

The structure-contour map for reflector R75 (fig. 38) shows an elliptical depression with R75 downwarped from about 210 m (689 ft) outside the crater down to 230 m (754 ft) beneath ground zero. The elliptical shape with the long axis parallel to the reef and the offset of the ellipse 150 m (492 ft) south of ground zero is well defined but not really understood. Downwarping of R75 begins at least 400 m (1,328 ft) southwest of ground zero, maybe as far as 700 m (2,296 ft). The downwarping of R75 to 230 m (754 ft) in OAK is considerably deeper than the downwarping of R75 in KOA to a depth of 180 m (590 ft).

The structure-contour map prepared for R100 shows an irregular surface varying between 325 and 350 m (1,066–1,148 ft) deep (fig. 39). An irregular, elongate depression occurs parallel to the reef with a 10- to 20-m (33–66 ft) downwarp. While R75 had a clear 20-m (66 ft) downwarp associated with OAK ground zero, the elongate depression of R100 is irregular enough to suggest a combination of pre-OAK relief with a 10-m (33 ft) or less additional downwarp due to the OAK detonation.

Structural Summary of OAK Crater Based on Multichannel Seismic Data

The seismic lines over the center of OAK crater show a transparent pond of sediments that extends down to 110 m (361 ft). In a water depth of 60 m (197 ft, corrected to Holmes and Narver datum), this 50-m-thick (164-ft-thick) transparent layer is interpreted as chaotically mixed debris and postevent sediment fill. Results from drilling this transparent sediment at OBZ–4 indicate that the boundary between "stratified, mixed rubble" and "stratified, unmixed rubble" occurred at 110 m (362 ft) (B_2 and B_3 layers of

Figure 34 (left). Northwest-southeast profile 112V1 at drill site OQT–19, OAK crater. *A*, Seismic display. *B*, Interpretation. Line 112 is perpendicular to the reef and 415 m (1,360 ft) southwest of OAK ground zero (GZ). Major disconformity numbers after B. Wardlaw, written commun., July 15, 1985.

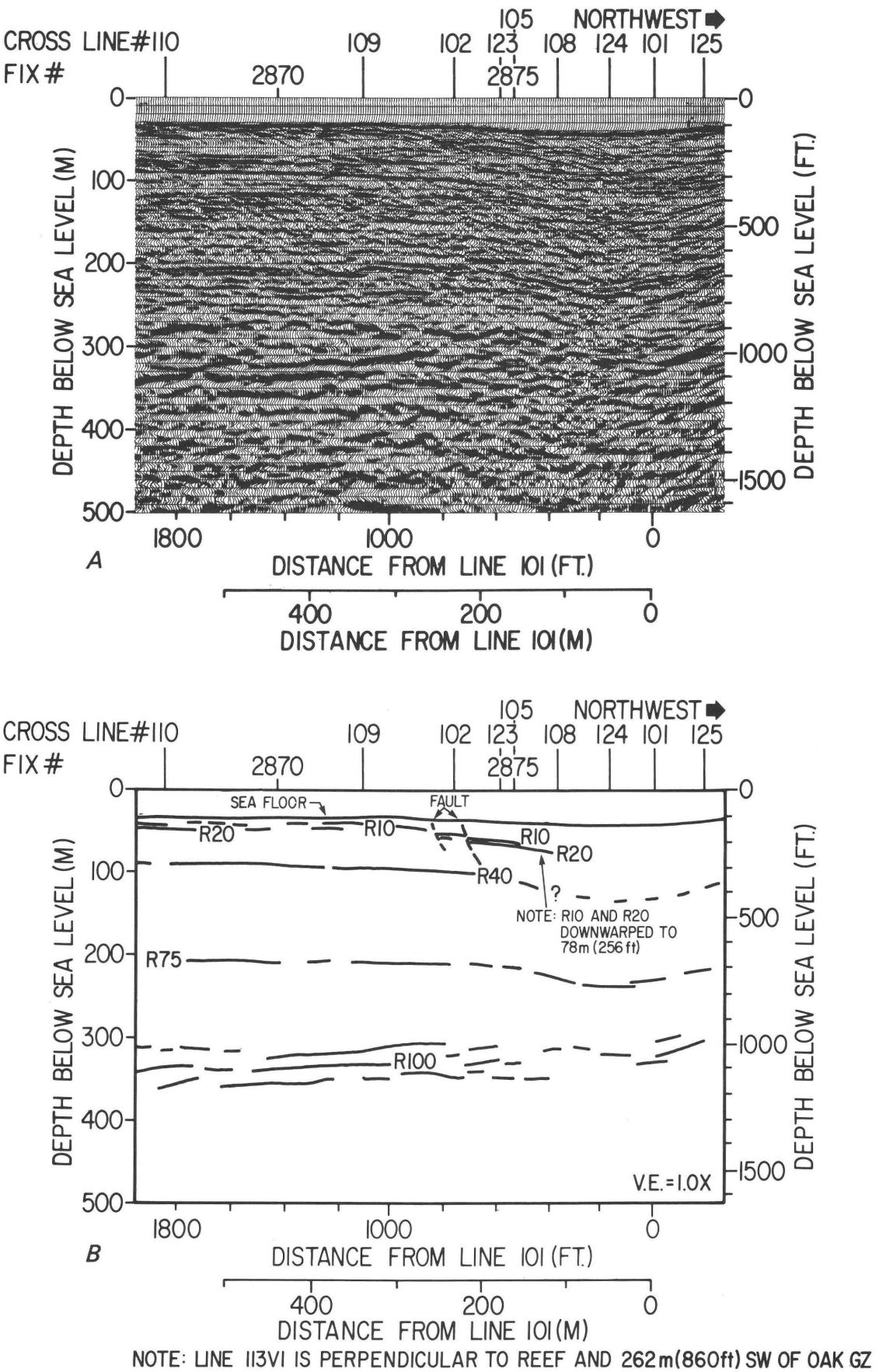

Figure 35. Northwest-southeast profile 113V1 near drill site OQT–19, OAK crater. *A*, Seismic display. *B*, Interpretation. Line 113 is perpendicular to the reef and 262 m (860 ft) southwest of OAK ground zero (GZ).

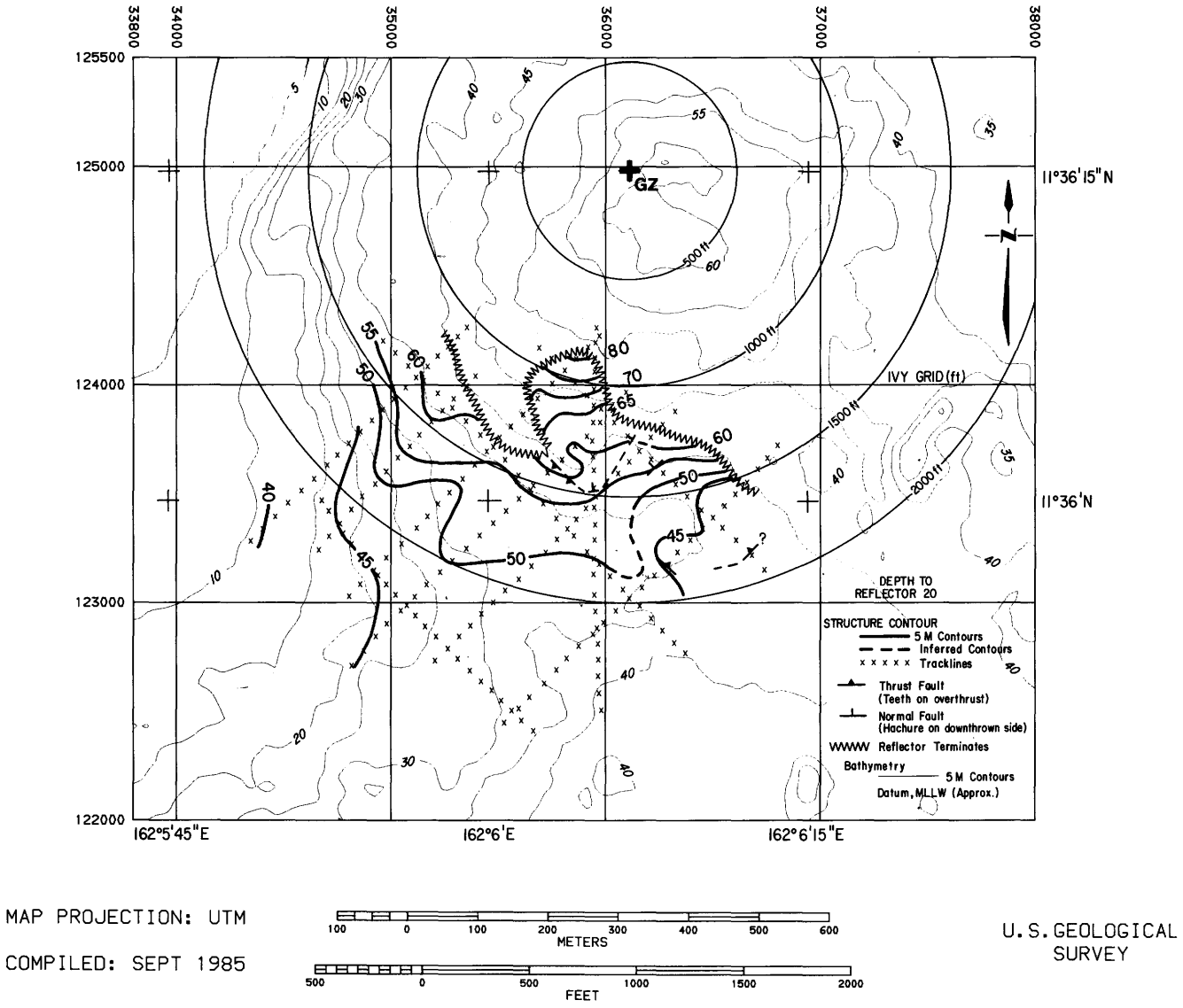

Figure 36. Structure-contour map, reflector R20, OAK crater. Thrust faults are dashed where inferred. GZ=ground zero.

B. Wardlaw, written commun., July 15, 1985). The lateral extent of the transparent sediment layer is obscured by side echoes and slumps near the rims of the crater but appears to be between 400 and 500 m (1,328–1,640 ft) from ground zero on lines 103V2 and 101V4 (figs. 22, 23). The base of this transparent sediment layer at 110 m (361 ft) is inferred to be the base of the transient crater.

A zone of intense fracturing extends from the base of the transparent sediments at 110 m (361 ft) down to approximately 180 m (590 ft) in the center of OAK crater (figs. 22, 24). Within this zone, the downwarped edges of reflectors R10, R20, and R40 become too intensely fractured to map within 250 to 400 m (820–1,328 ft) of OAK ground zero.

Beyond the zone of intense fracturing, downwarping of coherent sedimentary reflectors can be observed at varying distances from and depths below OAK ground zero. Downwarping of the R10 and R20 reflectors was demonstrated with the single-channel seismic data which showed that some effects of cratering could be observed out to 750 m (2,460 ft) to the southwest and 900 m (2,952 ft) to the northeast (chap. C, fig. 13, this volume). The single-channel data showed downwarping of R10 and R20 continuing to within 400 to 450 m (1,312–1,476 ft) of ground zero where the reflectors were either truncated or too deep to be detected. The multichannel seismic system confirmed these data, but especially southwest of ground zero, the system was able to trace R20 to within 250 m (820 ft) of ground zero. At distances of more than 750 m (2,460 ft) southwest of ground zero, R20 occurs at approximately a 40-m (133 ft) depth (fig. 36). The multichannel seismic lines parallel to the reef show that downwarping of R10 and R20 begins between 550 and 750 m (1,804–2,460 ft) from ground zero

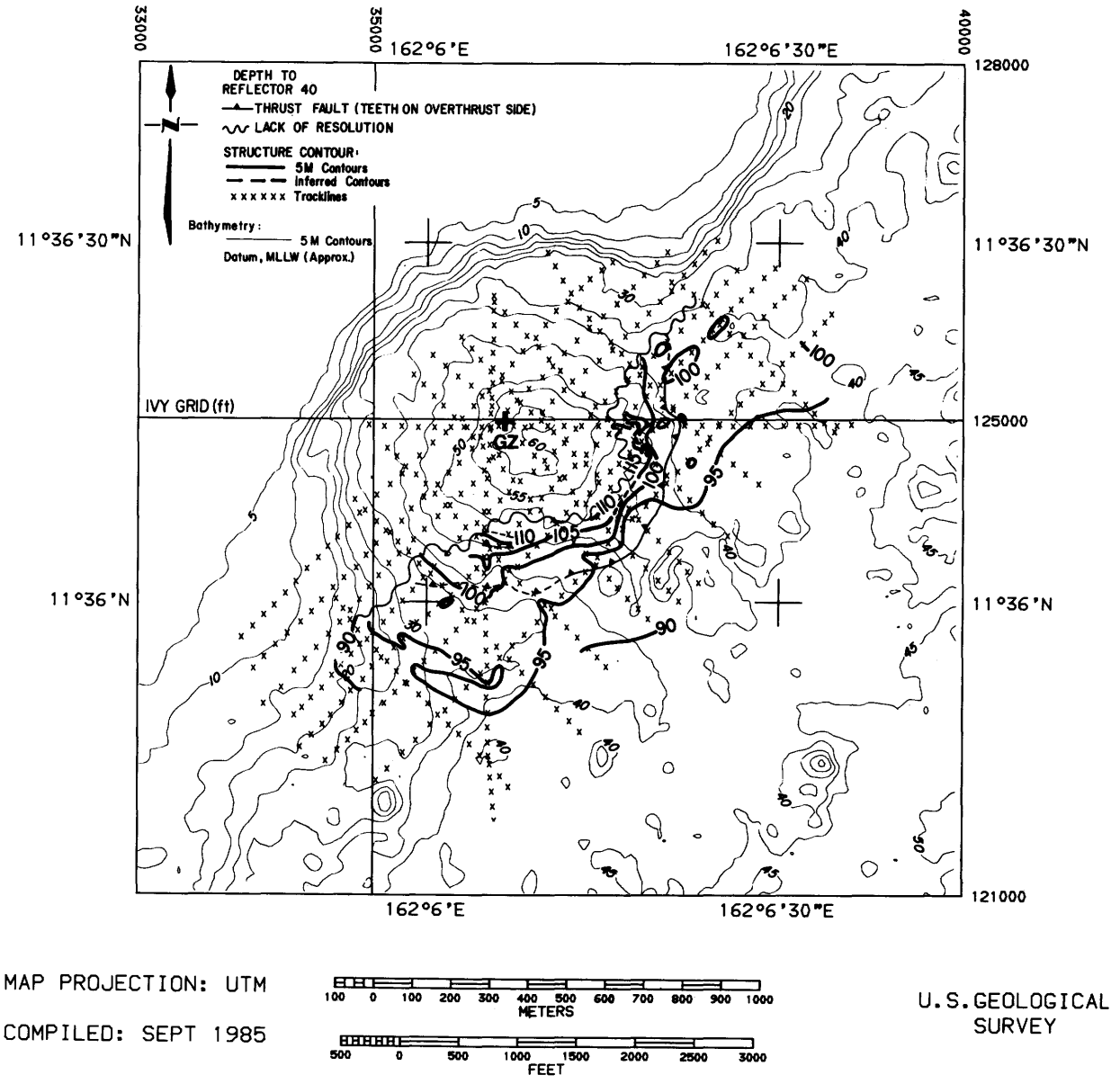

Figure 37. Structure-contour map, reflector R40, OAK crater. Thrust faults are dashed where inferred. GZ=ground zero.

(figs. 23, 24, 32, 33). A gradual downwarp occurs from 40 m (131 ft) in the southwest to a depth of 80 m (262 ft) at 250 m (820 ft) from ground zero where R20 is either truncated or obscured by fracturing. It is important to note that only a few small faults (1–2 m, or 3–6 ft) were observed to disrupt R10 and R20 over this broad zone of downwarp.

Downwarping at the next deeper level can be observed with reflector R40 which shows downwarp effects beginning between 400 and 500 m (1,312–1,640 ft) from ground zero (figs. 29, 30). R40 drops from a level of approximately 95 m (312 ft) outside the crater to a depth of 115 m (377 ft) at a distance of 300 m (984 ft) from ground zero before becoming too fractured to map (fig. 37).

The next deeper level of downwarp can be mapped on reflector R75 which occurs at a depth of approximately 210 m (689 ft) outside the crater (fig. 38). R75 downwarps to 230 m (754 ft) near OAK ground zero. R75 begins downwarping at distances up to 350 m (1,148 ft) southwest of ground zero (fig. 38).

The deepest level of possible downwarped reflectors can be inferred from reflector R100 which occurs at a depth of 325 to 350 m (1,066–1,148 ft) outside the crater (fig. 39). Approximately 10 m (33 ft) of downwarp are suggested on R95 in the 80-in^3 watergun line parallel to the reef over OAK ground zero (line 101V5, fig. 10) and on R100 in the 15-in^3 watergun line over the same location (fig. 23). Inspection of line 103V2 perpendicular to the reef (fig. 22) shows clear downwarp of reflectors to approximately 280 m

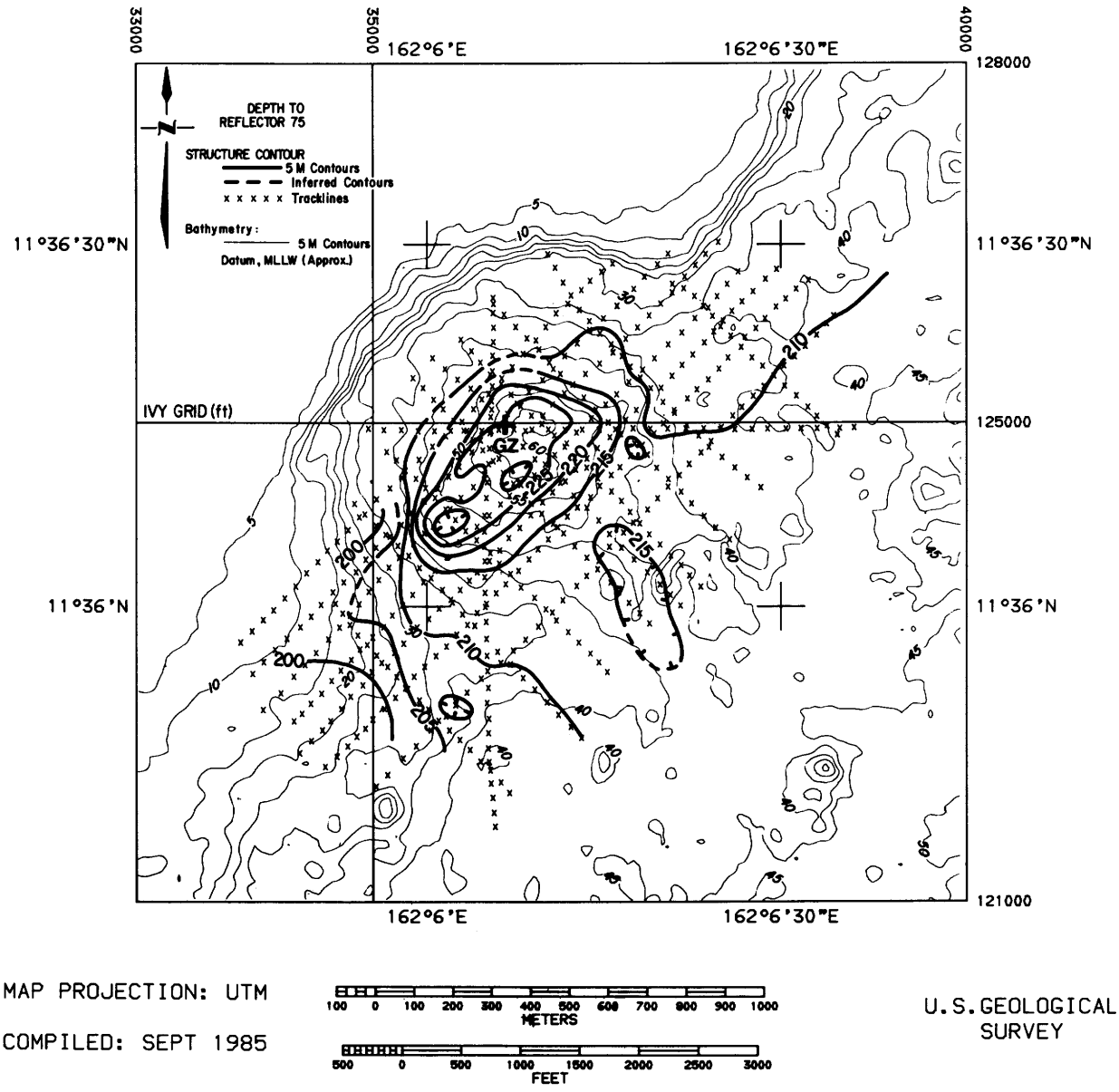

Figure 38. Structure-contour map, reflector R75, OAK crater. GZ=ground zero.

(918 ft), and this has been interpreted as the base of "moderate fracturing and depression." The possible 10-m (33 ft) downwarp of R100 is getting down within the random natural variations in depth to R100 outside the crater area. Therefore, the maximum depth of moderate downwarp or depression effects, that is, those downwarps greater than 10 m (33 ft), is 280 m (918 ft).

The check-shot velocities from the OAK ground zero site, OBZ–4, also show that the interval velocities at ground zero are 10 to 30 percent slower than the reference sites down to a depth of 300 m (984 ft). Because the check-shot interval velocities were averaged over the 250- to 300-m (820–984 ft) interval, the 280-m (918 ft) depth of "moderate fracture and depression" observed on line 103V2 is consistent with the check-shot data. A depth of 280 m (918 ft) is considered the best overall estimate of damage effects due to the OAK event, on the basis of a combination of multichannel and check-shot velocity data.

The preliminary drilling results indicate a slightly deeper level of downward displacement at 325 m (1,065 ft) with "undisplaced, fractured" rock extending down to 340 m (1,115 ft) (B. Wardlaw, written commun., July 15, 1985). The overall consistency between the seismic and drilling results from OAK crater is excellent. While the drill-hole data are generally the most accurate absolute measure of depth, the seismic data still provide the best relative measure of trends between the drill holes.

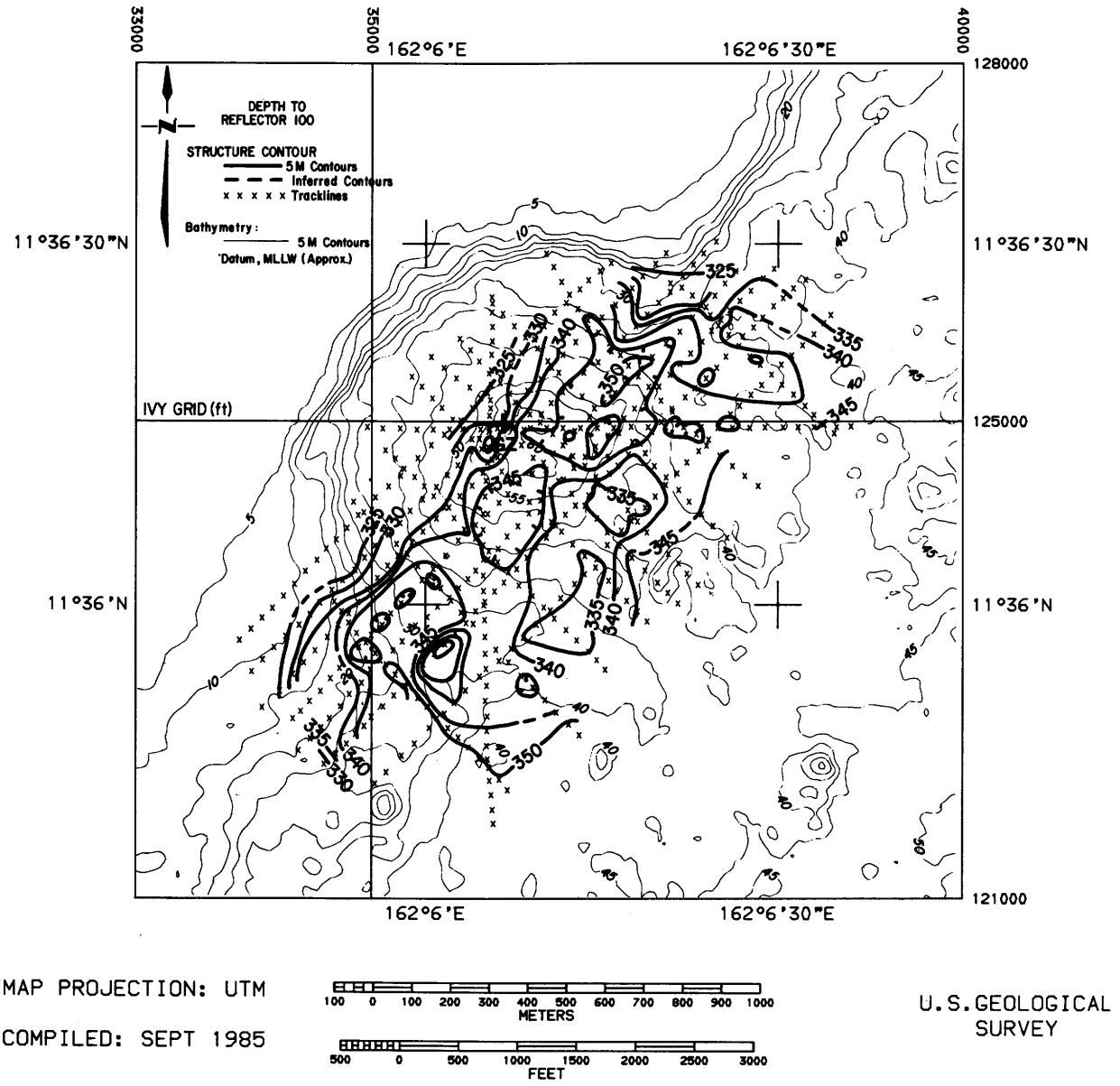

Figure 39. Structure-contour map, reflector R100, OAK crater. GZ=ground zero.

REFERENCES

Gray, W. C., 1979, Variable norm deconvolution: Palo Alto, Calif., Stanford University, Ph.D. thesis.

Ristvet, B. L., Tremba, E. L., Couch, R. F., Fetzer, J. A., Goter, E. R., Walter, D. R., and Wendland, V. P., Geological and geophysical investigations of the Eniwetok nuclear craters: Air Force Weapons Laboratory Technical Report TR–77–242, Kirtland Air Force Base, New Mexico 87117, 263 p.

Tremba, E. L., Couch, R. F., Ristvet, B. L., 1982, Enewetak Atoll Seismic Investigation (EASI): Phases I and II (final report): Air Force Weapons Laboratory Technical Report TR–82–20, Kirtland Air Force Base, New Mexico 87117, 124 p.

Chapter E

Seismic-Refraction Survey of OAK Crater

By H. D. ACKERMANN, J. A. GROW, and J. M. WILLIAMS

U.S. GEOLOGICAL SURVEY BULLETIN 1678

SEA-FLOOR OBSERVATIONS AND SUBBOTTOM SEISMIC CHARACTERISTICS OF OAK AND KOA CRATERS, ENEWETAK ATOLL, MARSHALL ISLANDS

CONTENTS

FIGURES

TABLE

Chapter E
Seismic-Refraction Survey of OAK Crater

By H. D. Ackermann[1], J. A. Grow[2], *and* J. M. Williams[1]

INTRODUCTION

Purpose

Two refraction lines were included in the data collected at OAK crater. These refraction measurements were augmented by stratigraphic data acquired by multichannel seismic-reflection techniques aboard *Egabrag II* and then by down-hole velocity data acquired aboard the drilling vessel.

We anticipated that refraction measurements would provide critical data concerning the velocity structure in the OAK crater area in comparison to the velocity structure of the undisturbed atoll. We hoped, thereby, to improve on the refraction data collected as part of project EASI (Enewetak Atoll Seismic Investigation) (Tremba and others, 1982) by using a variety of sound sources such as 15-in^3 and 80-in^3 water guns, a 540-in^3 airgun, and numerous recording channels.

Setting

Although a low sea state is ideal for profiling, interpretation of seismic data collected in an atoll is difficult because of the discontinuous and porous nature of the sedimentary strata. The level of detail desired to decipher crater structure requires closely spaced source and receiver points. OAK crater was formed on the edge of the reef plate, half in consolidated reef plate sediments and half in unconsolidated to poorly consolidated lagoonal sediments. This geometry resulted in refraction sideswipe from the reef front and possibly from the steep crater walls.

Previous Refraction Work

Raitt (1957) carried out the first refraction measurements at Enewetak Atoll. The measurements comprised four lines in the atoll and five outside. One unique characteristic of these data was that receiving geophones for several lines were set 76 m (250 ft) below the surface in the hole drilled at Elugelab Island (Ladd and others, 1953), which was later destroyed by the MIKE detonation. Six layers were identified with the following velocities: 2.44, 3.06, 4.15, 5.59, 6.90, and 8.09 km/s (8,000; 10,000; 13,600; 18,400; 22,600; 26,500 ft/s). The first two layers correlated with carbonate rock overlying a volcanic third layer which had been drilled both on Elugelab and Medren (Elmer) Islands (chap. A, fig. 1, this volume) (Ladd and others, 1953; Ladd and Schlanger, 1960). Raitt's shallow-depth results will be discussed in more detail near the end of this section.

No further refraction data were collected until 1971–72 when approximately 15 km (8 nmi) of lines were run mostly on Aranit (Aomon, or Sally) and Runit (Yvonne) Islands (Henny and others, 1974) as part of Project PACE (Pacific Atoll Cratering Experiment). Subsequently, approximately 76 km (41 nmi) of refraction lines were run on 12 islands in the atoll, and 30 km (16 nmi) of marine data were collected in various craters plus one 1,000-m (3,280 ft) line off Enjebi (Janet) Island as part of project EXPOE (Exploratory Program on Enewetak) (Ristvet and others, 1978). Two of these lines were shot in KOA-MIKE craters, but they defined only the top surface of one layer below the sea floor. None were run at OAK crater, but several lines were shot on the islands nearest the crater, Biken (Leroy) and Bokoluo (Alice) (Ristvet and others, 1978).

The last refraction data collected prior to this study are five lines in OAK and KOA craters and off Enjebi (Janet) Island as part of Project EASI (Tremba and others, 1982). Three zones were defined below OAK crater by combining refraction and reflection data. The first, from the crater floor to 87 m (285 ft) below it, has a velocity of 1,530 m/s (5,000 ft/s); the second, extending to a depth of 141 m (462 ft), has a velocity of 1,770 m/s (5,800 ft/s); and the third, and deepest, has three zones ranging in velocity from 2,010 to 2,440 m/s (6,600–8,000 ft/s). (See fig. 30, Tremba and others, 1982.) A similar model was developed for KOA (Tremba and others, 1982).

In the shallow sediments, Raitt (1957) determined a lagoonal velocity function which increases from 1.9 km/s (6,200 ft/s) in reef detrital material to about 2.4 km/s (7,900 ft/s) in partly consolidated calcareous sediments at a depth of about 106 m (348 ft); another increase to 3.0 km/s (10,000 ft/s) is observed at a depth of about 600 m (1,969 ft), also in partly consolidated calcareous sediments. In marked contrast to these results, Henny and others (1974) showed that the onshore velocities of the reef plate surrounding the lagoon may exceed 3.0 km/s (10,000 ft/s) at

[1]U.S. Geological Survey, Branch of Regional Geophysics, Denver, Colo. 70225.
[2]U.S. Geological Survey, Branch of Oil and Gas, Denver, Colo. 70225.

only 50 m (160 ft) of depth compared to 700 m (2,300 ft) in the lagoon as determined by Raitt.

Reynolds (see appendix B, Tremba and others, 1982) did a refraction study both at OAK crater and at a nearby reference area using a sparker sound source and two hydrophone receivers. He concluded that within 60 m (200 ft) of the sea surface, the reference area contains several stringers, or solution unconformities, each only a few meters thick, which are cut off within OAK crater. In addition, the velocity within the crater to a depth of about 150 m (490 ft) is slightly less than that at the reference site, whereas below 150 m, the velocities at the crater are, if anything, slightly greater than those at the reference site.

METHODS

Sites for deployment of hydrophones were selected on the basis of bathymetric and seismic data collected during Project EASI (Tremba and others, 1982). These sites lay along two refraction lines passing close to OAK ground zero. The longer line, 3.8 km (or 2.1 nmi), of 23 sonobuoy sites lay roughly parallel to the reef (reef line R1), and the shorter line, 1.5 km (or 0.8 nmi), of 7 sonobuoy sites was perpendicular to it (lagoon line R2) (fig. 1). Source-point positions extended several kilometers beyond the ends of the reef line and also beyond the southeast end of the lagoon line.

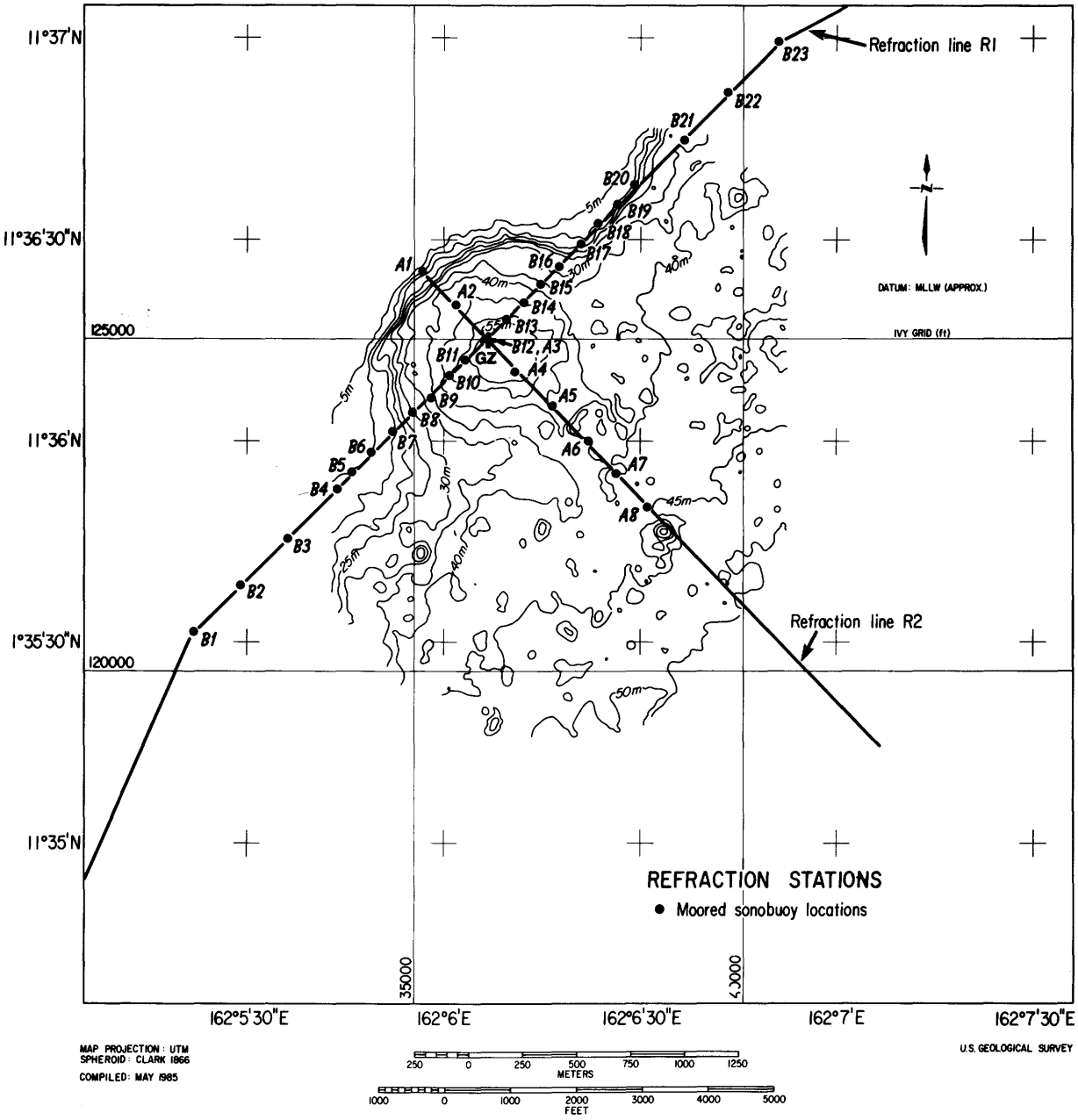

Figure 1. Locations of refraction lines R1 (the reef line) and R2 (the lagoon line) and hydrophone positions at OAK crater, Enewetak Atoll. GZ=ground zero.

Sonobuoys were attached to Norwegian floats 0.6 m (2 ft) in diameter that were taut-line moored with polypropylene line 1 cm (3/8 in.) in diameter to anchors weighing about 35 kg (77 lb). Buoys not within about 40 m (130 ft) of the desired site were repositioned and resurveyed. The configuration of a mooring is depicted in figure 2.

The recording systems comprised several components. Refraction Technology (Ref Tek) 18L low-frequency, analog, reusable radio sonobuoys were used for transmission of seismic data to the research vessel. Companion HS-1 FET (Field Effect Transistor) suspension hydrophones coupled the acoustic pressure wave to the radio telemetry system. Each buoy had an associated whip antenna cut to length for the transmission frequency of each channel. The adjustable gain of each buoy was set at 0 dB. In areas of shallow water, cables from sonobuoys to hydrophones were shortened to keep hydrophones off the bottom. Maximum length of the cables was 18.3 m (60 ft).

The sonobuoy receiving system consisted of a dual high-gain directional antenna that enabled reception of radio signals while approaching or departing each sonobuoy along the line. The signal was amplified by 20 dB prior to a Ref Tek-64 antenna distributor which split the radio signal to three Ref Tek-20 receiver mainframes, each of which incorporated 10 Ref Tek-19 receiver modules. The receiver modules were configured to minimize any adjacent receiver crosstalk. The seismic analog data were monitored using a galvo-recorder and recorded digitally by a 24-channel Texas Instrument DFS-V seismic data acquisition system in SEG–B nine-track magnetic tape format.

The survey was conducted over a period of 3 days, during which three passes were made along the two lines (fig. 1) with 15-in^3 and 80-in^3 water guns and a 540-in^3 airgun towed by *Egabrag II* at approximately 3 kn (150 cm/s). Shot-point spacings were approximately 6 and 12 m (20 and 40 ft) for the 15-in^3 and 80-in^3 water guns and 37 m (120 ft) for the 540-in^3 airgun.

Ship position was fixed every 20 seconds with the Motorola Falcon IV miniranger system. Because there was no provision for recording fix positions on the data tapes, shot locations were obtained at regular intervals by manually correlating fix positions with field file numbers recorded on tape headers. Final shot positions were obtained by interpolation from a 1:6,000-scale map of fix positions.

Seismic-refraction record sections for each receiving station were produced at the U.S. Geological Survey (USGS) processing center in Denver, Colo. A 100-ms automatic gain control operator, which effectively suppressed background noise prior to the onset of initial refraction arrivals, was applied to each seismic trace. Both filtered and unfiltered versions of the data were generated, and both were used to pick arrivals.

The three different energy sources (15- and 80-in^3 waterguns, 540-in^3 airgun) were used to provide a broad range of choice between frequency spectrum, signal amplitude, and data density. In the final analysis, the data from the 540-in^3 airgun were superior despite the gun's lower repetition rate which resulted in fewer traces per recording station and a lower data density. The rapid signal attenuation due to the porous nature of the coral sediments necessitated a large amplitude signal. The signal from the water guns contained a 30-ms-long precursor to the main pulse, causing difficulty in delineating initial onsets. The thin solution unconformities (Tremba and others, 1982) were transparent to all three energy sources.

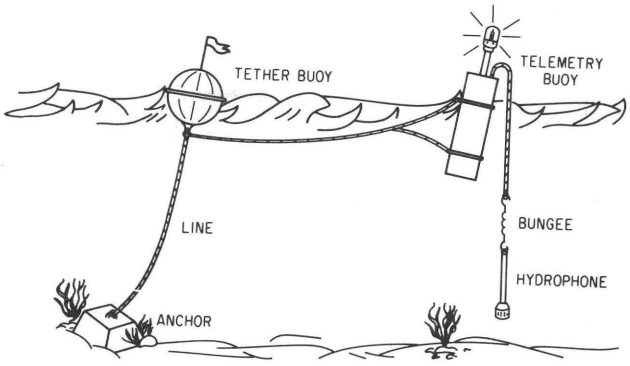

Figure 2. Sonobuoy mooring configuration.

Data quality was generally good. Typical examples of seismograms, in compressed form, are shown in figures 3 and 4. The most severe problem encountered was crossfeed between channels on the northeast end of the reef line resulting in some loss of data. The most severe case is shown in figure 5. Independent measurements of sonobuoy receiver locations showed a drift of roughly 30 m (100 ft), but relative locations with respect to source positions could be determined within a few meters. Another complication was that the track of the recording vessel did not lie precisely along the line of sonobuoys, resulting in a few mis-ties on reciprocal times along the reef line by as much as 15 to 20 ms. The distance between the source and individual sonobuoys was most often less than 50 m (160 ft). Stations A2, A8, and B15 malfunctioned. Such problems with individual channels were readily overcome by the large quantity and redundancy of collected data.

Large numbers of recording stations and closely spaced shot points are essential in areas of varying subsurface conditions such as those at OAK crater. Methods of interpreting such closely packed and overlapping data sets fall into the realm of engineering seismology (Ackermann and others, 1982).

RESULTS

The computer-processed results are presented as depth-distance diagrams, velocity sections which show layers of increasing velocity that may vary laterally (fig. 6). The upper boundary of each layer represents the path of a

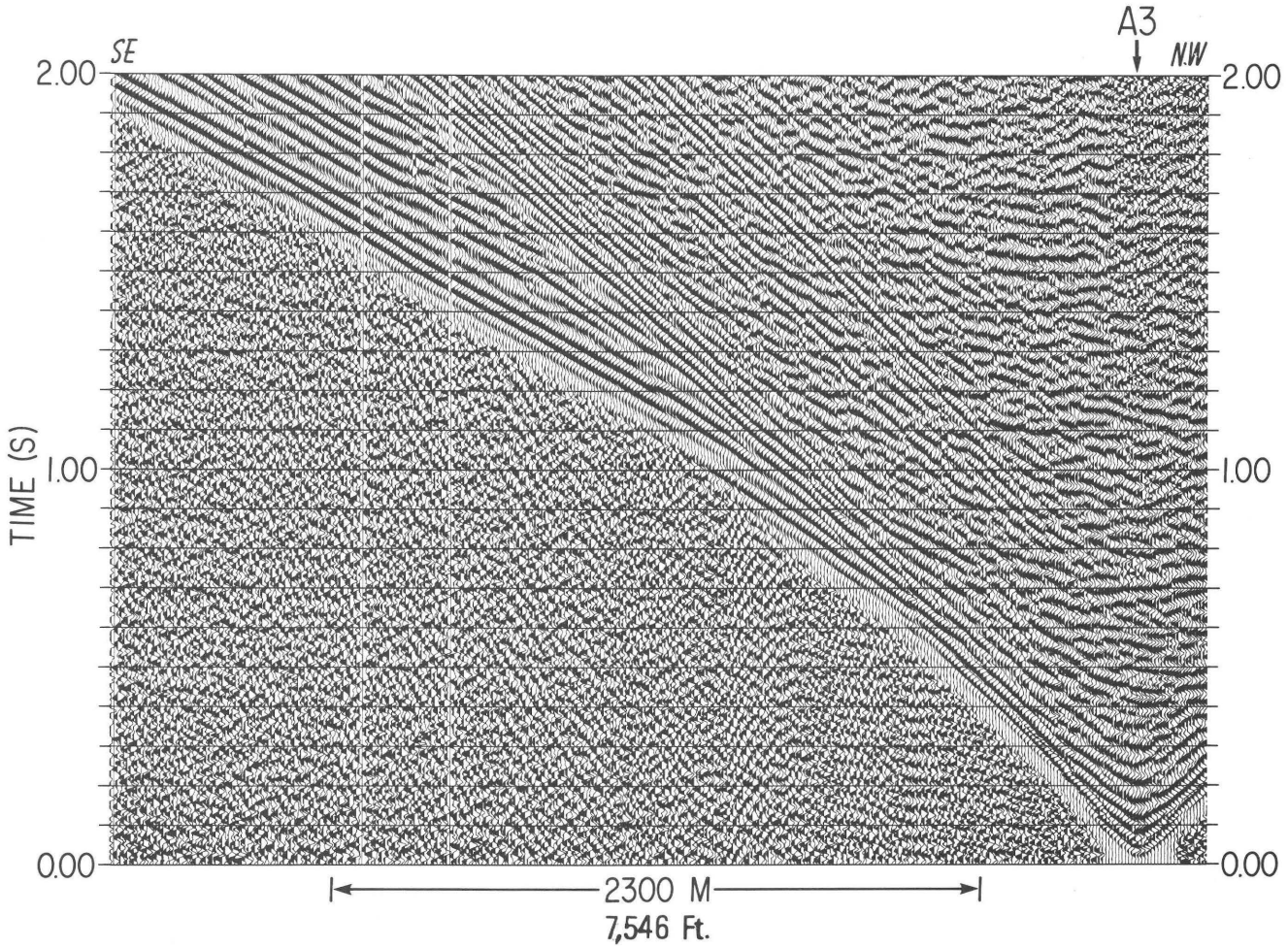

Figure 3. Seismogram for recording station A3 (fig. 1) from 80-in^3 watergun.

seismic ray that propagated from the source point to a receiver along a subsurface velocity discontinuity where the velocity is assumed to increase abruptly with depth. This upper boundary is called a horizon. Horizons represent ray paths which can cut across or transect geological or physical layers, as in OAK crater where ray paths cut across the crater fill (fig. 7), because it has approximately the same velocity as the fractured and porous rocks on the flanks. Velocity sections show the paths of rays; therefore, the shape of the crater could not be resolved from the refraction results. Information about the nature of the rocks or material along the ray paths could be deduced from the value and variations in velocity along them.

Refraction Sideswipe

At an apparent depth of about 600 m (2,000 ft), the ray velocity for the reef line is about 4.3 km/s (14,000 ft/s) compared to only 2.9 km/s (9,500 ft/s) beneath the lagoon line, suggesting an unrealistic anisotropy ratio of 32 percent. A velocity of 4.3 km/s implies dense rocks, perhaps limestone or fractured intrusive or lava flows, but not porous coral reef sediments found beneath back-reef or lagoon. However, the work of Henny and others (1974) proves that velocities within the reef are substantially higher than those in the lagoon (Raitt, 1957) and at depths of several hundred meters onshore may attain values of 4.3 km/s (14,000 ft/s). Because the reef line was offset only a short distance from the reef edge, the apparent discrepancy is readily resolved; it appears that the 4.3-km/s (14,000 ft/s) velocity simply represents sideswipe from a wave refracted along the reef edge. The reef-edge sideswipe originated from shallow depths, perhaps less than 100 m (330 ft). On land, experience has been that refraction sideswipe from steep discontinuities is seldom recorded because the direction of the returning wave is essentially perpendicular to the geophone orientation. Hydrophones, however, respond equally well to horizontal and vertical pulses.

This result severely limited analysis of the reef-line data. Reef-edge refractions arrived at the recording stations ahead of the slower arrivals from beneath the crater, resulting in the hidden-layer problem. Efforts at solving this problem were virtually fruitless. Therefore, the major portion of the interpretations for horizons deeper than the approximate

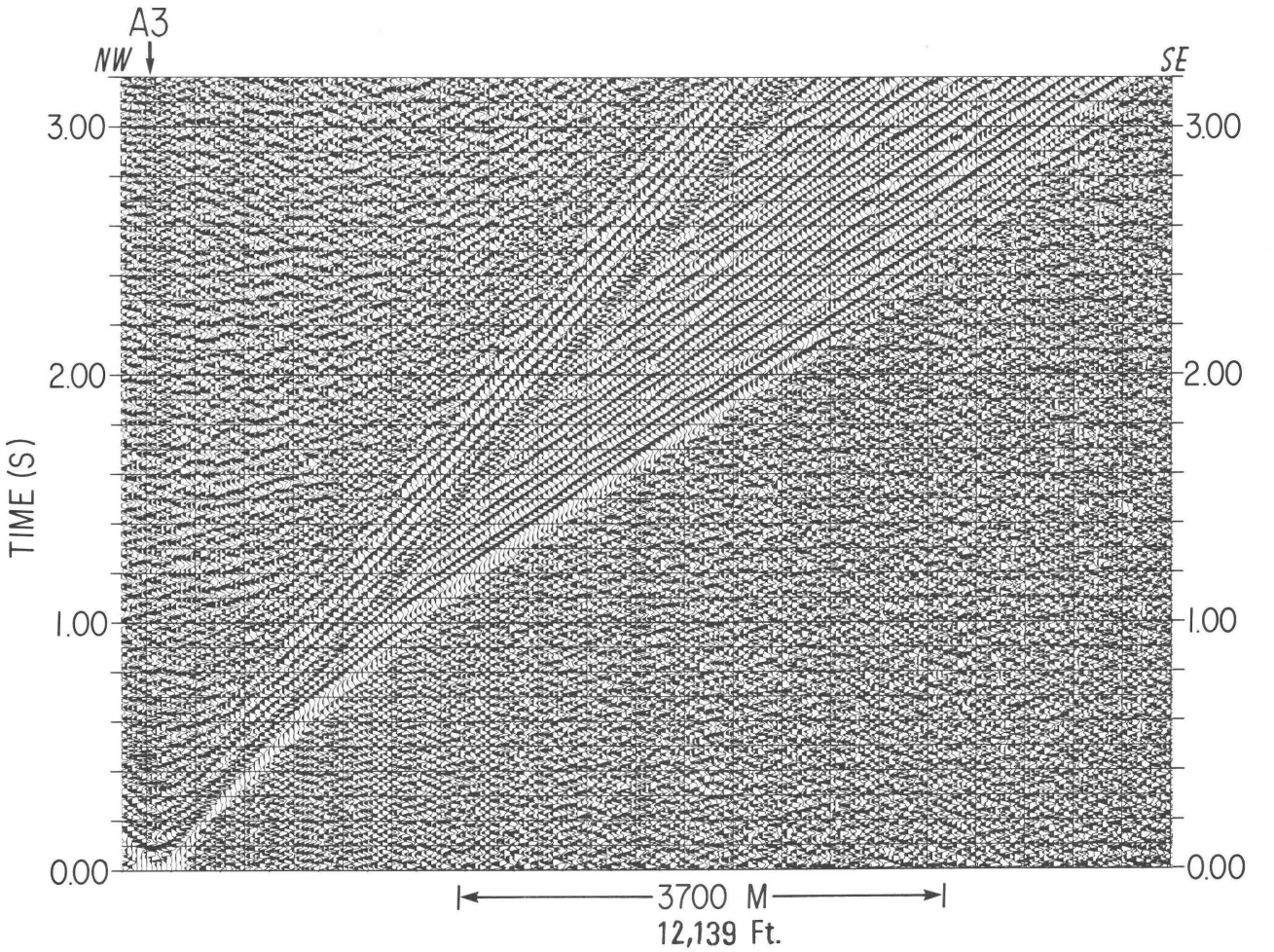

Figure 4. Seismogram for recording station A3 (fig. 1) from 540-in^3 airgun.

transient crater floor were obtained from the lagoon line using the six operational hydrophones. Data from the reef line, with its greater concentration of receiver stations and hence greater resolving power, were used to determine the shallower horizons.

Shallow Crater Structure—Horizons 1, 2, and 3

Signal returns were obtained from five horizons; that is, five critically refracted ray paths were observed. Computed ray paths and velocities for horizons 1, 2 and 3 of the lagoon line are shown in figure 6. Although horizons are bowed toward the crater interior, the true crater structure is not evident because of the small contrasts in velocity between undisturbed materials outside the crater area and those materials within the crater.

No returns were observed from the sea floor, indicating that the velocities of the porous shallow reef deposits outside the crater area and the shallow debris beneath the crater floor are indistinguishable from the velocity of sea water (about 1.54 km/s, or 5,050 ft/s). The initial critically refracted ray (horizon 1) outside the crater area was recorded from subsea-floor depths of between 5 and 30 m (16–100 ft) with propagation velocities between 1.7 and 1.8 km/s (5,600–5,900 ft/s). Beneath the crater floor, it was recorded from 10 to 20 m (30–70 ft) with velocities between 1.6 and 1.7 km/s (5,200–5,600 ft/s). The difference in velocity is small and almost indistinguishable. Data from horizon 2 were observed only on the northeast side of ground zero, with velocities between 1.8 and 1.9 km/s (5,900–6,200 ft/s). The third recorded critical ray again has remarkably similar propagation velocities both outside and inside the crater—2.0 to 2.3 km/s (6,500–7,500 ft/s) outside and 1.8 to 2.1 km/s (5,900–6,900 ft/s) inside. At ground zero, the path of this ray agrees well with the estimated base of the floor of the transient crater. (See chap. D, this volume.) Because of the lack of contrast in velocities, the minimum-time ray path for horizon 3 does not follow the crater floor but grazes it and travels through deeper coral-reef deposits.

The reversed travel-time curves, including extrapolations (Ackermann and others, 1982) from which horizon 3

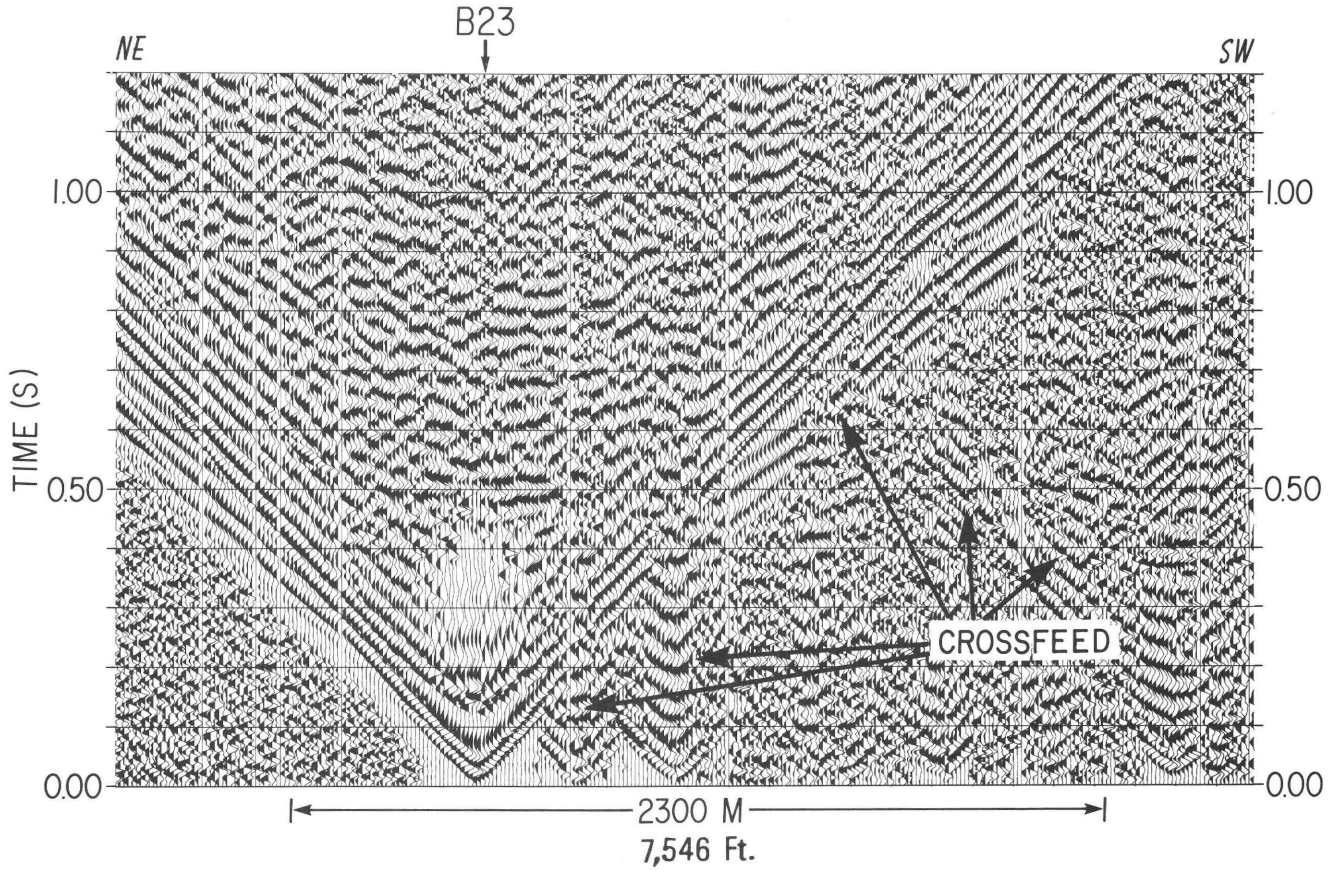

Figure 5. Seismogram for recording station B23 (fig. 1) showing the worst case of crossfeed between channels.

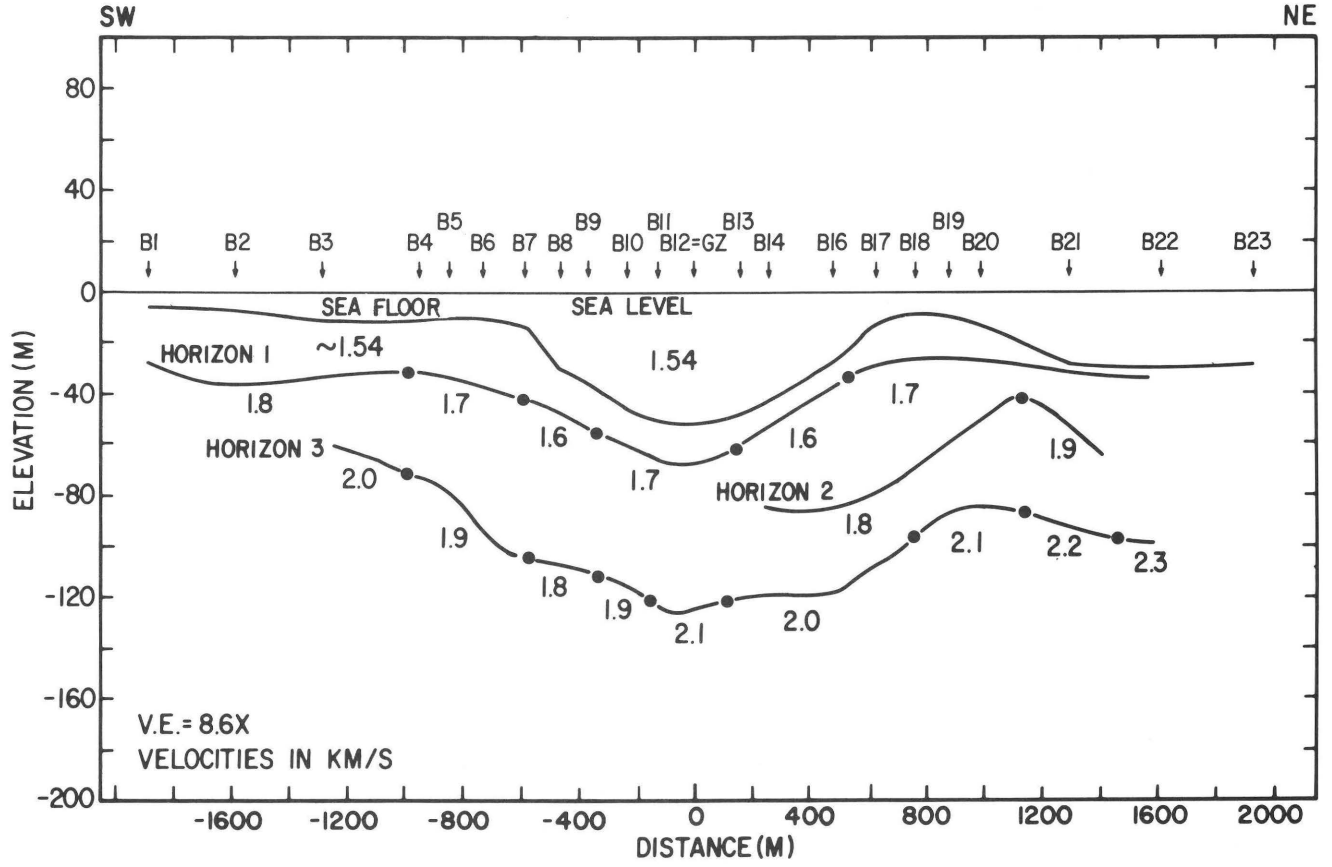

Figure 6. Velocity section for horizons 1, 2, and 3 at OAK crater interpreted from the reef-line data (line R1, fig. 1). Solid circles indicate boundary between velocity values. GZ=ground zero.

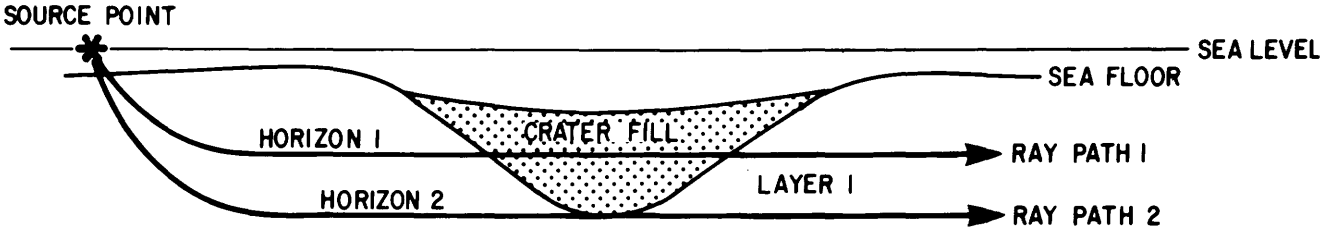

Figure 7. Two hypothetical ray paths, one of which transects crater-fill material and another that passes beneath it.

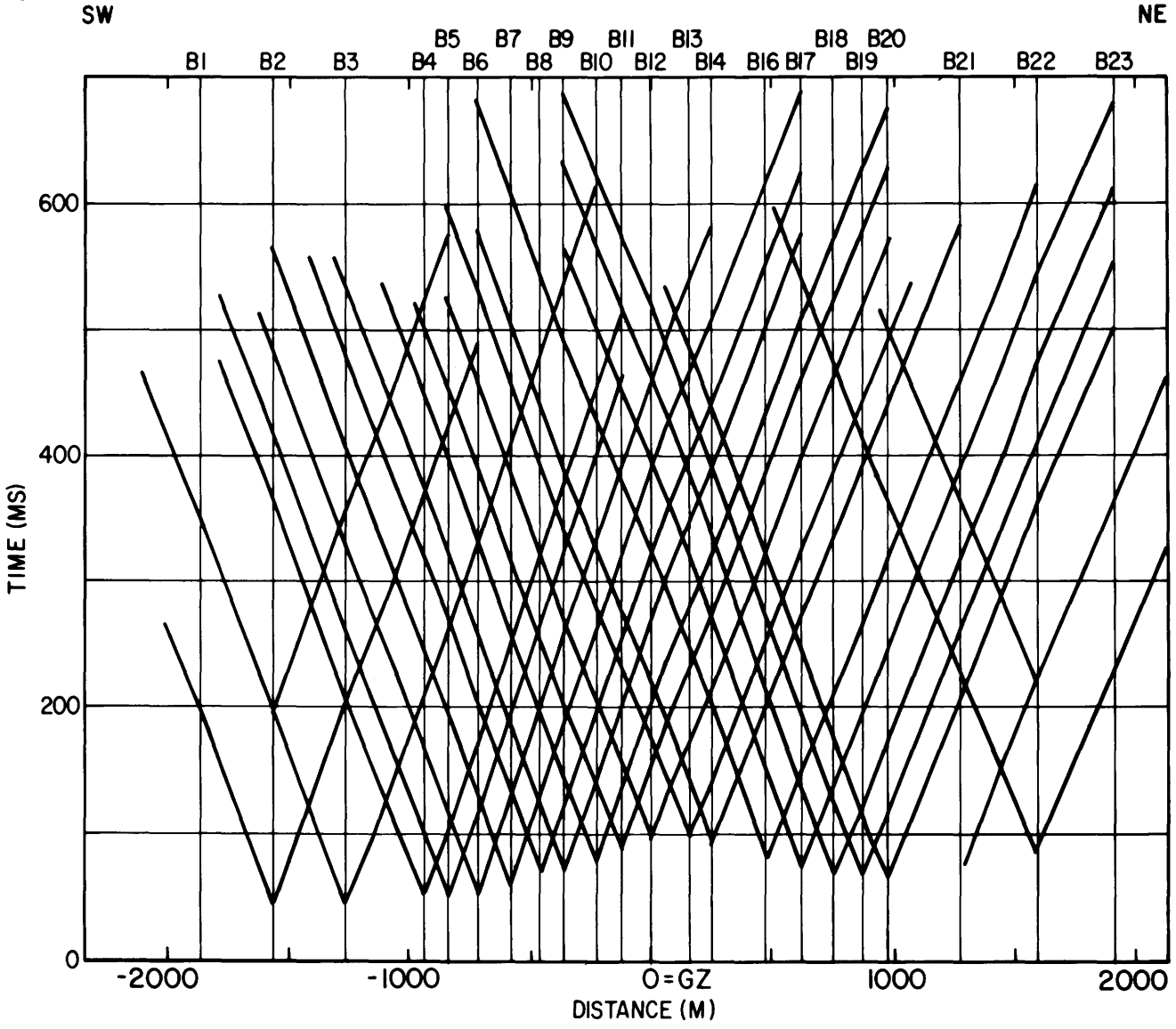

Figure 8. Extrapolated travel-time curves for horizon 3 from all of the receiver stations (B1–B23) on the reef line (fig. 1). Note the increase in delay time toward ground zero (GZ) (sta. B12).

was computed, are shown in figure 8. Note the steady increase in delay time approaching station B12 at ground zero where this ray path is approximately tangent to the transient crater floor.

Figure 9 shows a diagrammatic interpretation of the physical significance of the ray paths of figure 6. Line AB outlines the approximate excavated zone based on a depth of 120 m (390 ft) at ground zero. (See chap. D, this volume)

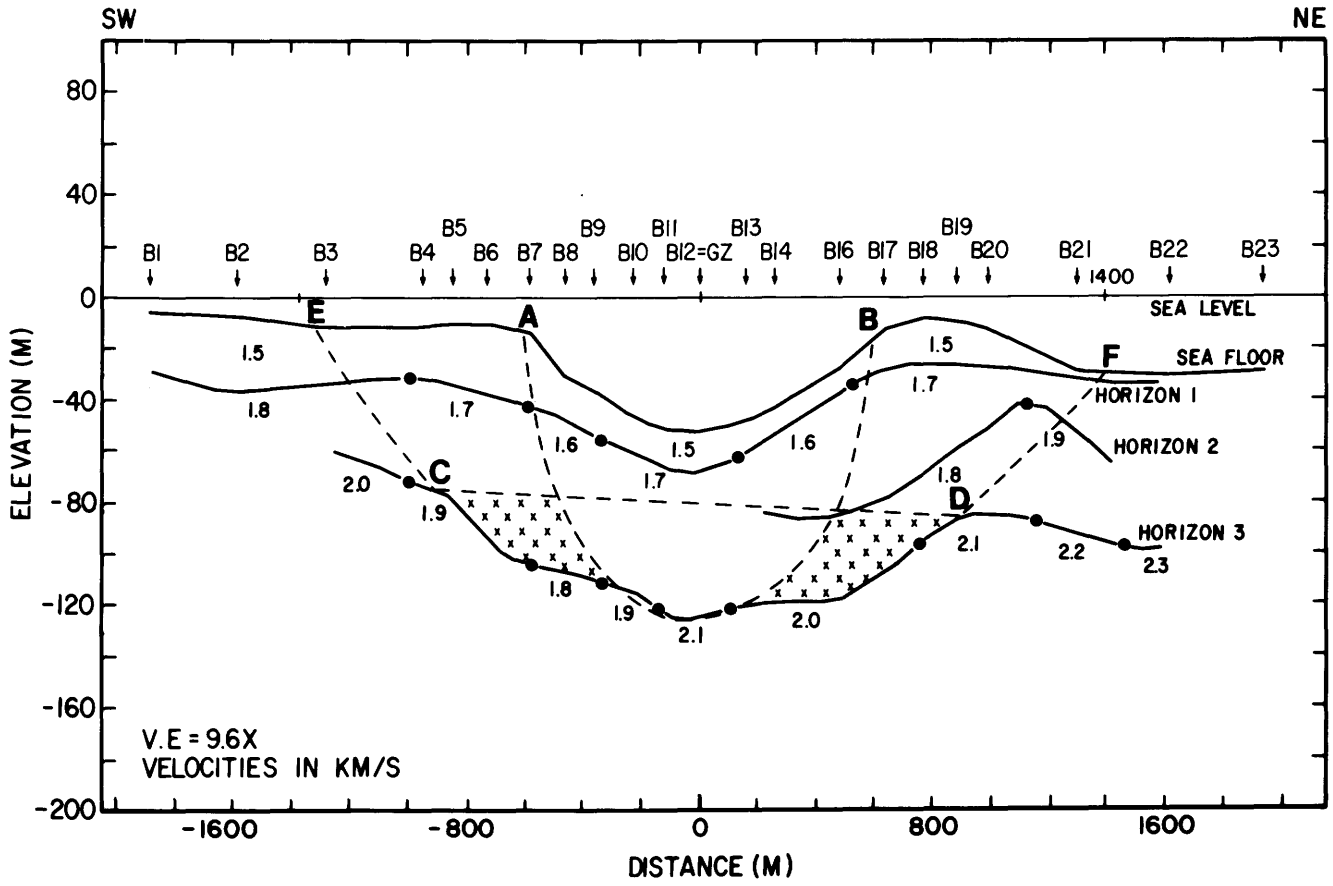

Figure 9. Interpretation of figure 6. Line AB encloses the initial excavation. Line CD estimates preevent horizon 3, and the x's below CD indicate highly fractured rock, reduced in velocity from preevent values of 2.2 to 2.3 km/s (7,200–7,550 ft/s) down to 1.7 to 1.9 km/s (5,600–6,250 ft/s). Lines CE and DF extrapolate this fractured zone to the sea floor. Solid circles indicate boundary between velocity values. GZ=ground zero.

and a maximum crater radius of about 600 m (2,000 ft). (See chap. A, this volume.) The ray representing horizon 1 warps downward beneath the crater with little change in velocity, conforming more to depth of the sea floor than to any other crater characteristic. Horizon 3, on the other hand, begins to warp downward well outside the probable transient crater and is tangent to it below ground zero. Dashed line CD was drawn to estimate the subhorizontal preevent horizon 3. A hypothetical preevent ray path would have approximately followed path CD, whereas the present minimum-time path bends beneath it, due not only to debris deposited in the bowl, but also to ruptures and fractures in wedges flanking both sides of the crater. Marked by x's in figure 9, these wedges, composing a ring or halo when viewed in three dimensions, constitute a large area, or volume, in which the blast phenomena lowered velocities from over 2 km/s (6,600 ft/s) to 1.7 or 1.8 km/s (5,600–5,900 ft/s). These wedges are projected toward the surface by dashed lines CE and DF and intersect the sea floor above the zone in which the velocity of horizon 3 reaches 2.2 to 2.3 km/s (7,200–7,500 ft/s); this velocity suggests the possibility that near-surface fractures may extend as far as 1,400 m (4,600 ft) from ground zero. Lines CE and DF are permitted to transect the layers below the sea floor on the assumption that additional fracturing only negligibly affected their initial in-place velocity, which was not much greater than that of sea water. Fracturing extending to a considerable distance from ground zero is also suggested by a reference boring which encountered fractured rock at distance of 1,325 m (4,347 ft) from ground zero (A. Schenker, oral commun., May 1985).

If blast-induced fractures exist at distances of over 1,000 m (3,300 ft) from ground zero, then the possible significance of the lateral increase in velocity of horizon 3 from 1.9 to 2.1 km/s (6,200–6,900 ft/s) beneath ground zero to 2.2 to 2.3 km/s (7,200–7,500 ft/s) under station locations B21 and B22 1,400 m (4,600 ft) northeast of ground zero must be evaluated. Is the lower velocity around the crater the result of blast-induced fractures, or is it due to the laterally varying nature of the coral reef deposits? Data from several sources suggest that 2.2 to 2.3 km/s (7,200–7,500 ft/s) is the in-place velocity of coral deposits in this area, approaching the velocity (2.4 km/s or 7,900 ft/s) measured by Raitt (1957) and Tremba and others (1982); and the

lower velocities of 1.8 to 2.1 km/s (5,900–6,900 ft/s) are the result of blast-induced fractures.

On the northeast side of the crater, the shallow-depth data from the reef line clearly indicate a slight increase in velocity with depth between horizons 1 and 3. (See horizon 2 in figs. 6 or 9.) The data are inadequate for attaching any other physical significance to them.

The shallow horizons beneath the lagoon line, computed from the 540-in^3 airgun data, are shown in figure 10. Although depth and velocity values on this line approximately agree with those on the reef line at ground zero, these data could not be interpreted in the same detail as were the reef-line data (figs. 6, 8) because only six operational hydrophones at larger intervals were emplaced there.

Deep Crater Structure—Horizons 4 and 5

Crater analyses for depths below 120 m (390 ft) were relegated to the lagoon-line data due to the interference by refraction sideswipe along the reef line. However, as shown in figure 1, the lagoon line could not be extended northwest of the crater, resulting in only single-ended (unreversed) seismic coverage from the deep structures beneath the crater. Therefore, an infinite number of solutions satisfying the data from greater depths are possible. The range of solutions was constrained to a large degree by the drilling results, which are described in some detail through the remainder of this section.

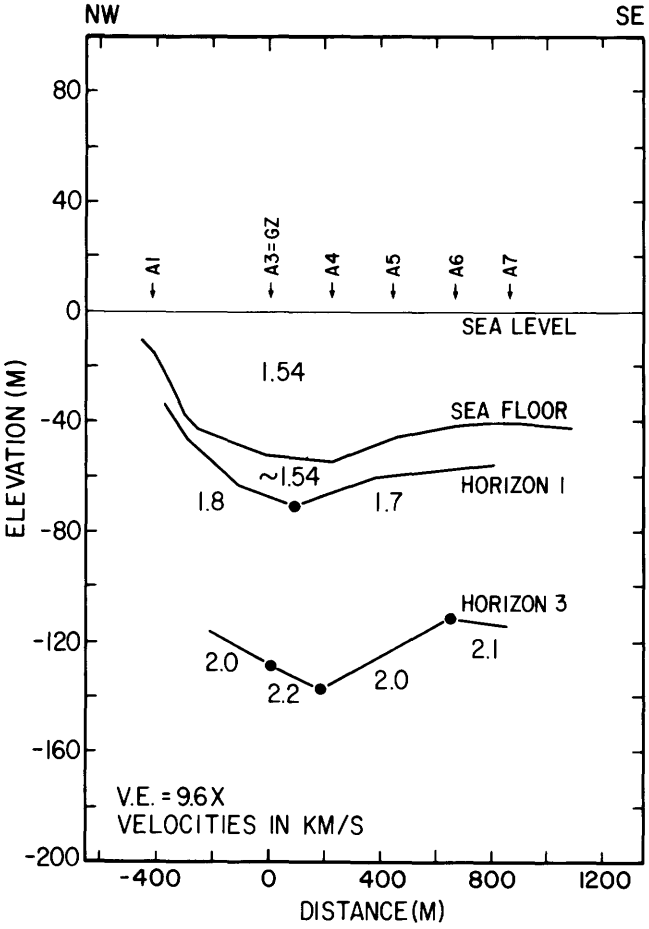

Figure 10. Velocity section for horizons 1 and 3 at OAK Crater interpreted from the lagoon-line data (line R2, fig. 1). Solid circles indicate boundary between velocity values. GZ=ground zero.

The travel-time curves for horizon 4 are shown in figure 11, where curves in parentheses and labeled A1 through A7 are from receiver positions A1 through A7. The travel-time curve in parentheses and labelled X represents the arrival times at all the six recording stations obtained with the source point at 1,790 m (5,870 ft) on the distance axis. The posted inverse slopes of curves A1 through A7 and the slope for curve X southeast of receiver position A6 suggest a subsurface ray velocity of approximately 2.8 km/s (9,200 ft/s)—or a horizon of negligible dip southeast of the crater with a velocity of about 2.8 km/s. An increased slope of curve X is observed northwest of receiver position A6 from the posted values of lower apparent velocity (fig. 11), suggesting that OAK crater and the fractured rocks around it have disrupted this travel-time curve.

Subsurface velocity distributions must satisfy curve X and curves A1 through A7. Through an iterative process, we obtained velocity distributions that also satisfy the velocity survey of the boring at ground zero. The process is simplified by first extrapolating both curve A7 and curve X to their origin points at 860 and 1,790 m (2,820–5,870 ft), respectively, with the inverse slope of 2.8 km/s (9,200 ft/s). These curves are labeled in figure 11 as Y and Z, respectively. Any solution that simultaneously satisfies curves X, Y, Z, and A7 will also satisfy curves A1 through A6.

Curves Y, Z, and A7, now representing reversed data, may be solved uniquely using the overlying velocity distribution of figure 10. The computer-generated output is shown by the horizontal row of open circles in the bottom right side of figure 12, representing a horizon or ray path approximately 300 m (1,000 ft) below sea level with a propagation velocity of 2.8 km/s (9,200 ft/s). Because curve X is unreversed in the subsurface, any set of velocity values within limits may be used to generate a subsurface profile of a ray path which satisfies it and the overlying velocity distribution. An initial value of 2.8 km/s generated the profile shown by the open circles in figure 13; namely, a horizontal bed southeast of station A6 which then drops precipitously an untenable 200 m (660 ft) within a distance of about 450 m (1,500 ft) below the crater floor. To raise horizon 4 beneath the crater, it is necessary to decrease its velocity, thereby implying that the rocks about 300 m (1,000 ft) beneath the crater floor are fractured. Successive iterations, gradually decreasing the velocity of horizon 4 to a limiting value of approximately 2.25 km/s (7,400 ft/s), resulted in figure 14. This solution is also untenable because the velocity survey

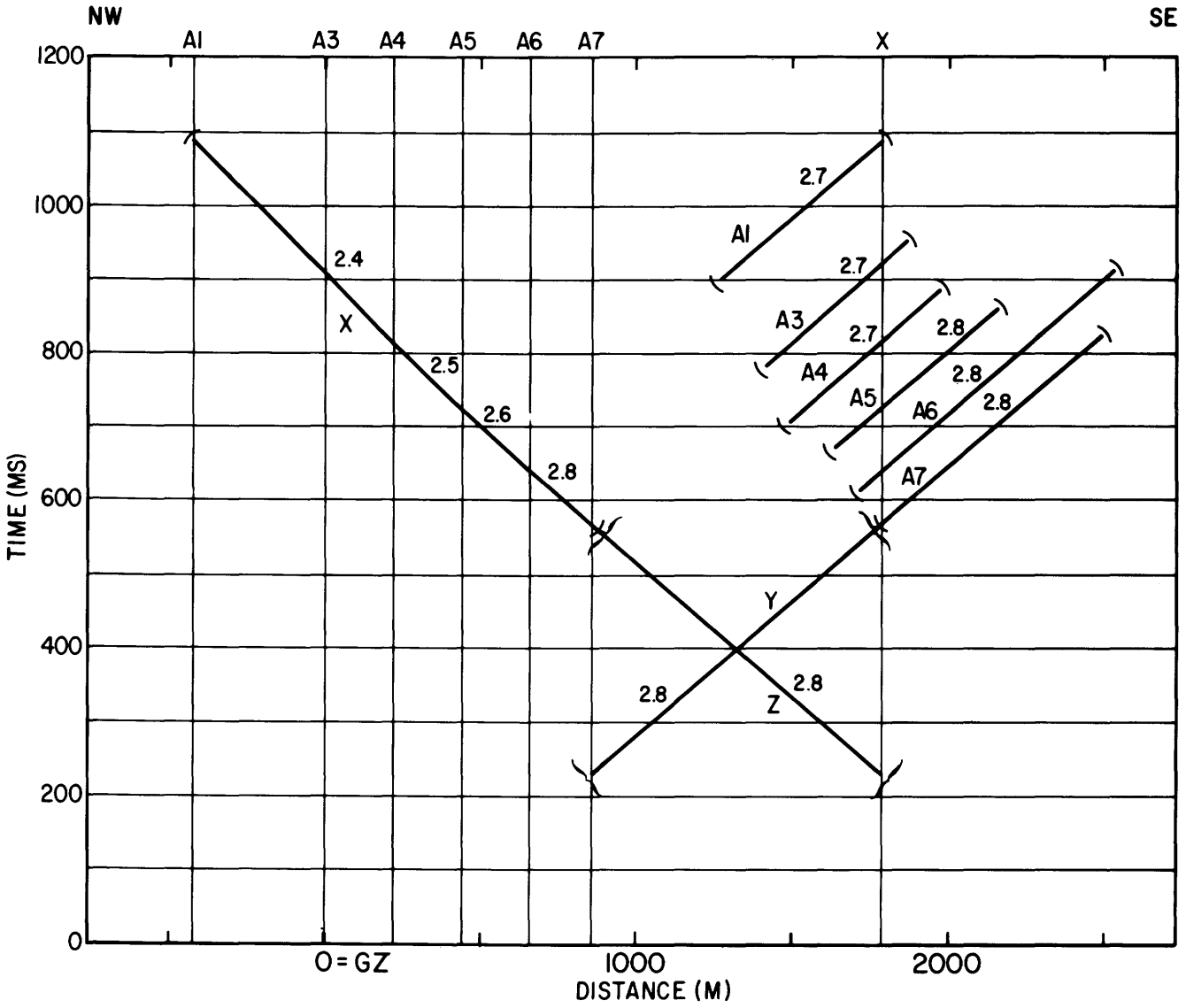

Figure 11. Travel-time curves for horizon 4. The line segments labelled A1 through A7 represent the data from receiver stations A1 through A7 (fig. 1), and the segment labeled X represents the arrival times recorded at the receiver stations with the source situated at point X on the distance axis. Curves Y and Z are extrapolations of curves A7 and X, respectively. Apparent velocities are in kilometers/second. Curves between parameters are measured data; curves between brackets are extrapolated data. GZ=ground zero.

in the ground-zero boring (table 1) showed that at approximately 300 m (1,000 ft) below sea level, the velocity increased abruptly from about 2.0 km/s (6,600 ft/s) to over 2.5 km/s (8,200 ft/s), not to 2.25 km/s (7,400 ft/s). The only way to attain a value as high as 2.5 km/s (8,200 ft/s) for horizon 4 beneath the center of the crater and yet satisfy the travel-time curves of figure 11 is to increase significantly the average velocity of the overlying materials outward from ground zero. Although in apparent contradiction to the ray velocities in figure 14, justification for tapering the velocities comes from three other sources: First are the results from the ground zero and reference borings. The latter were drilled on the reef line 1,325 m (4,347 ft) northeast of ground zero. A comparison of the velocity survey results (table 1) shows a significant velocity difference in the intervals between 100 and 300 m (330–980 ft) below sea level. The velocities below ground zero are lower. Second, refraction results from the reef line (fig. 6) suggest that velocities of refracting horizon 3 increase outward from the center of the crater. Third, the results of Raitt (1957) and Tremba and others (1982) in undisturbed sediments indicate that velocities below 100 m (330 ft) depth are 2.4 km/s (7,900 ft/s) and not the 2.0-km/s (6,600 ft/s) average determined from the ground-zero hole.

For the final set of computations in this iterative process, we estimated the average velocities for the material in layer 3 as 2.0 km/s (6,600 ft/s) in the center of the crater (consistent with the ground-zero velocity survey), increasing to 2.2 km/s (7,200 ft/s) between stations A4 and A5, and to 2.3 km/s (7,500 ft/s) beyond station A6, approximately

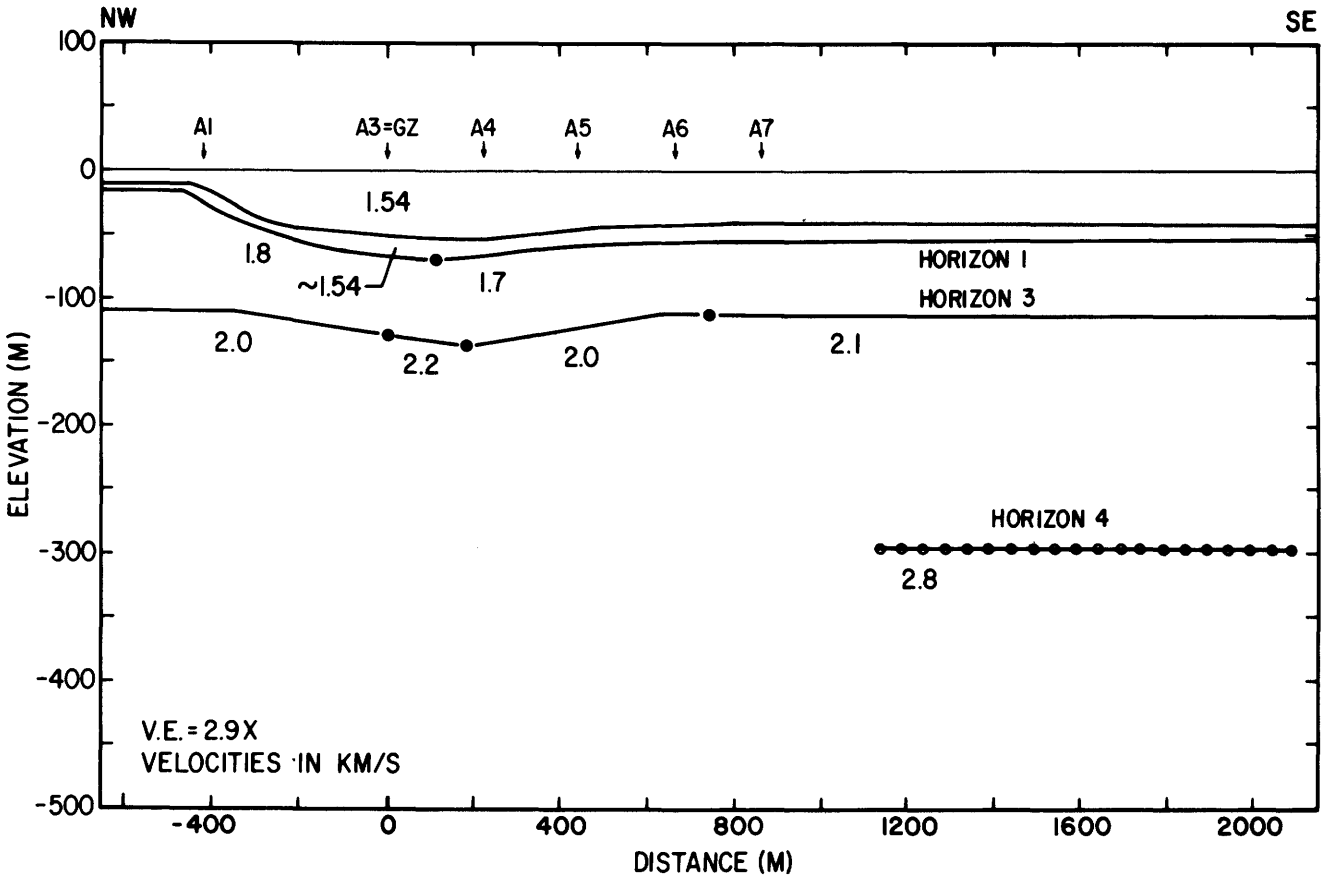

Figure 12. Profile of horizon 4 southeast of OAK crater. Profile was computed using the overlying velocity distribution obtained from figure 10 and the travel-time curves Y, Z, and A7 of figure 11. Solid circles indicate boundary between velocity values. Open circles are computed depth points connected by a best-fit line. GZ=ground zero.

Table 1. Interval velocities measured in boreholes at the OAK ground zero site and the reference site
[See fig. 19; SL, sea level; - - -, below depth of penetration]

Depth interval		Reference hole		OAK ground-zero hole		Difference	
m	ft	m/s	ft/s	m/s	ft/s	m/s	ft/s
SL–50	SL–164	1,543	5,062	1,543	5,062	0	0
50–100	164–328	1,634	5,360	1,634	5,360	0	0
100–150	328–492	2,058	6,751	1,650	5,413	408	1,338
150–200	492–656	2,513	8,244	2,016	6,614	497	1,630
200–250	656–820	2,294	7,526	2,165	7,103	129	423
250–300	820–984	2,778	9,114	1,961	6,433	817	2,680
300–350	984–1,148	---	---	2,538	8,326	---	---
350–400	1,148–1,312	---	---	2,632	8,635	---	---
400–450	1,312–1,476	---	---	2,273	7,457	---	---
450–500	1,476–1,640	---	---	2,674	8,772	---	---
500–550	1,640–1,804	---	---	2,513	8,244	---	---

650 m (2100 ft) from ground zero (fig. 15). We note that these are average velocities in a layer, which may exceed the ray velocity recorded from the upper surface. The sea-floor topography and the crater bowl have also been removed from figure 15 because of their negligible effect on vertical travel times.

Trial velocity values from horizon 4 were then successively iterated until a nearly horizontal profile satisfying the travel-time curves of figure 11 was obtained. This model (fig. 15) shows horizon 4 to be about 350 m (1,150 ft) deep, with a velocity of 2.4 km/s (7,900 ft/s) below ground zero that increases outward to 2.7 km/s (8,900 ft/s) 640 m (2,100

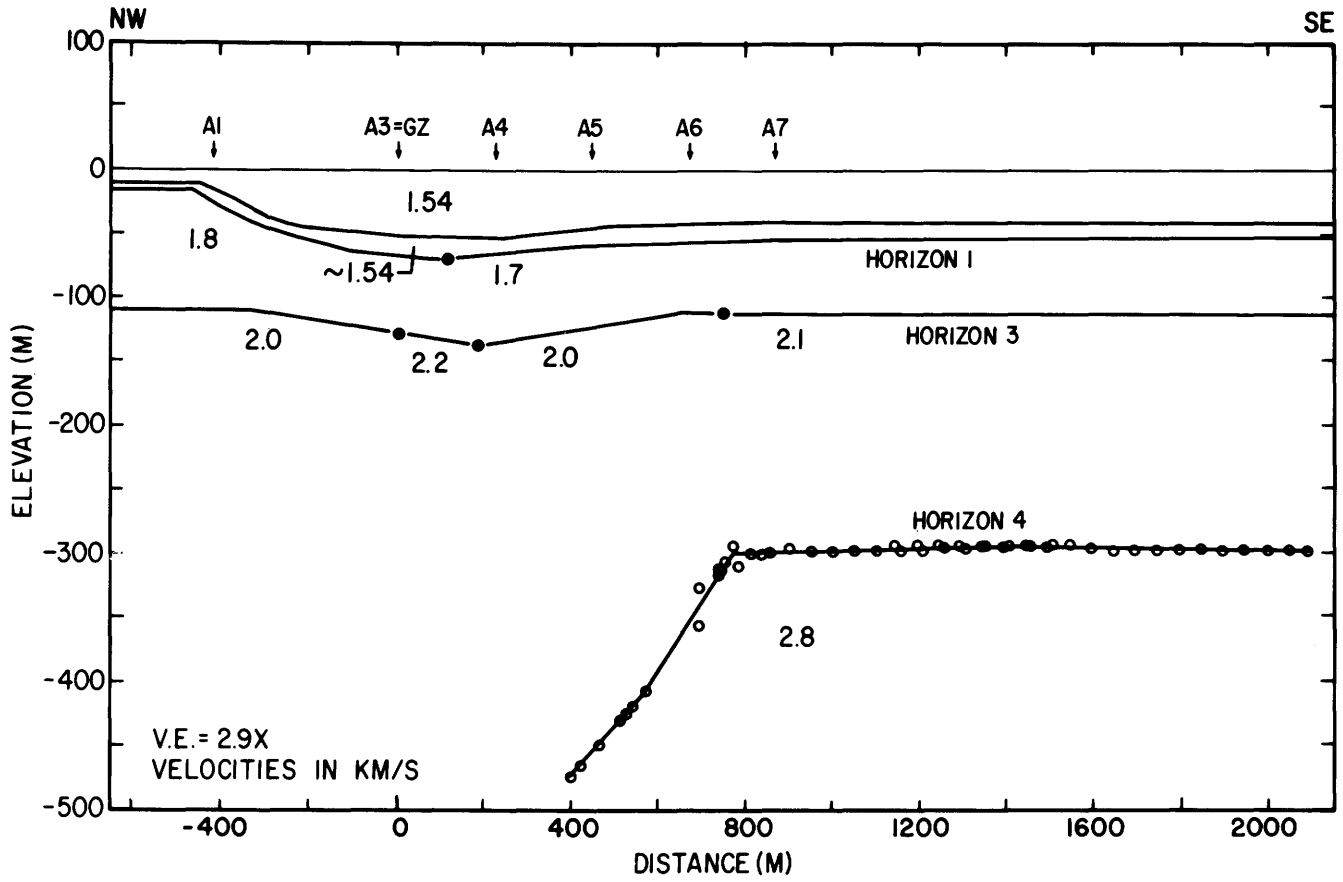

Figure 13. Profile of horizon 4 assuming its velocity to be 2.8 km/s. Profile was computed from the travel-time curves of figure 11 and the overlying velocity distribution obtained from figure 10. Solid circles indicate boundaries between velocity values. Open circles are computed depth points connected by a best-fit line. GZ=ground zero.

ft) from ground zero and 2.8 km/s (9,200 ft/s) beyond 900 m (2,950 ft) from ground zero.

This profile mis-ties the drilling results for horizon 4 at ground zero by 60 m (200 ft) of depth and 0.15 km/s (490 ft/s) of velocity. However, the computer analysis showed that by using a velocity of 2.5 km/s (8,200 ft/s) for horizon 4 below ground zero, a slightly greater downwarp towards the center of the crater is introduced, increasing the mis-tie there by an additional 30 m (100 ft). One way of raising the entire profile the required 60 m would be to decrease all velocities below horizon 3 by roughly 0.35 km/s (1,100 ft/s). However, this approach would severely compromise the well-velocity survey results. A more realistic approach is to force horizon 4 to dip downward toward the center of the lagoon by lowering the southeast end of the profile and raising the northwest end. We did this by modifying curves Y and Z in figure 11. A trial run produced the profile shown in figure 16, raising horizon 4 on the crater side by the desired amount and downwarping it toward the crater interior but with a velocity of only 2.4 km/s (7,900 ft/s).

The tie with drilling data at ground zero can undoubtedly be further improved by readjusting the average velocities of layer 3 and performing additional iterative computations on the data from horizon 4. However, we believe that further attempts at fine-tuning are unwarranted due to the limited data from the lagoon line. The data for greater depths are not reversed; there were only six working receiver stations, and coverage into the lagoon was insufficient to obtain an unambiguous precrater reference profile.

Refraction arrivals from horizon 5 were analyzed in the same manner as those for horizon 4. The travel-time curves are shown in figure 17. The overlying velocity distribution used is shown in figure 15, with the exception that a depth of 500 m (1,640 ft) below sea level was chosen as a cutoff beneath which lateral changes in velocity and thus differential fracturing were not permitted. A uniform velocity of 2.5 km/s (8,200 ft/s) was assumed for the velocity below a 500-m (1,640 ft) depth.

Analysis of the travel-time curves for horizon 5 resulted in a horizon at approximately a 700-m (2,300 ft) depth (fig. 18) with a corresponding ray velocity of a little over 2.9 km/s (9,500 ft/s), which does not appear to change laterally to the southeast of OAK ground zero.

The remainder of this section presents conclusions inferred from the analysis of horizons 4 and 5 of the lagoon line.

The rocks beneath ground zero, down to and including a hard layer (horizon 4) at approximately a 300-m (1,000

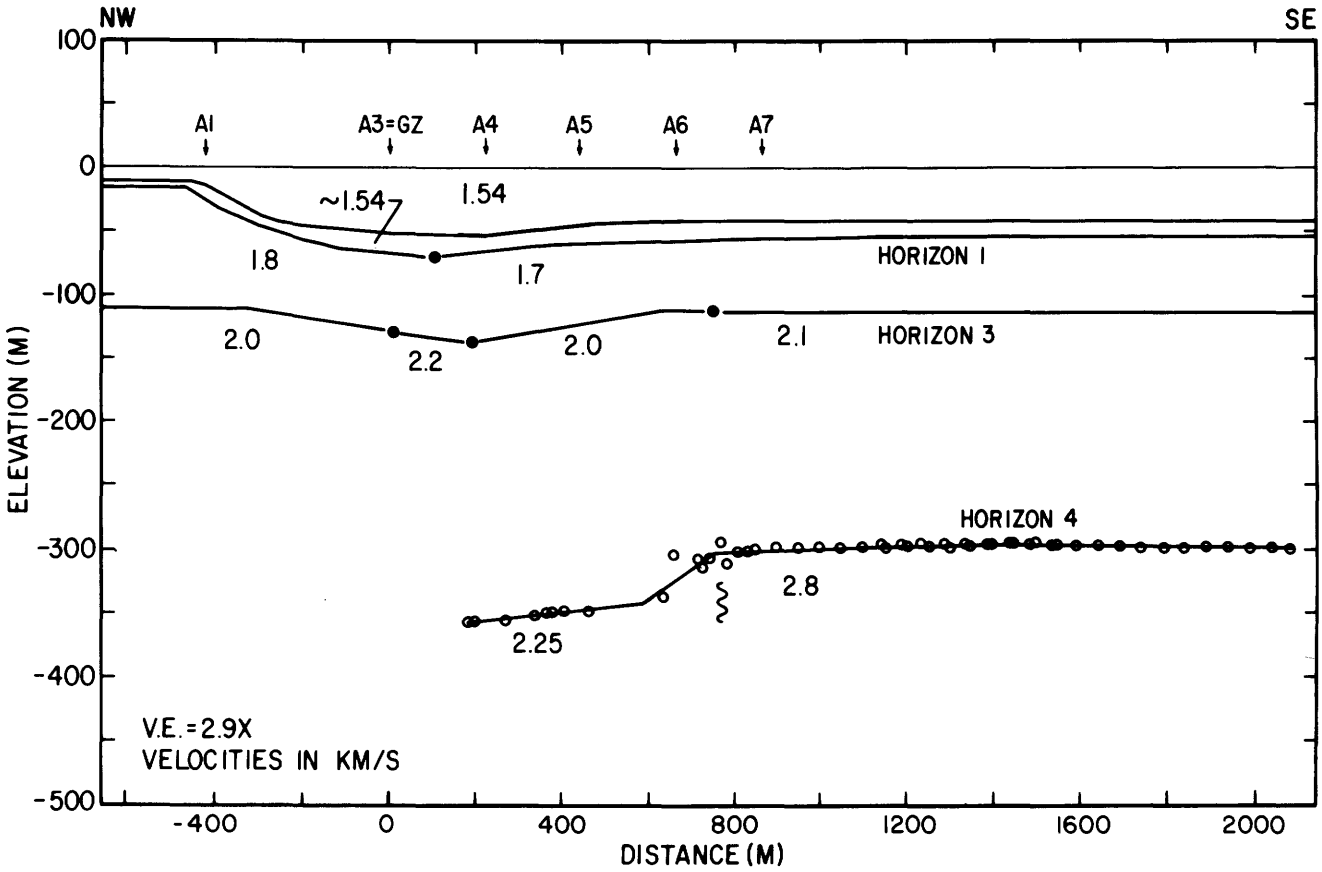

Figure 14. Profile of horizon 4 assuming that its velocity changes abruptly from 2.8 to 2.25 km/s (9,200–7,400 ft/s) 800 m (2,625 ft) from ground zero (GZ). Profile was computed from the travel-time curves of figure 11 and the overlying velocity distribution obtained from figure 10. Solid circles indicate boundaries between velocity values. Open circles are computed depth points connected by a best-fit line.

ft) depth, have a lower velocity than those in the surrounding undisturbed area and hence are fractured.

Velocities and, thus, fractures taper radially from the crater center. Between ground zero and 650 m (2,100 ft) radially to the southeast, the average velocity of the 200-m-thick (660-ft-thick) layer 3 increases from 2.0 km/s (6,600 ft/s) to about 2.3 km/s (7,500 ft/s), thus approaching the value of 2.4 km/s (7,900 ft/s) assumed for undisturbed rock. However, the critically refracted ray velocity for horizon 3 (fig. 10) tends to be less than that of the average layer velocity, suggesting that fractures near the surface of this layer extend further from ground zero than they do at depth. For example, on the reef line, critically refracted ray velocities do not reach 2.3 km/s (7,500 ft/s) until roughly 1,400 m (4,600 ft) from ground zero.

The velocity of layer 4, approximately 300 m (1,000 ft) deep, also increases radially from 2.4 to 2.5 km/s (7,900–8,200 ft/s) at ground zero to 2.7 km/s (8,900 ft/s) between 640 m (2,100 ft) and 800 m (2,600 ft) from ground zero. Assuming a value of 2.8 km/s (9,200 ft/s) for undisturbed rocks in layer 4 suggests that fracturing in this layer may extend further from ground zero than in the overlying softer materials.

The depth of fracturing in layer 4 cannot be determined. Layer 5 with a 2.9-km/s (9,500 ft/s) velocity at approximately a 700-m (2,300 ft) depth does not appear to be fractured, and the crater delay times for this horizon can essentially be accounted for by velocity decreases above the level of horizon 4. Our interpretations suggest a maximum depth of 500 m (1,600 ft) beneath which no fracturing occurs. It is likely that layer 4 is a thin bed less than 100 m (330 ft) thick, which acted as a wave guide or channel for seismic energy, explaining why fractures in this layer may radiate further from ground zero than in the overlying layer.

Finally, figures 15 and 16 suggest a possible 10- to 20-m (30–60 ft) downwarp of horizon 4 toward the center of the crater. However, the analysis of the fine structural details of this layer may have been carried out beyond the limits of data accuracy.

A GENERALIZED CRATER MODEL

Figure 19 depicts our final generalized crater model. The shallow features are inferred from the analysis of the reef line and the deep ones from the lagoon line. Therefore,

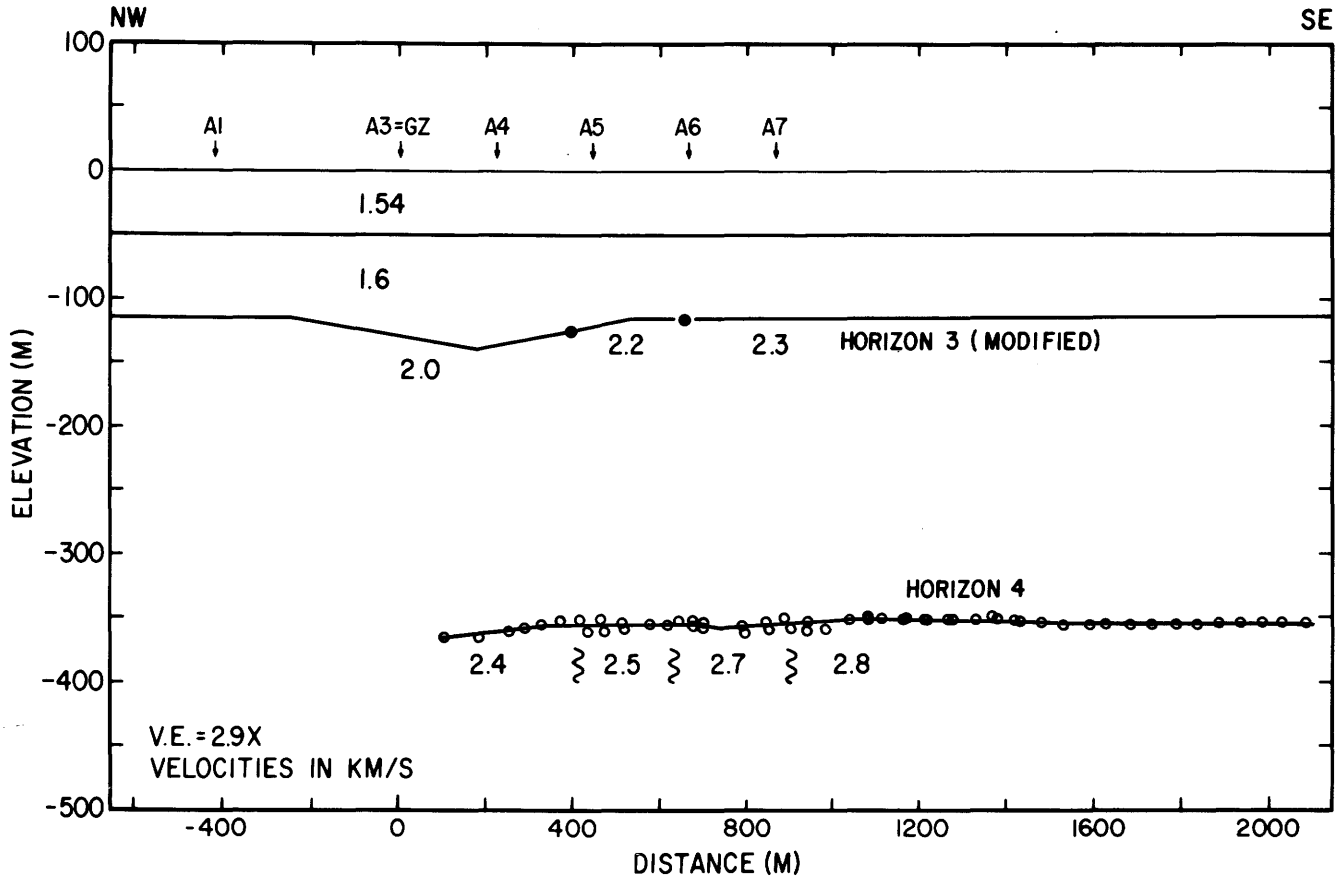

Figure 15. Profile of horizon 4 assuming that its velocity changes gradually from 2.8 km/s (9,200 ft/s) 850 m from ground zero (GZ) to 2.4 km/s (7,900 ft/s) at ground zero. Profile was computed from the travel-time curves of figure 11 and with the additional constraint that the velocity of the overlying material grades from 2.0 km/s (6,600 ft/s) at ground zero to 2.3 km/s (7,500 ft/s) 700 m from ground zero. Solid circles indicate boundaries between velocity values. Open circles are computed depth points connected by a best-fit line.

the problem of possible crater asymmetry, due to the high-density rocks composing the reef, has not been addressed.

Figure 19 shows four zones, A through D, outlined with heavy lines. Each zone includes an area, or volume in three dimensions, in which velocities are less than those of the surrounding country rock. The velocity reduction is due to fracturing produced by the OAK event. Individual zones are labeled with a range of velocities rather than a single value because velocities increase with distance from ground zero. In zone C, for example, the velocity below ground zero is 2.0 km/s (6,600 ft/s); nearer the crater margin where fractures diminish, it increases to 2.2 km/s (7,200 ft/s).

Zone A probably represents the infill of the transient crater which was excavated below the level of preevent horizon 3. It could not be distinguished by the refraction travel-time data from the surrounding ruptured and fractured coral (zone B) because of the small velocity differential (1.6–1.7 km/s vs. 1.7–1.8 km/s, or 5,200–5,600 vs. 5,600–5,900 ft/s) between them. Hence the boundaries of zone A (120-m, or 390-ft, depth; and 600-m, or 2,000-ft, maximum radius) had to be obtained from seismic reflection data (chap. C and D, this volume).

The base of zone B, defined by the reef-line data, surrounds the transient crater. It is characterized by a wedge (in cross section) shown by x's in figure 19; the wedge is adjacent to and surrounds the crater floor. This wedge represents highly fractured rock because the velocity in it has been lowered by about 33 percent, from 2.3 to 2.4 km/s (7,600–7,900 ft/s) preevent to 1.7 to 1.8 km/s (5,600–5,900 ft/s) postevent. Rocks in zone B that are shallower than those in preevent horizon 3 have undergone little change in velocity (from 1.8–1.9 km/s to 1.7–1.8 km/s, or 5,900–6,200 to 5,600–5,900 ft/s). This similarity does not mean

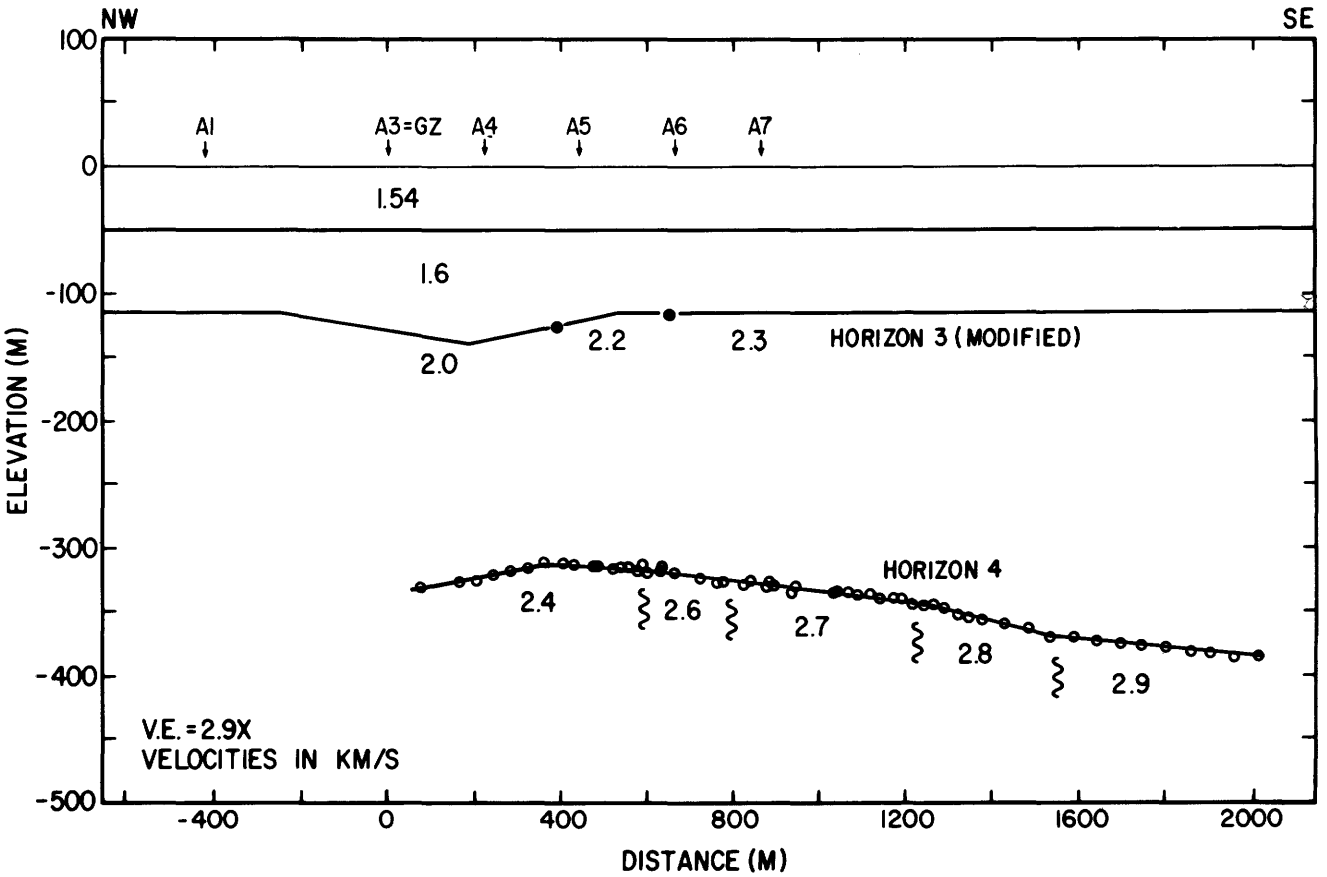

Figure 16. Profile of horizon 4 modified from that of figure 15 by introducing a southeast dip toward the lagoon. Solid circles indicate boundaries between velocity values. Open circles are computed depth points connected by best-fit line. GZ=ground zero.

that the rocks above preevent horizon 3 have not been altered but rather that their initial porosity was not significantly changed by fracturing. For example, the velocity of crater debris, completely rearranged from its initial state, is only slightly less than the velocity of the undisturbed materials at depths of less than 70 m (230 ft). Zone B has been extrapolated above horizon 3 to intersect the sea floor, suggesting that near-surface fractures may extend radially out about 1,400 m (4,600 ft) from ground zero.

Zones C and D were defined from the lagoon-line data with additional control from the velocity surveys in the ground zero and reference holes and the results of the refraction surveys of Raitt (1957), Ristvet and others (1978), and Tremba and others (1982). In zone C, which extends from below zone B to a depth of about 300 m (1,000 ft), the velocities of the country rock have been lowered from 2.3 to 2.4 km/s (7,500–7,900 ft/s) to 2.0 to 2.2 km/s (6,600–7,200 ft/s). It is floored by a high-velocity bed of unknown thickness represented by horizon 4, which had a preevent velocity of approximately 2.7 to 2.8 km/s (8,900–9,200 ft/s) that has been reduced to values of 2.4 to 2.6 km/s (7,900–8,500 ft/s) below the crater floor. These reduced velocities are shown in figure 19 as zone D. Reduced velocities in zone D extend radially 640 to 800 m (2,100–2,600 ft/s) from ground zero. The reference boring, 1,325 m (4,347 ft) from ground zero, also penetrated assumed event-induced fractures at approximately a depth of 300 m (984 ft) (A. Schenker, oral commun., May 1985).

Refraction travel-time delays from horizon 5, approximately 700 m (2,300 ft) deep, may be attributed entirely to lowered velocities in zones A through D, suggesting that fracturing extends at most 100 to 150 m (330–500 ft) beneath horizon 4 or to a maximum depth of about 425 m (1,400 ft). The denser rocks of layer 4 may have acted as a barrier to fracturing at greater depths.

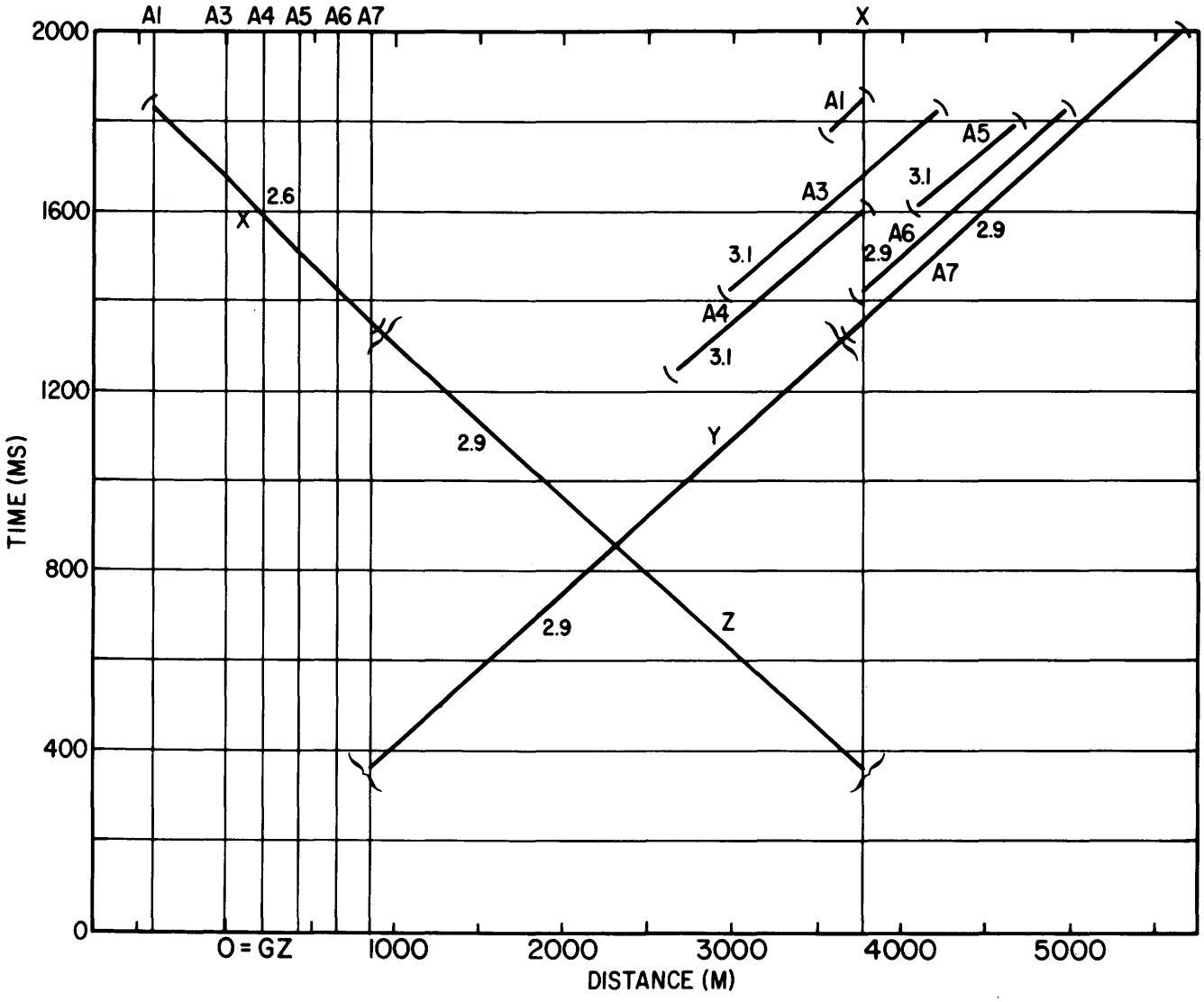

Figure 17. Travel-time curves for horizon 5. The line segments labeled A1 through A7 represent the data for receiver stations A1 through A7 (fig. 1), and the segment labeled X represents the arrival times recorded at the receiver stations with the source situated at point X on the distance axis. Curves Y and Z are extrapolations of curves A7 and X, respectively. Apparent velocities are in kilometers/second. Curves between parentheses are measured data; curves between brackets are extrapolated data.

Figure 18 (top right). Profile of horizon 5 computed from the travel-time curve of figure 17, using a velocity of 2.9 km/s (9,500 ft/s). The assumed overlying velocity distribution is that of figure 15, except for the velocity reversal at 500-m (1,640 ft) depth. Solid circles indicate boundaries between velocity values. Open circles are computed depth points connected by a best-fit line. GZ=ground zero.

Figure 19 (bottom right). Final interpreted model of OAK crater showing four zones (labeled A through D) in which velocities have been altered by the OAK event. Small x's indicate zone of highly fractured rock. Reference is the position of drill hole OAR–2 (See fig. 21, chap. D, this volume.) GZ=ground zero.

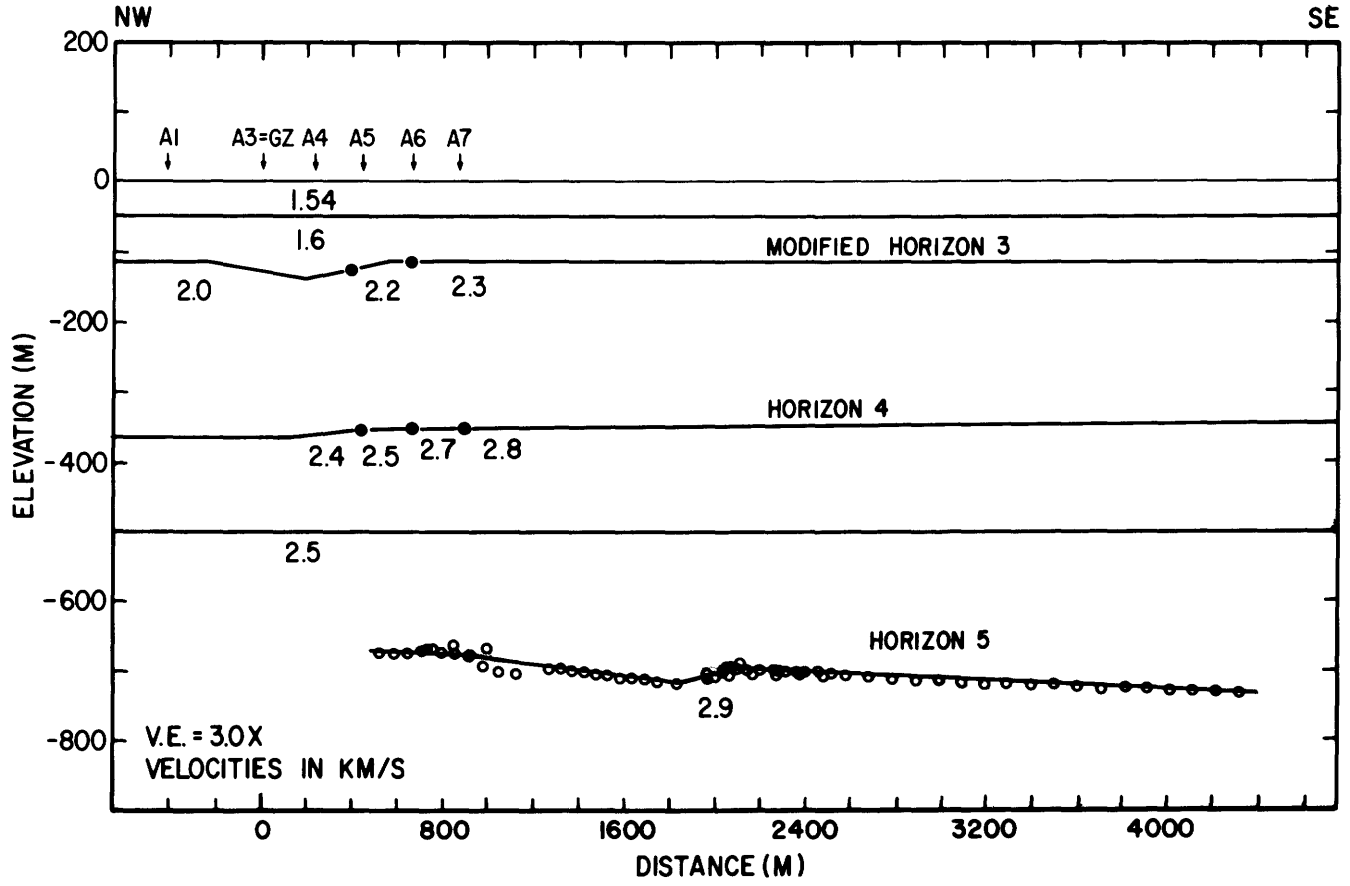
NW
SE
200
0
-200
-400
-600
-800
ELEVATION (M)
A1
A3=GZ
A4
A5
A6
A7
1.54
1.6
MODIFIED HORIZON 3
2.0
2.2
2.3
HORIZON 4
2.4
2.5
2.7
2.8
2.5
HORIZON 5
2.9
V.E. = 3.0X
VELOCITIES IN KM/S
0
800
1600
2400
3200
4000
DISTANCE (M)

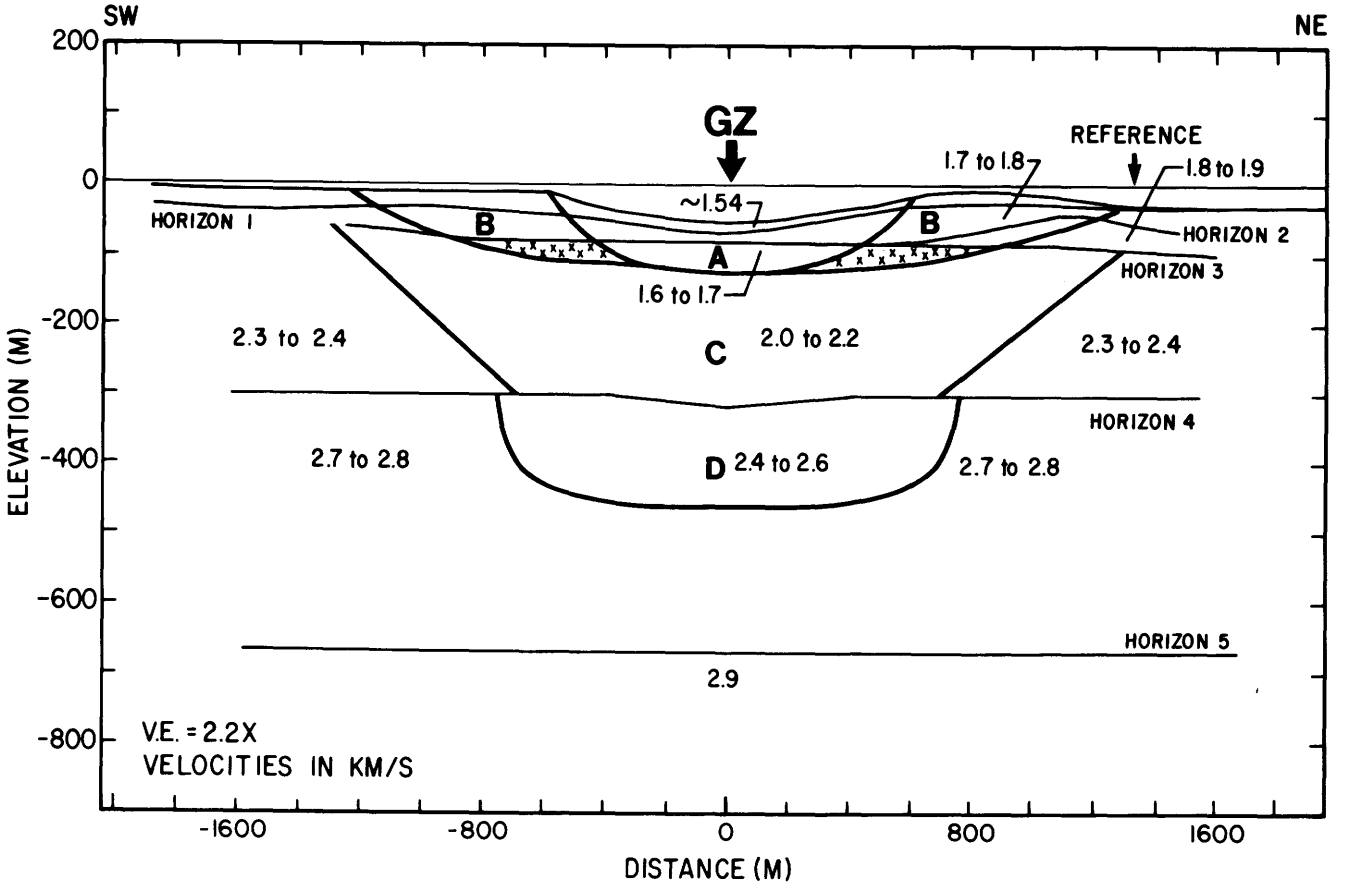
SW
NE
200
0
-200
-400
-600
-800
ELEVATION (M)
GZ
REFERENCE
1.7 to 1.8
1.8 to 1.9
~1.54
HORIZON 1
B
B
A
HORIZON 2
HORIZON 3
1.6 to 1.7
2.3 to 2.4
C
2.0 to 2.2
2.3 to 2.4
HORIZON 4
2.7 to 2.8
D 2.4 to 2.6
2.7 to 2.8
HORIZON 5
2.9
V.E. = 2.2X
VELOCITIES IN KM/S
-1600
-800
0
800
1600
DISTANCE (M)

REFERENCES

Ackermann, H. D., Panbratz, L. W., and Dansereau, D. A., 1982, A comprehensive system for interpreting seismic-refraction arrival-time data using interactive computer methods: U.S. Geological Survey Open-File Report 82-1065, 265 p.

Henny, R. W., Mercer, J. W., and Zbur, R. T., 1974, Near surface geologic investigations at Eniwetok Atoll: Proceedings of the Second International Coral Reef Symposium 2, Great Barrier Reef Committee, Brisbane, p. 615–626.

Ladd, H. S., Ingerson, E., Townsend, R. C., Russell, M., and Stephenson, H. K., 1953, Drilling on Enewetak Atoll, Marshall Islands: American Association of Petroleum Geologists, v. 37, p. 2257–2280.

Ladd, H. S., and Schlanger, S. O., 1960, Drilling operations on Enewetak Atoll: U. S. Geological Survey Professional Paper 260–Y, p. 863–903.

Raitt, R. W., 1957, Seismic refraction studies on Eniwetok Atoll: U.S. Geological Survey Professional Paper 260–S, p. 685–698.

Ristvet, B. L., Tremba, E. L., Couch, R. F., Fetzer, J. A., Goter, E. R., Walter, D. R., Wendland, V. P., 1978, Geologic and geophysical investigations of the Enewetak nuclear craters: Air Force Weapons Laboratory Technical Report TR–77–242, Kirtland Air Force Base, New Mexico 87117, 263 p.

Tremba, E. L., Couch, R. F., Ristvet, B.L., 1982, Enewetak Atoll Seismic Investigation (EASI): Phases I and II (final report): Air Force Weapons Laboratory Technical Report TR–82–20, Kirtland Air Force Base, New Mexico 87117, 124 p.

Chapter F

Observations of OAK and KOA Craters from the Submersible

By R. B. HALLEY, R. A. SLATER, E. A. SHINN, D. W. FOLGER, J. H. HUDSON, J. L. KINDINGER, and D. J. RODDY

U.S. GEOLOGICAL SURVEY BULLETIN 1678

SEA-FLOOR OBSERVATIONS AND SUBBOTTOM SEISMIC CHARACTERISTICS OF OAK AND KOA CRATERS, ENEWETAK ATOLL, MARSHALL ISLANDS

CONTENTS

FIGURES

Chapter F
Observations of OAK and KOA Craters from the Submersible

By R. B. Halley[1], R. A. Slater[2], E. A. Shinn[3], D. W. Folger[4], J. H. Hudson[3], and J. L. Kindinger[4], *and* D. J. Roddy[5]

INTRODUCTION

Purpose

The purpose of this part of the study was to observe and document characteristics of the crater bottom, to collect rock samples, and to make detailed observations of such important features as scarps, slumps, and debris. We used a research submersible, which was essential for conducting comprehensive reconnaissance surveys at all depths and especially in waters more than 30 m (100 ft) deep where scuba dive time was limited and where sharks were common.

Setting

Most submersible dives were conducted within Enewetak lagoon in the crater areas of OAK, KOA, and MIKE in waters between 5 and 60 m (16–197 ft) deep (figs. 1–3). Current speeds were less than 50 cm/s (1.0 kn), and waves were less than 1 m (3.3 ft) high, except during rare local squalls. Visibility varied from less than 1 m (3.3 ft) to more than 30 m (100 ft) but was commonly about 5–10 m (16–33 ft). Water temperature was 28±1 °C. On several dives, we examined control areas as far as 2 km (1.1 nmi) into the lagoon from the craters.

In 1984, we made 2 dives outside the atoll in a rockfall area off MIKE crater to a maximum depth of 198 m (650 ft) and, in 1985, 13 dives to a maximum depth of 359 m (1,180 ft). There, gentle swells did not interfere with diving, but abundant sharks precluded supporting scuba observations.

Previous Work

During July and September 1981, eight dives were made with the submersible *Makalii* as part of Project EASI (Enewetak Atoll Seismic Investigation) (Tremba and others, 1982). Six dives took place in OAK crater, one in KOA crater, and one outside the cratered areas. The observations made during these dives are incorporated into the following discussion of our results.

METHODS

During July and August of 1984, we conducted 144 dives aboard the research submersible *Delta*, which was operated by MARFAB, Torrence, Calif. (figs. 1, 2; appendix). The two-person submersible dove on 29 consecutive days, averaging 5 dives per day, with a maximum of 10 dives in 1 day. *Egabrag II*, support vessel for both submersible and scuba operations, monitored the submersible's location and depth continually during all reconnaissance, sampling, and demonstration dives, except when *Halimeda* or a whaler was used in shallow water or when equipment aboard *Egabrag II* malfunctioned.

The submersible was tracked from *Egabrag II* with a Honeywell Hydrostar Navigation System that was interfaced with the Motorola FALCON IV Miniranger System used to position *Egabrag II*. Inaccuracies in positioning the submersible developed in three situations: (1) when *Egabrag* was directly above the submersible; (2) when the submersible was rapidly ascending or descending; and (3) when the submersible was more than four times its depth away from *Egabrag*. The first situation occurred rarely; the second situation occurred when the submersible was crossing steep slopes inside the craters and patch reefs outside of OAK crater; the third situation was initially a problem in shallow water but subsequently was corrected by placing the Miniranger System aboard *Halimeda* or a whaler and tracking a float attached to the submersible. Some of the submersible locations may be inaccurately plotted in shallow water or in areas where slopes were steep.

During reconnaissance dives, video recordings were made of all sea-floor features along each track, and separate sound recordings were made of observers' comments. A 1.3-cm (0.5 in.) VHS video system was used for recording all observations and the observer's narrative from within the submersible. The recorder was powered by a 12-volt motorcycle battery in the submersible to allow as much as 2 hours

[1]U.S. Geological Survey, Branch of Oil and Gas Resources Denver, Colo. 80225.

[2]U.S. Geological Survey, Consultant, Oxnard, Calif. 93030.

[3]U.S. Geological Survey, Branch of Oil and Gas Resources, Fisher Island Station, Miami, Fla. 33139.

[4]U.S. Geological Survey, Branch of Atlantic Marine Geology, Woods Hole, Mass. 02543.

[5]U.S. Geological Survey, Branch of Astrogeophysical Studies, Flagstaff, Ariz. 86001.

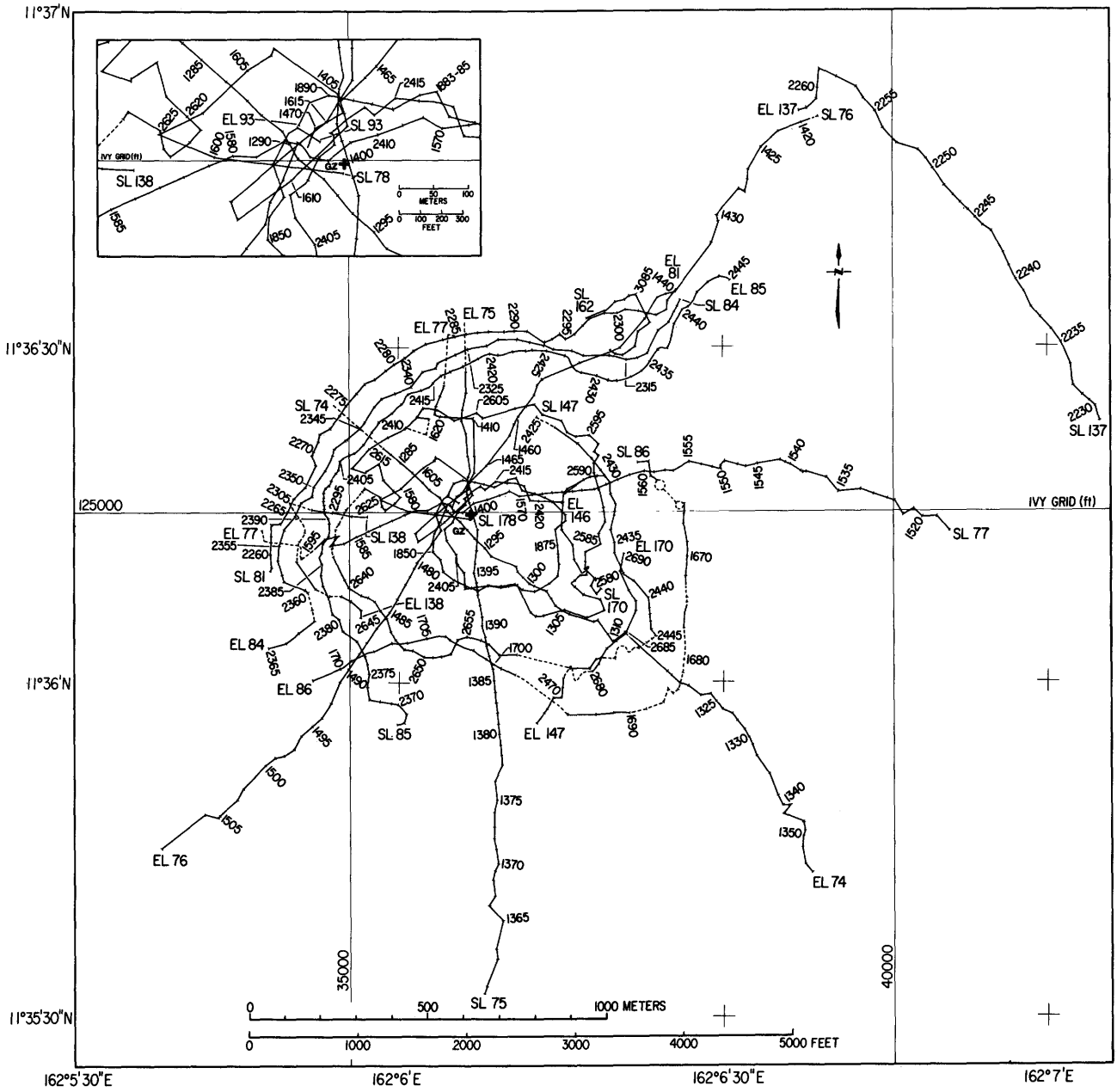

Figure 1. Location of 1984 submersible dive tracks in OAK crater. SL 75=start line 75; EL 76=end line 76. Navigational fixes shown by tics on dive tracks, annotated with fix number at 5-fix or greater intervals. Tracks dashed where location uncertain. GZ=ground zero.

of continuous recording on a TS 120 video tape. The camera displayed date, title, and elapsed time in the field of view throughout a dive. During dives, the elapsed time on the screen was repeated verbally, so that it would be recorded on the audio track along with verbal descriptions of the bottom, Greenwich time, depth, and navigation fix numbers. A second recording (audio only) of the observers' comments was also made during most dives. The 43 observation dives averaged 1 hour and 20 minutes in duration; some were as long as 2 hours and 30 minutes, and others as short as 20 minutes. The dives included six transects through ground zero and along several contours in each crater; the observations on these dives served as a framework for subsequent dives to investigate specific features.

During rock sampling dives, we attached a nylon mesh bag to the starboard side of the submersible's hull. The observer manipulated the submersible's mechanical arm and claw to pick up rock samples and deposit them in the sample bag. Up to 22 kg (48 lbs) of samples were collected at 59 sites (chap. G, fig. 1, table 1, this volume). Usually one dive was devoted to each site.

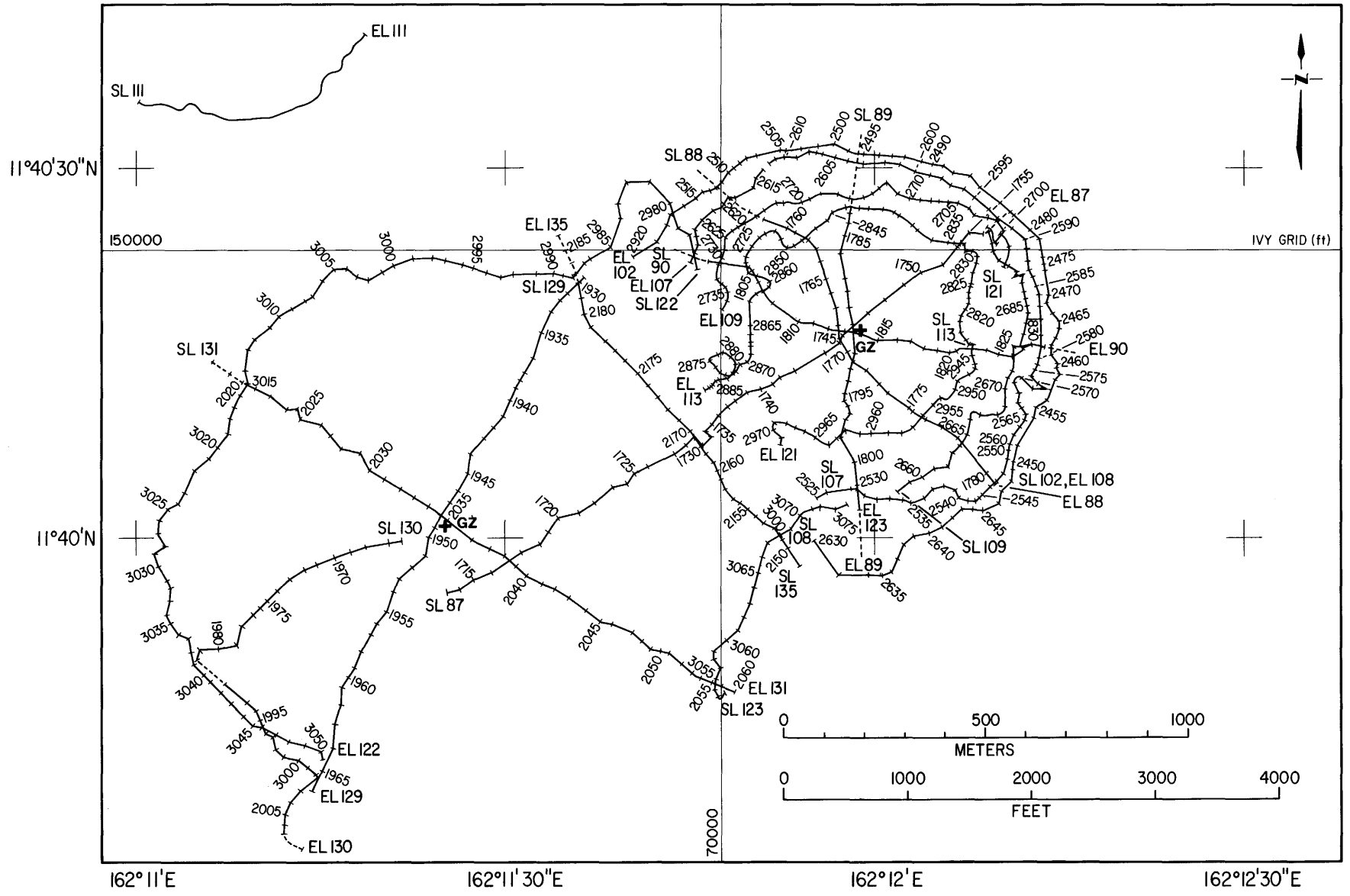

Figure 2. Location of 1984 submersible dive tracks in KOA and MIKE craters. SL 87=start line 87; EL 87=end line 87. Navigational fixes shown by tics on dive tracks, annotated with fix number at 5-fix or greater intervals. Tracks dashed where location uncertain. GZ=ground zero.

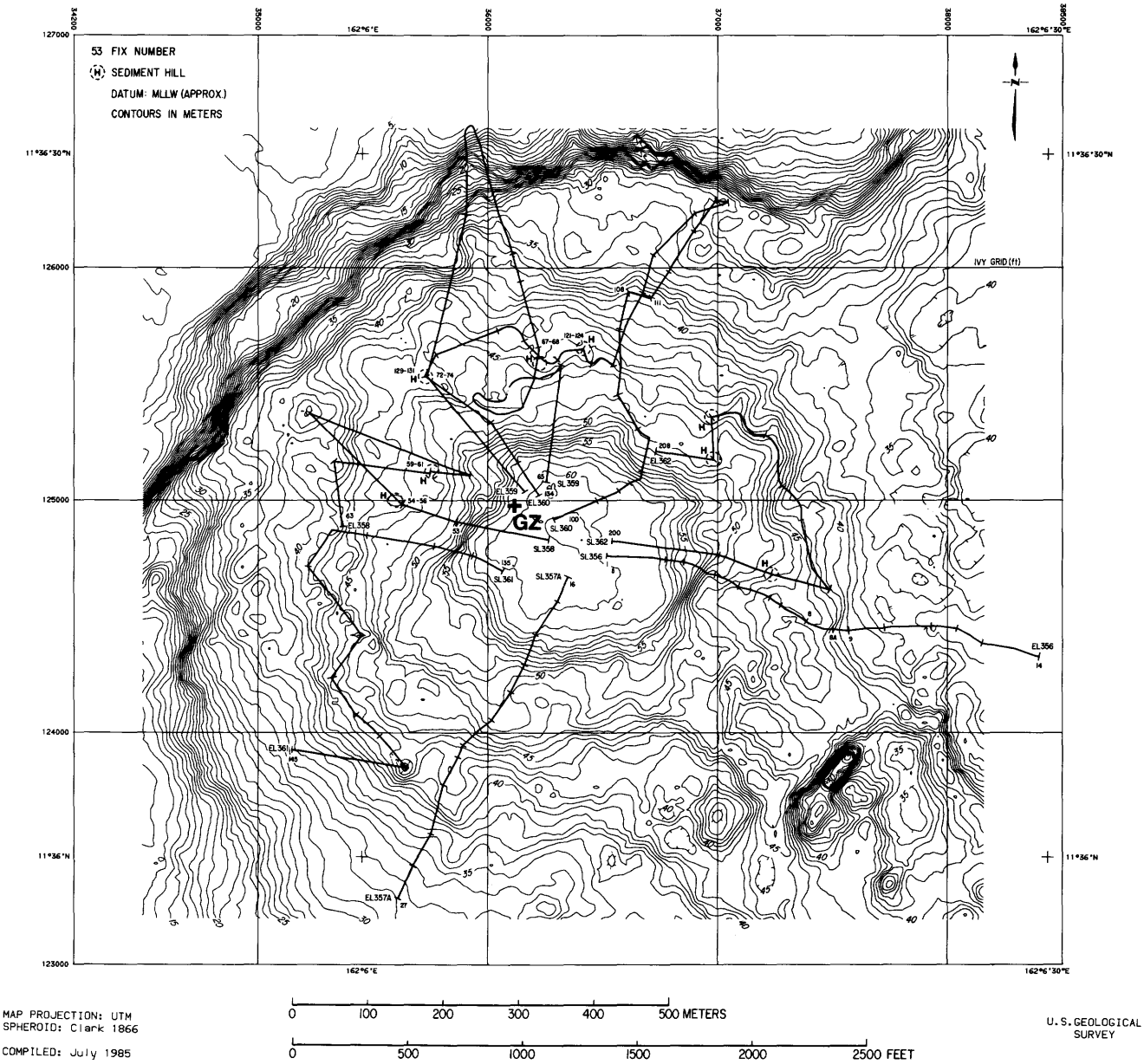

Figure 3. Location of 1985 submersible dives in OAK crater. Shown are positions of sediment hills (H) in the crater terrace area. (See fig. 4*A*.) SL 356=start line 356; EL 356=end line 356. Navigational fixes shown by tics on dive tracks, annotated with fix number at 5-fix or greater intervals. GZ=ground zero.

Forty-five field demonstration dives, averaging about 30 minutes each, were conducted for visiting project scientists and administrators, other project personnel, and for visiting officials from the Marshall Islands.

In 1985, 57 dives were conducted. Of these, 29 were in OAK, 13 in KOA, 13 outside the atoll off MIKE crater, and 2 near Medren Island. Most dives were made so that members of the Defense Nuclear Agency could observe and study important characteristics of each crater. No navigation was available except for seven dives in OAK that were specifically designed to document and sample critical features observed the previous year.

During those seven dives, the submersible towed a float that was tracked by a whaler equipped with the Falcon IV Miniranger System. Because the submersible traversed the crater slope over considerable depth changes, inaccuracies in this method of positioning were inevitable. These errors were later corrected by comparing submersible observations with features on a 1:1,500-scale bathymetric map contoured at a 0.5-m (1.5 ft) interval. The corrected tracks are shown in figure 3.

RESULTS

Observations from the submersible have been grouped into areas with similar bottom sediment and physiographic characteristics. Some of these areas correlate with the provinces defined on the basis of bathymetry in chapter A of this volume, for example, the crater floor, inner slope, and terrace in OAK crater. Other areas show less correlation. It should be emphasized that the boundaries of these areas are estimated from the submersible. The swath of visibility generally averaged about 20 m (67 ft) wide along the track of the submersible and area boundaries, particularly lagoonward of ground zero, and the boundaries should be taken as approximate.

OAK Crater

OAK crater lies on the leeward side of Enewetak Atoll, 12 km (6.5 nmi) from MIKE crater, the nearest other blast site. Apparently, little sediment has washed from the adjacent reef flat into the crater during the 27 years since it was formed (Tremba and others, 1982). Aerial photographs clearly show ejecta rays tens of meters wide and hundreds of meters long on the adjacent reef flat until the 1970's, but these have now mostly eroded away. We have superimposed the map of bottom characteristics and the 5-m bathymetric contours on an aerial photograph of the crater to show their relations to the reef plate (fig. 4*B*).

In OAK crater, the provinces defined from the submersible are: (1) crater floor, (2) inner slope, (3) terrace, (4) fluted slope, (5) benches, (6) talus slope, (7) hummocky sea floor, and (8) reef plate (fig. 4*A*,*B*). The dive results are discussed by province.

Crater Floor

Within the 59-m (194 ft) isobath (fig. 4*A*), the deepest part of OAK crater, the flat floor is covered by very fine-grained sediment (figs. 5, 6*A*). Although the sediment contains a mix of sand (2 mm–62 μm), silt (62 mm–4 μm), and clay (less than 4 μm), a predominance of silt and clay causes the sediment to be cohesive; therefore a clump of this material picked up with the claw of the submersible stays intact.

The crater floor is gently undulating. Its surface is smooth or is pockmarked with 2- to 5-cm-diameter (0.8- to 2-in.-diameter) funnel-shaped holes constructed by burrowing organisms, perhaps crabs, anemones, or worms (figs. 6*D*,*E*). Shrimp mounds, volcano-shaped piles of sediment, generally 15 to 20 cm (6–8 in.) high, are widely scattered throughout this area (figs. 6*A*–*C*). About three mounds are present in every square meter of the crater floor.

The sediment surface of the crater floor is widely covered by a thin brown microbial mat, presumably constructed of algae and bacteria. It is disrupted by the slightest disturbance. Along the outer edge of the crater floor and in depths greater than 50 m (164 ft) are hundreds of echinoids (sea urchins) (fig. 6*F*). The echinoid groups appear to be grazing on the brown microbial mat, which was removed to reveal white sediment where they had grazed. Individual echinoids are about 5 cm (2 in.) in length and are covered by fragile spines. Groups contain as many as 50 individuals per square meter (11 ft^2) and may cover tens of square meters of the sea floor. Scattered among and apparently moving with the echinoid groups are helmet shells (gastropods) averaging 10 to 30 cm (8–12 in.) in diameter. They evidently are feeding on the echinoids.

The flat crater floor represents the present level of infilling of the central crater area. The primary mechanism of infilling today appears to be deposition of fine-grained sediment that is transported in suspension to this deep and restricted portion of the crater, supplemented perhaps by sediment moving down the common gully thalwegs (chap. A, fig. 9, this volume). These crater floor sediments are the most fine-grained, most porous, and least dense of any encountered in the crater.

Movement of sediment as a traction load may also account for transport of some sediment to the crater floor. During June 1985, currents of about 50 cm/s (1 kn) were observed moving sediment along the bottom. Such currents appear to be short-lived, possibly associated with extreme tidal ranges, and none lasted more than a few hours.

Inner Slope

The base of the inner slope lies 100 m (330 ft) from the geometric center of the crater at about the 59-m (194 ft) isobath (fig. 4*A*). Although this slope averages only about 6–8°, it is locally as steep as 17°. The slope area is 75 to 100 m (246–328 ft) wide along the radius of the crater and extends 200 to 260 m (650–853 ft) beyond the geometric center of the crater. The top of the inner slope falls between the 54- and 49-m (177 and 161 ft) contours.

The microbial mat-echinoid-helmet community seems to be restricted to the low energy and poor circulation area of the lower inner slope and the crater floor (figs. 7*A*–*C*). Groups of grazing echinoids were not seen above about 53 m (175 ft) on the crater wall.

The surface sediments change slightly from the base of the inner slope, where they are extremely muddy and similar to the sediment on the crater floor, to the upper edge, where they contain more silt and sand (fig. 7*D*). The cohesiveness of the sediment reflects this textural change. No material coarser than sand was observed on the inner slope.

The inner slope forms an inner bowl, within the central crater area, that is partially filled with sediment to produce the flat floor of the crater. Probably because the inner slope has been modified by physical and biological sediment movement, no fault scarps are evident. Single-channel high-resolution seismic data do not show any coherent reflectors that extend as close to ground zero as this area (see chap. C,

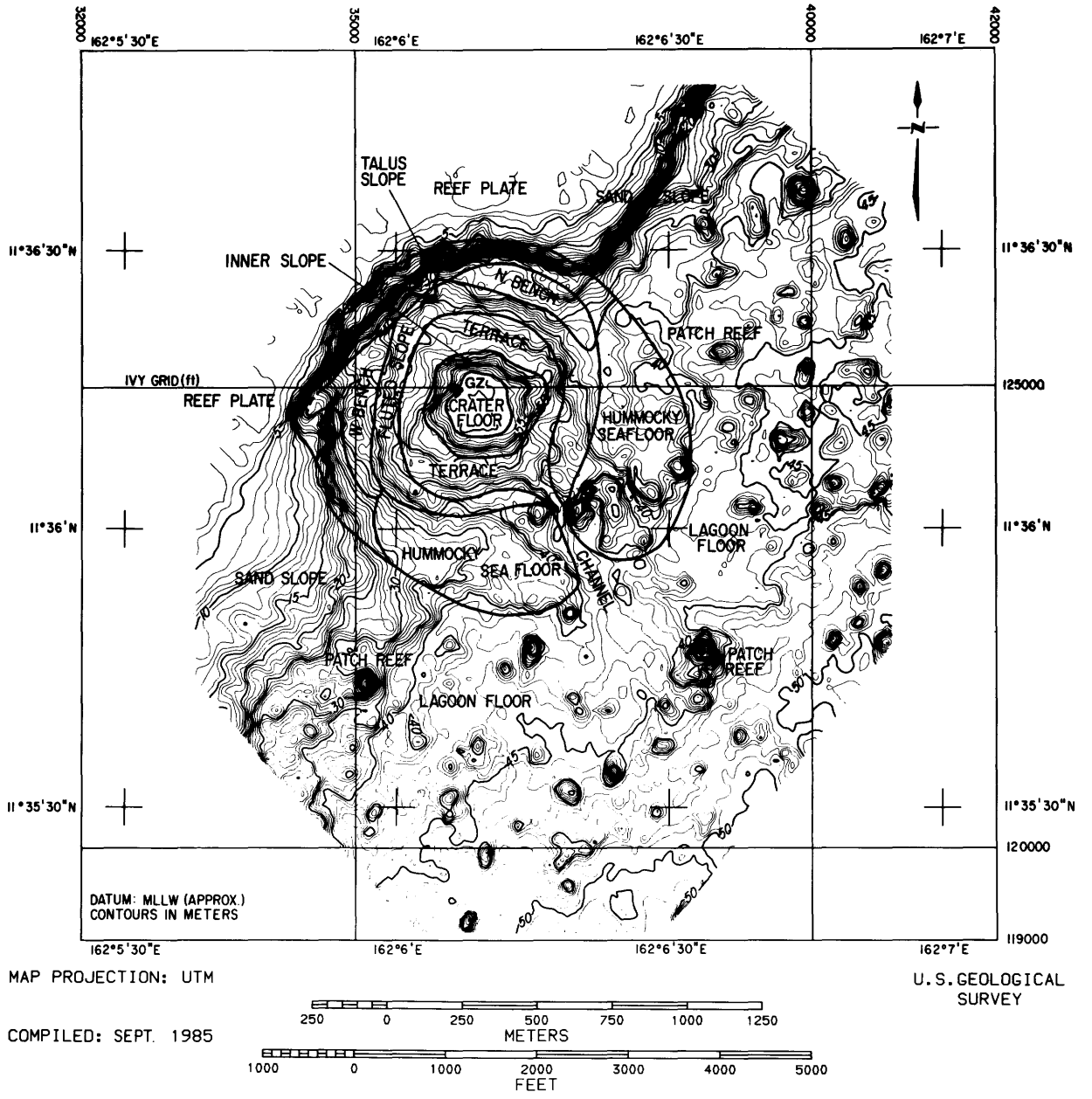

Figure 4A. Areas with similar bottom sediment and physiographic characteristics in OAK crater superimposed on 1-m bathymetry.

this volume); however, they do show complex downfaulting that may, at least in part, be responsible for the terrace and slope.

Terrace

From the top of the inner slope to a distance of 310 to 427 m (1,017–1,400 ft) from the geometric center of the crater is the terrace area, rising gently (2–3°) to the outer slope of the crater wall (fig. 4*A*). The terrace ranges from 100 to 200 m (330–660 ft) wide and is widest on the reef and lagoon sides of the crater.

The sediment on the terrace varies in character, depending on depth, proximity to the reef, and local topography. In most places, sediments are more sandy and burrowed than are sediments that cover the inner slope or crater floor. The most characteristic features in this depth zone are large shrimp burrows and mounds, up to 0.3 m (1 ft) high and 1 m (3 ft) in diameter, often so close together that they overlap. The mounds are most common at the outer edge of the terrace and decrease in frequency toward the inner slope. In addition, the benthic flora and fauna are more diverse here than those deeper in the crater. Common features on the

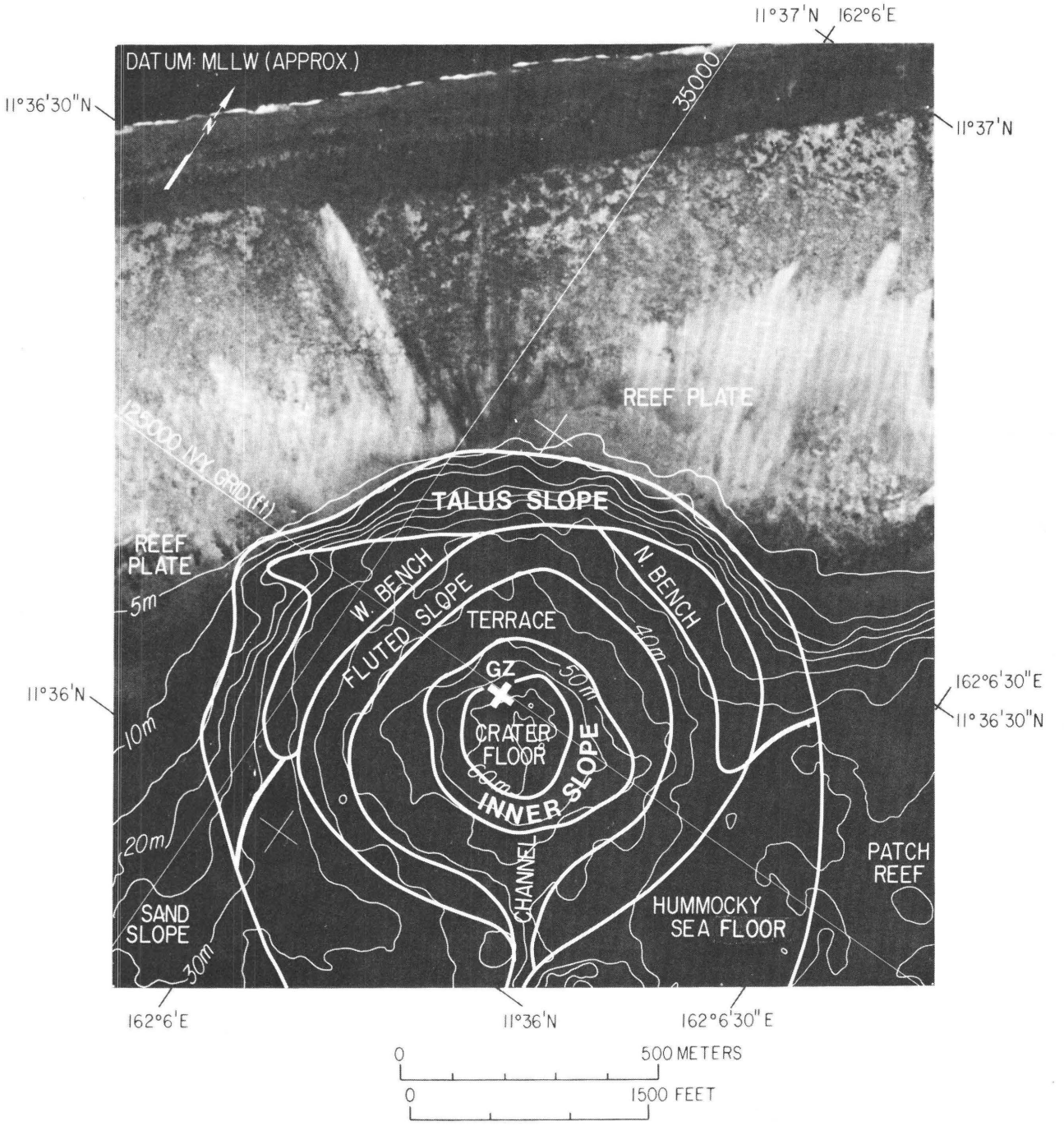

Figure 4*B*. Areas with similar bottom sediment and physiographic characteristics and 5-m bathymetry superimposed on vertical aerial photograph of OAK crater to show their relation to the reef plate. (Photograph courtesy of B. L. Ristvet.)

terrace surface are *Callianassa* sp. mounds, large burrowing anemones (up to 25 cm, or 10 in., in diameter, figs. 8*A*–*D*), small burrowing anemones (about 5 cm, or 2 in., in diameter), and a variety of calcareous and noncalcareous green and brown algae.

Smaller terraces or steps, less than 1 m (3 ft) high and having slopes less than 20°, lie within the terrace. Commonly, between two and five steps were observed on any transect across the terrace area. All are oriented with steep slopes facing ground zero. Some steps rise up to level portions of the terrace, and others slope slightly (a few degrees) away from ground zero, thus reversing the inward slope of the crater wall for short distances. Steps are 30 to 100 m (100–330 ft) apart and are oriented circumferentially with respect to the geometric center. Most occur on the reef side of the crater. The origin of these ridges is unknown, but they may be related to faults, slumps, and dewatering features (see chap. C, this volume).

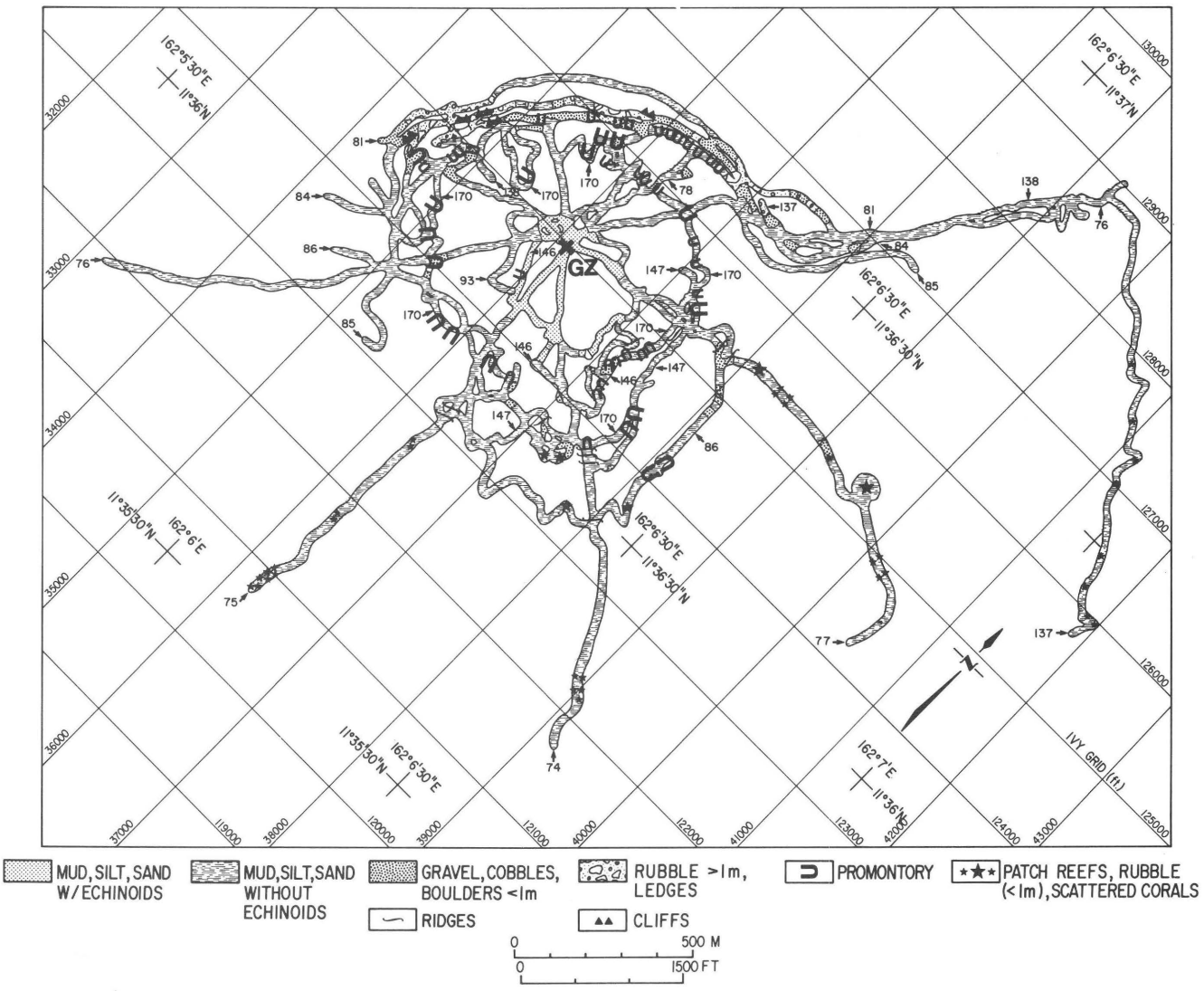

Figure 5. Generalized sea-floor characteristics along submersible dive tracks in OAK crater. The width of the tracks approximates the swath of visibility (20 m average). Track numbers shown with small arrow. GZ=ground zero.

Within the area of the terrace, we observed many small sediment hills apparently made up in part of dark-brown, coarse detritus. They contrasted with the surrounding finer textured terrace sediments. In 1985, we located eight of the hills with the Miniranger System (fig. 3) but observed others during dives when the navigation system was not being used. Most hills that we observed lie in the terrace area, but they may be more widespread. They are less than 3 m (10 ft) high and are round or elongate. Some reach dimensions of 5 to 10 m (16–33 ft) across and up to 30 m (100 ft) long, usually elongated in the direction of a crater circumference. Most hills contain granules (2–4 mm) and pebbles (4–64 mm) and even, in one area, a few cobbles (64–256 mm) (fig. 8*E*). Coarse material is concentrated near the tops of hills, possibly due to winnowing. The coarse material often consists of dark-brown coral fragments, typical of sediment that was cored 230 m (755 ft) below bottom (T. W. Henry and J. I. Tracey, oral commun., April 1985). Thus, the sediment hills may be composed in part of material transported upward by waters escaping from fractures to the sea floor from strata that were dewatering due to the compressional effects of the blast. Similar features have been noted in KOA crater (B. L. Ristvet, written commun., July 1984).

Also in the terrace area are large, gentle hills and swales, a hundred meters in width, that radiate from the crater center; they are obvious on the bathymetric map (fig. 4*A*) but are too large to be obvious with limited visibility from the submersible.

No rocks crop out and there is no evidence of debris blocks on the terrace; the rocks may have been buried by finer textured ejecta or by a veneer of crater sediments.

Fluted Slope

The fluted slope lies at the outer edge of the terrace, where the angle of the slope increases to as much as 20°.

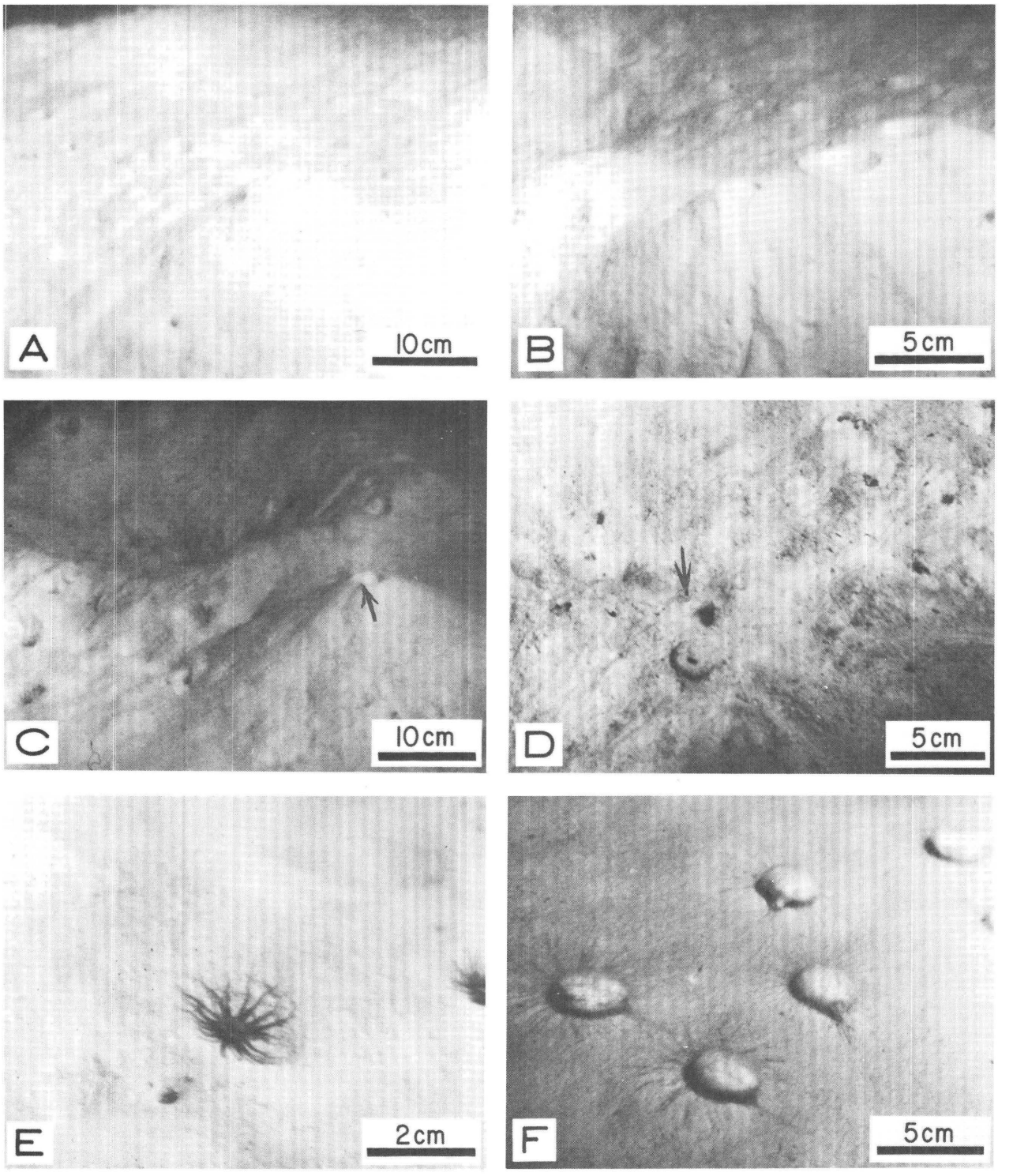

Figure 6. Features of the OAK crater floor: *A*, Isolated *Callianassa* burrow mound on pockmarked sea floor. *B*, Multiple *Callianassa* burrow mounds with groove produced by sediment slide down side of mounds in foreground. *C*, *Callianassa* mound (arrow) in foreground with depression of unknown origin in background. *D*, Small burrow (arrow) with radiating track pattern around opening. *E*, Tentacles of a worm that produces small burrows in crater floor. *F*, Echinoids commonly found at edges of crater floor.

(See figs. 3, 4*A*.) Gentle hills and swales extend from the terrace through the fluted slope (fig. 4*A*). But the fluted slope surface is mainly characterized by smaller promontories and reentrants (fig. 5); it is steepened by these promontories and is gentle where they are absent. The fluted slope surface merges with the back-reef talus slope on the north-

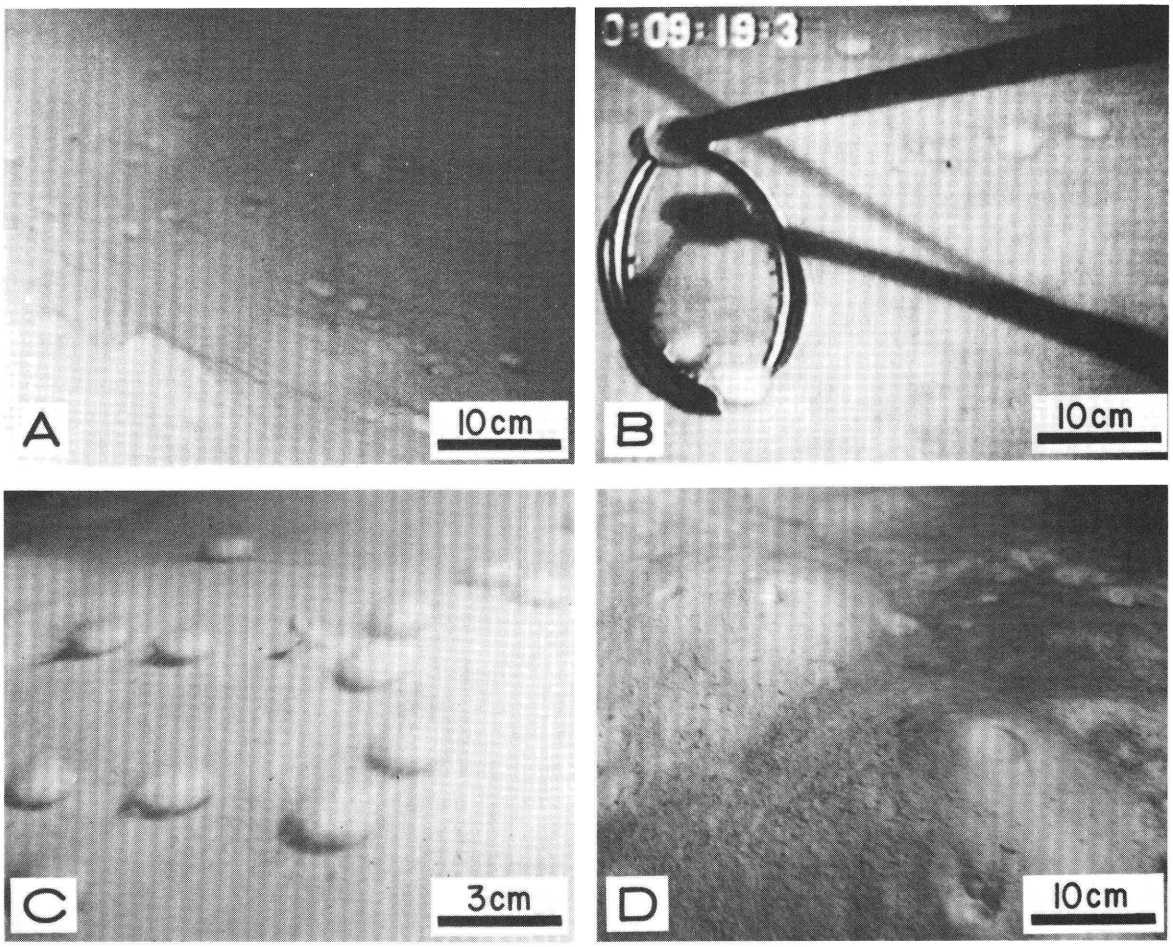

Figure 7. Features of the OAK inner slope: *A*, Isolated *Callianassa* mound and echinoids. *B*, Submersible arm and claw sampling echinoids on current-smoothed inner slope. *C*, Field of echinoids browsing on inner slope. *D*, *Callianassa* burrow mounds composed of slightly coarser sediment than those on the crater floor (compare with fig. 6*B*).

west (reef) side of the crater and with hummocky sea floor on the southeast (lagoon) side.

The promontories are a few meters high and several tens of meters wide and long. They are flat-topped, project into the crater, and merge smoothly upslope. The sides of the promontories are typically covered with fleshy macroalgae and scattered corals. Promontories are about as wide as the areas that separate them, producing a fluting effect on the scale of tens of meters. We did not see any promontories elongated parallel to radials (rays). Some promontories are covered by sand, silt, and clay, and others by gravel and cobbles, particularly on the side facing ground zero (figs. 9*A*–*E*). It is these rocky terrains that we commonly sampled for debris blocks. (See chap. G, this volume.)

The promontories may be mounds of debris that lie outside the transient crater, or they may be ridges that have been incised by postblast erosional processes within the transient crater, similar to but larger than the ridges in LACROSSE crater illustrated by Ristvet and others (1978, fig. 5.17).

Hummocky Sea Floor

Two areas of hummocky sea floor, one east of and one south of ground zero, are separated by a channel leading from the central crater area to the lagoon floor (fig. 4*A*). The areas of hummocky sea floor contain mounds or hills, some of which are up to 10 m (33 ft) high. Some of these hills appear to be mounds of debris; others are patch reefs that have been eroded or partially buried by debris. Areas between them look like the lagoon floor (fig. 9*B*) as does the channel leading from the lagoon to the crater. The southern area is less rough and more like lagoon floor than the eastern area.

Within this and the fluted slope areas, debris mounds were identified as close as 305 m (1,000 ft) to ground zero and as far away as 640 m (2,100 ft). The area covered by debris is at least 335 m (1,100 ft) wide in some areas. The mounded portion of the debris blanket is easily recognized from the submersible, but flatter portions of the blanket may extend beyond the mounds where it is hard to recognize.

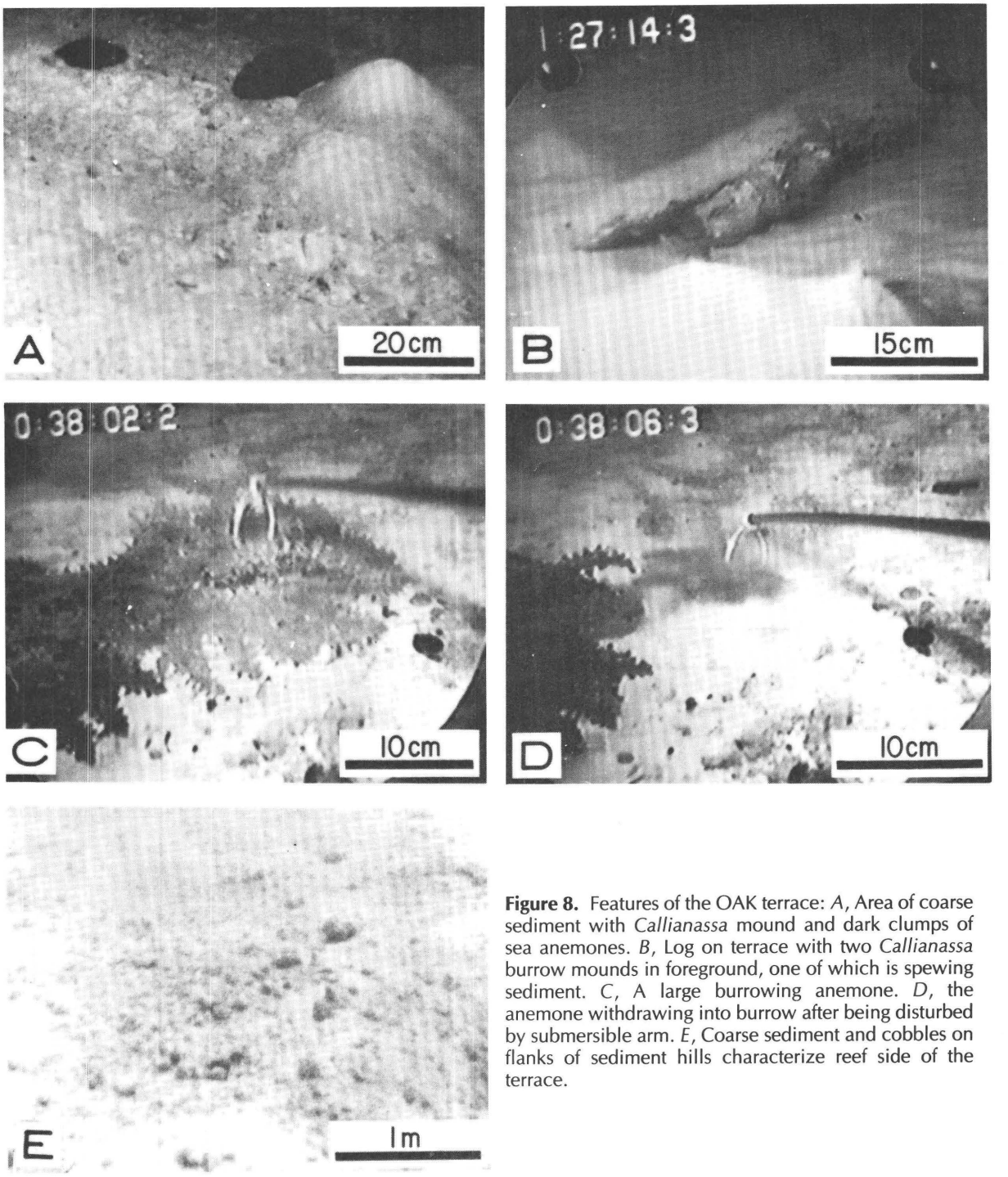

Figure 8. Features of the OAK terrace: *A*, Area of coarse sediment with *Callianassa* mound and dark clumps of sea anemones. *B*, Log on terrace with two *Callianassa* burrow mounds in foreground, one of which is spewing sediment. *C*, A large burrowing anemone. *D*, the anemone withdrawing into burrow after being disturbed by submersible arm. *E*, Coarse sediment and cobbles on flanks of sediment hills characterize reef side of the terrace.

Beyond the mounded debris (outward from ground zero) are small sediment ridges (figs. 4*A*, 5) parallel to the circumference of the crater, several tens of meters long, a meter to several meters high, and up to 15 m (50 ft) wide. They are generally larger than those in the crater terrace.

Benches

Prominent benches up to 5 m (16 ft) high and as much as 200 m (660 ft) long, occur roughly parallel to the crater circumference north and west of ground zero (fig. 4*A*). Much of their surface is covered by fleshy and calcareous algae (figs. 10*A*,*B*). They generally lie in water between 30 m (100 ft) and 40 m (130 ft) deep, but a particularly large feature on the western bench may be traced upward to water as shallow as 20 m (66 ft) (fig. 4*A*). It may be a break in the talus slope as interpreted in figure 10 of chapter A (this volume). The benches appear to pinch out against the talus slope northwest of ground zero. Perhaps the western and

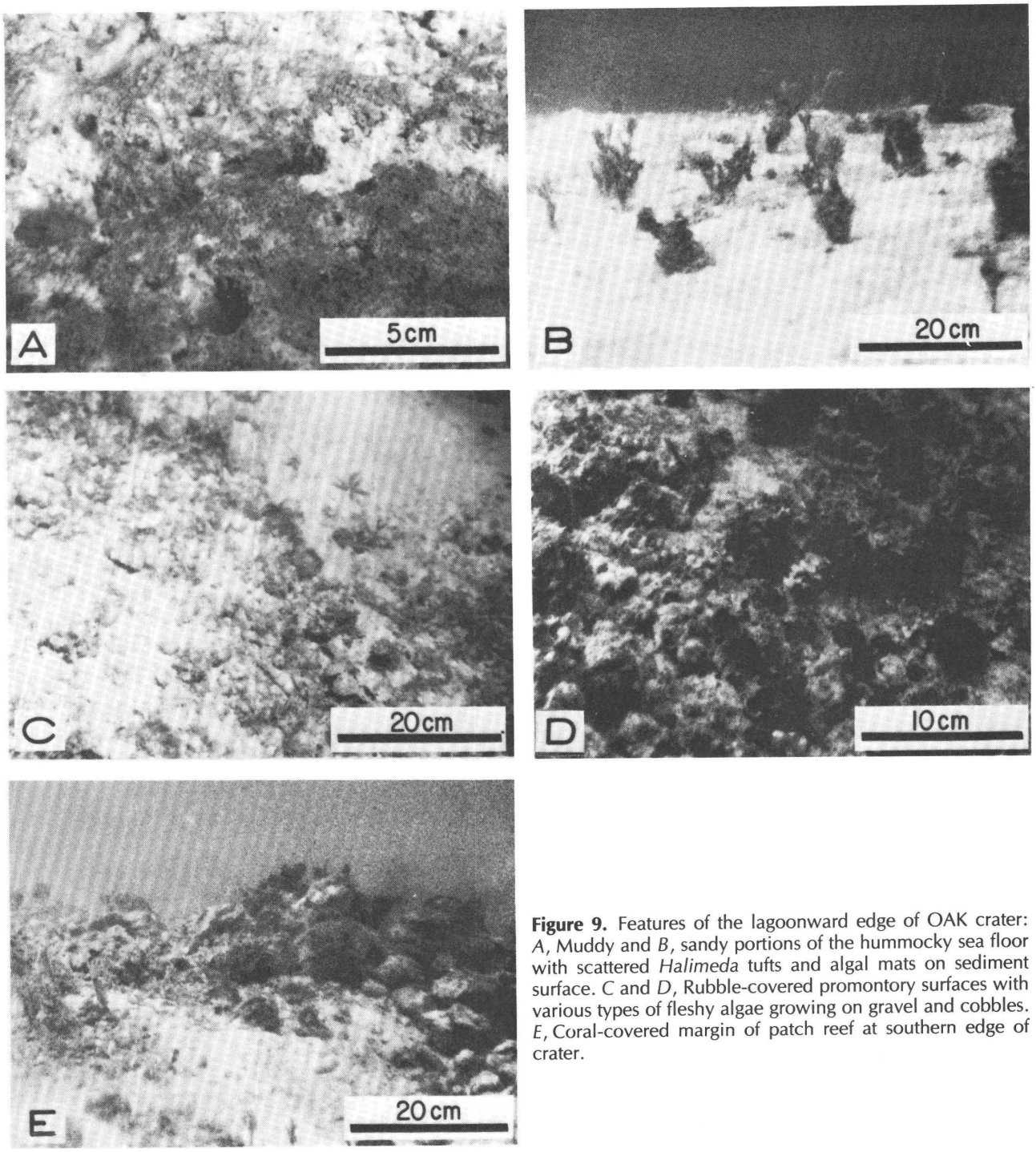

Figure 9. Features of the lagoonward edge of OAK crater: *A*, Muddy and *B*, sandy portions of the hummocky sea floor with scattered *Halimeda* tufts and algal mats on sediment surface. *C* and *D*, Rubble-covered promontory surfaces with various types of fleshy algae growing on gravel and cobbles. *E*, Coral-covered margin of patch reef at southern edge of crater.

northern benches are actually connected, forming a continuous feature along the reef side of the crater but with the central part buried beneath talus.

As with some other features observed from the submersible, the origin of the benches cannot be determined from their surface characteristics and must await additional subsurface exploration. Their position below the talus slope and the absence of similar features on the lagoon side of the crater suggests that they may have slumped from the talus slope to their present position. If so, the reef plate must have been stripped away prior to slumping because we found no evidence of it on the benches.

Talus Slope and Reef Plate

Along the reef on the northwest side of OAK crater, the benches and fluted slope merge with a talus slope (fig. 4*A*). The talus slope, composed mainly of sand and reef plate rubble, covers much of the steepest parts of the crater wall. Some terraces in the talus slope may have been formed

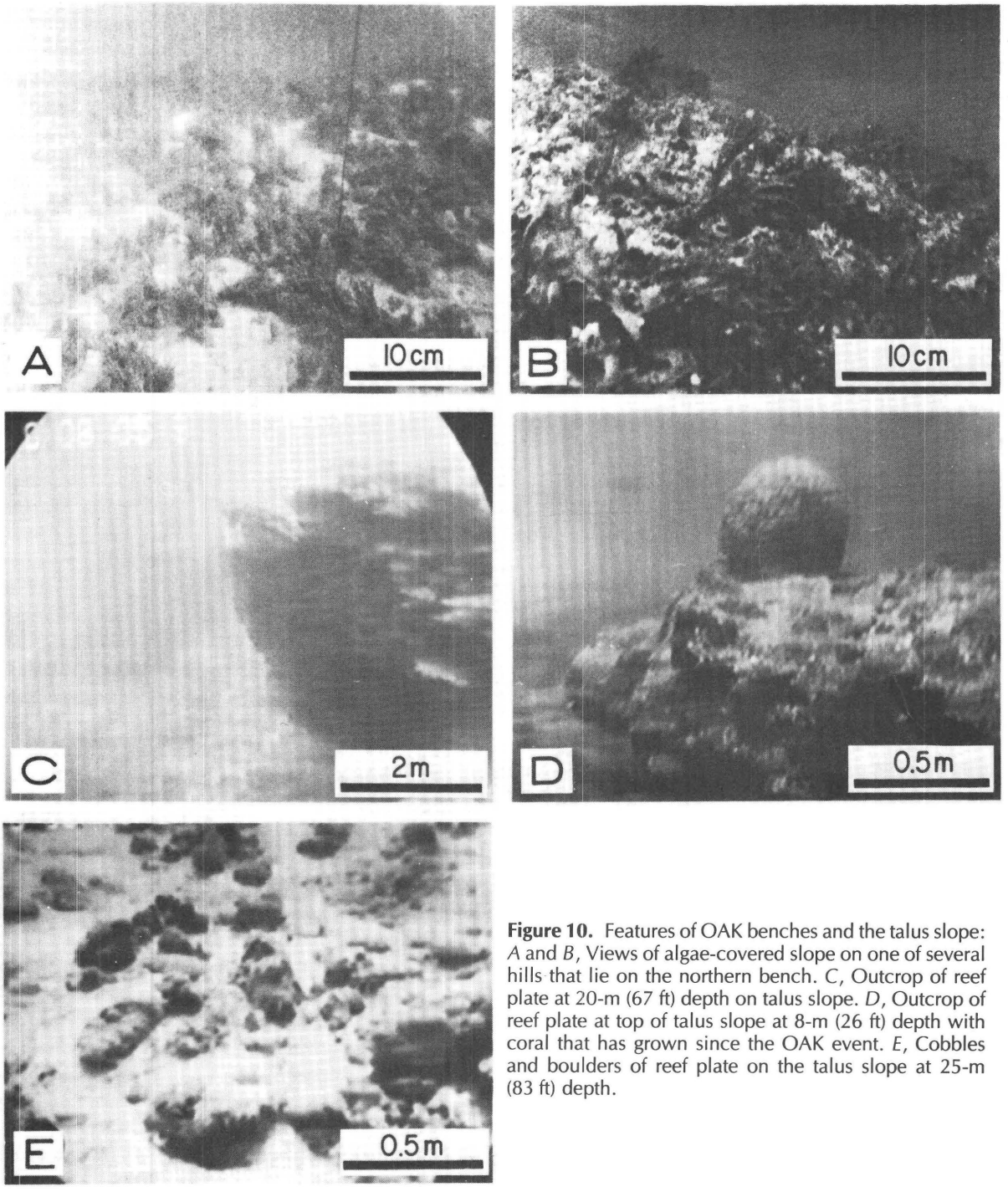

Figure 10. Features of OAK benches and the talus slope: *A* and *B*, Views of algae-covered slope on one of several hills that lie on the northern bench. *C*, Outcrop of reef plate at 20-m (67 ft) depth on talus slope. *D*, Outcrop of reef plate at top of talus slope at 8-m (26 ft) depth with coral that has grown since the OAK event. *E*, Cobbles and boulders of reef plate on the talus slope at 25-m (83 ft) depth.

by reef plate that is partly covered by sand. Other terraces on the slope probably comprise slumps that have moved or are moving material into the crater. Numerous small (1–5 m, or 3–16 ft) sand slumps were noted; however, some other areas have been stabilized by scattered algal plants and mats.

The top of the talus slope is rimmed by the lagoonward edge of the reef plate, rock that is formed of cemented reef rubble and occurs in a band several hundred meters wide lagoonward of the living reef (fig. 4*A*). The reef plate is partly exposed above the talus slope where it forms prominent escarpments as much as 5 m (16 ft) high (figs. 10*C*,*D*). Where the slope has a thicker veneer of sand, it barely protrudes. In other areas, there seems to be no reef plate at all; it may have been stripped away during the blast. (See chap. H, fig. 23, this volume).

The reef plate commonly underlies water less than 1 m (3 ft) deep, but it has been depressed along the edge of the crater to about 20 m (65 ft) at its closest point to ground

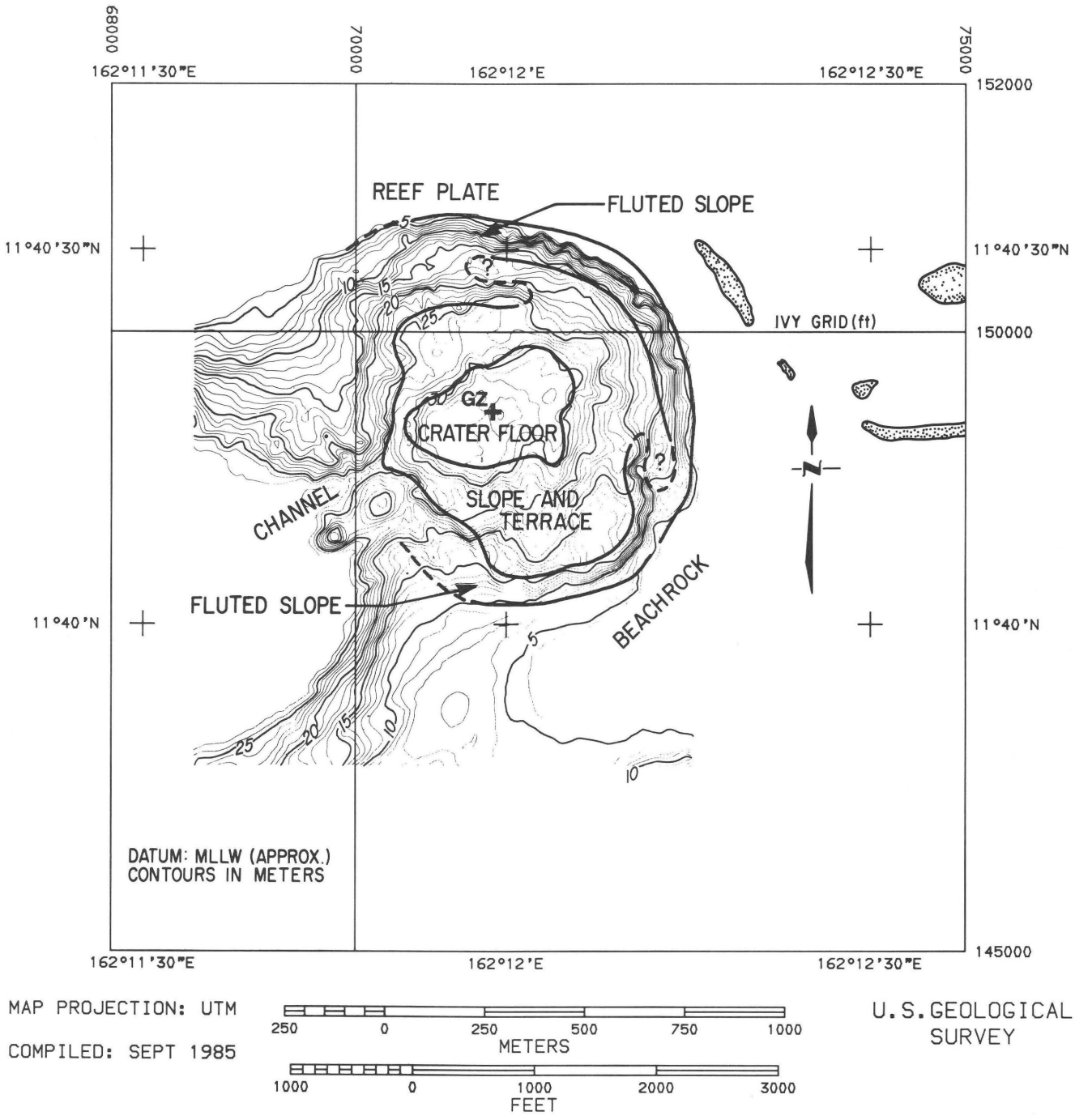

Figure 11*A*. Areas with similar bottom sediment and physiographic characteristics of KOA crater superimposed on 1-m bathymetry. GZ=ground zero.

zero (figs. 10*C*,*D*). The escarpment at the lagoonward edge of the reef plate is obviously eroding away from the crater. The original crater rim may have been several tens to as much as 100 m (330 ft) closer to ground zero. Evidence of this retreat are large blocks, boulders, and cobbles of reef plate that have slid downslope from the escarpment and cover the talus slope in many areas (fig. 10*E*). Where the slope is covered by sand, it presumably overlies much coarser reef plate detritus.

KOA Crater

KOA crater lies in a more windward position than OAK on the Enewetak Atoll in an area of considerable carbonate-sand production; as a result, sand islands have developed along this portion of the reef and beachrock has formed in the surficial sediments. Beachrock is lithified, well bedded, and contains moderately to steeply dipping layers of lithified beach sand. It forms around and beneath

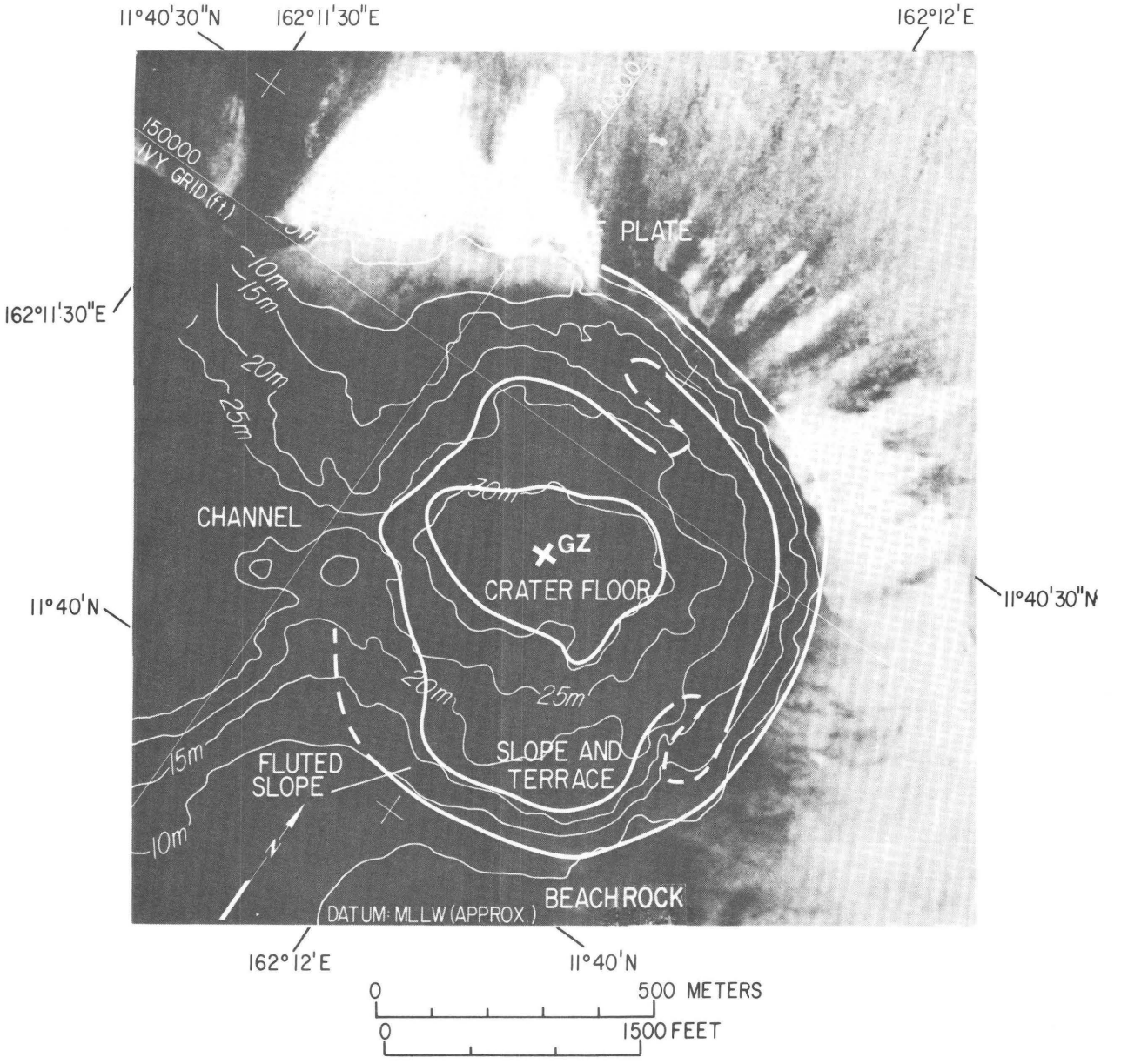

Figure 11*B*. Areas with similar bottom sediments and physiographic characteristics and 5-m bathymetry superimposed on vertical aerial photograph of KOA crater to show their relation to the surrounding reef plate and beachrock.

islands as the result of the precipitation of naturally occurring carbonate minerals between sand grains. At the KOA site, reef plate lies along the seaward (reefward) side of the crater, and both reef plate and beachrock lie along the other sides of the crater (fig. 11*B*). Major features and sediment texture of KOA crater are shown in figures 11*A* and 12. Figure 11 shows the provinces in KOA defined from the submersible. They include: (1) crater floor, (2) slope and terrace, (3) fluted slope, and (4) reef plate.

Crater Floor

The crater floor at KO*A* (fig. 11*A*) dips gently toward ground zero from a water depth of about 30 m (100 ft) to 33 m (108 ft); it is covered by sandy mud that appears to be coarser than the sediment on the floor of OAK crater, and it is covered by mounds 15 to 30 cm (0.5–1 ft) high that surround the burrows of *Callianassa* sp. shrimp. Large burrowing anemones, 15 to 20 cm (0.5–0.7 ft) across, lie widely scattered between the burrow mounds.

We observed no rock or gravel on the crater floor. Though visibility was poor (often <1 m, or 3 ft), we could see bottom sediments from the lower ports of *Delta*. Because the visibility was limited, large features might have been missed; however, no large features were encountered during several crater transects.

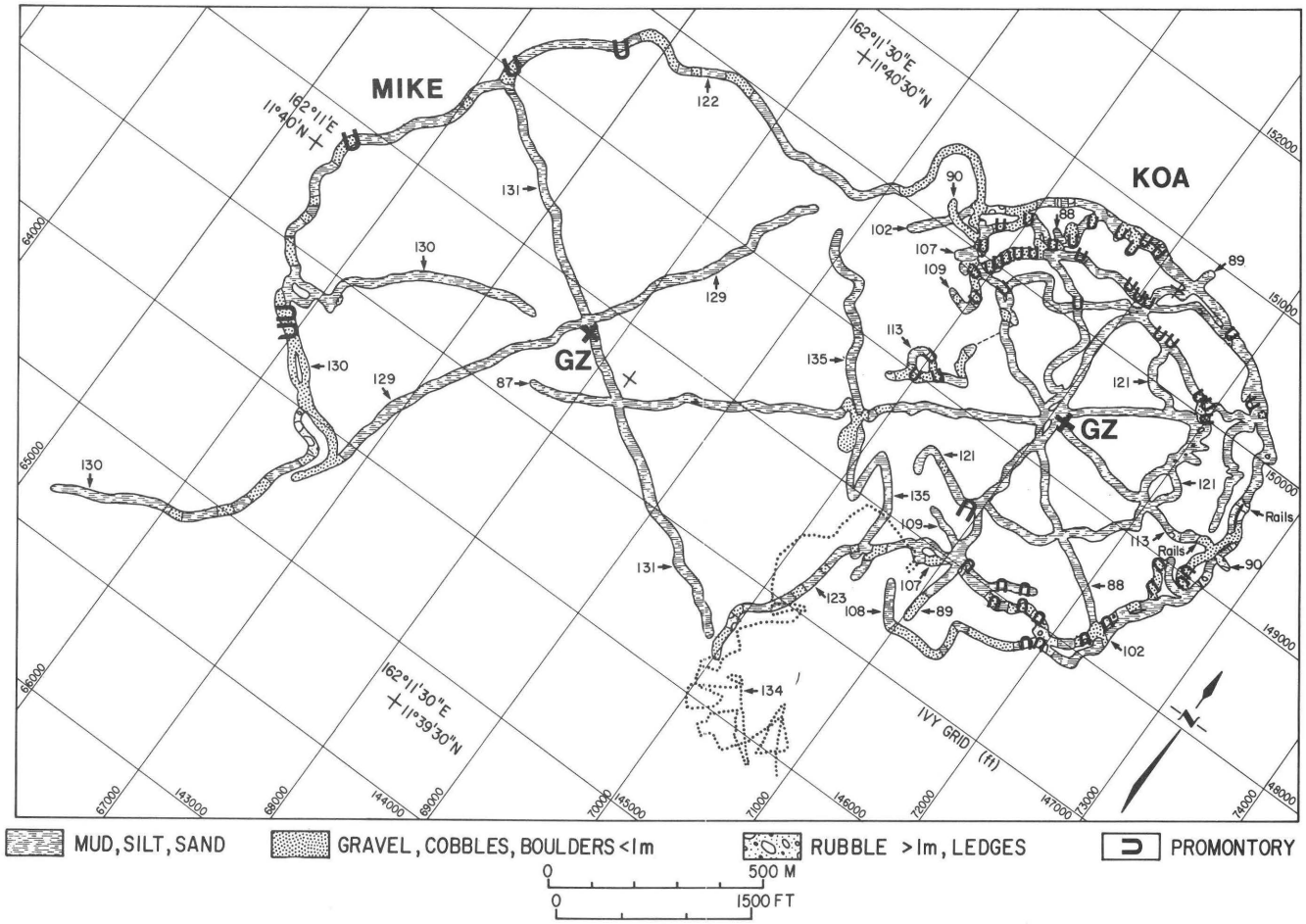

Figure 12. Generalized sea-floor characteristics along submersible dive tracks in KOA and MIKE craters. The width of the tracks approximates the swath of visibility (20 m average). Track numbers shown with small arrows. GZ=ground zero.

The crater floor of KOA, in contrast to that of OAK, appears to be receiving considerably more and coarser sediment that apparently is swept from the reef flat on the north and northeast sides of the crater. Sediment deposited on the crater floor is quickly reworked by burrowing organisms and is blended with older sediments.

Slope and Terrace Area

The crater floor is surrounded by a distinct but gentle slope area (fig. 11*A*). Slight variations of slope suggest that terraces are present in this area, but they are difficult to delineate from submersible observations. The sediments appear identical to those of the crater floor. The slope area lies at distances between 150 and 400 m (492–1,312 ft) from ground zero and extends from depths of 30 m (100 ft) to depths as shallow as 15 to 20 m (49–66 ft). The area of low relief around the crater floor (fig. 11*A*) is equivalent to the inner slope and terrace of OAK crater. No hills or steps were observed in this area. Although an inner slope and terrace may be differentiated on the basis of bathymetry (chap. A, fig. 18, this volume), no such distinctions were possible from the submersible. The entire sea floor in this area appears to be gently sloping, silty, and muddy sand burrowed by *Callianassa* sp.

Fluted Slope

At a radius of about 300 m (1,000 ft) from ground zero, the wall of KOA is scalloped or fluted by a series of reentrants and promontories similar to those in OAK (figs. 4*A*, 11*A*). Promontories are a few tens of meters wide, several meters high, are steep-sided toward ground zero, and merge gradually with the slope away from the crater

center. These reentrants caused the submersible to follow a sinuous course during dives along contours in this area. The promontories of KOA are covered with sand, gravel, and coarse rubble like those observed at OAK.

At the top of the fluted slope, the rim of the crater takes on different aspects. Southwest of ground zero, KOA is connected to MIKE through a 25-m-deep (82-ft-deep) channel. To the north, the crater wall is rimmed by reef plate; to the southeast and south, the crater wall is rimmed by beachrock. The sediment surface of the crater wall is mostly covered by sand which appears to be thicker on the northeast and east sides where the influx of detritus from the reef is greatest. On the northwest and southeast sides, there is a significant contribution of coarser material, composed of beachrock, reef plate, and living coral.

Where the crater is shallower than 25 m (82 ft), mostly fluted slope, the bottom is covered by patches of fleshy and calcareous macroalgae, commonly *Halimeda* sp., *Dictyota* sp., *Caulerpa* sp., and *Padina* sp. In some areas, these plants completely cover the bottom; elsewhere, they are widely scattered. There is only the most general correlation of the abundance of the plants with depth. The major controls of their distribution are not known.

The complex bathymetry of the area between the craters, made up of mounds and channels, probably resulted from several of the cratering events which were sited near this area (chap. A, fig. 17, this volume).

Slabs and outcrops of beachrock that occur on the south and southeast margins of the crater represent remnants of rocks that were originally beneath islands and along the lagoonward margins of islands in the KOA area. The bedding in undisturbed beachrock is typically steep and may be mistaken for rotated horizontal bedding.

MIKE Crater

MIKE crater has a large, flat, burrowed crater floor, probably indicating substantial sediment filling. The crater is rimmed with material that is more coarse than that found on the crater floor. Several promontories occur around the crater margin, some capped by coarse rubble and boulders. The promontories lie at a distance of about 550 m (1,800 ft) from MIKE ground zero (fig. 12).

Forereef Dives

In 1984 and 1985, we made 15 submersible dives along the seaward edge of the atoll near MIKE and KOA craters. These were reconnaissance dives to examine a natural portion of the forereef slope and to compare it with a slump scarp that was formed by a submarine rockfall (fig. 13*A*) created in the area during or shortly after the KOA event. Photographs (Ristvet and others, 1978) show that the escarpment was not present on November 8, 1952, after the MIKE event; but it is present on June 3, 1958, after the KOA event.

The natural slope is characterized in this area by three zones: (1) the reef plate, crest, and near forereef, which extend from sea level to 16 m (52 ft), with slopes of less than 10°, (2) the bypass slope, from 16 to 275 m (52–900 ft), with slopes of 55° that decrease to 35° near the base; and (3) a talus slope below 275 m (900 ft) with slopes that are less than 35°. Vertical walls, grooves and chutes, common on Caribbean forereef slopes (Enos and Moore, 1983) are sparse on the northwestern slope of Enewetak.

The slump scarp comprises three units that were differentiated initially by surficial appearance: (1) a rough near-vertical wall from the reef crest to 76 m (250 ft) composed mainly of coral, with common rubble-covered ledges (fig. 13*B*); (2) a vertical to overhanging wall from 76 m (250 ft) to 220 m (720 ft) that is massive and fractured, with smooth, blocky surfaces (figs. 13*C,D*); and (3) inclined strata from 220 m (720 ft) to more than 400 m (1,310 ft), composed of hard, dense white limestone and dolomite (fig. 13*E*). Caves occur in all three units. Open, cement-lined fractures and voids layered with cements are most common in the middle unit. Exposed on the southeastern side of the scarp are forereef boulder beds dipping at 30° toward the open sea. The steeper (55°) dipping natural surface truncates these beds, revealing the erosional nature of the bypass slope.

REFERENCES

Couch, R. F., Jr., Fetzer, J. A., Goter, E. R., Ristvet, B. L., Walter, D. R., and Wendland, V. P., 1975, Drilling operations on Eniwetok Atoll during Project EXPOE: Air Force Weapons Laboratory Technical Report TR–75–216, Kirtland Air Force Base, New Mexico 87117, 270 p.

Enos, Paul, and Moore, C. H., 1983, Fore-reef slope environment, *in* Scholle, P. A., Bebout, D. G., and Moore, C. H., Carbonate depositional environments: American Association of Petroleum Geologists, Memoir 33, p. 507–538.

Ristvet, B. L., Tremba, E. L., Couch, R. F., Jr., Fetzer, J. A., Goter, E. R., Walter, D. R., and Wendland, V. P., 1978, Geologic and geophysical investigations of the Eniwetok nuclear craters: Air Force Weapons Laboratory Technical Report TR–77–242, Kirtland Air Force Base, New Mexico 87117, 298 p.

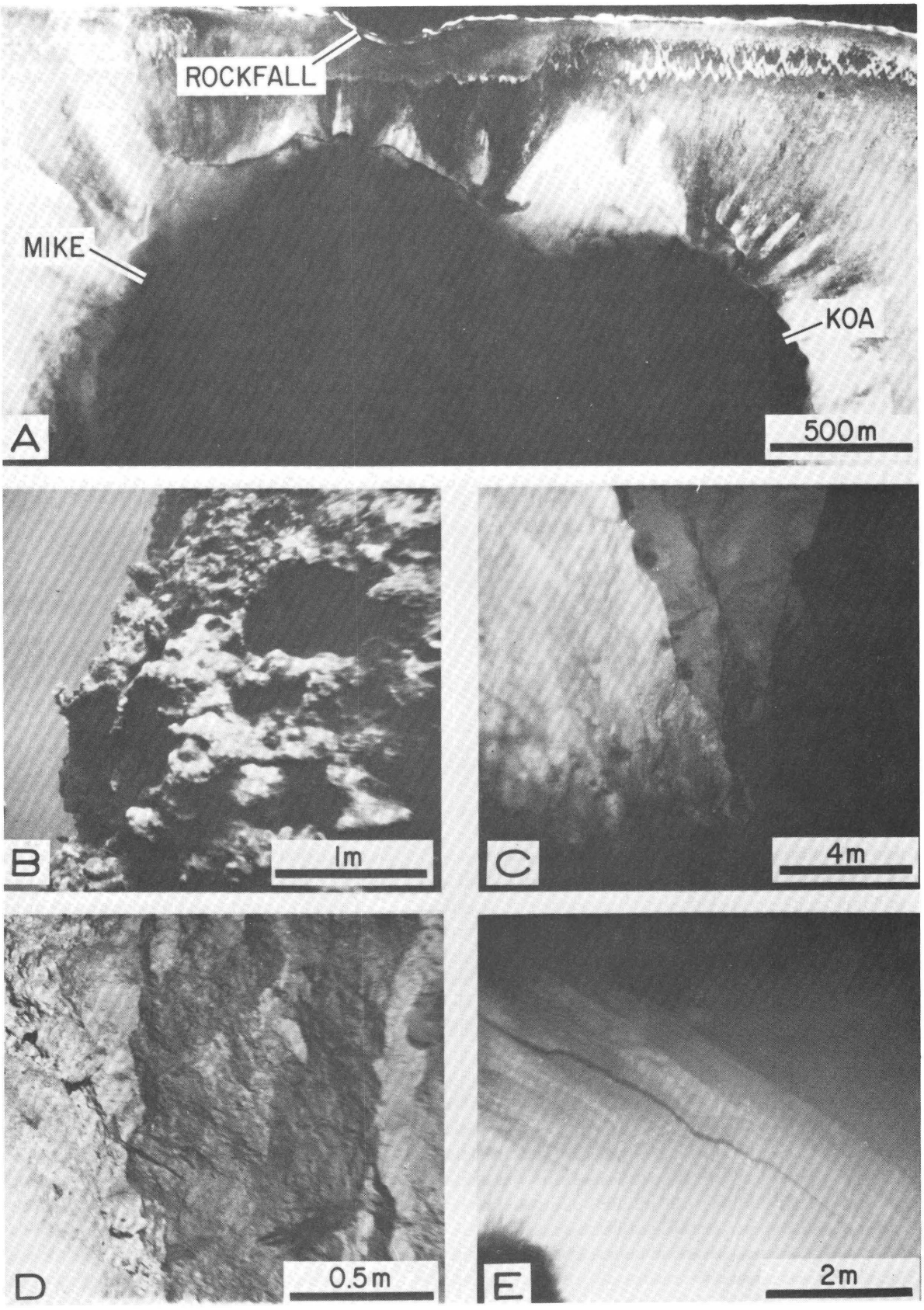

Figure 13. Features of the rockfall area seaward of MIKE: *A*, Vertical aerial photograph of MIKE and KOA craters, showing rockfall area on outer reef. (Photograph courtesy of B. L. Ristvet). *B*, Rough, near-vertical wall at 76-m (250 ft) water depth. *C*, View looking down a vertical to overhanging massive and fractured limestone wall at 168-m (550 ft) water depth. *D*, Close-up photograph of *C*, showing detailed features including a vertical fracture. *E*, Slope of dense white limestone and dolomite at 332 m (1,090 ft).

Appendix

Chapter F - Appendix

SUBMERSIBLE DELTA LOG

OAK and KOA Crater Survey
Enewetak Atoll

15 July-10 August 1984

DIVE no.	JULIAN DAY- Local Date/ Greenwich Date	TIME Local/ G.m.t.(Z)	LOCATION	DESCRIPTION Pilot Observer Mission
73	197-15JUL84 198-16JUL84	1230-1245 0030-0045Z	GZ OAK	SLATER SHINN TEST
74	"	1330-1530 0130-1330Z	OAK	SLATER SHINN TRANSECT
75	"	1610-1720 0410-0520Z	OAK	SLATER HALLEY TRANSECT
76	198-16JUL84 198-16JUL84	0858-1104 2058-2304Z	OAK	SLATER FOLGER TRANSECT
77	198-16JUL84 199-17JUL84	1215-1400 0015-0200Z	OAK	SLATER SHINN TRANSECT
78	"	1520-1710 0320-0510Z	OAK	PRIVITT HALLEY CRATER FLOOR SURVEY
79	199-17JUL84 "	0940-1110 2140-2310Z	OAK	SLATER FOLGER RECCO REEF
80	199-17JUL84 199-200- 17-18JUL84	1155-1250 2355-0050Z	OAK	SLATER FOLGER RECCO REEF

DIVE no.	JULIAN DAY- Local Date/ Greenwich Date	TIME Local/ G.m.t.(Z)	LOCATION	DESCRIPTION Pilot Observer Mission
81	199-17JUL84 200-18JUL84	1325-1500 0135-0300Z	OAK	SLATER FOLGER TV REEF MARGIN 7-M CONTOUR
82	"	1542-1626 0342-0426Z	OAK	PRIVITT RISTVET ORIENT.
83	"	1634-1716 0434-0516Z	OAK	PRIVITT BRAMLETTE ORIENT.
84	200-18JUL84 "	0935-1035 2135-2235Z	OAK	SLATER HALLEY TV REEF RECON 18-M CONTOUR
85	200-18JUL84 200-201 18-19JUL84	1122-1250 2322-0050Z	OAK	SLATER HALLEY TV REEF RECON 30-M CONTOUR
86	200-18JUL84 201-19JUL84	1410-1545 021--0342Z	OAK	SLATER HALLEY TV RECON LAGOON EJECTA BLANKET
87	201-19JUL84 "	0850-0953 2050-2153Z	KOA	SLATER FOLGER TRANSECT
88	201-19JUL84 "	1029-1109 2229-2309Z	KOA	PRIVITT FOLGER TRANSECT
89	201-19JUL84 201-202 19-20JUL84	1130-1205 2330-0015Z	KOA	PRIVITT HALLEY TRANSECT

DIVE no.	JULIAN DAY- Local Date/ Greenwich Date	TIME Local/ G.m.t.(Z)	LOCATION	DESCRIPTION Pilot Observer Mission
90	201-19JUL84 202-20JUL84	1231-1321 0031-0121Z	KOA	SLATER FOLGER TRANSECT
91	" "	1525-1555 0327-0355Z	OAK	SLATER SEVIN SURVEY
92	" "	1607-1637 0405-0437Z	OAK	SLATER KREYENHAGEN SURVEY
93	202-20JUL84 "	0931-1106 2131-2306Z	OAK	SLATER KREYENHAGEN SURVEY CRATER FLOOR
94	202-20JUL84 203-21JUL84	1220-1245 0020-0045Z	OAK	SLATER JONES ORIENT.
95	"	1300-1320 0100-0120Z	OAK	SLATER DAI ORIENT.
96	"	1325-1405 0125-0205Z	OAK	SLATER SCHENKER ORIENT.
97	"	1417-1440 0217-0240Z	OAK	SLATER BROWN ORIENT.
98	"	1449-1509 0249-0309Z	OAK	SLATER SEVIN ORIENT.
99	"	1524-1545 0324-0345Z	OAK	SLATER MATTHEWMAN ORIENT.
100	"	1553-1608 0353-0408Z	OAK	SLATER HOLLAR ORIENT.

DIVE no.	JULIAN DAY- Local Date/ Greenwich Date	TIME Local/ G.m.t.(Z)	LOCATION	DESCRIPTION Pilot Observer Mission
101	203-21JUL84 "	0928-0950 2128-2150Z	KOA	SLATER SHINN BOW PLANE SEARCH
102	"	1019-1149 2219-2349Z	KOA	SLATER SHINN TV
103	203-21JUL84 204-22JUL84	1300-1329 0100-0129Z	KOA	PRIVITT SEVIN ORIENT.
104	"	1345-1430 0145-1230Z	KOA	PRIVITT JONES ORIENT.
105	"	1452-1522 0252-0322Z	KOA	PRIVITT DAI ORIENT.
106	"	1539-1605 0339-0405Z	KOA	SLATER KREYENHAGEN ORIENT.
107	204-22JUL84 "	0852-1052 2052-2252Z	KOA	SLATER HALLEY TV
108	"	1111-1157 2311-2357Z	KOA	SLATER HALLEY TV
109	204-22JUL84 205-23JUL84	1307-1452 0107-0252Z	KOA	SLATER RODDY TV
110	"	1523-1623 0323-0423Z	KOA	PRIVITT JOHNSON BOW PLANE SEARCH

DIVE no.	JULIAN DAY- Local Date/ Greenwich Date	TIME Local/ G.m.t.(Z)	LOCATION	DESCRIPTION Pilot Observer Mission
111	205-23JUL84 205-23JUL84	0915-1115 2115-2315Z	OUTSIDE ATOLL OFF MIKE	SLATER HALLEY TV
112	205-23JUL84 205-206 23-24JUL84	1140-1310 2340-0110Z	AA	SLATER SHINN TV
113	206-24JUL84 207-25JUL84	1435-1645 0235-0445Z	KOA	SLATER RODDY TV
114	207-25JUL84 "	0924-1017 2124-2217Z	OAK	SLATER RODDY TV
115	"	1040-1111 2240-2311Z	OAK	SLATER RODDY TV
116	207-25JUL84 208-26JUL84	1340-1415 0140-0215Z	KOA	PRIVITT RISTVET RAIL SURVEY
117	"	1420-1445 0220-0245Z	KOA	SLATER RODDY TV
118	"	1456-1519 0256-0319Z	KOA	SLATER RODDY TV
119	"	1536-1612 0336-0412Z	KOA	PRIVITT NUNES ORIENT.
120	"	1433-1655 0233-0455Z	KOA	PRIVITT TRUMBORE ORIENT.
121	208-26JUL84 "	1015-1153 2215-2353Z	KOA	SLATER HALLEY TV

DIVE no.	JULIAN DAY- Local Date/ Greenwich Date	TIME Local/ G.m.t.(Z)	LOCATION	DESCRIPTION Pilot Observer Mission
122	208-26JUL84 209-27JUL84	1315-1500 0115-0300Z	MIKE	SLATER HALLEY TV
123	"	1543-1618 0343-0418Z	MIKE	SLATER HALLEY TV
124	209-27JUL84 "	0944-1110 2144-2310	OAK	SLATER PRIVITT TV
125	209-27JUL84 209-210 27-28JUL84	1140-1222 2340-0022Z	OAK	SLATER PRIVITT SAMPLING
126	209-27JUL84 210-28JUL84	1255-1320 0055-0120Z	OAK	SLATER PRIVITT SAMPLING
127	"	1340-1440 0140-0240Z	OAK	SLATER PRIVITT SAMPLING
128	"	1505-1625 0305-0425Z	OAK	SLATER PRIVITT SAMPLING
129	210-28JUL84 "	1004-1059 2204-2259Z	MIKE	SLATER RODDY TV
130	210-28JUL84 210-211 28-29JUL84	1134-1247 2334-0047Z	MIKE	SLATER RODDY TV
131	210-28JUL84 211-29JUL84	1331-1435 0131-0235Z	MIKE	SLATER RODDY TV
132	"	1534-1614 0334-0414Z	ENGEBI	SLATER RODDY TV

DIVE no.	JULIAN DAY- Local Date/ Greenwich Date	TIME Local/ G.m.t.(Z)	LOCATION	DESCRIPTION Pilot Observer Mission
133	"	1640-1820 0440-0620Z	ENGEBI	PRIVITT JOHNSON ORIENT.
134	211-29JUL84 "	1020-1145 2220-2345Z	MIKE	PRIVITT RODDY TV
135	211-29JUL84 212-30JUL84	1350-1445 0150-0245Z	KOA	PRIVITT RODDY SAMPLING
136	212-30JUL84 "	1019-1124 2219-2324Z	SW OF OAK	SLATER HALLEY TV
137	212-30JUL84 212-213 29-30JUL84	1235-1345 0035-0145Z	NW OF OAK	SLATER RODDY TV
138	212-30JUL84 213-31JUL84	1437-1532 0237-0332Z	OAK	SLATER RODDY TV
139	213-31JUL84 "	1006-1036 2206-2236Z	OAK	SLATER KINDINGER SAMPLING
140	"	1056-1130 2256-2330Z	OAK	SLATER KINDINGER SAMPLING
141	213-31JUL84 214-1AUG84	1237-1252 0037-0052Z	OAK	SLATER KINDINGER SAMPLING
142	"	1313-1345 0113-0145Z	OAK	SLATER KINDINGER SAMPLING

DIVE no.	JULIAN DAY- Local Date/ Greenwich Date	TIME Local/ G.m.t.(Z)	LOCATION	DESCRIPTION Pilot Observer Mission
143	"	1413-1443 0213-0243Z	OAK	SLATER KINDINGER SAMPLING
144	"	1500-1524 0300-0324Z	OAK	SLATER KINDINGER SAMPLING
145	214-1AUG84	1015-1020 2215-2220Z	OAK	SLATER SHINN ABORT
146	214-1AUG84 214-215 1-2AUG84	1030-1210 2230-0010Z	OAK	SLATER SHINN TV
147	214-1AUG84 215-2AUG84	1322-1426 0122-0226Z	OAK	SLATER SHINN TV
148	"	1505-1613 0305-0413Z	OAK	PRIVITT HUDSON SAMPLING
149	215-2AUG84 "	1012-1045 2212-2245Z	OAK	SLATER PRIVITT SAMPLING
150	215-2AUG84 215-216 2-3AUG84	1110-1204 2310-0004Z	OAK	SLATER HUDSON SAMPLING
151	215-2AUG84 216-3AUG84	1300-1315 0100-0115Z	LAGOON	PRIVITT JOHNSON INSPECT REEF
152	"	1345-1410 0145-0210Z	OAK	PRIVITT MEYERS RAD MEAS.
153	"	1426-1520 0226-0320Z	OAK	SLATER HUDSON SAMPLING

DIVE no.	JULIAN DAY-Local Date/ Greenwich Date	TIME Local/ G.m.t.(Z)	LOCATION	DESCRIPTION Pilot Observer Mission
154	"	1553-1638 0353-0438Z	OAK	SLATER HUDSON SAMPLING
155	216-3AUG84	1016-1059 2216-2259Z	OAK	SLATER KINDINGER SAMPLING
156	"	1109-1149 2309-2349Z	OAK	SLATER KINDINGER SAMPLING
157	216-3AUG84 217-4AUG84	1236-1314 0036-0114Z	OAK	SLATER KINDINGER SAMPLING
158	"	1336-1400 0136-0200Z	OAK	SLATER KINDINGER SAMPLING
159	"	1415-1445 0215-0245Z	OAK	PRIVITT JAMES ORIENT.
160	"	1506-1534 0306-0334Z	OAK	SLATER KINDINGER SAMPLING
161	"	1554-1610 0354-0410Z	OAK	SLATER KINDINGER SAMPLING
162	217-4AUG84 217-218 4-5AUG84	1114-1328 2324-0128Z	OAK	SLATER SHINN TV
163	217-4AUG84 218-5AUG84	1451-1542 0251-0342Z	OAK	SLATER HUDSON SAMPLING
164	"	1553-1649 0353-0449Z	OAK	SLATER HUDSON SAMPLING

DIVE no.	JULIAN DAY- Local Date/ Greenwich Date	TIME Local/ G.m.t.(Z)	LOCATION	DESCRIPTION Pilot Observer Mission
165	"	1925-2025 0725-0825Z	ENGEBI	PRIVITT WILSON RECCO
166	218-5AUG84	0945-1053 2145-2253Z	OAK	SLATER SHINN SAMPLING
167	"	1118-1154 2318-2354Z	OAK	SLATER KINDINGER SAMPLING
168	218-5AUG84 218-219 5-6AUG84	1237-1337 0037-0137Z	OAK	SLATER HUDSON SAMPLING
169	218-5AUG84 219-6AUG84	2015-2150 0815-0950Z	ENGEBI	PRIVITT JOHNSON RECCO
170	219-6AUG84 219-220 6-7AUG84	1000-1230 2200-0030Z	OAK	SLATER HALLEY TV
171	219-6AUG84 220-7AUG84	1309-1344 0109-0144Z	OAK	SLATER HALLEY SAMPLING
172	"	1405-1440 0205-0240Z	OAK	PRIVITT JOHNSON SEARCH FOR SAMPLE BAG
173	"	1455-1535 0255-0335Z	OAK	SLATER HALLEY SAMPLING
174	"	1551-1636 0351-0436Z	OAK	SLATER HALLEY SAMPLING

DIVE no.	JULIAN DAY- Local Date/ Greenwich Date	TIME Local/ G.m.t.(Z)	LOCATION	DESCRIPTION Pilot Observer Mission
175	220-7AUG84 "	0950-1035 2150-2235Z	OAK	SLATER KINDINGER SAMPLING
176	"	1058-1123 2258-2323Z	OAK	SLATER KINDINGER SAMPLING
177	220-7AUG84 221-222 7-8AUG84	1141-1230 2341-0030Z	OAK	SLATER KINDINGER SAMPLING
178	220-7AUG84 221-8AUG84	1307-1343 0107-0143Z	OAK	SLATER KINDINGER SAMPLING
179	"	1356-1420 0156-0220Z	OAK	SLATER KINDINGER SAMPLING
180	"	1445-1520 0245-0320Z	OAK	SLATER KINDINGER SAMPLING
181	"	1506-1555 0306-0355Z	OAK	SLATER KINDINGER SAMPLING
182	"	1603-1628 0403-0428Z	OAK	SLATER KINDINGER SAMPLING
183	221-8AUG84 "	0951-1016 2151-2216Z	OAK	SLATER HUDSON SAMPLING
184	"	1031-1056 2231-2256Z	OAK	SLATER HUDSON SAMPLING
185	"	1107-1142 2307-2342Z	OAK	SLATER HUDSON SAMPLING

DIVE no.	JULIAN DAY- Local Date/ Greenwich Date	TIME Local/ G.m.t.(Z)	LOCATION	DESCRIPTION Pilot Observer Mission
186	221-8AUG84 221-222 8-9AUG84	1153-1222 2353-0022Z	OAK	SLATER HUDSON SAMPLING
187	221-8AUG84 222-9AUG84	1334-1411 0134-0211Z	OAK	SLATER HUDSON SAMPLING
188	"	1421-1446 0221-0246Z	OAK	SLATER HUDSON SAMPLING
189	"	1454-1527 0254-0327Z	OAK	SLATER HUDSON SAMPLING
190	"	1546-1620 0346-0420Z	OAK	SLATER HUDSON SAMPLING
191	"	1636-1701 0436-0501Z	OAK	SLATER HUDSON SAMPLING
192	222-9AUG84 "	1004-1034 2204-2234Z	OAK	SLATER KINDINGER SAMPLING
193	"	1054-1124 2254-2324Z	OAK	SLATER KINDINGER SAMPLING
194	222-9AUG84 222-223 9-10AUG84	1141-1211 2341-0011	OAK	SLATER KINDINGER SAMPLING
195	222-9AUG84 223-10AUG84	1235-1300 0035-0100Z	OAK	SLATER KINDINGER SAMPLING
196	"	1319-1342 0119-0142Z	OAK	SLATER KINDINGER SAMPLING

DIVE no.	JULIAN DAY- Local Date/ Greenwich Date	TIME Local/ G.m.t.(Z)	LOCATION	DESCRIPTION Pilot Observer Mission
197	"	1359-1415 0159-0215Z	OAK	SLATER KINDINGER SAMPLING
198	"	1429-1448 0229-0248Z	OAK	SLATER KINDINGER SAMPLING
199	"	1504-1524 0304-0324Z	OAK	SLATER KINDINGER SAMPLING
200	"	1535-1615 0335-0415Z	OAK	SLATER KINDINGER SAMPLING
201	"	1630-1700 0430-0500Z	OAK	PRIVITT PAROLSKI RECCO
202	223-10AUG84 "	1000-1046 2200-2246Z	OAK	SLATER HALLEY TV
203	"	1104-1124 2304-2324Z	OAK	SLATER HALLEY TV
204	223-10AUG84 224-11AUG84	1220-1300 0020-0100Z	OAK	PRIVITT HALLEY

Chapter G

Preliminary Analyses of OAK Debris Samples

By R. B. HALLEY, R. P. MAJOR, K. R. LUDWIG,
Z. L. PETERMAN, and R. K. MATTHEWS

U.S. GEOLOGICAL SURVEY BULLETIN 1678

SEA-FLOOR OBSERVATIONS AND SUBBOTTOM SEISMIC CHARACTERISTICS OF OAK AND KOA CRATERS, ENEWETAK ATOLL, MARSHALL ISLANDS

CONTENTS

FIGURES

TABLES

Chapter G
Preliminary Analyses of OAK Debris Samples

By R. B. Halley[1], R. P. Major[1], K. R. Ludwig[2], Z. L. Peterman[2], *and* R. K. Matthews[3]

INTRODUCTION

Purpose

The OAK event produced debris that lies on the reef plate and on the lagoon floor around the crater. In this pilot effort, we are attempting to ascertain, within narrow limits, which subsurface horizons were the sources of the debris samples. To do this, we have correlated physical and chemical properties of debris samples recovered in the lagoon (fig. 1) with those of samples recovered from EXPOE (Exploratory Program on Enewetak) hole XEN–3, drilled on the south shore of Enjebi (Janet) Island (see fig. 9d, Couch and others, 1975), and with samples recovered from hole KAR–1 (see chap. D, fig. 2, this volume) drilled during 1985 south of KOA crater as part of the second phase of this program.

METHODS

We take several approaches to correlating the debris samples with samples from the core borings. These approaches include assessment of lithology and petrography and analyses of cathodoluminescene characteristics, trace elements, carbon and oxygen isotopes, and strontium isotopes. Most of these methods require samples having distinctive characteristics that can be correlated with specific strata found in the drill holes. The last two techniques rely on known temporal changes and can supply independent measures of age.

The locations of bottom samples collected in OAK crater are shown in figure 1. Preliminary data concerning the samples are presented in table 1. Pleistocene or older rocks were found at 21 of 59 sample sites. Pleistocene and older sediments as used here indicate strata that have been mineralogically altered in freshwater prior to and during a lowering of sea level about 18,000 years ago. Presently, except for crater areas, Pleistocene and older rocks are not exposed at the surface of the atoll and are generally covered by 10 to 20 m (33–66 ft) of younger sediments. Recovery of such rocks at the sea floor indicates that they have been transported from the subsurface during cratering and are probably debris or ejecta. Some of this material may have been airborne (ejecta), but we shall use the more inclusive term, debris.

In the lagoon, debris occurs as close as 300 m (984 ft) and as far as 640 m (2,100 ft) from ground zero at OAK; most was found at distances greater than 350 m (1,150 ft). It is not known to what degree this material has been redistributed by currents or waves.

About 80 percent of the samples consist of coral fragments that are not distinct from each other or from coral recovered from numerous horizons in core borings. The remaining 20 percent of the samples consist of a variety of limestone clasts that are more distinctive in their lithologic and geochemical character and therefore may be correlatable with sediments cored near the blast area. No sampling was conducted in KOA because debris in the area could have come from other nearby events.

LITHOLOGY

On the basis of the limestone classification of Dunham (1962), most of the limestone debris are packstones and wackestones. Three samples were grainstones. Typical debris limestones are shown in figure 1. They are commonly well lithified, and some show features, such as brown discoloration and vuggy porosity, associated with prolonged subaerial exposure during times of lowered sea level.

Debris was initially compared to cores from hole XEN–3 acquired during the EXPOE project (Couch and others, 1975; Ristvet and others, 1978) and from core KAR–1 acquired during the second phase of this study near KOA crater. Better correlations obviously can be made with samples from cores nearer OAK crater; such cores presently are being analyzed but are not yet available.

Most of the debris samples are well-lithified limestones. In the cores examined thus far, similar limestones occur primarily at solution unconformities (Couch and others, 1975). Many of these unconformities developed when the rocks were at the surface during periods of lowered sea level. Several of them are correlative, some as shallow as 7 m (23 ft) below the sediment surface in the OAK area. At KAR–1, which is about 12 km (6.5 nmi) from OAK

[1]U.S. Geological Survey, Branch of Oil and Gas Resources, Denver, Colo. 80225.

[2]U.S. Geological Survey, Branch of Isotope Geology, Denver, Colo. 80225.

[3]Brown University, Geology Department, Providence, R.I. 02912.

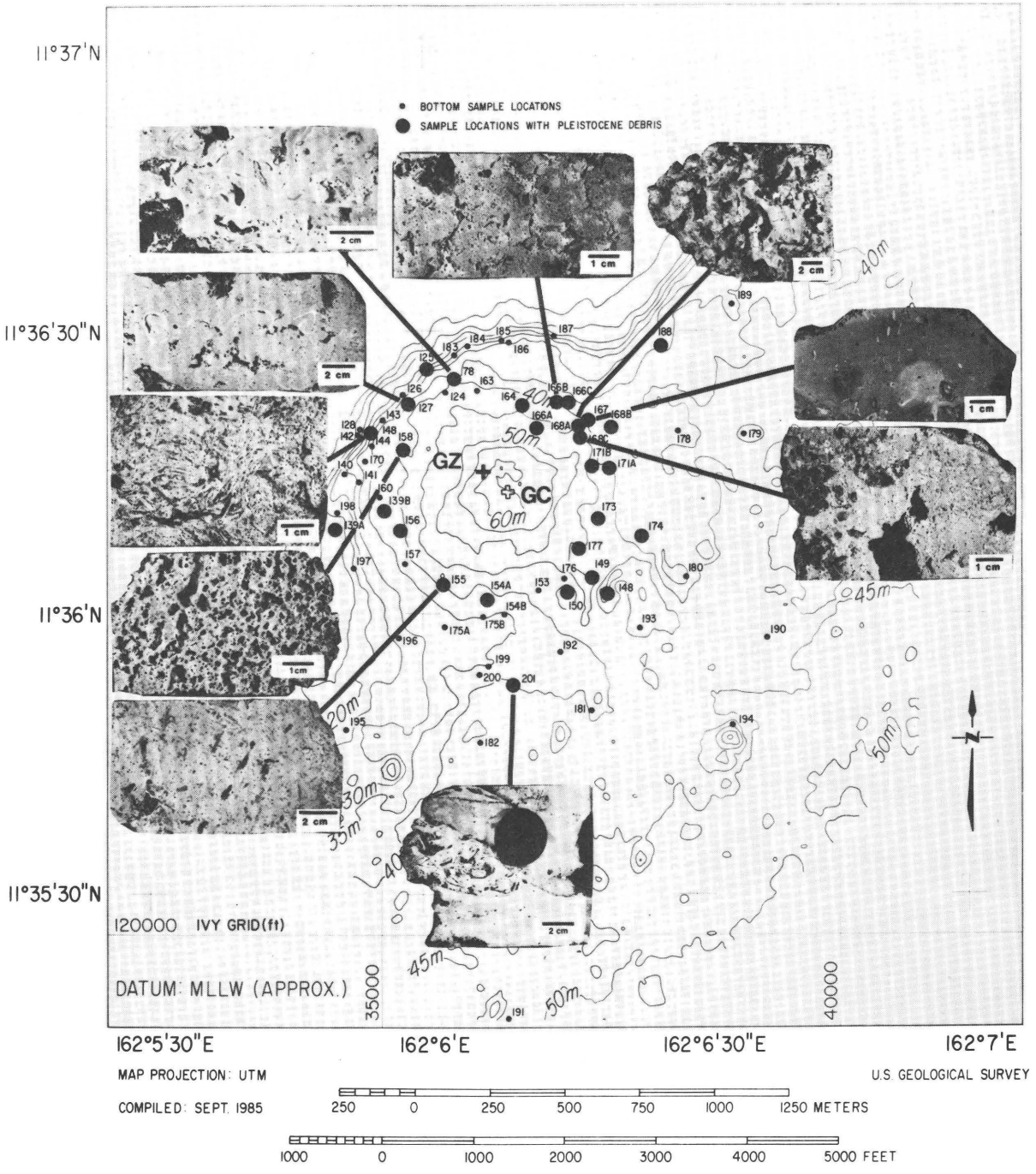

Figure 1. Debris sample locations and bathymetry in OAK crater with photographs showing lithology of Pleistocene or older limestones. Sample from locality 158 is a grainstone with most grains dissolved during alteration in fresh water. All other samples are packstones and wackestones in the terminology of Dunham (1962). Examples from sites 78, 168A, and 168C illustrate vuggy porosity and brown discoloration suggesting alteration at a solution unconformity. GZ=ground zero; GC=geometric center. Contour interval is 5 m.

ground zero, the uppermost horizons are not as well lithified as the debris samples. Presumably, much of the debris sampled around OAK comes from deeper horizons which, at KAR–1, lie about 20 to 30 m (66–100 ft) below bottom.

Some of the petrographic variations in debris are shown in figure 2. One sample exhibits bright luminescent bands of calcite cement (fig. 2*F*) which should be easy to recognize if it is present in core samples.

Table 1. Preliminary data on bottom samples from OAK crater

[Sample sites are shown in figure 1; samples combined at sites are noted with letter (A,B,C). X=Pleistocene age or older; N=age not determined. ---, no thin-section prepared and no coral or rock fragments recovered]

Sample site	Navigational fix	No. of samples	No. of thin sections	No. of coral fragments	No. of rock fragments	Pleistocene age
78	1622	7	6	6	1	X
124	1912	1	1	1	---	N
125	1915	6	8	4	2	N
126	1918	17	9	15	2	N
127	1921	11	5	4	7	X
128	1926	17	10	5	11	N
139	2329	3	1	3	---	X
140	2339	1	1	1	---	N
141	2343	1	1	1	---	N
142	2348	1	1	1	---	N
143	2351	7	2	7	---	N
144	2355	1	2		1	N
148	2481	4	4	3	1	X
149	2488	5	4	3	2	Probable X
150	2504	3	2	3	---	X
153	2518	4	3	4	---	N
154A	2521	4	4	4	---	X
154B	2525					
155	2527	6	5	6	---	X
156	2536	4	5	2	2	X
157	2539	5	3	5	---	N
158	2546	1	2		1	X
160	2549	4	1	4	---	N
163	2551	5	1	5	---	N
164	2558	5		5	---	Probable X
166A	2565	6	3	5	1	X
166B	2561					
166C	2560 (gravel)					

Table 1. Preliminary data on bottom samples from OAK crater—*Continued*

[Sample sites are shown in figure 1; samples combined at sites are noted with letter (A,B,C). X=Pleistocene age or older; N=age not determined. ---, no thin-section prepared and no coral or rock fragments recovered]

Sample site	Navigational fix	No. of samples	No. of thin sections	No. of coral fragments	No. of rock fragments	Pleistocene age
167	2569	3	3	3	---	X
168A	2571	7	5	4	3	X
168B	2575					
168C	2573					
170	2630	2	---	2	---	N
171A	2694	5	4	5	---	X
171B	2691					
173	2698	6	2	6	---	X
174	2701	4	3	3	1	X
175A	2703	3	1	3	---	N
175B	2707					
176	2714	3	1	3	---	N
177	2721	1			1	X
178	2725	4	2	4	---	N
179	2729	5	2	5	---	N
180	2736	9	3	9	---	N
181	2742	5	2	5	---	N
182	2745	2	---	1	1	N
183	2749	2	1	2	---	N
184	2751	1	---	1	---	N
185	2756	1	---	1	---	N
186	2764	3	---	3	---	N
187	2869	5	1	5	---	N
188	2772	3	2	2	1	Probable X
189	2774	2	---	2	---	N
190	2780	2	1	2	---	N
191	2784	2	---	2	---	N

Table 1. Preliminary data on bottom samples from OAK crater—*Continued*

[Sample sites are shown in figure 1; samples combined at sites are noted with letter (A,B,C). X=Pleistocene age or older; N=age not determined. ---, no thin-section prepared and no coral or rock fragments recovered]

Sample site	Navigational fix	No. of samples	No. of thin sections	No. of coral fragments	No. of rock fragments	Pleistocene age
192	2787	1	1	1	---	N
193	2791	8	4	7	1	N
194	2797	4	1	4	---	N
195	2803	3	3	3	---	N
196	2809	2	3	2	---	N
197	2812	1	2	1	---	N
198	2814	5	5	4	1	N
199	2821	3	3	3	---	N
200	2824	3	2	3	---	N
201	2827	1	1	1	---	X
125	1915	6	8	4	2	X
Total		246	160	203	42	
				Coral: rock = About 5/1		

TRACE ELEMENTS AND STABLE ISOTOPES OF CARBON AND OXYGEN

In core XEN–3, 175 samples were analyzed for magnesium, strontium, iron, and manganese as well as for carbon and oxygen-isotope ratios. These data are presented in table 2 and in figures 3 and 4. Analyses for the same elements in 10 debris samples are presented in table 3.

Some of these measurements can be used to estimate the preevent depth of debris samples. First, magnesium values of 1 percent or greater are limited to depths of less than 16 m (52 ft) in hole XEN–3 (fig. 3). Two selected debris samples (table 3, sites 125B, 147) have magnesium values that suggest that they are from this interval. Second, samples with $\delta^{18}O$ of less than -3.75 occur deeper than 14 m (46 ft) in XEN–3 (fig. 4), and seven debris samples have $\delta^{18}O$ less than -3.75 (table 3). Third, samples with $\delta^{13}C$ less than -5.0 are not found above 67 m (220 ft) (fig. 4), and two debris samples have $\delta^{13}C$ less than -5.0 (table 3). These data suggest that a geochemical profile of a core near OAK may provide the basis for estimating the original depth of debris samples. Further statistical analyses of these data combined with mineralogical analyses will establish the reliability of such correlations.

Several of the debris samples have uncommonly negative values for both oxygen and carbon, as may be expected from rock samples that originate near subaerial exposure horizons (Allen and Matthews, 1982). These isotopic analyses support lithologic inferences that debris samples may be derived from well-lithified limestones at or near solution unconformities.

STRONTIUM ISOTOPY AND PALEONTOLOGICAL STUDIES

A continuously changing, unidirectional marker during the Tertiary that left a record in OAK debris samples can be used to establish age and original depth of debris much more precisely than the comparative methods described above. Two such markers exist—one provided by the ratio of strontium isotopes 87 and 86 in marine carbonates, a ratio that has increased steadily through the time interval represented by OAK debris, and the other provided by evolutionary changes of organisms.

Paleontologic study of Enewetak material presently is focused on establishing a zonation in reference cores and documenting the disruption of this zonation in crater and

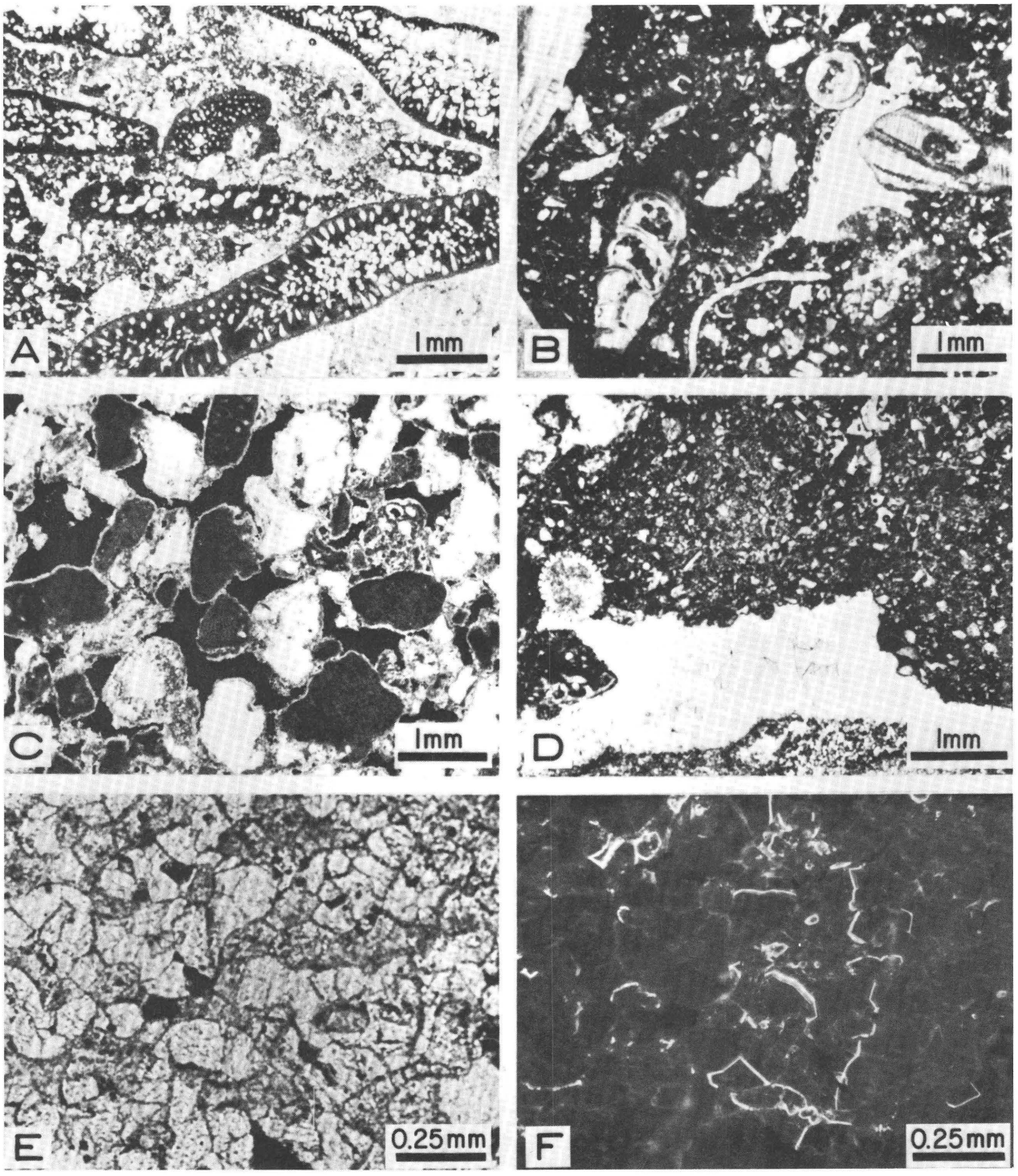

Figure 2. Photomicrographs showing petrographically distinct limestones from OAK debris samples. *A*, Algal (*Halimeda*) packstone. *B*, Mollusk (gastropod and bivalve) wackestone. *C*, Coral and algal grainstone. *D*, Echinoderm packstone with calcite-filled vugs. *E*, calcite cement in plain light. *F*, same as *E* during cathodoluminescence showing bright luminescent zones.

Table 2. Geochemical characteristics of samples from core XEN–3

[---, no data; ppm, parts per million]

Depth of sample (ft)	Depth of sample (m)	Mg (%)	Sr (ppm)	Fe (%)	Mn (ppm)	$\delta^{18}O$	$\delta^{13}C$
10	3.04	1.8	5,600	0.02	6.0	−1.94	2.13
11.3	3.44	1.9	5,100	.04	7.0	−2.81	1.50
18	5.48	2.3	4,100	.10	13.0	−2.67	.98
20	6.09	2.2	4,700	.09	10.0	−2.53	1.27
22.5	6.85	.33	7,500	.02	<4.0	−2.84	.21
24.5	7.46	.51	7,300	.01	5.0	−3.28	.39
27.5	8.38	---	---	---	---	−2.12	1.43
28.4	8.65	.73	7,200	<.005	<4.0	−3.57	.50
33	10.0	1.0	6,700	.05	6.0	---	---
40	12.1	.66	7,200	.03	<4.0	−3.38	.34
47.7	14.5	.36	7,600	.05	8.0	−3.00	−.08
48	14.6	2.0	4,500	.27	44.0	−2.88	.99
51.7	15.7	.48	5,100	.01	5.0	−4.41	−.54
53.8	16.3	.36	5,100	.04	9.0	−4.72	−.64
54.7	16.6	.57	5,200	.07	12.0	−3.86	−.19
57.1	17.4	.51	4,800	<.005	<4.0	−4.94	.11
57.5	17.5	.42	5,200	.01	<4.0	3.67	.68
58.5	17.8	.59	3,700	<.005	<4.0	−4.89	−.15
59.5	18.1	.67	3,100	.007	<4.0	−5.29	−.61
60.8	18.5	.62	3,200	.03	7.0	−4.53	−1.18
63	19.2	.51	4,200	.02	6.0	−4.46	.01
63.7	19.4	.43	4,500	.02	6.0	−4.17	−.41
64	19.5	.49	4,000	.02	6.0	−4.62	−.27
64.5	19.6	.54	4,400	.05	11.0	−4.33	−.05
64.7	19.7	.23	5,900	.005	<4.0	−3.90	−1.75
66	20.1	.46	3,900	.02	5.0	−4.37	−1.03
67.7	20.6	.47	4,500	.06	10.0	−4.36	−.26
68.7	20.9	.71	2,700	.05	12.0	−5.96	−.99
70.4	21.4	.22	7,400	.01	<4.0	−2.54	1.84
72.1	21.9	.41	5,000	.02	5.0	−3.97	.26
73.3	22.3	.38	5,600	.03	7.0	−4.00	.52
75	22.8	.34	4,900	.005	<4.0	−3.77	.26
76.2	23.2	.57	4,200	.4	10.0	−4.82	−.53
76.5	23.3	.54	2,100	.01	5.0	−5.63	−1.70
77.8	23.7	.33	5,500	.01	<4.0	−4.14	−1.38
79.7	24.2	.43	3,700	.01	5.0	−4.74	−1.59
80.8	24.6	.57	2,900	.02	6.0	−4.70	−1.81
82	24.9	.50	3,800	.02	6.0	−4.68	−1.76
82.5	25.1	---	---	---	---	−4.62	−1.90
82.8	25.2	.63	2,500	.02	7.0	−4.68	−2.35
84.8	25.8	.33	6,200	.02	4.0	−4.58	−.71
86	26.2	.57	4,200	.03	8.0	−5.19	−.86
87	26.5	.55	3,900	<.005	<4.0	−4.56	−.29
88	26.8	.36	5,900	.007	<4.0	−3.87	−.07
89	27.1	.23	6,900	.01	<4.0	−4.30	−1.15
89.5	27.2	.76	3,100	.03	8.0	−4.88	−1.41
89.8	27.3	.68	4,000	.07	12.0	−3.96	.13
91.4	27.8	.72	3,600	.02	5.0	−4.41	−.17
92.8	28.2	.59	3,600	.01	<4.0	−4.44	−.52
93.3	28.4	.71	3,500	.02	5.0	−4.17	−.41
94.5	28.8	.54	4,200	.01	<4.0	−4.16	−.27
95.8	29.1	---	---	---	---	−3.81	.09
96.8	29.5	0.31	6,500	0.02	<4.0	−4.49	−.79
98.3	29.9	.60	4,300	.007	<4.0	−3.82	.25
100	30.4	.62	4,100	.04	6.0	−4.25	−.26
100.2	30.5	---	---	---	---	−3.68	.28
103.5	31.5	.50	5,000	<.005	<4.0	−4.61	−.58
104.5	31.8	.62	3,900	.007	<4.0	−4.72	−.28
107.2	32.6	.48	6,400	.06	10.0	−3.61	.16
108.1	32.9	.62	4,300	.03	5.0	−4.09	−.17
110.2	33.5	.55	4,900	.02	<4.0	−4.44	.24
111.2	33.8	.57	4,500	.007	<4.0	−4.39	.15
113	34.4	.52	5,000	.007	<4.0	−4.20	.69
113.7	34.6	.54	4,700	.009	<4.0	−4.21	.25
113.9	34.7	.58	4,400	.04	6.0	−4.23	−.01
114.1	34.7	.28	6,800	<.005	<4.0	−3.71	−.06
114.2	34.8	.40	6,100	.02	4.0	−3.55	.31
115.6	35.2	.45	4,100	.007	<4.0	−3.56	1.24
116.1	35.3	.84	2,800	.01	<4.0	−4.67	.45
118.1	35.9	.63	4,400	.08	12.0	−3.80	.53
120	36.5	.62	4,900	.07	10.0	−3.59	.41
122.9	37.4	.66	4,000	.007	<4.0	−4.62	.20
124	37.7	.54	4,200	.007	<4.0	−4.46	.02
126.6	38.5	.59	4,600	.02	5.0	−4.09	.23
128.3	39.1	.21	7,200	<.005	<4.0	−3.10	1.30
130.2	39.6	.57	4,200	.02	<4.0	−4.50	.14
131.2	39.9	.59	4,700	.03	4.0	−3.94	.48
132.0	40.2	.55	4,900	.007	<4.0	−4.22	.21
132.6	40.4	---	---	---	---	−3.09	.22
133.4	40.6	.37	2,400	.008	4.0	−5.15	−2.01
134.5	40.9	.18	7,700	.02	<4.0	−3.06	−.25
135.8	41.3	.53	4,600	.008	<4.0	−3.84	.46
137.2	41.8	.55	4,200	<.005	<4.0	−4.18	.59
140	42.6	.51	4,700	.008	<4.0	−3.93	.64
141.9	43.2	.44	4,400	.02	<4.0	−3.53	−.84
143.7	43.7	.45	3,500	.02	<4.0	−4.64	−1.65
145.4	44.3	.60	3,500	.02	<4.0	−5.06	−1.07
147.6	44.9	.50	4,200	.01	<4.0	−4.56	−.81
149.3	45.5	.37	5,500	.01	<4.0	−3.72	.12
151.2	46.0	.33	6,100	.02	<4.0	−3.88	.64
152.2	46.3	.56	4,700	.07	13.0	−4.40	−.46
153.5	46.7	.68	5,200	.16	26.0	−3.78	.22
155.3	47.3	.42	4,900	.03	5.0	−4.54	−.11
157.3	47.9	.28	6,500	.02	<4.0	−3.20	−.12
158.9	48.4	.38	5,200	.01	4.40	−3.49	.16
162.0	49.3	.39	5,800	.008	<4.0	−3.16	1.07
163.9	49.9	.42	4,900	.008	4.0	−4.34	−1.13
165.8	50.5	.25	5,300	<.005	<4.0	---	---
167.0	50.9	.28	4,400	.01	<4.0	−4.51	−1.16
169.8	51.7	.22	4,900	.008	<4.0	−4.49	−1.74
170.6	51.9	.32	5,800	.01	<4.0	−3.03	.02
172.1	52.4	.41	2,400	.02	4.0	−5.45	−1.83
174.7	53.2	.32	4,900	.008	<4.0	−4.25	−2.43
176.0	53.6	.44	4,900	.03	6.0	−3.72	−.86
178.8	54.4	.29	5,200	.02	6.0	−4.30	−2.17

Table 2. Geochemical characteristics of samples from core XEN–3—*Continued*

[---, no data; ppm, parts per million]

Depth of sample (ft)	Depth of sample (m)	Mg (%)	Sr (ppm)	Fe (%)	Mn (ppm)	$\delta^{18}O$	$\delta^{13}C$
180.7	55.0	0.34	5,800	0.01	<4.0	−3.44	−0.09
181.6	55.3	0.38	5,100	0.02	5.0	−3.56	−0.35
82.3	55.5	0.32	4,300	<0.005	<4.0	−4.32	−2.40
184.9	56.3	0.37	5,400	<0.005	<4.0	−4.16	−1.05
186.9	56.9	0.19	5,500	0.01	<4.0	−4.08	−2.21
189.8	57.8	0.25	5,600	0.01	<4.0	---	---
191.3	58.3	0.30	3,800	0.01	<4.40	−4.75	−2.19
192	58.5	---	---	---	---	−4.80	−0.59
193	58.8	---	---	---	---	−4.21	−2.07
195	59.4	---	---	---	---	−4.91	−3.25
195.8	59.6	---	---	---	---	−4.81	−4.22
196.5	59.8	---	---	---	---	−3.37	−0.78
197	60.0	0.24	4,400	0.02	<4.0	−5.25	−3.11
197R	0	---	---	---	---	−4.47	−1.97
200	60.9	0.41	3,800	0.07	10.0	−4.53	−2.50
205.1	62.5	0.47	4,100	0.008	<4.0	−4.79	−0.62
208	63.3	---	---	---	---	−4.79	−0.67
209	63.7	---	---	---	---	−4.62	−1.76
210	64.0	---	---	---	---	−5.08	−1.54
211	64.3	---	---	---	---	−5.69	−0.25
212	64.6	---	---	---	---	−5.57	−0.38
213	64.9	0.47	3,900	0.04	8.0	---	---
213.2	64.9	---	---	---	---	−4.90	−0.89
214.0	65.2	0.38	4,100	<0.005	<4.0	−4.66	−0.49
217.2	66.2	0.45	4,100	0.008	<4.0	−5.24	0.05
218.3	66.5	0.35	4,400	0.02	<4.0	−4.81	0.03
220.6	67.2	---	---	---	---	−4.86	−0.18
222	67.6	---	---	---	---	−4.46	−1.04
223	67.9	---	---	---	---	−5.64	−5.67
223.2	68.0	---	---	---	---	−6.45	−7.11
223.5	68.1	---	---	---	---	−5.50	−7.71
224	68.2	---	---	---	---	−3.47	−1.15
76.5	23.3	.54	2,100	.01	5.0	−5.63	−1.70
225	68.5	---	---	---	---	−4.46	−2.36
228.3	69.5	---	---	---	---	−3.97	1.54
229.3	69.8	.53	3,100	.04	5.0	−4.31	−2.86
230.4	70.2	.59	3,800	.02	4.0	−4.62	−1.32
232	70.7	.54	4,300	.01	<4.0	−5.02	−1.32
234	71.3	.54	4,200	<.005	<4.0	−4.32	−1.06
235.3	71.7	.50	4,300	.02	<4.0	−4.55	−2.20
237.3	72.3	.37	5,000	.02	<4.0	−4.11	−2.20
239.6	73.0	.44	4,700	.007	<4.0	−4.43	−1.17
241.6	73.6	.50	3,800	.008	<4.0	−4.56	−1.63
243.2	74.1	.25	4,400	.005	<4.0	−4.49	−2.21
245.2	74.7	.27	4,200	.04	4.0	−4.48	−2.07
247.0	75.2	.24	5,000	.04	<4.0	−4.97	−2.04
249.0	75.8	---	---	---	---	−4.35	−1.76
249.9	76.1	---	---	---	---	−5.71	−8.12
251	76.5	---	---	---	---	−4.01	−2.48
251.8	76.7	.31	1,400	<.005	<4.0	−5.61	−5.12
252.7	77.0	.29	570	.04	<4.0	−5.97	−6.69
261.3	79.6	.19	6,500	.02	<4.0	−5.12	−3.34
263.3	80.2	.49	3,300	.008	<4.0	−5.29	−2.49
264.7	80.6	0.53	3,400	0.01	<4.0	−4.92	−1.83
268.6	81.8	.36	3,900	.007	<4.0	−4.18	−2.25
271.1	82.6	.21	3,400	<.005	<4.0	−5.19	−2.98
273.1	83.2	.22	3,600	.03	<4.0	−4.45	−2.24
274.9	83.7	.46	4,100	.02	<4.0	−4.55	−3.00
275	83.8	.12	7,700	.02	<4.0	−4.10	−.97
276.3	84.2	.51	2,800	.008	<4.0	−5.32	−4.15 (suspect)
276.6	84.3	.22	2,700	.02	<4.0	---	---
278.1	84.7	.69	3,100	.02	<4.0	−4.70	−2.98
280.8	85.5	.62	3,200	.02	<4.0	−4.40	−2.02
283	86.2	.66	2,900	.02	<4.0	−4.93	−2.86
284.1	86.5	.45	3,400	<.005	<4.0	−4.58	−3.29
286.3	87.2	.39	4,800	.02	<4.0	−3.93	−1.68
288.1	87.8	.92	3,800	.30	43	−3.65	−1.23
293.2	89.3	.30	6,200	.04	<4.0	−4.01	−1.38
296.5	90.3	.54	3,600	.01	<4.0	−5.89	−1.93

transition cores. A few of the debris samples contain enough characteristic microfossils to place them within this biostratigraphic zonation.

Table 4 presents data from analyses of 21 debris samples from OAK crater. Sr isotope analyses are given as epsilon-Sr, which is defined as

$$\text{Epsilon-Sr} = \left(\frac{(^{87}Sr/^{86}Sr)\ \text{sample}}{(^{87}Sr/^{86}Sr)\ \text{modern seawater}} - 1 \right) \times 10^4$$

The $^{87}Sr/^{86}Sr$ of seawater is taken from a modern clam shell from Enewetak. Similarly, calculated epsilon units from the data of DePaolo and Ingram (1985) indicate a rate of change of −0.524 epsilon units per million years (fig. 5). Using this relation, an age may be estimated for each debris sample (table 4).

Analyses of samples from KAR–1 have allowed us to construct a profile of epsilon-Sr for the core (fig. 6). The original depth of debris samples may be estimated by comparing epsilon-Sr of debris with the KAR–1 profile. A similar profile should be constructed for a core near OAK crater as soon as analyses are available.

Figure 3 (above right). Strontium and magnesium profiles for core XEN–3. (See table 2.)

Figure 4 (below right). Oxygen and carbon isotope profiles for core XEN–3. (See table 2.)

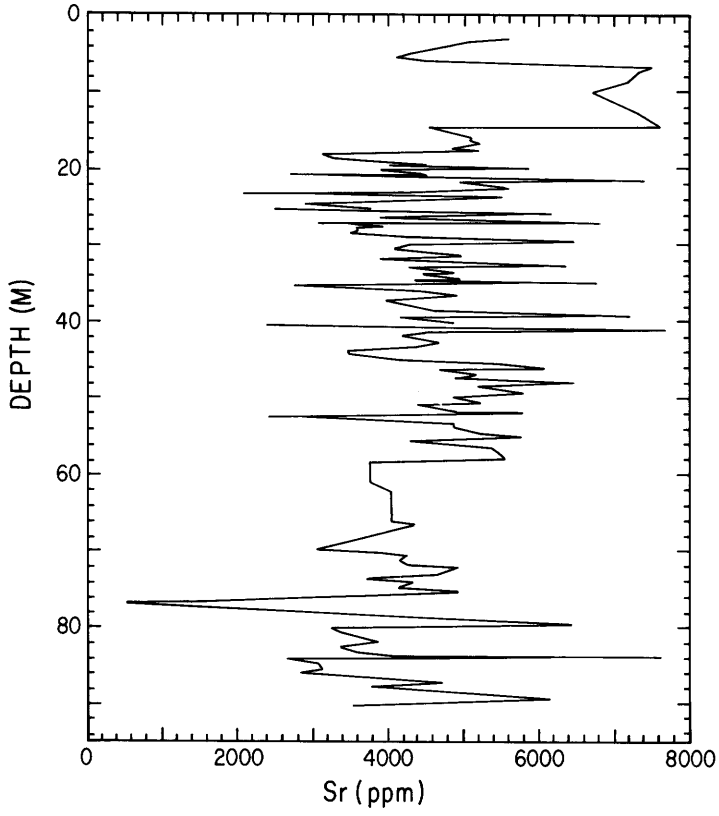
DEPTH (M)
0
20
40
60
80
0
2000
4000
6000
8000
Sr (ppm)

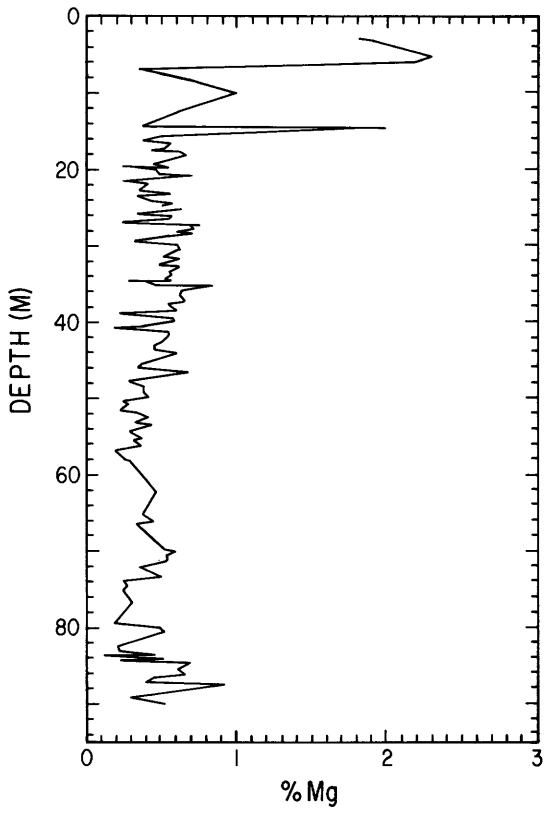
DEPTH (M)
0
20
40
60
80
0
1
2
3
%Mg

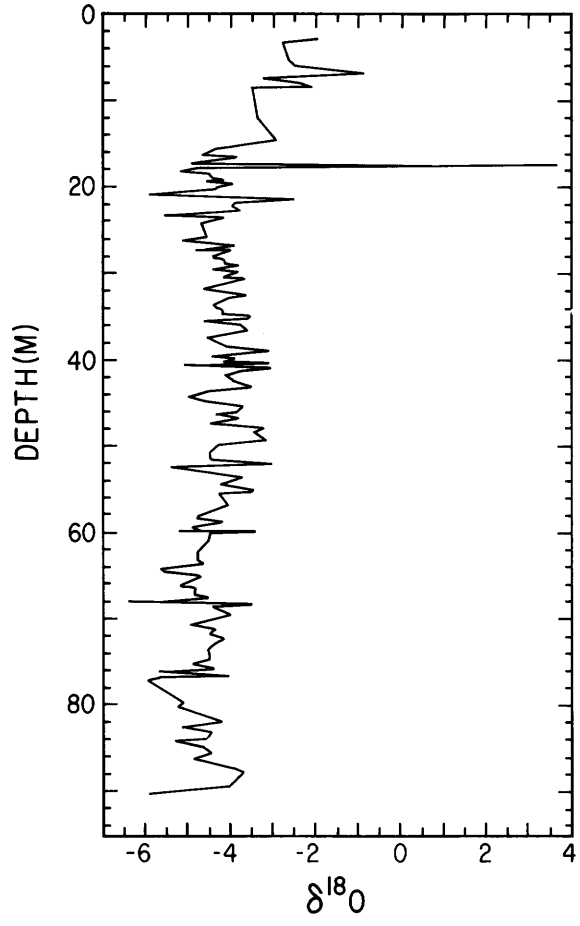
DEPTH(M)
0
20
40
60
80
-6
-4
-2
0
2
4
δ18O

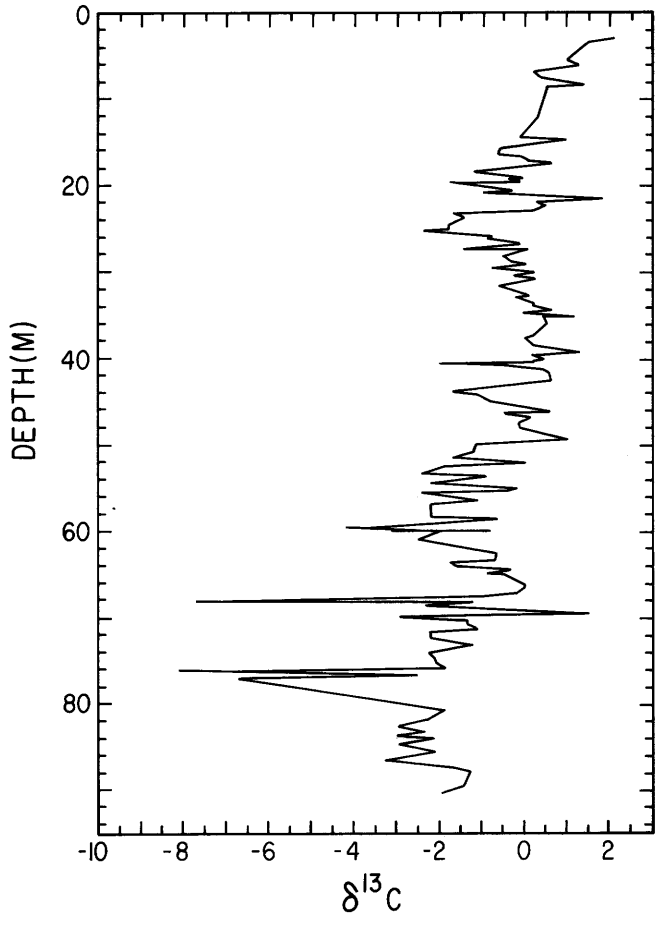
DEPTH(M)
0
20
40
60
80
-10
-8
-6
-4
-2
0
2
δ13C

Table 3. Chemical and isotopic analyses of selected OAK debris samples

[Sample sites are shown in figure 1; ppm, parts per million]

Sample site	Mg (%)	Sr (ppm)	Fe (%)	Mn (ppm)	$\delta^{18}O$	$\delta^{13}C$
78	0.35	520	0.008	<4.0	−6.16	−5.83
125B	4.9	1,600	.02	6.0	−0.86	2.55
125A	.38	1,500	.008	<4.0	−5.94	−6.28
127	.15	7,900	.01	<4.0	−1.48	+1.95
147	1.0	5,500	.005	<4.0	−3.40	+1.08
156	.36	4,800	.008	<4.0	−3.94	.58
158	.47	1,600	.008	<4.0	−4.87	−1.92
166B	.44	990	<.005	<4.0	−5.05	−3.42
168A	.40	3,000	<.005	<4.0	−5.08	−3.59
201	.33	2,300	.008	<4.0	−4.49	−0.74

The depth distribution of 21 OAK debris samples is shown in figure 7. The distribution suggests that the majority of samples fall in the depth range of 30 to 60 m (100–200 ft). With proper calibration, debris samples can probably be located to within ±6 m (20 ft) of their original depth.

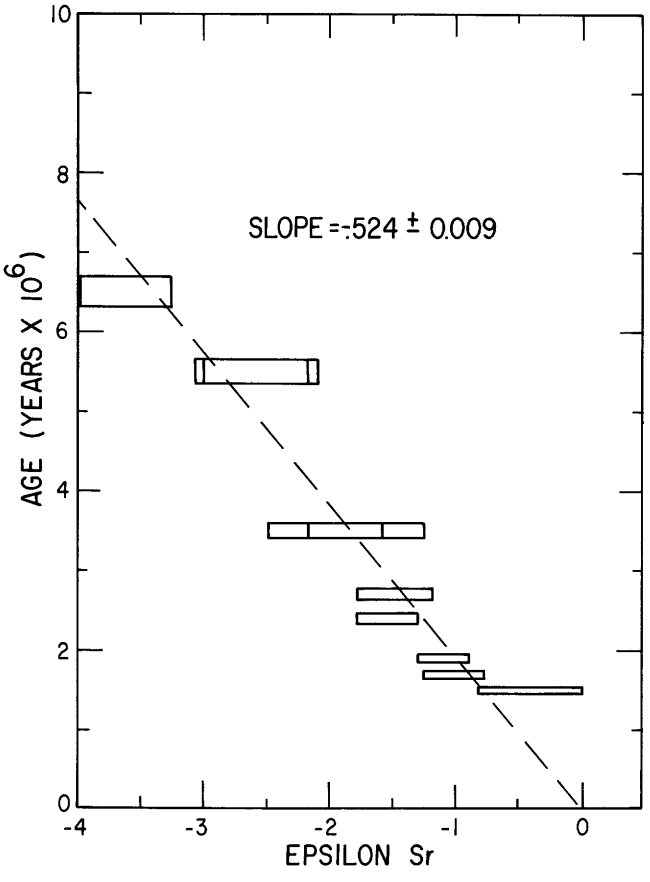

Figure 5. Rate in change of strontium isotope ratio in seawater during the last 8 million years, based on eight analyses of DePaolo and Ingram (1985), for core KAR–1. Columns indicate analytical error.

CONCLUSION

Of the various techniques used to analyze OAK debris, recent advances in Sr isotope analyses offer most promise for establishing original depths of samples. Analyses of error indicate that epsilon-Sr may be measured to within ±0.2 and perhaps to within ±0.1 units, resulting in an age estimate to within ±100,000 to ±200,000 years and a depth estimate within roughly ±6 m (20 ft).

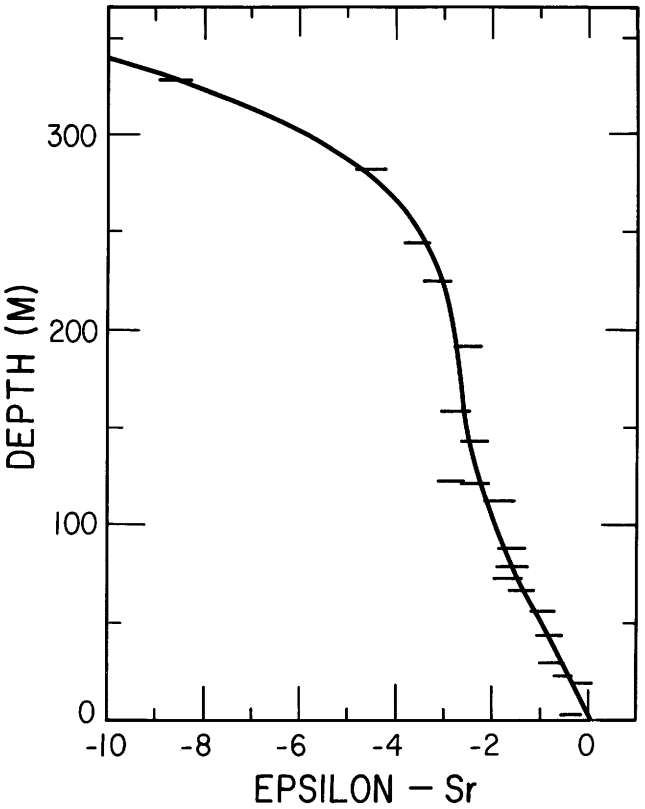

Figure 6. Change in seawater strontium during the last 8 million years, from data published by DePaolo and Ingram (1985). Horizontal bars show analytical error.

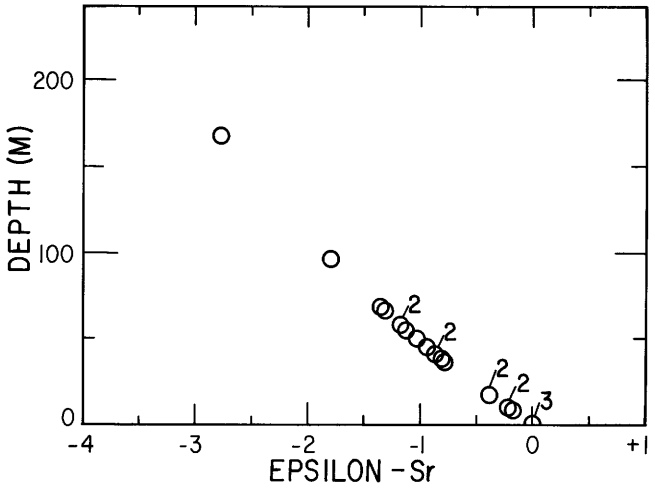

Figure 7. Depth estimates for OAK debris samples using KAR–1 for calibration. Each open circle represents one data point except where more (2, 3) are indicated.

Table 4. Strontium analyses from OAK crater debris samples

Sample sites are shown in figure 1.

Epsilon-Sr is defined as the difference, in parts per 10,000, between the $^{87}Sr/^{86}Sr$ ratio of the sample to the $^{87}Sr/^{86}Sr$ ratio of a modern clamshell standard.

The calculated age is based on DePaolo's data (DePaolo and Ingram, 1985) for late Tertiary carbonates, which indicate a rate of change of 0.524 epsilon units per million years. The calculated depth is based on the relationship we observed for preliminary data on samples from undisturbed core KAR–1, and has an uncertainty of roughly 15 m (50 ft).

Sample site	Epsilon −Sr	Age (Ma)	Estimated preevent depth below sea floor	
			(m)	(ft)
125A --------	−1.18±.15	2.25 ±.28	58	190
125C --------	−.4 ±.13	.76 ±.24	18	58
150 ----------	−.39±.15	.74 ±.28	17	57
158 ----------	−1.32±.14	2.51 ±.26	66	216
166B --------	−2.78±.18	5.3 ±.34	167	547
166C --------	−.82±.18	1.56 ±.34	38	126
167A --------	−.95±.2	1.81 ±.38	45	148
168A --------	−.87±.18	1.66 ±.34	41	134
168C --------	−1.8 ±.24	3.43 ±.45	96	314
171A --------	−1.13±.23	2.15 ±.43	55	180
171BD ------	−1.04±.16	1.98 ±.3	50	164
171(5) ------	−.88±.16	1.67 ±.3	41	136
173B --------	−.78±.15	1.48 ±.28	36	119
174 ----------	−1.18±.15	2.25 ±.28	58	190
174(1) ------	−1.36±.14	2.59 ±.26	68	224
178 ----------	.15±.16	−.29 ±.3	0	0
179 ----------	.16±.14	−.31 ±.26	0	0
180D --------	−.22±.15	.41 ±.28	10	32
188 ----------	−.18±.17	.335±.32	8	26
189 ----------	−.01±.12	.45 ±.22	1	3
191 ----------	−.23±.14	.43 ±.26	10	33

REFERENCES

Allen, J. R., and Matthews, R. K., 1982, Isotope signatures associated with early meteoric diagenesis: Sedimentology, v. 29, p. 797–817.

Couch, R. F., Jr., Fetzer, J. A., Goter, E. R., Ristvet, B. L., Walter, D. R., and Wendland, V. P., 1975, Drilling operations on Eniwetok Atoll during Project EXPOE: Air Force Weapons Laboratory Technical Report TR–75–216, Kirtland Air Force Base, New Mexico, 270 p.

DePaolo, D. J., and Ingram, B. L., 1985, High-resolution stratigraphy with strontium isotopes: Science, v. 227, p. 938–941.

Dunham, R. J., 1962, Classification of carbonate rocks according to depositional texture, *in* Ham, W. E., ed., Classification of carbonate rocks: American Association of Petroleum Geologists Memoir 1, p. 108–121.

Ristvet, B. L., Tremba, E. L., Couch, R. F., Jr., Fetzer J. A., Goter, E. R., Walter, D. R., and Wendland, V. P., 1978, Geologic and geophysical investigations of the Eniwetok nuclear craters: Air Force Weapons Laboratory Technical Report TR–77–242, Kirtland Air Force Base, New Mexico 87117, 298 p.

Chapter H

Scuba Observations of OAK and KOA Craters

By E.A. SHINN, J. L. KINDINGER, R. B. HALLEY, and J. H. HUDSON

U.S. GEOLOGICAL SURVEY BULLETIN 1678

SEA-FLOOR OBSERVATIONS AND SUBBOTTOM SEISMIC CHARACTERISTICS OF OAK AND KOA CRATERS, ENEWETAK ATOLL, MARSHALL ISLANDS

CONTENTS

FIGURES

TABLE

Chapter H
Scuba Observations of OAK and KOA Craters

By E. A. Shinn[1], J. L. Kindinger[3], R. B. Halley[2], *and* J. H. Hudson[1]

INTRODUCTION

Purpose

For complete characterization of the craters, direct observations were essential, especially around the critical rim areas. Such direct observations were made by a team of scuba divers, all of whom were geologists with extensive experience in reef carbonates. The goals of the scuba team were: (1) to describe and sample the areas of the crater in waters less than 30 m (100 ft) deep; (2) to document with photographs, 16-mm movies, and color videotapes those features pertinent to the understanding of crater evolution in the marine environment; (3) to search for upturned or overturned strata which might be useful in differentiating the transient crater margin from the apparent crater margin; (4) to obtain rock cores from the reef flat and other areas not accessible by a drill ship.

Setting

Scuba diving was limited to certain areas due to such factors as water depth, water clarity, and sharks. Almost all of KOA crater could be reached within the practical 30-m (100-ft) working depth limit for scuba diving, although the lagoonward rim of OAK crater was inaccessible (chap. A, figs. 1, 7, 16, this volume). Water clarity, especially in KOA crater, was occasionally the most restrictive factor. Sharks were abundant enough to discourage scuba diving on the seaward side of the reef opposite MIKE and KOA craters, but they were not a major problem in the lagoon. The environment for diving in the lagoon was usually ideal; winds were light and sea state low.

The OAK device was fired from a barge anchored in 4 m (14 ft) of water near the reef edge (figs. 1, 2). Following the explosion, the 4-m (14 ft) contour lay about 500 m (1,640 ft) northwest of ground zero where waters had been deepened to 60 m (197 ft).

[1]U.S. Geological Survey, Branch of Oil and Gas, Fisher Island Station, Miami Beach, Fla. 33129.

[2]U.S. Geological Survey, Branch of Oil and Gas, Federal Center, Denver, Colo. 80225.

[3]U.S. Geological Survey, Branch of Atlantic Marine Geology, Fisher Island Station, Miami Beach, Fla. 33129.

Previous Work

The first intensive geologic work at Enewetak began in the late 1940's prior to nuclear testing, during Operation Crossroads. The geologic work was limited to bottom sampling with grabs and to rock coring with rotary rigs on islands and exposed reef flats. The results of that research are contained in many papers collected in U.S. Geological Survey (USGS) Professional Paper 260. Scuba diving was not yet in general use for research purposes during Operation Crossroads. Subsequently, extensive shallow coring, accomplished with a truck-mounted rotary rig, and seismic profiling were carried out on various islands as part of project PACE (Pacific Atoll Cratering Experiment) and project EXPOE (Exploratory Program on Enewetak). The results of these studies, which provided most of the background data for this chapter, are summarized by Couch and others (1975) and by Ristvet and others (1978). These studies were followed by project EASI (Enewetak Atoll Seismic Investigation) which mainly dealt with seismic profiling but which also employed submersibles and scuba diving in both craters (Tremba and others, 1982). During each of these previous studies, most scuba diving was apparently carried out by U.S. Navy divers rather than by geologists.

METHODS

During the second leg of the current marine field study, the team of scuba divers operated from *Halimeda* (fig. 2 of the Introduction to the volume), while other scientists manned the submersible *Delta* operated from *Egabrag II*. Because all divers, including the submersible pilot, were geologists with extensive experience in coral reef areas, the continuity of observations was assured by interchanging personnel on a day-to-day basis. During the third leg, scuba divers operated from *Halimeda* while seismic operations were being carried out aboard *Egabrag II*.

The submersible's range and bearing were monitored continuously from *Egabrag II*, but locating features and objects identified by scuba divers was more complex. Some sites of interest were buoyed and their position later established with the Miniranger navigation system mounted aboard *Halimeda* or on one of the whalers. In shallow

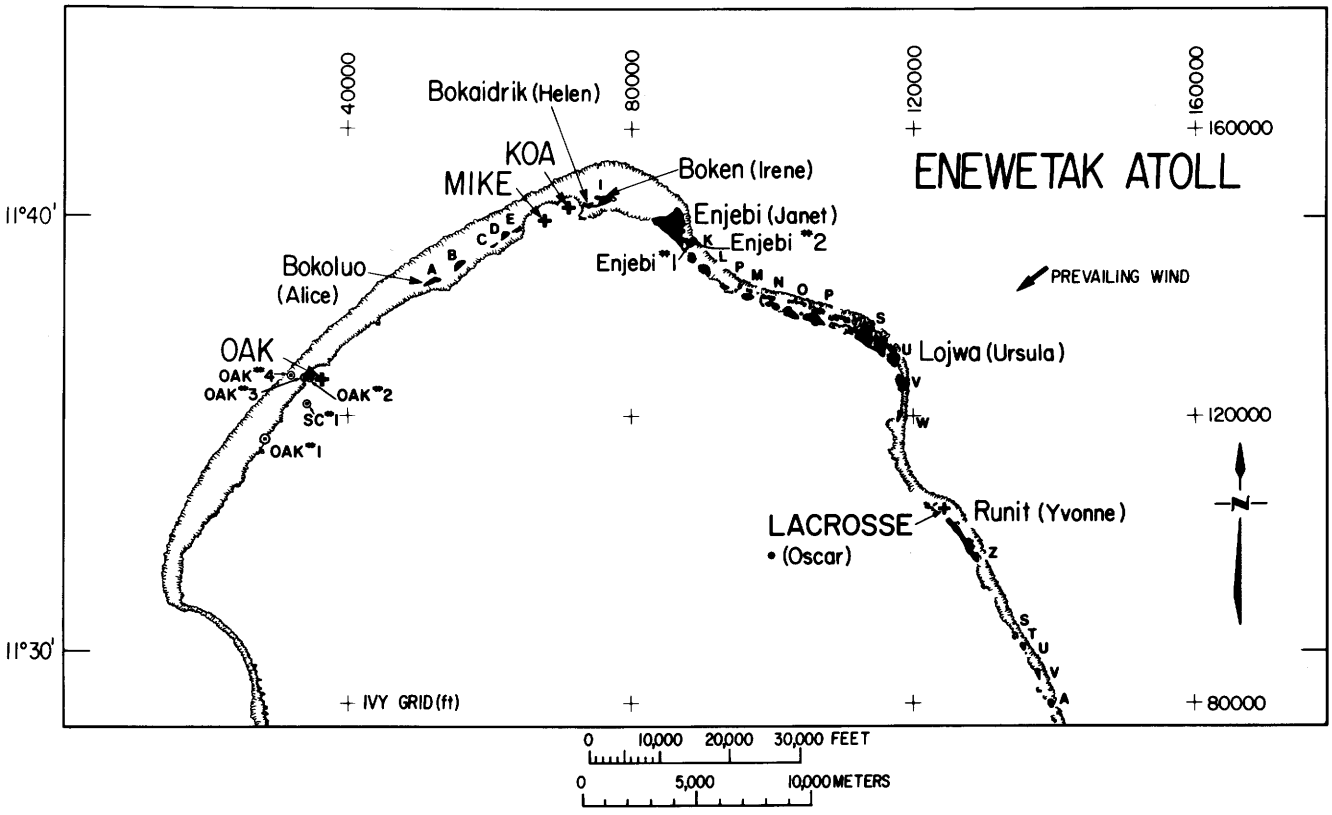

Figure 1. Map of Enewetak Atoll showing locations of OAK and KOA craters and approximate locations of core holes (OAK nos. 1–4, Enjebi nos. E1,E2; SC no. 1) drilled with diver-operated drill. Letters, such as A, B, and C, are the first initials of site names. (See table 1 of the Introduction to the volume.)

waters on the reef, positions of cores and sample stations were estimated.

For coring, *Halimeda* carried both a hydraulic pump and a water pump to operate the hydraulic drill. The hydraulic pump circulates oil at approximately 1,000 psi (pounds per square inch) at a rate of 8–9 gal/min (or 30–34 L/min) to drive the drill, and the low-pressure water pump circulates seawater used for drilling fluid. The hydraulic drill rig (figs. 3, 4), which can be used both above and below water, includes 1.5-m (5 ft) core barrel and 1.5-m (5 ft) lengths of standard drilling rod. The rig is capable of drilling to depths of 15 m (50 ft) in most limestone. It is generally used in water less than 15 m (50 ft) deep because of diver decompression constraints.

Tungsten-carbide face-flush bits, which cut 4.5-cm (1.75 in.) diameter cores, were used for most drilling, and a similar size diamond bit was used in hard limestone near the reef edge. Short, large-diameter cores of reef limestone and living coral heads were obtained using a 10-cm (4 in.) diamond masonry bit. Taken in sections, several 10-cm cores totaling as much as 3 m (10 ft) long, were removed from coral heads. When used in this mode, the drill was hand-held by one or two divers. A smaller hydraulic drill was also used to sample rock and coral. The small drill, about the size of a household electric drill, was used to take short, 0.6-m (2 ft) cores that were 6.5 cm (2.5 in.) in diameter. All the hydraulic drills were driven by the hydraulic pump in the boat via a 61-m-long (200-ft-long), 1.3-cm-diameter (0.5-in.-diameter) plastic high-pressure (2,000 psi maximum working pressure) hydraulic hose equipped with stainless steel quick-disconnect fittings.

Figure 2 (right). *A*, Oblique aerial photograph, looking northwest, of the leeward (west) side of Enewetak Atoll, showing the estimated ground zero (GZ) before detonation of OAK device. The band of coral to right of ground zero is the lagoonward termination of cemented reef flat, or reef plate. Ground zero is located over uncemented carbonate sand. Water depth in lower left-hand corner of photograph is greater than 30 m (100 ft). (Photograph courtesy of B. L. Ristvet.) *B*, Similar view to figure *A*, showing OAK crater in 1984, approximate locations of three diver-drilled cores, and location of 30-m-diameter (100-ft-diameter) secondary crater. Position of ground zero (GZ) is estimated.

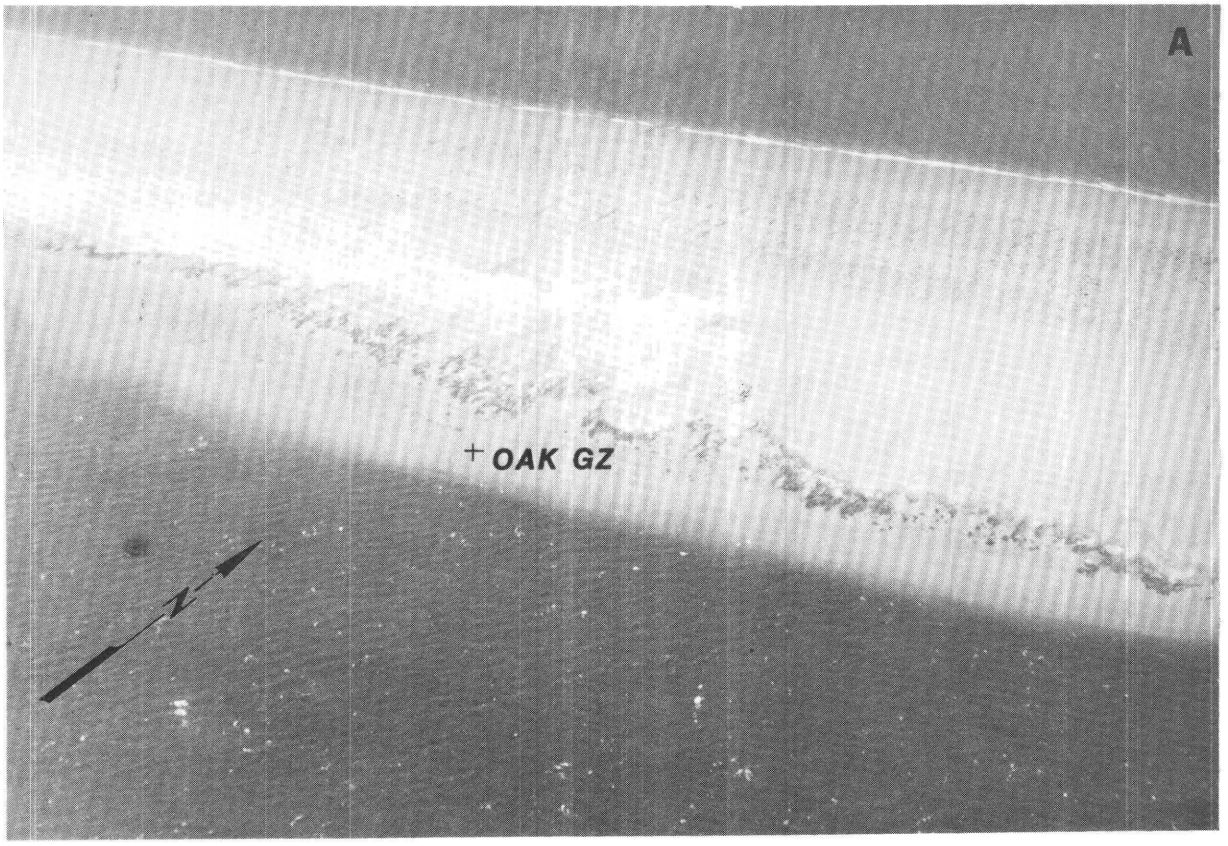
A
+ OAK GZ
N

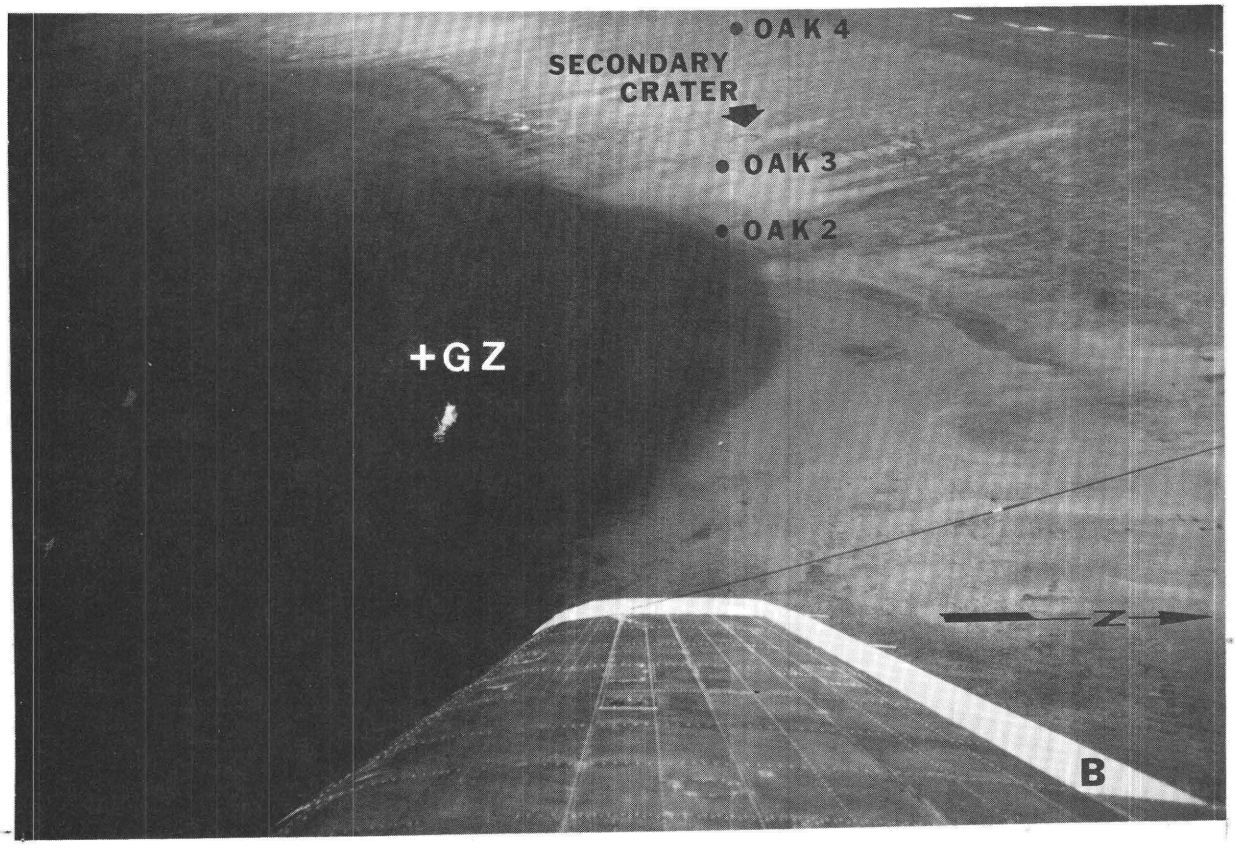
• OAK 4
SECONDARY CRATER
• OAK 3
• OAK 2
+GZ
N
B

Figure 3. Coring rig set up on reef flat at site of Enjebi core no. E1. (See fig. 1.) Hydraulic power source and water pump are aboard *Halimeda*. Photograph taken at high tide. At low tide, reef flat was exposed and boat was aground.

Still photographs were taken underwater with Nikonos cameras using subsea 150-watt strobes; 16-mm movies were taken both above and below the water with a Bolex movie camera in an underwater housing. Videotape records were made with a miniature JVC 1.3-cm (0.5 in.) VHS camera and recorder in a plastic underwater housing fitted with two battery-powered 100-watt movie lights.

A device called an airlift was constructed aboard *Egabrag II* to dig holes through sand cover. It consists of a 4.6-m (15 ft) length of 15-cm-diameter (6-in.-diameter) thin-walled aluminum tubing with a garden hose fitting near one end (fig. 5). A length of hose connects the airlift to an air compressor aboard *Halimeda*. Underwater, the end of the tube is pointed down into the bottom sediment. Air, pumped into the tube through the garden hose, rushes up the tube, creating suction that draws sediment into the tube at the bottom end and ejects it from the upper end. The tube is usually slanted so that the material coming out of the upper end does not fall back into the hole being excavated. The slightest current usually is sufficient to carry the suspended sediment from the working area. The airlift was used to dig six shallow holes along a transect at OAK and one deep (1.5 m, or 5 ft) hole in 18 m (60 ft) of water at KOA.

Figure 4 (right). Hydraulic coring machine at site of OAK core no. 2 in 9 m (30 ft) of water near edge of OAK crater. (See fig. 1.) Submersible *Delta* is in background.

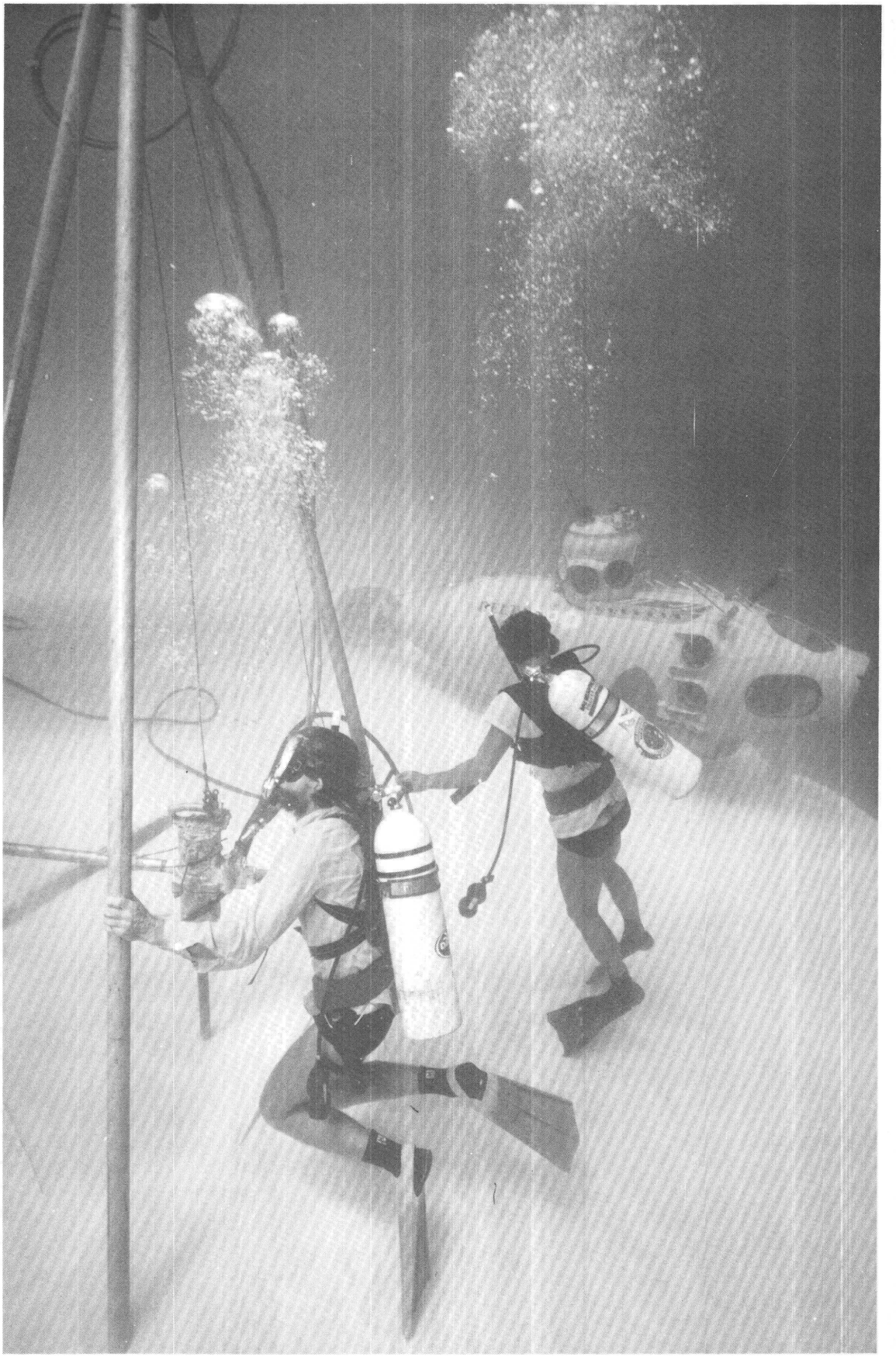

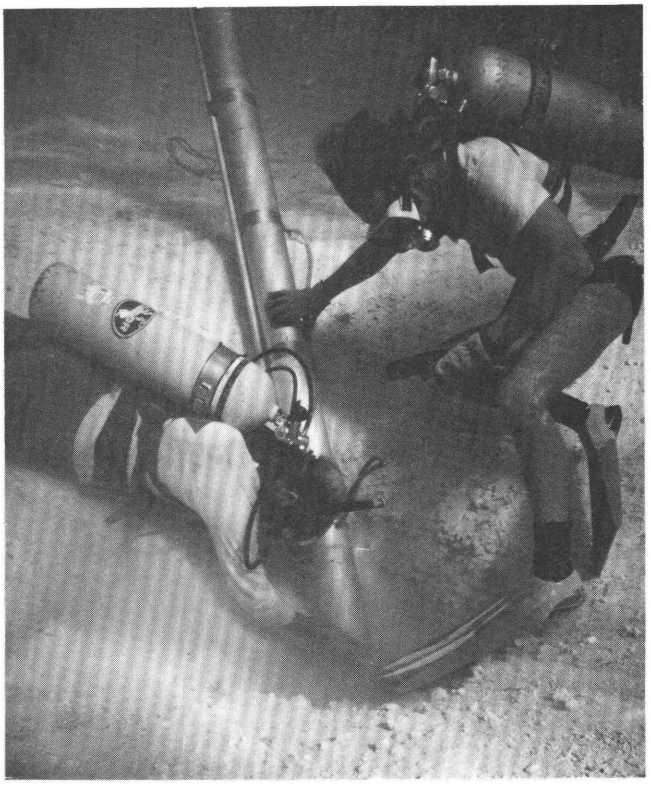

Figure 5. Digging a pit in carbonate sand with the airlift. Location is pit closest to OAK crater.

RESULTS

Baseline Data

To establish baseline data, we made underwater observations of reef flats and lagoonal patch reefs out of the area affected by the blast. We also drilled two cores on the windward-facing reef flat near Enjebi (see figs. 6, 7) and one core on the leeward-facing reef flat (lagoonal side) south of OAK (figs. 8, 9). The OAK core no. 1 was useful for comparison with three cores (OAK nos. 2, 3, 4) drilled in a transect extending from the edge of OAK crater to a position near the seaward margin of the reef flat. Pleistocene limestone was not reached in OAK core nos. 2, 3, or 4 (fig. 9).

The sediments, which were penecontemporaneously cemented, consist mainly of coral fragments, coralline algae, fragments of various calcified green algae, and whole in-place corals. Near the high-energy, wave-battered reef margin, thin flat-lying corals dominate. In cross section, these corals appear as a series of flat to undulose plates interlayered with sediment (fig. 10). Farther from the reef margin, larger massive corals as well as finger corals increase in number. The massive and branching corals, which have high relief, cannot survive the battering by waves on the reef margin. Lagoonal sediments consist mainly of sand-size algal and coral fragments and, in some areas, almost pure foraminiferal sands.

Diagenesis on the Reef Flat

Previous coring during Operation Crossroads, PACE, and EXPOE convincingly demonstrated that the degree of cementation and hardness of the reef-flat rock increases toward its seaward edge. Conversely, cementation decreases gradually toward the lagoon; a point is reached where cementation abruptly ceases and the sediment is unconsolidated. The cementation gradient was very pronounced in the Enjebi cores (figs. 6, 7). Core no. E–1 was successfully drilled on the reef flat 230 m (755 ft) from the reef edge using a carbide bit. The same carbide teeth were immediately stripped at the location of core no. E–2, 34 m (110 ft) from the reef edge, and a diamond bit had to be used instead. Figures 6 and 7 show that both cores were in the Holocene layer of reef-flat rock, or reef plate. In the lower portion of both cores, we encountered uncemented Holocene carbonate sand. The increase in cementation near the reef margin is probably related to increased wave action which pumps supersaturated seawater (the cement source) through the sediment and rock pores. The cement is mainly aragonite and high-Mg calcite. This reduction in cementation from reef edge to backreef has been documented elsewhere in modern reef sediments (James and Ginsburg, 1979; Shinn and others, 1982) and on Enewetak in deeper units by Ristvet and others (1978). In the older units, especially those of Pleistocene age, the relationship is complicated by an overprint of freshwater diagenesis. Each time relative sea level dropped, the rocks and sediments were subaerially exposed and penetrated by meteoric water, which caused cementation and leaching within the first meter or two of the sediment or rock surface. Because of the subaerial diagenesis overprint, submarine-cemented unconformities can be traced lagoonward to a point where the horizon had been lithified entirely with freshwater cements consisting of low-Mg calcite.

OAK core no. 1 was drilled about 3.5 km (1.9 nmi) southwest of OAK crater on the reef flat (fig. 1) a few meters from the abrupt change from rock to sediment. The environmental situation there is considerably different from that on the northeast reef flat where the Enjebi cores were drilled. On the west side of the atoll, the lagoonal edge of the reef flat receives considerable wave action because the prevailing northeasterly winds pass over 15 to 20 km (8–11 nmi) of open lagoon (fig. 1). The deep water and long fetch allow waves as high as 1.3 m (4 ft) to develop during 25-kn (12.5 m/s) winds. Swells as high as 1.5 m (5 ft) are not uncommon during winter. Because of this constant wave action, the lagoonal side of the reef flat has some of the characteristics of the windward (seaward) side of the reef where corals grow in abundance and reef flat sediments are moderately well cemented. Particularly large coral heads (*Porites lutea*) grow along a narrow depth zone (3–5 m, or 10–15 ft) of water just lagoonward of the reef flat. The reef flat is barely awash at spring low tide. Safe drilling sites on the lagoonal side of the reef flat were difficult to find,

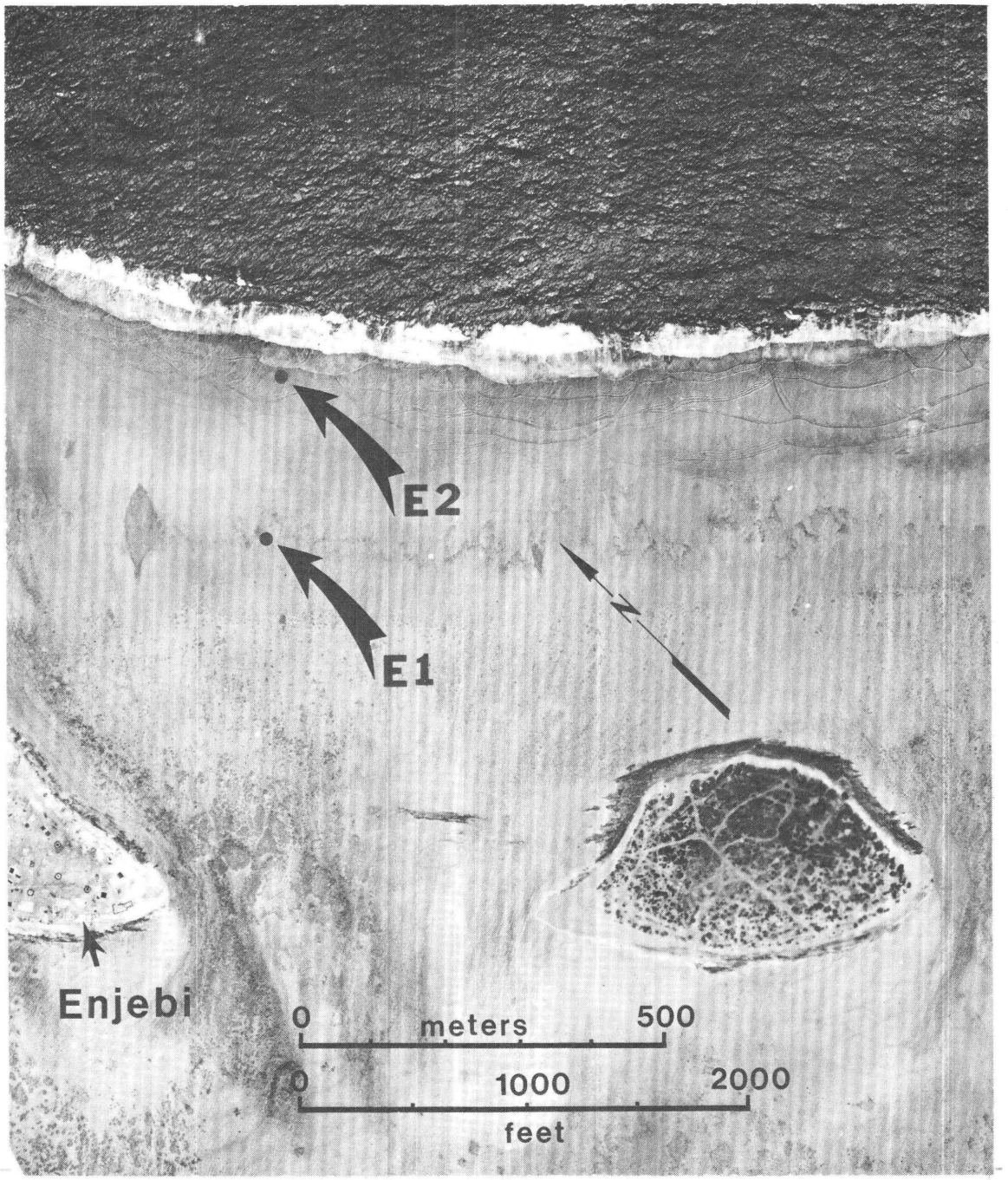

Figure 6. Aerial photograph showing approximate location of Enjebi core nos. E1 and E2 on reef flat. (See fig. 1.) (Photograph taken in 1944; courtesy of B. L. Ristvet.) Scale is approximate.

because *Halimeda* could be easily driven onto the reef by breakers. To drill OAK core no. 1, *Halimeda* was anchored with three moorings in a small, 3-m-deep (10-ft-deep), cove-like reentrant within the reef flat, and the drill, drill rods, and tripod were set up on the reef flat about 10 m (33 ft) away. Water at OAK core no. 1 was less than 30 cm (1 ft) deep at low tide. The approximate location of OAK core no. 1 is shown in figure 1, and a cross-section sketch (fig. 11) shows the depth of cementation. From 1.5 to 1.8 m (5–6 ft) downhole, Holocene sediment comprised uncemented carbonate sand; underlying Pleistocene sediment was cemented.

Figures 12 and 13 are aerial views of the windward reef flat on the east side of Enewetak Atoll and the leeward reef flat on the west side of the atoll. The windward or seaward side (fig. 12) is ornamented with spectacular spurs and grooves of erosional origin (fig. 14). They are similar to those described by Cloud (1959). On the west (leeward)

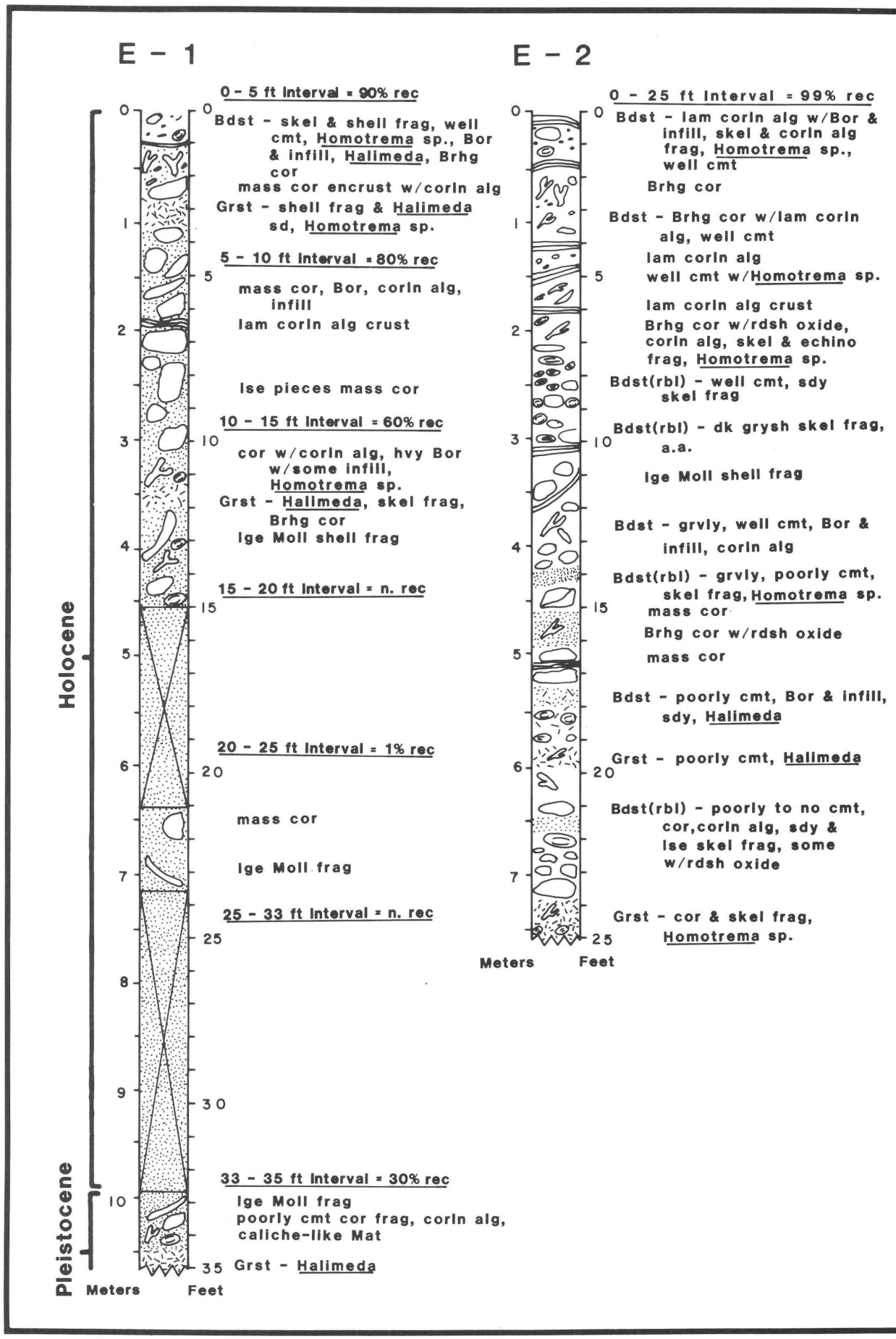
E - 1
0 - 5 ft interval = 90% rec
Bdst - skel & shell frag, well cmt, Homotrema sp., Bor & infill, Halimeda, Brhg cor
mass cor encrust w/corln alg
Grst - shell frag & Halimeda sd, Homotrema sp.
5 - 10 ft interval = 80% rec
mass cor, Bor, corln alg, infill
lam corln alg crust
lse pieces mass cor
10 - 15 ft interval = 60% rec
cor w/corln alg, hvy Bor w/some infill, Homotrema sp.
Grst - Halimeda, skel frag, Brhg cor
lge Moll shell frag
15 - 20 ft interval = n. rec
20 - 25 ft interval = 1% rec
mass cor
lge Moll frag
25 - 33 ft interval = n. rec
33 - 35 ft interval = 30% rec
lge Moll frag
poorly cmt cor frag, corln alg, caliche-like Mat
Grst - Halimeda
Holocene
Pleistocene
Meters
Feet
E - 2
0 - 25 ft interval = 99% rec
Bdst - lam corln alg w/Bor & infill, skel & corln alg frag, Homotrema sp., well cmt
Brhg cor
Bdst - Brhg cor w/lam corln alg, well cmt
lam corln alg
well cmt w/Homotrema sp.
lam corln alg crust
Brhg cor w/rdsh oxide, corln alg, skel & echino frag, Homotrema sp.
Bdst(rbl) - well cmt, sdy skel frag
Bdst(rbl) - dk grysh skel frag, a.a.
lge Moll shell frag
Bdst - grvly, well cmt, Bor & infill, corln alg
Bdst(rbl) - grvly, poorly cmt, skel frag, Homotrema sp.
mass cor
Brhg cor w/rdsh oxide
mass cor
Bdst - poorly cmt, Bor & infill, sdy, Halimeda
Grst - poorly cmt, Halimeda
Bdst(rbl) - poorly to no cmt, cor,corln alg, sdy & lse skel frag, some w/rdsh oxide
Grst - cor & skel frag, Homotrema sp.
Meters
Feet

Figure 7 (left). Lithology of Enjebi core nos. E1 and E2. (See fig. 1.) Pleistocene was reached in E1 at approximately 10 m (33 ft).

The following abbreviations in figures 7-9 are mostly after Swanson (1981):

a.a.	as above
alg	algae
Bdst	boundstone
Bor	bored
brhg	branching
chlky	chalky
cmt	cemented
cor	coral
corln	coralline
dk	dark
echino	echinoid
encrust	encrusted
frag	fragment
grsh or grysh	grayish
Grst	grainstone
grvly	gravelly
infill	infilled
hvy	heavy (-ily)
lam	lamina (-ated)
lge	large
lse	loose
mass	massive
Mat	material
Moll	mollusc
n.	no
Pkst	packstone
rbl	rubble
rdsh	reddish
rec	recovery
sd	sand
sdy	sandy
skel	skeletal
sol	solution
sp.	species (singular)
spp.	species (plural)
tn	tan
w/	with
wh	white
whsh	whitish

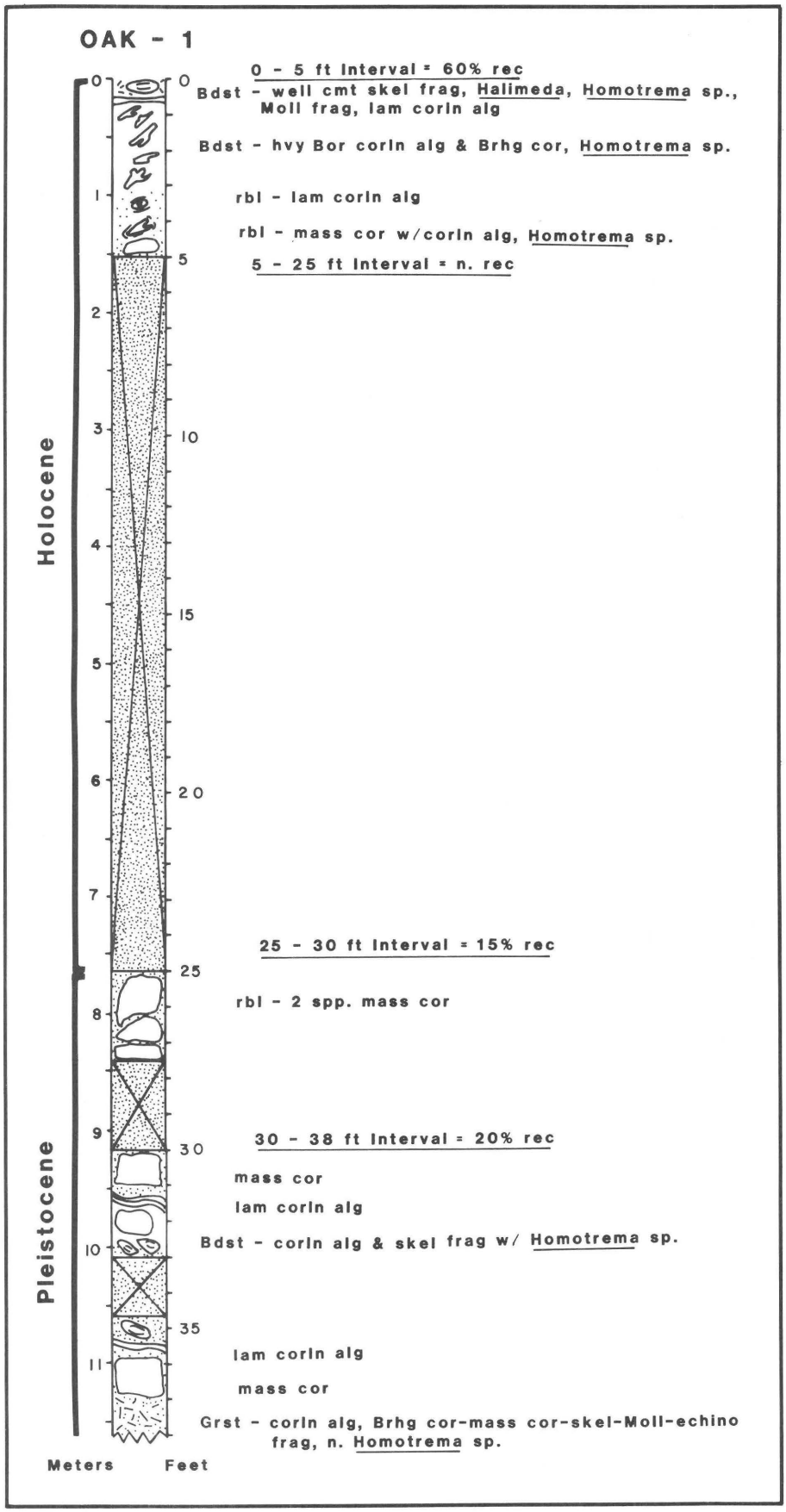

Figure 8 (right). Lithology of OAK core no. 1 drilled south of OAK crater. (See fig. 1.) Note the significant section of uncemented carbonate sand below cemented reef plate. Rock presumed to be Pleistocene in age was encountered at approximately 7.5 m (25 ft).

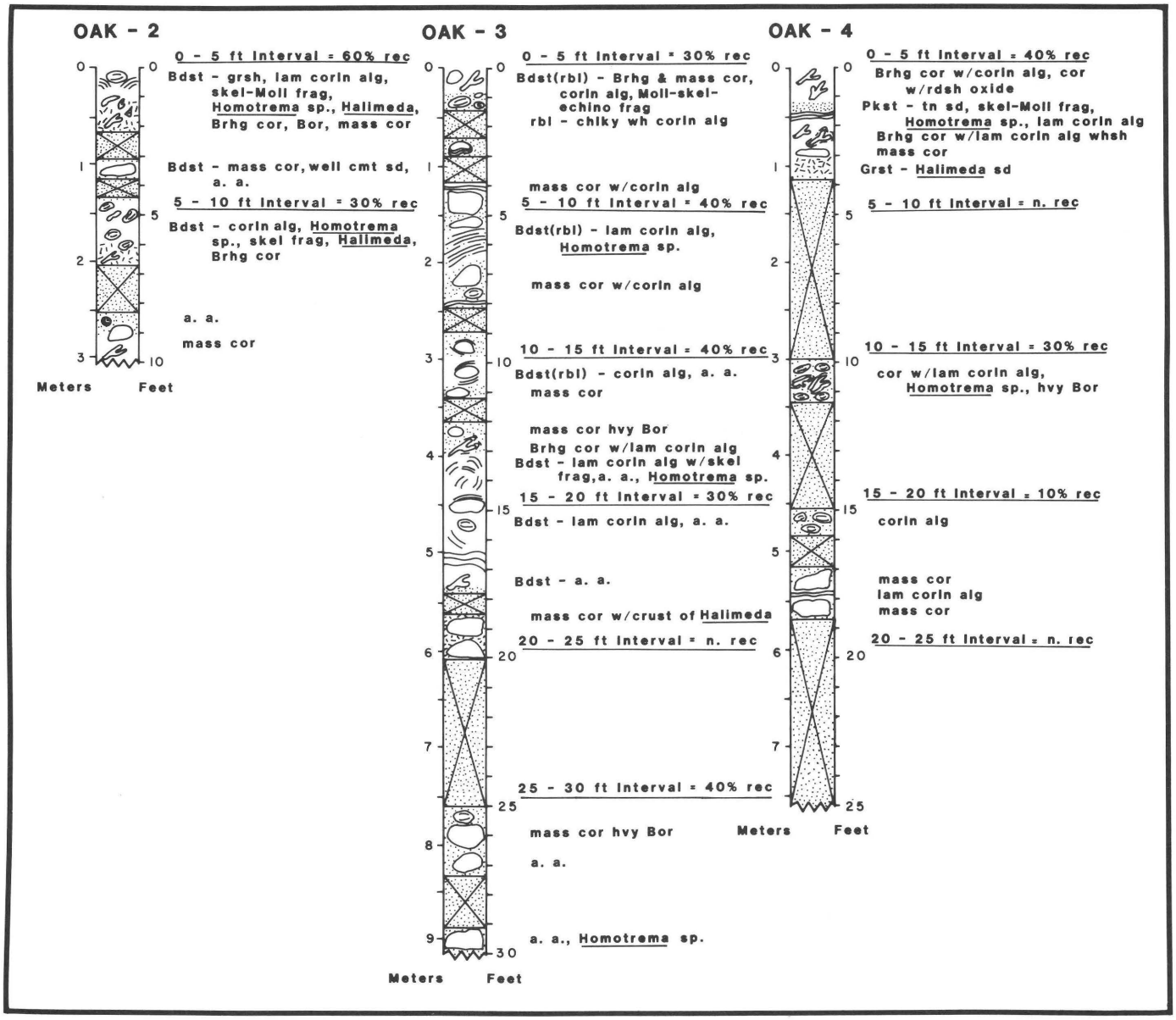

Figure 9. Lithology of three cores drilled in a transect near OAK crater. (See fig. 1.) OAK core no. 2 could not be drilled deeper because of fractured rock. Recovery of core was poor in OAK core no. 3 also due to fracturing, but thickness of cemented reef plate was approximately 6 m (20 ft). Pleistocene limestone was not reached in OAK core no. 3. Rock in OAK core no. 4 was not fractured, and only the upper meter was cemented. The remainder of the core was mainly uncemented carbonate sand and coral debris. (See definitions of abbreviations, previous page.)

reef flat, spurs and grooves are mostly lacking and the dropoff is precipitous (fig. 15). On the west (seaward) side of the atoll, the water depth increases from only 30 cm (1 ft) to over 100 m (330 ft) over a distance of less than 20 m (66 ft). Spurs are poorly defined there and appear to be more constructional than erosional. (See Shinn, 1963; Shinn and others, 1981, for a discussion of constructional versus erosional spurs and grooves.) On the east (seaward) margin,

Figure 10 (right). Selected slabs of core from Enjebi transect. Two slabs below the scale are from 4 ft (1.3 m) downhole in the highly cemented E2 corehole drilled 33 m (108 ft) from the reef edge. (See fig. 6.) Voids in E2 sample are lined with amber coating of aragonite, and rock is extremely hard. Material is mainly cemented coral. Two slabs above the scale are from same interval in core E1 drilled 210 m (690 ft) from reef edge. E1 sample consists mostly of poorly cemented carbonate sand.

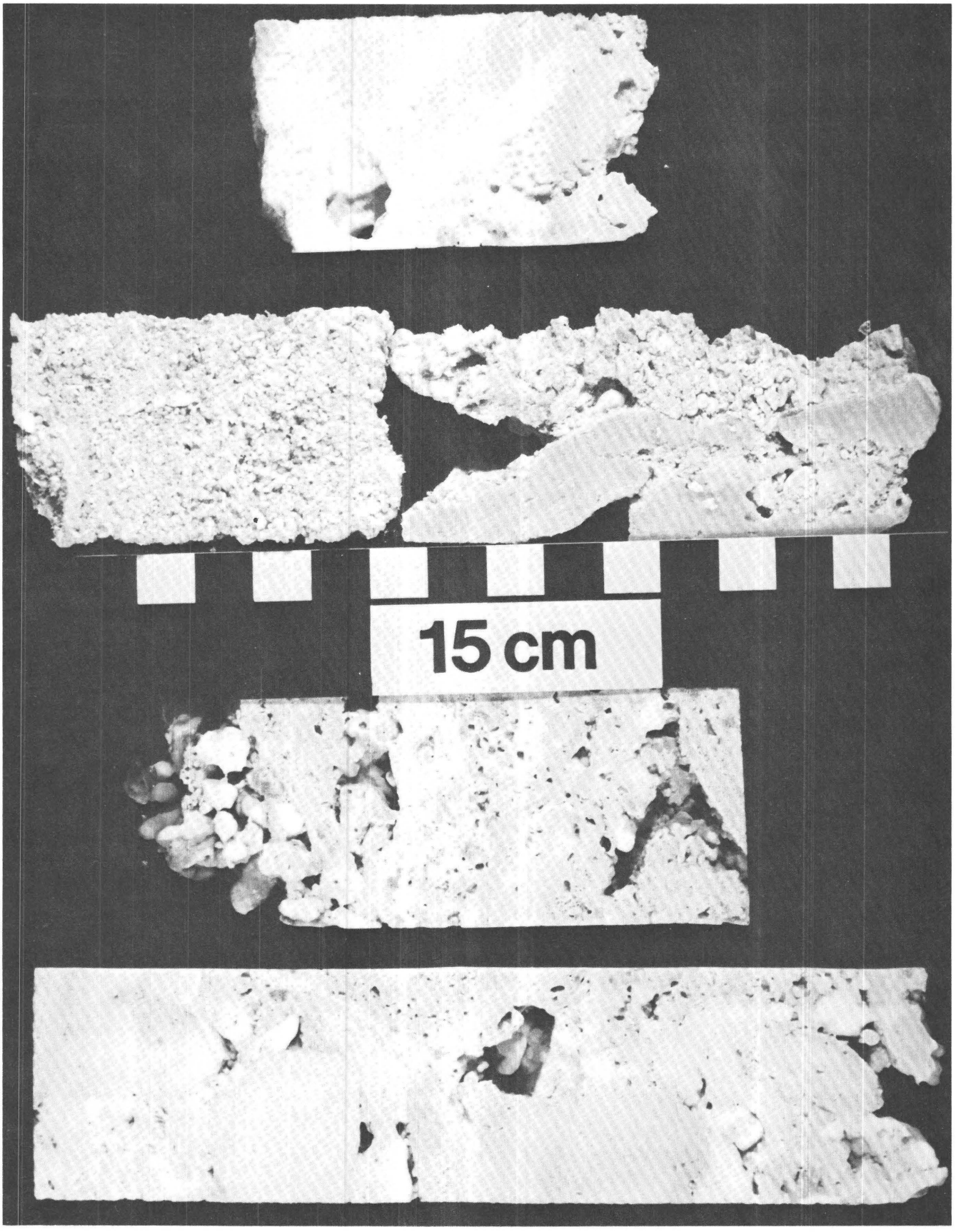
15 cm

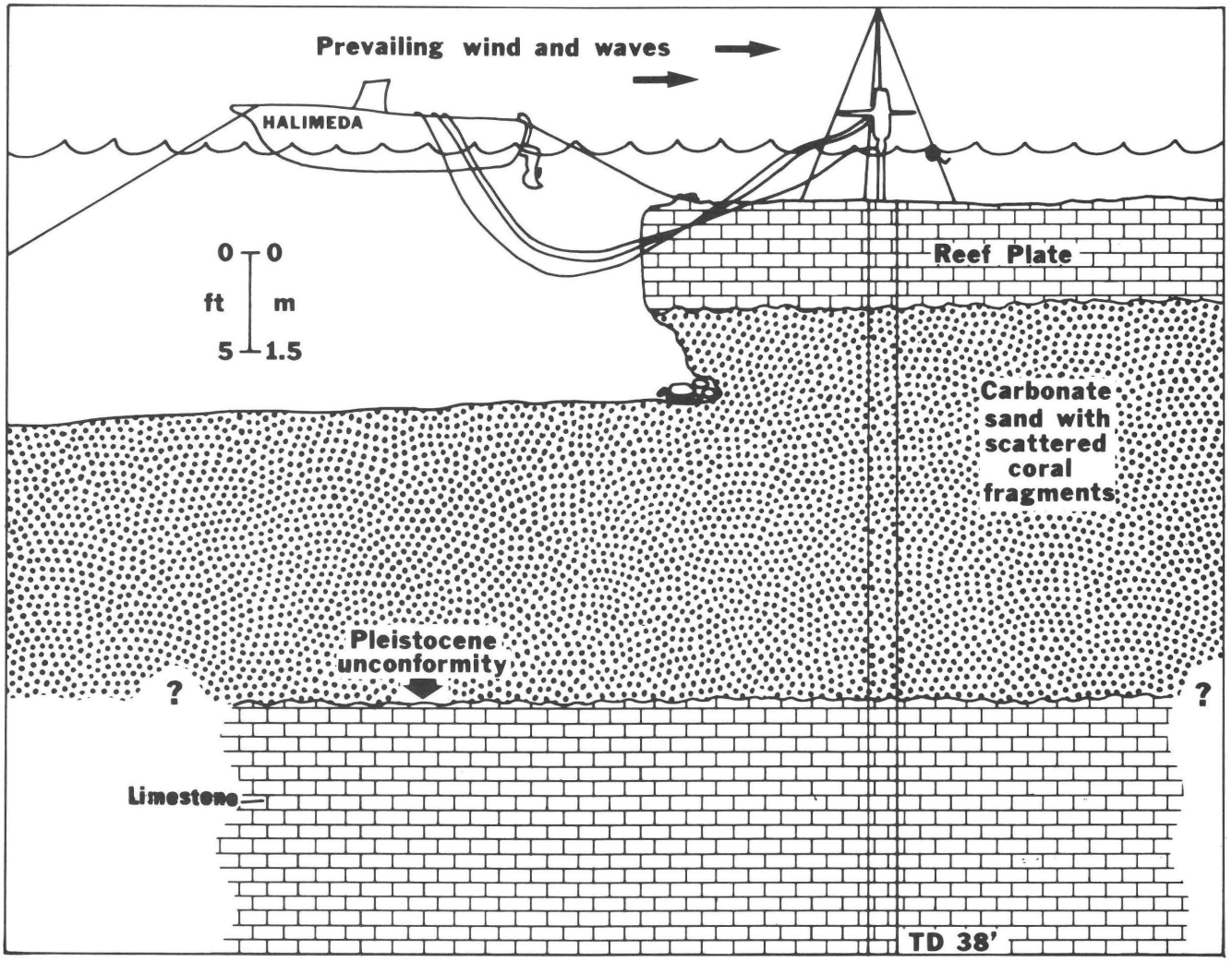

Figure 11. Schematic diagram showing drilling set-up and generalized lithology at location of OAK core no. 1. (See fig. 1.)

however, erosional spurs and grooves extend 30 to 100 m (100–330 ft) or more seaward from the exposed reef flat into water that is as much as 10 m (33 ft) deep in places. The major dropoff, where depths in excess of 100 m (330 ft) begin, lies another few hundred meters seaward along most of the east margin.

Small patch reefs, consisting mainly of large massive head corals, occur in 3 to 6 m (10–20 ft) of water lagoonward of both the east and west reef flat, as they do near the island of Biken (Leroy). This zone is more than a kilometer wide. It is only a few hundred meters wide between the islands of Bokoluo (Alice) and Enjebi (Janet). (See fig. 1 in the Introduction to the volume.) Within the lagoon, numerous patch reefs rise up to or near the surface from depths greater than 30 m (100 ft).

The width of the reef flat is variable, 200 to 300 m (656–984 ft) wide along the east side of the atoll and as much as 1 km (0.54 nmi) or more on the southwest side of the atoll and in the transitional zone to the north. In the vicinity of KOA and MIKE craters, the reef flat was originally more than 1 km (0.54 nmi) wide (fig. 1). Nuclear devices shot here were, for the most part, on the reef flat, although the reef plate apparently was not thick or well cemented, according to Ristvet and others (1978) and our observations.

Observations of OAK Crater Area

Two large, upside-down, 3-m-diameter (10-ft-diameter) *Porites lutea* head corals lie high on the reef flat both northeast and southwest of OAK crater (fig. 16). These heads served as useful landmarks throughout the study, and both are located within 50 m (164 ft) of the lagoonal margin of the reef flat. Heads reaching this diameter grow only in a narrow zone on the lagoonal side of the reef flat, and these heads apparently were emplaced upon the reef flat by the OAK event. Large storm waves capable of moving coral heads most often come from the seaward side, where no

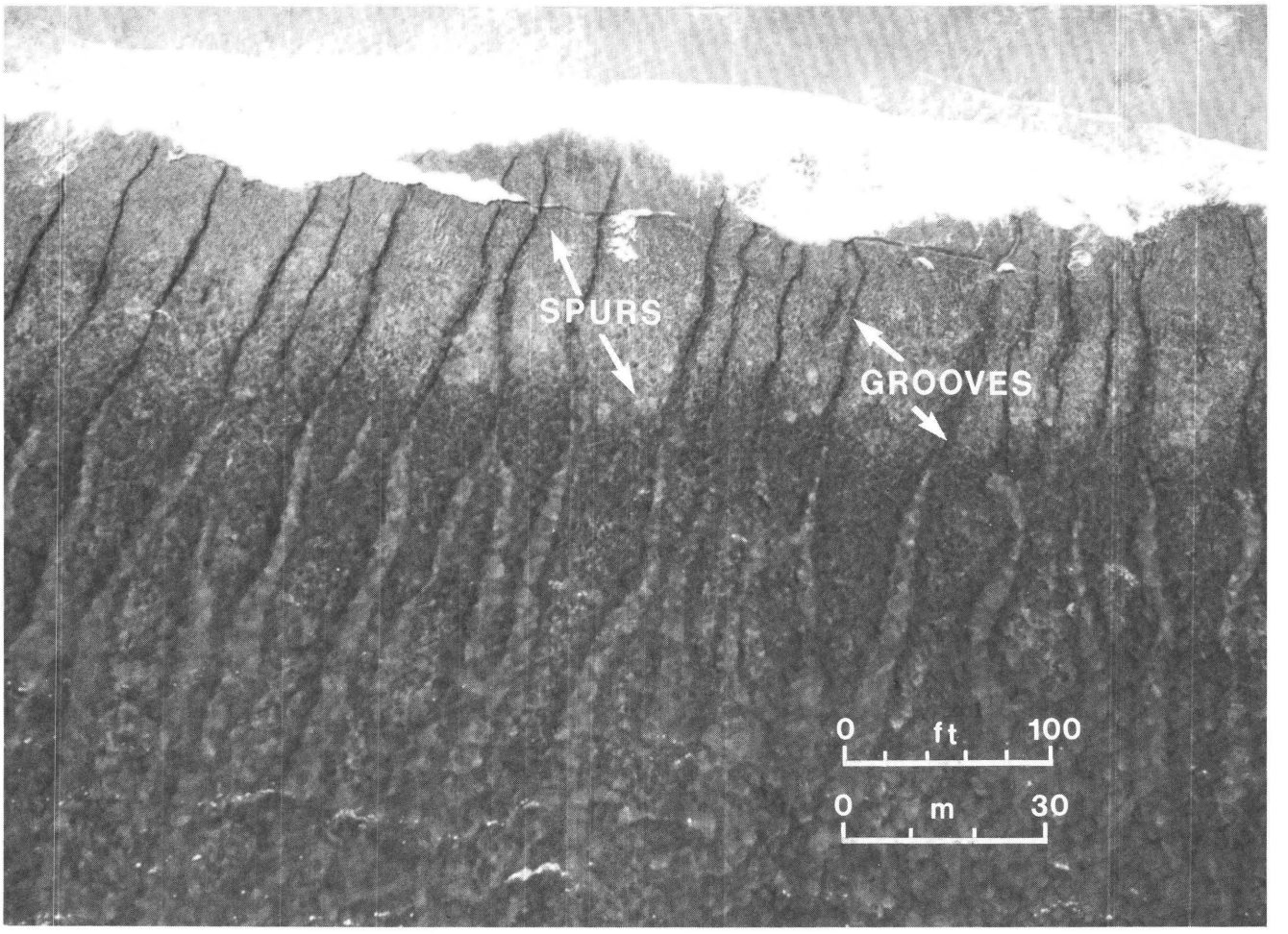

Figure 12. Aerial view of seaward margin of windward (east) reef flat showing well-developed erosional spurs and grooves. Grooves have overhanging edges near surf zone and in places form tunnels perpendicular to reef front. Scale is approximate.

similar heads were observed. Other debris is scattered over the flats which, at low tide, protrude above water both northeast and southwest of the crater. Few rocks like those in figure 16 are visible above water on the reef flat northwest of ground zero. Following a survey of overburden thickness, which was conducted by probing through unconsolidated sediment to the reef plate with a metal rod (fig. 17), we concluded that the area has subsided from 1 to 2 m (3.3–6.6 ft).

Scour Marks on the Reef Flat

Pronounced ripple-like grooves oriented normal to the trend of the reef occur intermittently along the lagoonal margin of the cemented reef flat. They measure roughly 5 to 10 cm (4–6 in.) high, are 10 to 15 cm (4–6 in.) wide, and are separated by grooves 10 to 15 cm (4–6 in.) wide (fig. 18). Although these features have the appearance of ripple marks often preserved on bedding surfaces of ancient limestone, they apparently were scoured by small pebbles and sand that wash back and forth as waves break on the reef flat eroding the reef plate. We used these features in addition to lithology to determine the origin of limestones found in 8 to 21 m (25–70 ft) of water along the west margin of OAK crater.

Rock Ledge on the West Rim

We made numerous scuba and submersible dives along the precipitous west rim of OAK crater to investigate the origin and age of the limestone and to determine if the rim was part of the transient crater or was created by postevent subsidence. Although much of the surface within about 200 m (656 ft) of the crater rim is covered with carbonate sand (fig. 19), a prominent rock ledge 1.5 to 2.5 m (5–8 ft) thick, crops out to form a precipitous escarpment. The ledge has been broken to form vertical and sometimes slightly overhanging scarps. Rock fragments and sandy sediment cover the lower part of the escarpment. The rubble slope, with some large boulders several meters in

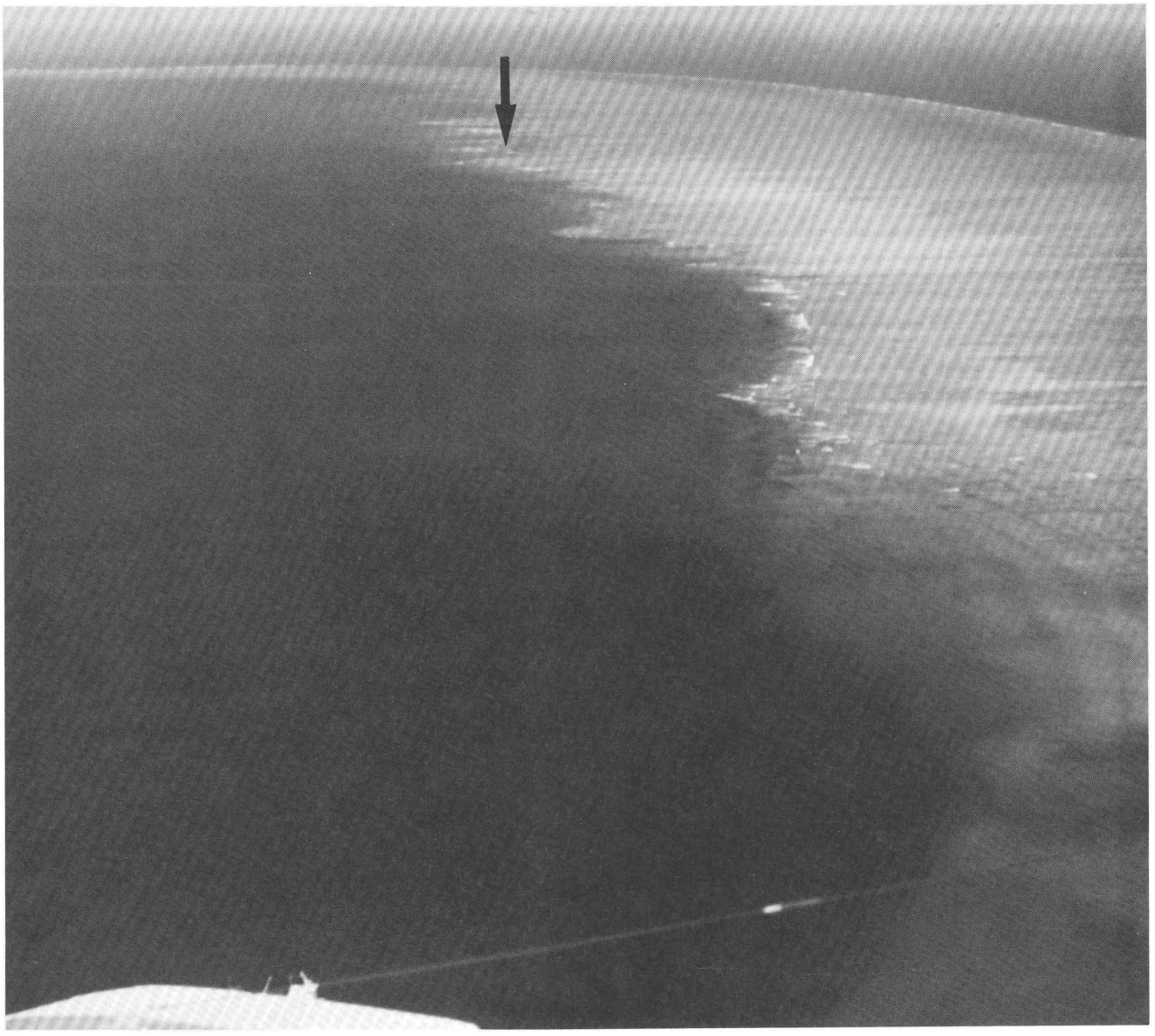

Figure 13. Aerial view of reef flat on leeward side of atoll in the vicinity of OAK crater. Prevailing wind produces waves which break on lagoon side of reef flat. View is to southwest, and approximate location of OAK core no. 1 is shown by arrow.

diameter, is sometimes as steep as 30° degree from the base of the escarpment to water at least as deep as 33 m (110 ft).

The surface of the rock ledge lies in water as shallow as 6 m (20 ft) to as deep as 22 m (70 ft). It can be traced laterally for 30 to 40 m (100–130 ft) in some places but in many places is covered by sand. The ledge is faulted, causing its depth to change dramatically. In one area in the center of the arc formed by the west rim of the crater, the ledge has been completely covered by sand and rubble for a distance of more than 100 m (330 ft).

Upturned Flap

Close to the area where OAK core no. 2 was drilled (see fig. 19), in 7 to 8 m (22–25 ft) of water, the ledge dips away from ground zero at an angle of about 10° (figs. 20*A*,*B*). Part of it is ornamented with ripple-like scour marks having the same spacing and orientation as those observed along the lagoonal margin of the nearby reef flat (fig. 20*A*). The presence of these scour marks, as well as the presence of red *Homotrema* sp. and the similarity of the rock matrix to that drilled at OAK core no. 1, are considered sufficient evidence that the rock forming the west margin of OAK crater is reef plate. In most places, it has subsided to a depth of about 12 m (40 ft), but at one locality it was observed as deep as 22 m (70 ft). Whether the upturned

Figure 14 (right). Underwater photograph showing smooth nature of spurs eroded by round coral boulders. Groove is about 1 m (3 ft) wide.

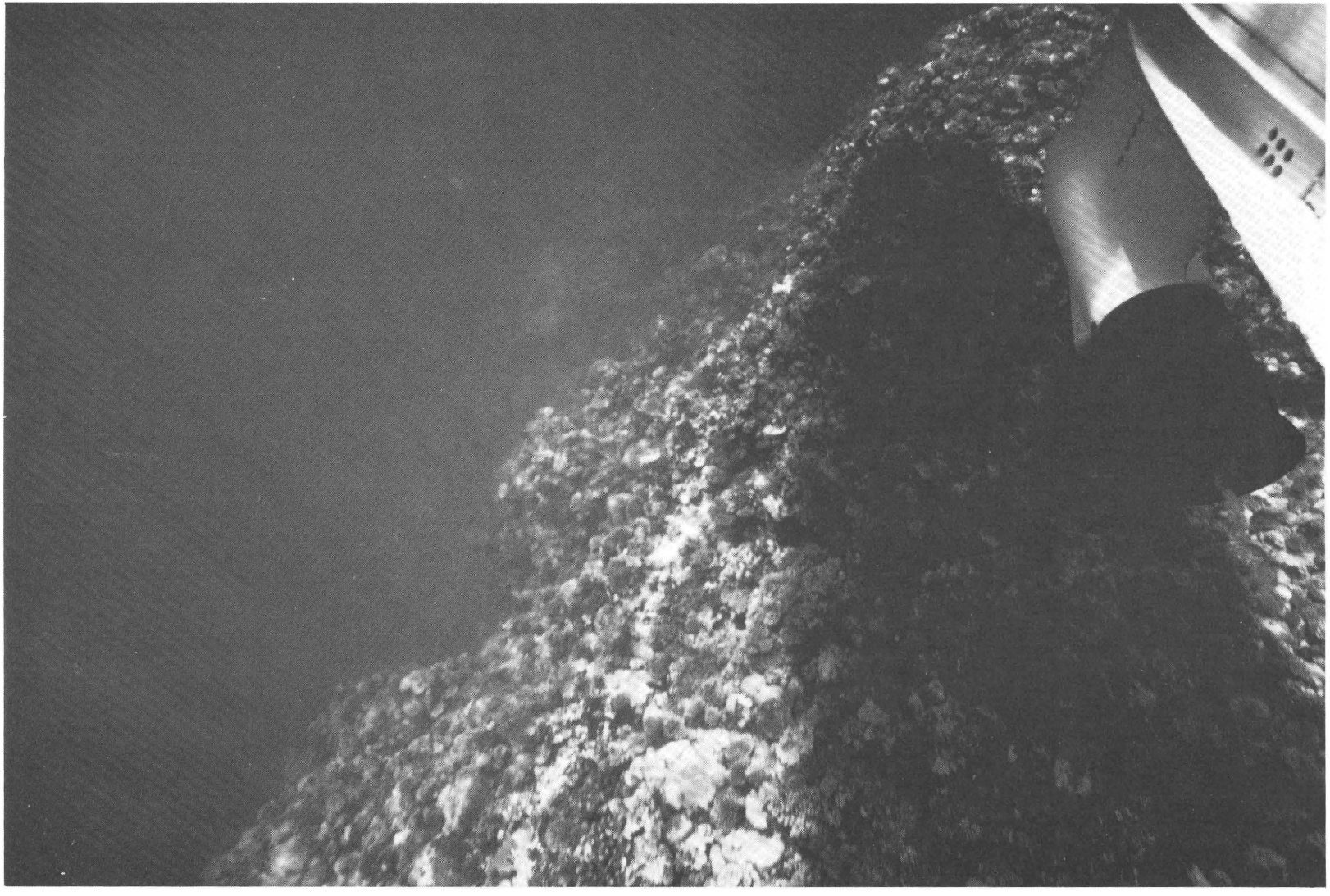

Figure 15. Underwater view looking down the precipitous slope on seaward (west) side of atoll. Propeller to right is only a few feet above bottom. Slope is approximately 80°, and spurs and grooves like those shown in figures 12 and 14 are absent. Propeller is about 0.25 m (0.8 ft) in diameter.

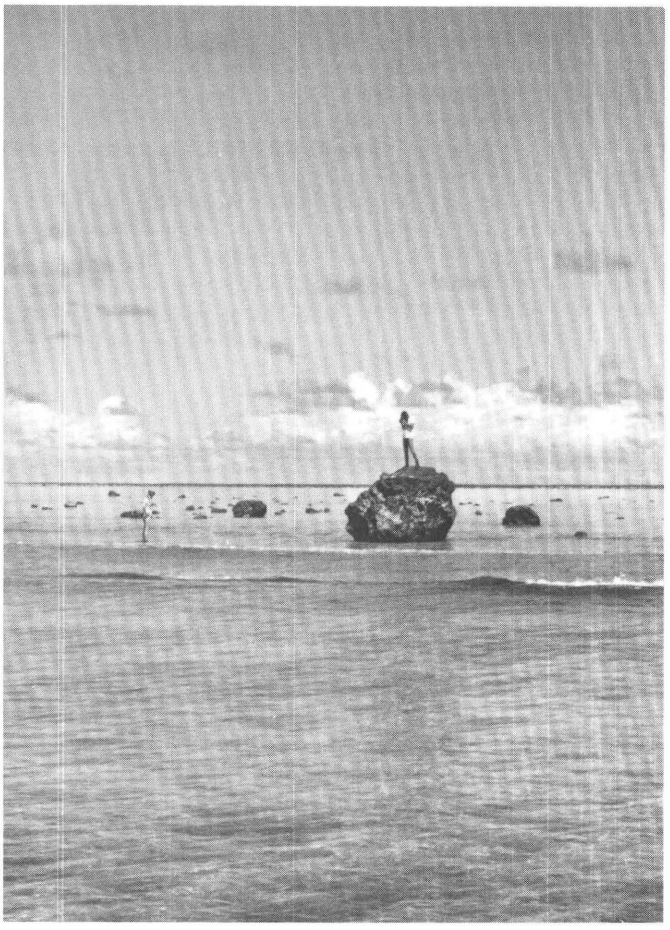

ledge, identical in appearance to portions of the upturned ledges surrounding LACROSSE crater (fig. 21), is an upturned flap or a rotated slump block was impossible to distinguish. A thick layer of sand covers much of it.

Oak Crater Transect

The observation of subsided reef plate with a possible upturned flap led to investigation of the reef flat west of the crater. Three core holes were drilled in a line. The first was located a few meters from the crater rim in 9 m (30 ft) of water (fig. 22); a second hole was placed in approximately 1.5 m (4 ft) of water and 244 m (800 ft) from the crater

Figure 16 (left). Large boulder (a single head of the coral *Porites lutea*) on reef flat southwest of OAK crater. Boulder was undoubtedly thrown there by the OAK event. Location of boulder is shown on figures 18 and 19. Man standing in water is in same position as in figure 18.

Figure 17 (below). Generalized map showing probe data parallel to reef flat opposite OAK crater. Data show the surface of reef plate is about 1 m (3 ft) deeper opposite the crater, indicating localized subsidence caused by the OAK event. Crater debris present adjacent to the crater on the reef flat does not protrude above water at low tide as it does northwest and southeast of the crater. *Porites lutea* boulder at left is the one shown in figure 16. See figure 19 for aerial photograph of same area. GZ=ground zero.

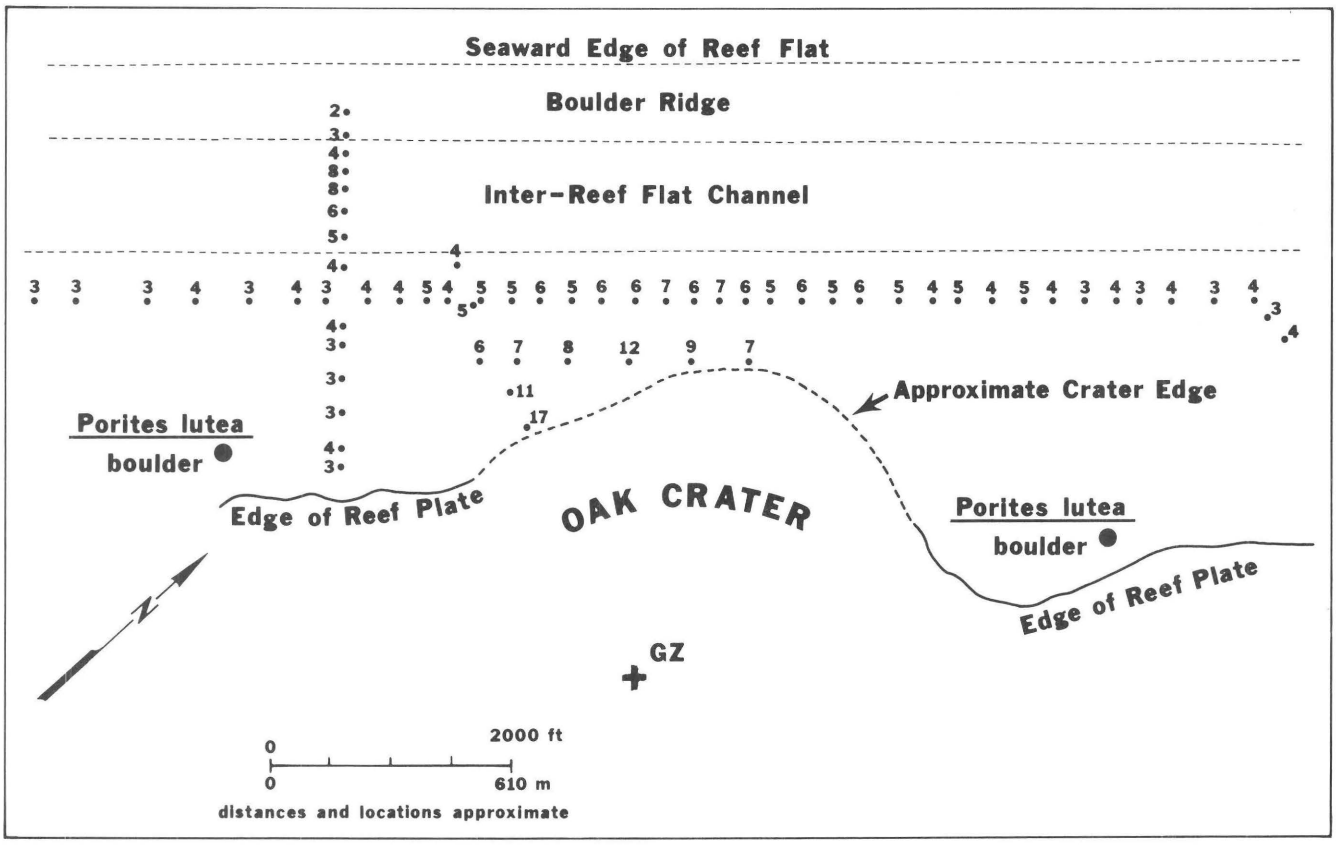

Figure 18. Photograph taken from atop boulder in figure 16 showing eroded ripple-like features in reef plate. Note cobbles in grooves and wave action which causes them.

margin; and a third was drilled near the seaward side of the reef flat about 823 m (2,700 ft) from the crater margin. Fracturing of the rock was evident in the two core sites closest to the crater, which were within the area affected by subsidence. The transect location is shown in figure 19. See figure 9 for lithologies. To obtain additional information, we dug six pits with the airlift through the sand cover along the transect line. The transect cross section is shown in figure 23. The pits allowed important observations of the underlying rock. First, there are no ripple-like grooves there, such as those we observed southwest of the crater area (fig. 18) and at the crater rim (fig. 20*A*); second, we observed no faunal borings in the rock (fig. 24*A*), whereas they are common southwest of the crater area; third, two large rock slabs were found to be exposures of reef plate and not slabs of debris. (See fig. 23 and detail in fig. 24*B*.) The slabs stand 30 to 100 cm (1–3 ft) above the surrounding rock, which is covered by 30 to 60 cm (1–2 ft) of sand. Apparently, the sand has filled in areas where about an equal thickness of reef plate has been stripped away by the blast. Why selective stripping occurred at this distance from the crater but not adjacent to the crater, where the scoured ripple-like features and bored surface are still intact, is not clear.

Unfortunately, no rock was encountered in the 1.5-m-deep (5-ft-deep) pit that we dug closest to the crater margin. The digging indicates that the reef plate does extend continuously beneath the sand from the crater rim to the point where it is exposed near OAK core no. 2. This observation suggests that the conclusions of Tremba and others (1982,

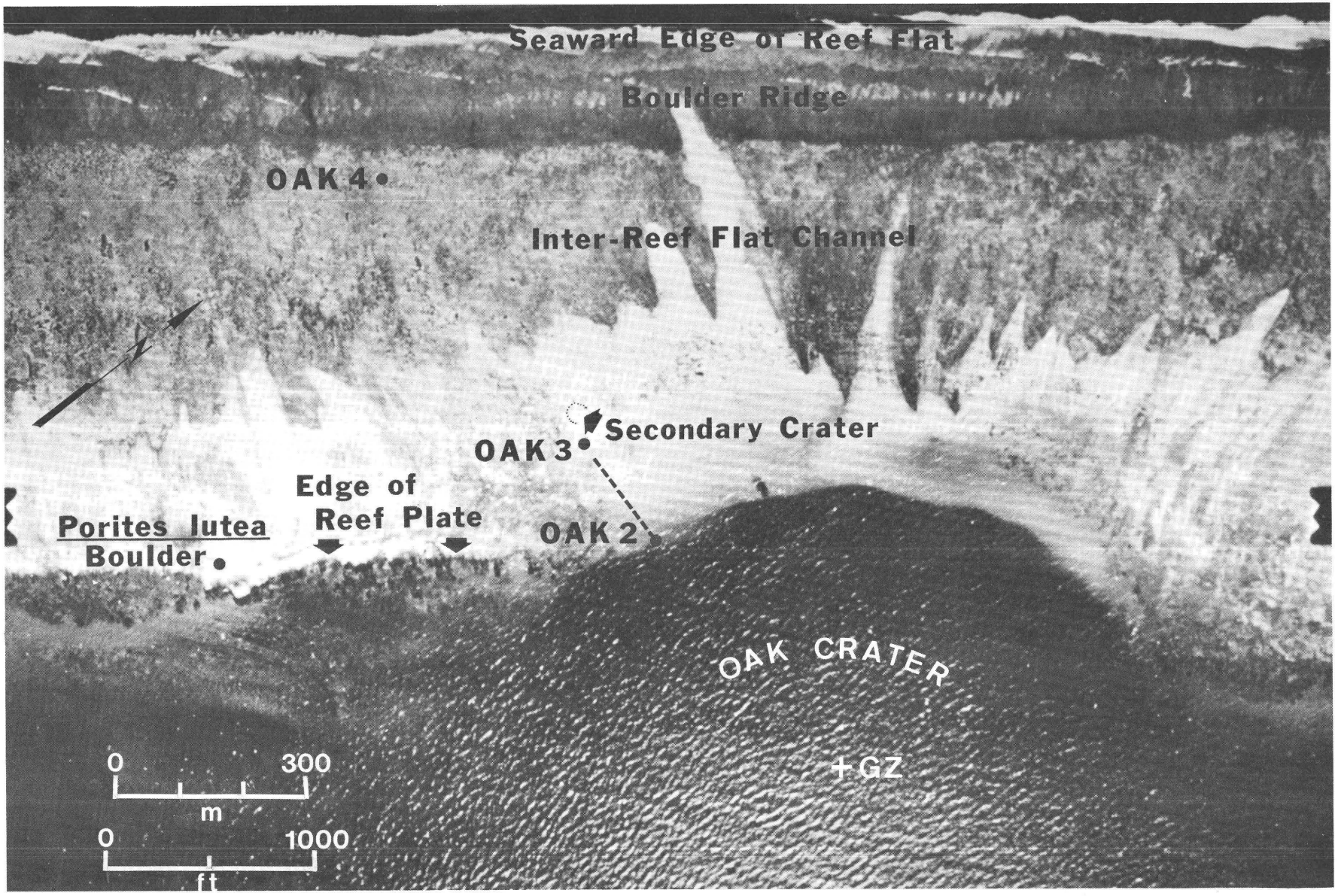

Figure 19. Aerial photograph of OAK crater taken in 1972 shows location of 30-m-diameter (100-ft) secondary crater (outlined by dots) and three core holes. Data from cores are shown in figure 9. Dashed line shows location of transect in figure 23. Most of the debris rays have been removed by subsequent storm waves. Locations and scale are approximate. (Photograph courtesy of B. L. Ristvet.)

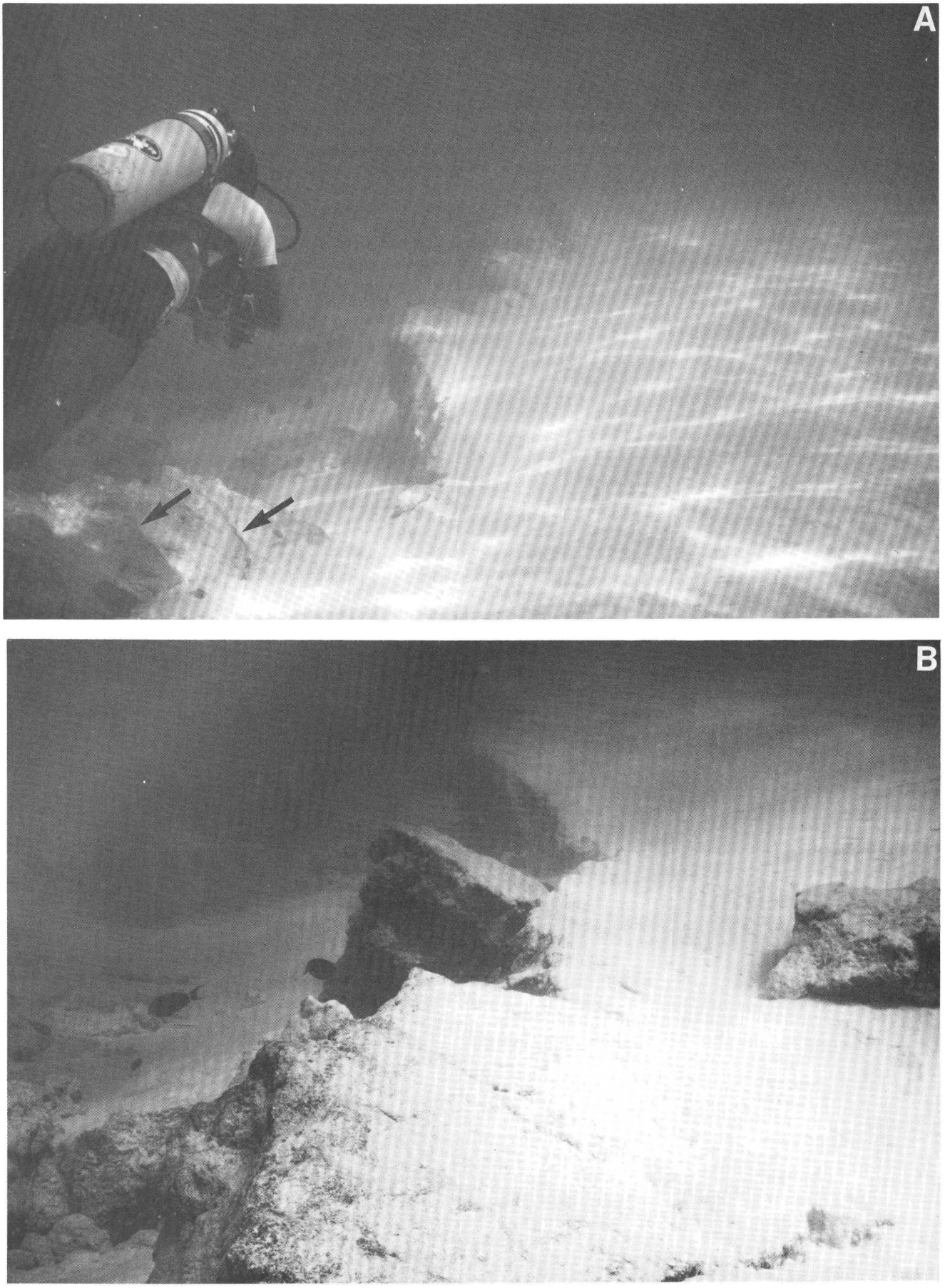
A
B

Figure 21. Upturned flap in reef plate at LACROSSE crater (fig. 1) on east side of atoll near Runit Island. Compare with figures 20*A* and *B*.

p. 70–71)—that the reef plate at the crater rim slid toward the crater a distance of about 90 m (300 ft)—may be incorrect. This transect is south of the location of reef plate that they suggested had moved, and their interpretation cannot be ruled out. To remove the thick layer of overburden in the area of the central escarpment required a larger airlift than we had available.

Fractures

The exposed reef plate contains numerous fractures and joints, especially near the site of OAK core no. 2. In addition, we observed several faults with down-to-the-crater displacement of 8.5 to 15 cm (3–6 in.). The rock contains pervasive microfractures (fig. 24*A*). These microfractures made drilling difficult because the angular chips continually jammed the core barrel. Fracturing was not apparent at the site of OAK core no. 4 farthest from the crater. At that site, only the upper 1.5 m (5 ft) of section was cemented. The sediment in the remainder of the hole down to 7.6 m (25 ft) was mostly uncemented carbonate sand with some coral debris.

Secondary Crater

We located a secondary crater along our transect, approximately 244 m (800 ft) from the crater rim and about 61 m (200 ft) from the site of OAK core no. 3 (fig. 19). The crater is 30 m (100 ft) in diameter and, for the most part, is surrounded by upturned reef plate. At extreme low tide, most of the upturned rocks protrude a few centimeters above the water surface (figs. 25*A*,*B*). Water in most of the sand-and-rubble-filled crater is less than 1.5 m (5 ft) deep at low tide, but at the western edge it is as deep as 4 m (13 ft), possibly due to wave and current scour of the bottom. The object that created this crater was not evident. If the crater

Figure 20*A* (top left). Subsided and upturned reef plate near location of OAK core no. 2. (See fig. 1.) Note ripple-like features on upturned rock below diver (arrows on crests). Features have same orientation and spacing as those shown in figure 18. Water depth 8 m (25 ft).

Figure 20*B* (bottom left). Expanded view of upturned reef plate shown in figure 20*A*.

Figure 22. The precipitous dropoff formed by subsided reef plate at location of OAK core no. 2. (See fig. 1.) Note fractures and postevent corals (*Porites lutea*) in foreground. Carbonate sand covers the rock except at edge. Water depth is 9 m (30 ft).

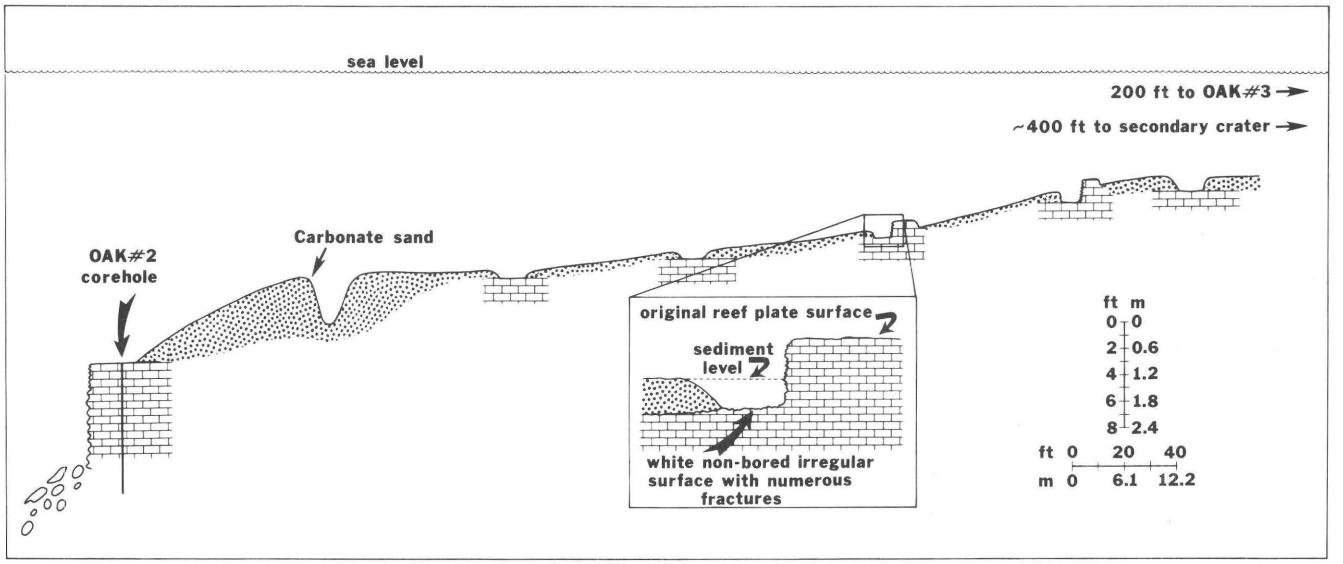

Figure 23. Cross section of pits, including OAK core no. 2, showing that subsided reef plate is continuous beneath sand. Much of the reef plate surface has been stripped by the OAK event and is shown in inset. See figures 1 and 19 for location; see also figures 24*A* and *B*. Water depth at each pit was measured within a period of 15 minutes to avoid errors caused by changing tide level.

is a secondary one, it is five times larger than those previously described by Ristvet and others (1978).

Patch Reef

A large patch reef is located about 2 km (1.1 nmi) southwest of OAK ground zero, just beyond the area covered by our bathymetric grid. (See SC no. 1, fig. 1). Its steep sides rise from a depth of 34 m (110 ft) to 9 m (30 ft). A sketch of the reef, which was named "Scorpion Conch Reef," is shown in figure 26*A*. Large fractures in it were probably caused by the OAK event (fig. 26*B*).

High-resolution seismic-reflection profiles indicate that many of the lagoonal patch reefs near OAK crater have accumulated over small Pleistocene topographic highs (chap. C, this volume). Many of the mounds sampled with the submersible in the eastern part of the crater are composed of Pleistocene or pre-Holocene reefal material (chap. F, this volume). Farther from ground zero, similar mounds are composed of living and dead Holocene corals. These observations suggested that many of the features closest to ground zero may be pre-Holocene coral mounds from which the Holocene cover has been stripped away by the blast.

Cores of the upper 8 m (25 ft) of the reef consist of slightly cemented coral and coralgal sand (recovery was poor) overlying uncemented sand between 8 and 12 m (25–35 ft); the latter was not recovered. No pre-Holocene rock was encountered. If Scorpion Conch Reef is like others in the lagoon, its Holocene cap may be in excess of 15 m (50 ft) thick.

Discussion

Like Ristvet and others (1978), we consider that the deepening of the reef flat opposite OAK crater (fig. 17) and the clearly evident down-to-the-crater subsidence and faulting (fig. 22) are the result of post-event subsidence, probably due to shock-induced liquefaction, grain reorganization, and dewatering. That such subsidence would have occurred instantaneously several hundred meters from ground zero is unlikely. Outside the vaporized area, expulsion of water controls localized subsidence, and the large numbers of tortuous interparticle pathways that escaping water would have to follow make it impossible for the water to escape quickly. Subsidence was probably greatest at ground zero and decreased with distance from it. How fast the reef plate subsided is not known. At KOA crater, Ristvet and others (1978) reported 2 m (6.5 ft) of subsidence just outside the crater rim associated with sand blows and water boils caused by escaping water. A similar situation undoubtedly took place at OAK.

The precipitous rock wall at the west margin of OAK may be the maximum extent of cratering at the time of the event, that is, the wall may be the transient crater rim. The upturned attitude of the reef plate, similar to the rim around LACROSSE crater, supports this hypothesis. The possibility that it is a rotated slab of slumped reef plate cannot be ruled out. We observed much of the crater rim wall dipping into the crater toward the area of maximum subsidence, which corroborates the geophysical results (chap. C and D, this volume).

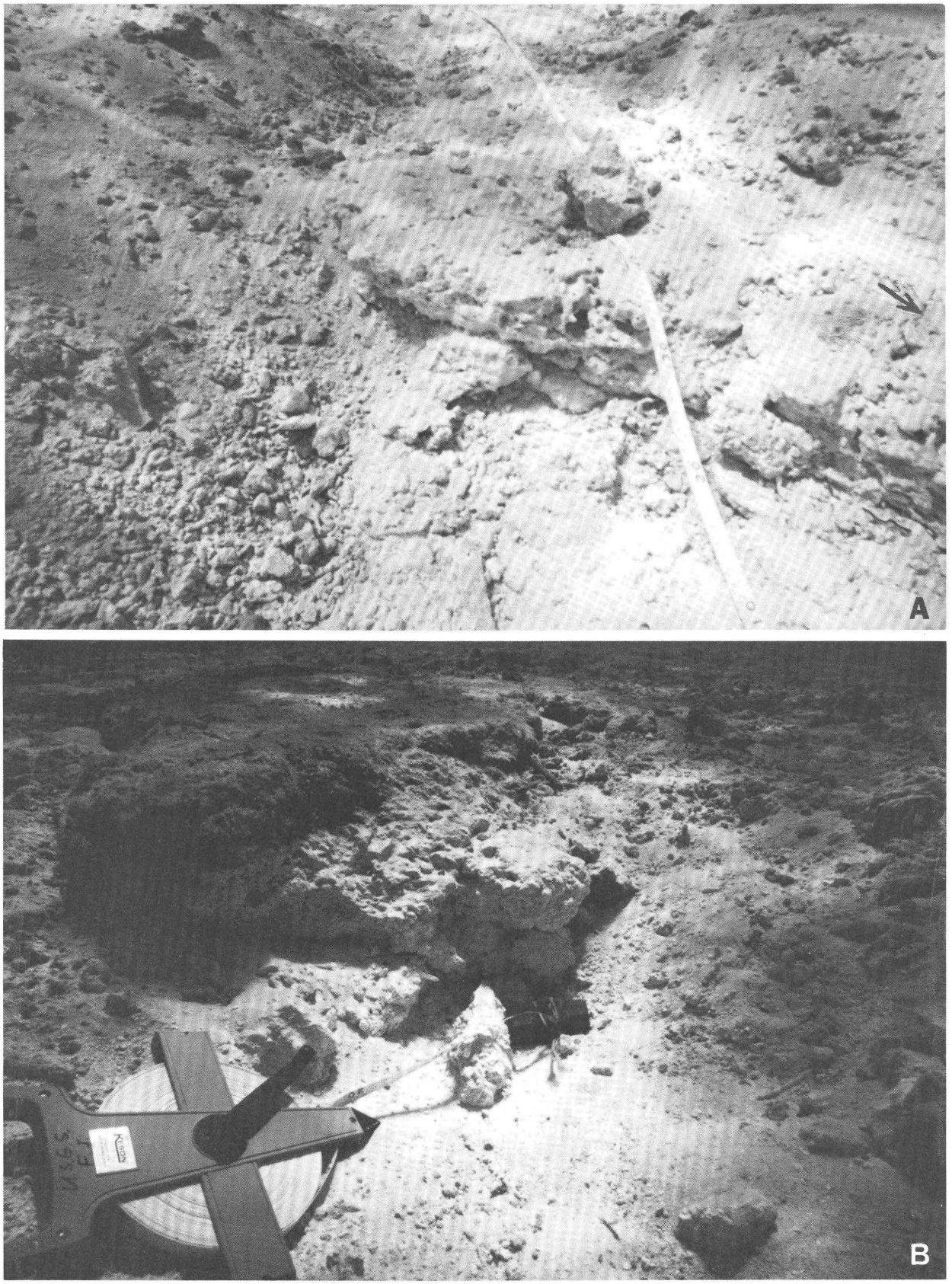

Figure 24. *A,* Surface of reef plate rock exposed in pit in figure 23. Note lack of pseudoripples and boring. Surface is irregular and fractured. Small fracture is visible at right-hand side of photograph (see arrow). Tape designations are in centimeters. *B,* Pit dug next to slab of rock showing that slab is actually a part of reef plate not stripped away. See inset in figure 23 for detail. Diameter of tape in spool is about 20 cm (8 in.).

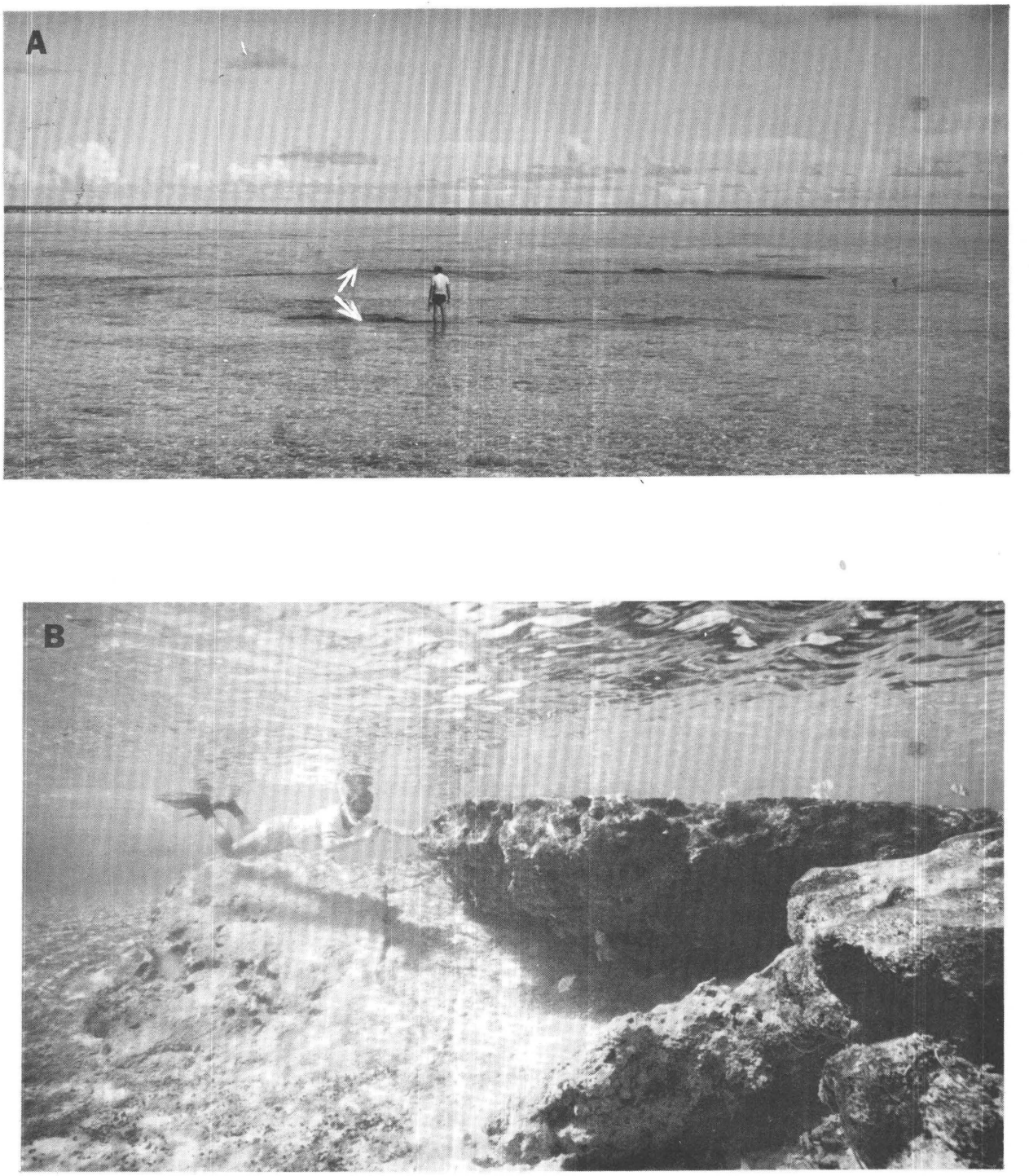

Figure 25. *A,* Upturned rim of secondary crater as exposed at low tide (see arrows). Man is facing northwest and standing on upturned rim. Crater is 30 m (100 ft) in diameter. *B,* Underwater view of interior of secondary crater showing part of upturned rim. Rim is exposed at low tide.

On the reef flat, post-Pleistocene material consists of well-cemented limestone, 1.5 to 2.5 m (5–8 ft) thick, that is underlain by 4.6 to 6 m (15–20 ft) of uncemented or poorly cemented sand; the sand, in turn, lies on cemented Pleistocene limestone. (See OAK core no. 1, figs. 8, 11; OAK core nos. 2, 3, fig. 9). The unconsolidated sand probably facilitated the removal and peeling of the cemented reef plate from the underlying Pleistocene limestone. Peeling back of the reef plate may have created an upturned flap found along much of the west wall of OAK crater. As the

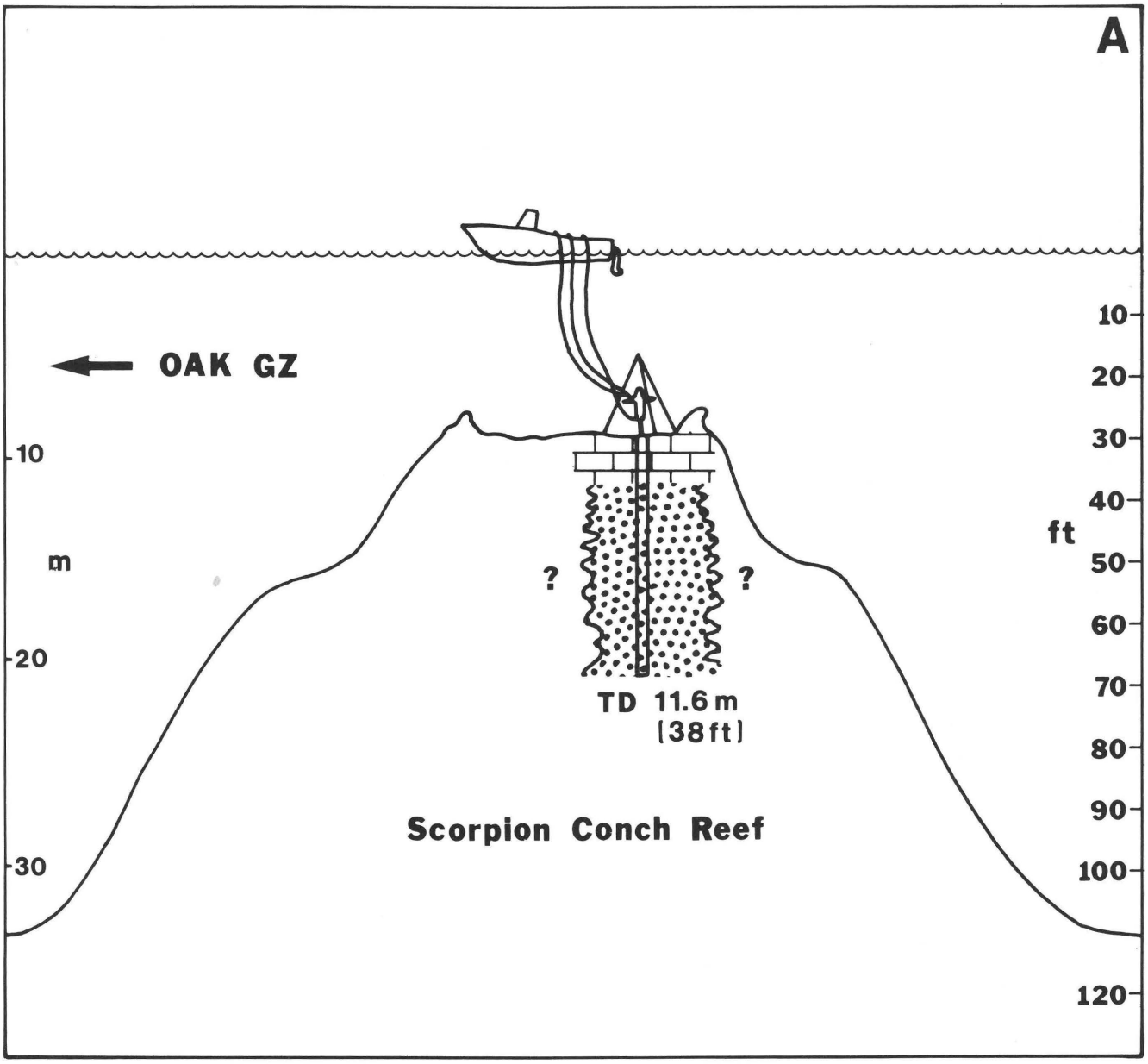

Figure 26*A*. Sketched cross section of Scorpion Conch Reef showing drilling location and thickness of section drilled. Brick pattern indicates slightly cemented coral and coralgal sand. Dots indicate uncemented coralgal sand. TD=total depth.

wall subsided, most of the upturned ledge apparently tilted back toward ground zero. Only in one area (figs. 20*A*,*B*) did the flap retain a dip away from ground zero. If this is correct, then the transient crater diameter may be approximated by the distance from this flap to ground zero, about 550 m (1,800 ft). The reef buttressed the blast, resulting in a wider distribution of debris in the lagoon (chap. A, B, and C, this volume).

The inrush of water to fill the crater excavated by the blast must have had significant effects on material in and around the crater. The sudden influx of water from the lagoonward side of the crater, where waters were about 45 m (150 ft) deep, undoubtedly transported much excavated material back into the crater and probably swept completely over the reef plate; however, its effect on the reef plate was probably less than elsewhere. The softer sediments in the lagoon were probably more affected by shock, by subsidence due to dewatering, and by erosion and deposition associated with the postblast rush of water back into the crater.

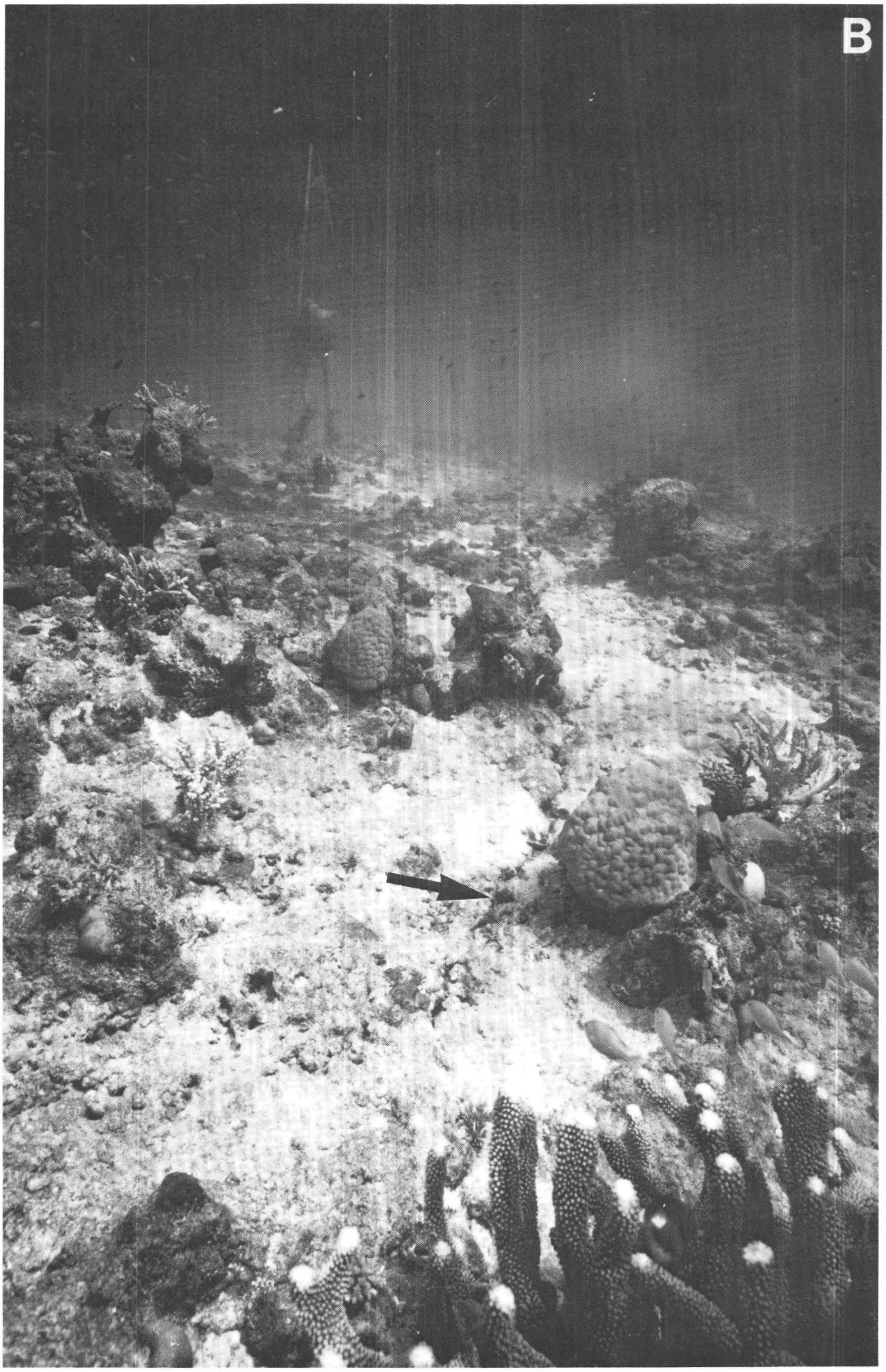

Figure 26*B*. Surface of Scorpion Conch patch reef at a depth of 9 m (30 ft). Arrow points to fracture in foreground. Coral head near arrow is approximately 1 m (3 ft) in diameter.

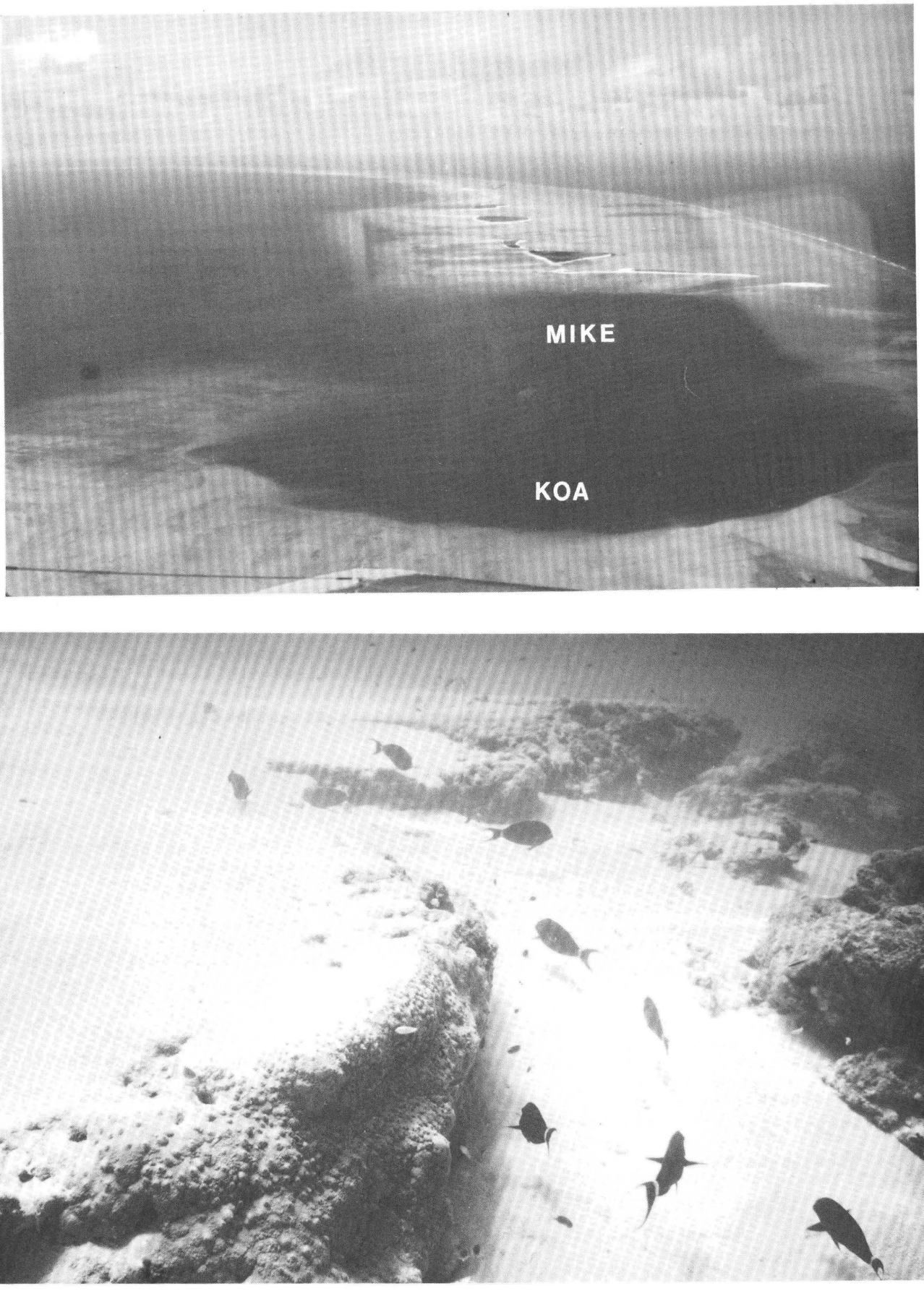
MIKE
KOA

Conclusions—OAK Crater

1. The west rocky escarpment of OAK crater is composed of subsided reef flat (upturned in one area) and may approximate the radius of the transient crater. On the northwest, reef-flat side of ground zero, therefore, we estimate that the transient crater radius is between 457 and 550 m (1,500–1,800 ft).
2. The transient crater wall northwest of ground zero subsided as much as 21 m (70 ft).
3. Cratering was greatly influenced by the geology; energy from the event followed paths of least resistance, that is, along changes in bedding and lithology.
4. Reef plate, 0.3 to 0.6 m (1–2 ft) thick, was stripped away as far as 122 m (400 ft) from the west crater rim.

Observations of KOA Crater Area

KOA was detonated in a geologically different setting from the one at OAK. KOA crater lies almost completely within a broad (greater than 1 km wide) reef flat, termed the "transitional area" by Ristvet and others (1978), at the northwest corner of the atoll, halfway between the windward east and northeast part of the atoll and leeward west rim of the atoll. The crater margins are clearly visible from the air, except on the southwest side where they merge with MIKE crater (fig. 27). Water surrounding the crater is less than 7 m (23 ft) deep in most places. To the northwest, the reef flat is only 30 to 60 cm (1–2 ft) deep at extreme low tides.

Because of KOA's location downwind from a reef flat thriving with sediment-producing organisms, the sedimentation rate, especially during storms, is high. High-resolution seismic-profile data (chapter C, this volume) indicate that about 9 m (30 ft) of postevent fill has accumulated. Because of this influx of sediment and the sluggish circulation of water in the crater, underwater visibility was seldom more than 6 m (20 ft). During one 3- to 4-day period in September, when winds blew from the west instead of the more common easterly direction, clear water moved into the crater, and underwater visibility improved to greater than 18 m (60 ft).

Diver Observations

The entire submerged margin of the crater, except for the part overlapping MIKE crater, was observed by two divers as they were towed behind *Halimeda*. The margin was even more thoroughly viewed from the submersible, which made dives along the 6-, 9-, and 18-m (10, 30, and 60 ft) isobaths. A ledge of rock is exposed near the north rim of the crater in 9 m (30 ft) of water (fig. 28); this ledge was documented thoroughly on video and with a 10-cm-diameter (4-in.-diameter) core, 60 cm (24 in.) long, to determine its age and composition. The rock is reef plate of Holocene age, similar to the reef plate that we observed at OAK crater. It is also identical to the rock we recovered in three cores collected from the reef flat north of KOA's rim, in 30 to 60 cm (1–2 ft) of water.

The ledge of rock (fig. 28) is slightly upturned; however, because of its limited exposure (the ledge lies parallel to the crater margin for about 12 m, or 40 ft), we could not determine if it was a rotated slab partly buried in sand or part of a more continuous layer that had been upturned. It is most likely a small dislocated slab that was not overturned but has been down-dropped about 9 m (30 ft) from its original position on the reef flat.

Most of the remainder of the the KOA crater margin consists of sediment. Along the north margin it is composed of sand-, pebble-, and cobble-size material that extends from 1.8 to 18 m (6–60 ft) of water depth. It lacks algal encrusters and appears to be freshly deposited. This sediment is probably frequently modified and supplemented by detritus transported into the crater from the adjacent reef flat.

Along the east margin, the slope is less steep than along the north margin, and the sediment is finer grained. Staghorn corals grow prolifically wherever rocks and manmade debris form a suitable substrate. We determined that massive head corals (*Porites lutea*) in the area began to grow on manmade objects within a year of the event. Other than the rock shown in figure 28, observations by scuba divers and from the submersible revealed few geological features useful to establishing the location of the transient crater margin. Manmade objects were discovered on the crater bottom; these objects provided data easily interpreted to indicate subsidence and a maximum crater diameter. The objects included a concrete test station, some railroad rails outside the crater in shallow water, and more significantly, a row of railroad rails in the crater in waters as much as 18 m (60 ft) deep. These objects are described below, beginning with those located in shallow water.

Concrete Test Structure

The remains of a large 43-m-long (142-ft-long) test structure (sta. 360.01), originally emplaced to test blast effects, were found in approximately 2.4 m (8 ft) of water 61 m (200 ft) from the east edge of the crater (figs. 29, 30). Preevent photographs (fig. 31) show that the structure was originally located on the island just above sea level. Ristvet and others (1978) determined that it subsided about 2 m (6 ft) within 8 days after the event (fig. 32). The station

Figure 27 (top left). Oblique aerial photograph looking westward, showing KOA and MIKE craters.

Figure 28 (bottom left). Slightly upturned Holocene reef plate in 9 m (30 ft) of water in a small area near north edge of KOA crater. Sand covers all but the edge of rock layer. Fish are approximately 0.3 m (1 ft) long.

COLLIMATOR STATION
RR Rails
Concrete Test Structure (Sta. 360.01)
N
0
30
m
0
100
ft
8 RR Rails

Figure 30. Concrete test structure shown in figures 29 and 31. Test structure had three separate parts. Upper surface of structure was 3.5 m (11.5 ft) above mean low water before KOA event.

originally was 558 m (1,830 ft) from ground zero (fig. 33), and its remains may have moved about 3 to 4 m (10–13 ft) closer to ground zero.

Shallow Railroad Rails

Near the concrete test structure is a line of railroad rails that were driven vertically into the bottom, spaced about 1.2 m (4 ft) apart for a distance of about 30 m (100 ft). The rails form a line tangential to the crater margin (fig. 29). In places, timbers connect the base of the rails (fig. 34). Head and branching corals, including one colony of *Pocillopora elegans* that is 2.2 m (7 ft) in diameter (fig. 35), grow on many of the rails. Many of the rails are bent away from ground zero.

More widely spaced rails along the same line extend for a distance of 30 m (100 ft) toward the crater margin. At the crater margin, they lead to a considerable amount of debris, consisting mainly of riprap and other rails that define a partly rectangular shape. The rails lie in water approximately 4.6 m (15 ft) deep outside the crater; some debris and rails extend down the slope into water as deep as 12 m (40 ft). Examination of old photographs, especially those in figures 36 and 37, shows that this is the location of the collimator station over which the line-of-sight (LOS) tube led from the housing of the device at ground zero to a bunker on Bokaidrik (Helen) Island. The line of rails leading toward the collimator station was part of the 7-m-wide (24-ft-wide) causeway shown in figures 31 and 36. Both the causeway and the collimator station were constructed of rails lined with timbers, driven into the reef flat and infilled with riprap and sand.

We verified the identity of the structure by locating the LOS supports (figs. 31, 36, 37). The remains of the 23-cm-wide (9-in.-wide) I-beams protrude 0.3 to 0.6 m (1–2 ft) from the bottom. They form a straight line leading from the bunker toward ground zero. We buoyed three of

Figure 29 (left). Vertical aerial view of the east margin of KOA crater showing location of a 43-m-long (142-ft-long) concrete test structure (Holmes and Narver sta. 360.01). Railroad rails northwest of the concrete structure are the remains of a causeway leading to the collimator station. Southwest of the structure, a set of eight rails extends into the crater to a depth of 8 m (25 ft). The east end of 28 more rails is marked by the circled cross at the lower left corner of the photograph. (Photograph courtesy of B. L. Ristvet.)

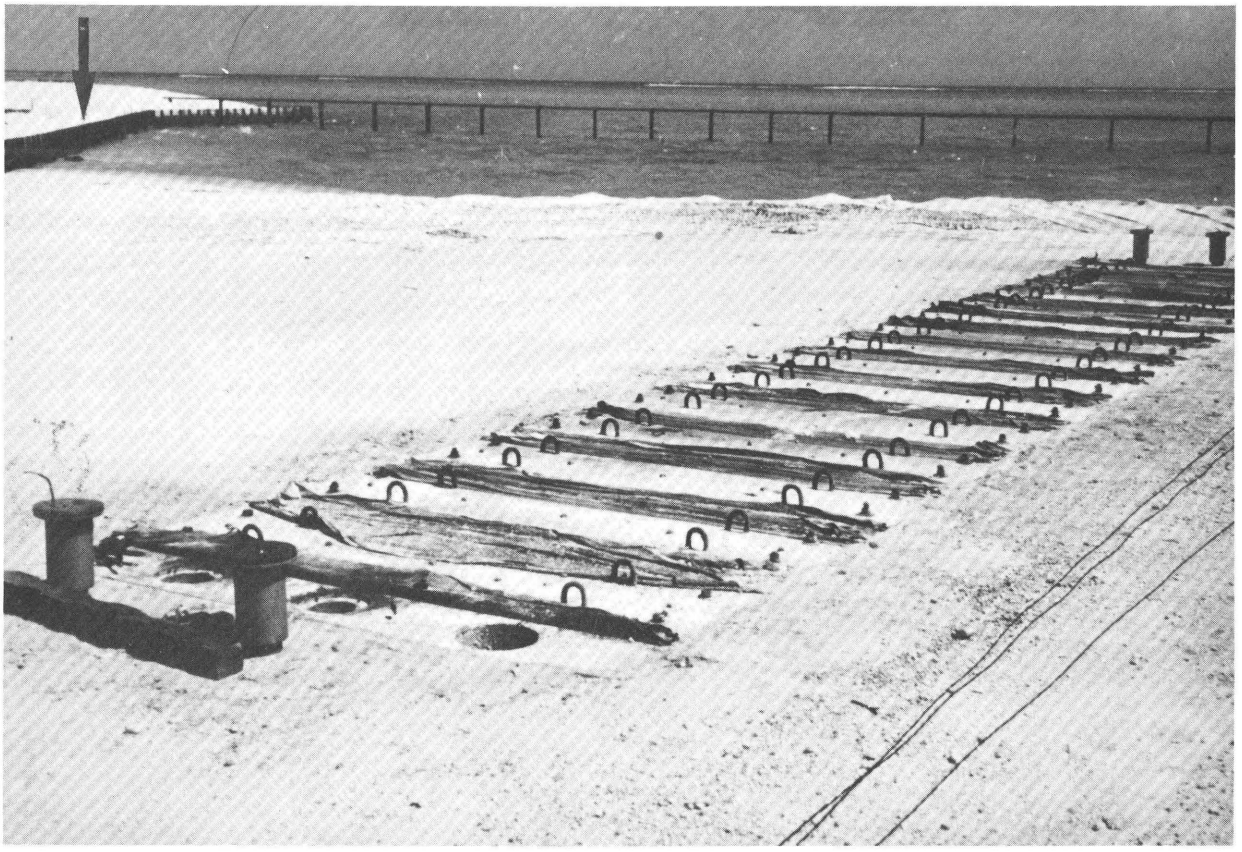

the beams with taut lines to establish their positions to aid the search for additional beams in the crater; none was found.

The rails that remained standing were all on the east side of both the collimator station and the causeway—the side away from ground zero. Preevent photography indicates that water depth at the time of construction was less than 1 m (3 ft). Maximum water depth was probably no more than 1.8 m (3 ft). Clearly, the tops of the rails visible in figure 34 were about 1 m (3 ft) above water when the photograph in figure 31 was taken.

The tops of the rails are now about 1.5 m (5 ft) below sea level. Subsidence took place as far as 100 m (330 ft) from the present edge of the sharp dropoff into the crater.

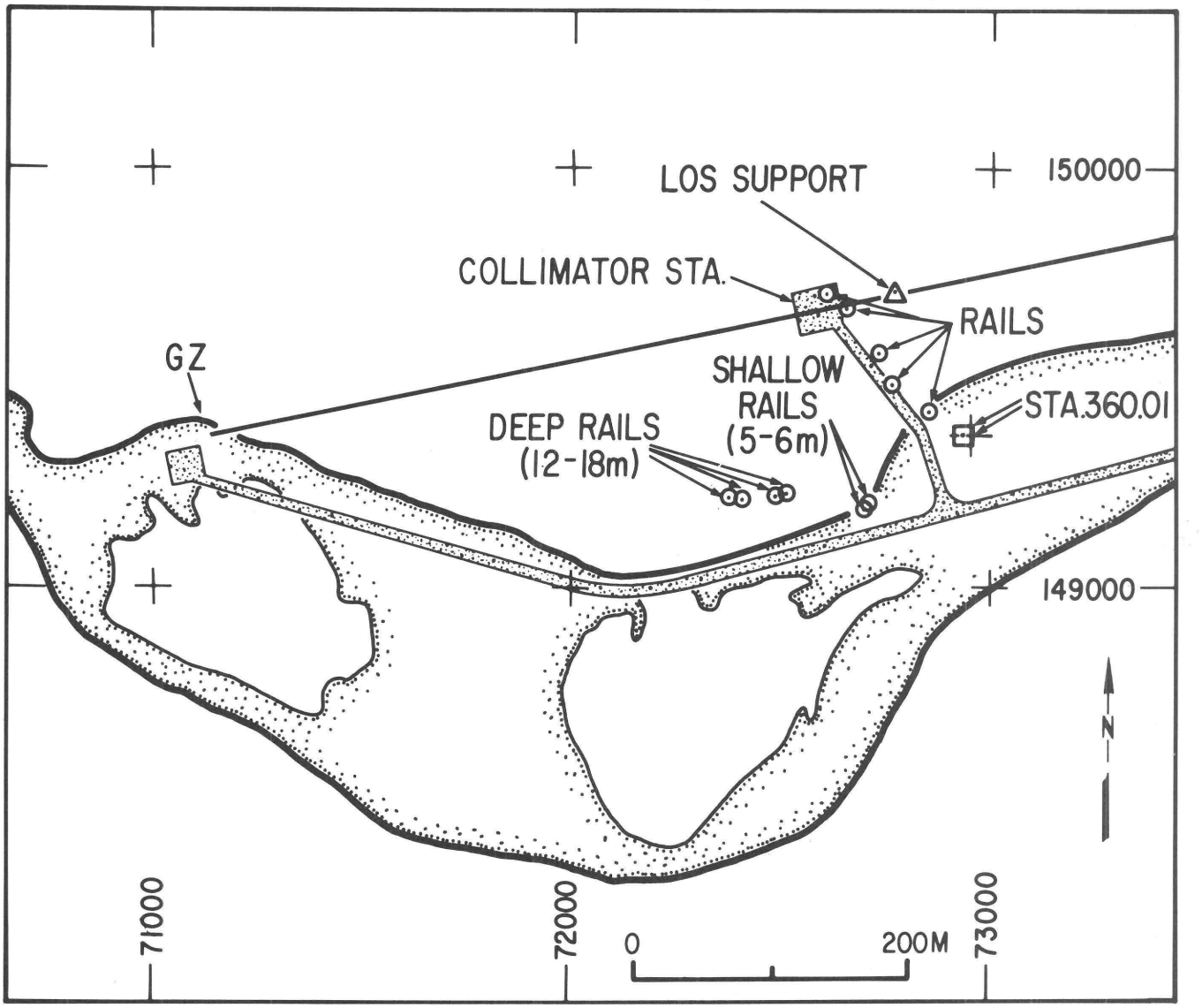

Figure 33. A diagram of the preevent KOA area taken from a photocopy of a Holmes and Narver drawing (courtesy B. L. Ristvet), showing the locations of various structures that we located underwater close to or in the crater. The buoy over the line-of-sight (LOS) I-beam support (triangle) and over station 360.01 (square) were located by H. V. Woodworth (of the Defense Mapping Agency) from shore with a theodolite. Most other buoys were located by the Miniranger System aboard a small boat. The Holmes and Narver location for station 360.01 (shown by a cross) is 4 m (14 ft) east of the position we buoyed.

Figure 31 (top left). North part of concrete test station 360.01 as it appeared before KOA event. Top of structure is 2.4 m (8 ft) wide and 3.5 m (11.5 ft) above mean low water. Note line-of-sight (LOS) tube on top of I-beams at top of photograph. LOS tube leads across collimator station at left and to KOA device shown in figure 37. Arrow shows vertical railroad rails used to make bulkhead of causeway leading to collimator station. Rails under arrow are same rails shown in figures 34 and 35. (Photograph courtesy of B. L. Ristvet.)

Figure 32 (bottom left). The northern part of station 360.01 subsided 2 m (6 ft) about 8 days after KOA event as it appears here. Note water level shown by arrow. (Photograph courtesy B. L. Ristvet.)

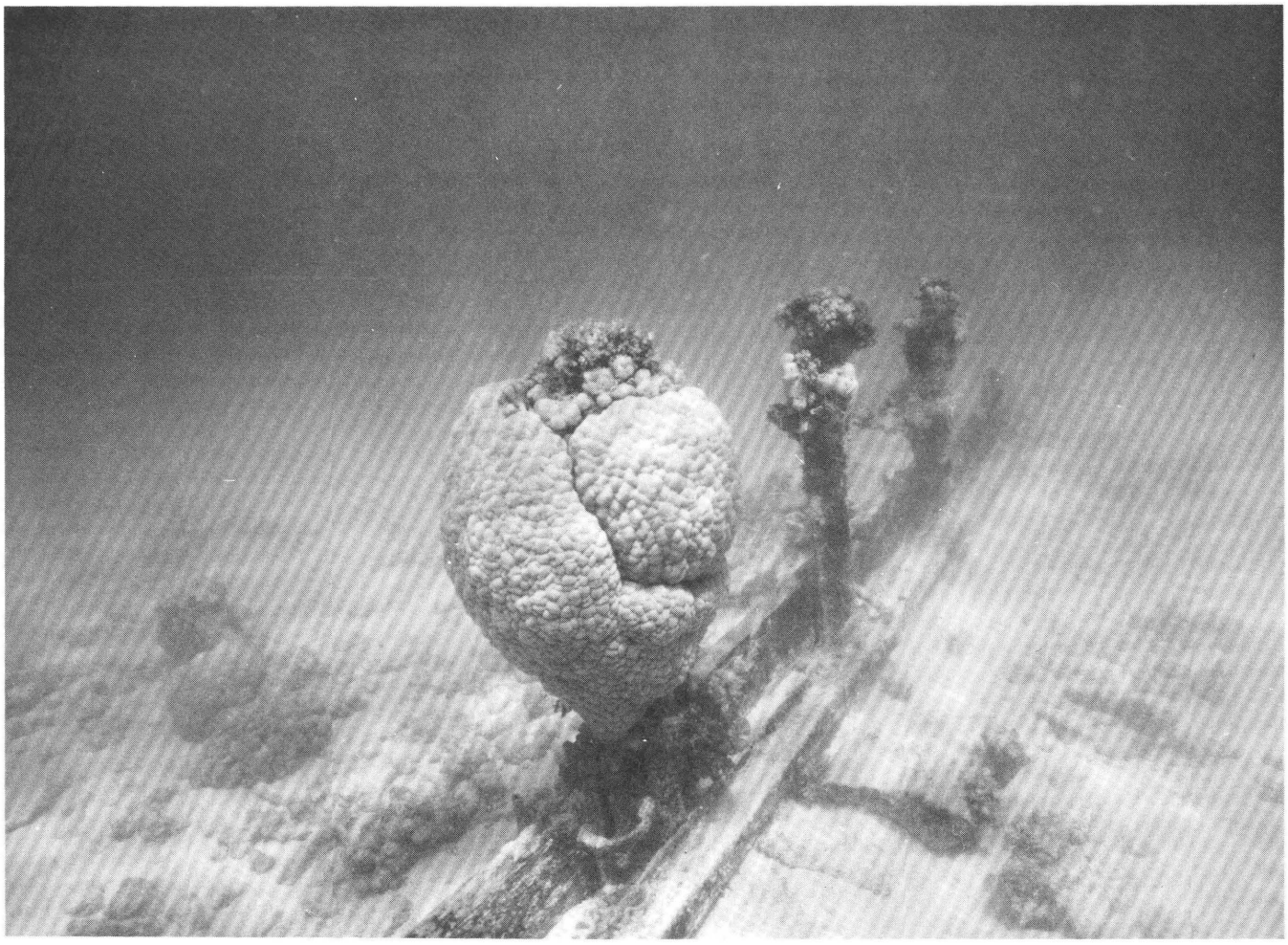

Figure 34. Line of rails with corals attached leading toward collimator station. View is to the north. Note timbers remaining at base of rails. These rails are the same as those shown by arrow in figure 31. Rails on side of causeway facing KOA ground zero were removed by the event.

Railroad Rails within KOA Crater

The most significant railroad rails were discovered in KOA crater during submersible reconnaissance dive no. 90. The rails were later buoyed and examined by scuba divers. The depth and spacing of the 28 rails was carefully determined, and the entire line was documented photographically and on videotape transects. The easternmost rail lies in 15 m (50 ft) of water; the line extends westward (toward ground zero) for a distance of 46 m (152 ft) into water that is 18 m (60 ft) deep (table 1). Most rails protrude above the bottom more than 1.8 m (6 ft), many are at least 3 m (10 ft) high, and one is 4.4 m (14.5 ft) long. Most are bent away from ground zero, and all have their flat bases oriented to the south (fig. 38). This set of rails is aligned with another set of eight rails that are located at the crater margin. The eastern end of this shallower line lies in 6 m (20 ft) of water (fig. 29) and extends westward into about 7.6 m (25 ft) of water. The bases of this line face south. No more rails were found in the area between the two sets of rails. Several cables, including one that was 10 cm (4 in.) in diameter and aluminum-shielded, extend into the crater from the site of

Figure 35. Detail of southernmost rail, which has a 2.2-m-diameter (7-ft-diameter) colony of *Pocillopora elegans* attached. Note timbers at base of line. Tape designations are in centimeters.

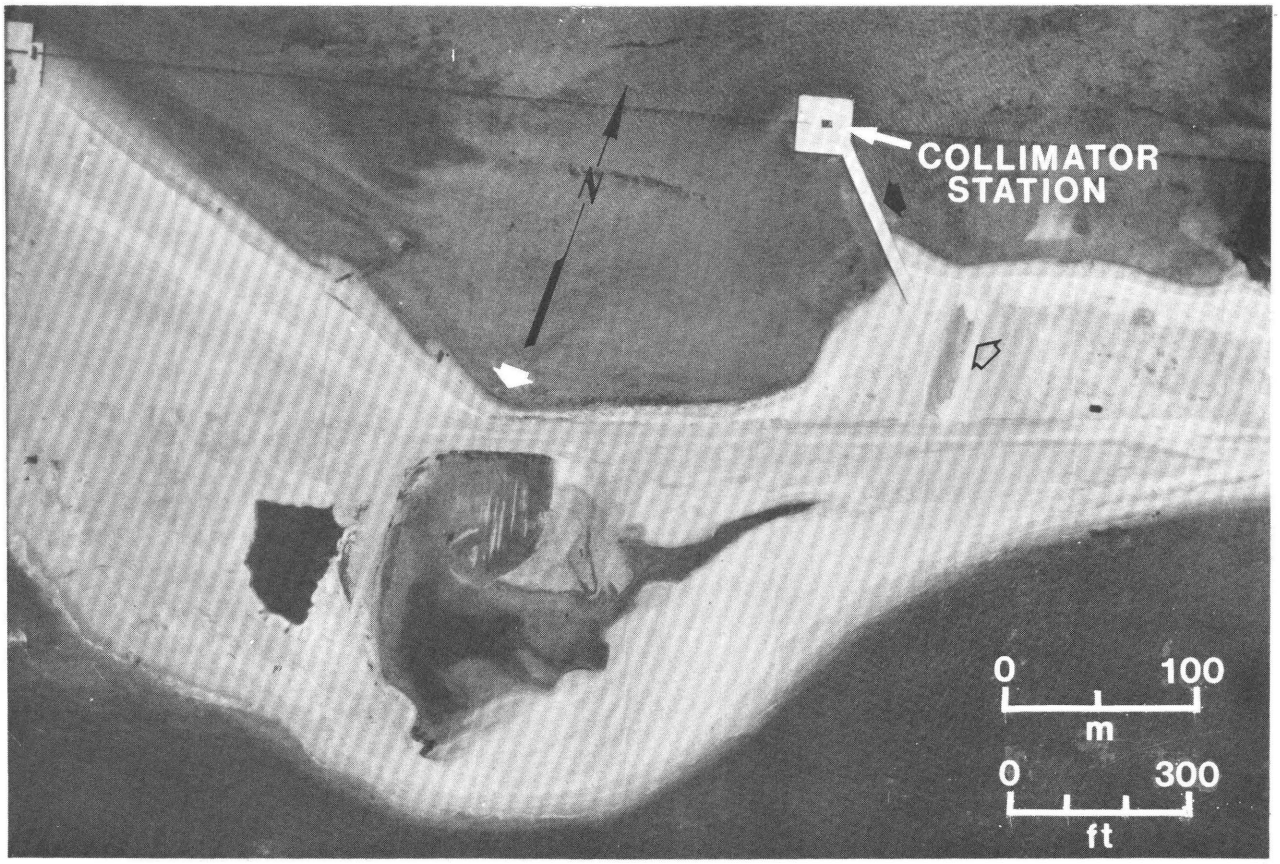
COLLIMATOR
STATION
N
0
100
m
0
300
ft


LOS TUBE
N

the shallow rails just south of the concrete structure shown in figure 29. The cables pass down into the sediment in about 6 m (20 ft) of water.

Using the hydraulic drill suspended from an airbag, a 3.7-m (12 ft) hole was cored 1 m (3 ft) north of the last rail in 18 m (60 ft) of water. The first 1.5 m (5 ft) of sediment was carbonate sand, which was not recovered; the remainder was rubble (probably riprap), and recovery was poor. Another site was cored 15 m (50 ft) closer to ground zero, and the same type of material was recovered. We dug a 1.5-m (5 ft) pit at the south side of the base of the last rail in 18 m (60 ft) of water. Most of the material there was sand, but the pit also contained riprap, tree limbs, and pieces of timber. The material appeared to be fill, possibly used to construct a causeway like the one that led to the collimator station.

All the rails were driven in with their flat bases oriented to the south, normal for rails used to hold back an earthen bulkhead or causeway on their south side. Timbers still attached to the collimator causeway (fig. 34) attest to this style of construction. Engineering drawings (dated December 27, 1957, Holmes and Narver) indicate that the rails shown in figure 34 were driven at least 1.2 m (4 ft) into "coral" and 1.8 m (6 ft) into sand. The timbers were attached to the base of the rails with 1.27-cm-diameter (1/2-in.-diameter) bolts.

The line of rails has a distinct bend in it. Most rails lie in an east-west line perpendicular to the crater margin, but between rails 16 and 17, the line bends 5–10° to the northwest toward ground zero.

The photographs and the Holmes and Narver diagrams of the preevent KOA area show a causeway located south of the deep rails (fig. 37). A bend in the causeway, shown by the arrow in figure 36, lies about 70 m (230 ft) west and 60 m (200 ft) south of the similar bend in the railroad rails, suggesting that the bend in the railroad rails is the same bend as in the causeway. If this is correct, the rails have moved at least 90 m (300 ft) to the northeast. Slumping, probably common in this area (chap. A, this volume), appears to have moved surface material to the northwest into the crater. It is improbable that a large portion of the bottom,

Figure 36 (top left). Pre-KOA event aerial photograph showing line-of-sight tube crossing to collimator station (solid white arrow), concrete test station 360.01 (open arrow), and curve in bulkheaded shoreline (wide white arrow). (Photograph courtesy of B. L. Ristvet.)

Figure 37 (bottom left). Aerial oblique photograph, looking east, of KOA device in water tank at lower right and line-of-sight tube leading from bunker in distance. Wide arrow indicates curve in bulkhead shown in figure 36. Riprap is visible below arrow. Cylindrical tank is 10 m (30 ft) in diameter. (Photograph courtesy of B. L. Ristvet.)

Table 1. Spacing of rails in KOA crater beginning in 18 m (60 ft) of water closest to ground zero and ending in 15 m (50 ft) of water farthest from ground zero

[GZ = ground zero]

Rail no.	Distance between rails (meters/feet)	Comments
1----0	0	Long, bent to N. large clump of staghorn coral at base.
2----1.6	5.3	Long, bent to N.
3----1.5	4.8	Clump of coral on top.
4----1.3	4.4	Short, 1 m (3 ft) high, staghorn between it and next rail.
5----1.2	4.1	Tall but broken.
6----0.9	2.9	Tall, 4.4 m (14.5 ft) and bent toward GZ, horizontal at top with coral, almost touches rail 5.
7----1.4	4.7	Short, less than 1 ft long, broken.
8----1.4	4.7	Long, bent toward GZ and S.
9----1.8	5.8	Tall, bent away from GZ.
10----2.0	6.4	Tall with clump of branching coral at base, top bent away from GZ.
11----2.4	7.8	Tall with clump of coral midway up.
12----2.0	6.7	Tall, bent away from GZ.
13----1.5	5.0	Tall, bent away from GZ.
14----1.6	5.2	Tall, bent away from GZ, clump of coral at top.
15----1.3	4.2	Tall, bent away from GZ.
16----1.4	4.7	Tall, bent away from GZ, coral at base, long space to next rail.
		Significant bend occurs between rails 16 and 17.
17----4.8	15.7	Tall, bent toward GZ?, long space to next rail, staghorn coral to N.
18----4.8	13.1	Tall.
19----1.8	5.8	Tall with parasol-shaped staghorn coral at base.
20----1.6	5.2	Medium size, staghorn coral to S.
21----1.3	4.4	Short with *Porites* on top, broken rails on bottom.
		Broken rail between rails 21 and 22, lots of debris, 4 rails on bottom.
22----1.4	4.5	Long, bent away from GZ.
23----1.3	4.2	Medium length, bent away from GZ, rail on bottom between rail 23 and 24.
24----1.3	4.2	Long, bent away from GZ and touching rail 25.
25----1.5	4.8	Long, bent away from GZ and touching rail 24, rail 25 is 3.5 m (11.6 ft) long.
26----1.2	4.0	0.9 to 1.2 m (3–4 ft) high, rail straight.
27----1.5	4.8	1 m (3 ft) high, straight.
28----1.6	5.4	0.2 m (0.8 ft) of rail bent away from GZ.

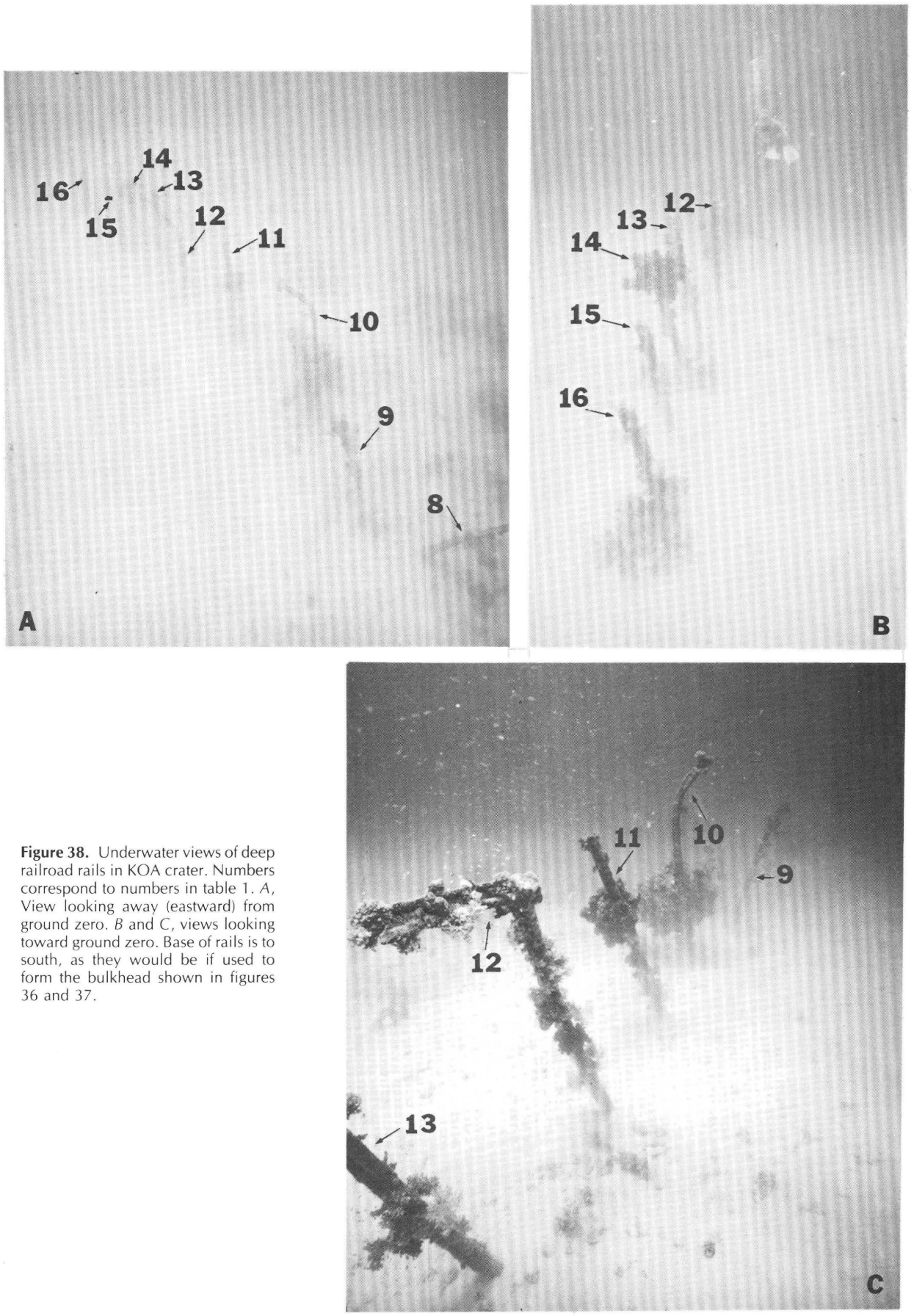

Figure 38. Underwater views of deep railroad rails in KOA crater. Numbers correspond to numbers in table 1. *A*, View looking away (eastward) from ground zero. *B* and *C*, views looking toward ground zero. Base of rails is to south, as they would be if used to form the bulkhead shown in figures 36 and 37.

at least 46.3 m or 152 ft long, could move 300 ft (90 m) away from ground zero while maintaining the linear integrity of 28 railroad rails.

After reexamining our techniques and records, the navigation fixes appear to be correct, and the rails are accurately located. Dives 90 and 109 both locate the rails in roughly the position shown. We moored buoys with taut lines over the deep rails, and the buoys were located with the Miniranger system aboard a small boat. These locations coincide closely with those established by the submersible (chap. F, this volume).

It is possible that the rails are at or close to their original positions and that they were not part of a structure included in the preevent documentation (fig. 33). If that is the case, the most craterward rail lies at 393 m (1,290 ft) from ground zero. Because we found materials in our core 15 m (50 ft) beyond the last rail that are similar to material at the last rail, we can subtract this value from the distance to ground zero; therefore, the resulting figure of 378 m (1,240 ft) may represent the maximum transient crater radius in this area.

If no rails were set at the locations they presently occupy, those in deeper water must have moved from their original locations at either the shoreline or the causeway. If we assume that the bend in the rails was acquired due to relative movement of the substrate, the need for a correlation with the bend in the causeway is eliminated. The line of rails can then at least be partially reconstructed by joining the shallow group with the deep group (fig. 33); this means that the deep rails must have moved about 56 m (184 ft) toward ground zero in a postblast slump. Thus the riprap that was drilled 15 m (50 ft) craterward of the deepest rail would have been about 430 m (1,411 ft) from ground zero before slumping took place. This distance probably represents a better estimate for the maximum transient crater radius in the southeast quadrant of the crater.

REFERENCES

Cloud, P. E., Jr., 1959, Geology of Saipan, Marianas Islands, Part 4—Submarine topography and shoal-water ecology: U.S. Geological Survey Professional Paper 280–K, p. 361–445.

Couch, R. F., Jr., Fetzer, J. A., Goter E. R., Ristvet, B. L., Tremba, E. L., Walter, D. R., Wendland, V. P., 1975, Drilling operations on Enewetak Atoll during Project EXPOE: Air Force Weapons Laboratory Technical Report TR–75–216, Kirtland Air Force Base, New Mexico 87117, 270 p.

James, N. P., and Ginsburg, R. N., 1979, The seaward margin of Belize barrier and atoll reefs: International Association of Sedimentologists Special Publication No. 3: Blackwell Scientific Publications, Oxford, England, 191 p.

Ristvet, B. L., Tremba, E. L., Couch, R. F., Jr., Fetzer, J. A., Goter, E. R., Walter, D. R., and Wendland, V. P., 1978, Geologic and geophysical investigations of the Eniwetok nuclear craters: Air Force Weapons Laboratory Technical Report TR–77–242, Kirtland Air Force Base, New Mexico 87117, 298 p.

Shinn, E. A., 1963, Spur and groove formation on the Florida reef tract: Journal of Sedimentary Petrology, v. 33, no. 2, p. 291–303.

Shinn, E. A., Hudson, J. H., Halley, R. B., Lidz, B., Robbin, D. M., and Macintyre, I. G., 1982, Geology and sediment accumulation rates at Carrie Bow Cay, Belize, *in* Rutzler, K., and Macintyre, I. G., eds., The Atlantic barrier reef ecosystem at Carrie Bow Cay, Belize, I: Structure and communities: Smithsonian Contributions to the Marine Sciences, v. 12, p. 63–75.

Shinn, E. A., Hudson, J. H., Robbin, D. M., and Lidz, Barbara, 1981, Spurs and grooves revisited: Construction versus erosion, Looe Key reef, Florida: Proceedings of the 4th International Coral Reef Symposium, Manila, Philippines, v. 1, p. 475–484.

Swanson, R. G., 1981, Sample examination manual: Methods in exploration series: American Association of Petroleum Geologists, 35 p., appendices 83 p.

Tremba, E. L., Couch, R. F., Jr., and Ristvet, B. L., 1982, Enewetak Atoll Seismic Investigation (EASI): Phases I and II (final report): Air Force Weapons Laboratory Technical Report TR–82–20, Kirtland Air Force Base, New Mexico 87117, 124 p.

*U.S. GOVERNMENT PRINTING OFFICE: 1986-491-405:20129


U.S. DEPARTMENT OF THE INTERIOR
March 3, 1849